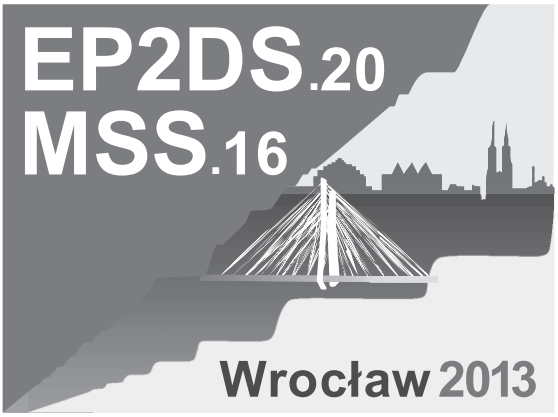

20th International Conference on

Electronic Properties of Two-Dimensional Systems

and

16th International Conference on

Modulated Semiconductor Structures

Abstracts

poster presentations

1 – 5 July 2013

Wrocław University of Technology Congress Centre

Wrocław, Poland

Dear Participants of EP2DS-20 and MSS-16,

Welcome to the joint conferences on *Electronic Properties of Two-Dimensional Systems (EP2DS)* and *Modulated Semiconductor Structures (MSS)*, organized by the Institute of Physics Wrocław University of Technology, in collaboration with the Institute of Physics, Polish Academy of Sciences.

The meeting has long tradition, reaching back to the first EP2DS conference organized by Professors John J. Quinn and Phillip J. Stiles at Brown University in 1976. It has been usually organized once in two years, alternately in America, Asia, and Europe. The last three editions took place in Genova, Italy (2007), Kobe, Japan (2009) and Tallahassee, USA (2011), and this year we have a privilege to host it for the first time in Poland.

Both conferences have established high reputation in the broad area of low-dimensional physics. EP2DS traditionally emphasizes fundamental physics, including transport and optical properties of electronic states in low-dimensional systems including graphene, nanotubes, and dielectric interfaces, while MSS addresses synthesis, processing and applications of modulated materials and novel systems including a broader range of carbon-based, hybrid, modulated organic, spintronic, and biologically based structures.

The topics highlighted by the 8 *plenary lectures* include fractional quantum Hall effect, graphene, topological insulators, quantum dots, condensates, and spintronics. *Special joint session* will also be devoted to Majorana fermions.

The conference host, *Wrocław University of Technology*, is a leading Polish university, ranked in the top five nationwide in academic quality and prestige.

The 1000 years old City of Wrocław, with the population over 600 000, is the capital of the south-western province of Poland "Lower Silesia". It is majestically situated on 12 islands on river Odra, linked by over 150 bridges. It is also the third largest Polish educational centre, with 170 000 students and 6 300 academic staff in 30 colleges, including Wrocław University of Technology as the largest one.

The Conference is proud of the Honorary Patronage of Polish Ministry of Science and Higher Education, National Centre for Research and Development, National Science Centre, Polish Physical Society, and Rector of Wrocław University of Technology. We also gratefully acknowledge financial support from Polish Ministry of Science and Higher Education, International Union of Pure and Applied Physics, and U.S. Army. The list of sponsors includes Comef, Newport, attocube, Raith, Hamamatsu Photonics Deutschland, SPS-Europe, Scontel, and PGE GiEK.

We look forward to welcoming you in Wrocław and wish you all a fruitful meeting and enjoyable time!

Jan Misiewicz Arkadiusz Wójs Jacek Kossut Tomasz Dietl

Committees

Organizers

Jan Misiewicz – Conference Chair
(*Institute of Physics, Wrocław University of Technology*)

Arkadiusz Wójs – Program Chair
(*Institute of Physics, Wrocław University of Technology*)

Jacek Kossut – EP2DS Chair
(*Institute of Physics , Polish Academy of Sciences, Warsaw*)

Tomasz Dietl – MSS Chair
(*Institute of Physics , Polish Academy of Sciences, Warsaw*)

International Advisory Committee

Gerhard Abstreiter	(*Germany*)	Charles Marcus	(*Denmark*)
Gunther Bauer	(*Austria*)	Bruce D. McCombe	(*USA*)
Fabio Beltram	(*Italy*)	Aron Pinczuk	(*USA*)
Sankar Das Sarma	(*USA*)	John J. Quinn	(*USA*)
Lloyd W. Engel	(*USA*)	C. N. R. Rao	(*India*)
Klaus Ensslin	(*Switzerland*)	David A. Ritchie	(*UK*)
Vladimir Fal'ko	(*UK*)	Michelle Y. Simmons	(*Australia*)
Alfred Forchel	(*Germany*)	Maurice Skolnick	(*UK*)
Christian Glattli	(*France*)	Robert A. Suris	(*Russia*)
M. Zahid Hasan	(*USA*)	Carlos Tejedor	(*Spain*)
Moty Heiblum	(*Israel*)	Paul Voisin	(*France*)
Yoshiro Hirayama	(*Japan*)	Klaus von Klitzing	(*Germany*)
Tae-Won Kang	(*South Korea*)	Enge Wang	(*China*)
Belita Koiller	(*Brazil*)	Robert M. Westervelt	(*USA*)
Leo P. Kouwenhoven	(*Netherlands*)	Qi-Kun Xue	(*China*)
Steven G. Louie	(*USA*)	Hou Zhi Zheng	(*China*)

EP2DS Program Committee

Jacek Kossut (Chair)	*Polish Academy of Sciences, Warsaw, Poland*
Manfred Bayer	*Technische Universität Dortmund, Germany*
Rolf J. Haug	*Leibniz Universität Hannover, Germany*
Philip Hofmann	*Aarhus University, Denmark*
Igor Kukushkin	*Russian Academy of Sciences, Chernogolovka, Russia*
Patricia Lustoza de Souza	*Pontifícia Universida de Católica, Rio de Janeiro, Brasil*
Alberto Morpurgo	*Université de Genève, Switzerland*
Daniela Pfannkuche	*Universität Hamburg, Germany*
Marek Potemski	*Grenoble High Magnetic Field Laboratoy, France*
Andrew Sachrajda	*National Research Council, Ottawa, Canada*
Mansour Shayegan	*Princeton University, USA*
Steven H. Simon	*University of Oxford, UK*
Adiel Stern	*Weizmann Institute of Science, Rehovot, Israel*
Seigo Tarucha	*University of Tokyo, Japan*
Arkadiusz Wójs	*Wrocław University of Technology, Poland*

MSS Program Committee

Tomasz Dietl (Chair)	*Polish Academy of Sciences, Warsaw, Poland*
Alexander V. Chaplik	*Russian Academy of Sciences, Novosibirsk, Russia*
Scott A. Crooker	*Los Alamos National Laboratory, USA*
Łukasz Cywiński	*Polish Academy of Sciences, Warsaw, Poland*
Jonathan Finley	*Technische Universität München, Germany*
Jean-Michel Gerard	*Service de Physique des Matériaux et des Microstructures (CEA/INAC/SP2M) Grenoble, France*
Shingo Katsumoto	*University of Tokyo, Japan*
Junichiro Kono	*Rice University, Houston, USA*
Hideo Ohno	*Tohuku University, Sendai, Japan*
Amalia Patane	*University of Nottingham, UK*
Raimundo Rocha dos Santos	*Universida de Federal do Rio de Janeiro, Brazil*
Ludvik Smrcka	*Akademie věd České republiky, Prague, Czech Republic*
Marzena Szymanska	*University of Warwick, Coventry, UK*
Alexander Tartakovskii	*University of Sheffield, UK*
Luis Vina	*Universidad Autónoma de Madrid, Madrid, Spain*

Local Committee

Jan Misiewicz (Chair)	*Institute of Physics, Wrocław University of Technology*
Adam Babiński	*Institute of Physics, University of Warsaw*
Leszek Bryja	*Institute of Physics, Wrocław University of Technology*
Paweł Machnikowski	*Institute of Physics, Wrocław University of Technology*
Paweł Podemski	*Institute of Physics, Wrocław University of Technology*
Katarzyna Roszak	*Institute of Physics, Wrocław University of Technology*
Grzegorz Sęk	*Institute of Physics, Wrocław University of Technology*
Piotr Sitarek	*Institute of Physics, Wrocław University of Technology*

Patronage

Ministry of Science and Higher Education, Poland

National Centre for Research and Development, Poland

National Science Centre, Poland

Polish Physical Society

Rector of Wrocław University of Technology, Poland

Financial Support

Ministry of Science and Higher Education, Poland

International Union of Pure and Applied Physics

U.S. Army Forward Element Command – Atlantic

Sponsors

COMEF Scientific & Research Equipment, Poland and Newport, Germany

attocube systems AG, Germany

Raith GmbH, Germany

Hamamatsu Photonics Deutschland GmbH, Germany

SPS-Europe B.V., The Netherlands

Scontel, Russia

PGE Górnictwo i Energetyka Konwencjonalna S.A., Poland

Social Program

The following special attractions are offered free of charge to all registered participants and accompanying persons.

Guided city excursions (Wednesday, 13.30 – 16.15)

We propose a few guided excursions around the most interesting places in Wrocław, e.g.:

The oldest part of the city: The Old Town includes the Gothic St. John's Cathedral, the Renaissance houses near the Market Square, the Baroque university and lots of fine examples of Art Nouveau and Functionalism.

The Centennial Hall and the Japanese Garden: The Centennial Hall is the most famous work of Wrocław Modernism. It was listed as a UNESCO World Heritage Site in 2006. The Japanese Garden located within Szczytnicki Park is one of the few traces of the 1913 World's Fair that was held in Wroclaw.

The Quarter of Tolerance: The Quarter of Four Temples also known as The Quarter of Tolerance is an old part of the city, where four religions coexist: Lutheran Protestantism, Orthodox Christianity, Catholicism and Judaism.

Conference Banquet (Wednesday, 19.30 – 21.00)

The Conference Banquet will take place in the splendid City Hall at the heart of our historic Market Square.

Music Concert (Thursday, 20.00 – 21.00)

The Music Concert is planned in Wrocław's magnificent Opera House located within walking distance of Market Square. Soloists of the opera will present the specially chosen repertoire.

Additional attractions are also available at modest fees (detailed information is available at registration desks).

1 July (Monday)

17.00 – 19.00

Poster sessions 1

EP2DS – MSS Joint session

Session sponsored by

LOT-QuantumDesign

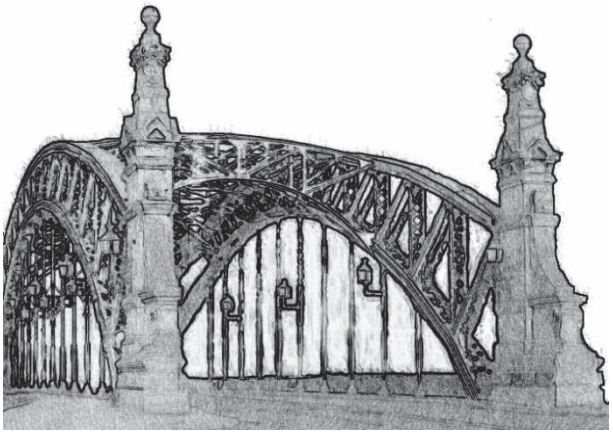

Zwierzyniecki Bridge

Screening property of bi-layer graphene investigated with scanning gate microscopy

Vishal Panchal [1,2], Alexander Tzalenchuk [1] and Olga Kazakova [1]

[1] *National Physical Laboratory, Hampton Road, Teddington, TW11 0LW, UK*
[2] *Royal Holloway, University of London, Egham Hill, Egham, Surrey, TW20 0EX, UK*

Devices fabricated out epitaxial graphene grown on SiC have shown great promise for commercialization [1,2]. However, due to the complicated growth procedures of epitaxial graphene, the best of samples contain ~95% single-layer (1LG) and ~5% bi-layer (2LG) graphene coverage [3]. Such samples have been shown to exhibit a work function difference of ~110±21 meV between 1LG and 2LG [4], which can affect the transport properties of graphene devices. Here, we investigate how the 2LG islands screen the local electric field produced by the scanning probe.

Scanning gate microscopy (SGM) is performed using an electrically conductive probe scanning the double-cross graphene Hall bar at a constant 15 nm lift height, while a DC bias voltage (V_g = +3 V) is applied to the probe. The device is current biased at I_{bias} = 10 μA and a lock-in amplifier, referenced to the mechanical resonance of the cantilever, measures the AC longitudinal voltage (V_{xx}) between the two crosses. The SGM image is generated by recording V_{xx}, pixel by pixel.

The SGM image (Fig. 1) shows a decrease in resistance of ΔR_4 = –80 mΩ with respect to the background when the probe is gating the 1LG channel. However, gating at the 2LG screens the electric field, restoring the resistance of the channel to the background value (dashed line #2). Moreover, gating at the 2LG located at the center of the channel has an opposite effect of increasing the resistance by R_4 = +70 mΩ (dashed line #1). Thus, we show that the presence of isolated 2LG islands can affect transport measurements. The screening efficiency will depend on geometry of 2LG domains and their exact position with respect to the leads. These measurements allow investigating the possible effect of decoupling between individual layers of graphene.

[1] V. Panchal *et al.*, J. Appl. Phys. **111**, 07E509 (2012).
[2] Y.-M. Lin *et al.*, Science **327**, 662 (2010).
[3] V. Panchal *et al.*, 12th IEEE Conf. on Nanotechnology (2012).
[4] O. Kazakova *et al.*, Crystals. **3**, in press (2013).

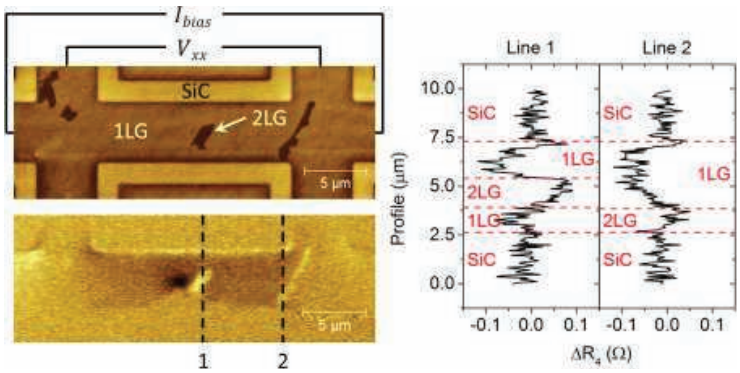

Pseudodiffusive conducance and Landa level hierarchy in biased graphene bilayer

Grzegorz Rut and Adam Rycerz

Marian Smoluchowski Institute of Physics, Jagiellonian University, Reymonta 4, PL–30059 Kraków, Poland

We demonstrate, by means of mode-matching analysis for the Dirac equation, that splittings of the Landau-level (LL) degeneracies associated with spin, valley, and layer degrees of freedom, directly affect the quantum-limited conductance of ballistic graphene bilayer. For wide samples ($W \gg L$), the Landauer-Büttiker conductance reaches the maximum $G \simeq se^2/(\pi h) \times W/L$ at the resonance via each LL, with the prefactor varying from $s = 8$ if all three degeneracies are preserved, to $s = 1$ if all the degeneracies are split. In the absence of bias between the layers, the degeneracies associated with spin and layer degrees of freedom may be split by manipulating the doping and magnetic field; the conductance at the zeroth LL is twice as large, while the conductance at any other LL equals to the corresponding conductance of graphene monolayer. The presence of bias potential allows one also to split the valley degeneracy. Our results show, that the charge transfer at each LL has pseudodiffusive character, with the second and third cumulant quantified by $\mathcal{F} = 1/3$ and $\mathcal{R} = 1/15$ (respectively). In case the electrochemical potential is allowed to slowly fluctuate in a finite vicinity of LL, the resulting charge transfer characteristics are still quantum-limited, approaching $\mathcal{F} \simeq 0.7$ and $\mathcal{R} \simeq 0.5$ in the limit of large fluctuations.

Magnetoplasmons in quasi-neutral epitaxial graphene nanoribbons

J. M. Poumirol[1], W. Yu[2], X. Chen[2], X. Chen[2], C. Berger[2], W. A. de Heer[2], M. L. Smith[3], T. Ohta[3], W. Pan[3], M. O. Goerbig[4], D. Smirnov[1], Z. Jiang[2]

[1]*National High Magnetic Field Laboratory, Tallahassee, FL 32310, USA.*
[2]*School of Physics, Georgia Institute of Technology, Atlanta, GA 30332, USA.*
[3]*Sandia National Laboratories, Albuquerque, NM 87185, USA.*
[4]*Laboratoire de Physique des Solides, CNRS UMR 8502, Univ. Paris-Sud, F-91405 Orsay cedex, France.*

We report on infrared transmission spectroscopy study of magnetoplasmons in quasi-neutral epitaxial graphene nanoribbon arrays [1]. The energy of the $L_{0(-1)} \rightarrow L_{1(0)}$ inter-Landau level transitions deviates from the characteristic $\sqrt{B}$ dependence observed in two-dimensional graphene. This behavior is explained as a signature of the upper hybrid mode formed between the Landau level transition and the plasmon resonance. The study of this hybrid mode allows us to probe the zero magnetic field plasmon resonance in the interacting regime, when a the strong decay of the plasmon mode induced by the coupling to electron-hole excitations takes place. The observed energy shift exhibits a peculiar ql_B^2 scaling behavior, which distinguishes it from the upper-hybrid mode in conventional two-dimensional systems and in highly doped graphene [3].

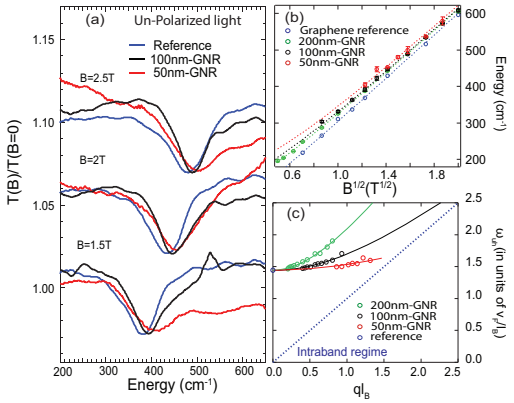

Figure 1: (a) Normalized magneto-transmission spectra of 2D graphene (blue), 100-nm-wide (black) and 50-nm-wide (red) Graphene nano ribbon (GNR) arrays measured with un-polarized IR light and at different magnetic fields. (b) $\hbar\omega_{uh}$ versus $\sqrt{B}$ for 2D graphene, 200-nm-wide, 100-nm-wide, and 50-nm-wide GNR array samples, a clear deviation from the linear behavior in observed for the GNR samples, following [2]. (b) Dispersion relation of the UHM, $\omega_{uh}(ql_B)$, in units of v_F/l_B. The data taken on the 2D graphene collapse on a single point (blue circle) at q=0. Dotted blue line indicates the boundary between the interband and intraband regimes.

[1] J. M. Poumirol et al. manuscript submitted to Phys. Rev. Lett.
[2] R. Roldán, J.-N. Fuchs, and M. O. Goerbig, Phys. Rev. B **82**, 205418 (2010).
[3] I. Crassee et al., Nano Lett. **12**, 2470 (2012) ; H. G. Yan et al., Nano Lett. **12**, 3766 (2012).

MoP4

Gate-dependent Kondo states in bilayer graphene

D. Mastrogiuseppe [1,2], A. Wong [3], K. Ingersent [3], S. Ulloa [1,2] and N. Sandler [1,2]

[1] *Department of Physics and Astronomy, and Nanoscale and Quantum Phenomena Institute, Ohio University, Athens, Ohio 45701-2979, USA*
[2] *Dahlem Center for Complex Quantum Systems and Fachbereich Physik, Freie Universität Berlin, 14195 Berlin, Germany*
[3] *Department of Physics, University of Florida, P.O. Box 118440, Gainesville, Florida, 32611-8440, USA*

One of the remarkable manifestations of cooperative phenomena in condensed matter physics is the many-body screening of a magnetic impurity placed in a metallic system, the *Kondo effect*. Although the physics underlying this effect in ordinary metals is well understood, microscopic symmetries can give rise to intricate features in the effective density of states of the host with profound consequences in the Kondo regime. Bilayer graphene (BLG) is an example of such a material with a gate-dependent gap and large pseudospin symmetry that provides an ample set of different microscopic environments for intercalated magnetic impurities. Combined to its easy tunability, BLG is an ideal material to study quantum phase transitions into various types of Kondo states.

We provide a full characterization of these transitions for a magnetic impurity intercalated in Bernal-stacked BLG and symmetrically coupled to carbon atoms on each layer, as a function of doping level of the system. Two factors determine the wealth of phases predicted: 1) the particular dispersion relation of BLG that gives rise to an interesting density of states with a discontinuity at the interlayer hopping energy; and 2) the properties of the microscopic coupling between the impurity and the layers that define different symmetries for the possible phases.

A multiband Anderson Hamiltonian that includes interaction and different hybridization environments describes the system. After an appropriate Schrieffer-Wolff transformation, we find the effective single-channel Kondo model with a strongly energy-dependent exchange coupling between conduction electron and impurity spins. This effective Kondo Hamiltonian reveals the possibility of driving the system through quantum phase transitions via changes in the chemical potential through gating or doping.

We use numerical renormalization group calculations to accurately describe the Kondo regime. Our calculations reveal zero-temperature transitions between local-moment and singlet strong-coupling phases under variation of band filling and/or energy of the impurity level. The latter show different regimes, such as conventional Kondo, pseudogap Kondo, and local-singlet ground states, distinguishable by their thermodynamic and spectral properties. We also obtain the Kondo temperature dependence with the chemical potential within the different regimes, which would be accessible via STM experiments.

Electronic transport in carbon nanotube-graphene junctions

P.T. Robert[1,2], R.-J. Du[1], F. Wu[1], A. Durand[1], F. Hennrich[1], M.M. Kappes[1,3,4], H.v. Löhneysen[1,2,4,5] and R. Danneau[1,2]

[1] *Institute of Nanotechnology, Karlsruhe Institute of Technology, Germany*
[2] *Institute of Physics, Karlsruhe Institute of Technology, Germany*
[3] *Institute of Physical Chemistry, Karlsruhe Institute of Technology, Germany*
[4] *DFG Center for Functional Nanostructures, Karlsruhe Institute of Technology, Germany*
[5] *Institute for Solid-State Physics, Karlsruhe Institute of Technology, Germany*

We have studied electronic transport through individual metallic carbon nanotube (CNT)-graphene junctions produced by atomic force microscope nano-manipulation. While our models demonstrate that a CNT has a very limited influence on the graphene sheet, i.e. that the charge transfer occurs only over few atomic raw [1], our electronic transport experiments show that the junction transparency is strongly gate-tunable depending on the resistance of the junction itself. We also observe that the junction resistance does not depend on the CNT-graphene overlapping distance. We explain the strong gate dependence of the resistance by the charge induced variation of the CNT-graphene distance. The absence of the junction length dependence of the resistance indicates that the charge injection occurs via a single point most likely to be at the end of the CNT [2].

[1] P.T. Robert, A. Durand, and R. Danneau, unpublished.
[2] P.T. Robert, R.-J. Du, F. Wu, F. Hennrich, M.M. Kappes, H.v. Löhneysen and R. Danneau, unpublished.

Ballistic interferences in suspended graphene: Theoretical modeling from contact to contact

Peter Rickhaus[1], Romain Maurand[1], Markus Weiss[1], Christian Schönenberger[1], Ming-Hao Liu[2], and Klaus Richter[2]

[1]*Department of Physics, University of Basel, Klingelbergstrasse 82, CH-4056 Basel, Switzerland*
[2]*Institut für Theoretische Physik, Universität Regensburg, D-93040 Regensburg, Germany*

Ballistic interferences in ultra-clean suspended graphene has been recently observed [Figs. 1(a)–1(b)], with transport simulation qualitatively agreeing with the experimental measurement also reported [Figs. 1(c)–1(d)]; see [1]. The interference stems from the Fabry-Pérot resonance within the cavities formed by the electrically induced pn junctions as well as by the graphene-contact interfaces, which are separated to each other longer than 1 micron in the experiment. In this presentation, full theoretical modeling of the ballistic transport, from one contact to the other through the suspended graphene, is illustrated. In qualitatively reproducing the experimentally measured conductance map, the transport simulation confirms the ballistic origin of the measured interferences and reveals the role played by the metal contacts.

[1] P. Rickhaus, R. Maurand, M.-H. Liu, M. Weiss, K. Richter, C. Schönenberger, arXiv:1304.6590.

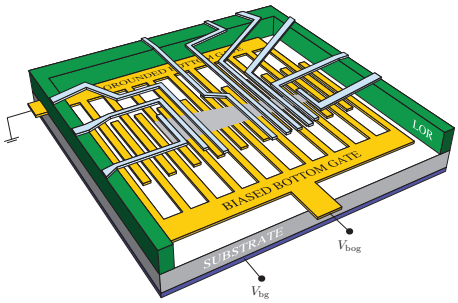

(a) Sketch of the suspended graphene device.

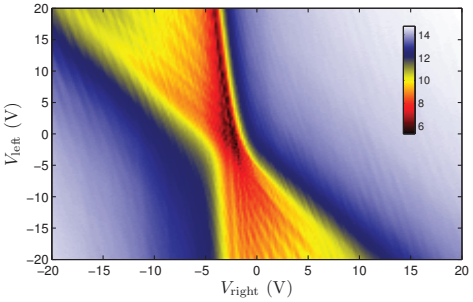

(b) Experimentally measured conductance map.

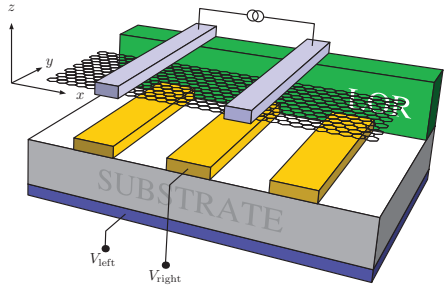

(c) Simplied sketch of the device for modeling.

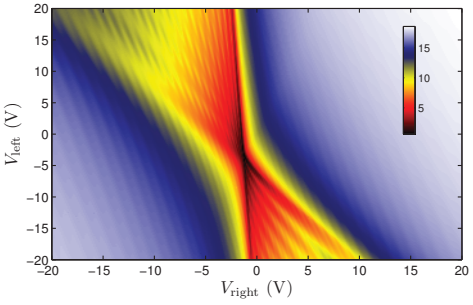

(d) Theoretically calculated conductance map.

Figure 1: Ballistic interferences measured and calculated in a two-terminal device with ultra-clean suspended graphene.

In-plane structural features of graphene on SiC revealed by TEM observations

J. Kuroki [1], W. Norimatsu[1] and M. Kusunoki[2]

[1] Department of Applied Chemistry, Nagoya University, Japan
[2] EcoTopia Science Institute, Nagoya University, Japan

Graphene has excellent electronic transport properties, therefore it is expected as a high quality semiconducting material. Thermal decomposition of SiC is one of the production methods of graphene. In this method, graphene layers formed on SiC (0001) and (000-1) faces show different structures and properties. Regarding the stacking structure, previous studies reported that graphene layers on SiC (0001) exhibited ABC stacking and are rotated by 30 º with respect to the SiC substrate [1]. On the contrary, the structure of graphene layers formed on SiC (000-1) is still controversial. In this study, we observed graphene layers on SiC {0001} surfaces by transmission electron microscopy (TEM). We succeeded to observe in the range of from the atomic scale to the sub-micrometer scale directly by using TEM and to analyze the in-plane structure of graphene on the SiC {0001} surfaces.

Commercially available on-axis 6H-SiC (0001) and 6H-SiC (000-1) single-crystal wafers were used. SiC (0001) substrates were graphitized at 1500 ºC in a vacuum (10^{-4} Torr), and SiC (000-1) substrates were graphitized at 1500~1800 ºC in 6-atm Ar atmosphere. We used EM-002B TEM at an electron accelerating voltage of 200 kV. Specimens for TEM observations were prepared by Ar-ion thinning or by exfoliation from the substrate. The number of graphene layers was counted directly by TEM observations along cross-sectional direction and the in-plane structure of graphene was analyzed by using plan-view observations and a fast Fourier transformation (FFT) treatment of the observed TEM images.

Figure 1(a) shows the planar TEM image of graphene layers on SiC (0001) and Figure 1(b) shows the FFT pattern of TEM plan-view image shown in Fig. 1(a). The FFT pattern shows one set of six-fold spots corresponding to graphene 1-100 reflections (indicated by yellow circles in Fig. 1(b)). This means that the graphene layers stacked with a 30 º rotation with respect to SiC. Figure 2(a) shows a TEM image of graphene layers transferred from SiC (000-1) substrate to the TEM micro-grid. Figure 2(b) shows an FFT pattern of a square area of about 100 nm in a TEM image of transferred graphene. The FFT pattern shows two sets of six-fold spots corresponding to graphene 1-100 reflections indicated by blue and yellow circles in Fig. 2(b). Presence of two sets of spots indicates graphene sheets with two different orientations and this means that graphene layers on SiC (000-1) stack with rotation within a single grain [2]. Dark field TEM images of graphene on SiC {0001} surfaces were also taken in order to observe the grain structure.

References:
[1] W. Norimatsu and M. Kusunoki, Phys. Rev. B. **81**, 161410 (2010).
[2] J. Kuroki, W. Norimatsu, and M. Kusunoki, e-J. Surf. Sci. Nanotech., **10**, 396 (2012).

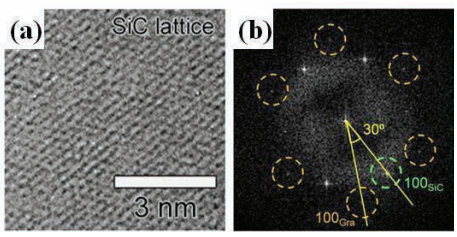

Fig. 1: (a) Planar TEM image of graphene on SiC (0001). (b) FFT pattern of TEM image Fig. 1(b).

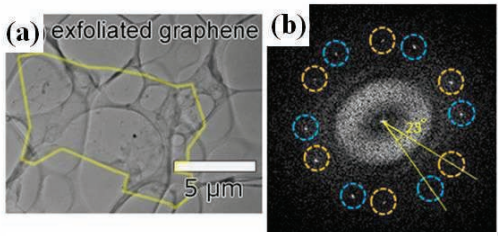

Fig. 2: (a) TEM image of graphene transferred from SiC (000-1) to carbon micro-grid. (b) FFT pattern of TEM image of exfoliated graphene.

Gap opening at the charge neutrality point of a graphene transistor on hBN

Francesca Chiappini[1], Steffen Wiedmann[1], Uli Zeitler[1], Konstantin S. Novoselov[2], Andre K. Geim[2], Roman V. Gorbachev[2], and Jan C. Maan[1]

[1] *Radboud University Nijmegen, Institute for Molecules and Materials and High Field Magnet Laboratory, Toernooiveld 7, 6525 ED Nijmegen, The Netherlands*
[2] *School of Physics and Astronomy, University of Manchester, UK;*

We have performed magneto-transport experiments in a high-mobility graphene transistor sandwiched between h-BN in magnetic fields up to 30 T. We find an exponentially increasing resistance at the charge neutrality point (CNP) when increasing the magnetic field and/or decreasing the temperature. This behaviour suggests a field-induced gap opening at zero energy. Additionally, resistance minima at filling factors $\nu=\pm1$ develop for B >8 T which indicates a full lifting of the four fold degeneracy of the zero-energy Landau level [1].

In order to probe the nature of the $\nu=0$ state in more detail, we have carried out experiments in tilted magnetic fields. Extracting the gap Δ_0 from the field and temperature dependence of the resistance at the CNP, $R_{CNP} \propto \exp(\Delta/2K_BT)$, yields $\Delta \approx 3$ meV at 8 T perpendicular field which is considerably larger than the bare Zeeman splitting. Together with the fact that Δ mainly scales with the perpendicular field component, this suggest a gap opening driven by exchange interaction, and thus, $\nu=0$ is not spin polarized.

Adding an additional in-plane field and leaving the perpendicular field component constant leads to a slight decrease of the resistance at the CNP which can be explained by an increased spin-splitting within the two level pairs above and below zero energy [2].

[1] Y. Zhang *et al.,* Phys. Rev. Lett. **96**, 136806 (2006).
[2] A. Veligura *et al.,* Phys. Rev. B **85**, 115412 (2012).

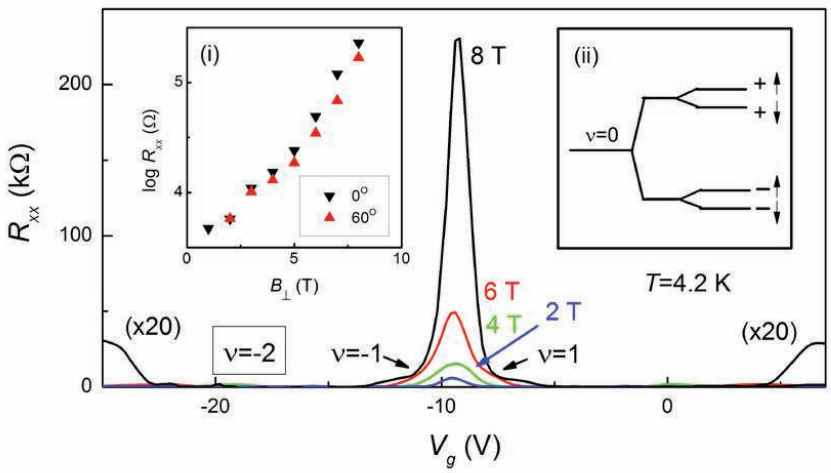

Fig. 1: Resistance as a function of gate voltage around the CNP. The inset (i) shows R_{CNP} as a function of the perpendicular field component for two tilt angles. Inset (ii) sketches the splitting scenario around $\nu=0$.

Hall-drag and magneto-drag in graphene via kinetic equation approach

M. Schuett,[1] P. M. Ostrovsky,[2,3] I. V. Gornyi,[1,4] M. Titov, [5] B. N. Narozhny,[6] and A. D. Mirlin [1,6,7]

[1] Institut fuer Nanotechnologie, Karlsruhe Institute of Technology, 76021 Karlsruhe, Germany
[2] Max Planck Institute for Solid State Research, Heisenbergstr. 1, 70569 Stuttgart, Germany
[3] L. D. Landau Institute for Theoretical Physics RAS, 119334 Moscow, Russia
[4] A. F. Ioffe Physico-Technical Institute, 194021 St. Petersburg, Russia
[5] Radboud University Nijmegen, Institute for Molecules and Materials, NL-6525 AJ Nijmegen, Netherlands
[6] Institut fuer Theorie der kondensierten Materie, Karlsruhe Institute of Technology, 76128 Karlsuhe, Germany
[7] Petersburg Nuclear Physics Institute, 188350 St. Petersburg, Russia.

Keywords: magneto-drag, Hall-drag, Boltzmann equation, hydrodynamic equations

Only since recently Coulomb drag measurements in Graphene have been available and right from the start they have been performed in the presence of a magnetic field as well [1]. In this work we calculate the magneto-drag and the Hall-drag resistivity at finite temperature for two graphene monolayers within the kinetic equation approach [2,3]. The presented theory is valid for the hydrodynamic regime $\tau_{dis}^{-1}\alpha_g^2 T \ll 1$ and appears there as hydrodynamic equations [2]. This way our theory corresponds to a microscopic formulation supporting a phenomenological Drude-like picture which for large concentrations equals the usual Drude form and for small concentration an effective two-band-Drude equation [4]. The theory presented allows for a qualitative description for arbitrary chemical potentials (see Fig. 1). An emphasis is put on the Hall-drag which is absent when derived from the standard Drude equation. Complete asymptotics of the magneto-drag and the Hall-drag resistivity are given. In particular, we have shown that the Hall-drag vanishes along the line of opposite carrier concentration in the layers. Additional we found non trivial concentrations at which the Hall-drag vanishes (see Fig. 1).

References:

[1] R.V. Gorbachev, A.K. Geim, M.I. Katsnelson, K.S. Novoselov, T. Tudorovskiy, I.V. Grigorieva, A.H. MacDonald, S.V. Morozov, K. Watanabe, T. Taniguchi, and L.A. Ponomarenko, Nature Phys. 8, 896 (2012).
[2] M. Schütt, P.M. Ostrovsky, M. Titov, I.V. Gornyi, B.N. Narozhny, and A.D. Mirlin. Phys. Rev. Lett. 110, 026601 (2013).
[3] B.N. Narozhny, M. Titov, M. Schütt, P.M. Ostrovsky, I.V. Gornyi, A.D. Mirlin, T. Tudorovskiy, M.I. Katsnelson, in preparation.
[4] M. Titov, R.V. Gorbachev, B.N. Narozhny, M. Schütt, P.M. Ostrovsky, I.V. Gornyi, A.D. Mirlin, T. Tudorovskiy, M.I. Katsnelson, A.K. Geim, and L.A. Ponomarenko, in preparation.

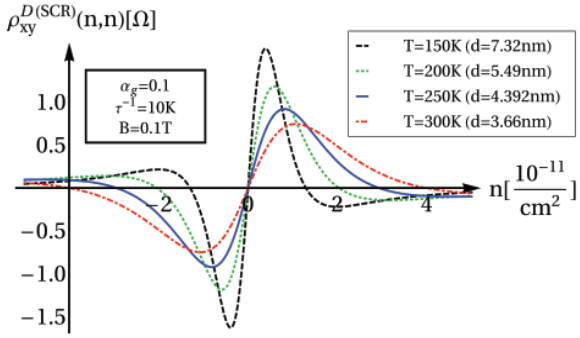

Fig. 1: **Right:** The Hall-drag resistivity for equal concentration varying temperature and distance.

Conductivity of chiral particles: Boltzmann-like analytical approach and finite-size Kubo formula simulation

Janik Kailasvuori[1,2], Bretislav Sopik[3], and Maxim Trushin[4]

[1] *International Institute of Physics, Universidade Federal do Rio Grande do Norte, 59078-400 Natal-RN, Brazil*
[2] *Max-Planck-Institut für Physik komplexer Systeme, Nöthnitzer Str. 38, 01187 Dresden, Germany*
[3] *Central European Institute of Technology, Masaryk University, Kamenice 735, 62500 Brno, Czech Republic*
[4] *University of Konstanz, Fachbereich Physik M703, 78457 Konstanz, Germany*

The sublattice degree of freedom of chiral carriers in graphene can be characterized by means of the pseudospin which is an additional quantum number formally similar to the real spin in spin-orbit coupled systems [1]. In chirally stacked N-layer graphene, the pseudospin makes N full rotations when the momentum winds around the Fermi surface resulting in the winding number $N_c = N$ [1]. There are quite a few speculations on the possibly important role of the pseudospin-coherent contribution in the electrical dc conductivity of graphene at low carrier concentrations [2, 3, 4, 5]. There is however no agreement whether this contribution really matters and can be extracted from the total conductivity. The main goal of the present work is to compare the exact numerical (finite-size Kubo) and approximated analytical (Boltzmann-like) pseudospin-coherent conductivities for an arbitrary N_c and in that way to figure out the correct approximation needed to derive the most reasonable analytical expression.

To investigate the relation between the winding number N_c and the conductivity of chiral carriers with the dispersion $E_k = \gamma k^{N_d}$ we start from the Hamiltonian

$$H_0 = \gamma k^{N_d} \begin{pmatrix} 0 & \exp(-iN_c\theta) \\ \exp(iN_c\theta) & 0 \end{pmatrix}, \qquad (1)$$

where k is the absolute value of the particle wave vector, $\theta = \arctan(k_y/k_x)$, and γ is a constant determined by the band parameters. In the special case of $N_d = N_c$ the Hamiltonian describes the low energy behaviour of carriers in chirally stacked multilayer graphene [1], but the general choice of $N_c \neq N_d$ makes it possible to distinguish the true pseudospin coherent conductivity contribution from the effects related to the change of the density of states. Using this Hamiltonian we compare the pseudospin-coherent Boltzmann-like conductivity in terms of the Fermi wave vector k_F and mean free path l with the corresponding finite-size Kubo conductivity computed in the spirit of [6] by means of the exact diagonalization of the total Hamiltonian $H = H_0 + V$ with V being point-like impurity potential which can be related to the mean free path l.

In the poster to be shown we discuss proper treatments of the collision integral in the Boltzmann equation for chiral particles as well as connections between our theoretical findings and the real electron transport in graphene.

[1] H. Min and A. H. MacDonald, Prog. Theor. Phys. Suppl. **176**, 227 (2008).
[2] M. Auslender and M. I. Katsnelson, Phys. Rev. B **76**, 235425 (2007).
[3] M. Trushin and J. Schliemann, Phys. Rev. Lett. **99**, 216602 (2007).
[4] J. Kailasvuori and M. C. Lüffe, J. Stat. Mech.: Theory and Experiment **2010**, P06024 (2010).
[5] D. Culcer and R. Winkler, Phys. Rev. B **78**, 235417 (2008).
[6] K. Nomura and A. H. MacDonald, Phys. Rev. Lett. **98**, 076602 (2007).

Influence of chirality on phonon-drag thermopower in monolayer and bilayer graphene

E. Wolf [1] **and D. Lehmann** [1]

[1] *Institute of Theoretical Physics, Technische Universität Dresden, 01062 Dresden, Germany*

Graphene possesses many unique features and due to its high electron mobility and high magnitude of thermoelectric power it is very attractive for applications. Recent realization of suspended monolayer graphene (MLG) and bilayer graphene (BLG) samples has made possible a direct probe of their intrinsic properties. A detailed study of the (intrinsic) scattering mechanisms, like electron-phonon-interaction, is therefore of large interest. A quite sensitive tool for investigating the coupling of electrons to acoustic phonon modes in 2D systems is the phonon-drag thermopower S^{g}. S^{g} arises from the momentum exchange between electrons and nonequilibrium phonons in the presence of a weak in-plane temperature gradient. There are two principal sources of the interaction between electrons and acoustic phonons in graphene. On the one hand electrons interact with acoustic phonons via a deformation potential proportional to the local contraction or dilatation of the lattice; on the other hand electrons couple to acoustic phonons by changes in bond length and bond angle between the carbon atoms [1]. The latter interaction can be described by an effective gauge field. While the deformation potential coupling is restricted to in-plane longitudinal acoustic (LA) phonons and out-of-plane (flexural) acoustic phonons (the latter coupling is by 2-phonon processes), the gauge field allows also coupling to in-plane transverse acoustic (TA) phonons.

In this study, we focus our attention on the effect that has chirality on the electron-phonon coupling and therefore on S^{g}. MLG and BLG not only exhibit a different low-energy electronic band structure, but also a different degree of electron chirality. While the charge carriers in MLG are massless quasiparticles characterized by a Berry phase of π, the electrons in BLG can be viewed as massive fermions with Berry phase 2π.

We have calculated S^{g} in doped MLG and BLG as function of temperature between 1K and 50K for different carrier densities. In contrast to former studies [2] where only LA phonons and an unscreened deformation potential interaction were considered, we have included the coupling by deformation potential and gauge field, the screening of deformation potential as well as the contributions of LA, TA and flexural phonons. For these purposes we have generalized the Cantrell-Butcher formalism [3] for the phonon-drag thermopower to allow also for 2-phonon processes.

For reasonable values of coupling constants and not too low temperatures our results show that the main contribution to S^{g} is due to the gauge field coupling by in-plane phonons. The chiral character of the electrons reduces both the contribution of deformation potential and the contribution of gauge field. However, the effect varies greatly, depending on the degree of chirality. With the change from MLG to BLG we observe for $T > 10\mathrm{K}$ a reduction of the contribution of the gauge potential and an increase of the contribution of the deformation potential. For temperatures below 10K the electron scattering by out-of-plane phonons cannot be neglected. Therefore we have also examined the differences between S^{g} in MLG and in BLG due to the coupling of electrons to flexural phonons.

[1] H. Ochoa et al., Phys. Rev. B **87**, 235416 (2011) and references therein.
[2] S. S. Kubakaddi, K. S. Bhargavi, Phys. Rev. B **82**, 155410 (2010); AIP Conf. Proc. 1349, 247 (2011).
[3] D. G. Cantrell and P. N. Butcher, J. Phys. C **20**, 1985 (1987); **20**, 1993 (1987).

Boundary Scattering in Ballistic Graphene

S. Masubuchi[1, 2], K. Iguchi[1], S. Morikawa[1], M. Onuki[1], K. Watanabe[1], T. Taniguchi[1], and T. Machida[2]

[1] *Institute of Industrial Science, University of Tokyo, Japan*
[2] *Institute for Nano Quantum Information Electronics, University of Tokyo, Japan*
[3] *National Institute for Material Science, Japan*

Charge carrier scattering at sample boundaries, boundary scattering, is a key element for understanding transport properties of graphene devices. To study boundary scattering effect, the charge carrier mean free path l_{mfp} has to be larger than the sample size. In this work, we report on the observation of anomalous magnetoresistance peaks due to diffusive charge carrier scattering at sample boundaries in ballistic graphene mesoscopic wires [1]. The magnetoresistance peak field scaled with the ratio of cyclotron radius R_c and wire width W as $W/R_c \sim 0.9$, different from that of classical semiconductor two-dimensional electron system $W/R_c \sim 0.55$.

We fabricated graphene/boron nitride mesoscopic wire devices using the mechanical transfer technique of monolayer graphene on hexagonal boron nitride substrate [Fig. 1 (a)]. The fabricated device exhibited high mobility $\mu \sim 70{,}000$ cm^2/Vs at $T = 4$ K. The mean free path of charge carriers reached ~1 μm at high charge carrier density $n \sim 3\text{x}10^{12}$ cm^{-2}. In magnetoresistance curves, we observed anomalous peak structures at magnetic fields B_{max} [colored region in Fig. 1 (b)]. The value of B_{max} scaled with the ratio of cyclotron radius R_c and sample width W as $W/R_c \sim 0.9$, indicating the magnetic commensurability effect between R_c and W. These observations indicate that the trajectories of charge carriers are bent by cyclotron motion and are scattered diffusively at the sample boundaries [inset in Fig. 1]. The proportionality constant between W and R_c differed from the case of conventional semiconductor two-dimensional electron system where $W/R_c \sim 0.55$ [1]. This observation suggests that the standard relation between R_c and W in semiconductor two-dimensional electron systems [2] has to be modified to explain the observed transport phenomena in graphene. Moreover, when the temperature was increased, the anomalous curves were retained up to room temperature. The temperature-dependent studies of resistivity indicate that the suppression of extrinsic charge carrier scatterings (optical phonon and impurities) compared to the conventional graphene on SiO_2 was the origin of the robust ballistic transport in graphene on hexagonal boron nitride.

[1] S. Masubuchi *et al.*, Phys. Rev. Lett. **109**, 036601 (2012).

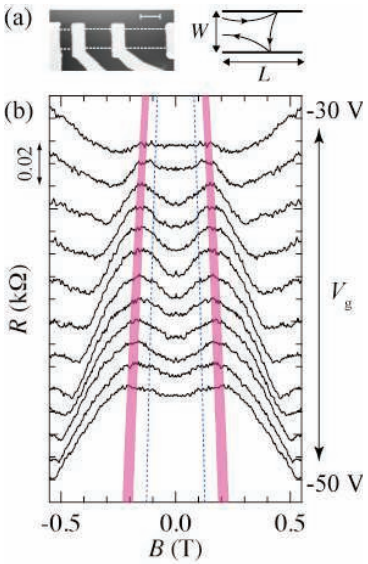

FIG. 1: (a) Atomic force microscopy image of the sample studied (b) Magnetoresistance curves at $T = 4$ K for gate-bias voltage $V_g = -30$, -32, ..., and -50 V (top to bottom). The blue dotted curves and colored area indicate the expected peak positions for $W/R_c = 0.55$ and 0.9 ± 0.1, respectively.

Spin Dependent Scattering in Graphene Systems: From Impurity Characterization to Birefringent Electron Optics

M. M. Asmar[1,2] and S. E. Ulloa[1,2]
[1] Department of Physics and Astronomy, Ohio University, Athens, OH 45701, USA
[2] Dahlem Center for Complex Quantum Systems, Freie Universität, Berlin, Germany

An important effect on the dynamics of spins in materials is the spin-orbit interaction (SOI), which reflects/arises from intrinsic lack of inversion symmetry in the lattice structure, or via broken symmetries in the system due to external or interfacial fields (Rashba interaction). Although intrinsic SOI is weak in graphene, the Rashba SOI can in fact be large due to strong local hybridizations by impurities of defects or by manipulation of substrates or applied gates [1]. Indeed, *resonant* scatterers, limiting electron mobility in graphene, appear likely due to impurities such as hydrogen or other adsorbed atoms, molecules, clusters of impurities or vacancies, or can be controllably implemented by metallic islands deposited on (or grown under) graphene. We have studied electron/hole transport in graphene under sizeable SOI and address theoretically some of the anticipated observables due to this effect.

We have developed analytical spinor solutions of the Dirac equation that include spin dependent observables, and use these to examine the role of SOI on scattering cross sections. By calculating the ratio of total to transport cross section at low energy we are able to probe the degree of isotropy of the scattering processes, and consequently probe the nature of the impurities and defects present in the graphene sample. We show that at low energies, this ratio of cross sections (equivalent to the ratio of scattering times obtainable from experiments [2]) can be nearly 1 (instead of 2, as expected with no SOI), to a degree that depends on the Rashba SOI strength. This suggests then a sample specific measurement of the important effective size of the SOI, especially if one is to consider spin transport.

Moreover, we show that Rashba SOI in graphene gives rise to optical *birefringence* in electron optics, which in essence reflects the intrinsic crystal structure even at long electronic wavelengths. This effect requires the presence of Rashba SOI, where different group velocities depend on the chirality of the electronic states, mimicking the light polarization dependence of the group velocities in optical birefringent materials. This can in principle be achieved via gated regions, and result in the formation of spinful cusps and caustics caused by the Veselago lens defined by the gate. Interestingly, this would be evident by the doubling of caustics and cusps produced by circular birefringent lenses, where the spacing between the two different *chiral cusps* is proportional to the strength of the Rashba interaction in the system [3].

[1] D. Marchenko *et al*., Nat. Commun. **3**, 1232 (2012).
[2] M. Monteverde *et al*., Phys. Rev. Lett. **104**, 126801, (2010).
[3] M. M. Asmar and S. E. Ulloa, Phys. Rev. B **87**, 075420 (2013).

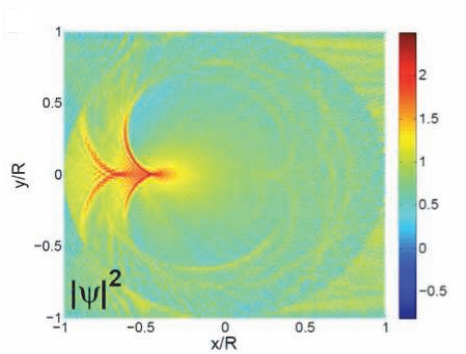

Fig. 1: Probability density patterns (scale bars show log of amplitudes, normalized to incident flux) resulting from the scattering of an incoming spin-up electron wave along the *x* direction towards a circular gate potential covering an area of radius *R*; the normal electric field reverses the carrier character from electron to hole and also generates and a Rashba spin-orbit field. The electronic dispersion in the gated region is modified, and this produces electronic *birefringence*, due to quantum mechanical effects that allow the presence of two chiral states.

MoP14

Gate Dependent Magnetophonon Resonance in Graphene

J. M. Poumirol[1], K. Myhro[2], Y. Kim[1], J. Ludwig[1], K. Myhro[2], J. Lau[2] and D. Smirnov[1]

[1]***National High Magnetic Field Laboratory, Tallahassee, FL 32310, USA.***
[2]***Department of Physics and Astronomy, University of California, Riverside, 92521 CA USA.***

The magneto-phonon resonance (MPR) effect is observed in semiconductors when the optical phonon energy coincides with the separation of two Landau levels (LLs). In graphene, the MPR can be described as a resonant mixing of inter-LL excitations and zone-center E_{2g} phonons into a combined mode, leading to a splitting proportional to the electron-phonon coupling [2],[3]. As a result, the Raman G-peak is expected to exhibit a series of filling-factor-dependent, multi-component anti-crossing structures as a function of applied magnetic field. Recently, we performed a polarization-resolved high-field magneto-Raman spectroscopy study of ungated, chemically doped graphene and identified three distinct types of G peak magnetic-field dependencies, providing a comprehensive experimental evidence of the MPR effect in graphene [1].

Here, we report a Raman spectroscopy study of MPR in gated single layer graphene in magnetic field up to 18T, demonstrating continuous tuning of the MPR lineshape by varying the carrier density. Tuning the gate voltage from -70V to 70V at constant magnetic field, we observe the progressive development of the low-field anticrossing branch corresponding to the fundamental MPR with $-1 \rightarrow 0$ and $0 \rightarrow 1$ inter-LL transitions, expected at approximately 25-30T. As the Fermi energy crosses the n=0 LL, a complex structure E_F dependent appear in the Raman spectra. This is because a higher (lower) occupancy of the n=0 LL reduces (enhances) the oscillator strength of the $0 \rightarrow 1$ transition due to the availability of filled and empty states in the involved LLs, whereas the same change in the electron density has the opposite effect on $-1 \rightarrow 0$ transition.

[1] Y. Kim, et al. arXiv:1211.6094v1 (manuscript submitted to Phys. Rev. Lett.)
[2] M. O. Goerbig et al. Phys. Rev. Lett. 99, 087402 (2007).
[3] T. Ando, J. Phys. Soc. Jpn. 76, 024712 (2007).

Novel highly conductive graphene-based materials

S. Russo[1], I. Khrapach[1], F. Withers[1], T. H. Bointon[1], D. K. Polyushkin[1], W. L. Barnes[1], M. F. Craciun[1]

[1] *Centre for Graphene Science, University of Exeter, Exeter (UK)*

The development of future flexible and transparent electronics relies on novel materials, which are mechanically flexible, lightweight and low-cost, in addition to being electrically conductive and optically transparent. Currently, tin doped indium oxide (ITO) is the most wide spread transparent conductor in consumer electronics. The mechanical rigidity of this material limits its use for future flexible electronic applications. The leading candidates to substitute ITO are graphene based materials. Graphene is an atomically thin conductive, transparent and flexible material. However, the use of graphene as a truly transparent conductor remains a great challenge because the lowest values of its resistivity demonstrated so far are above the values of commercially available ITO. Chemical functionalization of graphene offers a simple way to improve the electrical properties of these materials.

Here we report novel graphene-based transparent conductors obtained by intercalating few-layer graphene (FLG) with ferric chloride (FeCl3). Through a combined study of electrical transport and optical transmission measurements we demonstrate that FeCl3 enhances the electrical conductivity of FLG by two orders of magnitude while leaving these materials highly transparent. We find that the optical transmittance in the visible range of FeCl3-FLG is typically between 88% and 84%, whereas the resistivity is as low as 8.8 Ω. These parameters outperform the best values found in ITO (i.e. resistivity of 10 Ω at an optical transmittance of 85%), making therefore FeCl3-FLG the best candidate for flexible and transparent electronics. The temperature and magnetic field dependence of the electrical transport properties show that this material is metallic with typical carrier concentration of n=3x1014 cm-2 and macroscopic hole mean free path close to 1μm. Analysis of Shubnikov-de Haas oscillations together with Raman spectroscopy show decoupling of FLG into isolated graphene monolayers providing several parallel hole gas. The unique combination of record low resistivity, high optical, transparency and macroscopic room temperature mean free path has not been demonstrated so far in any other doped graphene system, and opens new avenues for graphene-based optoelectronics.

[1] I. Khrapach, F. Withers, T. H. Bointon, D. K. Pplyushkin, W. L. Barnes, S. Russo, M. F. Craciun, Adv. Mater. 24, 2844 (2012).

Infrared spectroscopy of hole doped ABA-stacked trilayer graphene

Nicolas Ubrig[1], Peter Blake[2], Dirk van der Marel[1] and Alexey B. Kuzmenko[1]

[1] *Département de Physique de la Matière Condensée , Université de Genève, CH-1211 Genève 4, Switzerland*

[2] *Graphene Industries Ltd, Manchester Centre for Mesoscience and Nanotechnology, University of Manchester, Manchester, M13 9PL, United Kingdom*

Using infrared spectroscopy, we investigate bottom gated ABA-stacked trilayer graphene subject to an additional environment-induced p-type doping. We interpret our experimental gate voltage-modulated reflectivity data using the Slonczewski-Weiss-McClure tight-binding model and the Kubo formula. This allows us to determine the charge densities and the potentials of the π-band electrons on all graphene layers separately. Further we can extract the interlayer permittivity due to higher energy bands and discuss connections to graphite[1].

[1] Ubrig et al., EPL 100, 58003 (2012).

Carrier Drift Velocity and Edge Magnetoplasmons in Graphene

Ivana Petkovic [1,2], F.I.B. Williams [1,3], Keyan Bennaceur [1], Fabien Portier [1], Patrice Roche[1], and D. Christian Glattli [1]

[1] *Nanoelectronics, SPEC, CEA Saclay, France.*
[2] *Laboratoire National de Métrologie et dEssais, 78197 Trappes, France.*
[3] *Institute for Solid State Physics and Optics, Wigner Research Centre for Physics, H-1525 Budapest, Hungary.*

We investigate electron dynamics at the graphene edge by studying the propagation of collective edge magnetoplasmon excitations. By timing the travel of narrow wave packets on picosecond time scales around exfoliated samples, we find chiral propagation with low attenuation at a velocity that is quantized on Hall plateaus [1]. We extract the carrier drift contribution from the edge magnetoplasmon propagation and find it to be slightly less than the Fermi velocity, as expected for an abrupt edge. We also extract the characteristic length for Coulomb interaction at the edge and find it to be smaller than that for soft depletion-edge systems. The ERC Advanced grant 228273 MeQuaNo is acknowledged.

[1] I. Petkovic, F.I.B. Williams, K. Bennaceur, F. Portier, P. Roche and D.C. Glattli, Phys. Rev. Lett. 110, 016801 (2013).

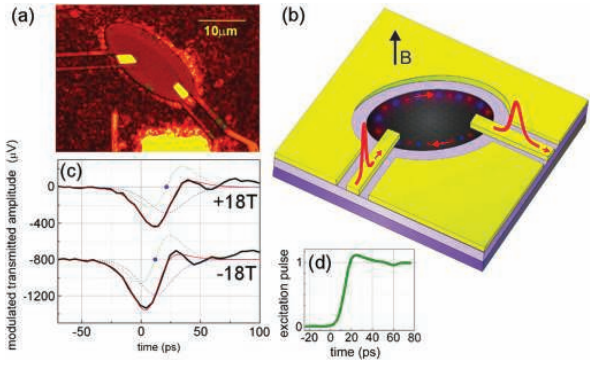

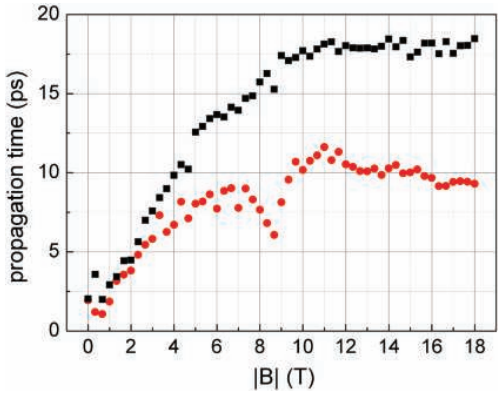

Upper figures: (a) Optical photograph of a graphene sample coupled to coplanar wave guides.
(b) Measurement configuration: An EMP wave packet excited by a 7 or 11 ps rise time 100 mV step function propagates along the edge.
(c) Demodulated responses, offset for clarity, constructed by subtraction of waveforms at a +/-15 V side gate potential for an 11 ps excitation. The arrival time difference arises from unequal left and right path lengths for oppositely directed magnetic fields.
(d) Direct measurement of the 7 ps rise time excitation pulse broadened to 13 ps by the receiver amplifier.

Lower figure: Propagation times between emitter and receiver structures as a function of the perpendicular magnetic field for opposing orientations..

MoP18

Spin-Polarized Electrons in Bilayer Graphene Flakes

P.A. Orellana[1], L.Rosales[1], L. Chico[2] and M. Pacheco[1]

[1] Departamento de Física, Universidad T. Federico Santa María, Casilla Postal 110V, Valparaíso, Chile,

[2] Departamento de Teoría y Simulación de Materiales, Instituto de Ciencia de Materiales de Madrid, CSIC, 28049 Cantoblanco, Spain.

In the last years, there has been much interest in exploring the unique properties of nanostructures for spintronic devices [1]. To this end, novel ways of generating and detecting spin-polarized currents have been explored. For instance, *Song et al.* [2] described how a spin filter might be achieved in open systems by exploiting the Fano-like resonances occurring in their transmission characteristics. The idea is to tune the system so that a transmission resonance for one spin channel coincides with an antiresonance for the opposite spin. In this way, a spin-polarized current arises.

Previous works have shown that graphene bilayer flakes exhibit Fano antiresonances in the transmission [3]. In this context, in this work we propose to exploit these antiresonances to produce spin-polarized currents in a graphene-based system by putting graphene bilayer flakes in contact with a magnetic insulator, such as EuO [4]. Exchange splitting is induced in the graphene flake due to the magnetic proximity effect [5]. This produces an opposite energy shift in the spin-up and down antiresonances in the conductance, yielding a spin polarization of the current. The feasibility of spin-polarized currents in graphene devices is important for the development of all-graphene electronics, which is one of the goals in the research.

We have describes the considered system by using a one-orbital tight-binding model, which we solve analytically within the single-mode approximation. We obtain an analytical solution for the spin-dependent transmission through bilayer graphene flakes. The comparison of this analytical result to the numerically computed transmission, obtained by a recursive Green function method, is excellent in the one-mode energy range. The analytical expression for the transmission allows us to explore thoroughly the parameter space, locating the most advantageous system sizes to obtain a net spin current.We have found that the maximum spin polarization is obtained when sharp antiresonances are produced in a plateau with maximum transmission. These correspond to quasi-localized states in the bilayer graphene flake. Thus, the tuning of the flake length is important to obtain a net spin current [6].

[1] S. Datta and S. Das Sarma, Appl. Phys. Lett. **56**, 665 (1990).
[2] J. F. Song, Y. Ochiai and J.P. Bird, Appl. Phys. Lett. **82**, 4561(2003).
[3] J. W. González , et al, Phys. Rev. B **81**, 195406 (2010); Phys. Rev. B **83**, 205402 (2011).
[4] H. Haugen, D. Huertas-Hernando and A. Brataas, Phys. Rev. B **77**, 115406 (2008).
[5] J. E. Tkaczyk and P.M. Tedrow, Phys. Rev. Lett. **61**, 1253 (1988).
[6] P.A. Orellana, L.Rosales, L. Chico and M. Pacheco, cond-matt: arXiv:1301.4974, submitted (2013)

Electronic and magnetic properties of zigzag edged triangular graphene flakes

Fadıl İyikanat[1], Ramazan Tuğrul Senger[2]
[1,2] *Department of Physics, İzmir Institute of Technology, İzmir, Turkey*

The graphene flakes we consider have equilateral triangular shapes with zigzag edges (n-TGF), where n denotes the number of edge hexagonal cells in one side of the triangle. Termination of these n-TGF structures with several elements (of the first two rows of the periodic table) and application of electric field to these flakes alter their electronic and magnetic properties.

In accordance with previous studies [1,2], we find that bare flakes have large spin magnetic moment values of 4(n-1) μB, whereas they reduce to (n-1) μB for full saturation of edges with Hydrogen, Lithium, Beryllium or Flour atoms. Moreover we have studied possible termination of other elements like Boron, Carbon and Nitrogen. Hydrogen and Flour atoms prefer to bind at the top of an edge Carbon atom. Unlike Hydrogen and Flour termination, the other atoms prefer to bind at the bridge sites.

Recent studies [3,4] show that the magnetic moments of triangular graphene flakes can be controlled by applied electric field. We show that the value of total spin polarization of triangular graphene flakes can be changed by tuning an applied in-plane external field. We demonstrate that, in these flakes total spin polarization can be reduced stepwise with the applied field. The electric field control of ferromagnetism in TGFs promises a new route for spintronic applications.

[1] H. Şahin and R. T. Senger, Phys. Rev. B 78, 205423 (2008).
[2] M. Ezawa, Phys. Rev. B76, 245415 (2007).
[3] Ma, Wen-Long, and Shu-Shen Li, Physical Review B 86.4 (2012): 045449.
[4] A. D. Güçlü, P. Potasz, and P. Hawrylak, Physical Review B 84.3 (2011): 035425.

Keywords: spintronic, triangular graphene flakes, electric field

Electron transport in graphene with one dimensional local strain

Hikari Tomori, Youiti Ootuka and Akinobu Kanda

Division of Physics and TIMS, Faculty of Pure and Applied Sciences, University of Tsukuba, Tsukuba, Ibaraki 305-8571, Japan

Graphene has a liner electronic dispersion relation near the Fermi level, leading to remarkable Dirac fermionic behaviors of carriers. One of the Dirac fermionic behaviors is the strain effect, in which lattice strain in graphene induces gauge fields. It was theoretically shown that strain-induced gauge fields can be tailored to modulate electronic states, forming 1D states, confinements and band gaps. [1,2] We focus on the one dimensional *local* strain which leads to the transport gap formation around the Dirac point. We aim to verify experimentally the modulation of electron transport by strain.

By using our original method [3], we fabricate two samples with different spatial variation of one dimensional strain. We confirm the strain by micro Raman spectroscopy (Figure 1), and compare the electron transport of these two samples (Figure 2). In the poster presentation, we report details of the experimental results.

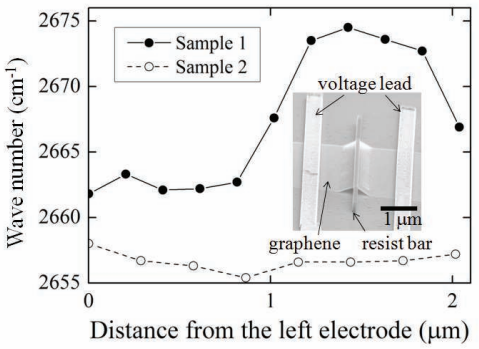

Figure 1. Spatial variation of the wave number of Raman 2D peak as a function of the distance from a voltage lead. Inset is an SEM image of a sample.

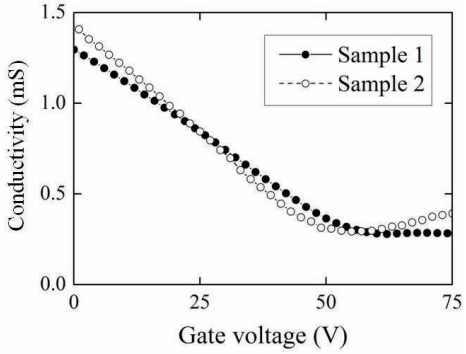

Figure 2. Gate voltage dependence of conductivity for samples 1 and 2.

[1] F. Guinea et al., Nat. Phys. **6**, 30 (2010).
[2] V. M. Pereira and A. H. C. Neto, Phys. Rev. Lett. **103**, 046801 (2009).
[3] H. Tomori et al., Appl. Phys. Express, **4**, 075102 (2011).

Floquet-Bloch theory and topology in periodically driven lattices

A. Gómez-León[1], and G. Platero[1]

[1] *Instituto de Ciencia de Materiales de Madrid (CSIC), Cantoblanco, 28049 Madrid, Spain*

Since the recent discovery of a new class of materials, the Topological Insulators, the search for topological transitions in condensed matter has become a prior task. Recently, the idea of inducing bands inversion in HgTe quantum wells by means of an ac potential was proposed [1] . In the present work we propose a theoretical formalism to describe topological phase transitions in systems which possess both spatial and time periodicities, i.e., periodic lattices driven by periodic time dependent electric fields. Our formalism allows to obtain effective hamiltonians for different driving regimes and to perform a complete topological classification of the system by means of the topological invariants. It is also general in the sense that it is suitable for describing different physical systems with arbitrary spatial dimension under ac fields for any frequency range, i.e., from adiabatic to diabatic or high frequency regimes[2] . We demonstrate that, at low frequencies, the Floquet hamiltonian for a D-dimensional system driven by a time periodic field is equivalent to a hamiltonian of a static system in D+1 dimension. leading to new topological properties which otherwise would be inaccesible. We show as well that different topological phases can be achieved by changing the lattice inter- site hoppings through the tuning of the ac field parameters. We show that the field amplitude controls the renormalization of the system parameters, while the frequency acts analogously to a DC electric field in the extra dimension. In particular, this last property relates the high frequency regime with the existence of Bloch oscillations and Landau-Zener transitions between bands, establishing a direct relation between diabatic regime and localization[3] . We illustrate our formalism with the analysis of an ac driven dimers chain[2] .

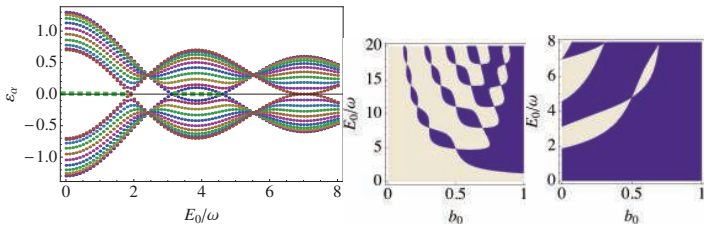

Figure 1: Left: Quasi-energy spectrum vs field amplitude for a dimers chain with hopping amplitudes ratio $\frac{\tau'}{\tau} = 0.3$ in the high frequency regime ($\omega \gg \tau$). Gapless modes in green dotted lines. Right: Phase diagram for the ac driven dimers chain with $\frac{\tau'}{\tau} = 0.3, 2$ (left and right respectively) as a function of the field amplitude and the intra-dimer distance b_0. Dark color means non-zero winding number. Note that non-trivial phases are possible for $\frac{\tau'}{\tau} > 1$ in diference with the undriven case.

*References

[1] Linder et al. , Nature Phys. **7**, 490 (2011).

[2] A. Gómez –León and G. Platero, submitted.

[3] N. Marzari et al., Rev. of Mod. Phys. **84**, 1419 (2012).

Electrical spin injection into graphene using h-BN tunnel barrier

Y. Inoue [1], **T. Yamaguchi** [1], **S. Masubuchi** [1,2], **S. Morikawa** [1], **M. Onuki** [1]
K. Watanabe [3], **T. Taniguchi** [3], **R. Moriya** [1] **and T. Machida** [1,2,4]

[1] *Institute of Industrial Science, University of Tokyo, Tokyo 153-8505, Japan*
[2] *INQIE, University of Tokyo, Tokyo 153-8505, Japan*
[3] *National Institute for Materials Science, 1-1 Namiki, Tsukuba 305-0044, Japan*
[4] *PRESTO, Japan Science and Technology Agency, Saitama 332-0012, Japan*

Graphene is a promising material for spintronics applications because of its long spin diffusion length. By inserting tunnel barrier in between a ferromagnetic electrode (F) and graphene, electrical spin injection and detection have been demonstrated in lateral graphene spin valve devices. So far, all of the reported experiments used either polycrystalline or amorphous tunnel barrier, thus obtained tunnel spin polarization is still few tenth of %. Fabrication of a high quality single crystal tunnel barrier between F and graphene is desired for much larger spin injection efficiency.

Recently, a hexagonal boron nitride (h-BN) has been recognized as another two-dimensional crystal system similarly to the graphene and used as high quality substrate for the graphene. It can be exfoliated to atomically thin layer, thus ideal material as a tunnel barrier. In this work, we fabricated graphene spin-valve device using a monolayer (ML) of h-BN as a tunneling barrier between F and graphene. From non-local magnetoresistance (MR) measurement, spin injection and detection has been demonstrated for the first time.

The device structure is schematically depicted in Fig. 1. By using dry transfer technique, a ML of h-BN is transferred on a 2-3 layer thick graphene. Ferromagnetic permalloy (Py) and non-magnetic (NM) Au/Ti electrodes are fabricated using EB lithography and EB evaporation. Two terminal I-V curve is measured in between F and NM electrodes at 30 K as shown in Fig. 2(a). I-V curve exhibits non-linear characteristics and suggests the successful fabrication of tunnel barrier in between FM and graphene. A non-local MR R_{NL} is measured as shown in Fig.2(b). We observed spin signal ΔR_{NL} of 0.4 Ω. ΔR_{NL} is robust against elevating temperature and ΔR_{NL}=0.3 Ω has been observed even at RT. We also measured Hanle curve in perpendicular magnetic field and extracted various important parameters such as spin diffusion constant and spin relaxation time which will be discussed at the presentation.

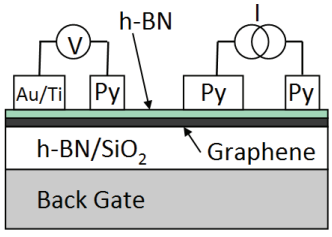

Fig. 1: Schematic illustration of the graphene spin-valve device with a ML thick h-BN tunneling barrier.

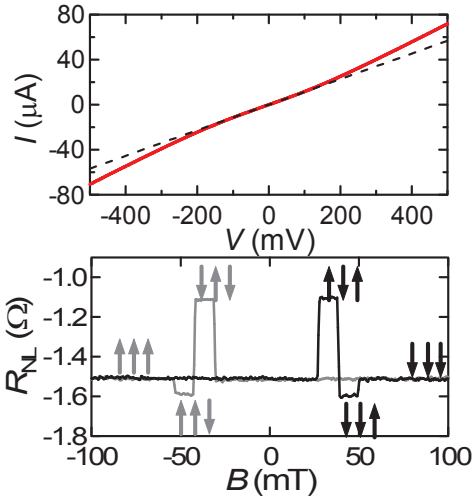

Fig. 2: (a) I-V and (b) R_{NL} measured at 30K. Arrows indicate magnetization direction of Py electrodes.

Electron and Optical Spectroscopies of Graphene Nanoribbons: Insights from Ab-Initio Calculations

D. Prezzi[1], A. Ferretti[1], S. Wang[1], A. Ruini[1,2], E. Molinari[1,2], P. Ruffieux[3], J. Cai[3], N.C. Plumb[4], L. Patthey[4], X. Feng[5], K. Müllen[5], C. A. Pignedoli[3], and R. Fasel[3,6]

[1] Istituto Nanoscienze, Consiglio Nazionale delle Ricerche, 41125 Modena, IT
[2] Dept of Physics, Informatics and Mathematics, University of Modena & Reggio, 41125 Modena, IT
[3] Empa, Swiss Federal Laboratories for Materials Science and Technology, 8600 Dübendorf, CH
[4] Swiss Light Source, Paul Scherrer Institut, 5232 Villigen, CH
[5] Max Planck Institut for Polymer Research, 55128 Mainz, Germany
[6] Department of Chemistry and Biochemistry, University of Bern, 3012 Bern, CH
Corresponding author: elisa.molinari@unimore.it

Graphene nanostructures have striking properties related to the lateral confinement that can open a band gap and induce semiconducting behavior. Key features connected to the tunability of electronic and optical properties as a function of structural parameters, e.g. width and edge structure of graphene nanoribbons (GNR), have been predicted theoretically (see e.g. [1-2]); however, only recently atomic control of GNR geometry (orientation, width and edge termination) was demonstrated [3]. These advancements in the fabrication procedure have thus allowed the first measurements of the band gap and the topology of the occupied bands of atomically precise armchair GNRs (AGNR's) by scanning tunneling spectroscopy (STS) and angle-resolved photoelectron spectroscopy (ARPES) techniques [4].
In this work we combine cutting edge theoretical and experimental techniques to study the electronic structure of a specific armchair nanoribbon (N=7, 7-AGNR). In particular we compare many-body perturbation theory calculations (performed at the GW level) with ARPES and STS data.

First principles calculations based on Density Functional Theory (DFT) were carried out for 7-AGNR, both isolated and on Au(111) substrate. Our findings clearly show a weak interaction between 7-AGNR and the Au(111) metal substrate. In order to compare ARPES and STS experiments, we have computed the self-energy corrections to the electronic structure by means of many-body perturbation theory, within the so-called GW approximation, which brings the gap to 3.7 ± 0.1 eV (the LDA value is 1.6 eV) [1]. We then estimated the gap reduction due to the presence of the metallic substrate by adding an image charge (IC) correction to the GW energy gap of the isolated GNR. Overall, this results in a theoretical estimate of the energy band gap of 2.3 to 2.7 eV for the 7-AGNR on Au(111), which is in very good agreement with the experimental value of 2.3 ± 0.1 eV.

The above results show that our ab-initio theoretical scheme can provide quantitative predictions for electron spectroscopies of nanoribbons on weakly coupled substrates such as Au. Recent results for optical excitations and excitonic effects will also be discussed, including the spectral evolution from molecular and polymer precursors to nanoribbons.

[1] D. Prezzi, D. Varsano, A. Ruini, A. Marini, and E. Molinari, Phys. Rev. B, 77 (2008) 041404; D. Prezzi, D. Varsano, A. Ruini, and E. Molinari, Phys. Rev. B, 84 (2011) 041401.
[2] C. Cocchi, A. Ruini, D. Prezzi, M. J. Caldas, and E. Molinari, J. Phys. Chem. C, 115 (2011) 2969.
[3] J. Cai et al, Nature, 466 (2010), 470.
[4] P. Ruffieux, J. Cai, N. C. Plumb, L. Patthey, D. Prezzi, A. Ferretti, E. Molinari, X. Feng, K. Mullen, C. A. Pignedoli, and R. Fasel, ACS Nano, 6 (2012) 6930.

MoP24

Counting molecular-beam grown graphene layers

Annette S. Plaut,[1] Ulrich Wurstbauer,[2] Aron Pinczuk,[2,3] Jorge M. Garcia,[4] and Loren N. Pfeiffer[5]

[1] *School of Physics, University of Exeter, Exeter EX4 4QL, UK*
[2] *Department of Physics, Columbia University, New York, NY 10027, USA*
[3] *Department of Applied Physics and Applied Mathematics, Columbia University, New York, NY 10027, USA*
[4] *MBE Lab, IMM-Instituto de Microelectronica de Madrid (CNM-CSIC), Madrid, E-28760, Spain*
[5] *Electrical Engineering Department, Princeton University, NJ 08544, USA*

We have used the ratio of the integrated intensity of graphene's Raman G peak to that of the silicon substrate's first-order optical phonon peak, accurately to determine the number of graphene layers across our molecular-beam (MB) grown graphene films [1]. We find that these results agree well both, with those from our own exfoliated single and few-layer graphene flakes, and with the results of Koh *et al.* [2]. We hence distinguish regions of single-, bi-, tri-, four-layer, etc. graphene, consecutively, as we scan coarsely across our MB-grown graphene. This is the first, but crucial, step to being able to grow, by such molecular-beam-techniques, a specified number of large-area graphene layers, to order.

[1] U. Wurstbauer *et al.*, Carbon **50**, 4822 (2012).
[2] Y.K. Koh *et al.*, ASC Nano **5**, 269 (2011).

Plasmons and single-particle excitations in single and double coupled graphene stripes

Marcos R. S. Tavares and Cesar E.P. Villegas

Centro de Ciências Naturais e Humanas, Universidade Federal do ABC, 09210-170, Santo André, SP, Brazil

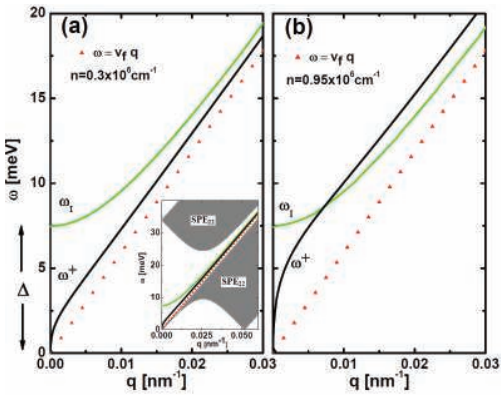

Fig. 1: The Plasmon modes for (a) n=0.3x10^6 cm^{-1} and (b) n=0.95x10^6 cm^{-1}. The inset shows the electron-hole continuum associated to the intrasubband transitions in the first excited state (hiperbolic relation dispersion).

The graphene electronic properties are unusual and arise as a direct consequence of the linear low-energy dispersion relation at the corners of the Brillouin zone, so that the low-lying excitations can be studied through the 2D Dirac Hamiltonian within a reliable approximation. The development of new experimental techniques, regarding control in growth and fabrication of nanostructures, have led to the design of new promising devices with potential applications in electronics, optoelectronics and photovoltaics. Nevertheless, despite the breakthroughs reached, further detailed studies concerning the single-particle excitations and plasmons in graphene-based nanostructures are required.

In this sense, we theoretically study the single-particle (SP) and collective excitations (plasmons) of Dirac Fermions confined in single and *double parallel nanostructures* formed by applying electric-magnetic barriers and also through patterning the graphene edges. We discuss the effects of the variation of controlled parameters, such as: i) induced gap; ii) barrier high and iii) width; and iv) doping, might have on the electronic properties of the system. Concerning the SP excitations, our results indicate that the character of the bound states is highly sensitive to the substrate induced gap. We also show that, through an adiabatic variation of the barrier intensity and nanostructure width, one might be able to control the current flux along the nanostructure. In addition, we study the plasmon modes of *double coupled* metallic armchair graphene nanoribbons (AGNRs) separated by distance L_b. For a single metallic AGNRs, we further show the plasmon dispersion dependence with the Fermi wavevector. Furthermore, we study the static dielectric function and found the absence of the logarithmic divergence at $q=2k_F$, which clearly suggests that plasmons in metallic AGNRs might be the most robust charge density oscillations occurring in quasi-one-dimensional electron systems. We also study the influence of L_b as well as the carrier densities over the acoustical and optical plasmon modes when double stripes are considered. Finally we address the dynamical screening properties of Fermion gas by considering a Fermi energy which fill out up to the second allowed state in the conduction band. We also found novel and interesting phenomena related to the Landau damped regions. Such effects arise as a direct consequence of the interaction of the linear dispersion (first state) with the hyperbolic dispersion (second state). Moreover, we found a strong influence of doping over the in-phase plasmon mode, whereas the out-phase plasmon mode remains robust, as shown in Fig.1.

[1] Marcos R.S. Tavares and Cesar E.P. Villegas, to be published.
[2] C.E.P. Villegas and M.R.S. Tavares, Appl. Phys. Letters, **101**, p. 163104, (2012); C. E. P. Villegas, and M. R. S. Tavares, et al., New J.Phys. **15** 023015 (2013).

High-performance graphene field-effect transistor and graphene spin-filter with atomically thin MoS_2 tunnel barrier

Nojoon Myoung[1], Kyungchul Seo[1], S. J. Lee,[2] and Gukhyung Ihm[1]

[1] *Department of Physics, Chungnam National University, Daejeon 305-764, Korea*

[2] *QSRC, Dongguk University, Seoul 100-715, Korea*

The excellent electronic properties of monolayer of graphene[1] have inaugurated the way for using layered materials in the post-silicon stage. Various layered structures have been used to fabricate vertical graphene heterostructures as an alternative device flatform based on graphene[2]. Graphene heterostructures with a thin MoS_2 layer are regarded as promising candidate systems for applications. Indeed, high current on/off ratio was observed in graphene/MoS_2 heterostructures. In this report, we present characteristics of tunneling current density through vertically stacked graphene/MoS_2 heterostructure as well as its applications.

We consider heterostructure, which consists of an atomically thin MoS_2 layer sandwiched by graphene as shown in Fig. 1. The MoS_2 layer of the heterostructure becomes a tunnel barrier for Dirac fermions, and both graphene layers play the role of high-quality source and drain electrodes. We can obtain the tunneling current through the MoS_2 insulating barrier as below

$$j\left(V_b, V_G\right) = j_0 \int_{-\infty}^{+\infty} D_S\left(E, V_b\right) D_D\left(E, V_b\right) T\left(E\right) \left[f_S\left(E, V_b, V_G\right) - f_D\left(E, V_b, V_G\right)\right] dE, \quad (1)$$

where $j_0 = \left(q v_F\right) / \left(2\pi L_0^3\right)$. We find the ratio of the tunneling current between an off-state and an on-state up to 10^6 at room temperature.

Moreover, we present not only the improvement in the current on/off ratio of the graphene/MoS_2 heterostructure but also an application of the heterostructure in spintronics by producing spin-dependent transport. First, we show that there emerge current peaks for a graphene/MoS_2/grarphene nanoribbon (GNR) heterostructure. This finding has potential for the use of the current peaks, resulting in the improvement of the current on/off ratio. Second, the existence of magnetic properties in few-layer MoS_2[3] can lead to the spin-polarized current in the graphene heterostructures. We show that the graphene heterostructure can be a perfect spin-filter for holes with the electron-hole asymmetric spin splitting of MoS_2[3].

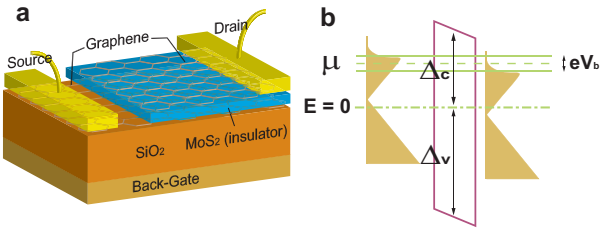

Figure 1: (a) Schematic view of various graphene/MoS_2 heterostructures. (b) Energetic diagram of the quantum tunneling model.

[1] A. H. Castro Neto *et al*, Rev. Mod. Phys. **81**, 109 (2009).
[2] L. Britnell *et al*, Science **335**, 947 (2012).
[3] E. S. Kadantsev, P. Hawrylak, Solid State Commun. **152**, 909 (2012).

Photoluminescence and Photocurrent of Thin Semiconducting Transition Metal Dichalcogenides

Nicolas Ubrig[1], Shangyun Jo[1,2], Alberto Ubaldini[1], Alexey B. Kuzmenko[1] and Alberto F. Morpurgo[1,2]

[1] *Département de Physique de la Matière Condensée , Université de Genève, CH-1211 Genève 4, Switzerland*
[2] *GAP, Université de Genève, CH-1211 Genève 4, Switzerland*

The interest in electronic and optical properties of Transition Metal Dichalcogenides (TMD) is rising since the exfoliation and the preparation of a MoS_2 single layer field-effect transistor[1]. It was also shown before that these family of compounds, in their bulk state an indirect bandgap semiconductor, undergo a transition to a direct bandgap semiconductor when thinned down to one flake[2].
In this work we present recent photoluminescence and photoconductivity measurements of exfoliated MoS_2, $MoSe_2$ and WS_2. The obtained flakes were contacted electrically through standard electron-beam lithography procedures. Through the top and/or back gate we probe the response of these systems as a function of an external electric field and doping. We thus study different effects in this compounds, e.g. the valley polarisation[3, 4] or the ambipolar transport[5], which make TMD a promising candidate for new nanotechnological applications.

[1] Radisavljevic et al., Nat. Nanotechnology 6, 147 (2011).
[2] Splendiani et al., Nano Lett. 10, 1271 (2010).
[3] Zeng et al., Nat. Nanotechnology 7, 490 (2012).
[4] Mak et al., Nat. Nanotechnology 7, 494 (2012).
[5] Braga et al., Nano Lett. 12, 5218 (2012).

MoP28

Effect of mechanical deformations in electronic properties of transition metal dichalcogenides

Mahdi Ghorbani-Asl, Pere Miró, Agnieszka Kuc, Thomas Heine
School of Engineering and Science, Jacobs University Bremen, Germany

Transition-metal dichalcogenides (TMDs) have recently attracted a great interest, particularly in their 2D monolayer forms, following comprehensive research on graphene. Despite the outstanding electrical properties of graphene, its application in nanoelectronic and nanophotonic devices is restricted due to zero band gap. The semiconducting TMD monolayers with extraordinary properties, such as distinct band gap, high carrier mobility and high thermal stability, are expected to have a promising potential in future nanoelectrodevices. Similar to graphene, 2D TMDs can be produced from their bulk material through liquid phase exfoliation process. Recently, these novel 2D systems have been used to fabricate first field-effect transistors, logical circuits and amplifiers [1,2].

We have found that the electronic structure of layered TMDs can be tuned by different strategies, such as quantum confinement, nanotube formation, substitutional doping or mechanical deformations [3-5]. In this work, electronic properties of TMD monolayers are studied as subject to mechanical deformations, namely strain and rippling. Under 2D-isotropic strain, the TMD monolayers change the semiconducting direct-gap character and become metallic for the deformations as large as 11%, what results in electrical conductivity at the Fermi level. On the other hand, the formation of ripples causes extreme quenching of the conductance. In addition, we have studied strain effects on the electronic and transport characteristics of TMD nanotubes.

References

[1] B. Radisavljevic, A. Radenovic, J. Brivio, V. Giacometti, A. Kis, *Nat. Nanotechnol*. **6**, 147 (2012).
[2] B. Radisavljevic, M. B. Whitwick, A. Kis, *App. Phys. Lett.* **101**, 043103 (2012).
[3] A. Kuc, N. Zibouche, T. Heine, *Phys. Rev. B* **83**, 245213 (2011).
[4] N. Zibouche, ,A. Kuc, T. Heine, *Eur. Phys. J. B* **85**, 49 (2012).
[5] M. Ghorbani-Asl, S. Borini, A. Kuc and T. Heine, submitted to *Phys. Rev. B* (2012), eprint arXiv:1301.3469.

Tuning electronic properties of transition-metal dichalcogenides

Agnieszka Kuc, Mahdi Ghorbani-Asl, Thomas Heine
School of Engineering and Science, Jacobs University Bremen, Germany

In 2011, transition-metal dichalcogenides (TMDs) have started their renaissance as potential materials for nano- and opto-electronics due to their extraordinary electronic properties arising from quantum confinement (exfoliation). Though known for over 40 years, bulk 3D TMDs are no threat to traditional silicon-based electronics. The situation has changed in 2011, when Nicolosi [1] and co-workers have shown that 3D TMDs are easy to process using liquid exfoliation and large-area single layers can be produced at low costs. Exfoliation to monolayers changes significantly electronic properties of TMDs. Kis and co-workers utilized this phenomenon and in the beginning of 2011 they produced the first field-effect transistor (FET) based on MoS_2 monolayer with mobility in the same range as for graphene nanoribbons and silicon thin films. [2] Shortly after, a logical circuits and amplifiers were produced. [3] Silicon-based FETs often suffer from heat dissipation. Therefore, to improve nanoelectronic devices one could replace silicon with materials that perform better at smaller scale, such as layered TMDs.
In this work, we have studied electronic properties of layered TMDs by means of quantum confinement, atomic substitutions, tube formation, layer stacking, and mechanical deformations. [4-6] Electronic and transport properties were investigated showing that the modifications mentioned above tune the electronic structure in a controlled way.

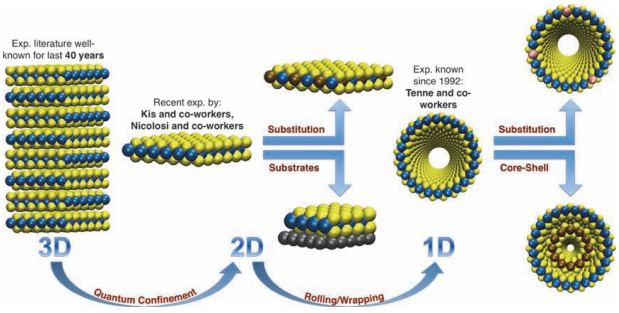

References
[1] Coleman, J. N.; Lotya, M.; O'Neill, A.; Bergin, S. D.; King, P. J.; Khan, U.; Young, K.; Gaucher, A.; De, S.; Smith, R. J.; Shvets, I. V.; Arora, s. K.; Stanton, G.; Kim, H.-Y.; Lee, K.; Kim, G. T.; Duesberg, G. S.; Hallam, T.; Boland, J. J.; Wang, J. J.; Donegan, J. F.; Grunlan, J. C.; Moriarty, G.; Shmeliov, A.; Nicholls, R. J.; Perkins, J. M.; Grieveson, E. M.; Theuwissen, K.; McComb, D. W.; Nellist, P. D.; Nicolosi, V. *Science* **331** (2011) 568.
[2] Radisavljevic, B.; Radenovic, A.; Brivio, J.; Giacometti, V.; Kis, A. *Nat. Nanotechnol.* **6** (2012) 147.
[3] Radisavljevic, B.; Whitwick, M. B.; Kis, A. *App. Phys. Lett*. **101** (2012) 043103.
[4] Kuc, A.; Zibouche, N.; Heine, T. *Phys. Rev. B* **83** (2011) 245213.
[5] Zibouche, N.; Kuc, A.; Heine, T. *Eur. Phys. J. B* **85** (2012) 1.
[6] M. Ghorbani-Asl, S. Borini, A. Kuc and T. Heine, submitted to *Phys. Rev. B.* (2012), eprint arXiv:1301.3469

Dielectric substrate and capping effects on optical properties of a few atomic monolayer MoS_2 sheets

D. Sercombe[1], S. Schwarz[1], O. Del Pozo-Zamudio[1], F. Liu[1], B. J. Robinson[2], E. A. Chekhovich[1], O. Kolosov[2], and A. I. Tartakovskii[1].

[1]*Department of Physics and Astronomy, University of Sheffield, S3 7RH, UK*
[2]*Department of Physics, University of Lancaster, Lancaster LA1 4YB, UK*

Molybdenum disulfide (MoS_2) is a promising layered material for use in Field Effect Transistors[1]. It also has unusual electronic properties such as an indirect-to-direct band gap transition and strong valley polarization[2]; with mono-molecular layer MoS_2 sheets showing bright photoluminescence (PL) up to room temperature[3]. In order to successfully integrate MoS_2 into opto-electronics devices both accurate control of light emission properties and a better understanding of thin film interactions with the environment are required. Here we use a combination of micro-PL and ultrasonic force microscopy (UFM) to show strong effects of SiO_2 substrate quality (in terms of roughness) and dielectric capping (SiO_2 and Si_xN_y) on the light emission from near-monolayer mechanically exfoliated MoS_2 sheets. In particular we find a notable variation in PL peak energy and lineshape between different sheets on the same substrate. We find that this variation is increased for rougher substrates grown by PECVD. We show, however, that such variation can be markedly suppressed, and in addition narrow PL linewidths obtained, when using atomically flat thermal oxide substrates and Si_xN_y capping (see Figure). Our interpretation of the improved reproducibility of the optical properties is supported by UFM measurements which were used to probe the elasticity of the MoS_2 sheets. We find that the stiffness of the sheet, characterising its adhesion to the surrounding dielectric layers, dramatically increases for smooth thermal oxide substrates, and is further improved by the capping. Based on both PL and UFM data, we relate the variation in the PL lineshape with variation of the strain and charging within the sheets. Thus our results indicate that optical properties can be controlled by appropriate choice of the dielectric substrate and capping, a key result providing a method for producing more consistently fabricated devices.

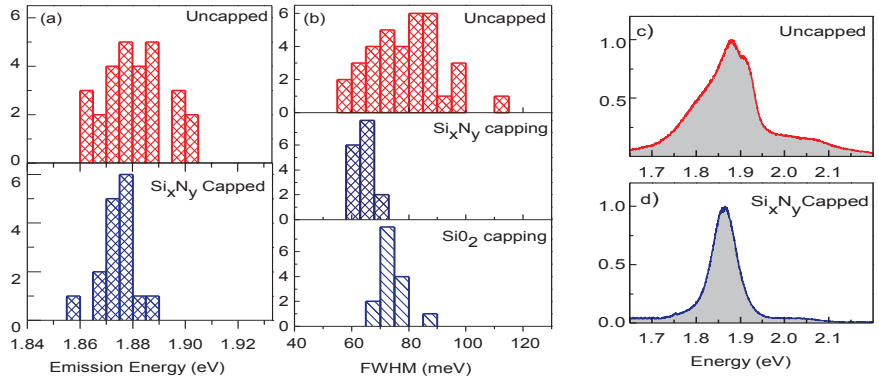

Histograms showing energy (a) and linewidths (b) of PL from capped and uncapped MoS_2 sheets. PL emission spectra for uncapped (c) and capped (d) MoS_2 sheets showing improved line-widths.

[1]Radisavljevic et. all. Nature nanotechnology, 6, 147–50. (2011)
[2] Zeng, H.; Dai, J.; Yao, W.; Xiao, D.; Cui, X. Nature nanotechnology 7, 490–3. (2012)
[3] Mak, K.; Lee, C.; Hone, J.; Shan, J.; Heinz, T. Physical Review Letters, 105, 2–5. (2010)

Tuneable photoluminescence emission from exfoliated InSe nanocrystals

G.W. Mudd[1], S. A. Svatek[1], O. Makarovsky[1], L. Eaves[1], A. Patanè[1], P. H. Beton[1], Z. D. Kovalyuk[2], G. V. Lashkarev[2], A. I. Dmitriev[2]

[1] *School of Physics and Astronomy, The University of Nottingham, Nottingham NG7 2RD, UK*
[2] *Institute for Problems of Materials Science, Ukrainian Academy of Sciences, Kiev, Ukraine*

The discovery of single-atomic layer graphene has led to a surge of interest in other anisotropic crystals with strong in-plane bonds and weak, van der Waals-like coupling between the atomic layers [1-2]. Here we report strong quantization effects and tuneable photoluminescence emission in mechanically exfoliated Bridgman-grown crystals of γ-rhombohedral InSe [3]. Figs.1a-c show scanning atomic force microscopy (AFM) and optical images, and height z-scans of a typical thin exfoliated flake. RT photoluminescence (PL) maps and corresponding spectra of the flakes are shown in Fig. 1(d-e). The near-band edge PL peak exhibits a strong blue-shift to higher photon energies hv with decreasing layer thickness h, consistent with 2-D quantum confinement of photo-excited carriers by the external surfaces of the flakes, see solid line fit in Fig. 1f obtained from a model based on the band parameters of InSe. The persistence of intense PL down to $h \sim 6$ nm and over periods of several weeks following exfoliation indicates that surface defects do not significantly impair radiative recombination. We exploit the high optical quality of exfoliated InSe layers to realize infrared photodetectors. Also, we discuss how nanoflakes of InSe could be used in combination with graphene electrodes to make novel optoelectronic nanodiodes.

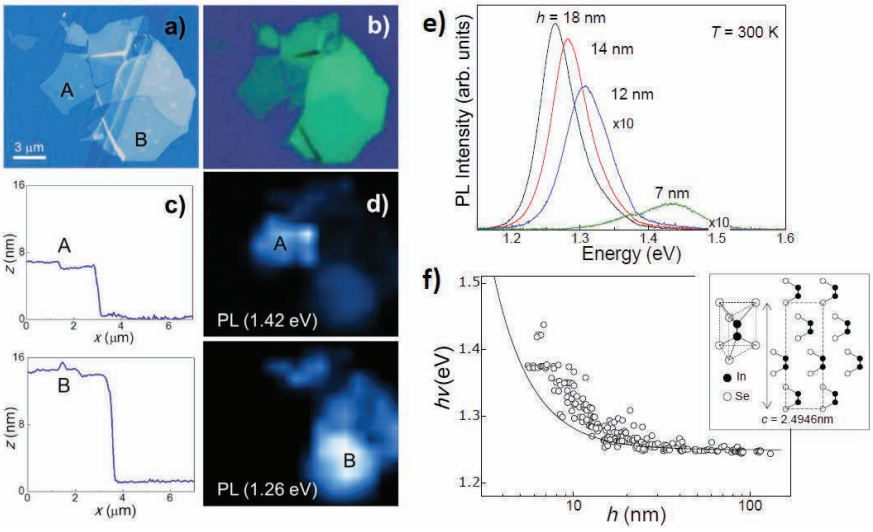

Figure: AFM **(a)** and optical image **(b)** of exfoliated InSe. The AFM z-profiles **(c)** and corresponding confocal micro-PL maps (**d**) reveal flat nanometer thick layers A and B. **(e)** Typical micro-PL spectra of InSe layers at $T = 300$K with peak energy strongly dependent on the layer thickness h **(f)**. The inset in (f) shows the crystal structure of γ-rhombohedral InSe.

[1] K.S. Novoselov et al., PNAS **102**, 10451 (2005).
[2] P.A. Hu et al., ACS Nano **6**, 5988 (2012).
[3] A. I. Dmitriev et al., Phys. Stat. Sol. (b) **162**, 213 (1990).

Photoluminiscence spectroscopy of thin sheets of Gallium Selenide

S. Schwarz[1], O. Del Pozo-Zamudio[1], D. Sercombe[1], E. A. Chekhovich[1], D. N. Borisenko[2], N. N. Kolesnikov[2], A. I. Tartakovskii[1]

[1]Department of Physics and Astronomy, University of Sheffield, Sheffield, S3 7RH, UK
[2]Institute of Solid State Physics, Russian Academy of Sciences, Chernogolovka 142432, Russia

Interest in atomically thin two-dimensional (2D) layered compounds, including metal chalcogenides, has increased in recent years due to unique physical properties of a few monolayer (ML) structures [1], and also growing effort in fabrication of novel heterostructures composed of layered materials. So far, main focus in studies of light-emitting layered materials was on MoS_2, which however shows dramatic decrease in photoluminescence (PL) for sheets with thicknesses above single ML [2]. Here we present low-temperature micro-PL (μ-PL) studies of thin sheets of mechanically exfoliated thin layers of GaSe capped with a thin SiN layer. We show that GaSe exhibit significantly brighter PL than MoS_2 around 2.05 eV for layers up to 160 nm thick. μ-PL enables observation of unusual sharp lines (with linewidths 3-10 meV) possibly originating from quantum-confined states in very thin dislocated layers embedded within quasi-bulk GaSe sheets. Our results indicate significant enhancement of exciton binding energies in such dislocated layers potentially enabling wider range of applications of GaSe in light emitting opto-electronic devices.

[1] Novoselov, K.S., et al., Nature 490, 192–200 (2012)
[2] Qing Hua Wang et al., Nature Nanotechnology 7, 699-712 (2012).
[3] Mooser E. et al., Il Nuovo Cimento, Vol. 18 B, N. 1, 164 (1973).
[4] PyngAn Hu et al., American Chemical Soc. Vol. 6, 7, 5988 (2012).

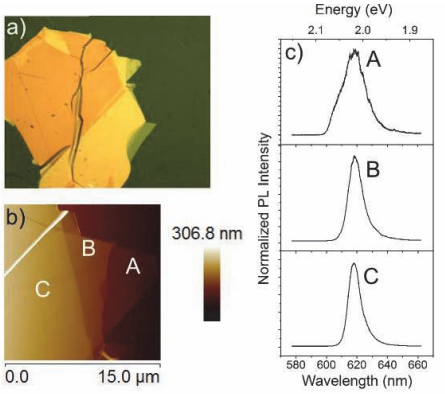

Fig.1. a) Optical image of a mechanically exfoliated GaSe thin flake. b) AFM image of a region of the flake shown in (a). Three different thicknesses are observed. c) Photoluminescence (PL) spectra measured for tree different places of the flake (A, B and C).

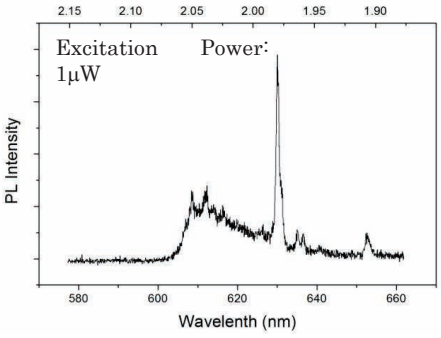

Fig.2. PL spectra of a GaSe thin flake measured with excitation power of 1 μW. Narrow lines appear with low excitation power at lower energies than the main PL line.

Band Gap Opening in Graphene on Transition Metal Dichalcogenides and Related Substrates

J .R. Wallbank[1], M. Mucha-Kruczyński[1,2] and V. I. Fal'ko[1]

[1] *Department of Physics, Lancaster University, Lancaster, LA1 4YB, UK*
[2] *Department of Physics, University of Bath, Claverton Down, Bath, BA2 7AY, UK*

It is often be desirable to open a band gap in graphene for use in electronic devises, however many techniques that do so also result in a reduction of the carrier mobility. In contrast, placing graphene on atomically flat crystal substrates often results in a dramatic increase in carrier mobility. Furthermore, an exactly aligned hexagonal substrate with a lattice constant exactly $\sqrt{3}$ times bigger than that of graphene, would result in a Kekulé distortion, inducing intravalley mixing and band gap opening at the Dirac point. Indeed there are many substrates, including certain transition metal dichalcogenides, that almost fit the requirement. However a slightly deviation from the $\sqrt{3}$ times bigger lattice constant or any misalignment angle will result in the formation of the quasi-periodic structure known as a moiré pattern.

The dominant effect of the moiré on graphene electrons can be described in terms of scattering using the simplest moiré harmonics, which, when combined with the symmetry of the system, allows the Hamiltonian to be written in terms of a small number of phenomenological, substrate dependant, parameters [1]. Like the Kekulé distortion, but in contrast to the thoroughly investigated case of graphene on substrates with comparable lattice constants [1], the $\sqrt{3}$ times bigger substrates result in intervalley scattering, allowing new parametric regimes to be explored.

We investigate the characteristic features that appear in the resulting graphene moiré miniband spectrum, systematically exploring the space of phenomenological substrate parameters. We show that the Dirac spectrum around zero energy always remains intact, in contrast with the Kekulé distortion. However, for a large parametric regime, a band gap is still opened by these substrates, but between the first and second moiré minibands. The remaining possibilities being that either the first and second minibands do not touch, although overlap on the energy axis, or, will touch at six highly anisotropic mini Dirac points.

[1] J. R. Wallbank, A. A. Patel, M. Mucha-Kruczynski, A. K. Geim, V. I. Fal'ko, arXiv:1211.4711 (2012)

Novel experimental technique of synthesis two-dimensional nanoparticles of autointercalated Niobium Diselenide

L.M. Chepyga[1], L.M. Kulikov[1,2] L.G. Akselrud[2]

[1] *Frantsevich Institute for Problems of Materials Science of NASU. 3, Krzhyzhanovsky Str., Kiev-142, 03680, Ukraine. E-mail: liudmylachepyga@ukr.net,*

[2] *Franko Lviv National University. 6, Cyril and Mefody Str., Lviv-79005, Ukraine. E-mail: akslev@googlemail.com*

Two-dimensional inorganic nanostructures as two-dimensional or graphene-like nanoparticles of d-transition metals dichalcogenides ("inorganic graphene-like nanostructures"; "2D nanostructures"; "ultrathin nanolayers") including 2H-MCh_2 nanostructures (M = Nb, Ta; Ch = S, Se; 2H-TaS_2 structural type; metallic type of conductivity) and their intercalated nanophases have been receiving great attention in recent years because they show unusual physical properties which are the result of a quantum size effect associated to their ultra-thin structure. These 2D nanosheets are now considered to be excellent candidates for future electronic applications. As demonstrated by groundbreaking advances such as superconductors and magnetic superlattices, 2D nanostructures play a pivotal role to realizing electronic, magnetic and optical properties.

The family of layered 2H dichalcogenides represents an interesting system in which charge-density-wave (CDW) order coexists with superconductivity. The CDW transition temperature decreases, while the superconducting critical temperature (Tc) increases from 2H-TaS_2 and 2H-$NbSe_2$ to 2H-NbS_2, suggesting that these two parameters compete. Indeed, as became known, in 2H-TaS_2 and 2H-$NbSe_2$, Tc increases under pressure while T_{CDW} decreases. After CDW order disappears, Tc remains approximately constant. All of anomalies, including an apparent anisotropy of the superconducting gap, is very important in physical research two-dimentional nanostructured systems.

Various techniques for nanostructured 2H-MCh_2 synthesis have been developed in the last decade or so. However, this methods are limited to the fabrication of a small amount of single-layer nanosheets materials with low reproducibility, which is disadvantageous for their application in electronic devices.

The nanosynthesis was carried out by "up-bottom" activated processes of intercalation (Li^+/H_2O) of autointercalated 2H-$Nb_{1.02(1)\div1.29(1)}Se_2$ micron powders. We studied the timing data of galvanostatic processes of intercalation with the potentiostat (PI-50-1, reference electrode – AgCl). The structural properties of dispersed powders were investigated by X-ray studies, SEM.

It was synthesized the homogeneous, anisotropic graphene-like 2H-$Nb_{1.02(1)}Se_2$ nanoparticles (2D, 2H-TaS_2 structural type) with average sizes of 22.7(7)–46.4(1.4) nm for [013] crystallographic direction, 61.9(1.7)–144(7) nm for [110] direction. Unit cell parameters (*a*, *c*) of 2H-$Nb_{1.02(1)}Se_2$ nanostructures correlate with average sizes of nanoparticles.

As a result of scanning electron microscopy flat (2D) 2H-$Nb_{1,02(1)}Se_2$ nanoparticles have correct hexagonal form with considerable anisotropy sizes of length and thickness. It form conglomerates and does not include other types of particles.

Graphen-like intercalated 2H-MCh_2 nanoparticles with wide structural-sensitive physical properties set are perspective for mentioned 2D nanomaterials design. 2D crystals can also be assembled in 3D heterostructures that do not exist in nature and have tailored properties, opening an entirely new chapter in condensed matter research.

Electronic properties of MoS_2-WS_2 heterojunction

K. Kośmider [1] **and J. Fernández-Rossier** [1,2]

[1] *International Iberian Nanotechnology Laboratory, Braga, Portugal*
[2] *Universidad de Alicante, Alicante, Spain*

The fabrication of electronic devices based on a single or a few layers of transition metal dichalcogenides , such as MoS_2 and WS_2, holds the promise of expanding the graphene revolution into an exciting new arena. Unlike graphene, the MoS_2 and WS_2 monolayers have a direct band gap in the 1.8eV range and, due to the strong spin orbit coupling (SOC) and the specifics of their atomic structure, they present strong spin-valley coupling. This has been demonstrated by means of optical pumping experiments which to valley polarized exciton population [1-3].

Here we study the electronic structure of a heterojunction made of two monolayers of MoS_2 and WS_2. Our first-principles density functional calculations [4] show that, unlike in the homogeneous bilayers, the heterojunction has an optically active band-gap, smaller than the ones of MoS_2 and WS_2 single layers. We find that that the optically active states of the maximum valence and minimum conduction bands are localized on opposite monolayers, and thus the lowest energy electron-holes pairs are spatially separated. Our findings portrait the MoS_2-WS_2 bilayer as a prototypical example for band-gap engineering of atomically thin two-dimensional semiconducting heterostructures.

We also find that, contrary to previous theory work, there is spin splitting at the K point both in the valence and the conduction band. We discuss the physical origin of the splitting at the conduction band and derive an effective Hamiltonian making use of Wannier functions and perturbation theory.

References:
[1] H. Zeng, J. Dai, W. Yao, D. Xiao, and X. Cui, Nature Nanotechnology **7**, 490 (2012).
[2] K.F Mak, K. He, J. Shan, and T.F. Heinz, Nature Nanotechnology **7**, 494 (2012).
[3] T. Cao, *et al.*, Nature Communications **3**, 887 (2012).
[4] K. Kośmider and J. Fernández Rossier, Physical Review B **87**, 075451 (2013).

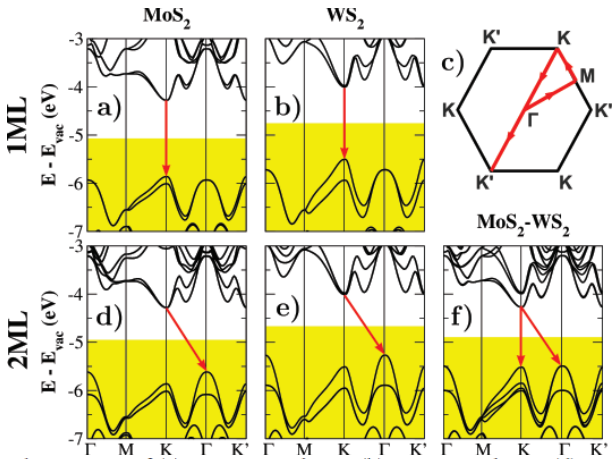

Fig.1: Band structures of (a) MoS_2 monolayer, (b) WS_2 monolayer, (d) MoS_2 bilayer, (e) WS_2 bilayer, and (f) MoS_2- WS_2 heterojunction. (c) Scheme of the Brillouin zone.

Energy spectrum, quantum Hall effect, and valley splitting in graphene on hexagonal boron nitride

Pilkyung Moon[1,2] and Mikito Koshino[1]

[1] *Department of Physics, Tohoku University, Sendai, 980–8578, Japan*
[2] *School of Computational Sciences, Korea Institute for Advanced Study, 130–722, Republic of Korea*

We theoretically investigate the electronic structure, quantum Hall effect, and valley splitting in graphene (monolayer and bernal-stacked bilayer) on hexagonal boron nitride. The beating of the mismatched lattices creates a superlattice potential, of which period can be much larger than intrinsic graphene. Using a low-energy approximation which incorporates the rigorous interlayer interaction [1], we describe the spectral evolution in a wide range of magnetic fields. We show that, at high magnetic field, even the zero energy Landau levels are completely reconstructed with a nonmonotonic sequence of quantized Hall conductivity (Fig. 1). And we find the lifting of valley degeneracy in this type of superlattice. The emergence of states with integer quantized conductance at noninteger filling of a single Landau level is well matched by the experimental results [2].

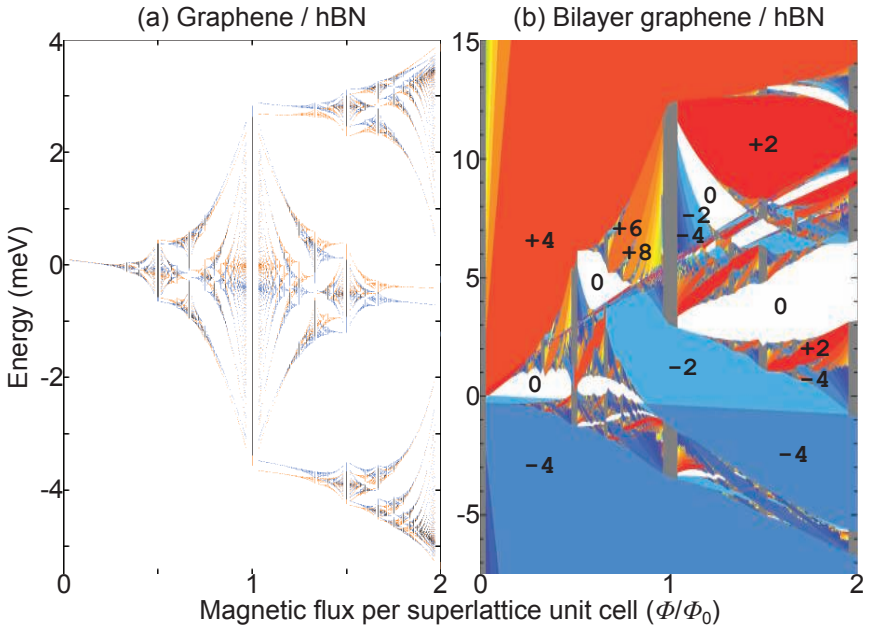

Figure 1: Energy spectrum of (a) monolayer graphene and (b) bernal-stacked bilayer graphene on hexagonal boron nitride with a 0° mismatch angle. The energy scale is chosen to highlight the lowest Landau level. The numbers in (b) label the quantized Hall conductivity in units e^2/h corresponding to each gap.

[1] P. Moon and M. Koshino, Phys. Rev. B **85**, 195458 (2012).
[2] C. R. Dean, L. Wang, P. Maher, C. Forsythe, F. Ghahari, Y. Gao, J. Katoch, M. Ishigami, P. Moon, M. Koshino, T. Taniguchi, K. Watanabe, K. L. Shepard, J. Hone, and P. Kim, arXiv:1212.4783 (2013).

Hyperbolic Spin vortices and Textures in Spinor Polariton Condensates

F. Manni[1], Y. Léger[1,2], Yuri G. Rubo[3], R. André[4] & B. Deveaud[1]

[1]*ICMP, École Polytechnique Fédérale de Lausanne (EPFL), CH-1015 Lausanne, Switzerland*

[2]*FOTON Lab, CNRS UMR6082, INSA 20 Ave des Buttes de Coësmes, CS14315, 35043 Rennes Cedex, France*

[3]*Centro de Investigación en Energía, UNAM, Temixco, Morelos, 62580, Mexico*

[4]*Institut Néel, CNRS, 25 Avenue des Martyrs, 38042 Grenoble, France*

* Corresponding author: francesco.manni@epfl.ch

Symmetry considerations and topological arguments are successfully employed to unveil intriguing analogies between natural phenomena that would otherwise appear different from each other. From cosmology down to quantum systems, the description of phase transitions passes through symmetry breaking arguments, which are associated with the generation of topological defects. In view of the study of such topological defects, Bose-Einstein condensates[1], superfluids and superconductors have proved to be prominent systems.

Extremely unconventional vorticity is predicted to occur in spinor quantum fluids, where the unique combination of quantum coherence and spin properties allows for the existence of quantized spin vortices, signatures of spontaneous breaking of the chiral symmetry in the system. Their observation and stability conditions represent an open and debated question. Spin topological entities are also expected to yield specific spatial structures - spin textures - in the condensate polarization structure.

Polaritons condensates have the unique advantage of non-destructive optical access to the condensate complex order parameter and spin properties. Spinor polariton condensates have recently been demonstrated, by identification of their fundamental fractional vortical excitations[2]. Higher order spin vorticity – spin vortices and monopoles - are predicted to occur in the systems[3], although up to now elusive to experimental observation.

In this work we demonstrate stable spin vortices, spontaneously arising in the steady state of a spinor polariton condensate. We provide a comprehensive measurement of the spin vortical entity, by complete characterization of the condensate spin texture. The observation proves occurrence of chiral symmetry breaking, which is the very mechanism underlying the formation of Dirac monopoles, conceivably paving the way for the identification of such non-classical entities with purely radial magnetic flux.

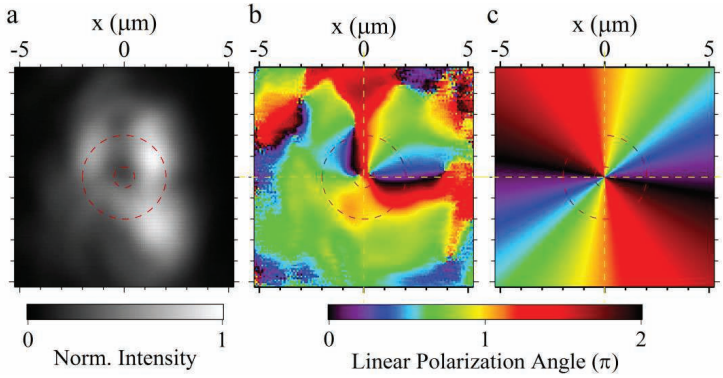

Fig. 1: (**a**) Polariton density distribution around the spin vortex core. (**b**) Measured and (**c**) theoretical linear polarization angle map, indicating the direction of the linear polarization when circumventing the spin vortex core in the Stokes parameters representation. Dashed red circles mark the vortex position.

[1] Davis, K. B., et al., Phys Rev Lett **75**, 3969-3973 (1995).

[2] Lagoudakis, K. G. et al., Science **326**, 974-976 (2009).

[3] Solano, M. T. & Rubo, Y. G., J Phys Conf Ser **210**, (2010).

MoP38

BEC-BCS-Laser Crossover theory of Exciton-Polariton Systems

M. Yamaguchi [1*], K. Kamide [1], R. Nii [1], T. Ogawa [1] and Y. Yamamoto [2, 3]

[1] *Department of Physics, Osaka University, Toyonaka, Osaka 560-0043, Japan*
[2] *National Institute of Informatics, Hitotsubashi 2-1-2, Chiyoda-ku, Tokyo 101-8403, Japan*
[3] *E. L. Ginzton Laboratory, Stanford University, Stanford, California 94305, USA*
[*] Corresponding author: yamaguchi@acty.phys.sci.osaka-u.ac.jp

In semiconductor exciton-polariton systems, Bose-Einstein condensation (BEC) of exciton-polaritons has been observed in recent years [1]. In contrast, this system is potentially capable of achieving the Bardeen-Cooper-Schrieffer (BCS) state and normal photon lasing in high-excitation regimes [2, 3], depending on quasi-equilibrium and non-equilibrium situations. The relationships among the BEC, BCS, and lasers are now one of the most exciting topics experimentally studied [4]. However, from a theoretical viewpoint, it is difficult to describe such phenomena in a unified way because the system includes many different types of physics, e.g. dissociations of electron-hole (e-h) pairs depending on the carrier densities, the non-equilibration of the system due to the pumping and losses, and so on.

In this study, within the Hartree-Fock approximation, we show a unified theory (BEC-BCS-laser crossover theory) [5] by extending the non-equilibrium Green's function for two-level systems [6]. The theory becomes identical to the BCS gap equation when the system is in quasi-equilibrium, whereas it results in the Maxwell-Semiconductor-Bloch equations describing the laser actions when non-equilibration of the system becomes essential. This means that we can discuss the BEC, BCS, laser physics by using only one theory. Furthermore, as a result of this theory, it is found that the single-particle spectral functions for the conduction and valence bands ($A_{cc}(\nu,\boldsymbol{k})$ and $A_{vv}(\nu,\boldsymbol{k})$) have quite simple expressions:

$$A_{cc/vv}(\nu;\boldsymbol{k}) = 2|u_{\boldsymbol{k}}|^2 L(\nu,\mp E_{\boldsymbol{k}}) + 2|v_{\boldsymbol{k}}|^2 L(\nu,\pm E_{\boldsymbol{k}}), \qquad (1)$$

where $u_{\boldsymbol{k}}$, $v_{\boldsymbol{k}}$, and $E_{\boldsymbol{k}}$ are the Bogoliubov coefficients and $L(\nu, \pm E_{\boldsymbol{k}})$ is the Lorentz function broadened by the e-h thermalization rate γ [7]. Here, one can notice that there are remarkable similarities to the superconductivities. The important point is, however, that Eq. (1) can be used *regardless of the BEC, BCS, and laser regime*.

In Fig. 1, we show typical peak positions of A_{cc} in a lasing regime, which is equivalent to the renormalized conduction-band structure. In this situation, μ corresponds to the laser frequency and the gap is opened mainly due to the Rabi splitting. Here, it should be noted that the existence of the gap indicates that there are light-induced e-h pairs even when the lasing occurs in contrast to the common belief. Such renormalization effects are also reflected in the gain spectra (not shown) which would be accessible by experiments. Details will be presented at the conference. This work is supported by the JSPS through its FIRST Program, and DYCE, KAKENHI 20104008.

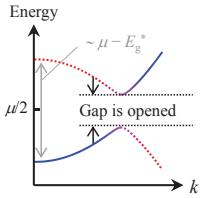

Fig. 1: Renormalized conduction band structure in the lasing regime. In this regime, μ is the laser frequency and E_g^* is the renormalized band gap due to the Coulomb interactions.

[1] J. Kasprzak *et al*, Nature **443**, 409 (2006).
[2] K. Kamide and T. Ogawa, Phys. Rev. Lett. **105**, 056401 (2010).
[3] L. S. Dang *et al*, Phys. Rev. Lett. **81**, 3920 (1998).
[4] J.-S. Tempel *et al*, PRB **85**, 075318 (2012); E. Kamman *et al*, New J. Phys. **14**, 023060 (2012).
[5] M. Yamaguchi, K. Kamide, T. Ogawa, and Y. Yamamoto, New J. Phys. **14**, 065001 (2012).
[6] M. H. Szymanska, J. Keeling, and P. B. Littlewood, Phys. Rev. Lett. **96**, 230602 (2006).
[7] M. Yamaguchi, K. Kamide, R. Nii, T. Ogawa, and Y. Yamamoto, arXiv:1301.4838 (2013).

Light-matter interaction between a two-dimensional electron gas and a micro-cavity

S. Smolka[1], W. Wuester[1,2], S. Faelt[1,2], F. Haupt[1], W. Wegscheider[2], A. Imamoglu[1]

[1] *Institute for Quantum Electronics – ETH Zürich, Wolfgang-Pauli-Strasse 16, 8093 Zürich, Switzerland*

[2] *Laboratory for Solid State Physics – ETH Zürich, Wolfgang-Pauli-Strasse 16, 8093 Zürich, Switzerland*

We report quantum optical studies on a two dimensional electron gas embedded in a semiconductor cavity by positioning a remotely doped GaAs quantum well between two distributed Bragg reflectors that form a λ-cavity. The coherent coupling of a photonic resonator and semiconductor excitons results into polaritons that are the fundamental ingredients to study quantum optical phenomena in the realm of cavity quantum electrodynamics [1, 2]. In the presence of an electronic reservoir, one could expect the exciton binding energy to vanish due to the screening of the Coulomb potential while the interaction between a hole created by a single photon absorption event and the continuum of electronic states leads to intriguing many-body phenomena such as the Fermi edge singularity [3, 4]. Theoretical predictions show that the case of an electronic reservoir model of two coupled oscillators describing a confined photon and exciton forming a polariton breaks down and the interactions are strongly modified by the continuum of states [5].

High resolution laser spectroscopy as well as confocal photo luminescence measurements at cryogenic temperatures are conducted to optically probe correlated many-body states emerging from the interaction between the cavity photon, the electronic reservoir and the photo-excited hole. A spatial tuning of the cavity resonance frequency allows us to directly access the signatures of strong coupling between optical excitations from the two-dimensional electron gas and the photonic mode. By changing the electron density the electronic Bohr radius and the binding energies can be modified. This alters the coupling strength of the electronic reservoir to the photonic mode linking the otherwise remotely connected research areas of cavity quantum electrodynamics and many-body physics.

[1] C. Weisbusch, M. Nishioka, A. Ishikawa, and Y. Arakawa, Phys. Rev. Lett. **69**, 3314 (1992).
[2] H.M. Gibbs, G. Khitrova, and S.W. Koch, Nature Photonics **5**, 275 (2011).
[3] G.D. Mahan, Phys. Rev. **153**, 882 (1967).
[4] M. S. Skolnick, *et al.*, Phys. Rev. Lett. **58**, 2130 (1987).
[5] N. S. Averkiev and M. M. Glazov, Phys. Rev. B **76**, 045320 (2007).

MoP40

Hybrid intersubband-intrasubband cavity polaritons

M. Załużny
Institute of Physics, UMCS, pl. M. Curie-Skłodowskiej 1, 20-031 Lublin, Poland

In the nonretarded limit the *n*-doped MQW slab supports the intersubband and intrasubband Coulomb modes [1]. When the MQW is embedded into a microcavity (MC), the resonant coupling between the ground cavity mode (c_1) and the intersubband Coulomb mode (with the frequency $\omega_{\rm IT}$) can be achieved. In this limit the formation of the intersubband cavity polariton (ICP) branches is possible [2,3]. In typical systems the frequency $\omega_{\rm IT}$ is much larger than the MQW plasma frequency ω_p. Consequently, the influence of the intrasubband plasmon modes (located below ω_p) on the behavior of the ICP branches can be omitted. We show that when condition $(\omega_p/\omega_{\rm IT})^2 << 1$ is not well fulfilled in the MQW-MC systems (see e.g. Ref. 3), the formation of the hybrid intersubband–intrasubband polariton branches becomes possible, provided that the mirrors are of the dielectric type.

Our approach is based on the "microscopic" implementation of the effective medium approximation [4]. For simplicity the dissipation and the dielectric mismatch are neglected. The results of the numerical calculations performed for the system with perfect dielectric mirrors are presented in Fig.1 [5].

The simultaneous coupling of the c_1 mode with the intersubband and intrasubband Coulomb modes can be equivalently considered as the photon mediated coupling between the intersubband and intrasubband plasmonic modes [6]. The inspection of Fig. 1 shows that the above mentioned coupling creates the hybrid ICP branch with an admixture of the intrasubband plasmon. The hybrid branch is blueshifted with respect to the "pure" ICP branch. As one can expect, practically only the lower ICP branch is affected by the intrasubband plasmons. At $k_x \approx 0.6\ k_{1,x}^{\rm res}$ and $\omega \approx 0.7\ \omega_{\rm IT}$ the considered branch crosses the c_1 mode and transforms into the upper intrasubband polariton branch with decreasing k_x.[5]. (k_x is the in-plane wave vector. Moreover, at $k_x = k_{1,x}^{\rm res}$ the frequency of the ground cavity mode $\omega_{\rm c1}(k_x)$ coincides with the intersubband frequency $\omega_{\rm IT}$.)

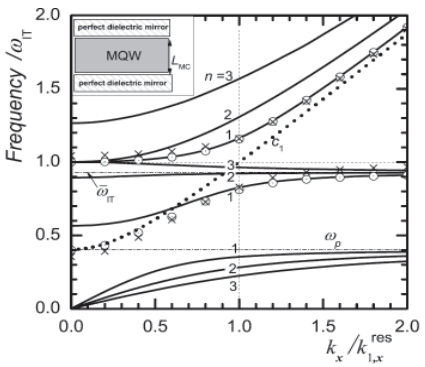

Fig. 1. The frequency of the three lowest order polaritonic branches (solid lines) and the ground photonic mode c_1 (dotted line) supported by the MQW-MC uniform system, with perfect dielectric mirrors, as a function of k_x. The geometry of the system is shown in the insert. The circles correspond to the lower and upper ICP branches calculated neglecting the presence of the intrasubband plasmons. The behavior of the above mentioned branches predicted by a well known two-oscillator model is also presented (crosses). The calculations have been performed for the system with $\omega_{\rm c1}(k_x = 0) = \omega_p = 0.4\ \omega_{\rm IT}$.

[1] A. C. Tselis and J. J. Quinn, Phys. Rev. B **29**, 3318 (1984).
[2] D. Dini, R. Kohler, A. Tredicucci, G. Biasiol, and L. Sorba, Phys. Rev. Lett. **90**, 116401 (2003).
[3] G. Günter *et al.* Nature **458**, 157 (2009).
[4] M. Załużny and C. Nalewajko, Phys. Rev. B **59**, 13043 (1999).
[5] M. Załużny and W. Zietkowski (to be published).
[6] V. Agranovich, H. Benisty and C. Weisbuch, Solid. Stat. Commun. **102**, 631 (1997).

Local modes in structures with multicomponent plasma

A.V.Chaplik

Institute of Semiconductor Physics, Novosibirsk, 630090, Russia

There exists a tight analogy between electron and plasmon spectra of crystals in the sense of influence of geometric defects. For example, a free surface results in formation of the Tamm states for electrons and the surface plasmon ("sqrt 2 – mode") provided mobile carriers in the bulk are available. If the Tamm band is not fully occupied a two-component plasma system arises that contains 2D and 3D plasmas. Yet another example of such a symbiosis of 2D and 3D plasmas is topological insulator with doping in the bulk.

In the first part of the present talk surface plasma oscillations are considered in such "2D + 3D" structure. It is shown that three regions of the dispersion law exist (with allowing for the retardation effects): linear dependence of plasmon frequency on the wave vector **k** for very small **k**, nearly linear dispersion for intermediate values of the wave vector (these two regions correspond to polaritons) and the third region (large **k**) gives the "shifted" 2D plasmon : const + sqrt **k**.

The second part deals with multilayer and lateral superlattices (SL) having one defective element meaning by that one layer or one quantum wire (for the case of lateral superlattice) with different value of the effective mass or electron concentration. This problem allows exact analytical solution with the aid of generating function for electrostatic potentials in the layers of multilayer SL or in the quantum wires of a lateral SL. As one could expect the local mode exists above the top of the plasmon band only if the carrier concentration in the defective layer exceeds the concentration in the regular layers. Its frequency is given by a simple analytical expression for multilayer SL whereas for lateral SL of quantum wires the local mode frequency is defined by a transcendental equation derived in the present work.

MoP42

Universality in condensation of exciton-polaritons

Michał Matuszewski and Emilia Witkowska

Instytut Fizyki Polskiej Akademii Nauk, Al. Lotników 32/46, 02-668 Warsaw, Poland

Phase transitions of second order taking place on a finite timescale exhibit a transition from adiabaticity to nonadiabaticity. Such phase transitions can lead to random formation of topological defects if symmetry is broken at the same time, as shown in numerous models ranging from the dynamics of the early Universe, superconductors, to liquid crystals. This process is described by the Kibble-Zurek mechanism which provides power-law scalings due to the underlying universality. We consider the condensation of exciton-polaritons, which is an example of an uncommon phase transtion, in which the transition connects an intrinsically nonequlilbrium state to a quasi-equilibrium state. We show that this process can lead to the formation of domains of polaritons and uncondensed excitons, and demonstrate scaling laws that give an estimate for the number of created defects.

[1] M. Matuszewski and E. Witkowska, arXiv:1212.0805.

The effect of magnetic field on the emission from exciton polaritons in semiconductor microcavity

B. Piętka, D. Zygmunt, J. Szczytko, J. Łusakowski
Institut of Experimental Physics, Faculty of Physics, University of Warsaw, Poland

P. Zięba, I. Tralle
Rzeszów University, Institute of Physisc, Mathematics & Natural Science Departement, Rzeszów, Poland

F. Morier-Genoud, B. Deveaud
Ecole Polytechnique Fédérale de Lausanne (EPFL), Lausanne, Switzerland

Exciton – polaritons in semiconductor microcavities attracted worldwide interest due to their potential in polariton based devices, possibility to create Bose-Einstein condensate and formation of a superfluid state with zero viscosity with many spectacular properties. These half-matter half-light quasi-particles, are composed of photon confined in microcavity and exciton resonance in quantum well coupled by strong interaction. The interaction modifies the dispersion of both resonances leading to two, upper (UP) and lower (LP), polariton branches of particular shape. The occupation of polaritons along the dispersion is governed by scattering with acoustic phonons leading to the thermal distribution (in a linear regime) and the polariton-polariton interactions leading to massive occupation of ground state with zero momentum (in a non-linear regime). The excitonic reservoir that supplies polaritons to the system is directly related to the number of particles in the final state.

In this study we use external magnetic field to influence the excitonic part of polaritons. The modification of the excitonic state close to zero momentum influence directly the LP and UP branches and with high momentum is modifying significantly the excitonic reservoir. The sample consists of a GaAs lambda microcavity sandwiched between two DBR AlAs/GaAs with one 8nm thick InGaAs quantum well. The polariton population is created non-resonantly. The sample is placed in a magnetic filed up to 5T at the cold finger of a cryostat in 4.5K. We image the full dispersion of LP and UP and we trace the evolution of energy, intensity and width of the emission lines in magnetic field.

We observe a strong influence of the magnetic field on the optical response of microcavity polaritons. First, we observe a global increase of the emission intensity showing that the relaxation from the excitonic reservoir towards polariton branches is enhanced. Second, the distribution of polaritons along the dispersion gets modified leading to the magnetically induced bottleneck effect. The shift in energy and Zeeman splitting are typical for the GaAs/GaInAs system and we describe it by a theoretical model of exciton in magnetic field coupled to photonic resonance in a cavity. We take into account the diamagnetic shift of excitons, cyclotron energy and the Zeeman splitting. The comparison between our theoretical model and experimental results gives us directly the measure of exciton oscillator strength modification in magnetic field. Moreover, we observe that the width of the emission lines is modified in magnetic field. The lines become narrower or broader depending on momentum and magnetic field value. We discuss this effect in terms of motional narrowing effect and possible magnetic field influence.

This work was supported by the Ministry of Higher Education grant 2011/01/D/ST7/04088.

MoP44

Optical control of vortex-antivortex lattices of polariton quantum fluids

D. Ballarini[1,2], R. Hivet[3], E. Cancellieri[3,4], F. M. Marchetti[4], M. H. Szymanska[5], C. Ciuti[6], E. Giacobino[3], D. Sanvitto[1,2], A. Bramati[3]

[1] Istituto Italiano di Tecnologia, IIT-Lecce, Via Barsanti, 73010 Lecce, Italy.
[2] NNL, Istituto Nanoscienze - CNR, Via Arnesano, 73100 Lecce, Italy.
[3]Laboratoire Kastler Brossel, UPMC-Paris6, École Normale Supérieure et CNRS, France
[4]Fìsica Teòrica de la Materia Condensada, Universidad Autònoma de Madrid, Madrid, Spain
[5]Department of Physics, University of Warwick, Coventry, United Kingdom
[6]Laboratoire Matériaux et Phénomènes Quantiques, Université Paris Diderot et CNRS, France

In quantum fluids, such as liquid helium and atomic Bose-Einstein condensates, vortex lattices have been observed as a consequence of an externally induced rotation [1]. The generation of vortex-antivortex (AV) lattices with total angular momentum L=0 has instead been observed only recently in a solid state system: exciton-polaritons in semiconductor microcavities under non resonant excitation [2]. Here we report on the coherent generation of polariton quantum fluids which create lattices of AV pairs, allowing for a complete control over the size and shape of the lattice geometry. Moreover, the true interacting effect of a condensate of polariton is revealed once the density is sufficiently high to allow for superfluid flow.
Exciton-polaritons are bosonic quasi-particles formed by the strong coupling between exciton and photon, which have shown to behave as a macroscopic quantum state both under resonant and non-resonant excitation. In particular, resonant excitation allowed for the observation and control of the flow of AV pairs, hydro-dynamically generated by artificial defects [3]. Extending these techniques, we have been able to study the formation of triangular and squared lattices of AV pairs under resonant excitation, demonstrating the existence of a power threshold above which the AV lattice disappears due to the strong interactions between polaritons (as shown in Fig.1). Below this threshold, the size of the unit cell is controlled by changing the energy of the excitation laser beam. Moreover, thanks to the out-of-equilibrium nature of polariton condensation, we have explored the formation process of this kind of topological excitations, and their organization in ordered structures, with a time resolution of few picoseconds.

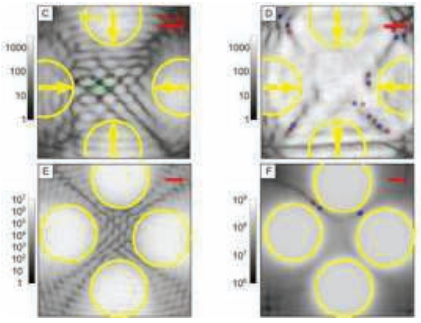

Figure 1. Four-pumps setup in the low power regime (C) and in the high power regime (D). A k=0.78μm^{-1} square lattice of vortex-antivortex pairs is formed in C and disappears in D. This nonlinear behaviour is due to the strong polariton-polariton interactions and it is correctly predicted by simulation based on the Gross-Pitaevskii formalism. E-F: Theoretical simulations run under the same conditions as in panels C and D, respectively.

[1] Yarmchuk et al, Phys. Rev. Lett. **43**, 214 (1979); Fetter et al, Rev. Mod. Phys. **81**, 647 (2009).
[2] Tosi et al, Nature Communications **3**, 1243 (2012).
[3] Sanvitto et al., Nature Photonics **5**, 610 (2011); G. Nardin et al., Nature Phys. **7**, 635 (2011).

Towards exciton polaritons at telecommunication wavelengths in GaAs-based microcavities

M. Pieczarka [1], P. Podemski [1], A. Musiał [1], K. Ryczko [1], A. Mika [1], M. Kozub [1], G. Sęk [1], J. Misiewicz [1], F. Langer [2], A. Forchel [2], S. Höfling [2], M. Kamp [2]

[1] *Institute of Physics, Wrocław University of Technology, 50-370 Wrocław, Poland*
[2] *Technische Physik, Physikalisches Institut, Universität Würzburg & Wilhelm Conrad Röntgen-Center for Complex Material, Am Hubland, D-97074 Würzburg, Germany*

Exciton polaritons are quasi particles resulting from a strong light-matter interaction between excitons and photons inside a high quality semiconductor microcavity. Their bosonic character and possible Bose-Einstein condensation give the opportunity to realize inversion-free emitter of coherent light which exhibits ultra-low threshold power.

Up to now, GaAs-based microcavities offered high optical quality with emission in the spectral range convenient for handling spectroscopic experiments employing standard and highly efficient Si-based detectors. In order to implement polariton lasers in optical telecommunication there is a need to extend the emission wavelength of the polariton systems further into the near infrared spectral range. This is possible in GaAs-based systems with properly chosen quantum well (QW) material. Particularly, insertion of multi-alloys as (In, Ga)(As, N, Sb) is a promising solution, offering both the spectral shift into the target range of 1.3 – 1.55 μm and the possible simultaneous oscillator strength increase [1] desired for enhanced exciton – photonic mode coupling.

We present optical investigations of GaAs-based planar microresonators with embedded quantum wells designed for the near infrared range. Reflection measurements together with angle resolved photoluminescence along the wafer radius (corresponding to different detuning between the exciton and cavity mode energy due to the wedge along the radius) were performed. Polariton eigenmodes emission in structures with embedded InGaAs quantum wells at the record wavelength of 1 μm was obtained and preserved to high temperatures up to 160 K with anticipation to significantly higher temperatures. The Rabi splitting of the eigenmodes in the investigated structures is approximately 7 meV and remains almost constant with temperature and, moreover, it is comparable with the expected exciton binding energy implying the very strong coupling conditions [2]. The latter explains forming the exciton-polaritons at temperatures corresponding to thermal energies exceeding the dissociation energy of Coulomb correlated electron-hole pairs in a quantum well. Diluted-nitride-based structures were also grown to obtain emission wavelengths in the telecom range, i.e. 1.3 μm. Significant improvement of the optical quality of InGaNAs quantum wells was gained by addition of antimony, which acts both as a surfactant for incorporation of N atoms into the structure during the epitaxial growth and as a fifth element of the quinary alloy. There will be discussed the current status of the exciton-photon coupling regime in this kind of InGaNAs(Sb)/GaAs QWs placed inside AlAs/GaAs resonators together with the system limitations and its possible future improvements.

[1] K. Ryczko, G. Sęk, J. Misiewicz, F. Langer, S. Höfling, and M. Kamp, J. Appl. Phys. **111**, 123503 (2012).
[2] J. B. Khurgin, Solid State Comm., **117**, 307 (2001)

Theory of 2D photon echo spectroscopy on quantum well intersubband dynamics

Thi Uyen-Khanh Dang[1], and Marten Richter[1]

[1] *Institut für Theoretische Physik, Nichtlineare Optik und Quantenelektronik, Technische Universität Berlin, Hardenbergstr. 36 EW 7-1, 10623 Berlin, Germany*

During the last decade coherent two dimensional spectroscopy, such as 2D photon echo, became an advanced tool for investigating correlations in semiconductors and in coupled pigments in the visible spectral range [1, 2, 3, 4]. Advances of the experimental techniques in IR and THz range suggest that an application of the 2D photon echo to the intra- and intersubband dynamics of quantum wells is possible[5]. We present a theoretical non-Markovian study of intra- and intersubband relaxation in quantum wells in the low density limit dominated by longitudinal electron-phonon coupling. The theoretical framework is used to calculate the 2D photon echo spectrum for intersubband transitions of a quantum well.

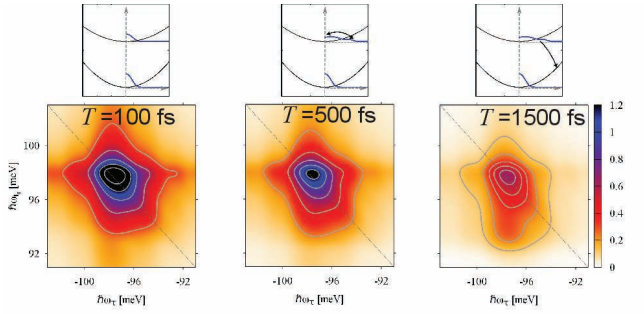

Figure 1: Calculated 2D photon echo spectra for different delay times T. Above the stepwise phonon induced density relaxation is sketched leading to the asymmetric 2D spectra .

The simulated signal is compared to the electronic density relaxation, where a stepwise relaxation through LO-phonon scattering to the minimum of the lower subband occurs. We identify the spectral signatures of the relaxation in the 2D photon echo, which are visible as an increasing asymmetry in the spectrum. Furthermore certain quantum pathways attributed to the intersubband relaxation can be pointed out, which have no equivalent in the visible. [6]

[1] X. Dai, A. D. Bristow, D. Karaiskaj, and S. T. Cundiff, Phys. Rev. A **82**, 052503 (2010).
[2] D. Karaiskaj, A. D. Bristow, L. Yang, X. Dai, R. P. Mirin, S. Mukamel, and S. T. Cundiff, Phys. Rev. Lett. **104**, 117401 (2010).
[3] G. Moody, M. E. Siemens, A. D. Bristow, X. Dai, D. Karaiskaj, A. S. Bracker, D. Gammon, and S. T. Cundiff, Phys. Rev. B **83**, 115324 (2011).
[4] T. Brixner, T. Mančal, I. V. Stiopkin, and G. R. Fleming, J. Chem. Phys. **121**, 4221–4236 (2004).
[5] W. Kuehn, K. Reimann, M. Woerner, and T. Elsaesser, J.Chem. Phys. **130**, 164503 (2009).
[6] T. U.-K. Dang, C. Weber, S. Eiser, A. Knorr, and M. Richter, Phys. Rev. B **86**, 155306 (2012).

Quantum plasmonics: strong-coupling between quantum emitters and surface plasmon polaritons

A. Gonzalez-Tudela[1], P.A. Huidobro[1], L. Martín-Moreno[2], FJ. García-Vidal[1], C. Tejedor[1]

[1] *Física Teórica de la Materia Condensada, Universidad Autónoma de Madrid, 28049, Madrid, Spain*
[2] *Instituto de Ciencia de Materiales de Aragón and Departamento de Física de la Materia Condensada, CSIC-Universidad de Zaragoza, E-50009, Zaragoza, Spain*

Propagating surface plasmon polaritons (SPPs) are well-known to have both a subwavelength light confinement and long propagation lengths [1]. Experimental evidence of the existence of Strong-Coupling(SC) between Quantum Emitters (QEs) and two-dimensional (2D) SPPs metallic systems [2], has not been accompanied by any rigorous theoretical interpretation.
We present a fully quantum mechanical description [3] of SPPs coupled to either one or many QEs in terms of a master equation for the density matrix containing both SPP's and excitstions of the QE's.
We start with single QE case determining the coupling to SPP's in a 2D geometry without the use of any fitting. We explore the parameters (lifetime, separation between QE and the surface, …) in which this SC regime could emerge. In this case, our main result is that SC appears when the SPP dispersion relation is extremely flat and coexisting with strong dissipation at the metal.
Then we study an ensemble of N QE's (Fig. 1) which requires the introduction of a collective mode for the excitations of the QE's. The main novelty of it resides in the fact that each QE contributes to the collective mode depending on its distance to the metallic surface. We incorporate the presence of dephasing and excitation mechanisms into the theoretical framework in order to be as close as possible to the experimental situation. Our formalism is able to reveal the key physical mechanisms that explain the reported phenomenology and also to determine the physical parameters that optimize the strong coupling (Fig. 2) [3].
Finally, we make predictions for experiments that could determine unambiguously, quantum effects. In particular, we show that coherent pumping of the SPP's with a well defined momentum produces a measurable second order coherence function $g^{(2)}(0)<1$ (Fig. 3) [3].

[1] T. W. Ebbesen *et al*, Physics Today **5**, 44 (2008).
[2] J. Bellessa *et al*, PRL. **93**, 036404 (2004), P. Vasa *et al*, PRL **101**, 16801 (2008). T. K. Hakala *et al* PRL. 103, 053602 (2009)
[3] A. Gonzalez-Tudela *et al,* PRL in press.

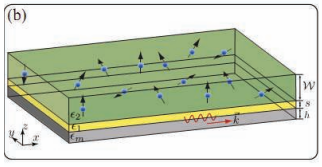

Fig. 1

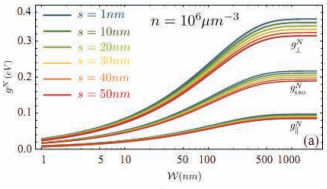

Fig. 2

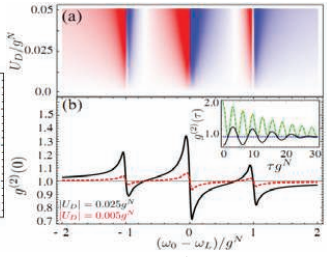

Fig. 3

Spin properties of bright polariton solitons in a semiconductor microcavity : The effect of polariton polarisation multistability

M. Sich [1], F. Fras [1], A. Gorbach [2], R. Hartley [2], E. A. Cerda-Mendez [3], K. Biermann [3], R. Hey [3], P. Santos [3], M. S. Skolnick [1], D. V. Skryabin [2], D. N. Krizhanovskii [1]

[1] *Department of Physics and Astronomy,University of Sheffield UK*
[2] *Department of Physics, University of Bath UK*
[3] *Paul-Drude-Institut, Berlin Germany*

Solitons are localised nondiffractive wavepackets, which can occur in a variety of non-linear systems. Light only solitons were observed in optical fibers and lasers, whereas matter only solitons are realised in cold atom systems. Recently, hybrid light-matter dissipative solitons were reported in strongly coupled semi-conductor microcavities[1]. These structures, where strong exciton-photon coupling results in the formation of 2D polaritons, have already demonstrated rich phenomena such as bistability, superfluidity and nonequilibrium condensation.

A notable specific feature of exciton polaritons arises from the fact that polaritons with parallel spins repel, while polaritons with opposite spins attract. Such spin anisotropy leads to polarisation multistability[2] where for a linearly polarized pumping laser the internal polariton field can be polarized either σ^+, σ^- circular or linear. The polariton spin multistability combined with the the fast picosecond response of bright solitons could also find applications in all-optical digital information processing.

Fundamentally, the soliton formation originates from the coexistence of pump bistability and parametric instability. In our experiment we use a CW pump to drive the system into the required conditions, and a ps-pulsed writing beam to trigger on demand the solitons[1].

Here we report the spin behavior of polariton bright solitons (see Fig. 1). Under a circularly polarised pump only soliton with a co-circular polarisation can be excited. This complete determination of the soliton spin state by the pump polarisation is consistent with spin conservative polariton-polariton scattering. For the case of a linearly polarised pump, the soliton spin state is conditional on the writing beam polarisation :

- $\sigma^{+(-)}$ solitons are turned on by a circular $\sigma^{+(-)}$ writing beam. The conversion of the linear polarisation of the pump to a circularly polarized soliton directly arises from the pump polarisation multistability, and opens the way for switch engineering with solitonic systems.
- With a linear writing beam, the solitons are found to be unpolarized. This could result either from a stochastic polarisation of the solitons pulse to pulse, or from the mixed nature of the soliton state. A statistical analysis, supported by correlation measurements, confirms the latter interpretation.

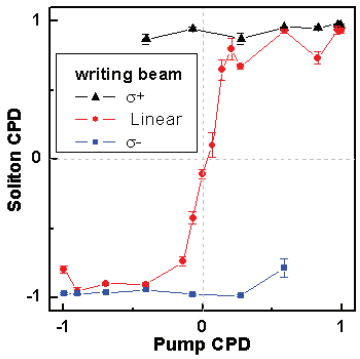

Fig 1. Soliton circular polairsation degree (CPD) as a function of pump circular polarisation degree recorded for the case of σ^+, σ^- and linearly polarized writting beam (triangles, squares and circles, respectively).

[1] M. Sich, D. N. Krizhanovskii *et al.*, Nature Photon. **6**, 50-55 (2012).
[2] N. A. Gippius, I. A. Shelykh *et al.*, Phys. Rev. Lett. **98**, 236401 (2007)

Nonequilibrium quantum cellular automata effect in a three-terminal triple quantum dot

Takashi Kobayashi, Takeshi Ota, Satoshi Sasaki and Koji Muraki

NTT Basic Research Laboratories, NTT Corporation, Atsugi 243-0198, Japan

Proposals on the exchange-only spin qubit [1] and electron spin entangler [2] have triggered growing interest in triple quantum dots (TQDs) for the exploration of new functionalities that exceed those of single and double quantum dots (DQDs). Recent studies indicate that TQDs are not only a promising candidate for applications to these quantum devices but also a platform for various correlation phenomena such as the quantum cellular automata (QCA) effect [3,4]. In this presentation, we report three-terminal transport measurements of a TQD. Detailed transport spectroscopy reveals a QCA effect, i.e., rearrangement of the ground-state charge configuration within the TQD that accompanies charge addition. Furthermore, we find that a transient charge configuration that occurs during transport through one channel dynamically induces a charge rearrangement and subsequent transport in the other channel, a phenomenon that can be termed a nonequilibrium QCA effect.

The TQD was defined in a GaAs/AlGaAs heterostructure by Ti/Au gates (Fig. 1). Each quantum dot (QD) has a separate electrical lead, which allows for the independent measurements of current I_L (I_R) through the left (right) DQD consisting of center and left (right) QDs and their sum $I_C = -I_L - I_R$. The upper panels in Fig. 2 show I_C measured in the few-electron regime for four different values of gate bias V_C, plotted as a function of gate biases V_R and V_L. Two sets of bias triangles, reminiscent of transport through DQDs, are observed. These triangles, which are separate at $V_C = -1.734$ and -1.814 V, merge to form complex features at intermediate V_C. The simultaneously measured I_R spectra (lower panels) allows us to clearly identify which DQD each bias triangle belongs to, revealing the existence of duplicated triangles at $V_C = -1.786$ V. Duplications of a bias triangles are explained by a QCA effect [3,4] as a consequence of the difference in the electrostatic coupling between the left and right QD pair and other pairs. Furthermore, we observe finite current flow outside the triangles. These signals originate from a QCA effect induced by transient occupations of the left (right) QD in the transport process through the left (right) DQD. Such a dynamic effect is specific to the nonequilibrium regime of three-terminal transport through a TQD.

[1] D. P. DiVincenzo et al., Nature **408**, 339 (2000).
[2] D. S. Saraga et al., Phys. Rev. Lett. **90**, 166803 (2003).
[3] L. Gaudreau et al., Phys. Rev. Lett. **97**, 036807 (2006).
[4] M. C. Rogge, R. J. Haug, Physica E **42**, 902-905 (2010).

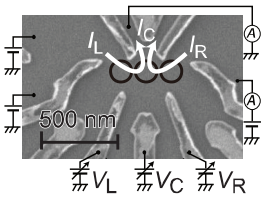

Figure 1: SEM image of the TQD sample.

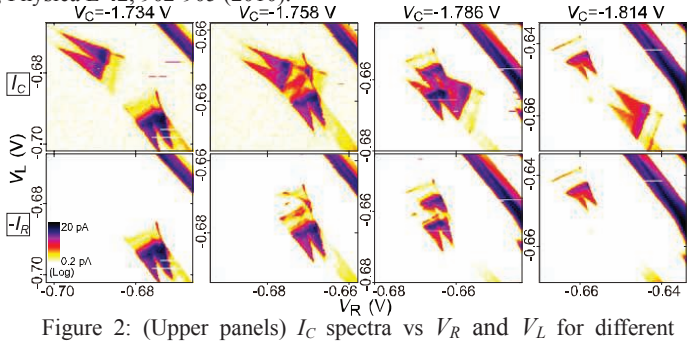

Figure 2: (Upper panels) I_C spectra vs V_R and V_L for different values of V_C. (Lower panels) simultaneously measured I_R spectra.

Transport via coherent state superpositions in triple quantum dots

M. Busl[1], G. Granger[2], L. Gaudreau[2,3], R. Sánchez[1], A. Kam[2], M. Pioro-Ladrière[3], S. A. Studenikin[2], P. Zawadzki[2], Z. R. Wasilewski[2], A. S. Sachrajda[2] and G. Platero[1]

[1] Instituto de Ciencia de Materiales de Madrid, CSIC, Cantoblanco, 28049 Madrid, Spain
[2] National Research Council, 1200 Montreal Road, Ottawa, Ontario, K1A 0R6 Canada
[3]Département de Physique, Université Sherbrooke, Sherbrooke, Québec J1K 2R1, Canada.

Spin qubits based on interacting spins in double quantum dots have been demonstrated successfully. Readout of the qubit state involves a conversion of spin to charge information, which is universally achieved by taking advantage of a spin blockade (SB) phenomenon resulting from Pauli's exclusion principle. SB manifests itself as a rectifier where current flows freely in one direction, but is blockaded in the other [1]. The blockade is found to be not perfect at zero magnetic field due to a mixing of singlet and triplet states in a field gradient resulting from the hyperfine interactions. These leakage currents are dramatically suppressed when a small external field splits off the triplet states from the singlet one. At present, more complex spin qubit circuits such as triple quantum dots are being developed. Here we show, both experimentally and theoretically, that in a linear triple dot SB becomes bipolar with current strongly suppressed in both bias directions and also that a new quantum coherent mechanism becomes relevant. In this mechanism, charge is transferred non intuitively via coherent states from one end of the linear triple dot circuit to the other, without involving the centre site [2]. We show that current only flows through the triple quantum dot when four configurations are degenerate, i.e. at quadruple points (QP). First, we focus on a QP where configurations of four and five electrons are degenerate. When a bias is applied in a magnetic field beyond ~10mT 'bipolar' SB is observed where current is suppressed in both bias directions. As the field is reduced to zero, SB leakage resonances are observed within the transport region. Of special interest are two very sharp resonances (marked as L-R in the figure) which correspond to alignment of states in the left and right dot but not in the centre and which result from a purely quantum coherent effect: electrons occupy states that involve their transference from one extreme to the other without ever visiting the centre. Such states have been invoked theoretically for possible applications such as spin bussing or quantum rectification. Further, we analyse another QP where configurations of two and three electrons are degenerate.

[1] K. Ono , D. G. Austing ,Y. Tokura and S. Tarucha, Science, **297**, 5585, (2002).
[2] M. Busl, et al, Nature Nanotechnology, in press. doi:10.1038/nnano.2013.7.

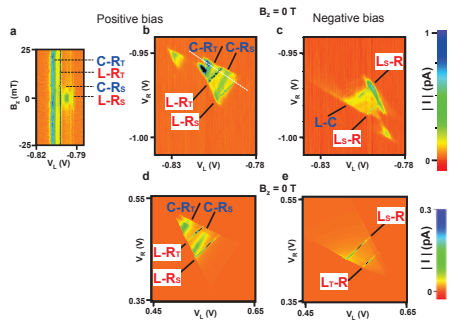

Figure 1. Leakage current through the TQD at quadruple points 5 and 6 for zero B. a) I(B) measured with a bias of 0.5 mV by sweeping $\mathbf{V}_L$ and $\mathbf{V}_R$ along the white dashed line in b). The dotted lines indicate the positions of the various resonances b–e), Results for a 0.5 mV bias of either polarity. Both for positive (b,d) and negative (c,e) bias and for experimental (b,c) and theoretical (d,e) results. One can clearly distinguish resonance lines with two different slopes: the L-R resonance lines, where (2,1,1) and (1,1,2) states are on resonance, and the steeper C-R resonance lines that occur when the energy of states (2,1,1) and (2,0,2) are aligned.

Two-path Transport Measurements with Bias Dependence on a Triple Quantum Dot

M. Kotzian[1], M.C. Rogge[1], K. Roszak[2], and R.J. Haug[1]

[1] *Institut fuer Festkoerperphysik, Leibniz Universitaet Hannover, Appelstrasse 2, 30167 Hannover, Germany*

[2] *Institute of Physics, Wroclaw University of Technology, 50-370 Wroclaw, Poland*

We present transport measurements on a lateral triple quantum dot with a star-like geometry and one lead attached to each dot. [1]

Technical and scientific improvement allow the fabrication of triple quantum dots and their detailed analysis. [2] The research on triple quantum dots is motivated by fundamental physics and by the fact that it can work as a single qubit. [3] It also is the smallest system with quantum dots being part of a qubit chain, which are needed for quantum computers.

Our sample design allows to simultaneously measure the conductance along two different paths with two quantum dots in each path. The structure is made with local anodic oxidation by AFM on a GaAs/AlGaAs heterostructure. By controlling the potentials via the four gates of the device triple points with two dots in resonance and quadruple points with all three dots in resonance can be established. [4,5] Using two of the leads as source contacts and one lead as a drain contact, signatures of three dots can be detected in both transport paths. This setup also provides the possibility of applying different bias voltages to the sources of the two transport paths and detecting excited states of the dots. Transport measurements in one path while varying the source-drain voltage on the other path show interesting features and prove the interaction between the transport paths. The measurement result is compared with a simulation of the electrostatics of the triple dot system.

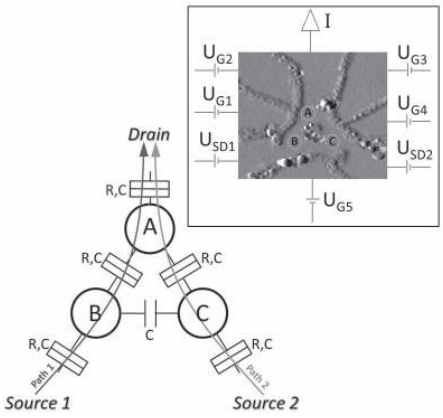

Figure 1: Schematic of the triple dot setup. Each of the dots is coupled to the other two and to one lead via tunneling barriers. The coupling between Dot B and C is of capacitive nature only.
Insert: AFM image of the triple dot structure defined by oxide lines. The applied gate voltages are labled U_{G1} - U_{G5} and the bias voltages U_{SD1} and U_{SD2}.

[1] M. C. Rogge, R. J. Haug, Phys. Rev. B **77**, 193306 (2008).
[2] D. Schrer, et al., Phys. Rev. B **76**, 075306 (2007).
[3] P. Hawrylak, M. Korkusinski, Solid State Comm. **136** (2005), pp. 508-512.
[4] L. Gaudreau, et al., PRL **97**, 036807 (2006).
[5] M. C. Rogge, R. J. Haug, New Journal of Physics **11**, 113037 (2009).

MoP52

MAGNETICAL CONTROL OF SPIN QUBITS IN QUANTUM WIRE

C. Kenfack Sadem [1,2], A. J.Fotué[1], L. C. FAI[1], M. TCHOFFO[1], R. M. Keumo Tsiaze[1] , J. E. Danga[1], and J. T. DIFFO[1].

1. University of Dschang, Faculty of Science, Department of Physics, Mesoscopic and Multilayer Structure Laboratory , Cameroon. Po Box: 67 Dschang - Cameroon
2. International Chair in Mathematical Physics and Applications, Univ. of Abomey-Calavi,Cotonou, Benin.
Email Address: kevinsadem@yahoo.fr

Abstract

The problem of control stimulates the analysis of qubit states in two levels system under the control of electromagnetic field. The ability to control the quantum state of a single electron spin in a quantum wire is at the heart of recent developments towards a scalable spin-based quantum computer. We investigated the influence of oscillating electromagnetic radiation field and the frequency of the parabolic confinement on a qubit. We compute the electron energy using supersymetry and, with the aid of Rotating Wave Approximation (RWA) we derived transition probability. For some values of the confinement, the transition probability becomes the Landau-Zener probability. It may also be seen that the high degrees of confinement (or high magnetic field) lead to an enhancement in the transition probability.

Keywords: Qubit transitions, electromagnetic field, quantum wire, transition probability and RWA.

Initialization of multiple quantum spins with non-equilibrium bias

Yasuhiro Tokura[1,2] and Toshihiro Kubo[1]

[1] *Graduate School of Pure and Applied Sciences, University of Tsukuba*
[2] *NTT Basic Research Laboratories, NTT Corporation*

Pauli spin blockade (P-SB) is one of the important phenomena to have a well-defined electron spin configurations with relatively easy setups and low-magnetic field.[1] The finite applied bias is essential to establish high spin states in coupled quantum dots (QDs), which is signatured by the suppression of the current through the series double QDs. P-SB is used in various experiments for accurate initialization and detection of the electron spins.[2, 3] Extension of the number of electron spins more than two is a critical step for the ‘scalable’ system for quantum information processing.

The purpose of this work is to theoretically argue the possibility of this direction. There are two ways to extend ordinary P-SB with two electrons and two QDs, which we call (1,1) P-SB, to three QD system:

- (2,1) configuration, where two QDs, QD1 and QD2, in the higher bias side and single QD, QD0, in the lower bias side, and there are tunnel couplings between QD1-QD0 and QD2-QD0 (Fig.1(a)).
- (1,2) configuration, where one QD, QD0, in the higher bias side and two QDs, QD1 and QD2, in the lower bias side, and there are tunnel couplings between QD0-QD1 and QD0-QD2 (Fig.2(b)).

In both configurations, we disregard the direct tunneling between QD1 and QD2. One electron transport in (2,1) configuration had been studied, and shows strong current suppression by the effect of coherent population trapping (CTP).[4] Here we found strong current suppression for two[5] and three electron states, however, in contrast to the conventional (1,1) P-SB, the spin state is mixed state because of CTP. In contrast, (1,2) configuration with three electrons shows current suppression with forming quadruplet spin dark state. We argue the level energy dependence of the leakage current and spin purity to compare recent experiments. *Part of this work is supported by Funding Program for World-Leading Innovative R&D on Science and Technology (FIRST).*

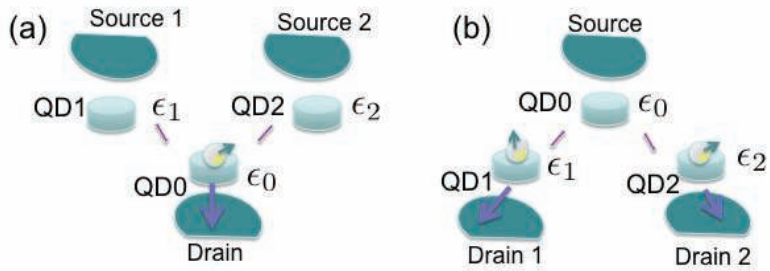

Fig.1 (a) Schematics of (2-1) P-SB, (b) (1-2) P-SB

[1] K. Ono, D. G. Austing, Y. Tokura, S. Tarucha, Science, **297**, 1313 (2002).
[2] F. H. L. Koppens, *et al.*, Nature **442**, 766 (2006).
[3] M. Pioro-Ladriere, *et al.*, Nature Physics **4**, 776 (2008).
[4] B. Michaelis, C. Emary, and C. W. J. Beenakker, Europhys. Lett., **73**, 677 (2006).
[5] C. Pöltl, C. Emary, and T. Brandes, Phys. Rev. B 80, 115313 (2009).

MoP54

The role of cotunneling processes in Andreev transport through quantum dot coupled to two ferromagnetic leads and one superconducting electrode

Piotr Trocha[1], **Ireneusz Weymann**[1]

[1] *Adam Mickiewicz University, 61-614 Poznań, Poland*

Quantum dot attached to one superconducting electrode and two normal leads allows to study nonlocal Andreev reflection phenomenon. Such a phenomenon has already been reported experimentally in hybrid structures consisting of two normal metal (or ferromagnetic) leads connected via tunnel barriers or point contacts to one common superconducting electrode. [1, 2, 3] In contrast to the direct Andreev reflection, where the hole is reflected back to the electrode from which the incoming electron originates, in nonlocal processes the hole is reflected into a second, spatially separated electrode. Recently, Cooper pair splitting has also been observed in quantum dot systems. [4, 5]

Here, we investigate local and nonlocal Andreev transport through the system consisting of single-level quantum dot coupled to one superconducting electrode and two ferromagnetic leads. We restrict our model to collinear magnetic configurations, i.e., parallel or antiparallel. To calculate basic transport characteristics like Andreev current, local and nonlocal conductance, we employ the real-time diagrammatic perturbation approach assuming weak tunnel coupling of the dot to the ferromagnetic leads. In turn, in the large superconducting gap limit the coupling to the superconductor can be arbitrary strong. The influence of cotunneling processes on the Coulomb blockade has been investigated.

[1] G. Deutscher and D. Feinberga, Appl. Phys. Lett. **76**, 487 (2000).
[2] D. Beckmann, H. B.Weber, and H. v. Löhneysen, Phys. Rev. Lett. **93**, 197003 (2004).
[3] S. Russo, M. Kroug, T. M. Klapwijk, and A. F. Morpurgo, Phys. Rev. Lett. **95**, 027002 (2005).
[4] L. Hofstetter, S. Csonka, J. Nygård, C. Schönenberger, Nature **462**, 960 (2009).
[5] L. G. Herrmann, F. Portier, P. Roche, A. Levy Yeyati, T. Kontos, C. Strunk, Phys. Rev. Lett. **104**, 026801 (2010).

Charge and spin Seebeck effects in hybrid quantum dot junctions

Karol Izydor Wysokiński

Institute of Physics, M. Curie-Skłodowska University, Radziszewskiego 10, Pl 20-031 Lublin, Poland

The study of thermoelectric transport in nanodevices is of theoretical and practical interest. Here we shall discuss two different devices. One consists of a molecule between two normal metallic electrodes and in the second case the device consists of the quantum dot placed between three electrodes: one normal metallic (N), other ferromagnetic (F) metal and the third superconducting (S). The main focus of the first model is to analyze strong coupling of charge and vibrational degrees of freedom, which may lead to effective attraction of electrons on a molecule. In this negative U model the pair tunneling is the main transport mechanism in the limit of weak coupling to the electrodes. In the second model due to the presence of ferromagnetic electrode the device is an efficient source of the pure spin current.

The molecule characterized by the negative effective charging energy $U<0$ has been modeled by the Anderson Hamiltonian. The electrical conductance, thermopower, and thermal conductance of the system have been calculated as a function of gate voltage in the weak coupling limit within the rate equation approach. In the linear regime the analytic formulas for the transport coefficients in the pair-dominated tunneling are presented. The effects found in the nonlinear transport include *inter alia* the rectification of the heat current. The sense of forward (reverse) direction, however, depends on the tuning parameter (distance from electron-hole symmetry point) and can be controlled by the gate voltage. We also discuss the quantization of the thermal conductance and the departures from the Wiedemann-Franz law.

The thermoelectric transport in the system composed of a quantum dot in contact with superconducting, ferromagnetic and normal metal electrodes can support pure spin current in the normal electrode. In the limit of a large superconducting gap and weak coupling between the dot and the electrodes we investigate the sub-gap charge and spin transport via Andreev mechanism using the standard master equation technique, which is known to be valid in the sequential tunneling regime. The Zeeman splitting of the dot level induces pure spin current in the ferromagnetic electrode under an appropriate bias. This opens a novel possibility to switch the spin current between two electrodes by electric means. The calculated spin and charge thermopower coefficients attain very large values, of the order of a few hundreds $\mu V\ K^{-1}$, and show similar dependences on the position of the on-dot energy level and temperature.

This work has been partially supported by the National Science Centre under the contract DEC-2011/01/B/ST3/04428

References:

1. **K. I. Wysokiński**
   Thermal transport of molecular junctions in the pair tunneling regime,
   Phys. Rev. B **82**, 115423 (2010).
2. **Karol I. Wysokiński,**
   Thermoelectric transport in the three terminal quantum dot,
   J. Phys. Condensed Matter **24,** 335303 (2012)

Counting statistics of single-electron capture by a dynamic quantum dot

L. Fricke[1], M. Wulf[1], B.Kaestner[1],V. Kashcheyevs[2], J. Timoshenko[2], P. Nazarov[2], F. Hohls[1], P. Mirovsky[1], B. Mackrodt[1], R. Dolata[1], T. Weimann[1], K. Pierz[1], H.W. Schumacher[1]

[1] *Physikalisch-Technische Bundesanstalt (PTB), Bundesallee 100, D-38116 Braunschweig, Germany*

[2] *Faculty of Physics and Mathematics, University of Latvia, Riga LV-1002, Latvia*

A renewed International System of Units (SI) strongly demands for a quantum-based current source relating the output current to the elementary charge e whose value will be fixed at redefinition [1]. A highly promising candidate for such a current source is the non-adiabatic single-electron pump [2, 3] exploiting a dynamic quantum dot forming out of a two-dimensional electron gas. Due to the dynamic tunnel barriers between the dot and the source/drain leads the dot can be driven by high frequencies since its population is not limited by tunneling constants. Recent measurements have qualified the pump accuracy to be better than 10^{-6} [4]. However, the exact initialization mechanism of these dynamic dots is still subject of current research.

Recently, a theoretical model of the probability of charge capture has been developed [5], including mainly three relevant energy scales for this process. These are the temperature (kT), the finite time scale for suppression of backtunneling (expressed by Γ_c) as well as the coupling of the rising source barrier to the energy levels of the quantum dot due to electrostatic cross talk (Δ_{ptb}). In the limit $\Gamma_c, \Delta_{ptb} \to 0$ the probability of charge capture follows a thermal distribution. In a second limit with $kT, \Gamma_c \to 0$, the previously predicted decay-cascade model [6] is reproduced.

To investigate these regimes and to identify the relevant processes in our samples, we combine such a dynamic quantum dot with highly-sensitive electrometers and perform counting measurements on the number of charges initialized on the dot and subsequently transferred to a measurement node. Using this architecture we are able to distinguish between these two limits and identify the decay-cascade regime as the dominating mechanism of charge capture in our sample [7]. Additionally, based on the relevant mechanism, we propose different strategies for further improvement.

Furthermore, an overview about the actual status of the self-referenced current source including an error-accounting scheme [8] will be given.

[1] 24th Resolution of the CGPM, available online via http://www.bipm.org/utils/common/pdf/24_CGPM_Resolutions.pdf.
[2] M. Blumenthal et al., Nature Physics **3**, 343 (2007).
[3] B. Kaestner et al., Phys. Rev. B **77**, 153301 (2008).
[4] S. Giblin et al., Nature Communications **3**, 930 (2012).
[5] V. Kashcheyevs, J. Timoshenko, Phys. Rev. Lett. **109**, 216801 (2012).
[6] V. Kashcheyevs, B. Kaestner, Phys. Rev. Lett. **104**, 186805 (2010).
[7] L. Fricke et al., Phys. Rev. Lett. accepted and arXiv:1211.1781.
[8] M. Wulf, Phys. Rev. B **87**, 035312 (2013).

Supercurrents in niobium-InSb nanowire Josephson junctions

R.S. Deacon[1], J. Sailer[2], A. Oiwa[2], T. Fuse[1], M.T. Deng[3], H.Q. Xu[3], S. Tarucha[2,4] and K. Ishibashi[1]

[1] Advanced Device Laboratory, RIKEN, Wako, Saitama 351-0198, Japan.
[2] The University of Tokyo, 7-3-1 Hongo, Bunkyo-ku, 113-8656, Japan.
[3]Division of Solid State Physics, Lund University, Box 118, S-221 00, Lund, Sweden.
[4]Center for Emergent Matter Science (CEMS), RIKEN, Wako, Saitama, 351-0198, Japan.

We will present preliminary results on the measurement of the supercurrent in Josephson junctions formed from InSb nanowires contacted with niobium source/drain leads. Our work is motivated by recent proposals for the realization of Majorana Fermions (MFs) in 1-D systems with strong spin-orbit interaction coupled to *s*-wave superconductors[1,2] and encouraging experimental results which hint at the detection of MFs[3-6]. We fabricate devices using both niobium deposited by electron beam evaporation and DC magnetron sputtering. Our devices show the signature of gate tunable switching current which persists to high magnetic fields (up to 3T). We are able to measure the ac-Josephson effect in this magnetic field range and observe the Shapiro step pattern. In addition we observe suppression and recovery of the switching current with increasing magnetic field indicating the influence of the Zeeman effect.

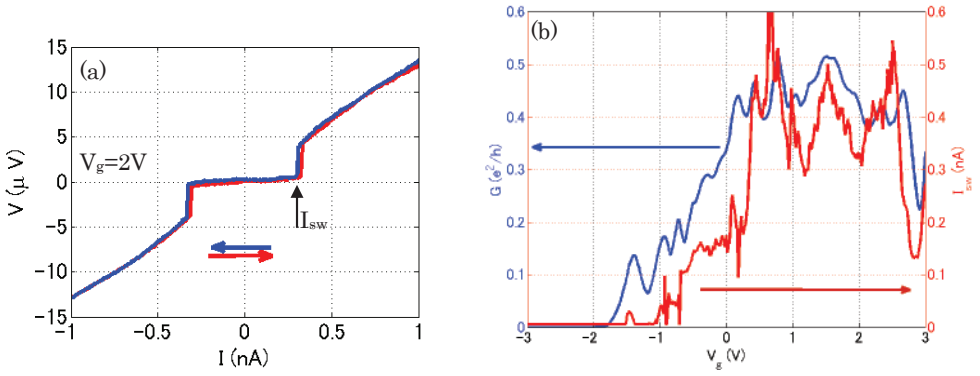

Figure (a) Example V-I trace showing the switching of the junction between supercurrent and normal branches. (b) Switching currents (red) and differential conductance (blue) measured as a function of the gate voltage.

[1] Y. Oreg *et al.*, Phys. Rev. Lett. 105, 177002 (2010)
[2] R. M. Lutchyn *et al.*, Phys. Rev. Lett. 105, 077001 (2010).
[3] V. Mourik *et al.*, Science 336, 1003 (2012)
[4] M. T. Deng *et al.*, Nano Lett. 12, 6414 (2012).
[5] L. P. Rokhinson *et al.*, Nature Physics, 8, 795 (2012).
[6] A. Das *et al.*, Nature Physics, 8, 887 (2012).

MoP58

Signature of Landau-Zener-Stückelberg interference in coherent charge oscillations of a one-electron double quantum dot

Takeshi Ota, Kenichi Hitachi and Koji Muraki

NTT Basic Research Laboratories, NTT Corporation, 3-1, Morinosato-Wakamiya, Atsugi, 243-0198, Japan

Recently, Landau-Zener (LZ) transitions have received renewed interest as an alternative approach to control single-qubit states. LZ transitions occur when a system is passed through an avoided crossing that arises from quantum mechanical coupling of two levels, where the transition probability is determined by the velocity, or the rate at which the Hamiltonian is varied. A single passage can serve as a coherent beam splitter for the incoming state. Successive sweeps through the avoided crossing back and forth induce multiple LZ transitions and thus interference between the superposition states generated on the incoming and outgoing passages. In analogy to optics, the final state also reflects the phase evolution between the two beam splitters. The effect, known as the Landau-Zener-Stückelberg (LZS) interference, has been demonstrated for superconductor charge and flux qubits [1] and semiconductor two-electron spin qubits [2].

Here we report the observation of LZS interference in coherent charge oscillations of a one-electron double quantum dot (DQD). The dot state is manipulated using high-frequency voltage pulses applied to the drain electrode and the charge state of the DQD is read out using nearby quantum point contact (QPC) charge sensor [Fig. 1(a)]. In order to achieve a nearly 50:50 beam splitter and thereby maximize the interference amplitude, the effective rise/fall time of the dot potential was controlled by tuning the dot-lead coupling. The QPC charge detection signal obtained in this way shows a characteristic oscillation pattern as a function of pulse duration and detuning ε, suggesting LZS interference [Fig. 1(b)]. The oscillations appear only for $\varepsilon > 0$, that is, when the system is passed though the resonance. By comparing experiment and numerical simulations, we show that there is a significant enhancement in the oscillation amplitude of the final state probability due to LZS interference. We also show that the LZS interference is relevant even without intentional pulse shaping and is thus inherent to charge qubits, whose anticrossing gap is comparable to the pulse rising/falling time.

[1] For example, S.N. Shevchenko, et al., Physics Reports 492, 1 (2010).

[2] J. R. Petta, et al., Science 327, 669 (2010).

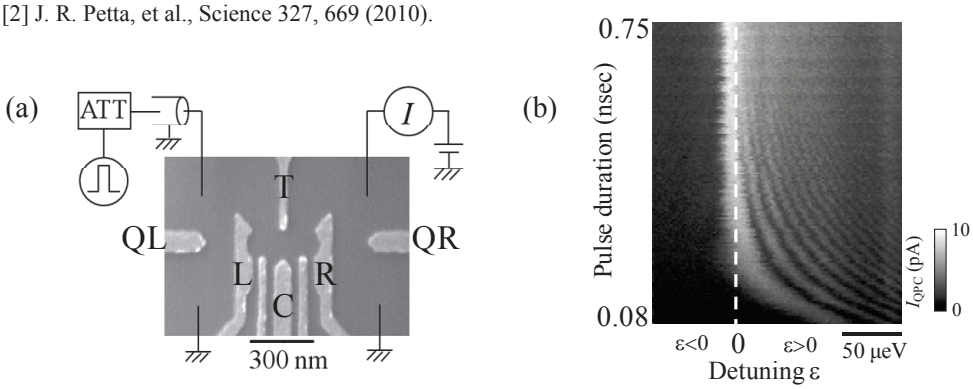

Fig. 1(a). Device structure and the experimental setup. The charge state of the DQD is measured by the QPC defined by the gates QR and R. (b) Pulse-induced QPC current I_{QPC} as a function of pulse duration and detuning ε.

Coherent electron transfer between distant quantum dots in a linear array

Floris R. Braakman[1], Pierre Barthelemy[1], Christian Reichl[2], Werner Wegscheider[2] and Lieven M. K. Vandersypen[2]

[1]*Kavli Institute of Nanoscience, Delft, The Netherlands*
[2]*ETH Zürich, Zürich, Switzerland*

Tunnel coupled quantum dots form the basis for electronic charge and spin qubits in semiconductors. The tunnel coupling gives rise to quantum coherent phenomena such as exchange oscillations of neighboring spins. However, tunnel coupling strength between non-neighbouring sites is negligible and it is therefore desirable to develop a form of long range coupling. In a linear array of three quantum dots, we demonstrate an effective tunnel coupling between the outer dots through virtual occupation of discrete levels in the center dot. The coupling strength depends strongly on the detuning between center and outer dot levels, in agreement with theoretical predictions. The observation of Landau-Zener-Stückelberg oscillations demonstrates the coherent nature of the coupling. The effective long-range tunnel coupling should also allow coherent exchange of remote spins.

Fano-interference in an optical transition from a neutral quantum dot to a correlated many-body state

F. Haupt[1], S. Smolka[1], M. Hanl[2], W. Wüster[1], J. Miguel-Sanchez[1], J. v. Delft[2] and A. Imamoglu[1]

[1] *Institute of Quantum Electronics - ETH Zürich, Wolfgang-Pauli-Strasse 16, 8093 Zürich, Switzerland*

[2] *Arnold Sommerfeld Center for Theoretical Physics, Ludwig-Maximilians-Universität München, D-80333 München, Germany*

The interaction between a local energy level and a continuum of states leads to fascinating quantum phenomena such as the Kondo effect [1] or Fano-type quantum interference. Here, we demonstrate a quantum interference between a discrete quantum dot (QD) energy level and a nearby Fermi reservoir (FR), that is modified by the scattering potential of the QD. [2] This interference is detected with resonant absorption measurements by tuning the neutral exciton (X^0) energy level with respect to the FR. [Fig. 1a)] We observe - in addition to the QD transition - an indirect transition, i.e. the generation of a hole in the quantum dot and an absorption of an electron in the FR. The line shapes show a pronounced asymmetry as well as broadening originating from the tunnel-coupling between dot and the FR. [Fig. 1b)] When the energy of the X^0 excitation is in the vicinity of or above the Fermi energy ε_F, the charge of the photo-excited QD hole cannot be fully screened by the optically excited electron and generates a scattering potential for the free electrons of the FR. [Fig. 1c)] This scattering potential modifies the wave-function of the FR and leads to a quench dynamics after absorption - a Fermi edge singularity. The experimental data are found to be in good agreement with theory using a numeric renormalization group model allowing us to determine the scattering potential strength. [3] The quantum interference between a QD and the FR is an important step to study the interplay between coherent laser excitation and an interacting many-body system.

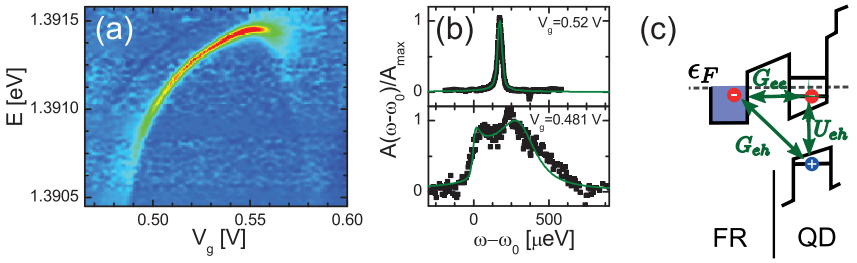

Figure 1: a) Absorption measurements as a function of applied gate voltage for the neutral exciton (X^0) transition from a strongly tunnel-coupled QD. [4] b) Representive absorption line shapes of the X^0 superimposed with our calculations (green curve). c) Schema depicts the effect of the scattering potentials in the sample structure (green arrows) between the QD and the FR electrons.

[1] C. Latta, F. Haupt, Nature **474**, 627 (2011).
[2] M. Heyl, S. Kehrein, Phys. Rev. B **85**, 155413 (2012).
[3] L. N. Oliveira, J.W. Wilkins, Phys. Rev. B **32**, 696 (1985).
[4] N. Kleemans, J. van Bree, Nature Physics **6**, 534-538 (2010).

Enhancement of thermoelectric efficiency in a quantum dot coupled to ferromagnetic electrodes due to Rashba spin-orbit coupling

Łukasz Karwacki[1], Piotr Trocha[1], and Józef Barnaś[1,2]

[1] *Faculty of Physics, Adam Mickiewicz University, 61-614 Poznań, Poland*
[2] *Institute of Molecular Physics, Polish Academy of Sciences, 60-179 Poznań, Poland*

Thermoelectric effects in spin-polarized transport through a quantum dot weakly coupled to two ferromagnetic leads via spin-conserving and Rashba-induced spin-nonconserving tunneling terms have been investigated theoretically by means of the non-equilibrium Green's function method. The Rashba term [1] leads to various interference phenomena, such as the Fano effect [2], which modify basic transport and electronic properties of the system.

We have analyzed spin-dependent transport through the system, especially such basic transport coefficients like conductance, heat conductance and thermopower. To evaluate the thermoelectric efficiency of the system, we have also calculated the dimensionless coefficient known as the figure of merit.

When the spin accumulation in the external leads becomes relevant, thermoelectric current leads to a spin voltage. Recently, this novel phenomenon has been observed experimentally in metallic magnets [3] and is referred to as the spin Seebeck effect. We have analyzed this effect by calculating spin counterparts of the transport coefficients mentioned above. Interplay between the Rashba-induced effective field and external magnetic field leads to enhancement of both charge and spin figures of merit, opening new possibilities for thermally-induced spin current generation.

[1] Q.-F. Sun, J. Wang and H. Guo, Phys. Rev. B **71**, 165310 (2005)
[2] P. Stefański, J. Phys.: Condens. Matter **22**, 505303 (2010),
[3] K. Uchida et al., Nature **455**, 778 (2008).

Determination of quantum dot parameters using quantum dot continuum transitions

Sandra Kuhn[1], **Andreas Knorr**[1] , **and Marten Richter**[1]

[1] *Institut für Theoretische Physik, Nichtlineare Optik und Quantenelektronik, Technische Universität Berlin, Hardenbergstrasse 36, 10623 Berlin, Germany*

A successful design of semiconductor quantum dot (QD) devices depends on the accuracy of the information about their structural properties [1]. We show, that spatial information about the bound QD states can be obtained by pump probe experiments [2] of optical transitions between bound QD states and continuum states [3].
The developed scheme to determine the spatial extension of bound states is applicable to self organized QDs embedded in bulk material and with modification also for QD wetting layer systems. In Fig. 1(a) interband and intraband transitions of a QD are illustrated.

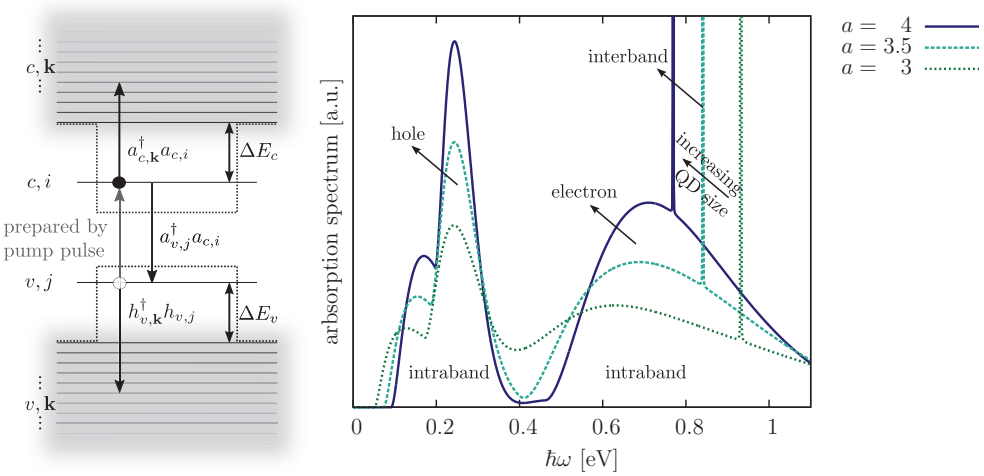

Figure 1: (a) Level scheme of the considered QD model. (b) Calculated absorption spectra for epitaxially grown InAs QD embedded in a GaAs bulk material and different QD sizes a for an excitation by the pump pulse of the ground exciton state.

We show theoretically that specific spectral information gained from pump probe experiments can be used to determine the spatial extension of bound states in QDs. Two steps are necessary: First, we separate the spectral contributions of electron, heavy hole and light hole intraband transitions of pump probe signals in frequency domain (Fig. 1(b)). Second, from the separated spectral contributions the absolute value of the corresponding intraband dipole moment can be obtained using analytical formulas. We show, that in first order approximation, the dipole moment is proportional to the derivative of the QD electron (hole) wave function in the wave number-space. This way, information about the spatial distribution of bound states can be obtained.

[1] C. Robert, C. Cornet et al., Phys. Rev. B **86**, 205316 (2012).
[2] F. Quochi, M. Dinu et al., Phys. Rev. B **67**, 235323 (2003).
[3] S. Sauvage, P. Boucaud et al., J. Appl. Phys. **82**, 3396 (1997).

Collective optical effects in multiple quantum dots

Anna Sitek[1,2], Andrei Manolescu[2], and Paweł Machnikowski[1]

[1] *Institute of Physics, Wrocław University of Technology, Wybrzeże Wyspiańskiego 27, 50-370 Wrocław, Poland*

[2] *School of Science and Engineering, Reykjavik University, Menntavegur 1, IS-101 Reykjavik, Iceland*

We study the effects resulting from the collective coupling of excitons residing in systems of two to four quantum dots to their radiative environment. The coupling to common photon reservoir leads to the appearance of rapidly decaying states and dark states which do not undergo radiative decoherence. The consequence of the co-existence of bright and optically inactive states is the vacuum-induced coherence effect which consists in a coherent excitation transfer from a bright state to the delocalized and decoherence-resistant one. In this presentation we specify the rapidly decaying states and amplitude combinations which form optically inactive superpositions, we also analyze the role of energy mismatch, coupling between the dots and dipole moments in the dynamics of excitons induced by collective coupling to the photon reservoir. We show that the destructive effect of the transition energy splitting can be overcome by an appropriate interplay of dipole moments which allows to observe perfectly stable states and thus spontaneous trapping of excitation in systems with technologically realistic energy mismatches even if the coupling between the systems does not exceed the transition energy difference by far [1].

Multiple quantum dots composed of two or more coupled quantum dots attract much attention due to the richness and complexity of their optical properties which have been manifested in many optical experiments [2]. One of the factors that affects the evolution of excitons confined in such structures is the collective coupling to the photon environment (superradiance) [3]. The investigation of these phenomena in quantum dot systems is essential for application of quantum information processing, since the dark superpositions do not undergo radiative decoherence and thus may be used for noiseless encoding of quantum information [4], while the short-living states show promise for optimization of lasers [5]. The collective effects are very sensitive to the homogeneity of the transition energy mismatches and may be destroyed in systems with energy splitting of the order of micro-electron-Volts which is below present technological feasibility. This effect may be considerably reduced by sufficiently strong coupling between the systems [6], but full stabilization of the collective effects in technologically realistic ensembles is possible only in systems with different dipole moments [1].

[1] A. Sitek, P. Machnikowski, Phys. Rev. B **86**, 205315 (2012).
[2] P. Borri *et al.*, Phys. Rev. Lett. **91**, 267401 (2003); C. Bardot *et al.*, Phys. Rev. B **72**, 035314 (2005); B. D. Gerardot *et al.*, Phys. Rev. Lett. **95**, 137403 (2005), D. F. Cesar *et al.*, Phys. Rev. B **72**, 195307 (2011).
[3] M. Scheibner *et al.*, Nat. Phys. **3**, 106 (2007).
[4] P. Zanardi, M. Rasetti, Phys. Rev. Lett. **79**, 3306 (1997); P. Zanardi, F. Rossi, Phys. Rev. Lett. **81**, 4752 (1998).
[5] A. A. Belyanin *et al.*, Laser Physics **13**, 61167 (2003); J. G Bohnet *et al.*, Nature **484**, 78 (2012).
[6] A. Sitek and P. Machnikowski, Phys. Rev. B **75**, 035328 (2007); Phys. Rev. B **80**, 115319 (2009); Phys. Rev. B **80**, 115301 (2009).

MoP64

Fine structures of triexcitons in single GaAlAs/AlAs quantum dots

M. Molas,[1,2*] A. A. L. Nicolet,[2] A. Babiński,[1] and M. Potemski[2]

[1] *Faculty of Physics, University of Warsaw, Hoża 69, PL 00-681 Warsaw, Poland*
[2] *Laboratoire National des Champs Magnétiques Intenses, CNRS-UJF-UPS-INSA, 25, avenue des Martyrs, 38042 Grenoble, France*

The electron-hole exchange interaction and anisotropy of the confinement potential of quantum dots (QDs) induce the fine structure splitting (FSS) of exciton (X) emission lines into two components which are usually linearly polarised in two perpendicular directions. The FSS of neutral excitons has been largely studied in the past providing valuable information on the electron-hole exchange interaction between carriers which occupy the ground-state conduction and valence band levels (*s*-shells). The FSS of the triexciton state (3X) which consists of two excitons in a singlet configuration on the *s*-shell and one exciton on the excited level (*p*-shell) was much less investigated, so far.

We report on polarization-sensitive studies of multiexcitonic emission from single GaAlAs/AlAs QDs. To test the attribution of the observed excitonic lines to a particular multiexcitonic configuration, the polarization-resolved single-photon correlation experiments were performed. Notably, the cascade recombination of a quadexciton (two electron-hole pairs in the singlet configuration on the *s*-shell, and two pairs in the singlet configuration on the *p*-shell) to the single exciton was observed [1]. With these experiments, the recombination lines due to neutral single- (X) and bi- (2X) exciton (energy range of the *s*-shell emission) and the emission due to tri- (3X) and quad- (4X) excitons (energy range of *p*-shell emission) have been identified.

The electron-hole exchange interaction of the unpaired exciton in the 3X state leads to the energy splitting (Δ_{3X}) similar to the splitting (Δ_X) of the neutral exciton. Investigating the polarization-resolved micro-photoluminescence, we measured both Δ_X and Δ_{3X} in more than twenty QDs. The Δ_{3X} can be observed as the splitting of the 4X→3X and/or 3X→2X emission lines. The polarization axes of two linearly polarized components of both exciton and triexciton were also studied. It was found that the alignment of polarization axes of X and 3X-split components is identical, with one of the axes being along the [110] crystallographic direction [2].

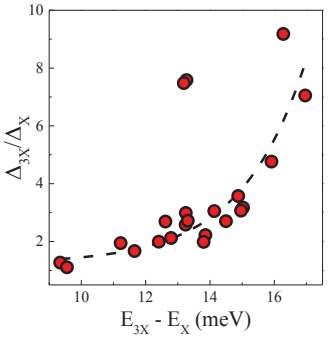

The ratio Δ_{3X}/Δ_X as a function of the energy separation between the 3X (*p*-shell) and the X (*s*-shell) emission lines. Dashed line is a guide to the eye.

It was found that the Δ_{3X} always exceeds Δ_X. As shown in the figure, the Δ_{3X}/Δ_X ratio increases monotonically with the energy separation (E_{3X}-E_X) between the 3X (*p*-shell) and X (*s*-shell) emission lines. This relationship can be understood in terms of different spatial extent of the *s*- and *p*-shell orbitals. This difference appears to be more pronounced for dots of small size (larger $E_{3X} - E_X$).

We believe that studies of both Δ_X and Δ_{3X} energy splitting can provide new and more precise information on QDs, revealing more details on electron-hole exchange interaction and the actual form of the confinement potential.

[1] Y. Arashida, Y. Ogawa, and F. Minami, Phys. Rev. B 84, 125309 (2011).
[2] M. Molas, K. Gołasa, B. Piętka, M. Potemski, and A. Babiński, Acta Phys. Pol. A 122, 988 (2012).

* corresponding author: maciej.molas@fuw.edu.pl

Aharonov-Bohm quantum rings in microcavities

A. M. Alexeev[1], **I. A. Shelykh**[2] **and M. E. Portnoi**[1]

[1] *School of Physics, University of Exeter, Stocker Road, Exeter EX4 4QL, UK*
[2] *Science Institute, University of Iceland, Dunhagi 3, IS-107, Reykjavik, Iceland*

Progress in nanolithography and epitaxial techniques has resulted in burgeoning developments in the fabrication of semiconductor nanostructures and optical microcavities. Cavity quantum electrodynamics addresses the interaction of an emitter embedded inside a microcavity with the cavity modes and the emission spectrum of the system. The luminescence spectrum of a microcavity coupled to a single quantum-dot-based emitter under incoherent continuous pumping has been studied extensively both theoretically and experimentally. This system possesses a rich spectrum, which maps transitions between quantized photon-dressed states of the light-matter coupling Hamiltonian.

There is a considerable current interest in non-simply-connected nanostructures, quantum rings, which have been obtained in various semiconductor systems [1-3]. The fascination in quantum rings is partially caused by a wide variety of purely quantum-mechanical effects, which are observed in ring-like nanostructures, including the celebrated Aharonov-Bohm effect resulting in magnetic-flux-dependent oscillations of various physical quantities. It has been shown that an external lateral electric field, which is known to reduce the ring symmetry and suppress the energy oscillations for the low-energy states, also modifies optical properties of the ring [4,5]. Namely, the application of a weak electric field leads to magneto-oscillations of frequency and the degree of polarization of optical transitions between the ground and first excited states which are typically in the THz range.

In the present work we examine a microcavity with an embedded quantum ring, which is pierced by a magnetic field and subjected to a lateral electric field. We calculate the luminescence spectrum of the system using the Lindblad master equation approach and demonstrate that it is strongly influenced by the pumping intensity and the quality factor of the cavity [6]. An additional degree of control can be achieved by changing the angle between the polarization plane of the pump and the external electric field. Optical properties of the considered system demonstrate a rich behavior which can be controlled by external electric and magnetic fields. These fields govern the electron spectrum and optical selection rules in a ring, which can be easily tuned to match the cavity modes.

[1] A. Lorke et al., Phys. Rev. Lett. **84**, 2223 (2000).
[2] E. Ribeiro et al., Phys. Rev. Lett. **92**, 126402 (2004).
[3] J.X. Chen et al., ACS Nano **3**, 173 (2009).
[4] A.M. Fischer, V.L. Campo, M.E. Portnoi, and R.A. Roemer, Phys. Rev. Lett. **102**, 096405 (2009).
[5] A.M. Alexeev and M.E. Portnoi, Phys. Rev. B **85**, 245419 (2012).
[6] A.M. Alexeev, I.A. Shelykh, and M.E. Portnoi, arXiv:1302.2138 (2013).

Temperature dependence of single quantum dot luminescence: influence of inter-dot coupling

N. A. Jahan,[1, 2,*], C. Hermannstädter[1], K. Akahane[3], M. Sasaki[3], H. Kumano[1] and I. Suemune[1]

[1]RIES, Hokkaido Univ., Japan, [2]Grad. School of Inform. Science and Technology, Hokkaido Univ., Japan, [3]National Institute of Information and Communications Technology, Tokyo, Japan

*Corresponding author: isuemune@es.hokudai.ac.jp

InAs quantum dots (QDs) grown on InP substrates can be used as sources of single photon and entangle photon pairs in the telecommunication bands. However, molecular beam epitaxy (MBE) growth of the InAs/InP system results in QD ensembles of rather high density (~10^{11}cm^{-2}) and thus photon generation from QDs may be affected by inter-dot coupling among neighboring QDs. In this paper we study the photoluminescence (PL) characterization of single InAs QDs grown on InP(311)B substrates and report a peculiar temperature dependence of single QD luminescence intensities. The observations are well explained with inter-dot carrier transfer through coupled excited states (CES) with correlated electron-hole escape mechanism.

4-ML InAs/$In_{0.53}Al_{0.22}Ga_{0.25}As$/InP(311)B QDs were grown by MBE at 470°C. The samples were etched into pillar structures with 100-nm diameters to select limited number of QDs. One of the pillars was excited with a 632-nm He-Ne laser with the power of 200 nW through an objective lens with NA=0.4. We observed sharp emission lines from individual QDs as shown in the inset of Fig. 1. Temperature dependence of the integrated PL intensities of individual sharp emission is shown for three major lines in Fig. 1. All the three lines show similar tendency but are not simple. For comparison, macroscopic-area PL measurements were performed on the as-grown InAs QD sample. The temperature dependence of the integrated PL intensity is shown in Fig. 2. Below 140 K, the integrated PL intensity is weakly temperature dependent. This suggests that the temperature dependence shown in Fig. 1 is not necessarily due to the change of recombination quantum efficiency.

We have studied the thermal activation energies from the data shown in Fig. 2 and derived two components; one with 22 meV dominating T<140 K and the other with 157 meV dominating T>140 K [1]. In the low temperature region corresponding to that of Fig. 1, we have measured the excited states of the QDs and compared with the thermal activation energy. The latter was almost half of the former, indicating the correlated electron-hole pair transfer from QDs to the neighboring QDs through coupled excited states [1]. Therefore the increase of the single QDs arises with the carrier transfer into the single QD and the decrease with the carrier escape to the neighboring QDs. In this temperature range the average lifetime increases with temperature and the overall intensity decreases with temperature. The mutual relation is quantitatively discussed based on the inter-dot carrier transfer indicated by Fig. 1. This work was supported in part by the SCOPE from the MIAC and Nano-macro materials, devices and systems alliance.

References: [1] N. A. Jahan, C. Hermannstädter, J-H. Huh, H. Sasakura, T. J. Rotter 2013 *J. Appl. Phys.* **113**, 033506.

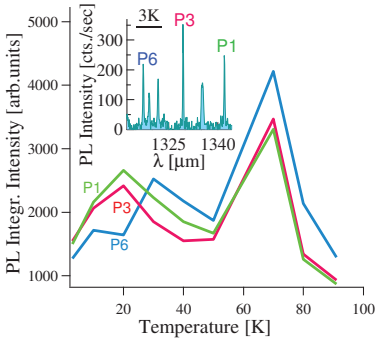

Fig. 1 PL spectrum observed from a 100-nm pillar and the temperature dependence of the integrated PL intensities of three individual sharp emission lines.

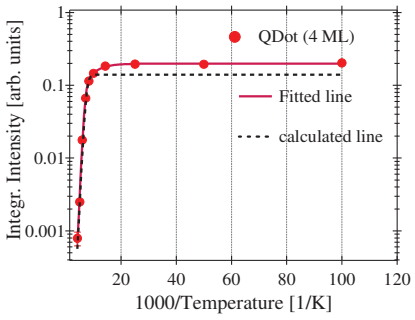

Fig. 2 Temperature dependence of the integrated PL intensity measured on macroscopic-area of QDs. Dashed line is for the purpose of identifying dominant temperature range of the two activation components [1].

Inter-sublevel transitions in single InAs/GaAs quantum dots

Daniel R. Stephan[1,2], Jayeeta Bhattacharyya[1], Manfred Helm[1,2], Yongheng Huo[3], Armando Rastelli[3,4], Oliver Schmidt[3] and Harald Schneider[1]

[1] *Institute of Ion Beam Physics and Materials Research, Helmholtz-Zentrum Dresden-Rossendorf (HZDR), Dresden, Germany*
[2] *Technische Universität Dresden, Dresden, Germany*
[3] *Institute for Integrative Nanosciences, IFW Dresden, Dresden, Germany*
[4] *Institute of Semiconductor and Solid State Physics, Johannes Kepler Universität, Linz, Austria*

In the past, inter-band transitions in quantum dots (QDs) have received an appreciable amount of scientific interest. However, inter-sublevel transitions have been studied much less extensively, likely because of their strongly non-radiative nature and because of limited availability of tunable sources for resonant excitation. In this work we explore the dynamics of inter-sublevel transitions in single InAs/GaAs self-assembled QDs. We combine the commonly used micro-photoluminescence (PL) technique with time-resolved detection and additional excitation by a free-electron laser. The experiment is carried out in the following way: the low-density QD sample is illuminated with a picosecond pulsed Ti:sapphire laser. PL from a single QD is coupled into a spectrometer, recording the spectrum with a CCD detector, as well as the time-resolved transient via the time-correlated single photon counting technique. Introducing a free-electron laser pulse tuned to the inter-sublevel transition energy excites carriers to a higher energy level, which decay back to the ground state non-radiatively with a relatively short time constant. These inter-sublevel dynamics causes quenching in the exponential PL decay of the energy of the ground state, which can be observed in time-resolved measurements. Whereas previous studies on inter-sublevel transitions have used QD ensembles[1-3], investigating single dots excludes many-dot effects such as inhomogeneous broadening and inter-dot transfer, which should lead to a better understanding of inter-sublevel carrier dynamics.

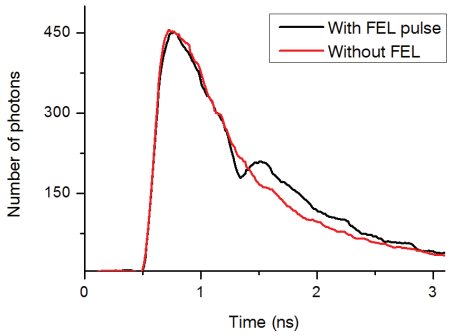

Fig. 1: Transients of the ground state PL line of a single QD, with and without free-electron laser (FEL) excitation. The measurement was taken at 5K with the FEL tuned to 87μm (14meV).

[1] J. Bhattacharyya, M. Wagner, M. Helm, M. Hopkinson, L. Wilson and H. Schneider, Appl. Phys. Lett. **97**, 031101 (2010).
[2] J. Bhattacharyya, S. Zybell, S. Winnerl, M. Helm, M. Hopkinson, L. Wilson, and H. Schneider, Appl. Phys. Lett. **100**, 152101 (2012).
[3] E. Zibik, T. Grange, B. Carpenter, N. Porter, R. Ferreira, G. Bastard, D. Stehr, S. Winnerl, M. Helm, H. Liu, M. Skolnick, L. Wilson, Nature Mater. **8**, 803 (2009).

MoP68

Photon extraction enhancement and suppression of multi-photon emission from an InAs quantum dot in a metal-embedded nanocone structure

X. Liu [1], T. Asano [1], S. Odashima [1], H. Nakajima [1,2], H. Kumano [1] and I. Suemune [1]

[1] *Research Institute for Electronic Science, Hokkaido University, Sapporo 001-0021, Japan*
[2] *Research Fellow of the Japan Society for the Promotion of Science, Tokyo 102-8472, Japan*

Semiconductor quantum dots (QDs) are potential candidates for bright single-photon sources in the context of quantum information processing and quantum communications. Significant progress has been made to achieve efficient single-photon sources.[1-4] Although photonic nanowires and distributed Bragg reflector microcavity pillars exhibited high photon-extraction efficiencies, mechanical stability related to their high aspect ratio and their stability to couple to outer photon-collection optics remain as challenging issues. In this abstract, we introduce a metal (silver)-embedded GaAs nanocone structure containing an InAs QD showing high photon extraction and suppression of multi-photon emission under quasi-resonant excitation.

The InAs QDs were grown on GaAs (100) substrate by metal organic molecular-beam epitaxy (MOMBE). To fabricate a tailored nanocone structure, electron beam lithography and dry etching processes were performed. Such a tailored structure was then deposited with a SiO_2 layer and Ag film. Sequential polishing followed by dry etching of GaAs was carried out for the fabrication of Ag-embedded nanocone structure including InAs QDs (see Fig. 1).

The μ-PL spectrum of an InAs QD in an Ag-embedded nanocone structure at 4 K is shown in the inset of Fig. 2(a). The PL peaks at 944 and 945.9 nm were determined as a neutral exciton (X^0) emission and a negatively charged exciton (X^-) emission, respectively. For the X^- line at saturation, the photon count rate was measured to be ~200 KHz as shown in Fig. 2(a) and the photon-extraction efficiency was 21.5% under 800 nm pulsed excitation with a repetition rate of 76 MHz. Considering the competition between the X^0 and X^-, our photon-extraction efficiency was as high as 24.6%. It can be seen that this newly developed structure exhibited an enhancement in photon extraction compared with our previous structure.[4] Second-order correlation function $g^{(2)}(\tau)$ was also measured under quasi-resonant excitation using 897 nm pulsed laser with a Hanbury-Brown and Twiss (HBT) setup.[5] Figure 2(b) shows the antibunching behavior of $g^{(2)}(\tau)$ without subtracting any background counts. The $g^{(2)}(0)$ was calculated to be 0.025, indicating strong suppression of multi-photon emission.

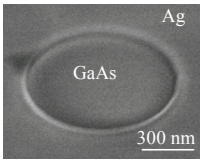

Fig. 1. Top-view SEM image of the Ag-embedded nanocone structure with removed substrate.

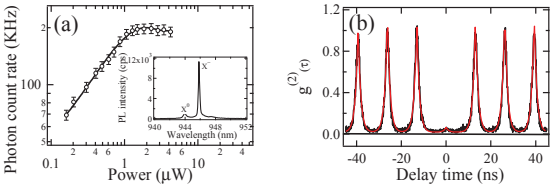

Fig. 2. (a) Photon count rate of the X^- line as a function of excitation power. The inset is the μ-PL spectrum. (b) $g^{(2)}(\tau)$ as a function of delay time τ. The red curve is the fit to the data.

[1] J. Claudon, J. Bleuse, N. S. Malik, M. Bazin, P. Jaffrennou, N. Gregersen, C. Sauvan, P. Lalanne, and J. Gerard, Nat. Photon. **4**, 174 (2010). [2] M. Pelton, C. Santori, J. Vučković, B. Zhang, G. S. Solomon, J. Plant, and Y. Yamamoto, Phys. Rev. Lett. **89**, 233602 (2002). [3] A. G. Curto, G. Volpe, T. H. Taminiau, M. P. Kreuzer, R. Quidant, and N. F. van Hulst, Science **329**, 930 (2010).[4] H. Nakajima, S. Ekuni, H. Kumano, Y. Idutsu, S. Miyamura, D. Kato, S. Ida, H. Sasakura, and I. Suemune, Phys. Stat. Sol. (C) **8**, 337 (2011). [5] R. Hanbury Brown and R. Q. Twiss, Nature **177**, 27 (1956).

Floating gate in a 2DEG island for electrostatically connecting distant quantum dots

T. Obata, M. Yamamoto, and S. Tarucha

Department of Applied Physics, University of Tokyo, Hongo, Bunkyo-ku, Tokyo 113-8656, Japan

Integration of multi-spin qubits has recently focused in the research frame of quantum computation with quantum dots (QDs). Manipulation of two individual single spins[1], control of spin singlet entanglement[2], and observation of long decoherence time and echo time by use of dynamical decoupling techniques[3] have been successively achieved . The next step is to scale up the quantum gates with more quantum dots. However, it is still challenging to address many quantum dots with sufficiently strong inter-dot couplings because it is crucial to accommodate gates and control lines to engineer larger scale QD systems. To solve these problems, it is theoretically proposed to use metallic materials as a floating gate for dipolar coupling between QDs, which can leave a larger space for making a complex electrical circuit[4]. We follow this concept to design the floating gate to connect two quantum dots 1μm apart. We prepare quantum dots defined in a 2DEG by Schottky gates and a floating gate defined in the same 2DEG by etching. We find that the floating gate in a 2DEG electro-statically couples the two quantum dots strong enough to control dipolar coupling between two spin qubits.

A scanning electron micrograph of our device is shown in Fig. 1. Two DQDs are separated by a 1μm long and 0.6μm wide 2DEG island. We find that two separated DQDs are capacitively coupled through the incompressive confined 2DEG island. We measure two sets of charge stability diagrams of the two DQDs as a function of two gate voltages for the two DQDs and find that when the number of electrons in one of the two DQDs is changed by one, the Coulomb peak positions for the other DQD is shifted, influenced by the change in the electrostatic potential of the first DQD. In addition, we observe that the inter-dot charge transition of one DQD also depends on the charge state of the other DQD. This is an indication that dipolar coupling between two qubits can be implemented by the floating gate. We also note that it is possible to turn on and off the coupling by a surface gate on the floating 2DEG[4]. We discuss these results and the possible extension of magnetic floating gates for the long range direct interaction of spin qubits[5].

[1] M. Pioro-Ladrière *et al.*, Nat. Phys. **4**, 776 (2008), T. Obata *et al.*, Phys. Rev. B **81**, 085317 (2010).
[2] R. Brunner *et al.*, Phys. Rev. Lett. **107**, 146801 (2011).
[3] H. Bluhm *et al.*, Nature Physics **7**, 109-113 (2010).
[4] L. Trifunovic *et al.*, Phys. Rev. X **2**, 011006 (2012).
[5] L. Trifunovic, F. L. Pedrocchi, and D. Loss, arXiv:1302.4017.

Ultra-Low Density GaAs Quantum Dots by Nanohole Filling

D. Sonnenberg [1], A. Graf [1], A. Küster [1], Ch. Heyn [1], and W. Hansen [1]

[1] *Institute of Applied Physics, University of Hamburg, Jungiusstr. 11, 20355 Hamburg, Germany*

We discuss the fabrication, as well as structural and optical properties of GaAs quantum dots with an ultra-low density of less than 10^6 dots per cm^2 uniformly over the whole wafer. We use the self-assembled local droplet etching (LDE) technique to drill nanoholes into AlGaAs surfaces and fill these holes partially with GaAs to form GaAs QDs of adjustable size in an AlGaAs matrix. The LDE is performed in a conventional molecular beam epitaxy system. First, group-III metal droplets, in our case Al, are deposited on a semiconductor surface at usual III-V MBE growth temperatures in Volmer-Weber growth mode under a very low arsenic background pressure F_{As}. After droplet deposition the sample is annealed, still without As supply. During annealing the Al droplets are transformed into nanoholes surrounded by an AlAs wall. At lowest possible F_{As} this leads to holes with a bimodal depth distribution, i.e., a relatively high number of shallow holes exists among some deep ones with a total density in the 10^8 per cm^2 range, as is visible in Fig. 1(a). By optimizing the As flux during the droplet deposition step, the formation of shallow holes can be suppressed, leading to only deep nanoholes, with an increased depth of ~30 nm and an ultra-low density typically in the 10^6 dots per cm^{-2} range (Fig. 1(c)). Apart from the influence of F_{As} on the hole density and depth (Fig. 1(d))[1], we also report on the influence of the process temperature [1] and droplet material amount [2] studied by atomic force microscopy (AFM).

By filling of the nanoholes with GaAs we obtained well separated, strain-free GaAs QDs. The ground-state emission energy of these QDs has been adjusted over an energy range from 1.56 eV up to 1.68 eV by the hole filling level [1]. The QDs show clear excitonic features with linewidths down to 100 µeV, setup resolution limited. High excitation power photoluminescence measurements demonstrate that also the quantization energy is precisely adjustable (Fig.1 (e-g)) [2].

The authors would like to thank the "Deutsche Forschungsgemeinschaft" for financial support via grant GrK 1286 and DFG-project HA2042/6-1.

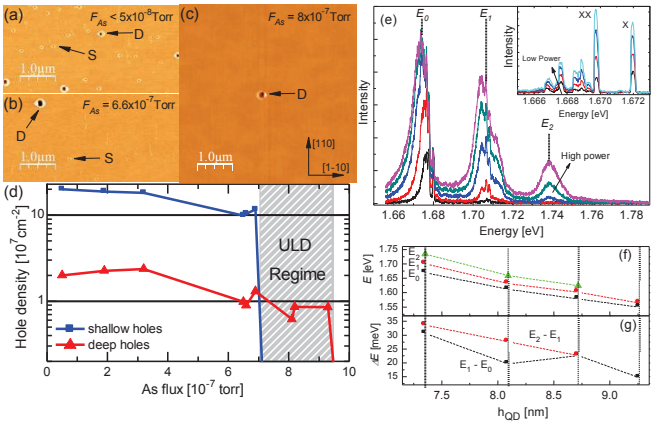

Fig.1: (a)-(c) AFM images of LDE samples with varied arsenic flux F_{As} during droplet deposition as indicated. (d) Density of shallow and deep holes in dependence of F_{As}. The lines are guides to the eye. [1] (e) High excitation power single-dot PL spectra at T=6 K from a single 7.3 nm high QD, with three broadened quantized shells E_0...E_2. In the inset, a low excitation power series of a dot is shown, were exciton X and biexciton peaks XX can be clearly identified by their power dependence. (f) Emission energies E_0...E_2 of the QD shells for samples with different QD height h_{QD}. (g) Comparison of the quantization energies ΔE in dependence of h_{QD} [2].

[1] D. Sonnenberg, A. Graf, V. Paulava, W. Hansen, and Ch. Heyn, Appl. Phys. Lett. **101**, 143106 (2012).
[2] D. Sonnenberg, A. Graf, V. Paulava, W. Hansen, and Ch. Heyn, J. Cryst. Growth http://dx.doi.org/10.1016/j.jcrysgro.2012.12.060.

Coupling and wavelength tuning of GaAs quantum dots

A. Küster [(1)], D. Sonnenberg [(1)], A. Graf [(1)], Ch. Heyn [(1)] and W. Hansen [(1)]

[1] *Institute of Applied Physics, University of Hamburg, Jungiusstr. 11, 20355 Hamburg, Germany*

We study a novel type of GaAs quantum dot molecules (QDM) fabricated by filling of nanoholes with a modulated material sequence. The samples were fabricated using molecular beam epitaxy (MBE) and the local droplet etching technique (LDE).[1] We have established the fabrication of highly uniform GaAs quantum dots (QD) by filling of LDE holes [2,3]. The fabrication of the present QDMs bases on the recently demonstrated drilling of ultra-low density nanoholes [3]. The nanoholes are etched in AlGaAs surfaces using Al droplets. The material sequence filled into the holes consists of GaAs to form a bottom QD, AlGaAs as tunnel barrier, and, again, GaAs to form an upper QD. Finally, the QDM is capped by an AlGaAs layer. Important parameters of the QDM such as individual quantum dot size and tunneling barrier thickness are adjusted by the respective filling amounts. In order to apply a vertical electric field, the QDMs were embedded in a gate structure as shown in Fig. 1a.

We investigate QDMs with varied tunnel barrier thickness to study coupling effects with excitation power dependent measurements. Fig. 1b presents typical power dependent photoluminescence (PL) spectra of a QDM. Two PL peaks are observed that we associate to emission from the individual QDs. The ratio of the integrated intensities of the ground state emission from the higher energetic QD_s and the lower energetic QD_l is presented in Fig. 1c as a function of the excitation power. The power dependence of the ratio clearly indicates non-resonant coupling within the QDM. [4] A reference sample with thicker tunnel barrier shows a constant ration indicating negelegible coupling (Fig. 1d). Furthermore, we studied the influence of a vertical electric field on the photoluminescence emission of our QDMs. We obtain Stark-shifts up to 25 meV, as shown in Fig. 1e.

The authors would like to thank the "Deutsche Forschungsgemeinschaft" for financial support via grant GrK 1286 and DFG-project HA2042/6-1

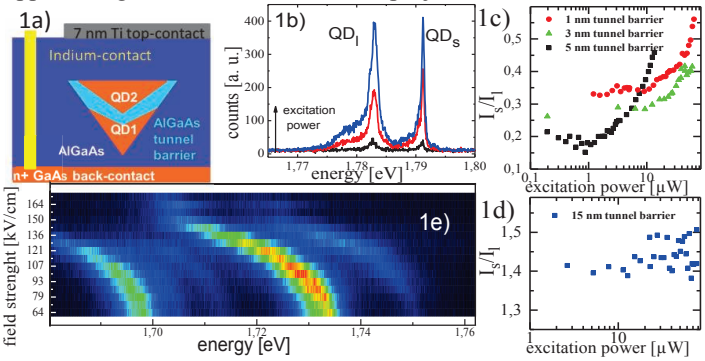

(a) Schematic sample structure of the QDM samples (b) PL spectra of a GaAs QDM at different excitation powers. (c) Intensity ratios I_s/I_l of the two QD's peaks of QDMs with different tunnel barrier thicknesses (d) I_s/I_l for a DQM with a 15 nm thick tunnel barrier (e) Electric field dependence of the ground-state emission depicted in color-encoded intensity

[1] Z.M. Wang et al. Appl. Phys. Lett. **90** (2007), 113120
[2] Ch. Heyn Appl. Phys. Lett. **94** (2009), 183113
[3] D. Sonnenberg et al. Appl. Phys. Lett. **101** (2012), 143106
[4] Reischel et al. Phys. Rev. B **76** (2007), 085338

MoP72

Electro-optical characterization of Ti/Au-ZnTe Schottky diodes with CdTe quantum dots

E. Zielony[1], E. Płaczek-Popko[1], P. Nowakowski[2], Z. Gumienny[1], A. Suchocki[2] and G. Karczewski[2]

[1]Institute of Physics, Wroclaw University of Technology, Wybrzeze Wyspianskiego 27, 50-370 Wroclaw, Poland
[2] Institute of Physics, Polish Academy of Sciences, al. Lotnikow 32/46, 02-668 Warsaw, Poland

We present the electric and optical spectroscopy techniques that have been applied to investigate ZnTe (*p*-type) – Ti/Au Schottky diodes containing a layer of CdTe self-assembled quantum dots (SAQDs). The reference ZnTe – Ti/Au diode without dots was also studied for comparison. Both samples were grown by molecular beam epitaxy technique. Raman measurements confirmed the presence of the CdTe layer while the photoluminescence (PL) spectra proved that CdTe quantum dots were formed in the investigated structure. The PL spectra revealed the CdTe QD electron-hole recombination energy equal to 2.1 eV at 10 K. Based on the temperature PL measurements the activation energy of photoluminescence quenching has been determined to be equal to 22 meV. Further confirmation for the QD formation has been obtained from the C-V characteristics which exhibited a step related to the charge accumulation at the QD states. DLTS spectra for the sample with QDs yield three hole-related signals with apparent activation energies equal to $E_{H1} = 0.16$ *eV*, $E_{H2} = 0.2$ *eV* and $E_{H3} = 0.4$ *eV*. For the reference ZnTe-Ti/Au diode solely single signal was observed of signature close to the level *H3* in the QD sample. Detailed characterization of the traps as well as the PL studies lead to the conclusion that the level *H2* is related to the defects located close to the QDs created during the growth while the other traps are associated with defects present in the ZnTe bulk material.

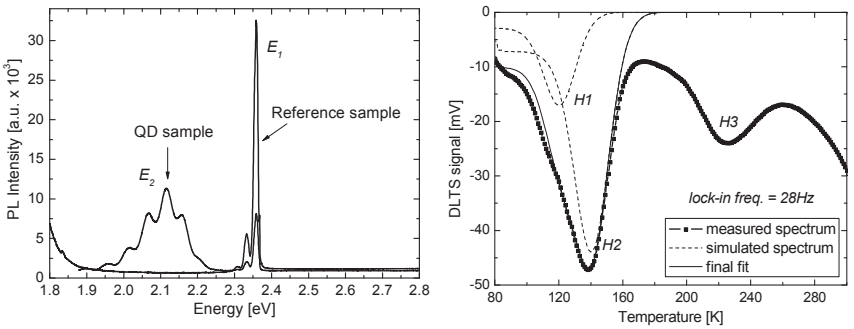

[1] E. Zielony, E. Płaczek-Popko, P. Nowakowski, Z. Gumienny, A. Suchocki and G. Karczewski, *Mat. Chem. Phys.* **134**, 821-828 (2012).

[2] E. Placzek-Popko, E. Zielony, J. Trzmiel, J. Szatkowski, Z. Gumienny, T. Wojtowicz, G. Karczewski, P. Kruszewski, and L. Dobaczewski, *Physica B* **404**, 5173 (2009).

Laser irradiation effects on the CdTe/ZnTe quantum dot structure studied by Raman and AFM spectroscopy

E. Zielony[1], E. Płaczek-Popko[1], A. Henrykowski[1], Z. Gumienny[1], P. Kamyczek[1], J. Jacak[1], P. Nowakowski[2] and G. Karczewski[2]

[1] *Institute of Physics, Wroclaw University of Technology, Wybrzeze Wyspianskiego 27, 50-370 Wroclaw, Poland*
[2] *Institute of Physics, Polish Academy of Sciences, al. Lotnikow 32/46, 02-668 Warsaw, Poland*

Micro-Raman spectroscopy has been applied to investigate the impact of laser irradiation on semiconducting CdTe/ZnTe quantum dots (QDs) structures. A reference sample (without dots) was also studied for comparison. Both samples were grown by molecular beam epitaxy technique on the *p*-type GaAs substrate. The Raman spectra have been recorded for different time of a laser exposure and for various laser powers. The spectra for both samples exhibit peak related to the localized longitudinal (LO) ZnTe phonon of a wavenumber equal to 210cm^{-1}. For the QD sample a broad band corresponding to the LO CdTe phonon related to the QD-layer appears at a wavenumber of 160cm^{-1}. With increasing time of a laser beam exposure and laser power the spectra get dominated by tellurium - related peaks appearing at wavenumbers around 120cm^{-1} and 140cm^{-1}. Simultaneously the ZnTe surface undergoes rising damage, with the formation of Te aggregates at the pinhole edge as reveal AFM observations. Local temperature of irradiated region has been estimated from the anti-Stokes/Stokes ratio of the Te modes intensity and it was found to be close or exceeding ZnTe melting point. Thus the laser damage can be explained by the ablation process.

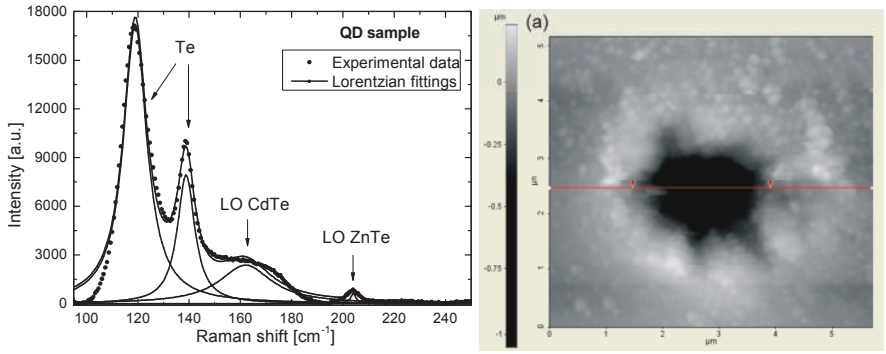

[1] E. Zielony, E. Płaczek-Popko, A. Henrykowski, Z. Gumienny, P. Kamyczek, J. Jacak, P. Nowakowski and G. Karczewski, *J. Appl. Phys.* **112**, 063520 (2012).

MoP74

Carrier confinement in stacks of InAs/GaAs sub-monolayer quantum dots: quantum dots or quantum wells?

Manus Hayne[1], Samuel Harrison[1], Matthew Young[1], Peter D. Hodgson[1], Robert J. Young[1], Andre Strittmatter[2], Andrea Lenz[2], Udo W. Pohl[2]and Dieter Bimberg[2]

[1] *Department of Physics, Lancaster University, Lancaster, LA1 4YB, UK*
[2] *Institut für Festkörperphysik, TU Berlin, Hardenbergstr. 36, 10623 Berlin, Germany*

Sub-monolayer quantum dots (SML-QDs) are formed by cycled deposition of <1 ML of InAs and a few MLs of GaAs. Cross-sectional scanning tunneling microscopy (X-STM) reveals that the samples comprise In-rich agglomerations with a large distribution of shapes and sizes (Fig. 1), embedded in an InGaAs quantum well (QW) [1]. Paradoxically, SML-QD photoluminescence (PL) is very bright and narrow (6 to 9 meV at 4 K), and SML-QD vertical-cavity surface-emitting lasers (VCSELs) can operate at up to 30 Gb/s [2]. Indeed, the very nature of the confinement is unknown: is the system zero- or two-dimensional?

We have used magneto-PL measurements at temperatures between 1.5 and 400 K in Faraday and Voigt geometry up to 17 T to probe the excitonic confinement of 3 SML-QD samples with a 10-fold stack of 0.5 ML of InAs separated by 1.5, 2.0 and 2.5 ML of GaAs. At low temperature the exciton Bohr radius is found to be 15 to 16 nm in all samples, i.e. the exciton extends laterally across several agglomerations (Fig. 1). Furthermore, the dependence of both the PL linewidth and the (Voigt geometry) diamagnetic shift on GaAs spacer thickness strongly implies that the vertical exciton extent is limited by the stack height (Fig. 1). *These results support the interpretation that the samples are quantum wells*. *In contrast, magneto-PL measurements at 350 to 400 K demonstrate dot-like states*: In high magnetic field (Faraday geometry) excited-state luminescence peaks become resolved, and display a field dependence that can be described by a Fock-Darwin spectrum (Fig. 2).

These paradoxes can be resolved by attributing *different dimensionalities of confinement to electrons and holes*. The agglomerations are too small to confine electrons, which are relatively light, so the electron wave-function is bounded vertically by the SML-QD stack, and the electrons see an InGaAs QW. This defines the exciton extent, and results in line-widths that are typical for (disordered) QWs [3]. The much heavier holes, on the other hand, are confined in the dot-like In-rich agglomerations with confinement energies ~9 meV.

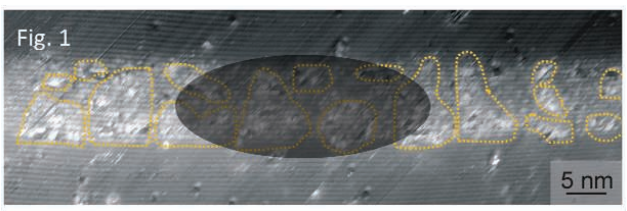

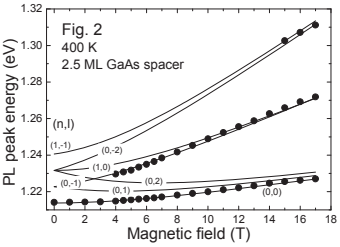

Fig. 1: Typical X-STM image of a SML-QD sample. The In-rich agglomerations are shown with dotted lines, while the shaded ellipse depicts the extent of the exciton (electron) wave function. Fig. 2: Magneto-PL peak positions (symbols) at 400 K for the sample with 2.5 ML GaAs spacers. The lines show the Fock-Darwin states. Similar behaviour was observed in all 3 samples.

[1] A. Lenz *et al*., Applied Physics Express **3**, 105602 (2010).
[2] N. N. Ledentsov *et al*., Nanoscale Res. Lett. **2**, 417 (2007).
[3] B. Bansal *et al*., Appl. Phys. Lett. **91**, 251108 (2007).

Fine structure of a biexciton in a quantum dot with magnetic impurity: Magnetic sensing of a spinless system

Marek J. Korkusinski[1], Anna H. Trojnar[1,2], Udson Mendes[1], Mateusz Goryca[3], Maciej Koperski[3], Tomasz Smolenski[3], Piotr Kossacki[3], Piotr Wojnar[4], and Pawel Hawrylak[1,2]

[1] *Quantum Theory Group, Security and Disruptive Technologies, National Research Council of Canada, Ottawa, Canada*
[2] *Department of Physics, University of Ottawa, Ottawa, Canada*
[3] *Institute of Experimental Physics, University of Warsaw, Warsaw, Poland*
[4] *Institute of Physics, Polish Academy of Sciences, Warsaw, Poland*

In molecular and solid state systems, localised spins are coupled to the spins of electrons residing in their environment due to the spin-spin exchange interaction. This coupling is exploited in techniques such as the nuclear (NMR) and electron (EPR) spin-based resonance, in which the localised spin is treated as a local probe. When the environment is in the spin singlet state, the localized spin does not interact with it directly except for the Kondo effect [1].

Here we demonstrate that spin-singlet few-electron systems such as pairs of holes or excitons confined in a quantum dot are probed by the spin of a magnetic impurity. Specifically, building on our earlier work [2], we show theoretically and experimentally that the ground state of a bi-exciton in a CdTe self-assembled quantum dot with a magnetic Mn impurity exhibits a fine structure due to electron-electron Coulomb and hole-Mn exchange interactions. The bi-exciton-Mn complex is described by a Hamiltonian which accounts for the electron and hole single-particle shell structure, quantum dot anisotropy, direct, short- and long-ranged electron-hole exchange and isotropic electron-Mn and anisotropic hole-Mn exchange interactions. Results of exact diagonalization of the microscopic bi-exciton-manganese ion model predicts a pattern of three pairs of states in the ground-state manifold, each pair labeled by the projection of the Mn spin. The origin of the fine structure is traced to the Mn-mediated interaction of spin singlet and excited spin triplet two-hole configurations. We show that the fine structure determines the relative positions of the bi-exciton emission maxima and can be derived from the bi-exciton and exciton emission spectra. Theoretical predictions are successfully compared with measured bi-exciton and exciton emission spectra of a single CdTe dot with a Mn ion in its center in samples fabricated in Grenoble [3] and Warsaw.

The coupling of the localized spin to the spinless environment enables imaging of nonmagnetic molecular and solid-state systems and is important for operation of electron spin-based qubits [4], operation of single-spin quantum memory [5], and nanomagnetism [6].

[1] J. Kondo, Progr. Theor. Phys. **32,** 37 (1964); A. Ote *et al.,* Nature Phys. **4**, 847 (2008).
[2] S.-J. Cheng and P. Hawrylak, Europhys. Lett. **81**, 37005 (2008); M. Goryca *et al.,* Phys. Rev. Lett. **103,** 087401 (2009); A. Trojnar *et al.,* Phys. Rev. Lett. **107**, 207403 (2011); A. Trojnar *et al.,* Phys. Rev. B **85**, 165415 (2012).
[3] L. Besombes *et al.,* Phys. Rev. B **71,** 161307 (2005).
[4] M. Korkusinski and P. Hawrylak, *Coded qubit based on electron spin,* in: *Semiconductor Quantum Bits,* edited by F. Henneberger and O. Benson, Pan Stanford Publishing, Singapore (2008).
[5] L. Besombes *et al.*, Phys. Rev. Lett. **93,** 207403 (2004); F. Qu and P. Hawrylak, Phys. Rev. Lett. **95,** 217206 (2005).
[6] S. T. Ochsenbein *et al.,* Nature Nanotechnol. **4,** 681 (2009); R. M. Abolfath *et al.,* Phys. Rev. Lett. **108,** 247203 (2102).

Optical spin control of a single Mn atom in a single quantum dot via the light hole exciton

D. E. Reiter[1], V. M. Axt[2], and T. Kuhn[1]

[1] *Institut für Festkörpertheorie, Universität Münster, Wilhelm-Klemm-Str. 10, 48149 Münster, Germany*

[2] *Theoretische Physik III, Universität Bayreuth, 95440 Bayreuth, Germany*

When a single Mn atom is doped into a semiconductor quantum dot (QD), new possibilities for spin control emerge. The strong exchange interaction between the exciton and the Mn spin leads to prominent features in the photolumescence spectrum, where instead of a single exciton line a set of six equidistant lines appears for a CdTe QD [1]. Due to valence band mixing previously dark excitons can become also visible in the spectrum [2]. In these QDs the uppermost valence band is considered as mostly heavy hole (HH) type. However, it is also possible to fabricate QDs where the uppermost valence band is of light hole (LH) type [3]. If a CdTe QD with a LH exciton doped with a single Mn atom is considered, the spectrum changes qualitatively and a set of twelve lines is expected [4].

In this contribution we discuss the possibility of spin control of the Mn atom via optical manipulation of the LH exciton and the signatures of the Mn spin dynamics in the signals of time-resolved optical measurements. We model a CdTe QD doped with a single Mn atom. For the exciton system we take into account the ground state without exciton, four single exciton states and one biexciton state. For circularly polarized light propagating along the growth axis, the two exciton states with spin ± 1 are bright, while the two exciton states with spin 0 are dark. In principle, when the LH exciton with an angular momentum of 1 interacts with the Mn spin, the Mn spin can flip by two, once by transferring the spin to the electron and once by spin transfer to the LH. However, because these states are off-resonant, no complete spin transfer is achieved. In the dynamical picture the spin transfer is reflected by exchange-induced Rabi oscillations of the occupations. A complete spin transfer of the Mn spin by two can be achieved by the usage of 2π pulses, which do not change the occupations of the states, but influence the coherences. For linearly polarized light propagating perpendicular to the growth axis, the exciton states with spin 0 become bright, while the other two exciton states become dark. Then by interaction of the LH exciton and the Mn spin a spin of 1 can be transferred. Using a sequence of pulses consisting of π pulses, which excite and de-excite the LH exciton, and 2π pulses, the Mn spin can be switched from a given initial state into all other eigenstates on a ps timescale [4]. When we compare this switching scheme to a previous switching scheme which includes also HH excitons [5], we find that the switching is much faster and a change of the Mn spin by one can be achieved, while the exciton system is returned to its ground state.

In a time resolved spectroscopy measurement the dynamics of the Mn spin can be followed. Because every Mn spin has its own spectral fingerprint, each switch of the Mn spin changes the position and strength of the lines appearing in the spectrum, which allows for an optical detection of the time-dependent Mn spin state.

[1] L. Besombes *et al.*, Phys. Rev. Lett. **93**, 207403 (2004).
[2] M. Goryca *et al.*, Phys. Rev. B **82**, 165323 (2010).
[3] Y. H. Huo *et al.*, arXiv preprint, arXiv:1208.6554, (2012).
[4] D. E. Reiter *et al.*, Phys. Rev. B **83**, 155322 (2011).
[5] D. E. Reiter *et al.*, Phys. Rev. Lett. **102**, 177403 (2009).

Electron spin relaxation in quantum dots: effect of the 3D shape

Juan I. Climente [1], Carlos Segarra[1] and Josep Planelles[1]

[1]Dept. de Química Física i Analítica, Universitat Jaume I, Castelló, Spain

Quantum confinement has a profound influence on the orbital motion of electrons, which is then felt by the spin degree of freedom through spin-orbit interaction (SOI). This has been exploited in two-dimensional electron gases to achieve unprecedented control on the electron spin, opening venue for new spin physics and spin-based applications. In the last decade, much of this knowledge has been transferred to the study of SOI effects in quasi-two-dimensional (electrostatic or self-assembled) quantum dots (QDs), enabling full control over individual spins.[1]

Yet, recent experiments have started addressing the spin dynamics of colloidal QDs, where the fully three-dimensional quantum confinement can be tailored to form a variety of shapes. [2, 3, 4] Structural anisotropies are known to have important consequences on spin-orbit coupling. Therefore, proper modeling of the 3D nature of SOI becomes essential to understand the properties and the possibilities of these systems.

In this presentation, we explore how the 3D confinement geometry affects the electron spin relaxation between Zeeman sublevels of zinc-blende QDs. As compared to the well-established case of quasi-2D systems, the additional (vertical) degree of freedom brings about a qualitatively different behavior. This allows us to generalize the role of the interaction between quantum confinement and SOI in the spin dynamics. In particular, we show that the conduction band Dresselhaus spin-orbit interaction is suppressed in spherical nanocrystals.[5] The suppression of the Dresselhaus term implies that spherical nanocrystals with wide gaps are essentially left with Rashba spin-orbit interaction alone, which is an ideal scenario for external control of spin degrees of freedom.

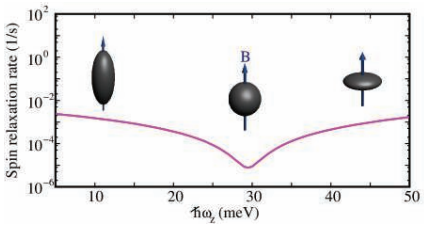

Figure: Electron spin relaxation rate in QDs with varying aspect ratio. Note the suppression for spherical QDs.

[1] D. Press, T. D. Ladd, B. Zhang, y Y. Yamamoto, Nature **456**, 218 (2008); R. Hanson, L. P. Kouwenhoven, J. R. Petta, S. Tarucha, y L. M. K. Vandersypen, Rev. Mod. Phys. **79**, 1217 (2007).
[2] G. D. Scholes, J. Kim, C. Y. Wong, V. M. Huxter, N. P. Sreekumari, K. P. Fritz, y S. Kumar, Nano Lett. **6**, 1765 (2006).
[3] L. Biadala, Y. Louyer, Ph. Tamarat, y B. Lounis, Phys. Rev. Lett. **105**, 157402 (2010).
[4] C. Y. Wong, J. Kim, N. P. Sreekumari, M. C. Nagy, y G. D. Scholes, J. Phys. Chem. C **113**, 795 (2009); V. M. Huxter, J. Kim, S. S. Lo, A. Lee, N. P. Sreekumari, y G. D. Scholes Chem. Phys. Lett. **491**, 187 (2010).
[5] J. Planelles, J. I. Climente, y C. Segarra, J. Phys. Chem. C **116**, 25143 (2012).

Effect of strain on the spin splitting of holes in GaAs/GaAlAs quantum wells

K. Ryczko, M. Kubisa and J. Misiewicz

Institute of Physics, Wroclaw University of Technology, 50-370 Wroclaw, Poland

The Zeeman splitting of holes in the ground valence subband of a strained GaAs quantum well is studied theoretically. We consider heterostructures grown on differently oriented substrates and subjected to a uniaxial stress along the growth direction. The g factor of confined hole states is obtained under a magnetic field directed parallel to the well plane. Calculations are performed in the framework of the Luttinger model, including the effects of bulk inversion asymmetry. The wave-vector and magnetic-field dependences of the spin splitting are fully taken into account. The g factor is evaluated numerically using the finite-difference method. We show that the spin splitting of the states close to the ground subband edge remains almost unchanged upon uniaxial tension, but increases rapidly with the compressive strain, as shown in Fig. 1. The increase of g factor occurs in structures with different orientations and is related to the strain-driven transition of the topmost subband from heavy-hole to light-hole type. For low-symmetry growth directions, applying a strain also modifies the anisotropy of the hole spin. We show that the high anisotropy of spin splitting, observed in the unstrained [113] wells [1], disappears under a compressive strain. In contrast, the spin splitting in the [110] wells, almost isotropic in the zero-strain case, becomes extremely anisotropic under small uniaxial compression. The anisotropy results from the strain-induced anticrossing of the topmost valence subbands and corresponds to the pinning of hole spin to the [11$\underline{2}$] axis [2]. We discuss the wave-vector dependence of the Zeeman splitting both in the limit of low and high magnetic fields.

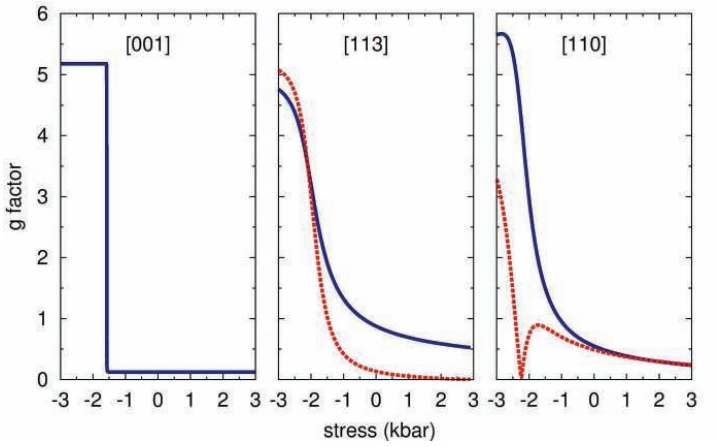

Fig. 1. Stress dependence of the g factor in 15-nm quantum wells with growth directions [mmn] = [001], [113], and [110], calculated at the subband edge (k = 0) for **B**||[nn($\underline{2}$m)] (solid lines) and **B**||[$\underline{1}$10] (dotted lines). The spin splitting in the [001] wells is isotropic.

[1] R. Winkler et al., Phys. Rev. Lett. **85**, 4574 (2000).
[2] M. Kubisa et al., Phys. Rev. B **83**, 195324 (2011).

Spin-induced time reversal symmetry breaking in an InGaAs mesoscopic ring with Rashba spin-orbit interaction

Fumiya Nagasawa[1], Makoto Kohda[1,2], and Junsaku Nitta[1]

[1] *Graduate School of Engineering, Tohoku University, Sendai 980-8579, Japan*
[2] *PRESTO, Japan Science and Technology Agency, Saitama 331-0012, Japan*

Elucidating the dynamics of spins in solid state systems is a key concept in modern spintronics. In previous studies [1, 2], spin-dependent decoherence has been investigated in an InGaAs-based two-dimensional electron gas (2DEG) subject to competition between Rashba spin-orbit (SO) and Zeeman couplings, the latter induced by a parallel magnetic field $B_{\parallel}$ to the 2DEG plane. It has been revealed that the decoherence is *a universal function* of the ratio of the Rashba SO coupling and the Zeeman energies (E_{SO} and E_{Z}, respectively). In this study, we investigate the spin-dependent decoherence in InGaAs mesoscopic rings, namely, in artificially defined interference paths.

An array of rings has been fabricated lithographically from an InGaAs quantum well. The radius of each ring is 0.61 μm. The perpendicular magnetic field dependence of the electrical resistance of the ring array has been measured as functions of gate voltage V_{g} and $B_{\parallel}$ at a temperature of 1.5 K. Due to ensemble averaging in the ring array, the time-reversal Altshuler-Aronov-Spivak (AAS) oscillations have been observed. We utilize the amplitude of the AAS oscillations, ΔR, to estimate the spin-dependent decoherence.

Suppression of ΔR in the in-plane $B_{\parallel}$-field has been observed (Fig. 1a). As shown in Fig. 1b, the suppression is a universal function of $(E_{\mathrm{Z}}/E_{\mathrm{SO}})^2$ for two dips of the ΔR oscillations (see the Inset of Fig. 1b), as observed in two-dimensional systems [2]. Not only that, the relative amplitudes $\Delta R_{1,2,3}$ (see Fig. 1a) can also be represented by a universal relation (Fig. 1c). The results suggest that the ratio $\tau_{\phi}(0)/\tau_{\mathrm{SO}}(0)$, with $\tau_{\phi}(0)$ being the phase-coherence time at $B_{\parallel} = 0$ and $\tau_{\mathrm{SO}}(0)$ the spin-relaxation time at $B_{\parallel} = 0$, is constant in our device. Thus, the universal relations studied in refs [1] and [2] are still valid for the ring array structure.

[1] F. Meijer, A. Morpurgo, T. Klapwijk, T. Koga, J. Nitta, Phys. Rev. B **70**, 201307 (2004).
[2] F. Meijer, A. Morpurgo, T. Klapwijk, J. Nitta, Phys. Rev. Lett. **94**, 186805 (2005).

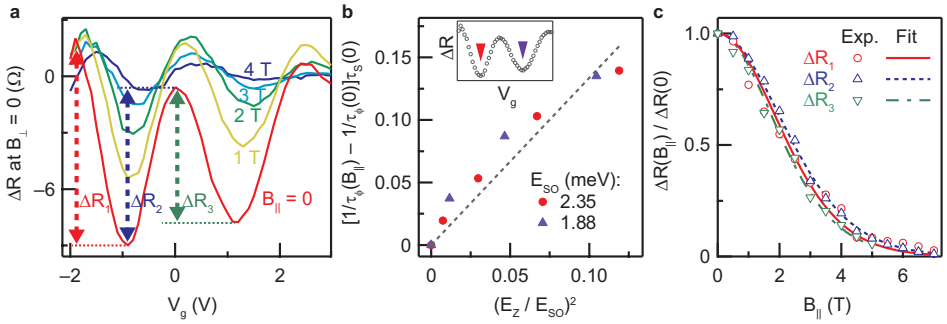

Figure 1: a, Amplitude of the AAS effect ΔR as a function of gate voltage V_{g} for varying in-plane $B_{\parallel}$-fields. b, Spin-induced dephasing rate $1/\tau_{\phi}(B_{\parallel}) - 1/\tau_{\phi}(0)$ multiplied by $\tau_{\mathrm{S}}(0)$, i.e., the spin-relaxation time at $B_{\parallel} = 0$, as a function of $(E_{\mathrm{Z}}/E_{\mathrm{SO}})^2$. Here, τ_{ϕ} is the phase-coherence time, E_{Z} is the in-plane Zeeman energy, and E_{SO} is the SO coupling energy. c, $B_{\parallel}$-field dependence of ΔR at different Rashba SO coupling strengths.

MoP80

Phonon-induced transparency in quantum dot molecules

Mark L. Kerfoot[1], Alexander Govorov[2], Davis Lu[1], Randall Babaoye[1], Allan S. Bracker[3], Daniel Gammon[3], Michael Scheibner[1]

1. School of Natural Sciences-Physics, University of California Merced, 5200 N Lake Rd., Merced CA 95343
2. Department of Physics and Astronomy, Ohio University, 45701, Athens Ohio
3. Naval Research Laboratory. 4555 Overlook Ave, SW, Washington DC 20375

Crystal lattice vibrations, i.e. phonons, have often been considered for the limitations they impose on quantum control and as sources of energy loss and noise in the crystalline-based components of modern technology. Here we report on the utilization of single phonons as a control parameter for the optical response of individual quantum dot molecules. As such, we demonstrate that phonons may enter the realm of mutual control of quantum states on the single particle level, which so far has been dominated by photons, electrons and spins.

Quantum dot molecules, i.e. coupled quantum dot pairs, provide an advantageous system as these individual particles can be made to interact and control each other. They possess highly tunable electronic, optical and spin properties [1]. We use quantum dot molecules to tune discrete optical transitions across tens of meV to enhance the interaction between excitonic states and optical phonons. In the presented case the interaction leads to an opto-mechanical mechanism by which the quantum dot molecule is rendered transparent by the quantized vibration of its own underlying lattice.

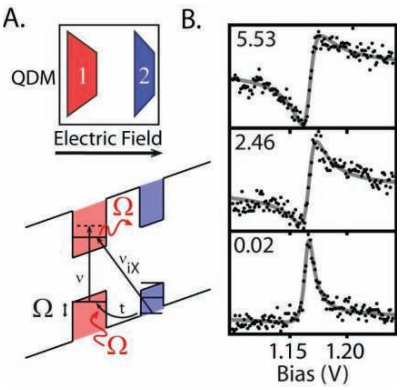

Figure 1 (A) Schematic of the structure (top) and the band diagram (bottom) of a QDM. In the band diagram the processes that lead to the phonon-induced Fano effect are indicated: optical absorption into the intradot optical polaron state, ν, optical absorption into the interdot exciton state, ν_{iX}, charge tunneling, t, with phonon emission and absorption, Ω. (B) Line scans of an interdot transition when it is in resonance with an intradot polaron at three different power levels (numbers in nW/μm^2).

We identify a Fano-effect as the physical mechanism behind this opto-mechanical transparency of the quantum dot molecule [2]. The Fano effect arises from quantum interference between two competing optical pathways, one associated with a discrete state and the other a continuum of states (Fig.1A). The result of this interference is a rapidly changing absorption lineshape verses the excitation energy. The Fano resonance is easily tunable (Fig.1B) and the consequent dips and peaks in absorption provide a switch to control quantum states. The universality of the Fano effect makes the concept of a vibration-induced decoupling from the environment transferable to a broad range of systems. We anticipate our results may provide an impetus for further investigations on the gainful use of phonons to provide greater control over individual quantum states, for example providing an on/off switch for optical state preparation and manipulation.

[1] Michael Scheibner, et al., "Essential concepts in the optical properties of quantum dot molecules" Solid State Comm. **149**, 1427-1435 (2009).
[2] Mark L. Kerfoot, et al., (manuscript in preparation).

Circularly Polarized Photoluminescence as a Probe of Spin Polarization and Interaction in GaAs/AlGaAs Quantum Hall Bilayers

L. Fernandes dos Santos[1], Yu. A. Pusep[1], L. Villegas-Lelovsky[2,3], V. Lopez-Richard[2],G. E. Marques[2], G. M. Gusev[4], D. Smirnov[5]

[1]*Instituto de Física de Sao Carlos, Universidade de Sao Paulo, 13560-970 Sao Carlos, SP, Brazil*
[2]*Departamento de Física, Universidade Federal de Sao Carlos, 13565-905 Sao Carlos, SP, Brazil*
[3]*Instituto de Física, Universidade de Brasília, 70910-900 Brasília, DF, Brazil*
[4]*Instituto de Física da Universidade de Sao Paulo, 05315-970 Sao Paulo, SP, Brazil*
[5]*National High Magnetic Field Laboratory, Tallahassee, Florida 32312, USA*

Circular-polarization-resolved magneto-photoluminescence was used to probe the spin character of electron and hole states in a GaAs/AlGaAs strongly coupled double-quantum-well system. In the low magnetic field regime shown in Fig.1(b), circular polarization and integrated photoluminescence intensities of the PL lines associated with symmetric and antisymmetric electron states present clear out-of-phase oscillations between integer values of the filling factor ν. These oscillations are caused by magnetic-field-induced changes in the population of the Landau levels (LLs) near to the Fermi level and may be understood in terms of a simple single-particle model [1]. In strong quantizing magnetic field regime ($\nu < 4$) shown in Fig.1(a), when the cyclotron energy dominates, the electron energy spectrum of this system is composed of four closely spaced LLs and it has spin and pseudospin (associated with layer) degrees of freedom. The interaction among electrons makes them accommodating over the LLs to minimize the total energy and thus, resulting in a new ground state. Direct evidences for interaction effects are: (i) the nonlinear dependencies of the LL energies on the magnetic field resulting in the symmetric-antisymmetric gap shrinkage at $\nu = 3$, (ii) the unexpected behavior of the integrated PL intensity and (iii) the changes in the electron polarization. Our observations indicate to depolarization of the ferromagnetic ground state at $\nu = 2$ due to exchange interaction [2].

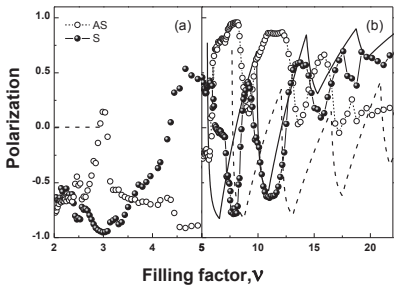

Fig.1. Polarizations of the PL lines assigned to the symmetric (closed circles) and antisymmetric (open circles) optical transitions measured as functions of the filling factor. Dashed line in panel (a) shows expected single-electron behavior, while full and dashed lines in panel (b) were calculated using multi-band k·p method.

[1] L. Fernandes dos Santos,Yu. A. Pusep,L. Villegas-Lelovsky,V. Lopez-Richard,G. E. Marques,G. M. Gusev,D. Smirnov,and A. K. Bakarov,Phy. Rev. B **86**, 125415 (2012).
[2] Yu.A. Pusep, L. Fernandes dos Santos, G. M. Gusev, D. Smirnov and A. K. Bakarov, Phys. Rev. Lett. **109**, 046802 (2012).

MoP82

Broken Translation Symmetry and Edge States

A. Matulis

Semiconductor Physics Institute, Center of Physical Sciences and Technology, Goštauto 11, LT-01108 Vilnius, Lithuania

The successive miniaturization of graphene-based electronic devices has triggered a broad interest in edge states that essentially influence the electronic band structure and electronic transport properties of nanometer-sized samples (see, for instance [1] and references there). The appearance and properties of these localized states depend sensitively on microscopic details of the edge, particularly these properties depend on the orientation of the edge in respect to the primitive vectors of the lattice like different so called *zigzag* and *armchair* edges in graphene. The mathematical description of the edge states is more complicated as compared with the bulk states because the edge breaks some translation symmetries, and this breaking is different for the above mentioned different edges. This feature isn't the prerogative of the particular graphene lattice but is inherent to any other lattice if the microscopic structure of it is taken into account.

The purpose of the present report is to illustrate the interplay of the above mentioned translation symmetry breaking and the particular properties of the edge states making use of the simplest model square lattice. In the case of the most symmetric edge (when its direction coincides with the primitive vector) we used the translation along the edge symmetry for transforming the two dimensional (2D) tight binding method equations to more simple 1D eigenvalue problem. The exact solution of the latter one was obtained by means of the Bethe's Ansatz which was checked by the numerical diagonalization. When the direction of the edge doesn't coincide with primitive vector the above mentioned symmetry is broken. Nevertheless it can be restored enlarging the primitive cell and the number of wave function components, what enables to use the above procedure. The edge state appears in the case when there is a force that keeps the electron close to the edge. The role of this force can be played by the additional local potential of atoms at the edge, or the modified electron tunneling amplitude along it. The influence of both these factors to the edge state properties is studied and the relation of them to the broken translation symmetry is traced. Thus, in the case of most symmetric edge the electron motion along it changes the effective local potential, and consequently, the edge state energy shift depends essentially on electron momentum along the edge, while in the less symmetric edge case the local potential and tunneling amplitude acts in a similar way.

[1] K. Wakabayashi *et al*, Sci. Technol. Adv. Mater. **11**, 054504 (2010).

Spin-orbit coupling as an intrinsic pinning mechanism for stripe orientation in high Landau levels

Inti Sodemann, Allan H. MacDonald
Department of Physics, University of Texas at Austin, Austin, Texas 78712
{sodemann,macdpc}@physics.utexas.edu

We propose that the source of the unidentified "native" anisotropy of the quantum Hall stripes phase in narrow quantum wells is the combined influence of Rashba and Dresselhaus spin-orbit interactions. Separately Rashba and Dresselhaus interactions have global rotational invariance, but this symmetry is lost when both terms are present so that [110] and $[1\bar{1}0]$ directions are not equivalent. We show that, to leading order in spin-orbit-coupling strength, the lowest energy stripe orientation is determined solely by the relative sign of the Rashba and Dresselhaus terms. When Rashba and Dresselhaus interactions have the same sign the preferred orientation is expected to be [110], in agreement with observations in GaAs. Within Hartree-Fock, we also estimate the anisotropy energy and find close agreement with its experimental determination from tilted magnetic field measurements.

MoP84

Insulating Phase in the Dynamically Nuclear Spin Polarized ν=2/3 Quantum Hall State

S. Tsuda [1], A. Fukuda [2], M. H. Nguyen [1], D. Terasawa [2] and A. Sawada [3]

[1] *Graduate School of Science, Kyoto University, Kyoto 606-8502, Japan*
[2] *Department of Physics, Hyogo College of Medicine, Nishinomiya, Hyogo 663-8501, Japan*
[3] *Research Center for Low Temp. and Mat. Sci., Kyoto Univ., Kyoto 606-8501, Japan*

Dynamic nuclear spin polarization (DNP) is one of the most promising techniques to manipulate nuclear spins to utilize spin-electronics device such as quantum processing. In the fractional quantum Hall state (QHS), the Landau level filling factor ν=2/3 QHS is suitable to carry out the DNP because of the affordable existence of the spin transition point. At the transition point where the spin-polarized and unpolarized domains are energetically degenerate, slow magnetic sweep greatly enhances the magnetoresistance R_{xx} [1] owing to the occurrence of the DNP through hyperfine interactions when electrons pass the domain wall [2]. However, the mechanism of the huge enhancement of the R_{xx} has not been revealed yet. One of the reasons is that such resistance-enhanced state (RES) is a transient state staying for several hundred seconds [3], and thus quick measurements are necessary to investigate the properties of the RES.

In this study, we have established the quick measurement scheme to observe the temperature dependence of the R_{xx} in the RES using the self-heating method by the large current, and confirm that the short-time application of the large current does not affect the intrinsic RES nature. Figure 1 demonstrates the temperature T dependence of the R_{xx} before and after the DNP. The DNP is carried out with 37.7 Hz and 60 nA AC current for about 30 min around ν=2/3. The R_{xx} is measured with a low frequency lock-in technique with small current of 5 nA. Surprisingly, the temperature derivative of the R_{xx} is negative after DNP in contrast to that it is positive before DNP. This fact indicates that the RES is an insulating state. Figure 2 shows the $R_{xx}/T - T^{-1/2}$ plot after DNP, implying that the solid line is a standard fit in the 2-dimensional Anderson insulator [4]. In the conference, we discuss relationships between the origins and mechanisms of the RES and an Anderson localization induced by nuclear spin polarization in detail.

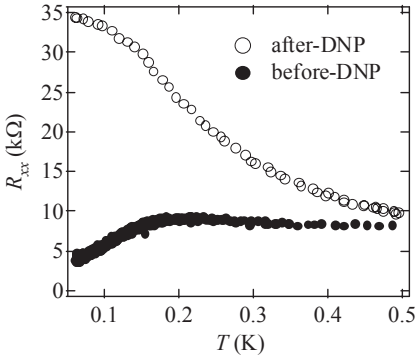

Fig. 1 Temperature dependence of the R_{xx} before and after DNP.

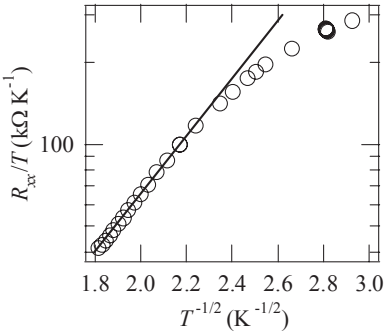

Fig. 2 $R_{xx}/T - T^{-1/2}$ plot after DNP.

[1] S. Kronmüller *et al*., Phys. Rev. Lett. **81**, 2526 (1998).
[2] S. Kronmüller *et al*., Phys. Rev. Lett. **82**, 4070 (1999).
[3] K. Iwata *et al*., J. Phys. Soc. Japan. **79**, 123701 (2010).
[4] Y. Ono, J. Phys. Soc. Japan. **51**, 237 (1982).

Shot noise of quasiparticles at local fractional quantum Hall states measured by a cross correlation technique

Masayuki Hashisaka [1], Tomoaki Ota [1], Koji Muraki [2] and Toshimasa Fujisawa [1]

[1] *Department of Physics, Tokyo Institute of Technology, Meguro, Tokyo, Japan*
[2] *NTT Basic Research Laboratories, NTT Corporation, Atsugi, Japan*

Edge channels (ECs) along the boundary of fractional quantum Hall (QH) states are regarded as chiral Luttinger liquids (CLLs). Charge tunneling between ECs through a quantum point contact (QPC) reflects fractional charge of quasiparticles [1] and CLL nature of ECs [2] as evidenced in shot noise measurements. On the other hand, measurement of current through a QPC in the QH regime suggested the importance to consider quasiparticle tunneling through the constriction region of a *local fractional QH state* [3]; even when the bulk filling factor (ν_B) is an integer, the local filling factor (ν_{QPC}) can be a fraction, since negative voltage applied to the split gate electrodes modifies the local electron density at the QPC. Here, we report the direct observation of fractional charge of quasiparticles at various ν_{QPC} by shot noise measurements. While the previous shot noise measurements have focused on the edge of the bulk fractional QH states, we are motivated to clarify quasiparticle tunneling through the local fractional QH state connected to the integer QH region.

Figure 1 shows the schematic of the device and the measurement setup. We inject DC current (I_1) from the Ohmic contact Ω_1 by applying a source-drain voltage (V_{sd}). The current I_1 flows to the QPC and is partitioned to I_2 and I_4, which are drained at Ω_2 and Ω_4. The current fluctuations ΔI_2 and ΔI_4 are converted to voltage fluctuations by cryogenic transimpedance amplifiers and measured with an analog-digital converter. We evaluate the shot noise caused at the QPC by calculating the cross-correlation $S_{21} = \langle \Delta I_2 \Delta I_4 \rangle$ in frequency band of 300 ~ 700 kHz. Figure 2 shows the typical V_{sd} dependence of S_{21} measured at 80 mK at magnetic fields of B = 8.8 T (ν_B = 1) and 4.4 T (ν_B = 2). The transmission probability T_1 of the EC of the lowest Landau level at V_{sd} = 0 is fixed at $T_1 \cong 1/3$ (Conductance from Ω_1 to Ω_4 is $G_{41} = e^2/3h$ at both bulk filling factors). The obtained S_{21} is negative due to the binominal distribution of quasiparticles. While the data at B = 4.4 T are well fitted by the calculation for free electrons (tunneling charge $e^* = e$: solid line), those at 8.8 T are close to the shot noise of $e^* = e/3$ at V_{sd} > 100 μV (dashed line). Moreover, we observed non-monotonic enhancement of the shot noise near V_{sd} = 30 μV, which indicates the CLL nature of ECs at local fractional QH states.

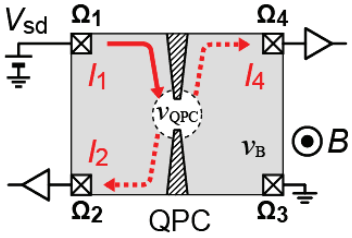

Fig. 1 Schematic of the device and the measurement setup.

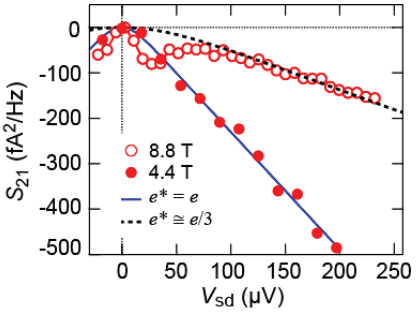

Fig. 2 Source-drain voltage (V_{sd}) dependence of S_{21} at $T_1 \cong 1/3$ at bulk filling factors of B = 8.8 T (open circles) and 4.4 T (filled circles).

[1] R. de-Picciotto *et al*., Nature **389**, 162 (1993); L. Saminadayar *et al*., Phys. Rev. Lett. **79**, 2526 (1999). [2] D. C. Glattli *et al*., Physica E **6**, 22 (2000); Y. C. Chung *et al*., Phys. Rev. B **67**, 201104(R) (2003). [3] S. Roddaro *et al*., Phys. Rev. Lett. 93, 046801 (2004).

MoP86

Giant Zeeman-splitting induced Spin Hall Effect in Dirac Fermions system in HgTe quantum wells

D.A.Kozlov [1,2], Z.D.Kvon [1,2], D.Weiss [3], N.N.Mikhailov[1], and S.A.Dvoretsky[1]

[1] *Instiutte of Semiconductor Physics, Novosibirsk, Russia*
[2] *Novosibirsk State University, Russia*
[3] *Regesburg University, Regensburg, Germany*

We report the observation of a giant nonlocal effect in Dirac point of a single valley gapless Dirac fermions system in HgTe quantum wells (QW) with the thickness d = 6.6 nm closed to the critical one corresponding to a transition from the direct to inverted band structure. We attribute this nonlocality to Zeeman splitting induced spin-Hall effect recently observed in graphene [1,2]. Unlike graphene the found nonlocality expands on macroscopic scale of several hundreds microns due to very long spin relaxation length.

The samples studied were the Hall bars with a width of 50 μm and a distance of 100 μm and 350 μm between voltage probes were fabricated by means of photolithography on the basis of (013)-oriented HgTe quantum wells with thickness 6.6 nm. As were shown recently in cyclotron resonance and weak localization experiments [3,4] in such kind of QW the system of single valley gapless 2D Dirac fermions is realized. Next, the ohmic contacts were prepared by annealing of indium. After that a double dielectric layer consisting of 100 nm SiO_2 and 200 nm Si_3N_4 was deposited at temperature 100°C. Then TiAu metallic gate was evaporated on the top of structure. The final device represented field effect transistor in which the conductivity of 2D electron system in HgTe QW was be able to change by applying the gate voltage V_g. The measurements of local and nonlocal resistance in the described samples were carried out in the temperature range 1.5 K – 10 K in a magnetic field up to 2 T by means of a standard Lock-in detection technique at frequencies 6–32 Hz with the excitation currents 1–100 nA through the sample. The main results are as follows:

1. At temperature range 1.5 – 25 K and in magnetic field range 0.3 – 1 T the nonlocal transport response (nonlocal resistance $\mathbf{R_{nonloc}}$) was observed at Dirac point of all studied samples while no nonlocal signal was seen out of its vicinity. Magnetic field dependence of nonlocal response has the threshold character with $B_{th} \approx 0.3$ T then at it saturates at B ≈ 0.5 T and does not change up to 1 T. As the temperature increases $\mathbf{R_{nonloc}}$ falls as $\mathbf{R_{nonloc} \approx T^{-1}}$.

2. At 1.5 K and B = 1 T nonlocality has the giant magnitude. The nonlocal resistance $\mathbf{R_{nonloc}}$ is in fact equals to local resistivity $\boldsymbol{\rho_{xx}}$ when the distance between current probes and potential ones is 100 μm. The increasing of this distance up to 350 μm leads to strong exponential fall of $\mathbf{R_{nonloc}}$.

3. Qualitatively the found nonlocality is very similar to that observed recently in graphene [1.2] and according to the theory developed in [2] can attribute to Zeeman splitting induced spin-Hall effect in Dirac point of the system studied. It means that giant nonlocal response reflects "giant" value of spin-Hall coefficient close to 1 as in graphene, which is 10^3 times bigger than in ordinary spin-Hall effect. But in comparison with graphene in our case nonlocality expands on much longer distance (several hundreds microns). We suggest that it is due to much higher Zeeman splitting in HgTe-based Dirac system than in graphene.

[1] D.A.Abanin, S.V.Morozov, L.A.Ponomarenko et al, Science, **332**, 328 (2011).
[2] D.A.Abanin, R.V.Gorbachev, K.S.Novoselov et al, PRL, **107**, 096660 (2011).
[3]. Z.D.Kvon, D.A.Kozlov, S.N.Danilov et al, JETP Letters, **94**, 816 (2011)
[4]. D.A.Kozlov, Z.D.Kvon, N.N.Mikhailov, S.A.Dvoretsky, JETP Letters, **96**, 730 (2012)

Two-phonon scattering in graphene in the quantum Hall regime

A. M. Alexeev and M. E. Portnoi

School of Physics, University of Exeter, Stocker Road, Exeter EX4 4QL, UK

One of the most distinctive features of graphene is its huge inter-Landau-level splitting in experimentally attainable magnetic fields resulting in the room-temperature quantum Hall effect. We have calculated the longitudinal conductivity due to two-phonon scattering in graphene in a quantizing magnetic field over a broad range of temperatures. The multi-phonon scattering mechanism [1] is known to be negligible for conventional two-dimensional systems under the quantum Hall conditions apart from exotic cases such as magneto-roton dissociation in phonon spectroscopy [2]. However, our calculations show that this mechanism dominates in the high-temperature quantum Hall regime in graphene, since at elevated temperatures the energy of an acoustic phonon with a wavevector comparable to the inverse magnetic length is much smaller than the temperature; therefore, a number of such phonons increases drastically. Single-phonon processes in pristine graphene in this regime remain suppressed due to momentum and energy conservation requirements. We show that the two-phonon scattering mechanism provides a significant error in Hall conductivity measurements, and it is therefore a major obstacle in using graphene as a room-temperature quantum Hall standard of resistance.

[1] V. N. Golovach and M. E. Portnoi, Phys. Rev. B **74**, 085321 (2006).
[2] V. M. Apalkov and M. E. Portnoi, Phys. Rev. B **66**, 121303 (2002).

Quantum point contacts in the fractional quantum Hall regime

S. Baer, C. Rössler, T. Ihn, K. Ensslin, C. Reichl, and W. Wegscheider
Solid State Physics Laboratory, ETH Zurich, 8093, Switzerland

Two-dimensional electron systems (2DES) at low temperatures and in strong magnetic fields show a rich spectrum of highly degenerate, incompressible ground states. Apart from the Laughlin sequence at filling factors ν = 1/m (m odd integer), other exotic states like the ν = 5/2 state have been observed [1]. Many properties of these states are unknown and of high interest for current research.

We investigate transport through quantum point contacts (QPCs) in the integer and fractional quantum Hall (FQH) regime. We study the influence of the potential shape of QPCs on the formation and the energy gap of fractional states in the channel. Fig.1a shows the transconductance of a tunable QPC on a high-mobility 2DES. Black regions correspond to integer and fractional quantum Hall states formed in the QPC or complete pinch-off. In the transition regime between different filling factors, resonances corresponding to the self-consistent formation of potential minima and maxima in the channel modulate the conductance. Finite bias measurements of these systems show a spectrum of conductance enhancement and suppression, currently not understood in detail. In the weak backscattering regime, we study the tunneling properties of the FQH states of the second Landau level. Fully quantized ν = 5/2 and ν = 7/3 states and pronounced reentrant integer quantum Hall states can be observed in the QPC (see Fig.1b). Finite bias measurements allow for an investigation of the tunneling properties of these states [2].

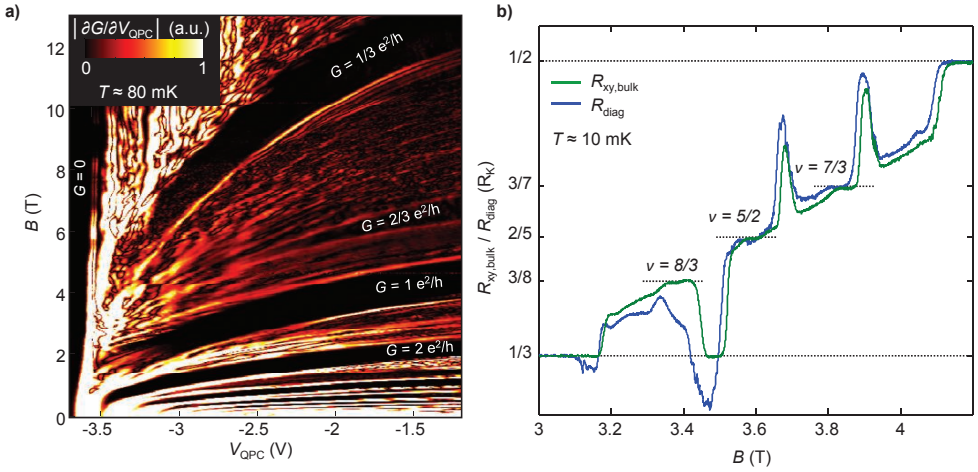

Fig. 1a: Transconductance through a QPC as a function of the gate voltage V_{QPC} and the magnetic field B. Black regions correspond to the transmission of integer or fractional quantum Hall states through the QPC. Fig 1b: R_{diag} and $R_{xy,bulk}$ (in multiples of R_K) as a function of the magnetic field. The diagonal resistance across the 1.2 µm wide QPC reveals a fully quantized ν = 5/2 and ν = 7/3 states with weak backscattering at the QPC constriction.

[1] R. Willett et al., Phys. Rev. Lett. **59**, 1776 (1987)
[2] I. P. Radu et al., Science **320**, 899 (2008)

Self-consistent transport and boundary conditions in finite quantum Hall devices

Tobias Kramer[1,2]

[1] *Institut für Theoretische Physik, Universität Regensburg, Germany, and*
[2] *Department of Physics, Harvard University, USA*

The theoretical result for the current-density distribution in Hall devices depends critically on the choice of boundary conditions at the source (injection) and drain contacts. In the classical limit, I show results from the (to my knowledge) first microscopic ab initio calculation [1] of the Hall potential of 10,000 interacting electrons, resulting in the potential shown in Fig. 1.

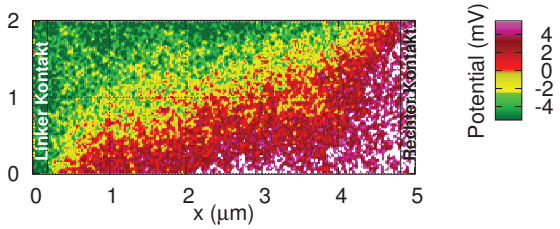

Fig. 1: Theoretical many-electron (10,000 Coulomb interacting electrons) computation of the classical Hall potential in a GaAs semiconductor device. The form of the Hall potential is directly linked to the boundary conditions at the injection source contact and requires a full account of electron-electron interactions [1].

In conventional semiconductor structures and graphene, a very similar potential to the one obtained in the classical case has been observed by various potential mapping methods, such as scanning probe microscopy and the photoelectric effect. On the theoretical side, this finding is surprising and shown to be incompatible with both, the edge state picture of the QHE and the bulk disorder picture of delocalized/localized states [1, 2]. I discuss how the different theoretical models of the QHE depend on the choice of boundary conditions and why the result show in Fig. 1 requires to solve the current distribution in a completely self-consistent fashion (including interactions) for a finite Hall device [2]. Both, the finite size and the self-consistently are often lacking in mesoscopic models of transport in a strong magnetic field and pose tremendous computational challenges. The usage of massively parallel graphics processing units (GPU) is crucial to obtain a self-consistent picture already for the classical case [1] and holds great promises to speed up fully quantum-mechanical simulations. I discuss how GPU computing can be applied to mesoscopic systems in an efficient way [3].

[1] T. Kramer, V. Krueckl, E. Heller, and R. Parrott *Self-consistent calculation of electric potentials in Hall devices* Phys. Rev. B, 81, 205306 (2010).
[2] T. Kramer, C. Kreisbeck, V. Krueckl, E. Heller, R. Parrott, and C.-T. Liang *Theory of the quantum Hall effect in finite graphene devices* Phys. Rev. B **81**, 081410(R) (2010).
[3] T. Kramer *electronic resource: GPU program resources available at* `http://quantumdynamics.wordpress.com/gpu`

MoP90

Non-Markovian spin transfer dynamics in optically excited diluted magnetic semiconductor quantum wells

M. Cygorek, C. Thurn, and V.M. Axt

Institut für Theoretische Physik III, Universität Bayreuth, 95440 Bayreuth, Germany

Diluted magnetic semiconductors (DMS) combine the versatility of the semiconductor host material with strong magnetic properties of the integrated dopants, making them promising candidates for future spintronic devices. A crucial step towards the realization of such devices is to gain a profound understanding of the exchange interaction between the spins of localized dopants and free carriers. In the literature, the exchange interaction is usually split up into the mean field part, which leads to a coherent precession of dopant and carrier spins around one another, and the spin dependent scattering part, which is responsible for spin transfer dynamics between the two spin subsystems. The latter effect is usually treated on the level of Markovian rate equations.

In this contribution we use a recently developed quantum kinetic approach [1] which explicitly accounts for the finite memory depth of the system to simulate the spin transfer dynamics in a (ZnMn)Se DMS quantum well.

We find pronounced signatures of a coherent exchange of spin between the electronic and the Mn subsystem: while an initially prepared total electron spin simply decays exponentially in the Markovian limit, time-dependent changes of the sign of the total electron spin are predicted by our quantum kinetic model [2]. Such non-Markovian features are usually connected to a large memory depth of the system. However, the spin memory function of the considered system turns out to decay on a sub-femtosecond timescale and, thus, more than three orders of magnitude faster than the electron spin. This seeming contradiction can be resolved by noting that in the Markovian limit not only memory effects are neglected but also the spin dependent electron redistribution over the carrier energies is missing, which in the full quantum kinetic equations occurs due to the energy-time uncertainty. The latter is crucial for the occurrence of sign reversals of the total electron spin, as we can show by artificially suppressing the redistribution of electronic energies while still accounting for the spin memory of the system [2].

Finally, we demonstrate that significant deviations from the Markov limit are most clearly observable if the spin polarized electrons are excited by two laser pulses of different color and opposite circular polarizations such that there is practically no net transfer of angular momentum from the laser field to the electronic system. Under these distinguished excitation conditions, the total electron spin should remain zero according to the standard Markovian rate equations for a DMS quantum well. In contrast, our quantum kinetic simulations predict a sizeable build-up of spin polarization in the conduction band which exhibits oscillations that persist for times much longer than the duration of the exciting laser pulses. These oscillations represent a clear signature of a coherent non-thermal exchange of spin between the electronic and the Mn subsystems.

[1] C. Thurn and V. M. Axt, Phys. Rev. B **85**, 165203 (2012).
[2] C. Thurn, M. Cygorek, V. M. Axt and T. Kuhn, ArXiv:1303.4322 (2013).

Dynamical spin reversion with spin polarized current

C. Hübner[1], B. Baxevanis[1], and D. Pfannkuche[1]

[1] *I. Institute of Theoretical Physics, Hamburg University*

Understanding the time evolution of a magnetization reversal process is crucial for the ongoing developments in logical spin structures. In our study based on a master equation approach we relate the dynamical properties of a quantum spin driven out of equilibrium to the excitation and relaxation processes involved. As a specific case our theoretical study provides inside into the dynamical switching processes between two fully spin polarized states of a Fe cluster absorbed on a Cu surface, probed with a spin polarized scanning tunneling microscope[1]. In this setup the polarized current switches the spin of the cluster between the two polarized states across an anisotropy barrier. Rates for the intermediate excitation and relaxation processes are calculated by taking into account cotunneling between the cluster and tip/surface. Excitation of the cluster arises due to inelastic spin transfer from the electron source. Fast relaxation is caused by coupling to the surface. We control the ratio between excitation and relaxation by changing the voltage between source and drain or varying the coupling of the cluster spin to the electron reservoirs. From the investigation of transient dynamics and the stationary limit, the current driven switching between the two fully spin polarized states can be expressed by a lifetime and an occupation probability. Both quantities are directly related to the in- and out-of-plane anisotropy of the cluster spin. Comparison between theory and measurement allowed us to extract the magnetic parameters unknown to the experiment. We also discuss the influence of temperature and external magnetic fields.

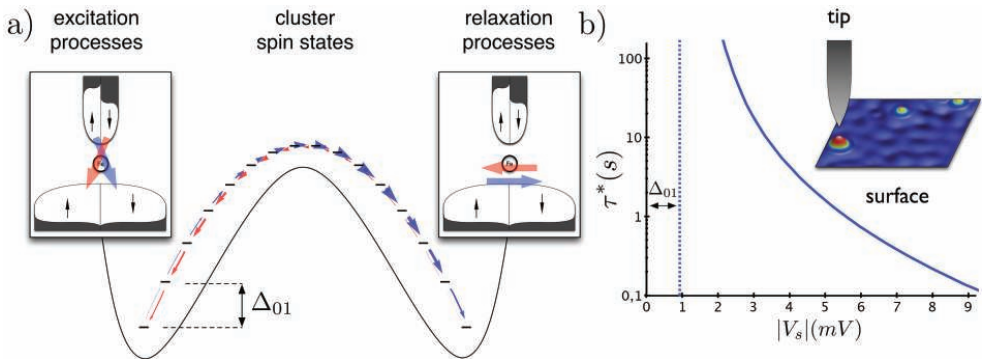

Figure 1: In a) an anisotropy potential with eigenstates of a $S = 15/2$ spin is displayed. Arrows represent the rates for excitation and relaxation processes. The mean lifetime is plotted in b) against the voltage between tip and surface in a scanning tunneling microscopy setup. Δ_{01} indicates the energy for the inelastic excitation out of the ground state.

[1] A. A. Khajetoorians, B. Baxevanis, C. Hübner, T. Schlenk, S. Krause, T. O. Wehling, S. Lounis, A. Lichtenstein, D. Pfannkuche, R. Wiesendanger, Science **339**, p. 55-59 (2013).

MoP92

Anisotropy of the RRKY interaction in ferromagnetic (Ga,Mn)As

Cezary Śliwa[1], Magdalena Birowska[2], Jacek A. Majewski[2], and Tomasz Dietl[1,2]

[1]*Institute of Physics, Polish Academy of Sciences, al. Lotników 32/46, 02-668 Warszawa, Poland*
[2]*Faculty of Physics, University of Warsaw, ul. Hoża 69, 00-681 Warszawa, Poland*

Ultrathin layers of the dilute ferromagnetic semiconductor (Ga,Mn)As have been studied recently by the method of subsequent chemical thinning and oxidizing steps [1]. The reported monotonic reduction of Curie temperature has been attributed to a gradient of the material properties (defect concentration) and the surface effect (donor traps). A vertical gradient of the effective magnetic anisotropy has been reported in [2]. In this contribution we investigate theoretically if the finite size itself may have an effect on the layer properties such as the perpendicular magnetic anisotropy. We also find that the microscopic mechanism which we consider significantly affects the predictions for the in-plane uniaxial component of the magnetic anisotropy.

The ferromagnetic interaction in (Ga,Mn)As is mediated by *p*-type carriers (RKKY interaction), which are subject to the spin-orbit interaction. Therefore, the anisotropy of the exchange interaction in the spin space is dependent on the spatial coordinates (relative position of the interacting spins or the wave vector of the applied perturbation). In the mean field approximation this translates into e.g. a thickness dependence of the perpendicular magnetic anisotropy. We find such a contribution to the magnetic anisotropy significant for layers thinner than about 10 lattice constants.

On the other hand, (Ga,Mn)As exhibits an in-plane uniaxial magnetic anisotropy, whose origin has been puzzling the researchers for a long time, and which we recently assigned to an asymmetry in the nanoscale distribution of the magnetic impurity predicted by an *ab initio* study [3]. Here, the spatial asymmetry of the impurity distribution translates into a contribution to the magnetic anisotropy, which is not captured by the Zener model [4] employed in [3].

We compare the total magnitude of the in-plane uniaxial anisotropy calculated according to this method (effective strains in the Zener model together with the RKKY contribution) with the results of a direct *ab initio* approach.

[1] O. Proselkov, D. Sztenkiel, W. Stefanowicz, M. Aleszkiewicz, J. Sadowski, T. Dietl, and M. Sawicki, Appl. Phys. Lett. **100**, 262405 (2012).
[2] H. Son, S. Chung, S. Yea, S. Kim, T. Yoo, S. Lee, X. Liu, and J. K. Furdyna, Appl. Phys. Lett. **96**, 092105 (2010).
[3] M. Birowska, C. Śliwa, J. A. Majewski, T. Dietl, Phys. Rev. Lett. **108**, 237203 (2012).
[4] T. Dietl, H. Ohno, F. Matsukura, J. Cibert, and D. Ferrand, Science **287**, 1019 (2000).

Chemical potential investigations of the surface of ferromagnetic-superconducting multilayers

K. Filar [1] , K. Rogacki [1,2] , P. Przyslupski [3] , V. I. Nizhankovskii [1]

[1] *International Laboratory of High Magnetic Fields and Low Temperatures, Gajowicka 95, 53-421 Wroclaw, Poland*
[2] *Institute of Low Temperature and Structure Research, Polish Academy of Sciences, Okolna 2, 50-422 Wroclaw, Poland*
[3] *Institute of Physics, Polish Academy of Sciences, Lotnikow Ave. 32/46, 02-668 Warsaw, Poland*

Chemical potential μ is the only one thermodynamical parameter which can be easy measured on low-dimensional systems like thin films or a two-dimensional electron gas. It is especially useful for multilayers because the properties of the topmost layer with thickness about the Debye screening length are investigated.

The method to measure the change of the chemical potential $\Delta\mu = \mu(H) - \mu(0)$ is based on the determination of the change in charge on the measuring capacitor consisting of the sample under investigation and the reference electrode. The idea is closely related to Lord Kelvin's investigations of the contact potential difference. In general, the contact potential difference differs from the chemical potentials difference by the magnitude of the potential difference of the double charged layers present at the surface of bulk metals. If the influence of a magnetic field on the capacitance C and in the work function of the reference electrode is negligibly small then $\Delta Q = -C\Delta\mu/e$, where e is the charge of current carriers.

Measurements of the chemical potential of superconducting and ferromagnetic films in stationary magnetic field were published many years ago [1]. The purpose of the present work is to investigate heterostructures consisting of superconducting and ferromagnetic layers [2]. The heterostructures were characterized by magnetic and transport measurements. Chemical potential investigations were done using the field-modulation technique that significantly increases the sensitivity of the method. Field was modulated at frequency 13.7 Hz with amplitude about 0.015 T. Charge was measured by the Keithley 642 Electrometer. For lock-in detection Signal Recovery 7265 and Signal Recovery 7225 were used.

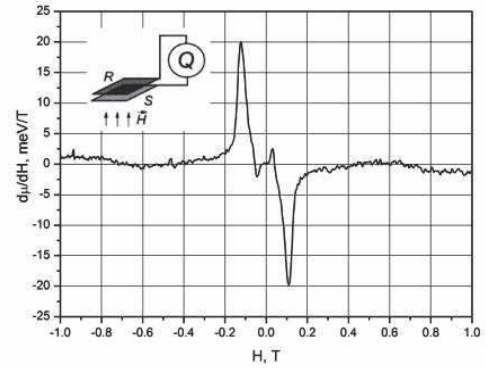

Figure on the left shows the results for $La_{0.7}Sr_{0.3}MnO_3$ epitaxial 90 nm film. Peculiarities observed in dependence of $d\mu/dH$ on magnetic field result from the behavior of magnetization and magnetostriction.

[1] V. I. Nizhankovskii, S. G. Zybtsev, Phys. Rev. B **50**, 1111 (1994).
[2] P. Przyslupski et al., Phys. Rev. B **69**, 134428 (2004).

MoP94

Selected physical properties of auto-catalytic GaAs:Mn nanowires grown by molecular beam epitaxy on silicon substrates

K. Gas[1]*, J. Sadowski[2,1], T. Kasama[3], A. Siusys[1], W. Zaleszczyk[1], T. Wojciechowski[1], J. F. Morhange[4#], A. Altintaş[5], H. Q. Xu[6] and W. Szuszkiewicz[1]

[1] *Institute of Physic PAS, al. Lotników 32/46, PL-02-668 Warszawa, Poland,*
[2] *MAX-IV laboratory, Lund University, Box 118, SE-221 00 Lund, Sweden,*
[3] *Center for Electron Nanoscopy, TUD, DK-2800 Kongens Lyngby, Denmark,*
[4] *Institut des Nanosciences de Paris, UMR 7588, UPMC, 4 pl. Jussieu, 75252 Paris, France,*
[5] *Division of Solid State Physics and the Nanometer Structure Consortium, Lund University, Box 118, SE-221 00 Lund, Sweden,*
[6] *Key Laboratory for the Physics and Chemistry of Nanodevices and Department of Electronics, Peking University, Beijing 100871, China*

GaAs nanowires (NWs) are attractive for potential applications in nanodevices, since they are built from a material which is widely used in optoelectronics. For functional devices the control over the polarity and concentration of charge carriers, i.e., doping of the given semiconducting materials is essential. However, since the growth of the NWs is governed by principles different from the case of bulk crystal or thin film growth, the doping mechanisms of a NW are still not fully recognized. Particularly interesting is doping GaAs NWs with Mn. In GaAs the Mn^{2+} ions occupying Ga sites and provides both magnetic moments, due to the spin polarisation of the half filled 3d shell, and acts as an effective acceptor, what opens possibility of using Mn-doped GaAs NWs for studying interesting phenomena associated with interactions between charge carriers or photons with localized, single Mn spins.

In this work we report on the results of our studies concerning the GaAs:Mn NWs. The NWs were grown in self-catalytic growth mode on oxidized Si(100) surface by MBE and characterized by SEM, TEM, PL, CL, Raman scattering and electron transport measurements. In order to analyze the influence of Mn presence on the physical properties of NWs the undoped GaAs NWs obtained in otherwise exactly the same manner as those containing Mn were also investigated. The results of resistivity measurements as a function of temperature showed that contrary to undoped GaAs NWs the Mn doped ones are conductive. The dependence of the I-V characteristics on the voltage applied to the substrate back gate revealed the p-type conductivity, confirming the acceptor character of Mn impurities embedded into NW. This finding is in agreement with the results of PL and CL measurements, which confirmed the presence of Mn^{2+} acceptors located at Ga sites of the GaAs host lattice of the NWs. An anomalous temperature dependence of the exciton emission was observed for the first time for such NWs and explained by the ionization of the acceptor states. Our measurements demonstrated that the upper limit of Mn content for the NWs obtained in the manner described above corresponds to the doping level, i.e., is much lower than the Mn/Ga flux ratio (about 3%) applied during the MBE growth. The direct evidence that a substantial accumulation of Mn takes place inside the catalyzing Ga droplets at the top of the nanowires only was also found.

This work was partially supported by the EU within European Regional Development Fund through grant Innovative Economy (POIG.01.01.02-00-108/09) and by the grant N N202 128639 from the Ministry of Science and Higher Education (Poland).

* Corresponding author: kgas@ifpan.edu.pl.
# Retired.

Magneto-intersubband oscillations of a wide quantum well in an electrically tuned triangular antidot lattice

J. C. B. Pomayna[1], F. G. G. Hernandez[1], G. M. Gusev[1], N. C. Mamani[2], Yu. A. Pusep[2], and A. K. Bakarov[3]

[1]*Instituto de Física, Universidade de São Paulo, Caixa postal 66318 - CEP 05315-970, São Paulo, SP, Brazil*

[2]*Instituto de Física de São Carlos da Universidade de São Paulo, Caixa Postal 66318 CEP 05315-970, São Carlos, SP, Brazil*

[3]*Institute of Semiconductor Physics, Novosibirsk 630090, Rusia*

The resistance of a two-dimensional electron system in a wide quantum well with a triangular antidot lattice has been measured under perpendicular magnetic field. The antidot potential was electrically tuned while the system has two occupied subbands in the magneto-intersusbband (MIS) oscillations. The experimental data shows the evolution of the MIS oscillations and the geometrical resonance (GR) peaks, due to the commensurability of the cyclotron radius and lattice period, as the system was driven by the external gate from unmodulated to strongly modulated system.

Spin accumulation at the Fe/Si interface and two types of Hanle characteristics

Tomotsugu Ishikura, Zhixin Cui, Keita Konishi, Joungeob Lee and Kanji Yoh

Research Center of Integrated Quantum Electronics, Hokkaido University, Sapporo, Japan

Electrical spin injection into semiconductor, especially silicon, has been intensely investigated. Evaluation of spin accumulation in three-terminal Hanle set-up has raised intense debate on the origin of too high spin accumulation voltage and too short spin lifetime [1 - 4]. Typical arguments were sequential tunneling through interface traps [2], stray field at the interface due to interface roughness [3] and magnetic-filed-dependent tunnel resistance [4]. These in various tunneling barrier materials such as Al_2O_3 or MgO so that the bias dependence characterization could not modify tunnel characteristics so much. Here we report the spin accumulation at the Fe/Si interface without dielectric tunnel barrier to understand the spin accumulation mechanism in three terminal Hanle effect.

Fabricated sample structure consists on n-type high phosphorus doped ($\sim 10^{19}$ cm^3) SOI wafer with ion plantation method. Fe electrodes were grown by MBE on n^+-Si. Non-local spin valve characterization revealed spin relaxation time of 7.45ns and spin diffusion length of 1.66μm as shown in Fig.1. Three-terminal Hanle-type was composed of Fe electrode of 150×200 μm^2 and Ni silicide electrodes were used for non-ferromagnetic contacts. Bias current dependence of three terminals Hanle measurement results is shown in Fig.2. Two types of Hanle-like signals were observed to overlap. From Lorenzian fitting, spin lifetime were of the order of 400 ps and 3 ns for wider and narrower peaks, respectively. Compared the nonlocal spin lifetime (7.45 ns), the value of narrower peaks seems to be consistent, suggesting that the narrower peak to be Hanle signal whereas broader and tall peaks to be originated from other mechanism such as magnetic field dependent tunnel resistance [4]. Figure 3 shows the biased current dependence of Hanle-type signal on bias current. Disappearance of wider peak at high bias suggests tunneling resistance related origin which is consistent with Uemura case[4].

[1] S. P. Dash et al., Nature **462**, 491 (2009) [2] M. Tran et al., Phys. Rev. Lett. **102**, 036601 (2009).
[3] S. P. Dash et al., Phys. Rev. B **84**, 054411 (2011). [4] T. Uemura et al., App. Phys. Lett. **101**, 132411 (2012)

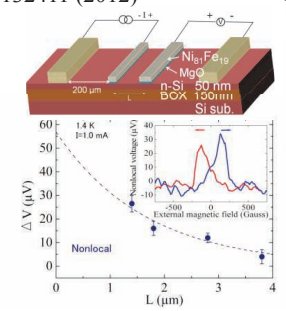

FIG .1. Nonlocal voltage as a function of length between ferromagnets including the schematics of nonlocal spin valve.

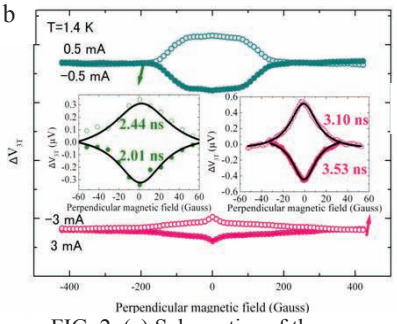

FIG. 2. (a) Schematics of three terminal Hanle geometry.
(b) Bias current dependence of three terminals Hanle effect at 1.3K.

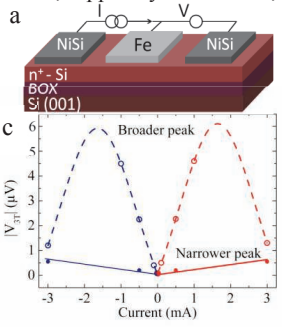

(c) Comparison of broader and narrower peaks dependence on biasd current in three terminal Hanle type signals.

Electron tunneling spectroscopy of 2D HgTe quantum well with inverted energy spectrum

Andrey A. Sherstobitov[1,2], Grigori M. Minkov[1,2], Aleksander V. Germanenko[2], Olga E. Rut[2], Nikolay N. Mikhailov[3],Sergei A. Dvoretski[3]

[1] *Institute of Metal Physics, UbRAS, Ekaterinburg, Russia.*
[2] *Ural Federal University, Ekaterinburg, Russia.*
[3] *Institute of Semiconductor physics, RAS, Novosibirsk, Russia.*

The progress in semiconductor technology allows us to get the high quality 2D heterostructures on gapless semiconductor HgTe. By the variation of the composition and width of the quantum well in this material we can tune the gap width and the energy spectrum. In particular at the well width of 6.3 nm this is the gapless semiconductor with Dirak like energy spectrum. Due to this fact these structures are attractive for experimentalists and theorists.

The electron tunneling spectroscopy is the tool to study the energy spectrum of semiconductor structures. In this method the differential conductivity of the contact between the metal and semiconductor separated by thin insulator is measured. In the simplest case the Fermi energy of semiconductor is independent on the applied voltage between the metal and semiconductor V_t. Then the applied voltage is equal to the difference between Fermi energies of metal and semiconductor. The differential conductivity of the contact is proportional to the density of states in the semiconductor at the Fermi energy of metal. So by the study of the differential conductivity versus V_t it is possible to obtain the energy spectrum of the semiconductor. In this work we present the study of the energy spectrum of 2D HgCdTe/HgTe/HgCdTe quantum well structure by this method.

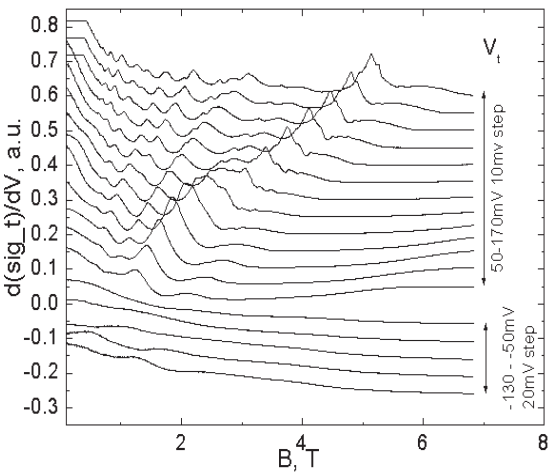

The samples was grown on [013] GaAs substrate. The width of quantum well HgTe was 20nm. Before preparation of the contacts (Al) the cap layer was partially etched by Br/Butanol based etchant. So we tune the conductivity of the barrier, in order to reach the measurable, but still tunneling, conductivity. It was found that the optimum conductivity is about few mkS. The measurement was carried out at the temperature (1.5-4.2) K in the magnetic fields up to 7 T.

The oscillations of the differential conductivity on V_t and the magnetic field were found in the investigated structures. Typical dependence of the differential conductivity on the magnetic field at different V_t is displayed on the figure. The analysis of these dependencies shows that, unlike the simplest case, in our case the Fermi level depends on V_t. The detailed analysis of the dependences allows us to shed light on the peculiarities of the spectrum of the two dimensional carriers and its dependence on the magnetic field in such interesting system.

This work has been supported in part by the RFBR (Grant Nos. 11-02-12126, and 12-02-00098).

MoP98

Transport via single and double quantum point contacts in 2D topological insulators

Chia-Wei Huang, Efrat Shimshoni, and Dmitry Gutman

Department of Physics, Bar-Ilan University, Ramat Gan, 52900, Israel

Sam T. Carr and A. Mirlin

Institute for Theoretical Condensed Matter physics, Karlsruhe Institute for Technology, Karlsruhe, Germany

We study transport properties of the helical edge states of 2D integer and fractional topological insulators (TI/ FTI), via one and two constrictions (quantum point contacts). Such constrictions can be made by adding a gate to the systems where the coupling between edge states on either side of 2D sample is electronically tuned by this gate. We study the stability of both the conducting (weak backscattering limit) and insulating fixed points (weak tunneling limit). Moreover, we explore interesting physics when double impurity is on resonance, leading to perfect transmission (weak backscattering limit) and Kondo physics (weak tunneling limit). Using renormalization group and duality mapping, we analyze phase diagrams for the following cases: (i) single constriction in FTI, which is a generalization of the single constriction in TI studied by J. Teo and C. Kane. (ii) two constrictions in TI, and (iii) two constrictions in FTI. We find different behaviors depending on interaction strength and particularly a regime where conductance is non-monotonic as a function of temperature in the experimentally accessible parameter regime

Transport properties of a 3D topological insulator on the basis of a strained high mobility HgTe film

D. A. Kozlov[1], Z. D. Kvon[1,2], D. Weiss[3], N. N. Mikhailov[1], S. A. Dvoretskiy[1]

[1] *A. V. Rzhanov Institute of Semiconductor Physics, 630090, Novosibirsk, Russia*
[2] *Novosibisk State University, 630090, Novosibirsk, Russia*
[3] *Regensburg University, 93053, Regensburg, Germany*

The discovery of 2D and 3D topological insulators (TI) has opened a new and exciting research field in condensed matter physics [1,2]. Recently a single Dirac cone has been observed by the angle resolved photoemission spectroscopy in the strained HgTe films [3]. However, there has been no clear evidence of the presence of 2D Dirac fermions in the transport properties in the mentioned above HgTe film. In our work we report the investigation of transport properties of a high mobility ($\mu = 4 \times 10^5\,\mathrm{cm^2/V{\cdot}s}$) 80 nm wide HgTe film furnished with a top gate. In our research we observed a controlled by the gate voltage transitions between three states: a 3D electron metal, 2D Dirac surface states and a 3D hole metal in the film. We performed transport measurements in a temperature range from 1.9 K to 15 K and in a magnetic fields up to 10 T and revealed several features and the whole of them are agreed with proposed model of three states. The gap in the energy spectrum of the film is found to be (15 meV), consistent with the recent calculations [3]. These main features observed are following:

1. Typical resistivity versus gate voltage dependencies $\rho_{xx}(V_g)$ at $T = 1.9\,\mathrm{K}$ in zero magnetic field is a smooth curve with a single maximum which corresponds Fermi energy near the top of the valence band. The gate voltage range corresponding TI state are bounded by valence band (E_v with arrow on a fig.) and conductive band (E_c on a fig.).

2. At the gate voltages corresponding to the Fermi level lying in the gap a quantum Hall effect is observed due to the 2D Dirac electrons from the two surfaces of the film.

3. When the Fermi level is outside the gap a scattering is detected between the 2D Dirac electrons and the bulk electrons/holes. Scattering with holes resulting in T^2-proportional positive temperature coefficient of resistance for $V_g < 2\,\mathrm{V}$.

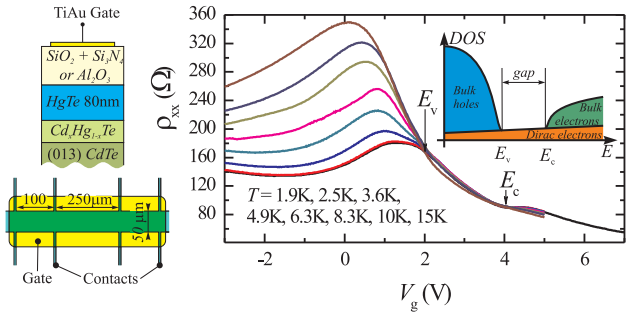

Figure 1: The sample schematic and $\rho_{xx}(V_g)$ dependence at zero magnetic field.

[1] M. Z. Hasan and C. L. Kane, Rev. Mod. Phys. **82**, 3045 (2010).
[2] X.-L. Qi and S.-C. Zhang, Rev. Mod. Phys. **83**, 1057 (2011).
[3] C. Brüne *et al.*, Phys. Rev. Lett. **106**, 126803 (2011).

MoP100

Spin polarization of surface states on (100) $Pb_{0.73}Sn_{0.27}Se$

B. M. Wojek[1], R. Buczko[2], S. Safaei[2], P. Dziawa[2], B. J. Kowalski[2], M. H. Berntsen[1], T. Balasubramanian[3], M. Leandersson[3], A. Szczerbakow[2], P. Kacman[2], T. Story[2], and O. Tjernberg[1]

[1] KTH Royal Institute of Technology, ICT Materials Physics, Electrum 229, 164 40 Kista, Sweden
[2] Institute of Physics, Polish Academy of Sciences, Aleja Lotników 32/46, 02-668 Warsaw, Poland
[3]MAX IV Laboratory, Lund University, P.O. Box 118, 221 00 Lund, Sweden

We present the experimental evidence for the spin polarization of the surface states on the (100) surface of $Pb_{0.73}Sn_{0.27}Se$ in the TCI phase as well as in the trivial one.
The recent discovery of topological crystalline insulators (TCI) [1-3] (stimulated by theoretical considerations [4,5]) widened the range of solids considered as hosting topologically protected surface states by systems from the family of IV-VI narrow band gap semiconductors. Our experiments aimed at revealing the topologically protected surface states on TCI, were successfully concluded by observation of such states on the (100) surface of $Pb_{1-x}Sn_xSe$ [1]. The properties of this solid solution are turned out to be particularly advantageous for studying the electronic structure of the TCI phase. In $Pb_{1-x}Sn_xSe$ crystals the strong relativistic effects result in a remarkable compositional evolution of their band structure leading to zero gap state for a specific composition $x=x_c$. For lower and higher Sn compositions the energy gap is open, but the parity of electronic states at band edges is reversed. The crystal with inverted parity of the states at the band edges (for $x>x_c$) hosts the topologically protected surface states. Thus, the properties of both TCI and trivial phases can be investigated in a single experiment, while the transition from one phase to another is induced by the change in temperature.
The experimental data were acquired by spin- and angle resolved photoelectron spectroscopy. The measurements were carried out at the I3 and I4 beamlines at the MAX-III synchrotron at MAX-lab, Lund University, Sweden. Since The band-structure inversion in $Pb_{0.73}Sn_{0.27}Se$ occurs at $T \approx 250$ K, the normal insulator phase was studied at T=300 K while the TCI phase at T=80 K. ARPES measurements confirmed the formation of the TCI phase below, but gapped states above the band-gap-inversion temperature. The spin-resolved experiments provided evidence for the spin polarization of surface states in both cases: TCI phase and normal insulator. The experimental results are coherent with the results of corresponding tight-binding band structure calculations. The spin polarization seems to be inherent to surface states in narrow-gap IV-VI semiconductors with the electronic band structure influenced by very strong spin-orbit interaction. The transition to the TCI phase induced by the band-symmetry inversion is related to the orbital degrees of freedom of electrons and holes but this also results, via spin-orbit interaction, in the spin polarization of electrons occupying both in-gap Dirac-metal surface states as well as the states close to the bottom of the conduction band and the top of the valence band.

[1] P. Dziawa, et al., Nat. Mater. **11**, 1023 (2012).
[2] Y. Tanaka, et al., Nat. Phys. **8**, 800 (2012).
[3] Su-Yang Xu, et al., Nat. Commun. **3**, 1192 (2012).
[4] Liang Fu, Phys. Rev. Lett. **106**, 106802 (2011).
[5] T.H. Hsieh, et al., Nat. Commun. **3**, 982 (2012).

Nonlocal transport near charge neutrality point in two-dimensional topological insulator

A.Rahim,[1] A.D.Levin,[1] G.M.Gusev,[1] Z.D.Kvon,[2,3], E.B Olshanetsky,[2] N.N.Mikhailov,[2] and S.A.Dvoretsky,[2]

[1]*Instituto de Física da Universidade de São Paulo, 135960-170, São Paulo, SP, Brazil*
[2]*Institute of Semiconductor Physics, Novosibirsk 630090, Russia*
[3]*Novosibirsk State University, Novosibirsk, 630090, Russia*

The two-dimensional (2D) topological insulator (quantum spin Hall insulator) is characterized by a bulk energy gap and boundary modes that are robust to nonmagnetic impurity scattering. The 2D quantum spin Hall insulator (QSHI) have been realized in HgTeCdTe quantum well with a width $W > 6.3nm$. Indeed, the presence of the edge state transport in the absence of magnetic field has been recently demonstrated both in the ballistic [1] and diffusive cases [2] in HgTe quantum wells. This novel state is driven by the intrinsic spin-orbit interaction, which leads to the formation of the helical edge modes with opposite spin polarization counter-propagating at a given edge. The resistance of samples longer than 1μm might be much higher than $h/2e^2$ due to the presence of the spin dephasing (electron spin flip backscattering on each boundary). Mechanisms of the back scattering are new and appealing task for theoreticians and is a matter of ongoing debate. An unambiguous way to prove the presence of edge state transport mechanism in a 2DTI are the nonlocal electrical measurements. The application of the current between a pair of the probes creates a net current along the sample edge, and can be detected by another pair of the voltage probes away from the dissipative bulk current path. It has been demonstrated that the resistance of HgTe quantum wells reveals a sharp peak, when the gate voltage induces an additional charge density, altering the quantum wells from an n-type conductor to a p-type conductor via a QSHI state[1, 2]. These behaviours resemble the ambipolar field effect observed in graphene [3].

The mechanism responsible for the observed peak in the local and nonlocal resistances near the charge neutrality point (CNP) in HgTe quantum wells relies on the combination of the edge state and bulk transport contributions with the backscattering within one edge as well as bulk-edge coupling both taken into account. When the gate voltage is swept through the CNP the local and nonlocal transport coefficients arise from the edge state contribution at CNP and short-circuiting of the edge transport by bulk contribution away from CNP.

In this paper we report on the observation and a systematic investigation of a local and nonlocal transport in HgTe quantum wells with inverted band structure corresponding to the QSHI phase. The measurements were performed in the different devices. The device A consists of three $4\mu m$ wide consecutive segments of different length $(2, 8, 32\mu m)$, and 7 voltage probes. The device B was fabricated with a lithographic length $6\mu m$ and width $5\mu m$. We provide details on the model taking into account the edge and bulk contribution to the total current. In the full edge + bulk transport model the density dependence of the local and nonlocal transport coefficients arises from bulk conductivity short circuiting the edge current away from the charge neutrality point. The model reproduces the key features of the data, in particular the density dependencies of the local and nonlocal resistivity.

[1] M. Konig et al, Science 318, 766 (2007)
[2] G.M.Gusev, Z. D. Kvon, O.A.Shegai, N. N. Mikhailov, S. A. Dvoretsky and J. C. Portal, Phys. Rev. B 84, 121202(R), (2011)
[3] S. Das Sarma, Shaffique Adam, E. H. Hwang, Enrico Rossi, Rev. Mod. Phys., 83, 407 (2011)

Berry-phase-controlled weak antilocalization and Josephson effects in HgTe topological insulator materials

Grigory Tkachov, Ewelina M. Hankiewicz, Hartmut Buhmann and Laurens W. Molenkamp

Wuerzburg University, Am Hubland, 97074 Wuerzburg, Germany

This work is focused on transport phenomena in topological insulators (TIs). Unlike conventional insulators, these novel nanomaterials exhibit nontrivial conduction properties originating from metallic-like boundary (edge or surface) states. The boundary states have a Dirac-cone energy bands (see Fig., left) characterized by nontrivial Berry phases. In this contribution, we demonstrate, both theoretically and experimentally, that the band Berry phases lead to unusual transport phenomena in HgTe TI materials:

(i) Weak antilocalization in HgTe nanostripes. As well known, in low-dimensional conventional systems electronic states tend to be localized by static disorder (e.g. due to impurities). Remarkably, this never happens in TI materials because the Berry phases hinder constructive quantum interference in the random disorder potential (see Fig., center). Moreover, we find that HgTe quantum wells exhibit weak antilocalization observable via a positive magnetoresistance. It is extremely strong in quasi-1D diffusive nanostripes with inverted band ordering and only weakly depends on the Rashba spin-orbit splitting, persisting even for zero splitting (see Fig., right). We propose a theoretical model that explains our findings in terms of the band Berry phases of single-valley Dirac fermions [1,2].

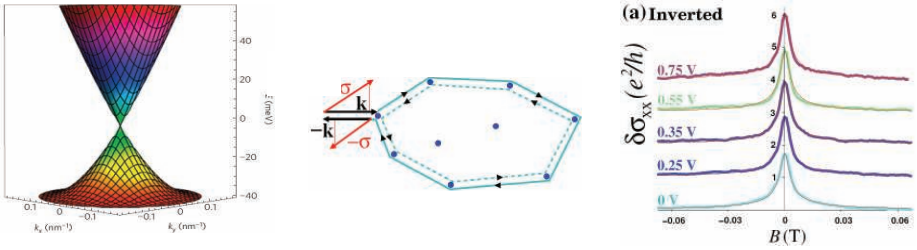

(ii) Zero-bias anomaly and topological midgap states in Josephson junctions. We also investigated transport in HgTe TIs with superconducting contacts. We observe and theoretically explain a zero-bias anomaly (pronounced resistance drop) resulting from Andreev reflection and the induced superconductivity on the TI surface [3]. Furthermore, in the TI Josephson junctions the Berry phase leads to topological midgap Andreev bound states [4] which are intimately related to Majorana fermions. We suggest schemes to detect these topological states in transport measurements.

Acknowledgments. This work has been supported by the German Research Foundation (DFG) through Grants No. HA5893/3-1 and No. TK 60/1-1

[1]. B. Buettner, C.X. Liu, G. Tkachov, E.G. Novik, C. Bruene, H. Buhmann, E.M. Hankiewicz, P. Recher, B. Trauzettel, S.C. Zhang, and L.W. Molenkamp, Nature Phys. **7** (2011) 418.

[2]. G. Tkachov and E. M. Hankiewicz, Phys. Rev. B **84** (2011) 035444.

[3]. L. Maier, J.B. Oostinga, D. Knott, C. Bruene, P. Virtanen, G.Tkachov, E.M. Hankiewicz, C. Gould, H. Buhmann, and L. W. Molenkamp, Phys. Rev. Lett. **109** (2012) 186806.

[4]. G. Tkachov and E. M. Hankiewicz, *Spin-helical transport in normal and superconducting topological insulators (Review Article)*, Phys. Status Solidi B **250** (2013) 215.

Topological protection length in HgTe/(Hg,Cd)Te quantum wells

G. Grabecki[1,2] , J. Wróbel[1,3],M. Czapkiewicz[1], Ł. Cywiński[1], S. Gierałtowska[1], E. Guziewicz[1], M. Zholudev[4,5], V. Gavrilenko[5], N. N. Mikhailov[6], S. A. Dvoretski[6], W. Knap[4], F. Teppe[4] and T. Dietl[1,7,8]

[1] *Institute of Physics, Polish Academy of Sciences, PL-02 668 Warszawa, Poland*
[2] *Department of Mathematics and Natural Sciences, College of Sciences, PL 01-938 Warszawa, Poland*
[3] *Institute of Physics, Rzeszów Uniwersity, PL-35 959 Rzeszów, Poland*
[4] *L2C, UMR Nº5221 CNRS, Université Montpellier 2, GIS-TERALAB, F-34095 Montpellier, France*
[5] *Institute for Physics of Microstructures, Russian Academy of Sciences, Nizhny Novgorod, 603950, Russia*
[6] *Institute of Semiconductor Physics, Siberian Branch, Russian Academy of Sciences, Novosibirsk, 630090, Russia*
[7] *Institute of Theoretical Physics, Faculty of Physics, University of Warsaw, PL-00 681 Warszawa, Poland*
[8] *WPI-Advanced Institute for Materials Research (WPI-AIMR), Tohoku University, Sendai 980-8577, Japan*

We present results of experimental studies of edge-channel transport down to 0.3 K in multiprobe Hall structures of modulation doped HgTe quantum wells (QWs) of the thickness $d = 8$ nm embedded between $Hg_{0.3}Cd_{0.7}Te$ barriers, the layout corresponding to a two-dimensional topological insulator (2D TI) [1]. The layers were grown by MBE [2], and the Hall bars of different linewidths (from 2 μm to 5 μm) have been patterned by e-beam lithography and wet-chemical etching. A top gate consisting of a 100 nm thick, HfO_2+Al_2O_3 composite (grown by atomic layer deposition) and a 30 nm thick gold film of the area $90 \times 90\,nm^2$ has been used for tuning the QW conductance between the n- and p-type. In the intermediate (depletion) regime the conductance of 2D TIs proceeds exclusively *via* helical edge channels, which gives rise to pronounced nonlocal resistances [3, 4]. In agreement with the expectation for the edge transport, our results show that the electric potential measured on consecutive contact probes distributed around the structure perimeter increases monotonically in this regime. Since this is only possible if current flows only along the edges, we conclude that no parasitic parallel conductance [5] affects our data. We also show that edge channel sections extending between the large contact probes can be treated as resistors connected in series, again in accord with the scenario of edge channel transport. On the other hand, the resistances of the edge channels are significantly higher than the quantized values predicted by the modified Landauer-Buttiker model [3], pointing to breaking of topological protection in channels that are 100 μm long. From both local and nonlocal resistance values, we estimate the topological protection length L_{tp} to be between 2 μm and 10 μm in our structures. Possible mechanisms accounting for finite values of L_{tp} will be discussed.

[1] M. König, et al., Science **318**, 766 (2007).
[2] M. Zholudev, et al., Phys. Rev. B **86**, 205420 (2012).
[3] A. Roth, et al., Science **325**, 294 (2009).
[4] G. M. Gusev, et al., Phys. Rev. B **84**, 121302 (2011).
[5] K. A. Kolwas, et al., phys. stat. sol. (b) **250**, 37 (2013).

MoP104

Level Spectroscopy of Dirac fermions in HgTe quantum wells

Yu. B. Vasilyev[1,2], J. Ludwig [2], J-M. Poumirol [2], N. N. Mikhailov[3], G. Yu. Vasileva[1,4], and D. Smirnov[2]

[1] *Ioffe Physical Technical Institute RAS, St. Petersburg, 194021, Russia*
[2] *National High Magnetic Laboratory, Tallahassee, Florida, 32310, USA*
[3] *Rzhanov Institute of Semiconductor Physics SB RAS, Novosibirsk, 630090 Russia*
[4] *St. Petersburg State Polytechnical University, St. Petersburg, 195251 Russia*

Predicted more than 60 years ago [1], the linear dispersion of low-energy charge carriers in a single layer of carbon atoms has recently been shown to exist in graphene [2]. When subjected to a magnetic field B, the characteristic linear dispersion of two-dimensional (2D) Dirac fermions $E = \pm c^* \hbar k$, where c^* is the electron velocity, transforms into a set of unequally spaced Landau levels (LLs) with energies $E_N = \mathrm{sgn}(N) \times c^* \sqrt{2e\hbar B|N|}$. The distinctive $\sqrt{B}$-dependent LL energies have been probed in infrared (IR) cyclotron resonance (CR) experiments enabling direct and accurate measurements of the band velocity c^* [3-5], the only parameter defining the linear dispersion.

Very recently, it has been shown that 2D Dirac fermions can be realized in CdHgTe-based semiconductor quantum wells (QWs) with an inverted band spectrum [6,7]. Magneto-transport experiments performed with gapless HgTe QWs indicated that there is a linear spectrum of particles when the well thickness (d) is close to the critical value of 6.3 nm, and Hall measurements show the anomalous sequence of quantum Hall plateaus specific to Dirac systems [8]. Unlike graphene, with its two spin-degenerate massless Dirac cones at two inequivalent points in momentum space, gapless HgTe QWs are an ideal system for studying Dirac fermions because of their single spin-degenerate Dirac valley at the Brillouin zone center. However, no spectroscopic measurements of the electron velocity c^* have been reported so far.

Here we report IR magneto-spectroscopy measurements of the cyclotron resonance of Dirac fermions in HgTe QWs. We studied two HgTe / CdHgTe QW samples (d=6.5 nm, 6.6 nm) grown by molecular beam epitaxy on a (013) GaAs substrate. All measurements were performed at 4.2 K in magnetic fields up to B= 17 T using a Bruker IFS 113 FTIR spectrometer in the range of 20 to 800cm^{-1}. Cyclotron resonances are clearly resolved with energy position that scales as $\sqrt{B}$ with the slope corresponding to an electron velocity $c^* = 6.37 \times 10^5 m/s$ in both samples. In one of the samples, the CR absorption line consists of two closely spaced minima. This indicates spin degeneracy lifting caused by the spin-orbit interaction, resulting in the appearance of two identical cones for the two spin directions.

Part of this work was supported by the Russian Foundation for Basic Research and the Russian Academy of Science. The measurements were carried out at the National High Magnetic Field Laboratory, which is supported by NSF Cooperative Agreement No. DMR-0654118, by the State of Florida, and by the DOE.

[1] P. R. Wallace, Phys. Rev. **71**, 622-634 (1947).
[2] K. S. Novoselov et al., Science **306**, 666 (2004).
[3] M. L. Sadowski et al., Phys. Rev. Lett. **97**, 266405 (2006).
[4] Z. Jiang et al., Phys. Rev. Lett. **98**, 197403 (2007).
[5] R. Deacon et al., Phys.Phys. Rev. B **76**, 081406(R) (2007).
[6] B. A.Bernevig, T.L. Hughes, & S.C. Zhang, Science **314**, 1757 (2006).
[7] M. König et al., Science **318**, 766 (2007).
[8] B. Büttner et al., Nature Phys. **7**, 418 (2011).

Light controlled spin polarization in two dimensional hole gases

H.V.A. Galeti [1], Y. Galvão Gobato [2], M.J.S.P.Brasil [3], M. Henini [4], G. Hill[5]

[1] Department of Eletrical Engineering, Federal University of São Carlos, São Carlos, Brazil
[2] Physics Department, Federal University of São Carlos, São Carlos, Brazil
[3]Gleb Wataghin Physics Institute, UNICAMP, Campinas, Brazil
[4]School of Physics and Astronomy, University of Nottingham, Nottingham, U.K
[5]Department of Eletronic and Eletrical Engineering, University of Sheffield, Sheffield,U.K

In this work, we have investigated the spin polarization from two dimensional hole gases (2DHG) in p-i-p GaAs/AlAs resonant tunneling diodes under magnetic field parallel to the tunnel current. We have studied the right (σ^+) and left (σ^-) circular polarization of the quantum well (QW) emission and contact layers as a function of the applied bias and laser intensity. We have observed several hole resonant peaks in the current-voltage characteristics curves and assign them to heavy-hole (HH1 and HH2) and light-hole resonances (LH1). The QW emission intensity is very sensitive to applied bias. We have observed that the QW polarization degree exhibits strong oscillations at hole resonances with values up to 46%. These oscillations depend strongly on the light intensity. A sign inversion is observed near the heavy hole resonance (HH2). The emission from contact layers show evidence of a spatially-indirect optical recombination between tunneling electrons and holes confined in *2DHG* at the accumulation layer (*e-2DHG*). The *e-2DHG* emission shows a negative circular polarization. We have observed that the sign of the circular polarization degree of both emissions can be reversed by increasing the light excitation. Finally, the polarization degree of both 2D gases in the accumulation layer and QW are very sensitive to applied voltage and the laser intensity.

Imaging magnetoelectric subband depopulation in ballistic constrictions

A. A. Kozikov [1], D. Weinmann [2], C. Rössler [1], T. Ihn [1], K. Ensslin [1], C. Reichl [1], and W. Wegscheider [1]

[1] *Solid States Physics laboratory, ETH Zürich, CH-8093 Zürich, Switzerland*
[2] *Institut de Physique et Chimie des Matériaux de Strasbourg, Université de Strasbourg, CNRS UMR 7504, 23 rue du Loess, F-67034 Strasbourg, France*

We have measured local transport through a stadium formed by two ballistic constrictions. The conductance through the stadium is measured at 300 mK as a function of the position of a biased metallic tip which is scanned across the sample. [1, 2]. We have observed a set of unexpected fringe patterns at the constrictions (Fig. 1a) and imaged the transition from electrostatic to magnetic depopulation of subbands in one of the constrictions in a perpendicular magnetic field. We interpret the fringes as a standing wave pattern between the AFM tip and the top gates leading to quantized conductance plateaus. The fringes form a checkerboard pattern (Fig. 1b), which precisely allows determining the number of transmitted modes in each of the tip-gate constrictions.

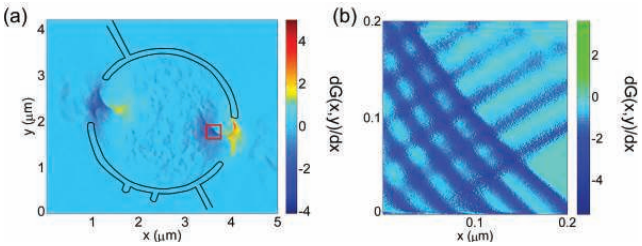

Figure 1. (a) Numerical derivative of the conductance through the stadium, d$G(x, y)$/dx, with respect to the x-axis as a function of tip position, (x, y). The position of the stadium is shown by black solid lines (top gates). (b) A zoom-in of the part (a red square in (a)) of right fringe pattern. The mentioned checker board pattern is clearly seen.

In the quantum Hall regime moving the tip inside the constriction brings edge channels closer together, which are backscattered one by one. This is seen in spatially resolved images as wide conductance plateaus, each of which corresponds to its own local filling factor. Classical and quantum simulations describe well most of our observations.

The coherent wave nature of electrons is widely studied using such interferometers as the Mach-Zehnder and Fabry-Perot. They were shown to be suitable for the investigation of exotic fractional and non-Abelian quantum Hall states. The control over the electron trajectories enclosing an Aharonov-Bohm flux is accomplished by applying a voltage to metallic top gates. A higher tunability can be achieved by using a moveable top gate. Our findings allow fine tuning potential landscape and tip position for further experiments to image Aharonov-Bohm oscillations at low and high (quantum Hall regime) magnetic fields. Not only the voltage, but also the gate-surface distance and the in-plain gate position can be changed. The variable strength and gradient of the induced potential, the control over the length and shape of electron waves or edge channels are advantages when using a moveable top gate.

[1] M. A. Topinka *et al*. Science. **289**, 2323 (2000).
[2] A. A. Kozikov *et al*. New J. Phys. **15**, 013056 (2013).

Effects of spin-orbit coupling on transport through a QPC modulated by a periodic potential

Sigurdur I. Erlingsson[1], **and Gunnar Thorgilsson**[1]

[1] *School of Science and Engineering*
Reykjavik University, Menntavegi 1, IS-101 Reykjavik
Iceland

The strength of the Rashba spin-orbit interaction can be measured via transport using different experimental setups [1], e.g. magnetoresistance measurements via Shubnikov-de Haas oscillations [2, 3], and weak anti-localization [5, 4]. Recently, it was proposed that the Rashba strength could be extracted from a charge conductance measurement of a parabolic quantum wire, with a quasi-periodic potential along the transport direction [6].

In this work we will expand on the proposal in [6]. By replacing the quantum wire with a quantum point contact (QPC), we are better able to address experimentally relevant systems. Starting from a 2DEG with Rasbha spin-orbit coupling we calculate charge transport through a QPC which in addition is modulated by a quasi-periodic potential, located in the constriction part of the QPC. The transport calculations are based on the recursive Green's function method. The quasi-periodic potential is chosen such that it will open up gaps in the density of states where the effect of the spin-orbit coupling is most prominent. This will lead to dips in the conductance through the system, and the position of the dips is determined by the strength of the Rashba coupling. Experimentally the quasi-periodic potential can be realized using finger gates [6]. The transport results are compared with energy spectra for the corresponding ideal periodic potential. The position of the dips match with the position of the gaps in the energy spectra. Thus, a relatively low number of finger gates, between 10-20 finger gates, can be sufficient to open up gaps.

Also, we will consider the case of a quasi-periodic magnetic field, induced by ferromagnetic finger gates. In this situation the dips will affect the two spin species differently, leading to spin polarized current through the QPC. We will study how different orientation of the magnetization of the finger gates affect the transport properties of the system.

[1] W. Zawadzki, and P. Pfeffer, Semicond. Sci. Tech. **19**, R1 (2004).
[2] J. Nitta, T. Akazaki, H. Takyanagi, and T. Enoki, Phys. Rev. Lett. **78**, 1335 (1997).
[3] G. Engels, J. Lange, T. Schäpers and H. Lüth, Phys. Rev. B **55**, R1958 (1997).
[4] T. Koga, J. Nitta, T. Akazaki, and H. Takyanagi, Phys. Rev. Lett. **89**, 046801 (2002).
[5] V.A. Guzenko, T. Schäpers, and H. Hardtdegen, Phys. Rev. B, **76**, 165301 (2007).
[6] G. Thorgilsson, J.C. Egues, D. Loss, and S.I. Erlingsson, Phys. Rev. B **85**, 045306 (2012).

MoP108

Scanning Gate Imaging of the 0.7 anomaly

A. Iagallo[1], N. Paradiso[1], S. Roddaro[1,2], C. Reichl[3], W. Wegscheider[3], S. Heun[1], and F. Beltram[1]

[1] *NEST, Istituto Nanoscienze-CNR and Scuola Normale Superiore, Pisa, Italy*
[2] *Istituto Officina dei Materiali CNR, Laboratorio TASC, Basovizza (TS), Italy*
[3] *Solid State Physics Laboratory, ETH Zurich, 8093 Zurich, Switzerland*

The origin of the so called "0.7 structure" in the transport characteristics of 1D mesoscopic devices represents a long standing puzzle, yet showing a continuously renewed interest for possible applications in spintronics [1]. Though several mechanisms have been proposed to explain such anomaly, a general consensus has not been achieved so far.

Among the proposed explanations are the formation of a quasi-bound state at a constriction entrance near pinch-off, quantum interference from scatterers within the electron phase coherence length from the constriction, and Kondo effect due to zero-dimensional systems inside the constriction itself acting as quantum dots. While a quasi-bound state is strictly linked to geometrical factors, being related to mode mismatch between the 1D channel and the large 2D reservoirs, the other two explanations involve the presence of point defects, such as charged impurities.

By using low temperature Scanning Gate Microscopy on GaAs/AlGaAs heterostructures in Quantum Point Contact geometry, we can definitively rule out zero-dimensional structures (e.g. charged defects and antidots) as the underlying origin of the 0.7 feature. The technique allows to identify with nanometric resolution [2] the presence of localized defects, which are detected as sharp fluctuations in the 2D charge density. On the other hand, Fig. 1(a) shows a typical SGM image of a clean QPC constriction, where the quantized conductance displays circular symmetry and no trace of charged spots is detected. Our results also weaken the hypothesis of a shallow bound state forming at the QPC entrance, because a small-amplitude local perturbation of the potential would induce charging and discharging of such a state, visible as concentric ring structures in a SGM image. As shown in Fig. 1(b), the characteristic features of the 0.7 structure survive also a strong perturbative action by the biased AFM tip, which would destroy the potential landscape and quench the quasi-bound state.

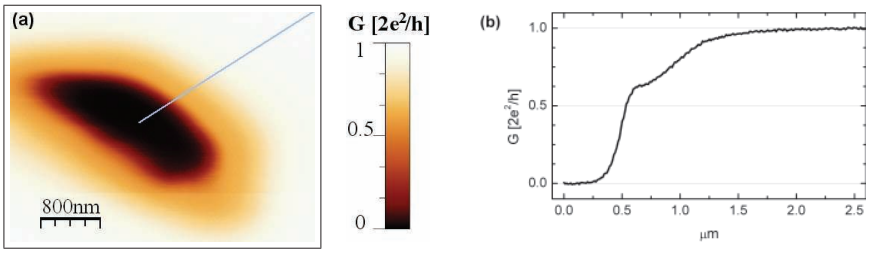

Figure 1: (a) SGM image of a QPC central region, spanning the conductance interval $0-2e^2/h$. A cutaway profile, obtained along the blue solid line, is shown in (b), where the plateau at G$< 2e^2/h$ is the signature of the 0.7 anomaly.

[1] A. M. Burke, O. Klochan, I. Farrer, D. A. Ritchie, A. R. Hamilton, and A. P. Micolich, Nano Letters **12**, 4495 (2012).
[2] N. Paradiso, S. Heun, S. Roddaro, G. Biasiol, L. Sorba, D. Venturelli, F. Taddei, V. Giovannetti, and F. Beltram, Phys. Rev. B **86**, 85326 (2012).

Optical characterization of strain-compensated $Ge/Si_{0.16}Ge_{0.84}$ multiple quantum wells on silicon-based germanium virtual substrate

P. H. Wu[1], Y. S. Huang[1,*], H. P. Hsu[2], C. Li[3], and S. H. Huang[3]

[1] *Department of Electronic Engineering, National Taiwan University of Science and Technology, Taipei, 106, Taiwan*
[2] *Department of Electronic Engineering, Ming Chi University of Technology, Taishan, Taipei 243, Taiwan*
[3] *Department of Physics, Semiconductor Photonics Research Center, Xiamen University, Xiamen 361005, People's Republic of China*

Recent progresses in Si photonics suggest that Si-based materials could provide a strong support for the technological integration of optical functions in CMOS microelectronics. In this perspective, SiGe alloys are of particular interest because they can be epitaxially grown on Si substrates and are compatible with a large number of standard Si processes and CMOS technology. Bulk mobilities of SiGe alloys with high Ge content are higher than those of Si for both electron and holes. Moreover, SiGe technology allows the integration on Si substrates of high speed electronics devices.

In Ge, the direct gap at the Γ point is only 140 meV above the indirect fundamental gap at room temperature and the direct gap energy is within the range of wavelengths used in telecommunications. Ge/SiGe multiple quantum well (MQW) structures with Ge-rich barriers have attracted more attention because their optical properties are expected to exhibit close analogies to those of III-V direct-gap semiconductors. Recently, a strong quantum Stark effect associated with the direct-gap interband transition has been observed in strained Ge/SiGe MQW on relaxed Ge-rich SiGe buffers by photocurrent and transmission spectroscopy and electro-absorption modulators based on this effect have also been demonstrated [1,2].

In this study, a strain-compensated $Ge/Si_{0.16}Ge_{0.84}$ multiple quantum well (MQW) structure grown on a Ge-on-Si virtual substrate (Ge-VS) was characterized by using temperature dependent photoreflectance (PR) and piezoreflectance (PzR) techniques. Signals from every relevant portion of the sample, including Ge-VS, MQW and barriers were observed. The band gap blue-shifted and valence band splitting in the vicinity of the direct band-edge transitions of Ge revealed that the Ge-VS is compressively strained. This result provides useful information for crystal grower. The existence of compressive strain actually is contrary to the direction of recent technological development trend, where tensile strain has been used to shift the direct transitions in Ge/SiGe MQW stacks closer towards the telecommunication C-band. A comprehensive analysis of the PR and PzR spectra led to the identification of various quantum-confined interband transitions. In addition, the parameters that describe the temperature dependence of the excitonic transition energies were evaluated and found to be similar to that of the bulk Ge.

[1] Y. H. Kuo, Y. K. Lee, Y. Ge, S. Ren, J. E. Roth, T. I. Kamins, D. A. B. Miller, and J. S. Harris, Nat ure 437, 1334 (2005).
[2] S. Tsujino, H. Sigg, G. Mussler, D. Chrastina, and H. von Känel, Appl. Phys. Lett. 89, 262119 (2006).

Signatures of Landau level crossings in a Two-Dimensional Electron Gas

Rayda Gammag[1] and Cristine Villagonzalo[2]

[1] *Asia Pacific Center for Theoretical Physics, POSTECH, Pohang, 790-784 Korea*
[2] *National Institute of Physics, University of the Philippines Diliman, Quezon City, 1101 Philippines*

A two-dimensional electron gas (2DEG) under a magnetic field $\vec{B} = B\cos(\theta)\hat{x} + B\sin(\theta)\hat{z}$ is studied. Here θ denotes the angle that $\vec{B}$ makes with the 2DEG plane. In addition to the Zeeman energy, the system is assumed to be under an asymmetric potential which is described by the Rashba term. The eigenvalues are solved analytically assuming that crossing Landau levels (LL) share equal probabilities [1]. In order to predict the behavior of thermodynamic quantities, the density of states (DOS) is simulated which take the form of a series of Gaussian.

The ratio of the DOS over its zero-tilt value DOS_0 is shown in Figure 1. We focus on the large tilt angles ($\theta > 80°$) where novel phenomena are observed.

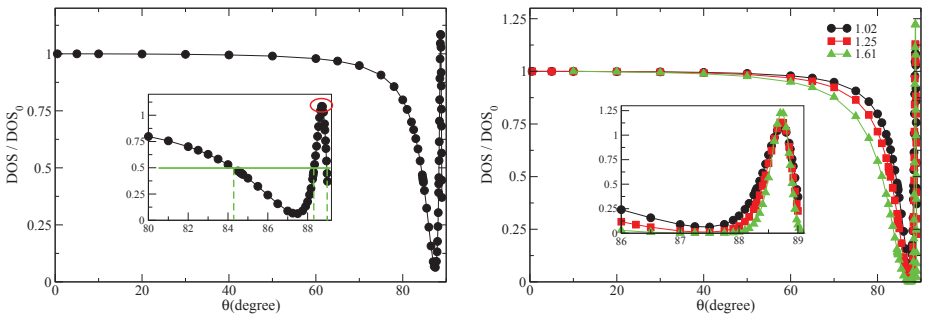

Figure 1: Left: The evolution of the peak height at $B_z \simeq 1.02$ T with increasing tilt angle. As indicated by the ordinate label, what is plotted here is the ratio of DOS(θ) over DOS(0°). The trend shows an increasing depth (or spin splitting) until it reaches a maximum around 87.5°. This is the angle where simultaneous LL crossings occur [3] and this phenomenon was observed experimentally [2]. Aside from the usual beating patterns, here we discover another way of detecting LL crossing imprint. The green solid line marks $\mathrm{DOS}/\mathrm{DOS}_0 = 0.5$ with three corresponding angles $\theta_{ps} \approx 84.2°, 88.3°, 88.9°$. At around these same angles do we observe the DOS phase reversal accompanying a minimized DOS amplitude [3]. One remarkable feature of this plot is the maximum peak surpassing DOS_0 around 88.7° as indicated by the red circle. This is contrary to expectations if one considers solely the prefactor of the DOS being proportional to B_z. In the perspective of LL crossing, however, this θ coincides to another crossing point (verified in the simulations although no longer shown here). Right: Qualitatively the same trend is followed by other Landau level peaks (found at other values of B_z) where the extrema are located at exactly the same values of θ.

[1] R. Gammag, C. Villagonzalo, Solid State Commun. **152**, 757 (2012).
[2] A.T. Hatke, M.A. Zudov, L.N. Pfeiffer, K.W. West, Phys. Rev. B **85**, 241305(R) (2012).
[3] R. Gammag, C. Villagonzalo, Solid State Commun. **156**, 16 (2013).

Formulating Transmission Probabilities of Arbitrary Potential in a 2-dimensional Quantum Chaotic Systems

Avik Kumar Mahata [1]

[1] *National Institute Of Technology, Materials Science and Engineering, MME Department, Trichy, Tamilnadu, India-620015*

In the following note I have tried to formulate the transmission probability for a 2-dimensional quantum well with finite potential barrier with a chaos inside the system. Analytical formula for transmission probability has been derived by different ways previously; Analytical Transfer Matrix Method is one of them and it has been tested experimentally. Here, I will be discussing the same tunneling with a magnetic field inside the tunnel and that magnetic field creates a chaos inside the well. There is a different scenario when we apply a magnetic field to the tunnel, like the Hamiltonian becomes time dependent. For an arbitrary infinite potential when we will be applying a magnetic field the electron moves to and fro inside the well, and for a finite potential barrier there is a finite probability that the electron pass through the barrier, but as the Hamiltonian becomes time dependent the calculation becomes very rigorous and difficult. Here, we use Random Matrix Theory to resolve the issue, and trying to formulate the transmission probability through an arbitrary but finite potential. In literature we can find Random Matrix Theory has been used to solve problems in Chaotic Quantum Dot problems. I adopt the same approach solving Quantum Tunneling problems for a Chaotic 2-Dimensional well.

PACS numbers: 73.40.Gk, 73.40.Lq, 85.30.De

MoP112

Quasi-ballistic transport in AlGaN/GaN heterostructures in extremely high electric fields

B. A. Danilchenko[1], N.A.Tripachko[1], A. E. Belyaev[2], S. A. Vitusevich[3*], H.Hardtdegen[3], H.Lüth[3]

[1]Institute of Physics, NASU, Pr. Nauki 46, Kiev 03028, Ukraine

[2]Institute of Semiconductor Physics, NASU, Pr. Nauki 45, Kiev 03028, Ukraine

[3]Peter Grünberg Institute, Forschungszentrum Jülich, Jülich D-52425, Germany

Electron transport in two-dimensional (2D) conducting channels of AlGaN/GaN heterostructures in extremely high electric fields at 4.2K has been studied. Sample's mesa was designed with a special geometry in order to achieve the electric field as high as possible without breakdown. We observed ballistic transport of 2D-electrons in the channel of an AlGaN/GaN heterostructure with reduced carrier concentration. In the ballistic transport regime, the highest carrier velocity attained was 6.8×10^7 cm/s at an electric field of 0.3 MV/cm in the channel. This velocity is 85% of the natural limit in the velocity predicted for the carrier transport based on the band structure of wurtzite GaN and is the highest ever achieved in semiconductors in an externally applied electric field. The results of our experimental studies are in good agreement with analytical and Monte Carlo theoretical predictions of high-energy carrier kinetics implying a negative mass state contribution to transport phenomena in GaN-based materials. These results provide evidence of approaching to the regime with negative differential conductivity (NDR), which is expected at a field of about 0.6MV/cm. The revealed ballistic transport regime with the highest drift velocity attained is an important step towards reaching the theoretically predicted region with NDR.

The rough estimations show that in our particular case the dissipated electric power density in the sample constriction reaches ~10^{12} W/cm^3. Thus, the further progress in the study of the transport phenomena in such huge electric fields requires overcoming the problem of efficient heat removal from the active region of the device.

Negative Magnetoresistance Induced by an Interplay of Smooth Disorder and Rare Strong Scatterers

L. Bockhorn[1], I. V. Gornyi[2], A. D. Mirlin[2], C. Reichl[3], D. Schuh[4], W. Wegscheider[3], and R. J. Haug[1]

[1] *Institut für Festkörperphysik, Leibniz Universität Hannover*
[2] *Institut für Nanotechnologie, Karlsruhe Institute of Technology*
[3] *Laboratorium für Festkörperphysik, ETH Zürich*
[4] Institut für Experimentelle und Angewandte Physik, Universität Regensburg

In a high mobility two-dimensional electron gas (2DEG) realized in a GaAs/AlGaAs quantum well we observe a strong negative magnetoresistance around zero magnetic field. Figure 1 shows a typical measurement of the strong negative magnetoresistance around zero magnetic field. We divide the strong negative magnetoresistance into two sections because of their different behaviors for different conditions. The huge magnetoresistance at larger magnetic fields depends strongly on the temperature and the electron density, while the peak around zero magnetic field is left unchanged [1, 2, 3, 4] at low temperatures. The crossover between the peak and the huge magnetoresistance is marked by a slight plateau in the longitudinal resistance around B_c=12 mT. The height of the peak is given by $\Delta\rho_{xx} = \rho_0 - \rho_{xx}(B_c)$.

The peak around zero magnetic is a two-dimensional effect, as concluded from tilted magnetic field measurements. In accordance with Mirlin *et al.* [5] we conclude that the peak around zero magnetic field is induced by a combination of smooth disorder and rare strong scatteres. The saturation of the longitudinal resistivity at B_c=12 mT is determined by the smooth disorder, while the height of the peak is dominated by the rare strong scatterers. The density of the strong scatterers n_S is determined by using the curvature of the peak, ρ_0 at zero magnetic field and $\rho_{xx}(B_c)$ at the crossover between the peak and the huge magnetoresistance. However the densities of the strong scatterers of our high mobility samples are much lower than expected from the estimated densities of background doping in our sample.

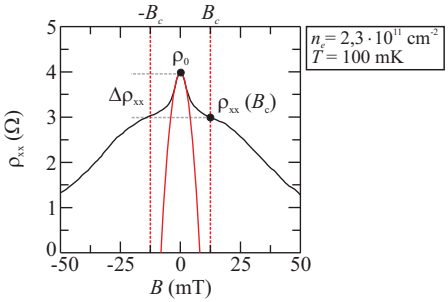

Figure 1: The longitudinal resistivity ρ_{xx} vs. the magnetic field B. The strong negative magnetoresistance is divided into the peak and the huge magnetoresistance.

[1] Y. Dai, R. R. Du, L. N. Pfeiffer, and K. W. West, *Phys. Rev. Lett.* **105**, 246802 (2010).
[2] L. Bockhorn, et al., *Phys. Rev. B* **83**, 113301 (2011).
[3] A. T. Hatke, et al., *Phys. Rev. B* **85**, 081304 (2012).
[4] I. V. Gornyi and A. D. Mirlin, *Phys. Rev. B* **69**, 045313 (2004).
[5] A. D. Mirlin, D. G. Polyakov, F. Evers, and P. Wölfle, *Phys. Rev. Lett.* **87**, 126805 (2001).

MoP114

Influence of doping on "exciton gas – electron-hole liquid" phase transition in SiGe quantum wells

A. F. Adiyatullin, V. S. Bagaev, V. S. Krivobok, S. N. Nikolaev and E.E. Onishchenko

Lebedev Physical Institute of Russian Academy of Sciences, Moscow, Russia

It is well known that for moderately doped Si and Ge crystals impurities serve as centers of nucleation for electron-hole liquid (EHL) and significantly lower the threshold for condensation. The influence of impurities on the formation of the quasi-2D condensed phase in semiconductor quantum well (QW) has not been studied yet. At the same time the unique features of quasi-2D EHL and the related "gas-liquid" phase transition have been observed recently for the systems based on SiGe/Si QW: condensation occurs at much lower excitation densities as compared with bulk Si, the phase transition is accompanied by the formation of unusual excitonic complexes, the barrier for electrons in SiGe layer results in a significant increase of EHL critical temperature [1,2]. In this work, we investigated the influence of boron impurity placed in the center of SiGe layer (or in close proximity to QW) on the many-body effects occurring in photoexcited SiGe/Si QW.

SiGe/Si samples with a single SiGe layer with a thickness of 5 nm and Ge content of 3-14.5% were grown by MBE on high-resistivity Si-substrates. In some samples boron δ-layer with a density of ~ 10^{10} cm^{-2} was placed at different distances from QW or in the centre of SiGe layer. Steady-state and time-resolved photoluminescence (PL) measurement have been used to study many-particle states and the related phase transitions in the QW.

In the time-resolved PL spectra of "pure" samples (without δ-layer) with Ge content of 3-6.9% quasi-2D EHL emission has been detected at low (5K) temperatures. For a wide range of times (< 1 mks) the EHL line shape as well as the decay time constant remained unchanged. For delay time > 2 mks after an excitation pulse the QW no-phonon emission line as well as its phonon replicas shifted to shorter wavelengths. A comparison of the spectra recorded at different temperatures revealed at least two recombination channels in addition to the EHL: free excitons (FE) and many-particle states (MPS). The exact nature of the MPS is the subject of debate. In particular, a sequential analysis of PL spectra in IR and visible regions indicates that MPS should include more than 4 particles (two electron and two holes). Decrease of the excitation power density in the steady-state experiments from 240 to 70 mW/cm^2 at T = 5 K leads to "pure" sample spectra transformation from EHL to MPS PL. At higher temperature (10 K) the collective states dissociate and FE role increases.

The dopant δ-layer incorporation in the QW center hardly affects on the sample spectrum at low temperature and high excitation level. The EHL emission lineshapes in the both doped and "pure" structures are matched together with high precision. This confirms a high structural quality of the samples and their characteristics identity. Decrease of excitation power up to 70 mW/cm^2 results in significant QW PL line narrowing without distinguishable line shift. This narrow line is observed at higher temperature contrary to EHL but is absent in "pure" sample spectra. So we can to attribute this line to the luminescence of the boron-bound excitons. The binding energy of bound exciton complex (BEC) is 6 meV for QW with 5% Ge content.

It has been shown that the QW doping leads to the BEC line appearance in the PL spectra. Also, the dopant δ-layer suppresses EHL formation at low excitation power density.

[1] V. S. Bagaev, V. S. Krivobok, S. N. Nikolaev et al., Phys.Rev.B **82**, 115313 (2010)
[2] V. S. Bagaev, V. S. Krivobok, S. N. Nikolaev et al., JETP Letters, **94**(1), 63-67 (2011)

Charge coherence and Fermi-edge singularity in dopant-based devices in silicon

B. Voisin[1], B. Roche[1], E. Dupont-Ferrier[1], X. Jehl[1], R. Wacquez[2], M. Vinet[2], S. De Franceschi[1] and M. Sanquer [1]

[1] *SPSMS, UMR-E CEA / UJF-Grenoble 1, INAC, 17 rue des Martyrs, 38054 Grenoble, France*

[2] *CEA, LETI, MINATEC Campus, 17 rue des Martyrs, 38054 Grenoble, France*

Single donors in silicon are attracting much attention in view of their potential use as qubits for quantum computing [1]. Their deep and sharp confinement potential induces a large valley-orbit splitting [2], which results in a single, spin-degenerate ground-state level well separated from all the other orbital levels. This is a favourable property to realize either single-donor spin qubits or two-donor charge qubits. Yet interactions with nearby fluctuating charges can be an important source of orbital dephasing. We have measured a charge coherence time T_2 of 0.3 ± 0.1 ns using Landau-Zener-Stückelberg interferometry in the first double-donor transistor in silicon [2, 3]. Through charge pumping experiments [4] we have studied the impact of the coupling to the source and drain leads on the dynamics of double-donor systems. In such doped devices, these donors strongly couple to ionized donors (charge fluctuators) located at the edges of the reservoirs. Short-range Coulomb interactions between these fluctuating charges and the electrons in the reservoirs can lead to a phenomenon known as Fermi edge singularity (FES) [5]. This effect can limit the orbital coherence of coupled donors [6].

To further explore the role of these fluctuating charges, we have measured resonant tunneling transport through donors implanted in a very short silicon nanowire. Experimental studies of the FES have so far been reported only for resonant tunneling vertical devices in III-V heterostructures [7]. Here, using a lateral device geometry, we have taken advantage of local gate electrodes to tune the different energy levels with respect to each other. A current peak is observed when the donor level aligns with the Fermi energy of the reservoir, followed by a power-law decrease of the current, which is in qualitative agreement with the theory of FES [5].

Acknowledgements: The authors thank H. Baranger, M. Houzet and J. Meyer for very fruitful discussions. This work is supported by the French ANR under Project SIMPSSON n 2010-Blan-1015.

[1] F. Zwanenburg *et al.*, accepted for publication in Rev. Mod. Phys., arxiv:1206.5202
[2] B. Roche, E. Dupont-Ferrier, B. Voisin, M. Cobian, X. Jehl, R. Wacquez, M. Vinet, Y.-M. Niquet, and M. Sanquer Phys. Rev. Lett. **108**, 206812 (2012).
[3] E. Dupont-Ferrier, B. Roche, B. Voisin, X. Jehl, R. Wacquez, M. Vinet, M. Sanquer and S. De Franceschi, accepted for publication in Phys. Rev. Lett., arXiv:1207.1884v1.
[4] B. Roche, R.-P. Riwar, B. Voisin, E. Dupont-Ferrier, R. Wacquez, M. Vinet, M. Sanquer, J. Splettstoesser and X. Jehl, accepted for publication in Nature Communications, arXiv:1212.1142.
[5] K. A. Matveev and A. I. Larkin, Phys. Rev. B **46**, 15337 (1992).
[6] Igor V. Yurkevich, Jim Baldwin, Igor V. Lerner, and Boris L. Altshuler, Phys. Rev. B **81**, 121305 (2010).
[7] A.K. Geim, P.C. Main, N. La Scala, Jr., L. Eaves, T.J. Foster, P.H. Beton, J.W. Sakai, F.W. Sheard, and M. Henini, G. Hill and M. A. Pate , Phys. Rev. Lett. **72**, 2061-2064 (1994).

MoP116

Electronic properties of TiO_2 films grown by atomic layer deposition

M. Tallarida, C. Das and D. Schmeisser

Brandenburg University of Technology, Applied Physics – Sensors, Konrad Wachsmann Allee, 17, 03046, Cottbus, Germany

We have studied the electronic properties of TiO_2 thin films grown by atomic layer deposition (ALD) by means of synchrotron radiation photoemission spectroscopy (SR-PES). The use of ALD for growing thin oxide films assures the homogeneity and complete coverage even of the first monolayer [1]. Samples, grown in-situ on Si substrates, had thickness ranging between 1 monolayer and 8nm, depending on the ALD parameters, i.e. number of cycles and oxygen precursors used. Thanks to the homogeneity of the samples we could investigate the electronic properties depending on film thickness and morphology. In particular we observed the evolution of the valence band and in-gap states with film thickness, by making use of resonant photoemission (resPES) at both the Ti2p and O1s edges. By means of X-ray absorption spectroscopy (XAS) we observed the intensity evolution of the main peaks at both the Ti2p and O1s edges, also related to the film thickness and homogeneity. The changes, previously observed for nanoparticles [2] and sputtered films [3], were alternatively addressed to quantum confinement [2] and to structural relaxations [3]. Based on both resPES and XAS results, we discuss the two hypotheses. We finally discuss the occurrence of linear dichroism at both Ti2p and O1s edges, depending on the film thickness and ALD preparation.

[1] Tallarida, M.; Schmeisser, D. *Semiconductor Science and Technology* **2012**, *27*, 074010.
[2] Vayssieres, L.; Persson, C.; Guo, J. H. *Applied Physics Letters* **2011**, *99*, 183101.
[3] Soriano, L.; Fuentes, G. G.; Quirós, C.; Trigo, J. F.; Sanz, J. M.; Bressler, P. R.; González-Elipe, A. R. *Langmuir* **2000**, *16*, 7066.

Imaginary time propagation code for large-scale two-dimensional eigenvalue problems in magnetic fields

P. J .J. Luukko[1], E. Räsänen[2]

[1]*Nanoscience Center, University of Jyväskylä, FI-40014 Jyväskylä, Finland*
[2]*Department of Physics, Tampere University of Technology, FI-33101 Tampere, Finland*

We present our open-source code [1, 2] for solving the single-particle, time-independent Schrödinger equation in two dimensions. Our program, `itp2d`, utilizes the imaginary time propagation (ITP) algorithm, and it includes the most recent developments in the ITP method: the arbitrary order operator factorization [3] and the exact inclusion of a (possibly strong) external magnetic field [4]. In our implementation we emphasize a modern and easily extensible design, simple and user-friendly interfaces, and an open-source development philosophy. Our program is able to solve thousands of eigenstates of a two-dimensional quantum system in a reasonable time with commonly available hardware. The main motivation behind our work is to allow the study of highly excited states and statistical properties of energy levels of two-dimensional quantum dots and billiard systems with a single versatile code, e.g., in research on quantum chaos. Furthermore, `itp2d` can be combined with real-space electronic-structure methods based on, e.g., density-functional theory.

Figure 1: Density plot of the 975th eigenstate of a particle in a box with a strong external magnetic field.

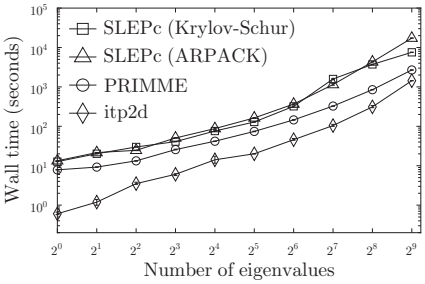

Figure 2: Elapsed wall time as a function of the number of solved eigenstates for four different programs, including our `itp2d`.

[1] P. J. J. Luukko, E. Räsänen, Comput. Phys. Commun. **184**, 769 (2013).
[2] `https://bitbucket.org/luukko/itp2d`
[3] S. A. Chin, Celest. Mech. Dyn. Astron. **106**, 391 (2010).
[4] M. Aichinger, S. A. Chin, E. Krotscheck, Comput. Phys. Commun. **171**, 197 (2005).

Phase transition of pinning modes in wide quantum wells

A. T. Hatke[1], B. Magill[1], Y. Liu[2], L. W. Engel[1], M. Shayegan[2], L. N. Pfeiffer[2], K. W. West[2], and K. W. Baldwin[2]

[1] *National High Magnetic Field Laboratory, Tallahassee, FL 32310, USA*
[2] *Princeton University, Princeton, NJ 08544, USA*

Recent transport studies of wide quantum wells (WQWs) [1] have revealed a reentrant integer quantum Hall effect (RIQHE) located in Landau filling factor (ν) ranges between 0.80 and 0.87 and interpreted as some type of pinned Wigner solid. The ν of the RIQHE is remarkably sensitive to the carrier density n.

Wigner solids, including those of quasiparticles or -holes, within the ν ranges of the integer quantum Hall effect (IQHE) [2] exhibit a microwave resonance. This resonance is understood as a pinning mode, in which quasiparticles or holes oscillate about their pinned positions. In this study, we investigate the microwave spectra for $0.8 \leq \nu \leq 1$ in WQWs, of width $w = 54$ and $w = 65$ nm with varying n. Fig. 1 (a) shows spectra ($w = 65$ nm and $n = 2.1 \times 10^{11}$ cm^{-2}) where the frequency response of the real part of the diagonal conductivity (Re(σ_{xx})) taken at many ν varying from 0.8 (top) to 1.0 (bottom) with a step of 0.01 is plotted.

On decreasing ν from 1 we observe a resonance peak, labeled A in the figure. A further decrease in ν results in the observation of an additional resonance, marked as B. In Fig. 1 (b) we plot the spectrum at $\nu = 0.9$. For this ν we observe both resonances and the spectrum can be fit to a double Lorentzian, consistent with two Wigner solid phases coexisting. The critical filling factor, ν_c, for crossover between the resonances is plotted as a function of n in Fig. 1 (c) for well widths of $w = 54$ and 65 nm. The phase farthest from $\nu = 1$ can be reasonably identified with the RIQHE of [1], which also moves closer to $\nu = 1$ as n increases. The observed coexistence of phases is consistent with a first order phase transition between two distinct Wigner solid phases.

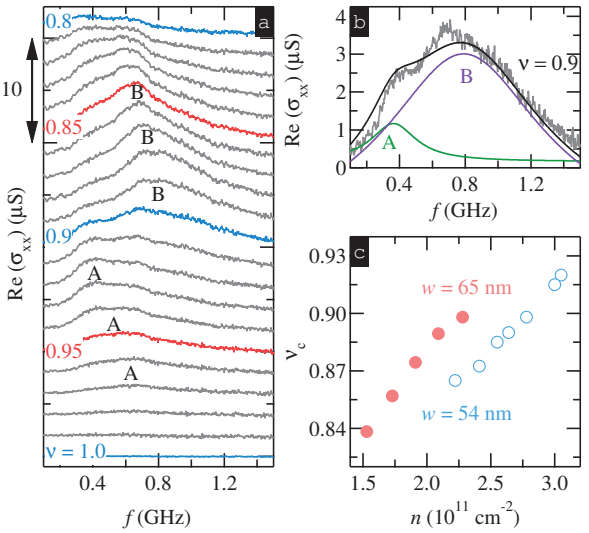

Figure 1: (a) Microwave spectra for $\nu = 0.8$ (top) to $\nu = 1.0$ (bottom) in step of 0.01 normalized to $\nu = 1$. Well width $w = 65$ nm and $n = 2.1 \times 10^{11}$ cm^{-2}. (b) Microwave spectra for $\nu = 0.9$ with double Lorentzian decomposition. (c) ν_c versus carrier density.

[1] Y. Liu, C. G. Pappas, M. Shayegan, L. N. Pfeiffer, K. W. West, and K. W. Baldwin, Phys. Rev. Lett. **109**, 036801 (2012).
[2] Y. Chen, R. M. Lewis, L. W. Engel, D. C. Tsui, P. D. Ye, L. N. Pfeiffer, and K. W. West, Phys. Rev. Lett. **91**, 016801 (2003).

Magnetotransport in nanostructured InAs-based High Electron Mobility Transistors

Olivio Chiatti[1], Sven S. Buchholz[1], Christian Heyn[2], Wolfgang Hansen[2], Saskia F. Fischer[1]

[1] *Neue Materialien, Institut für Physik, Humboldt-Universität zu Berlin, D-10099 Berlin*
[2] *FG Wachstum, Institut für Angewandte Physik, Universität Hamburg, D-20148 Hamburg*

The controlled creation, manipulation and detection of spin-polarized currents by electrical means is of high interest. Here we investigate narrow-gap semiconductors with large spin-orbit coupling. Nanostructures can be used to filter specific momentum modes and possibly to create and detect spin-polarized currents [1, 2].

We use wafers with a InAs/InGaAs/InAlAs double quantum well structure [3], containing a shallow two-dimensional electron gas at about 45 nm depth (Fig. 1a). At 4.2 K the carrier density is $n \approx 3 \times 10^{11}$ cm^{-2} and the mobility $\mu \approx 1 - 9 \times 10^4$ Vs/cm^2 in the dark. We fabricate Hall-bars and quantum point contacts (QPCs) with in-plane gates (Fig. 1b), using micro-laser and electron-beam lithography and wet chemical etching, in order to investigate spin-polarized currents when asymmetric gate-voltages are applied.

The in-plane gates are successfully employed to vary the QPC width and the QPCs show conductance quantization from 300 mK up to 1.8 K (Fig. 1c). Applying asymmetric gate-voltages shifts the onset of the conductance curves and DC-bias measurements indicate a shift in the subband structure. Here, we present the results of our magnetotransport measurements and discuss their implications for investigations of the spin-orbit coupling in InAs.

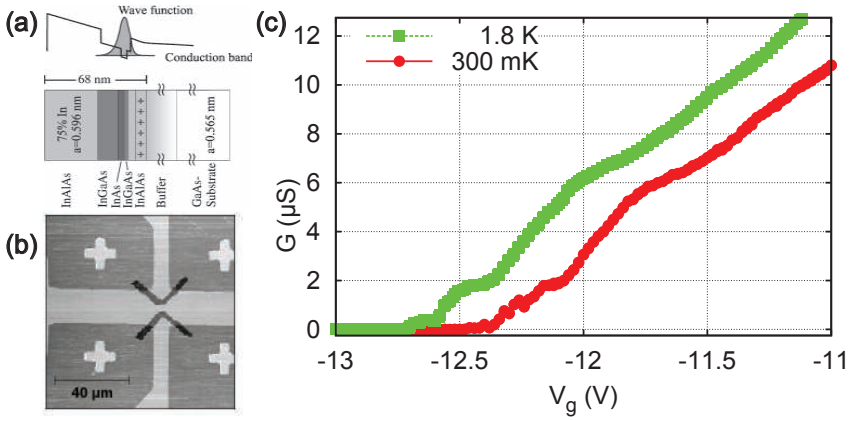

Figure 1: *a*) Scheme of the layer sequence, conduction band and electronic wavefunction of the wafer (from [3]). *b*) Atomic force microscopy image of a QPC. The width and length of the constriction are approximately 1.5 μm and 6 μm, respectively. *c*) Conductance G as a function of gate voltage V_g of a QPC similar to *b*, at two different temperatures.

[1] R. H. Silsbee, *J. Phys.: Condens. Matter* **16**, R179 (2004).
[2] P. Debray *et al.*, *Nature Nanotech.* **4**, 759 (2009).
[3] C. Heyn *et al.*, *J. Crystal Growth* **251**, 832 (2003).

Landau-Zener theory: slow and fast noise in nanoscale systems

A.B. Tchapda*, C. Kenfack Sadem, M.B. Kenmoe, J. Diffo , A. Fotué, and L.C. Fai

University of Dschang, Condended Matter Division, Mesoscopic and Multilayer Structure,PO.Box 67 Dschang, Cameroon
** E-mail address: tchap2007@yahoo.fr*

This work research investigates the effect of transition probability of noise in Landau-Zener theory using the perturbation expansion method compare to Kayanuma's investigation. We use perturbation expansion method to study the off-diagonal noise in x-directions that we called X-noise model and another general case is the existence of off-diagonal noise in both x and y direction with so-called XY-noise model. We use this perturbation expansion to find a general formula of transition probability for the case of slow noise (slow fluctuation) and fast noise (fast fluctuation). We have shown that the results based on the perturbation expansion method for the slow noise (transition probability versus LZ parameter) for the case of XY-model are in full agreement with Kayanuma's perturbative treatment for X-noise model. We demonstrated that the perturbation expansion method can be easily generalized that for the investigation of XYnoise model, but also for the case of fast fluctuation.

Keywords: Landau-Zener transition probability, noises and perturbation.

Effects of Valley Polarization on Spin Polarization in a Silicon 2DEG

V.T. Renard [1], B. A. Piot [2], Y. Niida [3,4], D. Tregurtha[4], A. Fujiwara[5], Y. Hirayama[3] X. Waintal[1], G. Fleury[6] and K. Takashina[4]

[1] *SPSMS, UMR-E 9001, CEA-INAC/UJF-Grenoble 1, France*
[2] *LNCMI-Grenoble, CNRS-UJF-UPS-INSA, France*
[3] *Graduate School of Science, Tohoku University, Japan*
[4] *Department of Physics, University of Bath, UK*
[5] *NTT Basic Research Laboratories, NTT Corporation, Japan*
[6] *SPEC-IRAMIS, CEA Saclay, France*

Understanding the physics surrounding the valley degree of freedom and harnessing it is becoming an area of growing research interest, on one hand due to possible valleytronics applications and issues related to silicon based quantum information processing, and on the other hand due to topical material systems such as graphene and MoS_2 also possessing this degree of freedom. In traditional semiconductor based 2-dimensional electron systems (2DES), extensive studies on AlAs quantum wells have revealed rich physics in which valley and spin both play similar but important roles in determining the properties of the 2DES. In particular, freezing one degree of freedom has strong effects on the 2DES's properties in relation to the other.

Here, we address the effect valley polarization has on spin polarization in silicon, by measuring in-plane magneto-transport with and without valley polarization. Valley degeneracy and polarization are achieved by using a (001) silicon-on-insulator based structure in which the valley splitting can be continuously enhanced in situ to 10's of meV [1].

At valley degeneracy, as known from numerous previous studies in silicon 2DESs, the in-plane magnetic field required to spin polarize the electrons (B_P) is much lower than expected from single particle considerations demonstrating the importance of electron-electron interactions. With valley polarization at high electron density, we find B_P to increase, but not nearly as much as the doubling expected from the single particle picture, also qualitatively consistent with previous work in AlAs [2].

As the density is reduced, the increase in B_P with valley polarization is suppressed further and remarkably, at the lowest density, we find B_P to decrease with valley polarization which is qualitatively opposite to single-particle expectations. i.e. at low enough density, it can be easier to spin polarize a valley polarized system than polarizing a valley degenerate one. Our data are interpreted in terms of electron-electron interactions and disorder and are directly compared to parameter free quantum Monte Carlo simulations [3] which show good agreement.

[1] K. Takashina, Y. Ono, A. Fujiwara, Y. Takahashi and Y. Hirayama. Phys. Rev. Lett. **96**, 236801 (2006)
[2] Y.P. Shkolnikov, V. Vakili, E.P. De Poortere and M. Shayegan. Phys. Rev. Lett. **92**, 246804 (2004)
[3] G. Fleury and X. Waintal. Phys. Rev. B **81**, 165117 (2010).

MoP122

Evidence for two-dimensional Wigner crystal formation in chemical potential measurements

Ding Zhang, Xuting Huang, Werner Dietsche, Klaus von Klitzing, and Jurgen H. Smet

Max Planck Institute for Solid State Research, Heisenbergstrasse 1, D-70569 Stuttgart, Germany

The evolution of the chemical potential of a 2-dimensional electron system was investigated within the quantized Hall regime. The measurement of this thermodynamic quantity was carried out using a closely spaced GaAs bilayer system, with top and bottom gates as well as separate contacts to each layer. Chemical potential variations in one layer were detected with high resolution by monitoring the induced resistance change in the neighboring layer [1, 2]. Apart from the well known rapid increase of the chemical potential when the lower lying Landau level became completely occupied and a higher lying Landau level got filled, two additional anomalies manifested themselves symmetrically around exact integer filling (Fig. 1 (a)). They were attributed to the formation of incompressible Wigner crystals of either quasiparticles or quasiholes [3]. Non-equilibrium dynamics was excluded as the origin of the extra jumps in the chemical potential [4].

The investigations were carried out at different densities, i.e. magnetic fields as well as temperatures. The ratio of the magnetic length l_B over the interparticle distance $l^* = 1/\sqrt{n^*}$ (n^* is the density of quasiparticles) did not vary with the B-field (Fig. 1 (b)). The anomalies vanished when the temperature exceeded around 400 mK, which is consistent with the melting behavior of a solid. More interestingly, the two anomalies got closer to the exact integer filling at higher temperatures. A linear extrapolation (Fig. 1 (c)) yields a temperature of 840 mK which marks the critical temperature for a Wigner crystal.

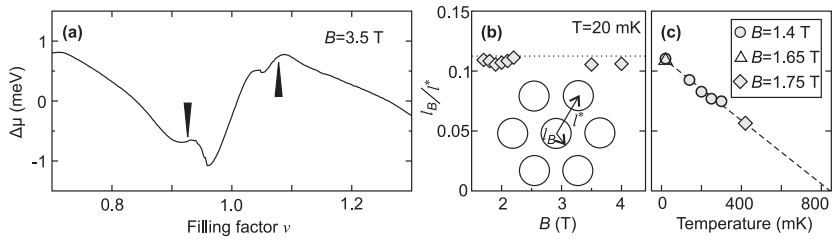

Figure 1: (a) Chemical potential measured around filling factor $\nu = 1$ at $B = 3.5$ T. Arrows mark the two anomalous features indicating the incompressible state of the Wigner crystal. (b)(c) Critical ratio l_B/l^* at which the anomalies appear plotted as a function of (b) the magnetic field B and (c) the temperature. Inset to (b) illustrates the two length scales: l_B–the magnetic length; l^*–the quasiparticle distance. Dotted line marks $l^*/l_B = 9$. Dashed line linearly extrapolates to a temperature of 840 mK at $l_B/l^* = 0$.

[1] L. H. Ho, et al., Appl. Phys. Lett. **96**, 212102 (2010).
[2] S. Kim, et al., Phys. Rev. Lett. **108**, 116404 (2012).
[3] Y. Chen, et al., Phys. Rev. Lett. **91**, 016801 (2003).
[4] L. H. Ho, et al., Phys. Rev. B **82**, 153305 (2010). E. Tutuc, et al., Phys. Rev. B **68**, 201308 (2003). W. Pan, et al., Phys. Rev. B. **71**, 153307 (2005).

Thermally and optically excited multi-channel transport at the interface of $LaAlO_3/SrTiO_3$ heterostructures

V. K. Guduru[1], A. McCollam[1], A. Granados del Aguila[1], S. Wenderich[2], A. Jost[1], M. K. Kruize[2], P. C. M. Christianen[1], G. Rijnders[2], A. Brinkman[2], H. Hilgenkamp[2], J. C. Maan[1] and U. Zeitler[1]

[1] *High Field Magnet Laboratory and IMM, Radboud University Nijmegen, NL.*
[2] *MESA+ Institute for Nanotechnology, University of Twente, Enschede, NL.*

We have performed magnetotransport experiments on a $LaAlO_3/SrTiO_3$ interface [1] with a 10 nm $LaAlO_3$ film, in magnetic fields up to 30 T. The temperature was varied in the range $T = 4.2$ K to 150 K and additionally the sample was illuminated with UV radiation at a fixed $T = 4.2$ K.

Our experimental results show that the low-temperature regime ($T \leq 4.2$ K) is dominated by one type of charge carriers, $n_1 \simeq 10^{14}$ cm^{-2}, with a lower carrier mobility, $\mu_1 \simeq 5$ cm^2/Vs, yielding a linear Hall resistance. Increasing T above 4.2 K or illuminating with UV light with an energy higher than the $SrTiO_3$ band-gap (3.65 eV) at a fixed $T = 4.2$ K, leads to a significant decrease of the resistance, a strong positive magnetoresistance appears and the Hall resistance becomes distinctly non-linear. We explain our observations by thermal or optical excitation of an additional high-mobility electron channel situated 6 meV above the low-mobility channel.

Our magnetotransport data can be quantitatively explained within a simple two-carrier model, where thermal activation (Fig. a) or UV illumination (Fig. b) creates a low-concentration (n_2) and high-mobility (μ_2) electron channel [2], in addition to an existing low-mobility one at 4.2 K. The carrier concentration and the mobility values of this second-electronic channel are extracted from a two-band model fits of the magnetoresistance and the non-linear Hall resistance.

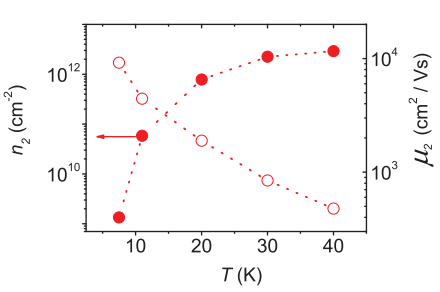

(a) Concentration (left axis, filled circles) and mobility (right axis, open circles) of thermally activated high-mobility electron channel as a function of temperature.

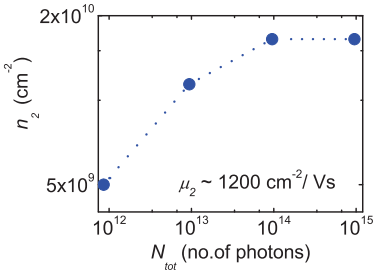

(b) Concentration (filled circles) of the photo-excited carriers as a function of illumination intensity expressed in terms of the photon number, N_{tot}, at 4.2 K.

[1] A. Ohtomo and H. Y. Hwang, Nature **427**, 423 (2004).
[2] V. K. Guduru *et al.*, Appl. Phys. Lett. **102**, 051604 (2013).

MoP124

Surface Magnetotransport due to Helical Edge State in the Organic Dirac Fermion System at the Quantum Limit

Toshihito Osada, Mitsuyuki Sato, Kazuhito Uchida, and Takako Konoike

Institute for Solid State Physics, University of Tokyo, Kashiwa 277-8581, Japan

It is known that the ν=0 quantum Hall (QH) state of undoped graphene is a spin-unpolarized insulating phase (QH insulator). In this paper, in contrast, we show that the spin-polarized ν=0 QH state with gapless edge mode (QH ferromagnet) is realized in another 2D massless Dirac fermion system, an organic conductor α-(BEDT-TTF)$_2$I$_3$ [1]. We present experimental evidences of QH ferromagnet by detecting surface transport due to its helical edge state.

In sufficiently strong magnetic field, the 2D massless Dirac fermion system with charge neutrality shows the ν=0 QH effect resulting from the breaking of four-fold (spin and valley) degeneracy of the n=0 Landau level. In the case that the spin splitting is dominant, the ν=0 QH state is the QH ferromagnetic phase with a gapless helical edge state, which consists of a pair of n=0 QH edge states with opposite spin and chirality (Fig.1(a)) [2]. In the multilayer system, the helical edge states contribute to the surface interlayer transport causing the saturation of interlayer resistance. The finite in-plane magnetic field breaks the interlayer coupling causing rapid increase of saturation resistance (Fig.2(a)).

Based on the above picture, we have performed two kinds of experiments on the saturation of interlayer resistance to confirm the existence of the helical edge state in α-(BEDT-TTF)$_2$I$_3$. (1) The saturated value was not scaled by sample sectional area (Fig.1(b)). This means that the saturation does not originate from bulk transport. (2) The saturated value became minimum when the magnetic field was parallel to the stacking direction. as expected (Fig.2(b)). These results strongly suggest the realization of the helical surface state.

In addition, we also report several experiments on the in-plane transport. The results suggests that the edge channel transport is dominant but dissipative. It is consistent with the fact that the helical edge state is not topologically protected because of the lack of time reversal symmetry.

[1] T. Osada, J. Phys. Soc. Jpn. **80**, 033708 (2011); *ibid*. **77**, 084711 (2008).
[2] T. Osada, Phys. Status Solidi B **249**, 962 (2012).

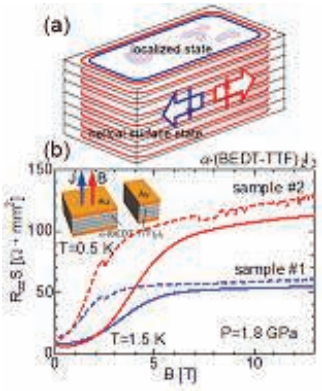

Fig. 1: (a) Concept of the helical surface state. (b) Saturation of interlayer resistance due to surface transport not scaled by sectional area.

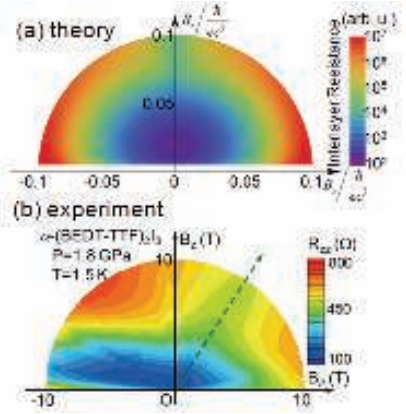

Fig. 2: Dependence of interlayer resistance on field orientation and strength. (a) theory, (b) experiment.

Two-photon quantum well infrared photodetectors in the THz-regime

Carsten Franke [1,2], **Harald Schneider** [1] **and Martin Walther** [3]

[1] *Helmholtz-Zentrum Dresden-Rossendorf*
[2] *Technische Universität Dresden*
[3] *Fraunhofer IAF Freiburg*

Two-photon quantum well infrared photodetectors (QWIPs) are interesting devices for the investigation of ultrashort pulses in the mid-infrared[1] and THz-regime[2]. In these devices the photocurrent shows a quadratical dependence on the intensity of the incoming radiation which is useful in autocorrelation experiments.

We are currently investigating two-photon QWIPs based on the GaAs/AlGaAs material system with an aluminum content lower than 5% in the barrier, which leads to absorption wavelengths above 50µm.

Here we present first measurements of the electronic and optical properties of our samples. We performed dark current measurements and observed large current discontinuities which can be attributed to impact ionization. Photocurrent spectra confirmed the expected absorption wavelengths and showed evidence of further signatures related to optical-phonons. We also present results of autocorrelation measurements at the free-electron laser FELBE at the Helmholtz-Zentrum Dresden-Rossendorf.

[1] H. Schneider, O. Drachenko, S. Winnerl, M. Helm and M. Walther, Appl. Phys. Lett. 89, 133508 (2006).
[2] H. Schneider, H. C. Liu, S. Winnerl, C. Y. Song, M. Walther and M. Helm; Optics Express 17, 12279 (2009).

MoP126

Tuning Fermi Contour Anisotropy of GaAs of Quasi-2D Electron and Hole Systems in Parallel Magnetic Fields

D. Kamburov, M.a. Mueed, M. Shayegan, L.N. Pfeiffer, K.W. West, K.W. Baldwin, and R. Winkler†

Department of Electrical Engineering, Princeton University, USA
†Department of Physics, Northern Illinois University, DeKalb, Illinois 60115, USA

In a quasi-2D carrier system with finite (non-zero) layer thickness, the coupling between the carriers' out-of-plane motion and an applied magnetic field ($B_{||}$) parallel to the sample plane could lead to a severe distortion of the energy bands and the Fermi contours (FCs). Such a distortion can affect devices and/or experiments which rely on ballistic transport of the carriers in the presence of a strong $B_{||}$ used, e.g., to spin-polarize the carriers.

Here we present both numerical calculations (Fig. 1) and experimental data that shed light on this field-induced anisotropy [1,2]. We show results for the FCs of both quasi-2D electrons and holes confined to GaAs quantum wells. As seen in Fig. 1, at $B_{||} = 0$ the FC is circular for electrons. With increasing $B_{||}$, the majority-and minority-spin FCs are deformed, and eventually the minority-spin FC disintegrates. In contrast to the electron case, the hole FCs are slightly anisotropic and split even at $B_{||} = 0$; the splitting is a result of the strong spin-orbit interaction. The hole FCs show much stronger splitting at finite $B_{||}$ and the anisotropy is much more pronounced for the majority spin FC (see, e.g., the contours for $B_{||} = 10$ T).

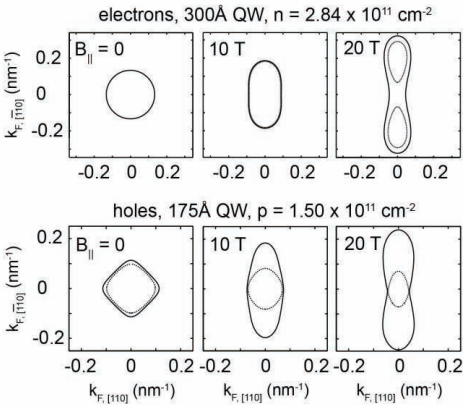

Fig. 1. Results of 8 x 8 Kane Hamiltonian calculations of the FCs. The majority- and minority-spin FCs are shown by solid and dotted lines. Top row: FCs for electrons confined to a 300-Å-wide GaAs quantum well. Bottom row: FCs for holes in a 175-Å-wide quantum well.

Experimentally, we use the commensurability between the quasi-classical orbits of the carriers with a periodic potential modulation [1-3] to measure the size of the Fermi wave vector k_F along both [110] and [$\bar{1}$10] as a function of $B_{||}$. We use a novel technique that allows us to apply a large $B_{||}$ as well as a small perpendicular field to induce the commensurability oscillations.

Our results agree semi-quantitatively with the numerical calculations given in Fig. 1 [1-3]. They demonstrate the *tuning* and *probing* of the GaAs 2D carrier dispersions and FC anisotropy through the application of $B_{||}$.

References:

[1] D. Kamburov *et. al*., preprint.
[2] D. Kamburov *et al.*, Phys. Rev. B **86**, 241302 (2012).
[3] D. Kamburov *et al.*, Phys. Rev. B **85**, 121305(R) (2012).

Spin–orbit coupling effect on a particle density correlation in a two–dimensional electron gas

M. Kołodziej and G. Harań

Institute of Physics, Politechnika Wrocławska,
ul. Wybrzeże Wyspiańskiego 27, 50-370 Wrocław

Symmetry breaking as an origin of significant physical phenomena, like magnetism or superconductivity, is an important issue in condensed matter physics. Particularly interesting is a presence or a lack of time–reversal and inversion symmetries which determine the symmetry of a superconducting groundstate. Their role has been extensively studied in experiment and theory in non–centrosymmetric superconductors [1]. A unique opportunity to control the time–reversal and inversion symmetry breaking is provided by the spin–orbit coupling interaction in two–dimensional systems where these two symmetries can be lifted by applying external magnetic or electric fields, respectively [2].

The spin–orbit coupling interaction, $\vec{\gamma}(\mathbf{k}) \cdot \hat{\sigma}$, is determined by the scalar product of a gyroscopic vector $\vec{\gamma}(\mathbf{k})$ and the spin operator $\hat{\sigma}$ with $\vec{\gamma}(\mathbf{k}) = \vec{\gamma}(-\mathbf{k})$ representing a time–reversal symmetry breaking and $\vec{\gamma}(\mathbf{k}) = -\vec{\gamma}(-\mathbf{k})$ standing for the inversion symmetry breaking. In both cases the interaction leads to the energy band splitting. We discuss the effect of the above two types of the spin–orbit coupling interaction on a density correlation function in a two–dimensional electron gas and conclude on a possible Cooper pair formation: dominated by the intraband pairing for a broken time–reversal symmetry and with a prevailing interband pairing for a broken inversion symmetry. We also point out that our result can be verified experimentally by the Fourier–transformed scanning tunneling microscopy of a single nonmagnetic impurity in two–dimensional or quasi two–dimensional electron systems [3].

[1] E. Bauer and M. Sigrist, Lecture Notes in Physics **847** (Springer 2011).
[2] M. Sigrist, Lectures on the Physics of Strongly Correlated Systems XIII, ed. A. Avella and F. Mancini (AIP, 2009).
[3] L. Capriotti, D. J. Scalapino, and R. D. Sedgewick, Phys. Rev. B **68**, 014508 (2003).

MoP128

Spin texture of bismuth bilayers: an *ab initio* calculation

Erika Nascimento Lima [1], **Tome M. Schmidt**[1]

[1] *Universidade Federal de Uberlandia*

Bismuth is a very heavy element whose electronic structure is very influenced by the spin-orbit coupling (SOC). Nowadays, surface states with strong SOC induce spin splitting, [1] that is promising for applications in spintronics. *Ab initio* calculations have been shown that Bi bilayers (BLs) present large Rashba splitting due to the significant SOC. Furthermore, it was predicted that Bi BLs can present spin quantum Hall (QSH) states. Few layers of Bi stacking along the (111) direction is predicted to be a topological insulator [2]. In this work, using first principles calculations we investigate the band structure and spin texture of Bi BLs stacking along the (111) direction. Our results show that for a certain number of BLs, Bi(111) present two surface states with opposite spin texture, forming a topological Dirac insulator. By increasing the number of BLs a transition to a metal occurs, suppressing the Dirac cone, but keeping a spin texture on the surface states.

[1] Yu M. Koroteev.et al, Physical Review Letters **93**, 046403 (2004).
[2] M. Wada et al, Physical Review B **83**, 121310 (2011).
[3] Liang Fu, C. L. Kane, Physical Review B **76**, 045302 (2007).

Fano profiles at the onset of the x-ray absorption spectra of SiO_2.

M. Städter, M. Tallarida & D. Schmeißer

Brandenburg University of Technology, 03046 Cottbus, Germany

Keywords: Fano profile, x-ray absorption, SiO_2

We analysed the x-ray absorption spectra at the Si2p edge of a 50nm thermal grown SiO_2 on a Si(111) substrate. At the onset of the spectra we found a characteristic Fano profile.

The Fano profile describes the result of the interference of two competing transition passes originating from a Si2p core hole. The photo-excited electron can either become excited into the valance band or into a discrete energetic state within the band gap. From the analysis of the spectroscopic profile we determine the details of that Fano interference. In particular, we derive the position of the discrete state. It is found to be 600meV below the conduction band minimum.

Our findings demonstrate that the fine structure in the Si2p XAS data are indeed assigned to oxygen deficient defects. The energetic position derived are in good agreement with theoretical data of Si dimer and trimer defects incorporated in the SiO_2 matrix. /1/

1 G. Pacchioni, G. Ieraò, Phys. Rev. B 57 (1998) 818.

In-plane stationary current in double-well structure

Matvey V. Entin[1] and Lev I. Magarill[1,2]

[1] *Institute of Semiconductor Physics, Siberian Branch, Russian Academy of Sciences, Novosibirsk, 630090 Russia*

[2] *Novosibirsk State University, Novosibirsk, 630090 Russia*

We study the in-plane stationary current caused by phototransitions between the states of a quantum well. The electric field of light $\mathbf{E}(t) = \mathrm{Re}\,(\mathbf{E}e^{-i\omega t})$ has both vertical and in-plane components. The stationary current originates from the periodic vibration of electrons between two non-equivalent quantum wells caused by the normal component of the alternating electric field with simultaneous in-plane acceleration/deceleration by the in-plane component of electric field $\mathbf{E}(t)$. First, the classical model of the process is developed. Namely, we consider electrons in the oscillator well in z direction. The classical Newton equation for an electron has the form $\ddot{\mathbf{r}}(t) + \Omega^2\mathbf{n}z(t) + \gamma\dot{\mathbf{r}}(t) = e\mathrm{Re}(\mathbf{E}e^{-i\omega t})/m$, where the liquid friction coefficient $\gamma = \gamma_0 + \gamma_1 z$ is introduced; $\mathbf{n}$ is the unit vector along z-axis. The solution in the first order in γ_1 reads

$$\overline{\dot{\mathbf{r}}(t)} = \frac{\gamma_1\omega e^2}{2\gamma_0 m^2}\mathrm{Im}\frac{(\mathbf{En})(\mathbf{E}^* - \mathbf{n}(\mathbf{nE}^*))}{(\omega^2 - i\gamma_0\omega)(\omega^2 - \Omega^2 + i\gamma_0\omega)}. \quad (1)$$

Here $\overline{(...)}$ denotes the time averaging. The stationary drift of electron leads to the stationary current $\mathbf{j} = en_s\overline{\dot{\mathbf{r}}(t)}$, where n_s is the surface electron concentration.

The quantum mechanism of the stationary current in double quantum well is conditioned by in-plane transition asymmetry which appears due to the indirect phototransitions with the participation of impurity scattering. Figure a,b and c show the sketch of a proposed experiment, the band structure of the system under consideration, and the scheme of phototransitions. The photocurrent has a resonant character corresponding to the equality of the photon energy to the distance between subbands Δ. The current appears in response to the linear-polarized light. The resulting current for the case of δ-like quantum wells is

$$\mathbf{j} = \frac{e^3 dn_s}{m\Delta}\frac{\tau}{(\Delta-\omega)^2\tau^2+1}(\mathbf{E} - \mathbf{n}(\mathbf{nE}))(\mathbf{nE})\frac{d^2}{2z_0^2}\frac{\beta(1-\beta^2)}{(1+\beta^2)^2} \quad (2)$$

Here β is the amplitude of mixing of the states in different wells, d is the distance between wells, τ is the intrawell relaxation time for scattering on Coulomb impurities. Estimates show that the current density in GaAs/GaAlAs structure can achieve maximum 3.6 μA/cm at electric field $E = 1V/cm$.

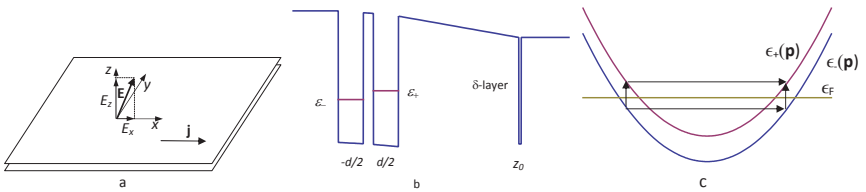

FIG. 1: a) Proposed experiment. The electric field of light $\mathbf{E}(t)$ is tilted in (x,z) plane. The stationary current is directed along the x-axis. b) The band structure. Quantum wells are centered in planes $z = \pm d/2$. The carriers are provided by the δ-layer of donors in the plane z_0. c) The transition amplitude is combined from vertical light-induced transition and impurity scattering non-conserving the in-plane momentum.

Linear polarization rotation study of the microwave radiation-induced magnetoresistance oscillations in the GaAs/AlGaAs system

A. N. Ramanayaka [1], Tianyu Ye [1], H-C. Liu [1], R. G. Mani [1], and W. Wegscheider [2]

[1] *Dept. of Physics & Astronomy, Georgia State University, Atlanta, GA 30303*
[2] *ETH-Zurich, 8093 Zurich, Switzerland*

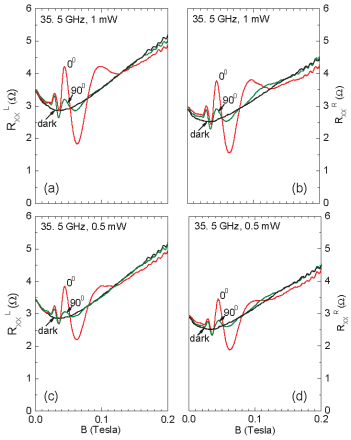

Fig. 1) Microwave-induced magneto resistance oscillations in R_{XX} at 1.5K are shown at f = 35.5 GHz for P = 1 mW in panels (a) and (b), and for P = 0.5 mW in panels (c) and (d). The R_{XX} measured on the left (right) side of the Hall bar is shown as R_{XX}^{L} (R_{XX}^{R}). Each panel shows a dark curve (black), a curve (red) obtained at θ = 0°, and a trace (green) obtained at θ=90°.

Microwave-induced zero-resistance states appear when the associated B^{-1}-periodic magnetoresistance oscillations grow in amplitude and become comparable to the dark resistance of the 2DES.[1] Existing theories, such as the displacement model, the inelastic model, the nonparabolicity model, and radiation-driven electron orbit model, have made differing predictions regarding the influence of the microwave polarization in the microwave radiation-induced oscillatory transport. For example, the inelastic model suggests polarization insensitivity.[see ref. 2 and refs. therein] We have investigated the effect of rotating, in-situ, the polarization of linearly polarized microwaves relative to long-axis of Hall bars. The results indicate that the amplitude of the magneto-resistance oscillations is remarkably responsive to the relative orientation between the linearly polarized microwave electric field and the current-axis in the specimen. [2]

For this experiment, we invented a new setup where circular symmetry allows the rotation of the antenna and the linear polarization with respect to the stationary sample. Figure 1 exhibits the R_{xx} vs. B at f = 35.5 GHz with a high mobility GaAs/AlGaAs Hall bar sample in the setup. Fig. 1(a) and (b) show the results obtained at a source-power P = 1 mW, while Fig. 1(c) and (d) show the same obtained at P = 0.5 mW. Here, a comparison of the red ($\theta = 0^0$) and green ($\theta = 90^0$) traces within any single panel of Fig. 2 indicates that the amplitude of the radiation-induced magneto-resistance oscillations is reduced at $\theta = 90^0$.[2]

We have also examined the detailed polarization angle, θ, dependence of the magnetoresistance oscillations at the oscillatory extrema by fixing the magnetic field and rotating θ at particular frequencies.[2] We found that the angular response of the extrema can be fit with $R_{xx}(\theta) = A \pm C \cos^2(\theta - \theta_0)$, where the + sign corresponds to the maxima and the – sign corresponds to the minima. Here, the fit extracted θ_0 differ substantially from zero, well beyond experimental uncertainty. Indeed, the data suggest that the θ_0 depends upon the extremum in question or B, and sgn(B). Such a large difference in θ_0 due to B-reversal was wholly unexpected.[2]

[1] R. G. Mani et al., Nature 420, 646 (2002); M. A. Zudov et al., Phys. Rev. Lett. 90, 046807 (2003).

[2] R. G. Mani, A. N. Ramanayaka, and W. Wegscheider, Phys. Rev. B 84, 085308 (2011); A. N. Ramanayaka, R. G. Mani, J. Inarrea, and W. Wegscheider, Phys. Rev. B. 85, 205315 (2012).

Commensurability oscillations in the thermoelectric power of unidirectional lateral superlattices

K. Koike, Y. Kato, A. Endo, S. Katsumoto, and Y. Iye

Institute for Solid State Physics, The University of Tokyo, Kashiwa, Chiba 277-8581, Japan

The magnetoresistance of a unidirectional lateral superlattice (ULSL) is well known to exhibit commensurability oscillations, which result from the commensurability between the cyclotron radius R_c and the period a of the unidirectional periodic potential modulation imposed on a two-dimensional electron gas (2DEG). Similar commensurability oscillations are theoretically predicted to be present also in the thermoelectric power [1] but, to the knowledge of the present authors, have never been experimentally verified thus far. In the present paper, we report our experimental observation of the commensurability oscillations in the thermoelectric power of ULSLs.

The device for the measurement is prepared from a GaAs/AlGaAs 2DEG wafer. We introduce 1D periodic potential modulation via strain-induced piezoelectric effect by placing an array of electron-beam resist having the period $a = 200$ nm on the surface of the wafer. As depicted in Fig. 1, the temperature gradient is introduced by heating the center of the Hall bar by an ac current $I_h = 70\ \mu$A, $f = 13$ Hz, and the resulting thermovoltage $V_{\alpha\beta}$ $(\alpha,\beta = x,y)$ is detected by picking out the component with the frequency $2f$ employing the standard lock-in technique. To investigate the anisotropic behavior, ULSLs with the orientation of the modulation both parallel and perpendicular to the temperature gradient are prepared on the device.

Two components of the thermovoltages, V_{xx} and V_{yx}, are plotted in Fig. 2 along with the magnetoresistivity ρ_{xx} measured in the same sample. Oscillations similar to those in ρ_{xx} are clearly observed in the thermovoltages, but with the phase difference of roughly $\pi/2$. In the thermovoltages, the oscillations are much more prominent in the off-diagonal component V_{yx} than in the longitudinal component V_{xx}, in marked contrast to the case for the resistivity. The oscillations behave basically in accordance with the behavior expected for the thermopowers in ULSLs pointed out in an earlier work by Endo and Iye [2].

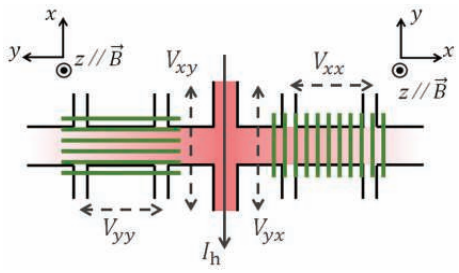

Fig. 1: Schematic diagram of the sample. The temperature gradient is introduced by ac heating current I_h. The direction of the principal axis of the modulation is defined as the x direction for both left and right ULSLs.

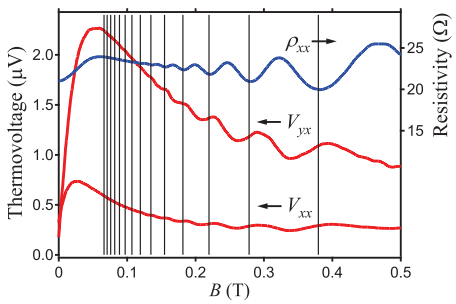

Fig. 2: Thermovoltages and magnetoresistance at $T = 3.4$ K. Vertical lines indicate the positions of the flat-band conditions, where ρ_{xx} takes minima.

[1] F. M. Peeters and P. Vasilopoulos, Phys. Rev. B **46**, 4667 (1992).
[2] A. Endo and Y. Iye, AIP Conf. Proc. 1339, 617 (2011).

Landau level crossing and anti-crossing of bilayer two-dimensional hole gas in Ge/SiGe quantum well

R. Moriya [1], Y. Hoshi [2], Y. Inoue [1], S. Masubuchi [1,3], K. Sawano [2], Y. Shiraki [2] N. Usami [4] and T. Machida [1,3]

[1] *Institute of Industrial Science, University of Tokyo, Tokyo, Japan*
[2] *Advanced Research Laboratories, Tokyo City University, Tokyo, Japan*
[3] *Institute for Nano Quantum Information Electronics, University of Tokyo, Tokyo, Japan*
[4] *Institute for Materials Research, Tohoku University, Sendai, Japan*

Recent development of crystal growth technology enable us to fabricate high mobility two-dimentional hole gas (2DHG). Particularly, the 2DHG in strained Ge is remarkable since it reveals large hole mobility and small effective mass almost comparable to that of electron. However, there have been only few studies on the quantum Hall effect (QHE) and its angular dependence of 2DHG in strained Ge/SiGe quantum well (QW). Since heavy hole of Ge does not couple with in-plane magnetic field, it was not possible to observe Landau level (LL) crossing of this material with a tilted magnetic field. Here we show, by using bilayer 2DHG in Ge/SiGe QW, clear LL level crossing and anti-crossing can be observed.

A QW consist of 20 nm $Si_{0.35}Ge_{0.65}$/20 nm Ge/20 nm $Si_{0.35}Ge_{0.65}$ is grown on $Si_{0.35}Ge_{0.65}$/Si(001) virtual substrate by using gas-source MBE. By introducing *p*-type doping on the top and bottom side of QW, bilayer 2DHG is created in the well. A sheet hole density of the bilayer 2DHG is 6.0×10^{11} and 7.3×10^{11} cm^{-2}, respectively, and average mobility is 35,000 cm^2/Vs. A Hall resistance R_{xy} and longitudinal R_{xx} is measured at 50 mK under the magnetic field $B_\perp$ perpendicular to the sample as shown in Fig. 1. Resistance minima appeared at the filling factor ν=(2N+2), because of the bilayer QHE. We measured magnetic field angle θ dependence of R_{xx} and plotted versus $1/\cos\theta$ as shown in Fig. 2. R_{xx} periodically changes with respect to $1/\cos\theta$, indicating this is due to the crossing of the LLs. Up to three-times of the crossing was observed within our measurement range. This is very distinct from single layer 2DHG sample where LL crossing was not observed within the same field range.

We also observed anti-crossing of the LLs (not shown). Furthermore, a weak anti-localization was observed in the low-field data of R_{xx}. Thus we think anti-crossing is due to the large spin orbit interaction of the 2DHG in Ge/SiGe QW. This system enables us to study various LL physics in high mobility 2DHG.

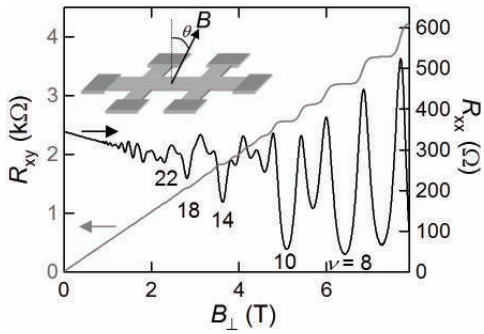

Fig. 1: Perpendicular magnetic field (θ = 0) dependence of R_{xy} and R_{xx}.

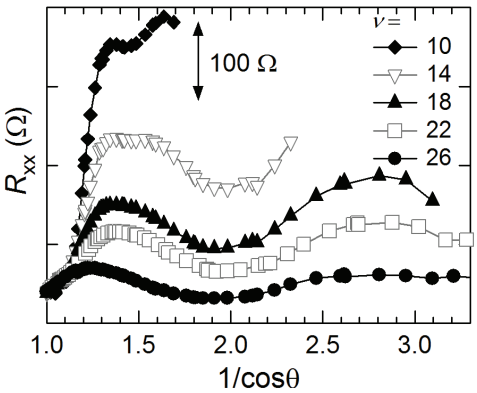

Fig. 2: R_{xx} vs. $1/\cos\theta$ at various ν.

MoP134

Quantum theory of the second-order electromagnetic response of a low-dimensional electron gas

S. A. Mikhailov

Institute of Physics, University of Augsburg, D-86135 Augsburg, Germany

The linear electromagnetic response of a uniform electron gas to a potential electric field is determined by the known Lindhard formula for the dielectric function $\varepsilon(q,\omega)$. This formula can be obtained within the self-consistent-field approach or in the random phase approximation. The function $\varepsilon(q,\omega)$ is related to the polarizability of the electron gas $\alpha(q,\omega)$ and can be analytically calculated for three-, two- and one-dimensional (3D, 2D, 1D) degenerate electron gases at arbitrary values of the wave vector q and the frequency ω.

In this work we derive simple analytical formulas which relate the *second-order* response functions, i.e. the second polarizability $\alpha^{(2)}(q,\omega)$ and the corresponding to $\varepsilon(q,\omega)$ second-order function, to the first-order (linear) ones. These formulas are valid for 3D, 2D and 1D electron gases obeying both Boltzmann and Fermi statistics (i.e. for an arbitrary relation between the chemical potential and temperature). For a degenerate nD electron gas (n=1,2,3) they allow one to analytically calculate the second-order response functions at arbitrary values of q and ω.

The calculated second-order response functions describe the second harmonic generation in the considered electron systems. It has been recently shown [1] that the excitation of the 2D electron gas by the electromagnetic wave with the frequency ω close to the 2D plasma frequency $\omega_p(q)$ should lead to a huge enhancement of the second harmonic intensity. The results of [1] were obtained in the long-wavelength and low-frequency limit (q and ω are small as compared to the Fermi wave vector and energy respectively). The new formulas obtained in this work are valid at arbitrary q and ω and allow one to get the optimal conditions for the second harmonic generation not restricted by the long-wavelength and low-frequency limits. They are valid both for quantum-well (2D) and for quantum wire (1D) systems.

This work is very important for development of semiconductor sources of sub-terahertz and terahertz radiation. The experimental technique of exciting the 2D and 1D plasmons in semiconductor GaAs/AlGaAs structures is very well developed and the mobility of GaAs samples is so high that the quality factor of plasma resonances $Q=\omega_p/\delta\omega_p$ can be much larger than unity, $Q>>1$. Since the intensity of the second harmonic was shown [1] to be proportional to Q^4 one should expect a very efficient frequency up-conversion at the 2D/1D plasmon frequencies. Our results may thus open a new research direction in fundamental and applied physics – the nonlinear plasmonics.

This work was supported by Deutsche Forschungsgemeinschaft.

[1] S. A. Mikhailov, Phys. Rev. **84,** 045432 (2011).

Nonlinear transport and inverted magneto-intersubband oscillations in a triple quantum wells

Z. S. Momtaz[1], G.M.Gusev[1], A.D.Levin[1] and A.K.Bakarov

[1] *Instituto de Física da Universidade de São Paulo, 135960-170, São Paulo, SP, Brazil*
[2] *Institute of Semiconductor Physics, Novosibirsk 630090, Russia*

A two-dimensional (2D) electron system in a perpendicular magnetic field shows magnetoresistance oscillations, known as Shubnikov-de Haas oscillations (SdH) originating from the sequential passage of the Fermi level through Landau levels. If more than one subband is occupied the possibility of intersubband transitions start to occur and leads to another kind of magnetoresistance oscillation. These oscillations, called magneto-intersubband oscillations (MIS) have been studied in single quantum wells with two occupied subbands [1] and recently in a double quantum well (DQW) system [2] and triple quantum wells [3]. MIS oscillations offer new possibilities in transport measurements, e.g. the determination of quantum lifetimes in regions where SdH oscillations are completely suppressed at high temperatures [2, 3]. The nonlinear transport in two-dimensional 2D electron systems placed in a perpendicular magnetic field has been extensively studied in the past in connection with the Hall-field induced resistance oscillations (HIROs) [4] and zero differential resistance state phenomena [5]. Recently novel nonlinear effects in DQW have been observed: with increasing current I, the amplitudes of the MIS oscillations decrease, until a flip of the MIS oscillation picture occurs.

In present paper we study the inverted MIS oscillations in TQW systems. A triple quantum well system consists of three quantum wells separated by thin barriers where electrons occupy three 2D subbands coupled by tunneling. Our samples are coupled GaAs triple quantum wells (TQWs) with a central well width of 20 nm and lateral well widths of 14 nm separated by a 1.4 nm barrier in a 2D electron gas with a mobility of 5×10^5 Cm^2/Vs.

The barrier widths are 1.4 nm and 2 nm, respectively. In our experiments, we have found that the current induced inversion of the magnetoresistance shows up in TQWs as a flip of the MIS oscillation pattern. We determine the critical magnetic field corresponding to the inversion of the quantum contribution to resistance for 3 different periods of MIS oscillations. Moreover, we compared the measurements for macroscopic size (500 μm) and mesoscopic size (5 μm) samples and found essential difference in the nonlinear transport behavior.

[1] V. Polyanovsky, Fiz. Tekh. Poluprovodn., S.-Petersburg **22**, 2230 (1988).
[2] N. C. Mamani et al., Phys Rev. B **77**, 205327, (2008).
[3] S.Wiedmann, N.C.Mamani, G.M.Gusev, O.E.Raichev, A.K.Bakarov, J.C.Portal, Phys. Rev. B **80**, 245306, (2009).
[4] C. L.Yang, J. Zhang, R. R. Du, J. A. Simmons, and J. L. Reno, Phys. Rev. Lett. **89**, 076801 (2002).
[5] A. A. Bykov, J.-Q. Zhang, S. Vitkalov, A. K. Kalagin, and A. K. Bakarov, Phys. Rev. Lett. **99**, 116801 (2007).

MoP136

Terahertz Transitions and Excitons in Narrow-Gap Carbon Nanotubes

C. A. Downing[1], R. R. Hartmann[2], I. A. Shelykh[3] and M. E. Portnoi[1]

[1]*School of Physics, University of Exeter, Stocker Road, Exeter, EX4 4QL, UK*
[2]*Physics Department, De La Salle University, Taft Avenue, Manila, Philippines*
[3]*Science Institute, University of Iceland, Dunhagi 3, IS-107, Reykjavik, Iceland*

We calculate the exciton binding energy in narrow band gap single-walled carbon nanotubes, accounting for the quasi-relativistic dispersion of electrons and holes. Exact analytical solutions of the quantum relativistic two-body problem are obtained for several limiting cases. We show that the binding energy scales with the band gap and conclude on the basis of the data available for semiconductor nanotubes that there is no transition to an excitonic insulator in quasi-metallic nanotubes and that their proposed THz applications [1] are feasible.

Depending on the presence of a metallic gate and the carrier density, excitons can be either described by a short-range electron-hole interaction potential [2] or by an unscreened cusp potential, similar to that considered by Loudon in the 1950s [3]. Our analysis shows that the Loudon potential is a good fit for the quasi-one-dimensional Coulomb potential, obtained by averaging the three-dimensional Coulomb potential with the envelope functions. We report exact analytic solutions for the quasi-relativistic Loudon problem for an exciton with a zero total momentum along the nanotube axis. The complex four-component structure of the electron-hole relative motion wavefunction, which is obtained when two graphene sublattices and two types of particles are taken into account, results in a counterintuitive dip in the shape of the particle density distribution within the exciton, shown in Figure 1.

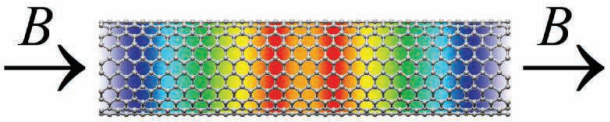

Figure 1. Distribution of the electron density in a 1s exciton assuming that the hole is in the center of the picture. Red and blue colors correspond to the highest and lowest values of density, respectively.

The vanishing exciton binding energy with decreasing of the energy gap removes for narrow-gap nanotubes the undesirable effect of strongly-bound dark excitons, which is known to suppress optical emission in semiconductor nanotubes [4]. However, the Coulomb interaction remains important as it smears the van Hove singularity in the one-dimensional density of states [5]. We report the resulting shape of the terahertz emission from narrow-gap carbon nanotubes with the Coulomb effects taken into account, for both the long-range and short-range interaction models.

[1] M. E. Portnoi, O. V. Kibis, and M. Rosenau da Costa, Superlattices Microstruct. **43**, 399 (2008).
[2] R. R. Hartmann, I. A. Shelykh, and M. E. Portnoi, Phys. Rev. B **84**, 035437 (2011).
[3] R. Loudon, Am. J. Phys. **27**, 649 (1959).
[4] J. Shaver and J. Kono, Laser & Photon. Rev. **1**, 260 (2007).
[5] T. Ogawa and T. Takagahara, Phys. Rev. B **43**, 14325 (1991).

Sharp current suppression at the triplet resonant tunneling in a two-electron double quantum dot

Sonia Sharmin[1], **Koji Muraki**[2], **and Toshimasa Fujisawa**[1]

[1] *Department of Physics, Tokyo Institute of Technology, Meguro-ku, Tokyo, 152-8551 Japan*
[2] *NTT Basic Research Laboratories, Atsugi 243-0198, Japan*

A two-electron system in a double quantum dot (DQD) provides the simplest and richest spin-dependent transport characteristics. The Pauli spin blockade (PSB) effect prohibits spin triplet (1,1)T states (one electron in each dot) to transfer to the doubly occupied singlet (0,2)S state. This effect disappears when doubly occupied triplets (0,2)T are energetically accessible. Here we focus on the triplet resonant tunneling from (1,1)T and (0,2)T, where a couple of sharp current dips on the top of the broad resonant tunneling peak are resolved. The experiment implies the importance of dynamic nuclear spin polarization (DNP), while the detailed mechanism of the sharp suppression remains veiled.

The system we focus upon involves four-fold (1,1) as well as three-fold (0,2)T and (0,2)S states in the transport window (Fig. 1(a)). Experimentally, current through a DQD fabricated in an AlGaAs/GaAs heterostructure is measured as a function of a gate voltage, which is converted into the energy detuning ε between (1,1) and (0,2)T. Current spectrum measured at magnetic field B = 100 mT exhibits clear PSB with a small leakage current (-400 μeV < ε << 0) and a triplet resonant tunneling peak (ε ~ 0), as shown in Fig. 1(b). Surprisingly, a sharp current dip appears around the top of the broad triplet resonant peak (marked by an arrow). This dip develops with increasing B up to a critical field B_C (~ 300 mT depending on the tunneling coupling t_P), above which the dip disappears and other multiple dips start to appear at slightly off-resonant conditions (ε < 0), as shown in Fig. 1(c).

In the absence of nuclear Overhauser effect, (1,1)S partially blocks the transport when the relaxation rate to the ground state (0,2)S is smaller than the triplet transport rate. The spectrum at B = 0 could be the case under the singlet spin blockade (SSB). At finite B (< B_C), net nuclear polarization arises from flip-flop transitions from (0,2)S, and actually the current enhancement (marked by a circle) suggests lifting SSB with an inhomogeneous Overhauser field ΔA. However, one of the eigenstates at ε = 0 remains close to the singlet $\left|(1.1)S\right\rangle - \frac{\Delta A}{t_P}\left|(0,2)T_0\right\rangle$ for small ΔA << t_P. This explains the suppression of current (SSB) at ε = 0, but not the sharp ε dependence. Although detailed analysis with Overhauser field is required, an intriguing three-level resonance with different spin states is anticipated at ε = 0. Electron-nuclear dynamics plays a role even when the current is not completely suppressed.

[1] K. Ono et al., Science 297, 1313 (2002). [2] Y. C. Sun et al., Appl. Phys. Lett. 101, 263108 (2012).

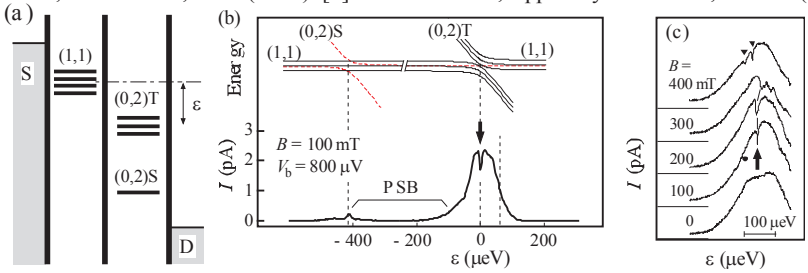

Fig. 1 (a) Energy diagram of a DQD. (b) Current spectrum. The inset shows a schematic energy diagram of singlet (dashed) and triplet states (solid lines). (c) Magnetic field dependence of the dip structure.

MoP138

N-V_{Si}–related center in non-irradiated 6H SiC nanostructure

N. Bagraev[1], E. Danilovsky[1], D. Gets[1], E. Kalabukhova[2], L. Klyachkin[1], A. Malyarenko[1], D. Savchenko[2,3], B. Shanina[2]

[1]Ioffe Physical-Technical Institute, Russia
[2]Lashkaryov Institute of semiconductor physics, NASU, Ukraine
[3]Institute of Physics, AS CR, Czech Republic

The nitrogen-vacancy (N-V) center in diamond and silicon carbide polytypic is well-known to be one of the best versions of a qubit that is able to demonstrate quantum computations at high temperature [1].

Here we present the first findings of the ordinary and electrically-detected ESR studies of the N-V_{Si}–related triplet center with spin state S = 1 in the planar p-type 6H-SiC nanostructure. This nanostructure was prepared by the non-equilibrium diffusion of boron under controlled injection of silicon vacancies (V_{Si}) at the temperature of T = 900^0C into the n-type 6H SiC (0001) wafer which was previously oxidized using the pyrolysis of silane. The quantum conductance, tunneling spectroscopy and SIMS measurements showed that the 6H-SiC nanostructure represents the ultra-narrow p-type quantum well, 2 nm, confined by the δ-barriers heavily doped with boron, 3 nm. The EDESR method by measuring the only magnetoresistance of the p-type quantum well under the high frequency generation from the δ-barriers appears to allow the identification of both the triplet center above noticed and the presence of the isolated silicon vacancies. Since the measurements of the positive magnetoresistance response under the high frequency generation were performed without any light illumination and injection of carriers from the contacts, the EDESR effects appear to result from the spin-dependent scattering of spin-polarized holes from the single paramagnetic centers at the edge channels of the p-type quantum well [2]. Therefore the resonant positive magnetoresistance data appear to be interpreted in terms of the interference transition in the diffusive transport of free holes between the weak antilocalization regime ($\tau_S > \tau_\varphi > \tau_m$) in the region far from the ESR of a paramagnetic point defect located inside edge channels and the weak localization regime ($\tau_\varphi > \tau_S > \tau_m$) in the nearest region of the ESR of that defect.

The ESR and EDESR data on the hyperfine (hf) structure related to the hf interaction with one ^{14}N nuclei seem to evidence that the triplet center is tentatively assigned to the N-V_{Si} defect. The striking result obtained in this work is that as distinct from the well-known N-V defects observed in the e-irradiated diamond as well as in the heavy n-irradiated and high temperature annealed n-type 6H SiC, the N-V_{Si} center has been found in the non-irradiated 6H-SiC nanostructure, with the larger value of the zero-field splitting constant D and anisotropic g-factor.

[1] J.R. Weber, W.F. Koehl, J.B. Varley, A. Janotti, B.B. Buckley, C.G. Van de Walle, and D.D. Awschalom, Proc. Natl. Acad. Sci. USA. **107**, 8513 (2010).
[2] N.T.Bagraev, V.A. Mashkov, E.Yu. Danilovsky, W. Gehlhoff, D.S. Gets, L.E. Klyachkin, A.A. Kudryavtsev, R.V. Kuzmin, A.M. Malyarenko, V.V. Romanov, Appl. Magn. Res. **39**, 113 (2010).

Ballistic electron transport in cascade of $n^+ - i - n^+$ homo- and heterodiodes.

V. V. Korotyeyev[1], V. A. Kochelap[1], and L. Varani[2]

[1] *Institute of Semiconductor Physics, NASU, Kiev, Ukraine*
[2] *Institut d'Electronique du Sud (CNRS UMR 5214), Universite Montpellier 2, Montpellier, France*

We present a self-consistent theory of ballistic electron transport in $n^+ - i - n^+$ homo- and heterodiodes for steady-state and high-frequency regimes. The theory takes into account real injection/exclusion processes at the $n^+ - i$ interfaces, space-charge effects in the base region and diffusive electron transport in contacts. Numerical results are obtained for $InAs$ diodes.

For the steady-state problem, we derive the spatial distributions of electron concentration, electric field and electrostatic potential, and calculate the current-voltage characteristics. We demonstrate that widely accepted simplifications and results, such as the virtual cathode approximation, the Child law and others, cannot be applied to describe semiconductor ballistic diodes for realistic values of the applied electric biases. We develop the theory of real-space transit-time resonance in ballistic diodes and determine the small-signal frequency-dependent response of these devices.

The negative dynamic resistance (NDR) effect is identified and studied. We show that the thermal spreading of injected electrons over the energy greatly affects the transit-time resonance and suppresses the NDR effect. The parameters of the diodes and working temperatures necessary to achieve the maximum NDR effect in the THz frequency range are determined. Finally, we discuss the use of the NDR effect to generate THz radiation. With this aim, we analyze the coupled system of the ballistic diode and the resonator TEM mode. The cascade structure of ballistic diodes gives the larger gain coefficients than single diode. For this cascade, the criterion of THz generation can be readily achieved for a reasonable number of ballistic diodes [1]. The results indicate the perspectives for the development of THz sources based on ultra-short ballistic devices.

[1] V. V. Korotyeyev, V. A. Kochelap, A. A. Klimov, G. Sabatini, H. Marinchio, C. Palermo, and L. Varani, Journal of Nanoelectronics and Optoelectronics **6**, 169 (2011).

MoP140

Light polarization control by H-assisted strain modulation in GaAsN/GaAs heterostructures

S. Birindelli [1], M. Felici [1], R. Trotta [2], A. Notargiacomo [3], A. Gerardino [3], S. Rubini [4], F. Martelli [4], M. Capizzi [1], A. Polimeni [1]

[1] *Dipartimento di Fisica, Sapienza Università di Roma, P.le A. Moro 5, Roma, Italy*
[2] *Johannes Kepler University, Linz, Austria*
[3] *IFN-CNR, Via Cineto Romano 42, 00156 Roma, Italy*
[4] *TASC-INFM-CNR, S.S 14 Km 163.5, 34149 Trieste, Italy*

Defect engineering via the spatially controlled formation of N-H complexes in *dilute nitrides* allows for modulating the electronic and structural properties of the host material in the growth plane [1]. In the work presented here, the surface of a $GaAs_{1-x}N_x$ (x=0.8%) sample was patterned by electron beam lithography with H-opaque Ti wires (width w=500 nm), oriented at different angles (0°, 22.5°, 45°, 67.5°, and 90°) with respect to the [110] crystallographic direction. After hydrogenation and Ti removal, a spatial modulation of both *band-gap energy* and *strain fields* was obtained in the growth plane.

Polarization-resolved *micro-photoluminescence* (μPL) measurements evidence a high *degree of polarization* (ρ) of the light emitted from single wires, due to the H-induced strain anisotropy [see Fig. 1(a-c)]. Further, the polarization angle is found to rotate with the wire orientation, suggesting a potential for light-polarization control via strain engineering. Also, ρ is maximum (minimum) for wires oriented at 0° and 90° (at 45°), highlighting the influence of the underlying crystal on the selection rules governing light emission from the wires.

Finally, atomic force microscopy (AFM) shows that the wires protrude by ~2 nm above the hydrogenated barriers [see Fig. 1(d-f)], due to the lattice distortion induced by the strain anisotropy. This could be useful for X-ray optics applications based on the *Berry-phase effect*, *i.e.*, on the giant translation undergone by X-rays traversing a deformed medium [2].

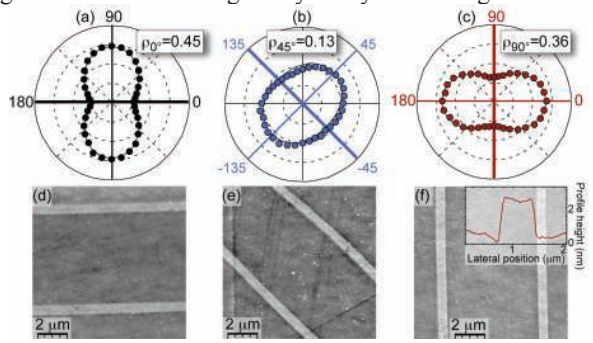

Figure 1. (a-c) Intensity (at T=10 K) of the μPL signal of single GaAsN wires (oriented at 0°, 45°, and 90° with respect to the [110] crystallographic direction), plotted as a function of the angle between the polarization vector and the [110] axis. The listed values of the degree of linear polarization (ρ) were obtained from the fitted curves, displayed as solid lines in the figure. (d-f) AFM images of the GaAsN wires. The contrast between the wires and the hydrogenated barriers is due to the ~2 nm protrusion associated with the H-induced strain anisotropy [see inset of panel (f)].

[1] R. Trotta *et al.*, Adv. Funct. Mater. **22**, 1782 (2012) and references therein.
[2] Y. Kohmura *et al.*, Phys. Rev. Lett. **110**, 057402 (2013) and references therein.

Fundamental limits to the Urbach tail in GaAs quantum wells

Rupak Bhattacharya [1], Richarj Mondal,[1] Pradip Khatua,[1] Alok Rudra,[2] Stefan Malzer,[3] G. Döhler,[3] Bipul Pal,[1] and Bhavtosh Bansal[1]

[1] *Indian Institute of Science Education and Research Kolkata, Nadia 741252, India*
[2] *Ecole Polytechnique Fededrale de Lausanne, CH-1015 Lausanne, Switzerland*
[2] *Max Planck Institute for the Science of Light, 91058 Erlangen, Germany*

Contrary to the predictions of band theory, it has long been experimentally observed that, the band edges of insulators are blurred with an exponential density of states that extends into the bandgap [1]. Interestingly the functional form of the spectral and the temperature dependence of these bandtail states is almost universal (Urbach rule) across insulators, irrespective of the magnitude of the bandgap or the strength and nature of disorder [1, 2]. Despite three decades of extensive work on quantum wells (QWs), this is the first comprehensive study of the bandtail states in a quasi-two-dimensional system, done not only with the aim of establishing the Urbach rule for GaAs QWs [Fig. (a)], but also to elucidate the origin of these tails at low temperature. A fundamental understanding of these bandtail states is relevant, e.g., in understanding the feasibility of laser cooling of semiconductors by anti-Stokes PL, and the limitations in treating the semiconductor ground state at par with the QED vacuum in context of phenomena like virtual photoconductivity.

Through low temperature electro-absorption (photoconductivity) measurements we have systematically verified the assumptions of a rigorous version [2] of the classic Dow-Redfield theory [1] that is also valid at low temperatures. We have found that broadening of the excitonic resonance due to the electric field of phonons is the fundamental mechanism for bandtailing in high quality QWs. At low temperatures (4K), this is essentially due to the zero-point phonon modes and gives a fundamental limitation to the Urbach energy, $E_u \sim 2$ meV. Furthermore, from the magnetic field dependence of the excitonic linewidths, we have inferred that the interface disorder of large correlation length found in samples of poor quality also strongly affects the bandtails [3].

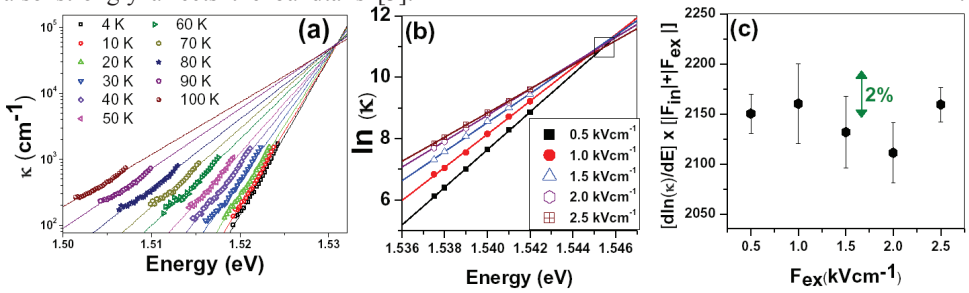

Figure: (a) Urbach rule in a high quality GaAs QW. (b) The exponential slope of the absorption coefficient κ below the energy gap is modified on application of in-plane electric field F_{ex}, in accordance with the Dow-Redfield theory. (c) $\kappa \sim \exp[C\,(E-E_0)\,/(|F_{in}|+|F_{ex}|)]$ predicts that product of the logarithmic derivative of the absorption coefficient times the total ($|F_{in}|+|F_{ex}|$) electric field should be constant. The electric field F_{in} due to the zero-point phonons is inferred to be 3kVcm^{-1}.

[1] J. Dow and D. Redfield, Phys. Rev. B **5**, 594 (1972).
[2] W. Schaefer and M. Wegener, Semiconductor Optics and Transport Phenomena, (Springer, 2002).
[3] K. Noba, Y. Kayanuma, and K. Nojima, Int. J. Mod. Phys. B **15**, 3908 (2001).

How to use type II InAs/GaSb superlattice structure to reach detection wavelength of 2-3 μm?

Jianliang Huang [1], Wenquan Ma [*1], Yang Wei [1], Yanhua Zhang [1], Kai Cui [1], Yulian Cao [1], Xiaolu Guo [1], and Jun Shao [2]

[1] *Institute of Semiconductors, Chinese Academy of Sciences, Qinghua East A35, Beijing 100083, China*
[2] *National Laboratory for Infrared Physics, Shanghai Institute of Technical Physics, Chinese Academy of Sciences, Shanghai 200083, China.*

Type II InAs/GaSb superlattice (SL) structure has many advantages for infrared photodetector applications and its detection wavelength is proved to be able to cover the range of about 3 to 30 μm by tuning the constituent layer thickness and the thickess ratio of InAs to GaSb. However, it has been an important aspect to push the detection wavelength into the short wavelength range of 2-3 μm by using the type II SL structure. This paper [1] tries to answer an important question: is it possible to use type II SLs to reach detection wavelength of 2-3 μm and how to realize it?

We reveal that a strong In intermixing occurs during the growth of InAs/GaSb SL structure. The In intermixing is strongly related to the growth temperature and can have a very big impact on the short period SL band structure and is the reason why a detection wavelength smaller than 3 μm can't be realized for a SL structure like InAs (3 ML)/GaSb (3 ML). Concretely, we find that the infrared photoluminescence (PL) peak of an InAs (8 Å)/GaSb (9 Å) SL structure is shifted from 5.8 to 4.0 μm at 77 K when the growth temperature is lowered from 380 to 340°C. This blueshift of the PL peak is attributed to the reduced In intermixing due to a lower growth temperature. To reduce the influence of the In intermixing on the SL band structure, besides lowering the growth temperature, another effective scheme is to increase the GaSb layer thickness in the SL structure. Experimentally, we find that the PL peak of an InAs (8 Å)/GaSb (21 Å) SL structure grown at 380°C reaches 2.7 μm at 77 K. By using this SL structure, the 50% cutoff wavelength of a *p-i-n* type of detector reaches 2.56 μm at 77 K.

[1] J. L. Huang, W.Q. Ma, Y. Wei, Y.H. Zhang, K. Cui, Y.L. Cao, X.L. Guo, and J. Shao, IEEE J. Quantum Electron. **48**, 1322 (2012).

Millisecond-range liquid phase recrystallization for III-V/Si heteronanojunction fabrication

S. Prucnal[1], S.Q. Zhou[1], F. L. Bregolin[1], X. Ou[1], M. O. Liedke[3], R. Huebner[1], M. Helm[1], J. Zuk[2], M. Turek[2], K. Pyszniak[2], A. Drozdziel[2], and W. Skorupa[1]

[1]*Institute of Ion Beam Physics and Materials Research, Helmholtz-Zentrum Dresden-Rossendorf, P.O. Box 510119, 01314 Dresden, Germany*
[2]*Maria Curie-Sklodowska University, Pl. M. Curie-Sklodowskiej 1, 20-035 Lublin, Poland*
[3]*Institute of Radiation Physics, Helmholtz-Zentrum Dresden-Rossendorf, P.O. Box 510119, 01314 Dresden, Germany*

The downscaling and stressor technology of Si based devices are extending the performance of the silicon channel to its limits. One promising solution for the performance progress which can overcome those limits is the integration of different functional optoelectronic elements within one chip.
We have developed a compact, CMOS compatible and fully integrated solution for the integration of III-V compound semiconductors with silicon technology for optoelectronic applications. The III-V nanostructured semiconductors are synthesized in silicon based matrixes using the combination of ion beam implantation and millisecond flash lamp annealing (FLA) techniques via ***millisecond range liquid phase epitaxy*** [1, 2]. In this paper we will present investigations of the microstructural, optical and electrical properties of InAs and InP nanostructures formed in silicon and on SOI wafers. The growth evolution of the III-V nanostructures during FLA and the influence of the annealing parameters on their crystallographic orientation, shape and size will be explored. Conventional selective etching was used to form the n-III-V/p-Si heterojunction. The current-voltage measurement confirms the heterojunction diode formation between *n-type* III-V quantum dots and *p-type* Si. The main advantage of our method is its integration with large-scale silicon technology, which also allows its application for the fabrication of Si-based optoelectronic devices.

[1] S. Prucnal, et al. NanoLett. **11**, 2814 (2011).
[2] S. Prucnal, et al. Nanotechnology, **23,** 485204 (2012).

MoP144

The electroluminescence from p^+-nanostructured Si – n-Si (100) heterojunctions

N. Bagraev [1], L. Klyachkin [1], R. Kuzmin [1], A. Malyarenko [1], V. Mashkov [2]

[1] *Ioffe Physical-Technical Institute of the Russian Academy of Sciences, St. Petersburg*
[2] *St. Petersburg State Polytechnical University, St. Petersburg*

The goal of the present work was to study the electroluminescence from novel heterojunctions that represent the p-type nanostructured Si (ns-Si) heavily doped with boron on the n- Si (100) wafer. These heterojunctions were prepared on the n-type Si (100) surface within frameworks of the planar diffusion silicon technology. It is well-known that the generation of excess fluxes of the silicon self-interstitials and vacancies occurs during the formation of an oxide overlayer on the Si (100) wafer. The fluxes have the preferred crystallographic directions along <111> and <100> axes, respectively, which allow the formation near the Si-SiO_2 interface the nanostructured layer produced by a set of self-interstitial microdefects confining longitudinal ultra-narrow, 2 nm, silicon quantum well (Si-QW) [1]. After preliminary oxidation, photolithography and etching, the non-equilibrium short-time boron diffusion from the gas phase should be carried out to passivate the dangling bonds and to transform the Si (100) wafer with the ns-Si layer into the ns-Si/Si p^+n heterojunctions. The high concentration of boron introduced during this process was controlled by the SIMS method and appeared to be equal to the value of 5×10^{21} cm^{-3}. The ns-Si/Si p^+n heterojunctions have been shown to represent the p-type Si-QW confined by wide band gap heterobarriers heavily doped with boron on the Si (100) wafer [1].

Room temperature electroluminescence from the heterojunctions studied was observed from visible to far infrared spectral range. The nanostructured silicon layer heavily doped with boron appeared to participate in the generation of visible light as a result of direct interband optical transitions in the 2 nm silicon microdefects. Highly linearly-polarized infrared electroluminescence, 1.16 μm, is originated from the heterointerface between the nanostructured barrier heavily doped with boron and the n-type Si (100) wafer. The intensity and degree of the linear polarization as well as the spectral shape of this infrared electroluminescence were studied as a function of temperature, excitation levels and the lateral voltage applied in the plane of the p+-n junction. The last one causes the quenching of the high degree of the linear polarization and the intensity of the electroluminescence. Intensive light emission in far infrared region seems to be started from the intraband optical transitions in nanostructured silicon layer. The results obtained show that the ns-Si/Si p^+n heterojunctions are able to exhibit a great potential for realizing the fully silicon-compatible optoelectronic devices in different spectral ranges.

[1] N.T. Bagraev, E.Yu. Danilovsky, W . Gehlhoff, L.E. Klyachkin, A.A. Kudryavtsev, R.V. Kuzmin, A.M. Malyarenko, V.V. Romanov, Journal of Modern Physics **2**, 256 (2011).

Influence of intervalley scattering on the metallic behavior in Si MOSFETs

V. T. Renard[1], I. Duchemin[2], Y. Niida[3], A. Fujiwara[4], Y. Hirayama[3] and K. Takashina[5]

[1] *CEA-INAC/UJF-Grenoble 1, SPSMS, UMR-E 9001, 17 rue des martyrs, 38054 Grenoble cedex 9, France*
[2] *CEA-INAC/UJF-Grenoble 1, SP2M, UMR-E 9001, 17 rue des martyrs, 38054 Grenoble cedex 9, France*
[3] *Graduate School of Science, Tohoku University, 6-3 Aramakiaza Aoba, Aobaku, Sendai, 980-8578 Japan*
[4] *NTT BRL, NTT Corporation, Atsugi-shi, Kanagawa 243-0198, Japan*
[5] *Department of Physics, University of Bath, Bath BA2 7AY, UK*

Whether or not electrons confined to two dimensions conduct electricity when the temperature approaches absolute zero remains a subject of intense research and controversy. It is well established that the metallic behavior is stronger in systems like silicon where valley degeneracy enhances interactions. However, little is known about the role of valley splitting and inter-valley scattering, two processes associated with valley degeneracy. After demonstrating that valley splitting could be electrically controlled in Si quantum wells [1], we have recently shown that valley splitting suppresses the metallic behavior in this system [2]. Here, we address the problem of inter-valley scattering which has previously been disregarded because of the lack of theoretical description.

We implement a recent theory of weak-localization magneto-conductivity (MC) with inter-valley scattering [3] to extract the inter-valley scattering time in our sample. Doing so not only allows us to demonstrate for the first time that the metallic behavior can be observed even in presence of strong inter-valley scattering, but also to show that this observation can be quantitatively explained by the interplay of electron-electron interactions and weak localization [4]. Our analysis leads to the solution of a long standing pivotal paradox concerning weak-localization and the metallic behavior in Si. This paradox had arisen from the observation a MC typical of weak-localization, while its characteristic logarithmic temperature dependence in zero field conductivity had been illusive in the metallic state. We show that this is due to a coincidental cancellation by effects of interactions between electrons at B=0 T (Figure 1).

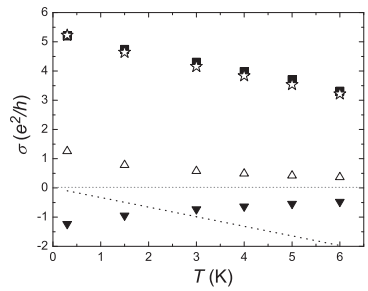

Figure 1: Measured conductivity (■) for $n = 3.9 \times 10^{15}$ m^{-2}, ballistic interaction correction (···), diffusive interaction correction (△), weak localization correction (▼) and the sum of Drude, WL, diffusive and ballistic contributions (☆).

[1] K. Takashina *et al.* Phys. Rev. Lett. **96**, 236801 (2006).
[2] K. Takashina *et al.* Phys. Rev. Lett. **106**, 196403 (2011).
[3] A. Kuntsevich *et al.* Phys Rev. B. **75**, 195330 (2007).
[4] V. T. Renard *et al.* cond mat (2013).

MoP146

Radiation losses in resonator measurement converters for scanning microwave microscopy

Yuriy Y. Gordiyenko, Dmytro A. Polietaiev and Bohdan V. Sokolenko

Taurida National V.I.Vernadsky University

In this document, we present the results of calculations on numerical model of the microwave converter with the coaxial measuring aperture are discussed. Conditions at which it is necessary to consider radiating losses are found.

Currently, scanning microwave microscopy (SMM) is widely used for the study of different materials and structures. The advantage of SMM is the opportunity to conduct research not only the surface of the sample, but the volume near the surface area. Almost all the work in this direction are experimental, without analyzing the characteristics of the probing devices and the optimization of the geometry of the probe to increase the spatial resolution [1].

Resonator measurement converters with coaxial measurement aperture (RMC CMA) have wide application in SMM [2]. In each of the above spheres optimal designing of such converters depends upon various criteria; however, it is practically demonstrated that the necessity of considering the radiation losses is found in both cases.

Usually simulation characteristics of RMC are based on the oscillatory mode of the electromagnetic field in the resonator. For closed systems it is quite admissible. But in RMC CMA influence of the object upon the resonator field is altering radiation properties of the measurement aperture.

Purpose of work is the calculation and analysis of RMC CMA with the influence of the sample and selection criteria when one can neglect of radiative losses.

For theoretical investigation of such a RMC it is necessary to find a total distribution of the electromagnetic field in the resonator and in the object from the solution to the Maxwell equations. The contribution of the radiation component in variation of the RMC Q-factor at the influence exerted by the object depends upon electromagnetic properties of the object and the aperture geometry. At the general setting of solution to this problem it is impossible to separate the indicated aspects (radiation and oscillatory loss).

The Q-factor is determined from the frequency dependence of the parameter S11 calculated using direct numerical methods for solving the Maxwell equations for field distribution on the basis of the finite elements technique [3] without considering active losses in the resonator walls.

It follows that only at $R_2/\lambda < 0,01$ and $tg\delta_2 > 10^{-2}$ there can be neglected the radiation losses as compared the oscillatory ones.

The performed investigations provide a convincing proof of the fact that while using coaxial measurement equipment in SMM of the dielectrics with $tg\delta_2 < 10^{-2}$, it is not allowed to neglect the influence of losses upon the radiation.

[1] L.F. Chen, C.K. Ong, C.P. Neo et al. Microwave Electronics Measurement and Materials Characterization (2004).
[2] Yu.Ye. Gordiyenko, N.I. Slipchenko, V.V. Petrov Radio Electronics and Informatics **3**: (2007).
[3] G.I. Marchuk, V.I. Agoshkov Introduction to the projection-grid methods (1981).

A movable light emitting area in resonant tunneling diodes

G. Pettinari [1,3], N. Balakrishnan [1], O. Makarovsky [1], R.P. Campion [1], A. Polimeni [2], M. Capizzi [2] and A. Patanè [1]

[1] *School of Physics and Astronomy, The University of Nottingham, Nottingham NG7 2RD, United Kingdom*
[2] *Dipartimento di Fisica, Sapienza Università di Roma, P.le A. Moro 2, 00185 Roma, Italy*
[3] *IFN-CNR, via Cineto Romano 42, 00156 Roma, Italy*

The ability to spatially localize and move on a micrometer scale the emitting region in a light emitting diode (LED) is relevant for a variety of applications, such as Lab-On-a-Chip experiments, bio-imaging, optoelectronic integrated circuits, etc. Such control has been achieved, recently, in organic LEDs and transistors [1], but with performances that are presently limited by the properties of the employed organic materials –such as low quantum efficiencies, low carrier mobilities, and temporal instabilities– and by uncertainties in the physical mechanisms underlying carrier recombination and light emission in these material systems. These drawbacks can be overcome in an inorganic LED, as shown in this work [2].

We report on the realization of a movable micrometer light emitting area in a resonant tunnelling LED (RTLED) containing a GaAs/AlAs quantum well (QW). This is achieved via post-growth hydrogen passivation of C-dopants on the *p*-type layer of the *p-i-n* RTLED. The resulting increase of resistivity combined with the resonant injection of carriers in the QW leads to an unusual spatial localization of the QW electroluminescence (EL) emission along a *ring,* whose size and position are controlled by the applied voltage; see Fig. 1. The formation of the ring is observed for temperatures up to T = 100 K with characteristics indicating a real possibility for this movable LED to be used up to liquid-nitrogen temperatures. An additional, important outcome of tailoring the resistivity of the *p*-type contact layer with hydrogen is the possibility of achieving *simultaneous resonant injection of both electrons and holes* under given bias conditions. This results in a tenfold increase of the QW EL intensity and a threefold increase in the peak-to-valley QW EL intensity ratio versus applied voltage, a figure of merit of a RTLED.

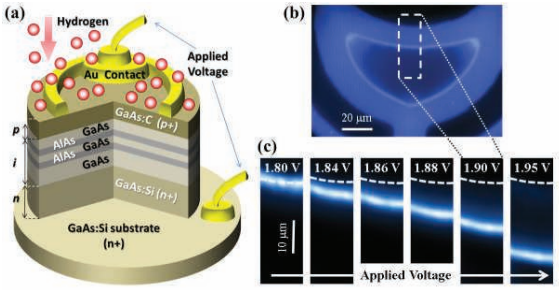

Figure 1. Sketch of a 200 μm-mesa *p-i-n* RTLED **(a)** and digital camera image of the EL emission intensity (at T = 9 K and V_{app} = 1.9 V) after post-growth hydrogen incorporation **(b)**. The neutralization of C-dopants in the region of the mesa exposed to hydrogen results in a localization of the QW EL emission along a ring, whose size and position are controlled by the applied bias **(c)**.

The successful realization of a movable micrometer-size LED in a compact and versatile solid state device will foster the development of innovative applications. Also, the controlled simultaneous resonant injection of carriers in the QW could be exploited for creating coherent excitonic states in electrically pumped quantum devices [3].

[1] B.B.Y. Hsu *et al*., Adv. Mater. **24**, 1171 (2012).
[2] G. Pettinari *et al*., *manuscript submitted for publication* (2013).
[3] A.J. Shields, Nature Phot. **1**, 215 (2007).

A customized THz quantum-cascade laser as the local oscillator for a heterodyne receiver at 4.745 THz

L. Schrottke[1], M. Wienold[1], R. Sharma[1], X. Lü[1], K. Biermann[1], A. Tahraoui[1], H. Richter[2], H.-W. Hübers[2,3], and H. T. Grahn[1]

[1] *Paul-Drude-Institut für Festkörperelektronik, Hausvogteiplatz 5–7, 10117 Berlin, Germany*
[2] *Deutsches Zentrum für Luft- und Raumfahrt, Institut für Planetenforschung, Rutherfordstr. 2, 12489 Berlin, Germany*
[3] *Technische Universität Berlin, Institut für Optik und Atomare Physik, Straße des 17. Juni 135, 10623 Berlin, Germany*

Quantum-cascade lasers [1] (QCLs) for the terahertz (THz) spectral region [2] are promising light sources for several spectroscopic applications and THz imaging. For practical use, however, the challenge consists in the simultaneous fulfillment of specifications for an entire set of operating properties such as lasing frequency, optical output power, and beam profile within a single device. At the same time, the lasers have to comply with the range of operating temperatures and pumping powers defined by the specific application.

We discuss the design and optimization of customized THz QCLs. As an example, we report on the development of a local oscillator used in a heterodyne receiver for the investigation of interstellar atomic oxygen. In this case, the source is required to emit in continuous-wave (cw) mode with a tuning range of about 5 GHz either just below or above 4.745 THz. For single-mode operation with the required tuning range, we fabricated distributed-feedback (DFB) lasers combining a single-plasmon QCL with a lateral first-order grating. Tuning is achieved by adjusting the effective refractive index of the resonator through the temperature inside the device by varying the driving current. Therefore, the QCL is required exhibit a sufficiently large wall-plug efficiency over a rather wide range of current densities, but with a negligible spectral shift of the gain maximum.

The design procedure includes the optimization of an appropriate design type using a self-consistent model based on classical rate equations. For this optimization, also reabsorption and negative differential conductivity has to be regarded. The wafers were grown by molecular-beam epitaxy. In order to improve the homogeneity of the about 10 μm thick active region, the growth rates were controlled using optical monitoring. Lasers with emission close to the target frequency can be operated in cw mode at low temperatures with more than 10 mW output powers and above 60 K with about 1 mW. The DFB laser ridges were fabricated by dry etching. For a DFB laser which shows emission covering precisely the required frequency range, we achieved an output power of about 0.5 mW for operation between 42 and 47 K in a mechanical (liquid-coolant-free) cooler. Under these conditions, the beam profile is almost circular [3].

The results demonstrate the potential of THz QCLs as well as the applicability of the rate-equation model. At the same time, we observed differences between nominally identical samples, which show the complexity of the QCL structures and reveal the remaining challenge for the growth and fabrication in order to achieve the highest possible output power at the target emission frequency in a single device.

[1] J. Faist, F. Capasso, D. L. Sivco, C. Sirtori, A. L. Hutchinson, and A. Y. Cho, Science, **264**, 553 (1994).
[2] B. S. Williams, Nature Photon. **1**, 517 (2007) and references therein.
[3] L. Schrottke, M. Wienold, R. Sharma, X. Lü, K. Biermann, R. Hey, A. Tahraoui, H. Richter, H.-W. Hübers, and H. T. Grahn, Semicond. Sci. Technol. **28**, 035011 (2013).

DFT simulation of the physical properties of AlN/GaN multiquantum well (MQWs) system

Pawel Strak[1], Pawel Kempisty[1], and Stanislaw Krukowski[1,2]

[1] *Institute of High Pressure Physics, Polish Academy of Sciences, Sokolowska 29/37, 01-142 Warsaw, Poland*

[2] *Interdisciplinary Centre for Mathematical and Computational Modelling, University of Warsaw, Pawinskiego 5a, 02-106 Warsaw, Poland*

Density functional theory simulations (DFT) were used to obtain physical properties of AlN/GaN multi-quantum wells (MQWs) systems. To overcome the Kohn-Sham band gap (BG) underestimation, we have applied a method proposed recently by Ferreira et al., called LDA-1/2 which approximately includes the self-energy of excitations in semiconductors, providing BG energies, effective masses, and band structures in very good agreement with experiment [1]. Systematic DFT studies were conducted to determine an influence of changing of the well/barrier width ratio on the properties of AlN/GaN MQW system such as the electric field, polarization charges and polarization dipoles within the well-barrier structure. It was shown that these fields depend critically on the well-barrier thickness ratio. A comparison of the fields proves that the DFT results recover basic trends predicted by the theory based on spontaneous and piezoelectric polarization, computed from the Berry-Phase approach in Ref. [2]. Generally, the fields obtained from the Poisson solution in the DFT calculations are greater than these predicted by the polarization models. We relate this error to the BG underestimation which was not corrected by the authors in the last reference. The field gives rise to Quantum Confined Stark Effect (QCSE), changing the energies of quantum states of the electrons and holes in the wells and also separating the wavefunctions of both quasiparticles in space. The overlap of these functions is calculated, showing considerable separation in space which significantly reduces the oscillator strength of the optical transitions, and consequently, the optical efficiency of nitride based light emitting diodes (LED) and laser diodes (LD), especially for wider structures. For wider barriers, the energies of the transition displays the crossover from narrow minima type where the parallel polarized transition has a lower energy to wide wells where the perpendicular polarized emission is lower in the energy scale. This is related to the crossover of the CH and LH/HH bands, as postulated in Refs [3, 4]. For the narrow GaN layers, the optical strength is higher for perpendicular polarized transitions which is in agreement with the experimental results in Ref. [5], where a stronger emission was observed for the c-axis direction. For wider wells, the strengths falls much faster for perpendicular polarization which indicates the important role of the band offsets. The results were also used for optaining a spatial distribution of the bands in structures with atomic resolution which allows direct estimation of the band offset.

[1] L.G. Ferreira, M. Marques, and L.K. Teles **78**(12), 125116 (2008).
[2] V. Fiorentini, F. Bernardini, F. Della Sala, A. Di Carlo, P. Lugli, Phys. Rev. B **60**, 8849 (1999).
[3] Y. Taniyasu and M. Kasu, Appl.Phys. Lett. **98**, 131910 (2011)
[4] K. Kamiya, Y. Ebihara, K. Shiraishi, and M. Kasu, Appl. Phys. Lett. **99**, 151108 (2011)
[5] Y. Taniyasu and M. Kasu, Appl. Phys. Lett. **99**, 251112 (2011)

Ab initio DFT simulation of the physical properties of InN/GaN multiquantum wells

Pawel Strak[1], Pawel Kempisty[1], and Stanislaw Krukowski[1,2]

[1] *Institute of High Pressure Physics, Polish Academy of Sciences, Sokolowska 29/37, 01-142 Warsaw, Poland*

[2] *Interdisciplinary Centre for Mathematical and Computational Modelling, University of Warsaw, Pawinskiego 5a, 02-106 Warsaw, Poland*

Ab initio DFT simulations of InN/GaN multiquantum wells (MQW) were used to obtain electric potential profile in the system that, after appropriate averaging procedure, reveal electric field in the wells and barriers, and also electric potential jumps at the interfaces. The field changes, and the potential jumps were used to obtain the density of the polarization charges and the dipole layer at InN/GaN interfaces, respectively. It was shown that polarization dipoles are confined within one double atomic layer, proving that they have different nature from the dipole layers emerging at the semiconductor surfaces or within p-n junctions.The obtained fields depend on both the well and the barrier thicknesses. DFT data are in good agreement with the continuum polarization analysis results that were obtained accounting the DFT determined potential jumps and using the standard polarization parameters. Built-in electric field causes a spatial separation of carriers, but one of the most important factors, from the point of view of efficiency of the light emission, is the overlap of the hole quantum states at the valence band maximum, and the electron states at the conduction band minimum. The efficiency proportional to the oscillator strength values was obtained from an implementation of the PAW method [1] in an existing plane-wave code supporting non norm-conserving Vanderbilt-type US PP's [2], the Vienna *ab initio* simulation package VASP [3] - [5]. To overcome the Kohn-Sham band gap (BG) underestimation, in comparison to the experimental ones, we have applied an empirical LDA+U correction method [6]. In parallel, a considerable insight was gained in the semiconductor structure properties, including the electronic dispersion relations and the density of states, both total and projected on the atomic layers. Semiconductor bands variation in space projected from partial density of states were inwestigated.

[1] P.E. Blchl, Phys. Rev. B **50**, 17953 (1994)
[2] D. Vanderbilt, Phys. Rev. B **41**, 7892 (1990).
[3] G. Kresse, and J. Hafner, Phys. Rev. B **47**, 558 (1993).
[4] G. Kresse, and J. Furthmller, Comput. Mat. Sci. **6**, 15 (1996).
[5] G. Kresse, and J. Furthmller, Phys. Rev. B **54**, 11169 (1996).
[6] A. I. Liechtenstein, V. I. Anisimov and J. Zaane, Phys. Rev. B **52**, R5467 (1995).

MCD OF CRYSTALLINE THIN FILM ORGANIC SEMICONDUCTORS

Naveen Rawat [1], Z. Pan [1], L. Manning [1], R. Waterman [1], S. McGill [2] and M. Furis[1]

[1]Material Science Program, University of Vermont, Burlington VT, USA
[2]The National High Magnetic Field Laboratory (NHMFL), Tallahassee, Florida, USA

Metal Phthalocyanines (MPc's) are organic p-type semiconductors used in light emitting diodes (LEDs), photovoltaic cells and field effect transistors (FETs). In the crystalline phase, they exhibit large mobilities (~1cm^2/Vs) and can also accommodate magnetic ions such as Cu, Co, or Mn in the center, making them exhibit paramagnetic and even ferromagnetic behavior [1]. Soluble organic thin films allow engineering of magnetic properties via control of the molecular stacking and possible creation of the organic analogues to diluted magnetic semiconductors (DMS) [2].

Magnetic Circular Dichroism (MCD) is extremely useful in understanding the correlations between excitons, spin exchange mechanisms and collective magnetic behavior of conduction electrons [3]. We investigated these exchange mechanisms in long range ordered crystalline MPc thin films. Non peripheral substituted Cobalt and Manganese Pc's were fabricated using a novel solution-based pen-writing technique [4]. MCD of Co-Pc shows signature of distinct transitions between ligand electronic states in the vicinity of the bandgap (fig 1a). The evolution of Zeeman splitting of specific MCD-active states is very well described by a Brillouin-like function with enhanced effective g-factors (fig 1b), analogous to DMS systems. MCD active states beyond 1μm have been observed for the first time in case of MnPc thin films (fig 1c). In the case of Mn-Pc, our measurements show stronger hybridization of ligand electronic states with the Mn d-orbitals. Future plans involve MCD experiments in high magnetic field at the NHMFL's new B=25T Split-Helix magnet facility [5] and SQUID measurements at the IFPAN, Poland.

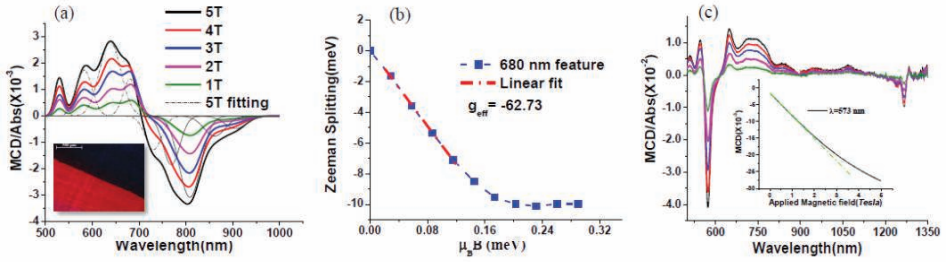

Fig. 1**: a)** MCD spectra of Soluble Co-Octabutoxy Pc with varying magnetic field up to 5T. Inset: Polarized image of thin film sample showing long range order (dark and bright grains correspond to different grain orientations, scale bar=0.5mm) **b)** Zeeman splitting of ligand electronic state (λ = 680nm) as a function of magnetic field. **c)** MCD spectra of Mn-Octabutoxy Pc with varying magnetic field up to 5T, Inset: field ramp at 573nm showing non linear evolution of MCD with increasing magnetic field.

[1] R. Zeis *et al*., Appl. Phys. Lett. **86**, 022103 (2005)
[2] T. Dietl, J. Phys.: Condens. Mat. **19,** 165204 (2007)
[3] K. Ando, Science **30**, 5782 (2006)
[4] R. L. Headrick *et al*., Appl. Phys. Lett. **92**, 063302 (2008)
[5] Z. Pan *et al.,* Magnet Lab Reports, Volume **18**, No.3, 14-15 (2011)

This work was supported by the NSF, MRI and CAREER programs: DMR- 0722451; DMR-0348354; DMR- 0821268; DMR-1056589

MoP152

Virtual crystal approximation versus valence band anticrossing model of the band structure in the (Ga,Mn)As and (Ga,Bi)As epitaxial layers.

O. Yastrubchak[1*], J. Sadowski[2,3], J. Z. Domagala[2], Ł. Gluba[1], J. Żuk[1] and T. Wosiński[2]

[1]Institute of Physics, Maria Curie-Skłodowska University in Lublin, Pl. Marii Curie-Skłodowskiej 1,20-031 Lublin, Poland
[2]Institute of Physics, PAN, 02-668 Warsaw, Poland
[3]MAX-Lab, Lund University, 22100 Lund, Sweden
yastrub@hektor.umcs.lublin.pl

The GaAs semiconductor alloy compounds containing Bi or Mn have emerged as potential candidates for novel microelectronic and spintronic applications. The band gap of the (Ga,Bi)As epitaxial layers red shifted considerably upon the addition of only a few atomic percent of Bi and exhibits other anomalous properties, such as a reduced temperature dependence as well as giant spin-orbit splitting. To explain these unusual features of the electronic structure of the (Ga,Bi)As epitaxial layers the band anticrossing (BAC) model was developed [1]. It was suggested in [2], that in the (Ga,Mn)As the valence band anticrossing interaction is observed as well.

We have investigated (Ga,Bi)As and (Ga,Mn)As layers and, as a reference, undoped GaAs layer, grown by LT-MBE. All the epitaxial layers were grown pseudomorphically on semi-insulating (001) GaAs substrates. The alloy compositions were determined from high resolution X-ray diffractometry (XRD) measurements. The photoreflectance (PR) spectroscopy enabled the determination the of the band gap values (E_0) and spin-orbit split-off (E_{SO}) band to conduction band optical transition in (Ga,Mn)As and (Ga,Bi)As epitaxial layers. Photoreflectance studies were supported by Raman spectroscopy.

The very large valence band anticrossing interaction is observed for (Ga,Bi)As epitaxial layers with 1% of Bi content. This interaction caused the strong red shift the of the energy values of E_0 as well as E_{SO} for this film with respect to that in reference LT- GaAs epi-layer.

In (Ga,Mn)As with a low (1–2%) Mn content and hole density close to that of the metal-insulator transition, the E_0 interband transition energy was blue shifted with respect to that in reference LT-GaAs. On the other hand, a substantial red shift, of 40 meV, of the E_0 energy was revealed in (Ga,Mn)As with the highest (6%) Mn content and a hole density corresponding to metallic side of the metal-insulator transition [3]. Nevertheless for all investigated (Ga,Mn)As epitaxial layers no energy value changes at E_{SO} optical transition are observed. These results support the idea assumes mobile holes residing in the valence band of GaAs and the Fermi level position determined by the concentration of valence-band holes. The blue shift of the E_0 in the (Ga,Mn)As with a low Mn content was interpreted as a result of the Moss-Burstein shift of the absorption edge due to the Fermi level location below the top of GaAs valence band. On the other hand, a substantial red shift of the E_0 in (Ga,Mn)As with the highest (6%) Mn content was interpreted in terms of a disordered valence band, extended within the band-gap, formed in highly Mn-doped (Ga,Mn)As as a result of merging the Mn-related impurity band with the host GaAs valence band.

[1] K. Albery, J. Wu, W. Walukievicz, K. M. Yu, O.D. Dubon, S.P. Watkins, C.X. Wang, X. Liu, Y.-J. Cho, and J. Furdyna, Phys. Rev. B 75 (4), 045203 (2007)
[2] K. Alberi, K.M. Yu, P.R. Stone, O.D. Dubon, W. Walukiewicz, T. Wojtowicz, X. Liu, J.K. Furdyna, *Phys. Rev. B* **78**, 075201 (2008)
[3] O. Yastrubchak, J. Zuk, H. Krzyzanowska, J.Z. Domagala, T. Andrearczyk, J Sadowski, T. Wosinski, *Phys. Rev. B* **83** (24), 245201 (2011)

III-V quantum light source and cavity-QED on Silicon

O. Del Pozo-Zamudio[1], I. J. Luxmoore[1], R. Toro[1], N. A. Wasley[1], E. A. Chekhovich[1], A. M. Sanchez[2], R. Beanland[2], A. M. Fox[1], M. S. Skolnick[1], H. Y. Liu[3] and A. I. Tartakovskii[1]

[1]Department of Physics and Astronomy, University of Sheffield, Sheffield, S3 7RH, UK
[2]Department of Physics, University of Warwick, Coventry CV4 7AL, UK33
[3]Department of Electronic and Electrical Engineering, University College London, London, WC1E 7JE

'On-demand' generation of single photons or entangled photon pairs is of fundamental importance for quantum cryptography [1], quantum lithography [2] and quantum information processing applications [3]. Successful generation of such non-classical light has been achieved using III-V semiconductor quantum dots (QDs) [4,5]. Recently, III-V QDs were also used in ridge lasers monolithically grown on silicon substrates [6], which provides first steps to unification of III-V based communication technologies with silicon photonics and electronics. Here we demonstrate single photon QD emission in photonic crystal nano-cavities fabricated from a III-V material grown by direct molecular beam epitaxy on a Si substrate. The high quality of the obtained III-V material and photonic structures is emphasized by observation of strong light-matter coupling between the two-level system of a single self-assembled InGaAs/GaAs QD and the optical field of a nano-cavity. This work [7] paves the way for the direct integration of quantum optical systems on a sustainable and low cost silicon platform, and will also enable in a long term unprecedented scalability of III-V quantum devices on large diameter Si substrates.

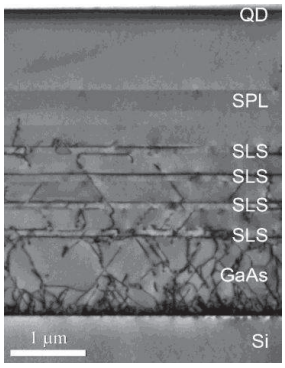

Fig.1. TEM image of the unprocessed sample, showing that threading dislocations are efficiently captured by the quantum well strain filters (marked SLS) and a short-period superlattice (SPL).

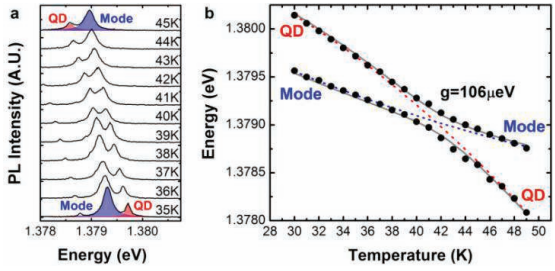

Fig.2. Strong coupling of an InGaAs/GaAs QD to the optical mode in an L3 nano-cavity in a photonic crystal fabricated from GaAs grown on Si (sample shown in Fig.1). The characteristic anti-crossing behaviour is observed in photoluminescence measurements carried out for different temperatures (a). The Rabi splitting, *2g*, exceeding 200 μeV is observed (b).

[1] Tittel, W., Brendel, J., Zbinden, H. & Gisin, N. Rev. Mod. Phys. 74, 145 (2002).
[2] Boto, A.N. et al., Phys. Rev. Lett. 85, 2733 (2000).
[3] O'Brien, J., Furusawa, A. & Vuckovic, J., Nature Phot. 3, 687 (2010).
[4] Yuan, Z. et al., Science 295, 102 (2002).
[5] Salter, C.L. et al., Nature 465, 594 (2010).
[6] Wang, T. et al, Opt. Exp. 19, 11381 (2011).
[7] Luxmoore, I.J.et al., Sci. Rep. 3, 1239 (2013).

MoP154

Nonlinear growth in the microwave reflection signal from the GaAs/AlGaAs 2DES in the regime of radiation-induced magnetoresistance oscillations

Tianyu Ye[1], R. G. Mani[1] and W. Wegscheider[2]

[1] *Georgia State University, Atlanta, GA 30303 USA*
[2] *ETH-Zurich, 8093 Zurich, Switzerland*

Microwave induced magnetoresistance oscillations (MIMOs) in the high mobility two dimensional electron system (2DES)[1, 2] have now been studied for more than a decade, using a variety of experimental methods. And, a number of theories including the displacement model, the inelastic model, the radiation-driven electron orbit model, and the non parabolicity model have been proposed to explain the observed phenomena. In order to better understand the physical contributions, we have studied microwave reflection from the high mobility 2DES and the correlation between microwave reflection and the observed MIMOs in transport .

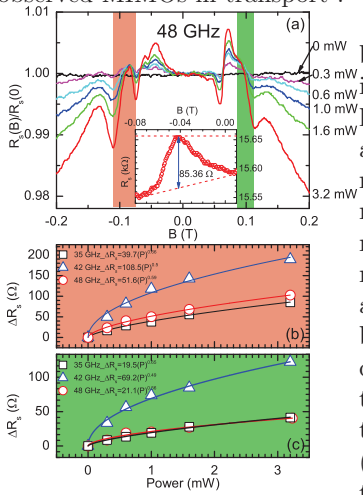

Figure 1: (a)Normalized R_s as a function of B for different microwave powers at 48 GHz and 1.5 K. The inset shows the determination of the amplitude of the R_s oscillation. (b) Amplitude of R_s oscillation on left dark region in (a) as a function of microwave power at different frequencies. (c) Amplitude of R_s oscillation on right dark region in (a) as a function of microwave power.

Microwave reflection was measured by a resistive bolometric sensor that lies right above the high mobility GaAs/AlGaAs heterostructure specimen. At liquid helium temperature both the diagonal resistance (R_{xx}) and bolometric resistance (R_s) that indicates microwave reflection were measured by four terminal lock-in technique in a ramped perpendicular magnetic field. With microwave illumination, R_{xx} exhibit MIMOs and, remarkably, R_s also exhibits oscillations in the same regime as MIMOs. Experiment indicates that the amplitude of both MIMOs and R_s oscillations increases with the microwave power, P. To highlight the oscillatory effects, the R_s with different microwave powers were normalized to zero magnetic field as in Figure 1(a). Figure 1(b) and (c) show that, as microwave power increases from 0 mW to 3.2 mW, the amplitude of the R_s oscillations increases nonlinearly with P. A fit of the growth of the R_s amplitude with P indicates a power law relation between the R_s amplitude and microwave power. From Fig. 1(b) and 1(c) it is apparent that the non-linear growth of the R_s amplitude is similar to observed growth of the MIMOs amplitude with P.[3] Both R_s oscillations and MIMOs amplitude appear to follow a power law as $A = A_0(P)^{\alpha}$, where A is the amplitude, A_0 is a constant, P is incident microwave power and α is the power law exponent. For both R_s oscillations and MIMOs, α is approximately 0.5. The results suggest that the remote sensor is able to sense the photo-excited state of the 2DES.

[1] R. G. Mani et al., Nature. **420**, 646 (2002).
[2] M. A. Zudov et al., Phys. Rev. Lett. 90, 046807 (2003).
[3] R. G. Mani et al., Phys. Rev. B **81**, 125320 (2010).

2 July (Tuesday)

17.15 – 19.00

Poster sessions 2

EP2DS – MSS Joint session

Wrocław Central Station

Weak localization in epitaxial graphene layers grown on (0001) SiC

M. Gryglas-Borysiewicz[1], A. Kwiatkowski[1], J. Przybytek[1], S. Butun[2], E. Ozbay[2], W. Strupiński[3], R. Stępniewski[1], M. Baj[1]

[1] *Institute of Experimental Physics, Faculty of Physics, University of Warsaw, ul. Hoża 69, 00-681 Warsaw, Poland*
[2] *Nanotechnology Research Center (NANOTAM), Bilkent University, Turkey*
[3] *Institute of Electronic Materials Technology, ul. Wólczyńska 133, 01-919 Warsaw, Poland*

We performed magnetotransport studies of the epitaxial graphene layers grown on semi-insulating (0001) SiC by CVD method [1]. The samples were processed by means of optical lithography into large hall bars (263μm x 526μm) with Ti/Au metallization for ohmic contacts. Resistivity tensor was measured in Oxford Instruments VTI system in temperatures ranging from room temperature down to 1.5 K and magnetic fields up to 12T.

Diagonal component of the resistivity tensor ρ_{xx} had a pronounced peak at B=0, attributed to a weak localisation, and oscillations at higher fields, superimposed on a rising background (see fig.1). In order to extract credible information about the parameters governing weak localisation, it is important to take this background into account. The rising background can successfully be simulated in terms of mobility spectrum [2]. Here, we applied two channel conductivity model combined with a weak localization correction to the conductivity proposed in [3] to simulate the full conductivity tensor. The parameters obtained will be discussed and compared to other approaches used in the literature.

References:
[1] W. Strupiński, K. Grodecki, A. Wysmołek, R. Stepniewski, T. Szkopek, P. E. Gaskell, A. Grüneis, D. Haberer, R. Bozek, J. Krupka, and J. M. Baranowski, Nano Lett., **11** (4),1786 (2011)
[2] M. Gryglas-Borysiewicz, B. Jouault, J. Tworzydło, S. Lewinska, W. Strupinski and J.M. Baranowski, Acta Phys. Pol. A **116,** 838 (2009)
[3] K. Kechedzhi, E. McCann, V.I. Fal'ko, H. Suzuura, T. Ando, and B.L. Altshuler, Eur. Phys. J. Special Topics **148**, 39–54 (2007).

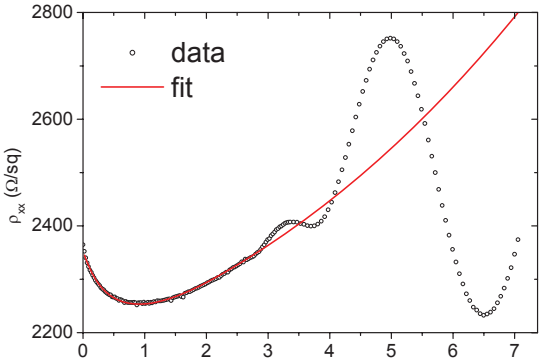

Fig.1. ρ_{xx} component of the resistivity tensor

Artificial graphene as a designer Dirac material

E. Räsänen[1], C. A. Rozzi[2], S. Pittalis[3], and G. Vignale[4]

[1] *Department of Physics, Tampere University of Technology, FI-33101 Tampere, Finland*
[2] *CNR – Istituto Nanoscienze, Centro S3, Via Campi 213a, I-41125 Modena, Italy*
[3] *Department of Chemistry, University of California, Irvine, California, USA*
[4] *Dept. of Physics and Astronomy, University of Missouri, Columbia, Missouri, USA*

Recent advances in creating *graphene-like systems from the two-dimensional electron gas* are leading to a new science of "designer Dirac materials" [1]. Artificial graphene can be created either by positioning molecules on a metal surface [2] or by arranging quantum dots in an adjustable honeycomb lattice (see Fig. 1 and Refs. [3, 4]). As our ability to control the quality of artificial graphene samples improves, so grows the need for an accurate theory of its electronic properties, including the effects of electron-electron interactions. Here we determine those effects on the band structure and on the emergence of Dirac points [4], and discuss future investigations and challenges in this exciting new field [5].

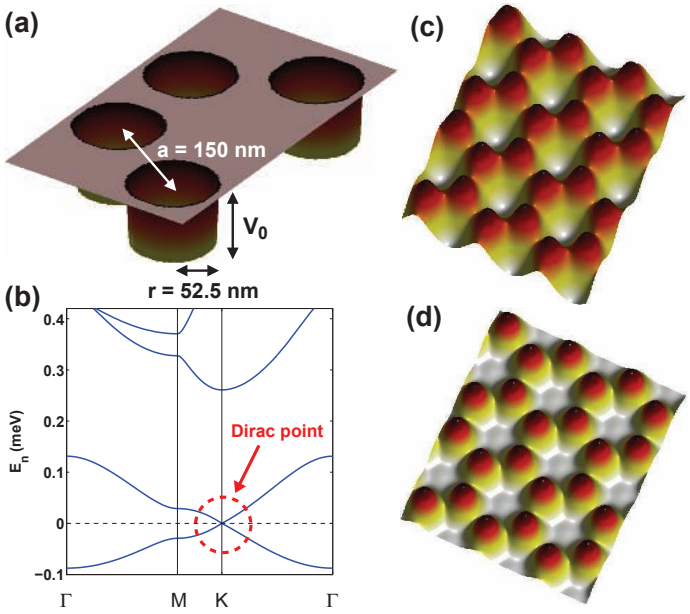

Figure 1: (a) Piece of the model potential for artificial graphene with tunable parameters. (b) Band structure exhibiting a Dirac point at the Fermi level. (c-d) Electron density without (c) and with (d) electron-electron interactions [4].

[1] Nature **483**, Issue 7389 (2012): Cover picture; News & Views by J. Simon and M. Greiner, p. 282; Letters by K. K. Gomes *et al.*, p. 306 (Ref. [2]) and Tarruell *et al.*, p. 302.
[2] K. K. Gomes, W. Mar, W. Ko, F. Guinea, and H. C. Manoharan, Nature **483**, 306 (2012).
[3] See A. Singha *et al.*, Science **332**, 1176 (2011) and references therein.
[4] E. Räsänen, C. A. Rozzi, S. Pittalis, and G. Vignale, Phys. Rev. Lett. **108**, 246803 (2012).
[5] E. Räsänen *et al.*, to be published (2013).

Transmission through silicene quantum barriers

Diana M. M. Gustin[1], *Marcos R.S. Tavares*[1], *G.-Q. Hai*[2], and *P. Vasilopoulos*[3]

[1] Centro de Ciências Naturais e Humanas, Univ. Federal do ABC, 09210-170, S. André, SP, Brazil
[2]Instituto de Física de São Carlos, Universidade de São Paulo, 13560-970, São Carlos, SP, Brazil
[3] Department of Physics, Concordia University,7141 Sherbrooke Ouest, Montreal, Canada H4B 1R6

Silicene is a monolayer of silicon atoms that form a two-dimensional honeycomb lattice similar to graphene's. It has attracted considerable attention due to its exotic electronic structure and its compatibility with current silicon-based electronic technology. The low-energy physics of silicene is described by Dirac electrons with relative large spin-orbit interaction, $\lambda = 3.9\, meV$, due to its buckled structure[1] with $l = 2.3 \times 10^{-2}\, nm$ the half distance between the A and B sublattices. Its band structure can be controlled externally by an electric field $E_z = 300\, meV/nm$. We theoretically explore resonant features in the electronic transmission T through barriers in silicene by studying T as a function of the electron's energy E (meV) and its angle of incidence θ. The incident electrons are assumed spin polarized and the barriers are formed by contact potentials. Our results show that the applied electric field can result in spin-resolved transmission channels. In addition, we critically compare the results with those through barriers in graphene. Important differences from the graphene's case[2] show up and are highlighted in the transmission $T^{\uparrow}$ and polarization $P = |T^{\uparrow} - T^{\downarrow}|/|T^{\uparrow} + T^{\downarrow}|$. A (E,θ) contour plot of T, for incident *spin-up electrons*, through a silicene barrier of length L=110 nm and height V=100 meV, is shown in Fig. 1(a). Notice the periodicity along the E axis for large θ. Figure 1(b) is the same contour as in Fig. 1(a) but for the values $\lambda = 0\, meV$ and $E_z = 0$ which pertain to a barrier on suspended graphene. Notice the absence of the transmission channel below 20 meV shown in Fig. 1(a). The contour plot in Fig. 1(c) shows the spin polarization P for a barrier on silicene. P increases strongly for energies near the top of the barrier and also for $E_+ = (\lambda + l * E_z)$ and $E_- = -(\lambda - l * E_z)$.---This work is sup-ported by CAPES, CNPq, and FAPESP, Brazil, and the NSERC grant OGP012756, Canada.

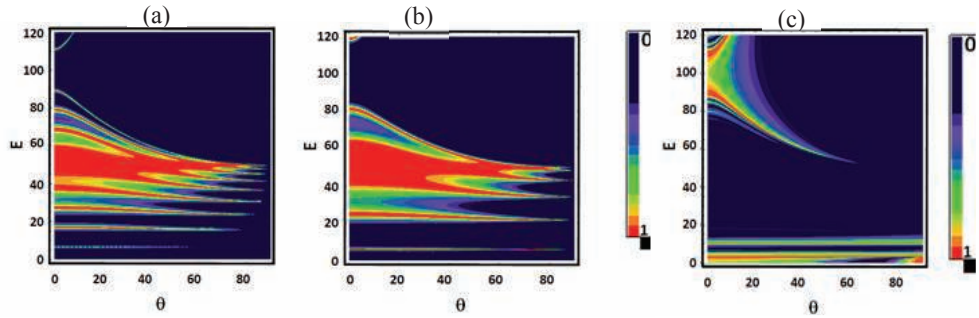

Figure 1. (a) (E,θ) contour plot of the transmission through a silicene barrier. (b) As in (a) for a barrier on suspended graphene. (c) (E,θ) contour plot of the polarization for a silicene barrier.

[1] Motohiko Ezawa, Phys. Rev. Lett. **109**, 055502 (2012).
[2] J. Milton Pereira Jr. *et al.,* Appl. Phys. Lett. **90,** 132122 (2007).

Determination of mobility in top and bottom surfaces of multilayer graphene placed on SiO_2/Si substrate

Akinobu Kanda, Yosuke Nukui, Hidenori Goto, Hikari Tomori, Youiti Ootuka

Division of Physics and TIMS, Faculty of Pure and Applied Sciences, University of Tsukuba, Tsukuba, Ibaraki 305-8571, Japan

We experimentally demonstrate that in a thick multilayer graphene sheet placed on a SiO_2/Si substrate, the mobility of the top surface, facing the vacuum, is about five times larger than that of the bottom surface, attaching to SiO_2, at room temperature. From the temperature dependence of the mobility, we argue that the dominant mechanism which deteriorates the mobility of multilayer and even *single* layer graphene is the Coulomb scattering originating from the charged impurities in the substrate.

The samples are dual-gated graphene devices with a suspended contactless top gate fabricated with a method reported in [1]. A highly-doped Si substrate covered with a SiO_2 layer was used as the back gate. We examined seven multilayer graphene (MLG) films with thickness t ranging from 0.9 to 5.3 nm, which were obtained by using mechanical exfoliation of kish graphite. We measured the top-gate voltage (V_{tg}) dependence of the conductance with the back gate grounded ($V_{bg} = 0$) and the V_{bg} dependence of the conductance with the top gate grounded at room temperature, 77 K and 4 K.

We estimate the mobility of the top surface and that of the bottom surface of MLG based on a simple model in which a MLG film is divided into three layers: the layers near the top (bottom) surface with thickness λ (layer A (C)) and the remaining central part (layer B), and we make two assumptions: 1) the mobility of layers A, B and C (μ_t, μ_0, and μ_b, respectively) are uniform in each layer, and 2) there is no change in the carrier density in each layer in the direction perpendicular to the surfaces. Under these assumptions, μ_t (μ_b) is calculated from the slope of the conductance, dG/dV_{tg} (dG/dV_{bg}), and sample dimensions.

We find that the ratio $r = \mu_b/\mu_t$ as a function of t steeply decreases around $t \sim 1$ nm and stays at a constant value of ~0.2 in thick MLG. The ratio slightly increases with decreasing temperature, but is around 0.25 for thick films at 4.2 K, indicating that the major electron scattering of graphene occurs at the bottom surface, and it survives even at low temperatures. This means that the mobility of graphene placed on a substrate can be improved by removing the charged impurities in the substrate.

[1] G. Liu, J. Velasco, Jr., W. Bao, and C. N. Lau, Appl. Phys. Lett. **92**, 203103 (2008).

Electronic multi-criticality in bilayer and trilayer graphene

Oskar Vafek[1]

[1] *National High Magnetic Field Lab and FSU, Tallahassee, FL 32310*

Electronic properties of bilayer graphene are qualitatively different from properties of two separate graphene single layers. The difference stems partly from the fact that the dispersion is no longer described by two isotropic Dirac cones near K and K' points. Rather, over wide energy range, the dispersion can be accurately described by two parabolically touching bands.

As a result, at the "neutrality point" the many-body effects are expected to lead to broken symmetry ground states. I will review current theoretical approach to electron-electron interaction driven many-body instabilities within the framework of Wilson RG. The role of competing interactions and the dependence of different ordering tendencies on the range of the interaction will be examined. In particular, I will argue that for longer range interaction giving predominantly forward scattering, the leading ordering tendency is towards a gapless electronic nematic state[1][4]. For shorter range interactions, such as in the Hubbard model, additional back scattering becomes comparable to the forward scattering and the leading ordering tendency is towards a gapped Neel antiferromagnet[2][3]. These results will be discussed in the context of recent experiments reporting signatures of broken symmetry states in suspended bilayer graphene.

Similar analysis will also be presented for ABC stacked trilayer graphene. There we find that the leading instability with forward scattering density-density interaction only is a mirror-breaking gapless state[5]. Addition of a small, but finite back scattering favors gapped phases[5], allowing us to make connections to the existing experiments on TLG. A fundamental symmetry difference between TLG and bilayer graphene (BLG) will be discussed. This symmetry difference is responsible for disfavoring nematic states in TLG under the same conditions that favor nematic states in BLG.

[1] Oskar Vafek and Kun Yang, PRB **81**, 041401(R) (2010).
[2] Oskar Vafek, PRB **82**, 205106 (2010).
[3] Robert E. Throckmorton and Oskar Vafek, PRB **86**, 115447 (2012).
[4] Vladimir Cvetkovic, Robert E. Throckmorton and Oskar Vafek, PRB **86**, 075467 (2012).
[5] Vladimir Cvetkovic and Oskar Vafek, arXiv:1210.4923.

Growth of boron-doped graphene by thermal decomposition of B_4C

W. Norimatsu [1], K. Hirata[1] and M. Kusunoki[2]

[1] *Department of Applied Chemistry, Nagoya University, Japan*
[2] *EcoTopia Science Institute, Nagoya University, Japan*

Graphene, a one-atom-thin carbon material with a honeycomb structure, is attracting extensive researchers after its discovery. It is widely known that wafer-scale graphene can be grown by thermal decomposition of silicon carbide [1]. In this case, annealing the SiC single crystal in a vacuum or in an argon atmosphere leads to the selective sublimation of the silicon atoms, and the remaining carbon atoms form graphene spontaneously on the semi-insulating SiC substrate. This is because the silicon atom is relatively easy to sublimate in a vacuum at high temperatures compared with the carbon atom. This face suggests that graphene can be grown by thermal decomposition of other carbides. In this study, we grew graphene by thermal decomposition of B_4C and investigated its features by high-resolution transmission electron microscope (HRTEM) observations.

We used B_4C particles for graphitization. B_4C particles with their size of about 0.5 μm were annealed at 1600~1900 ºC in a vacuum furnace (~10^{-4} Torr). Transmission electron microscope (TEM) observations and electron energy loss spectroscopy (EELS) measurements were carried out using Topcon EM-002B-, JEM-2010F- and ARM200F-type TEMs at an accelerating voltage of 200 kV.

Figure 1 shows an HRTEM image of graphene grown at 1700 ºC. Graphene layers were observed as dark line contrasts. In the B_4C area in this image, B_{12} clusters can be seen as bright dots. As is seen in the image, graphene layers were grown on the two-dimensional (003) plane consisting of B_{12} clusters. Graphene was also grown on (101) and (-102) surfaces. Figure 2 shows a low-magnification image of graphene on B_4C, together with its carbon and boron mapping images analyzed by EELS measurement. In graphene region, boron atoms were clearly present, suggesting that boron atoms were doped into graphene lattice. Our EELS spectrum obtained from graphene region had a strong boron peak. This is the direct evidence of doped boron in graphene layers.

References:
[1] W. Norimatsu and M. Kusunoki, Phys. Rev. B. **81**, 161410 (2010).
[2] W. Norimatsu, K. Hirata and M. Kusunoki, *J. Phys.: Condens. Matter*, **24**, 314207 (2012).

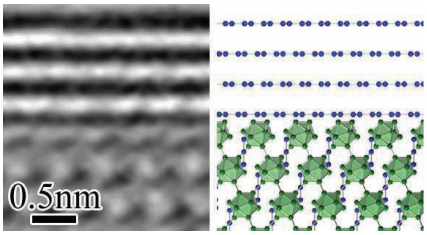

Fig. 1: TEM micrograph and its model of graphene grown on B_4C.

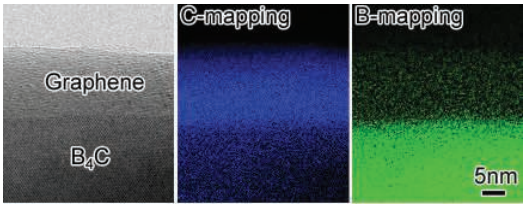

Fig. 2: TEM images and C- and B-mapping images obtained by EELS analysis.

Splitting of the zero-energy Landau level in epitaxial graphene on SiC

K. Takase, H. Hibino and K. Muraki

NTT Basic Research Laboratories, NTT Corporation, Atsugi, Kanagawa, 243-0198, Japan

Zero-energy states in high fields in graphene have been widely studied for a variety of physics associated with the lifting of fourfold spin and valley degeneracy using high-mobility samples exfoliated from graphite [1]. For epitaxial graphene on SiC, on the other hand, the ground states at zero energy still remain unexplored, since accessing the charge neutrality point without deteriorating sample qualities has been difficult. Using top-gated devices in both Hall-bar and Corbino geometries, we demonstrate lifting of spin/valley degeneracy in epitaxial graphene at high fields, which manifests as a double peak in longitudinal conductivity (σ_{xx}) around $\nu = 0$. The energy gap associated with the Landau level (LL) splitting is estimated from transport spectroscopy that we recently developed [2] as well as from temperature (T) dependence of longitudinal resistance R_{xx}.

The Hall-bar sample with width 40 μm and length 200 μm was fabricated from epitaxial graphene grown on 6H-SiC(0001). At $T = 8$ K, R_{xx} at $\nu = 0$ increases almost linearly with B, whereas at $T = 1.6$ K, it rapidly increases with B [Fig. 1(a)], indicating strongly insulating behavior at high B. Converting the measured R_{xx} and Hall resistance, the latter fluctuating around zero, into σ_{xx} reveals a double peak with a minimum at $\nu = 0$, signaling the splitting of the zero-energy LL [Fig. 1(b) top]. At $\nu = 0$, σ_{xx} is thermally activated, which corroborates the insulating behavior of the $\nu = 0$ state. Direct measurement of σ_{xx} using a Corbino device finds LL splitting of similar magnitude.

We estimated the energy gap Δ at $\nu = 0$ in two ways. First, the T dependence of R_{xx} at 16 T can be well fitted by $R_{xx} \sim \exp(\Delta/2k_BT)$ with the Boltzmann constant k_B [Fig. 1(c)], yielding $\Delta \sim 7$ K at 16 T. Second, we analyzed the trajectories of the σ_{xx} peaks mapped vs. V_g and B. The mapping reveals parabolic, instead of linear, fan diagram that reflects the relativistic graphene LLs, because, in the presence of high-density interface states, the Fermi energy of graphene varies in proportion to V_g [2]. We find that at high B the positions of the split σ_{xx} peaks are quite close to those of $\nu = \pm 1$ [Fig. 1(b) bottom]. Analyzing these data gives the upper bound of the gap, which can be crudely estimated to be 15 K at 16 T. In the conference, we will discuss the underlying physical mechanism of the $\nu = 0$ gap.

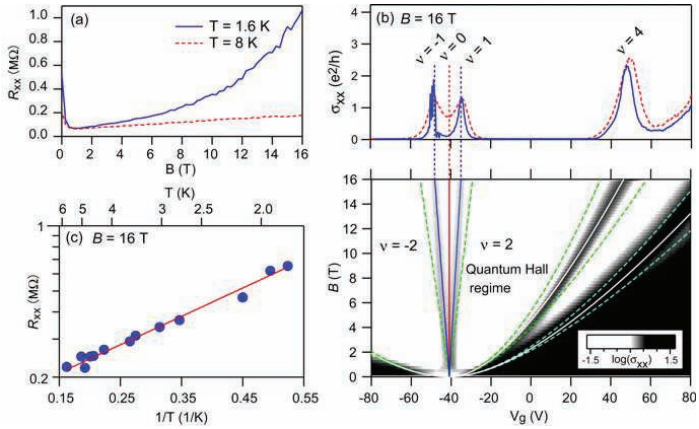

Fig. 1(a) R_{xx} at $\nu = 0$ vs. B at $T = 1.6$ and 8 K. (b) Top: σ_{xx} vs. V_g at $B = 16$ T. Bottom: σ_{xx} vs. V_g and B. Solid lines indicate $\nu = 0$, ±1, ±4, and 8, and dashed ones mark borders between integer and non-integer fillings. (c) R_{xx} at $\nu = 0$ vs. $1/T$ at $B = 16$ T. The solid line shows Arrhenius equation with $\Delta = 7$ K.

[1] A. F. Young *et al*., Nat. Phys. **8**, 553 (2012). [2] K. Takase *et al*., Phys. Rev. B **86**, 165435 (2012).

Emergent Dirac cones and valley Hall states in gated multilayer graphenes

Takahiro Morimoto[1], and Mikito Koshino[2]

[1] *Condensed Matter Theory Laboratory, RIKEN, Saitama, 351-0198, Japan*
[2] *Department of Physics, Tohoku University, Sendai, 980-8578, Japan*

There are growing interests in multilayer variants of graphene such as bilayer and trilayer, which support chiral quasiparticles, characterized with non-trivial Berry phases. There, the trigonal-warping deformation of the energy band, which is intrinsic to graphite-based systems, gives rise to small Dirac cones near Dirac point in these multilayers. The Lifshitz transition, in which the Fermi circle breaks up into separate parts, takes place at a small energy scale around a few meV. On the other hand, it is possible to modify the band structure of multilayer graphenes by applying an electric field perpendicular to the layer, using external gate electrodes attached to the graphene sample. While it has been argued that, for bilayer graphene a perpendicular electric field opens a band gap, and, for ABA trilayer graphene it causes a band overlap, a situation where both the interlayer asymmetry and the trigonal warping are in effect has not been fully discussed so far.

Motivated by these, we study the electronic structures of ABA (Bernal) stacked multilayer graphenes in uniform perpendicular electric field, and show that the interplay of the trigonal warping and the potential asymmetry gives rise to a number of emergent Dirac cones nearly touching at zero energy [1] . The band velocity and the energy region (typically a few tens of meV) of these gate-induced Dirac cones are tunable with the external electric field. In ABA trilayer graphene, in particular, applying an electric field induces a non-trivial valley Hall state, where the energy gap at the Dirac point is filled by chiral edge modes which propagate in opposite directions between two valleys. In four-layer graphene, in contrast, the valley Hall conductivity is zero. A nontrivial valley Hall state generally occurs in asymmetric odd layer graphenes and is related to a hidden chiral symmetry which exists only in odd layer graphenes.

[1] Takahiro Morimoto and Mikito Koshino, Phys. Rev. B **87**, 085424 (2013).

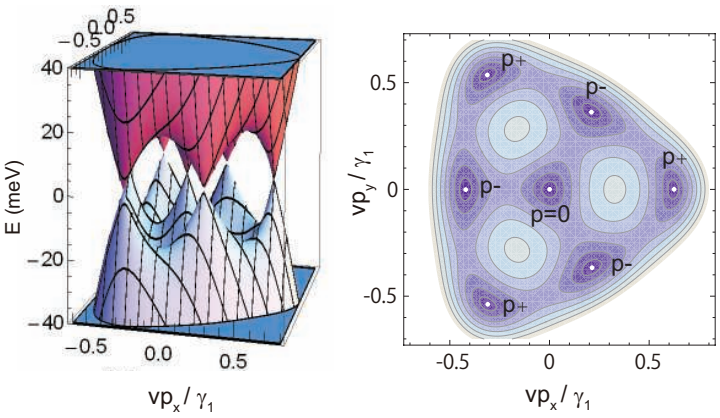

Figure 1: Band structures of ABA trilayer graphene in a perpendicular electric field with a trigonal warping effect, depicted in 3D plot (left panel) and contour plot (right).

Landau levels of disordered massless Dirac fermions when the Dirac cones are both shifted and tilted

T. Honda[1], Y. Hatsugai[2], H. Aoki[3], and T. Kawarabayashi[1]

[1] *Department of Physics, Toho University, Funabashi, Japan*
[2] *Institute of Physics, University of Tsukuba, Tsukuba, Japan*
[3] *Department of Physics, University of Tokyo, Hongo, Japan*

Particles governed by the massless Dirac equation are now realized not only in graphene [1] but also in various classes of systems encompassing an organic metal (with tilted Dirac cones) [2], molecular graphene [3] and cold atoms on optical lattices [4, 5]. While usually Dirac cones appear in pairs with the opposite Berry phases (which is dubbed the fermion doubling), theoretically a model has been proposed in which the doubling is lifted, where the half-integer contributions to the Hall conductivity result in different sequence of Chern numbers with extra plateaus [6]. While involving seemingly artificial complex transfer energies, this can be realized in cold atoms on optical lattices, where the Hall conductivity can be detectable [5]. On the other hand, usual wisdom is that the chiral symmetry causes the doubled Dirac cones, and that the symmetry protects sharp (δ-function like) zeroth Landau levels against disorder. So it becomes an intriguing question to ask what will happen to the zeroth Landau level in the singled-out Dirac cone.

With this background, we explore numerically the effect of disorder on the Landau levels for a lattice model where the energy offset between two Dirac cones can be controlled by an imaginary hopping between the next nearest-neighbor (NNN) sites. Previously, we have shown that for a disorder in the nearest-neighbor (NN) hopping, the $n = 0$ Landau levels become anomalously sharp as the Dirac cones are energetically shifted even when the disorder is short-ranged, quite unlike the case of the degenerated cones [7]. In the present paper, we extend the analysis to various other cases. Specifically, we are interested in the effect of tilted (as well as shifted) Dirac cones, which is realized by introducing a real part in the NNN hopping. While the tilting of the cones destroys the chiral symmetry, we can introduce a *generalized* chiral symmetry which protects the sharp $n = 0$ Landau levels [8]. Here we find that the $n = 0$ Landau levels indeed remain sharp even in the shifted cones when the disorder respects the generalized chiral symmetry [9]. By contrast, a disorder in the NN hopping, which destroys the symmetry, the sharpness is degraded when the cones are tilted (Fig. 1) .

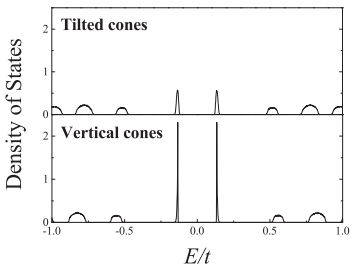

Fig. 1: Landau levels for Dirac cones with an energy shift $\delta E/t = 0.28$ (t: the NN hopping) for the bond disorder. The central two peaks are the $n = 0$ levels.

[1] K.S. Novoselov et al., Nature **438**, 197 (2005).
[2] N. Tajima et al. Phys. Rev. Lett. **102**, 176403 (2009).
[3] K.K. Gomes et al, Nature **483**, 306 (2012).
[4] L. Tarruell et al., Nature **483**, 302 (2012).
[5] F. Mei et al., Phys. Rev. A **84**, 023622 (2011).
[6] H. Watanabe, Y. Hatsugai, H. Aoki, Phys. Rev. B **82**, 241403(R) (2010).
[7] T. Kawarabayashi, T. Honda, H. Aoki, Y. Hatsugai, AIP Conference Proceedings, in press (arXiv:1208.2307).
[8] T. Kawarabayashi, Y. Hatsugai, T. Morimoto, H. Aoki, Phys. Rev. B **83**, 153414 (2011); Int. J. Mod. Phys.: Conf. Series **11**, 145 (2012).
[9] T. Honda et al., in preparation.

A new path for superconducting graphene

C. Tonnoir [1], C. Chapelier [1], A. Kimouche [2], J. Coraux [2], B. Delsol [3], B. Gilles [3]

[1] *SPSMS, UMR-E 9001, CEA-INAC/UJF-Grenoble 1, 17 rue des martyrs, F-38054 Grenoble cedex 9*
[2] *CNRS Grenoble – Institut Néel, 25 rue des Martyrs, BP 166, F-38042 Grenoble cedex 9*
[3] *Grenoble INP – SIMAP, 1130 rue de la Piscine, BP 75, F-38402 Saint-Martin-d'Hères cedex*

Whereas a tunable Josephson super-current has been observed in graphene long time ago [1], inducing superconducting properties in graphene remains very challenging. One reason comes from the difficulty to prepare a good interface between graphene and the superconducting metal which is usually deposited on top of the graphene layer. In this work, we developed a new and reliable method to induce superconductivity in graphene by growing graphene on top of a thin Rhenium film.

Scanning tunneling microscopy (STM) studies with atomic resolution reveal large flat terraces of our samples fully covered with graphene and the existence of a moiré superstructure of 2.3nm periodicity, which is typical of graphene on lattice mismatched substrates [2]. The superconducting properties of graphene on Rhenium have been probed by low temperature tunneling spectroscopy performed at 50 mK. We observed a very homogeneous superconducting state below a superconducting transition temperature $T_c \geq 2K$, significantly higher than the critical temperature of bare Rhenium films. The density of states at energy much higher than the superconducting gap reveals features which are position dependent on the moiré pattern, indicating different local coupling strengths of the graphene layer with the Rhenium substrate. We also made more disordered samples with areas partially covered with amorphous carbon. In this situation, a spatial evolution of the superconducting proximity effect shows up between the regions displaying a moiré pattern and the disordered ones. We analyzed this evolution in the framework of mesoscopic superconductivity theories.

The superconducting properties of graphene on Rhenium have been further characterized under a perpendicular magnetic field of a few hundred Gauss. A disordered array of vortices has been observed and the electronic density of states of the vortex core has been obtained. This opens new possibilities in the quest of zero mode states in the vortex core of graphene [3].

[1] H.B. Heersche et al., *Nature* **446**, 56-59 (2007)
[2] E. Miniussi et al., *PRL* **106**, 216101 (2011)
[3] R. Jackiw and P. Rossi, *Nucl. Phys. B* **190**, 681 (1981)

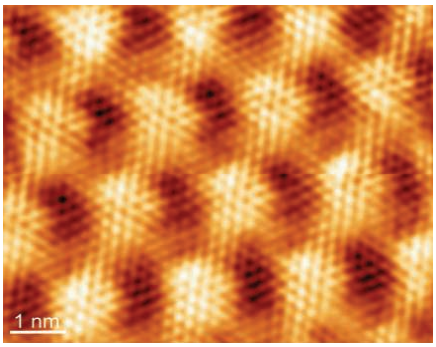

STM image of graphene on Rhenium with atomic resolution on the moiré pattern.

Transition from weak localization to strong localization regime in the bilayer graphene

D. Terasawa [1], A. Fukuda[1], Y. Ohno[2], and K. Matsumoto[2]

[1] *Department of Physics, Hyogo College of Medicine, Nishinomiya, 663-8501 Japan*
[2] *The Institute of Scientific and Industrial Research, Osaka Univ., Ibaraki, 567-0047 Japan*

Weak localization (WL) effect occurs in a broad range of disordered conductors including graphene, two-dimensional honeycomb lattice of carbons. It is suppressed by the external magnetic field B, and the longitudinal resistance R_{xx} decreases as increasing B. The WL in graphene is attributed to the chiral nature of valley degree of freedom [1]. The WL in graphene has been studied extensively [2,3], however, there still remain unknown aspects in the behavior of R_{xx} in the presence of B. Here we report on the resistance fluctuation that is observed in the bilayer graphene sample at low temperatures.

The sample is fabricated by the method of mechanical exfoliation of natural graphite. The bilayer flake is deposited on the SiO_2 surface separated by 300nm from n^+ Si substrate and cooled by the helium-free refrigerator. The mobility is approximately 2,500 cm^2/Vs at room temperature. Figure 1 (a) shows the longitudinal resistance R_{xx} as a function of V_g for 17 K and 7 K. After anneal, we find that Dirac point shifts to V_g = -36 V. R_{xx} increases as temperature decreases, and R_{xx} shows a reproducible oscillation at 7 K. Figure 1 (b) shows R_{xx} at different values of V_g marked by arrows in Fig. 1 (a) as a function of B. We see that every traces of R_{xx} decreases in the presence of B and takes a minimum value, then gradually increases as B further increases. This behavior is well explained by the competition between the suppression of the WL in the low B and the strong localization in the high B. Moreover, we find that the trace of R_{xx} at V_g = -42.7 V, which corresponds to the minimum point in the oscillated R_{xx} at B =0 T, takes the minimum at a smaller B value (~ 0.2 T) than the other two traces that takes the minimum at approximately ~0.5 T. We compare the results with the theory [1] and discuss the intervalley scattering rates in the conference.

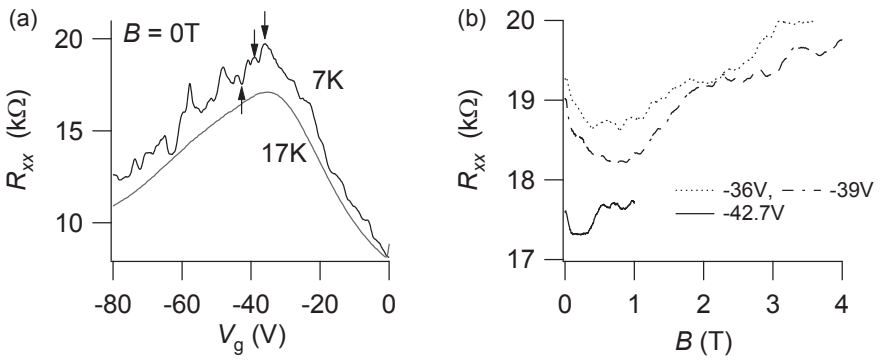

Figure 1 (a) R_{xx} as a function of V_g for different temperatures at 17 K and 7 K at B =0 T. (b) R_{xx} at different values of V_g corresponding to the position marked by arrows in (a) as a function of B.

[1] E. McCann, *et al*., Phys. Rev. Lett., **97** 146805 (2006).
[2] R. V. Gorbachev *et al.*, Phys. Rev. Lett. **98**, 176805 (2007).
[3] F. V. Tikhonenko, *et al.*, Phys. Rev. Lett. **100**, 056802 (2008).

Optical absorption in twisted bilayer graphene

Pilkyung Moon[1,2] and Mikito Koshino[1]

[1] *Department of Physics, Tohoku University, Sendai, 980–8578, Japan*
[2] *School of Computational Sciences, Korea Institute for Advanced Study, 130–722, Republic of Korea*

Recent epitaxial growth technique realized twisted bilayer graphene in which two layers are stacked with a random rotation angle [1]. We theoretically investigate the optical absorption property of twisted bilayer graphenes with various stacking geometries, and demonstrate that the spectroscopic characteristics serve as a quite robust fingerprint to identify the rotation angle between two layers [2]. We find that the optical absorption spectrum consists of a series of characteristic peaks ranging from terahertz to ultraviolet frequencies, which are associated with the van Hove singularity in the superlattice band structure (Fig. 1). We calculated the optical conductivity in two different methods, the tight-binding model and the effective mass model based on the Dirac equation, and found that the effective model nicely reproduce the tight-binding results for small rotation angles, and also analytically explain the optical selection rule which is peculiar to twisted bilayer graphene. Our results not only give a convenient way to identify the geometry of twisted bilayer graphene but also provides useful information for opto-electronic application.

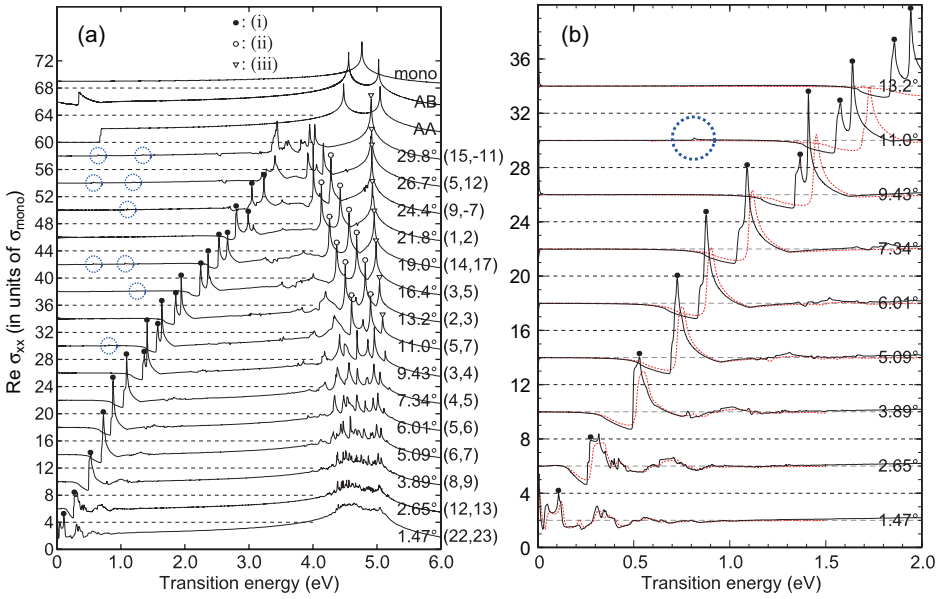

Figure 1: Dynamical conductivities of twisted bilayer graphenes with various rotation angles in (a) wide and (b) narrow frequency ranges. Peaks marked with symbols represent the excitations associated with three different types of van Hove singularity. Dashed (blue) circles indicate the tiny peaks which appears only when the actual lattice period L is larger than the Moiré period L_{M}.

[1] C. Berger *et al.*, Science **312**, 1191 (2006).
[2] P. Moon and M. Koshino, arXiv:1302.5218 (2013).

Tuning of quantum interference in top-gated graphene

A. Iagallo[1], S. Tanabe[2], S. Roddaro [1,3], M. Takamura[2], H. Hibino[2], S. Heun[1], and F. Beltram[1]

[1] *NEST, Istituto Nanoscienze-CNR and Scuola Normale Superiore, Pisa, Italy*
[2] *NTT Basic Research Laboratories, NTT Corporation, 3-1 Morinosato Wakamiya, Atsugi, Kanagawa, Japan*
[3] *Istituto Officina dei Materiali CNR, Laboratorio TASC, Basovizza (TS), Italy*

The chiral nature of quasiparticles in graphene gives rise to a number of peculiar magnetotransport phenomena such as a nonzero Berry phase resulting in half-integer quantum Hall effect and negative magnetoresistance. Quantum interference effects in graphene are nowadays theoretically well understood, based on the interplay between different chirality-breaking scattering mechanisms and dephasing time. From an experimental point of view, in high quality graphene, the low density of short-range scatterers allows the Berry phase to manifest as a Weak Antilocalization (WAL) dip in the magnetoresistance [1]. As the π-phase contribution is averaged out by chirality breaking scattering, enhanced backscattering results in the usual Weak Localization (WL) correction. Essential in driving the transition between WAL and WL regimes is the possibility of tuning the charge density in the graphene monolayer.

The quest for monolithic integration of devices recently moved the interest towards Epitaxial Graphene (EG) on SiC, which has reached high mobility and uniformity on the wafer scale [2]. Despite such interest, the interplay between localization and chirality is still rather unexplored for EG grown on the Si face, where only positive magnetoresistance due to electron localization has been observed so far [3].

We report on quantum interference measurements in top-gated Hall bars epitaxially grown on the Si face of SiC, where the transition from WL to WAL regime was achieved varying the temperature and charge density. We analyzed the relative weight of the scattering mechanisms affecting the conductance in the different density regions. The results stress the role of SiC based devices as a promising technology for graphene coherent electronics.

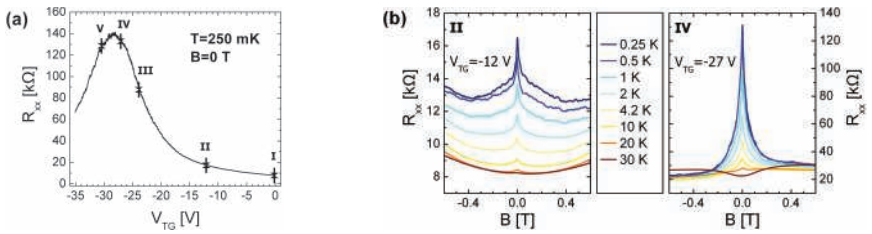

Figure 1: (a) Longitudinal resistance R_{xx} as a function of top gate voltage V_{TG}, showing a maximum at the charge neutrality point. The values of V_{TG} selected for magnetoresistance measurements are indicated. (b) The amplitude of the WL peak decreases as the temperature is increased (point II), evolving into a WAL dip for sufficiently low charge density (point IV).

[1] F. V. Tikhonenko, A. A. Kozikov, A. K. Savchenko, and R. V. Gorbachev, Phys. Rev. Lett. **103**, 226801 (2009).
[2] S. Tanabe, Y. Sekine, H. Kageshima, M. Nagase, and H. Hibino, Phys. Rev. B **84**, 115458 (2011).
[3] S. Lara-Avila, A. Tzalenchuk, S. Kubatkin, R. Yakimova, T. J. B. M. Janssen, K. Cedergren, T. Bergsten, and V. Fal'ko, Phys. Rev. Lett. **107**, 166602 (2011).

Magnetoresistance of high mobility graphene in parallel magnetic fields

J. Wakabayashi, S. Shiraishi, W. Wang

Department of Physics, Chuo University, 1-13-27 Kasuga, Bunkyo-ku, Tokyo 112-8551, Japan

It is well known that there are ripples in graphene suspended in space or placed on a substrate. Due to the presence of ripples, a magnetic field applied parallel to the two dimensional plane of graphene creates locally the magnetic field component normal to the surface of ripples according to the gradient of the local surface against the magnetic field. Because ripples vary in size and in curvature from place to place, a random magnetic field with zero mean is produced and, hence, a system of Dirac fermions in random magnetic fields is formed. Investigations of electrical transport properties of Dirac fermions in random magnetic fields coupling with ripples are interesting.

Recently, the magnetoresistance of graphene in parallel magnetic fields has been investigated.[1, 2, 3] However, the samples used have low mobility approximately 2.0×10^3 cm^2/Vs to 3.5×10^3 cm^2/Vs and it was not clear whether the transport properties observed is intrinsic to Dirac fermions or not. In the present paper we report the experimental results obtained using graphene with high mobility about 2×10^4 cm^2/Vs exfoliated onto a Si/SiO_2 substrate at a temperature of 1.9 K. The upper left inset of the figure shows the gate voltage dependence of resistivity ρ_{xx} and $\sigma_{xx} = \rho_{xx}^{-1}$ in zero magnetic field and the upper right inset shows QHE results at B = 13 T. These results confirm the present graphene has high quality enough to investigate the intrinsic properties of Dirac fermions in random magnetic fields.

We have measured magnetoresistance applying the parallel magnetic field $B_{//}$ between -15 T and +15 T along the source-drain direction at several gate voltages. The negative magnetoresistance due to the weak localization and the normal component of the random magnetic field was small in contrast to the previous experiments. [1, 2] The magnetoresistance $\Delta\rho = \rho(B_{//}) - \rho(0)$ was approximately parabolic against $B_{//}$ and we have determined the coefficient a by fitting the equation $\Delta\rho = aB_{//}^2 + b$ to the data. The main panel of the figure shows the carrier density dependence of the coefficient a. The blue lines represent $|n|^{-3/2}$ dependence predicted by the semiclassical calculation. [1] The experimental results in the carrier density $|n| > 1 \times 10^{11}$ cm^{-2} have shown good agreement with the result of semiclassical calculation. However, the coefficient a shows saturation in the range of $|n| < 1 \times 10^{11}$ cm^{-2}. We discuss these results combining with the results of AFM measurements of the ripples.

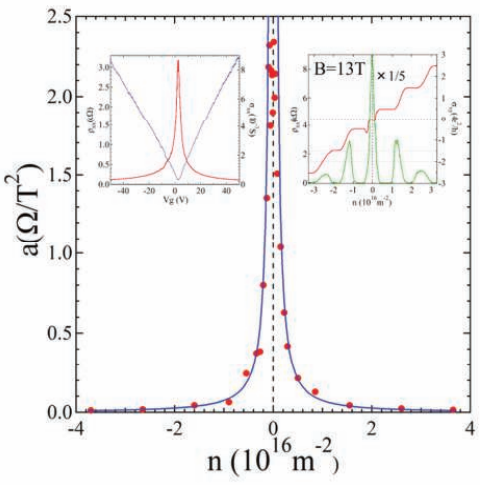

References:
[1] M. B. Lundeberg and J. A. Folk, *Phys. Rev. Lett.* **105**, 146804 (2010).
[2] J. Wakabayashi and T. Sano, *J. Phys.: Conf. Ser.* **334,** 012039 (2011).
[3] J. Wakabayashi and K. Sano, *J. Phys. Soc. Jpn.* **81,** 013702 (2012).

Infrared Photoresponse of High-Mobility Graphene in the Quantum Hall Regime

S. Masubuchi[1, 2], M. Onuki[1], M. Arai[1], K. Watanabe[1], T. Taniguchi[1], and T. Machida [1, 2, 4]

[1] *Institute of Industrial Science, University of Tokyo, Japan*
[2] *Institute for Nano Quantum Information Electronics, University of Tokyo, Japan*
[3] *National Institute for Material Science, Japan*
[4] *PRESTO-JST, Saitama, Japan*

The linear electronic band structure of graphene has lead to the formation of unequally and uniquely spaced Landau levels in graphene. Here, we report on the infrared photoresponse of high-mobility graphene devices due to the cyclotron resonance. In photoresponse signals, we observed two types of signals. The photovoltaic photoresponse was dominant at high temperature (T > 20 K) and low bias currents (I < 100 nA), whereas the bolometric effect was dominant at low temperature (T < 20 K) and high bias current (I > 100 nA). The photovoltaic photoresponse was sustained even up to T = 180 K.

We fabricated graphene/boron nitride Hall-bar devices using the mechanical transfer technique of graphene on hexagonal boron nitride. The fabricated device exhibited high mobility $\mu \sim 110{,}000$ cm^2/Vs at T = 4 K. The sample was irradiated by CO_2 laser light with the wavelength of λ = 10.6 μm. In the photoresponse signals measured at high temperature (T > 20 K) and zero bias current, positive and negative photoresponse signals (ΔV) were emerged at $\nu = \pm 2$ quantum Hall states [Fig. 1(b)]. The amplitude of ΔV was independent of I, indicating that the photoresponse signal was due to photovoltaic effect. On the other hand, when ΔV were measured at low temperature (T < 10 K) and finite bias current I = 100 nA, ΔV were emerged at quantum Hall transition regions between ν = -6 -> -2, -2 -> 2 and 2 -> 6. The amplitude of ΔV was linearly dependent on I and decayed quickly as the temperature was raised, indicating that the photoresponse signal was due to bolometric photoresponse.

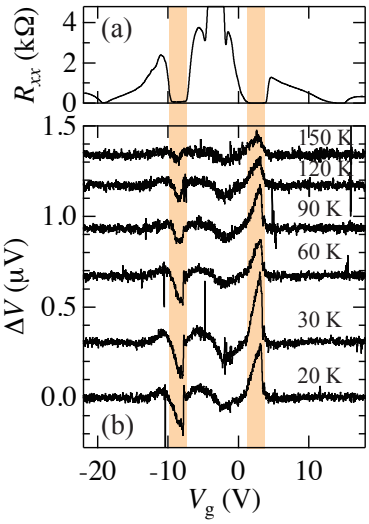

FIG. 1: (a) Longitudinal resistence R_{xx} and (b) photovoltaic response ΔV as a function of back-gate bias voltage V_g measured in magnetic fields of B = 8 T.

These results were in contrast to the case of the conventional low-mobility graphene on SiO_2, where the photoresponse signal was limited to bolometric effect. This observation suggests the emergence of intrinsic photoresponse in graphene by improving the charge carrier mobility. When the temperature was raised, the photovoltaic signal was sustained up to T = 180 K, indicating the possibility for developing high-temperature operating IR detectors using graphene.

Spin-polarized currents of Dirac fermions at cyclotron resonance

C. Zoth[1], P. Olbrich[1], P. Vierling[1], K. M. Dantscher[1], G. V. Budkin[2], S. A. Tarasenko[2], V. V. Bel'kov[2], D. A. Kozlov[3], Z. D. Kvon[3], N. N. Mikhailov[3], S. A. Dvoretsky[3], and S. D. Ganichev[1]

[1] Terahertz Center, University of Regensburg, Regensburg, Germany
[2] A.F. Ioffe Physical-Technical Institute, St. Petersburg, Russia
[3] Institute of Semiconductor Physics, Novosibirsk, Russia

We report on the observation of giant spin-polarized photocurrents in HgTe-based quantum well (QW) samples of width close to the critical thickness, at which a gapless state and the Dirac spectrum emerge [1]. The study of the photocurrent, accompanied by the measurements of radiation transmission as well as Shubnikov-de Haas and quantum Hall effects, reveals that the current enhancement is caused by cyclotron resonance (CR) in a Dirac fermion system. We develop a microscopic theory of the effect and show that the current originates from spin-dependent scattering of carriers heated by radiation.

The excitation of a MBE-grown (013) oriented HgTe/$Hg_{0.3}Cd_{0.7}Te$ QW sample with low power terahertz (THz) radiation of *cw* CH_3OH THz laser operating at a frequency of 2.54 THz results in a *dc* electric current caused by the photogalvanic effect. Applying a magnetic field perpendicular to the QW plane and studying the field dependence of the photocurrent, we observe that the current exhibits a resonance with a magnitude exceeding the photocurrent at zero magnetic fields by several orders of magnitude [2]. We observed that the magnetic field B_c at which the resonant photocurrent emerges can be tuned from negative to positive values by changing the type of carriers in the same sample applying optical doping [3]. Moreover the value of B_c depends on free carrier concentration and increases with rising Fermi energy. For our QW samples with the carrier density $(1 - 10)\cdot10^{10}$ cm^{-2} and THz radiation with the photon energy $\hbar\omega$ = 10.35 meV, the resonant photocurrent appears at correspondingly low magnetic fields B_c = 0.42 – 1.2 T. The photocurrent data, accompanied by measurements of radiation transmission as well as Shubnikov-de Haas and quantum Hall effects, give evidence that the enhancement of the photocurrent is caused by cyclotron resonance in a Dirac fermion system. From the resonance positions measured for several electron densities we find that the electron Fermi velocity is almost constant, being about $7\cdot10^5$ m/s. The value is in a good agreement with the electron velocity for 2D Dirac fermions in HgTe/HgCdTe QWs of critical thickness, $v = 6.3\cdot10^5$ m/s, obtained from the energy dispersion calculated in [1]. The strong dependence of the CR position on the carrier density indicates the Dirac character of the energy spectrum in the QWs with an energy-independent electron velocity. The resonant photocurrent is also detected in HgTe-based QW samples with the width L_w = 20 nm, which are characterized by a quadratic dispersion. Here CR, proved by the same experimental methods, is observed at a substantially larger magnetic field $B_c \sim 3$ T, with its position barely dependent on the carrier density.

The microscopic origin of the current is discussed in terms of the cyclotron motion, spin-dependent scattering and Zeeman splitting. We show that the current is spin-polarized and its enhancement comes from three constructively contributing factors: strong spin-orbit coupling, large *g*-factor in HgTe/HgCdTe QWs, and efficient radiation absorption at CR.

[1] B. Büttner *et al.*, Nature Phys. **7**, 418 (2011).
[2] P. Olbrich *et al.*, preprint http://arxiv.org/abs/1301.4572.
[3] Z.D. Kvon *et al.*, JETP Lett. **94**, 816 (2011).

Magnetic field response of graphene nanostructures

Mikito Koshino [1] **and Yuya Ominato** [1]

[1] *Department of Physics, Tohoku University, Sendai, Japan*

We theoretically study the anomalous magnetic field response of graphene flakes and ribbons. The recent developments in fabrication techniques realized a variety of graphene nanostructures with various shapes and sizes. Here we show that a finite-sized graphene, or "a piece of Dirac metal", behaves in non-trivial manner in presence of magnetic field, due to the coexistence of massless Dirac spectrum and the quantum confinement. We show that the orbital magnetic susceptibility rapidly changes between diamagnetism and paramagnetism as a function of Fermi energy in accordance with the level structure. Remarkably, the total susceptibility varies in proportion to cube of the system size even though the system is two dimensional. The diamagnetism of graphene flakes is fairly strong and can be observed using the magnetic field alignment in a solvent. When graphene flakes are randomly stacked in the perpendicular direction, the whole system exhibits an analogue of Meissner effect, where the external magnetic field is significantly screened inside the sample.

[1] Y. Ominato and M. Koshino, Phys. Rev. B 85, 165454 (2012).
[2] Y. Ominato and M. Koshino, arXiv:1301.5440v1 (2013).
[3] M. Koshino and T. Ando, Phys. Rev. B 81, 195431 (2010).

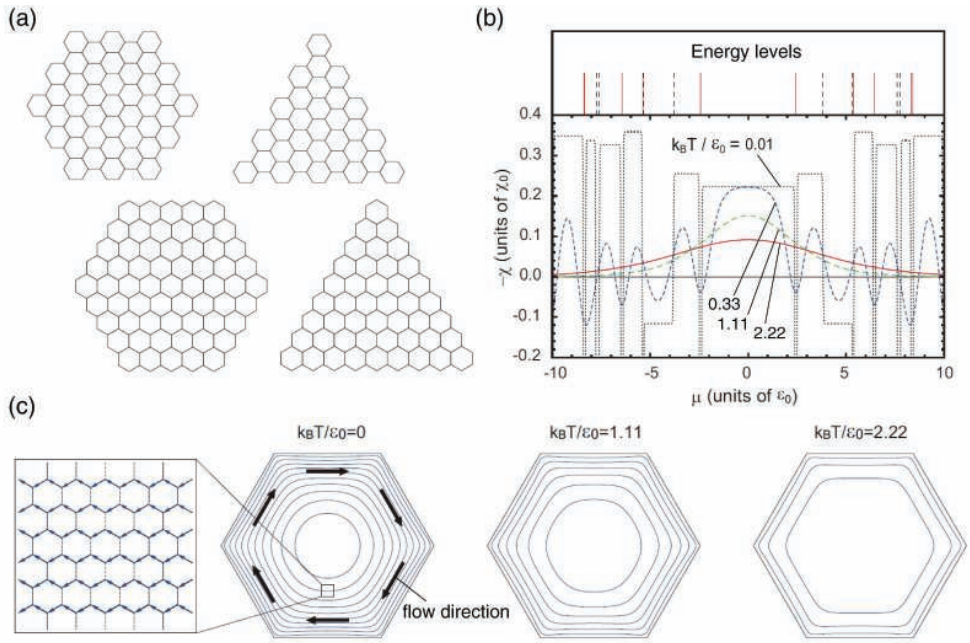

(a) Atomic structures of graphene flakes. (b) Orbital magnetic susceptibility as a function of the chemical potential of a hexagonal armchair graphene flake. (c) Diamagnetic current distribution in a hexagonal graphene flake in several different temperatures.

Annealing-induced magnetic moments in epitaxial graphene detected by spin precession measurements

B. Birkner[1], D. Pachniowski[1], A. Sandner[1], M. Ostler[2], T. Seyller[3], J. Fabian[4], M. Ciorga[1], D. Weiss[1], and J. Eroms[1]

[1] *Institute of Experimental and Applied Physics, University of Regensburg, 93040 Regensburg, Germany*
[2] *Lehrstuhl für Technische Physik, University of Erlangen-Nürnberg, 91058 Erlangen, Germany*
[3] *Technische Universität Chemnitz, 09107 Chemnitz, Germany*
[4] *Institute of Theoretical Physics, University of Regensburg, 93040 Regensburg, Germany*

Epitaxial graphene grown on SiC presents a viable route towards large-scale integration of graphene-based spintronics devices. Recently, two experimental groups realized spin transport in epitaxial graphene, but with vastly different spin relaxation times in different measurement configurations [1,2]. Also, the material system SiC/graphene seems much more complex than exfoliated graphene, and localized states can influence spin transport [3]. This motivated our experimental study of spin transport in epitaxial graphene before and after annealing at 150 °C in vacuum. Surprisingly, even these moderate conditions lead to considerable modifications in spin transport. We observe a reduction of the spin relaxation time and length upon annealing and, at first sight, a discrepancy between the charge diffusion constant and spin diffusion constant. This can be resolved by assuming local magnetic moments, which were shown to lead to an enhanced effective g-factor [4]. Here we also present the temperature dependence of the effective g-factor, which shows a 1/T-dependence, as expected for paramagnetic moments [5].

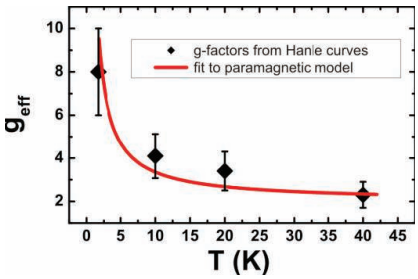

Figure 1: Temperature dependence of the effective g-factor after annealing

[1] B. Dlubak, M.-B. Martin, C. Deranlot, B. Servet, S. Xavier, R. Mattana, M. Sprinkle, C. Berger, W. A. De Heer, F. Petroff, A. Anane, P. Seneor, and A. Fert, Nature Physics **8**, 557 (2012).
[2] T. Maassen, J. J. van den Berg, N. IJbema, F. Fromm, T. Seyller, R. Yakimova, and B. J. van Wees, Nano Lett. **12**, 1498 (2012).
[3] T. Maassen, J. J. van den Berg, E. H. Huisman, H. Dijkstra, F. Fromm, T. Seyller, and B. J. van Wees, Phys. Rev. Lett. **110**, 067209 (2013).
[4] K. M. McCreary, A. G. Swartz, W. Han, J. Fabian, and R. K. Kawakami, Phys. Rev. Lett. **109**, 186604 (2012).
[5] B. Birkner, D. Pachniowski, A. Sandner, M. Ostler, T. Seyller, J. Fabian, M. Ciorga, D. Weiss, and J. Eroms, Phys. Rev. B **87**, 081405(R) (2013).

Electron – Phonon Couplings and Fano Resonances in Epitaxial Graphene Bilayer

J.M.Baranowski[1,2], W.Strupinski[1], M.Mozdzonek[1], K.Grodecki[1,2], and P. Osewski[1]

1.Institute of Electronic Materials Technology, Wolczynska 133, Warsaw, POLAND
2. Faculty of Physics, University of Warsaw, Hoza 69, Warsaw, POLAND

Keywords: graphene bilayer, Raman active mode, optical active mode, Fano shape line,

A vast majority of the optical studies of graphene have been performed by Raman spectroscopy, whereas infrared techniques that can provide complementary information, due to different selection rules, remain largely unexplored. Fourier transformed infrared attenuated total reflection spectroscopy (FTIR-ATR) and infrared reflectivity together with Raman measurements of epitaxial hydrogenated graphene bilayers grown on 4H-SiC(0001) by CVD are presented and discussed. The intercalation of hydrogen under a buffer and a single graphene layer was performed at high temperatures in the range 1000^0C – 1200^0C.

The FTIR-ATR measurements using polarized light revealed the Si – H stretch mode at 2128cm^{-1}, which proves that the SiC(0001) surface is saturated with hydrogen. The obtained bilayers are hole-doped (p = 1.3 – 1.6x10^{13} cm^{-2}), with the carrier mobility of 3000cm^2/Vs – 3500cm^2/Vs at 300K. In addition to the Si – H stretch line, a strong absorption is observed in both FTIR-ATR and reflectivity in the vicinity of the well-known Raman G band (close to1590cm^{-2}). However, the absorption line (detected in the reflection from the SiC substrate through the graphene bilayer) is shifted to a lower energy with respect to the Raman G line by about 10cm^{-1}, as shown in Fig. 1. This is the manifestation of an effect that in a plane optical phonon in the center of the Brillouin zone (G band) of bilayer graphene consist of an in-phase-mode (even parity) - being the Raman active one (RM), and an out-of-phase-mode (odd parity) - being the infrared active one (OM) [1]. Due to a large hole concentration, the RM and OM are no longer degenerate and the OM is shifted to a lower energy with respect to the RM. Such splitting between the Raman and optical modes of the G line was earlier reported only for a freestanding gated graphene bilayer in the electric fields [1].

In addition to finding the split between the energy of the Raman and infrared active modes we observed that the OM is of a Fano shape. The Fano shape of the infrared active G line was found in reflectivity and in FTIR-ATR, as well. Such Fano line shape of the optical mode of the G line was also earlier reported in the freestanding gated graphene bilayer [2]. The Fano shape absorption line, particulary strong in FTIR-ATR (Fig. 2) is observed for the first time for the graphene bilayer without influence of the electric field. The presence of Fano resonance indicates that infrared active G phonon mode is interacting with a continuum of hole excitations within the graphene bilayer valence band.

[1] Jan Yan et al., Phys. Rev. B 80 241417 (2009)
[2] A.B. Kuzmenko et al., Phys. Rev. Lett. 103, 116804 (2009)

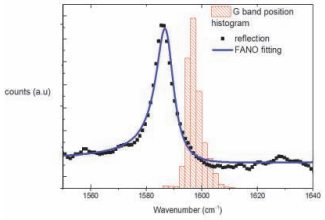

Fig. 1. The optical mode (OM) observed in reflectivity and the histogram of the Raman (RM) mode versus infrared wavenumber.

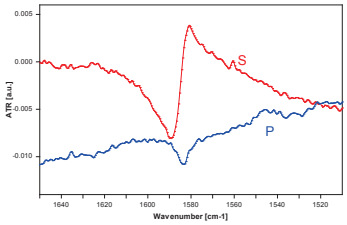

Fig. 2. The Fano resonance of the OM mode observed in s and p polarization in FTIR-ATR measurement.

Electron-electron interactions in non-equilibrium bilayer graphene

Weizhe Edward Liu [1], Allan H. MacDonald [2] and Dimitrie Culcer [1,3]

[1] *ICQD, Hefei National Laboratory for Physical Sciences at the Microscale, University of Science and Technology of China, Hefei 230026, Anhui, China*
[2] *Department of Physics, The University of Texas at Austin, Austin TX 78712, USA*
[3] *School of Physics, University of New South Wales, Sydney NSW 2052, Australia*

Conducting steady-states of doped bilayer graphene have a non-zero sublattice pseudospin polarization. In this talk, I will demonstrate that electron-electron interactions renormalize this polarization even at zero temperature, when the phase space for electron-electron scattering vanishes. We have shown that, because of the strength of interlayer tunneling, electron-electron interactions nevertheless have a negligible influence on the conductivity which vanishes as the carrier number density goes to zero [1]. The influence of interactions is qualitatively weaker than in the comparable cases of single-layer graphene or topological insulators, because the momentum-space layer pseudo spin vorticity is 2 rather than 1. Our study has reliesd on the quantum Liouville equation in the first Born approximation with respect to the scattering potential, with electron-electron interactions taken into account self-consistently in the Hartree-Fock approximation and screening in the random phase approximation. Within this framework the result we have obtained is exact.

[1] Weizhe Edward Liu, A. H. MacDonald, and Dimitrie Culcer, Physical Review B 87, 085408 (2013).

Spin Hall effect in graphene with fluctuating Rashba field

A. Dyrdał[1], **J. Barnaś**[1,2]

[1] *Faculty of Physics, Adam Mickiewicz University in Poznań*
[2] *Institute of Molecular Physics Polish Academy of Sciences, Poznań*

The crucial issue of spintronics is pure electrical control of the spin degree of freedom. One of the phenomena allowing such a control is the spin Hall effect (SHE) [1, 2], that originates from spin-orbit coupling in the system and leads to spin current (or spin accumulation) flowing perpendicularly to an external electric field. The spin Hall effect strongly depends on the type of spin-orbit coupling and may be either of intrinsic or extrinsic origin. The extrinsic SHE is associated with scattering mechanisms (skew scattering and side jump) on impurities and other defects, while the intrinsic SHE is a consequence of a nontrivial trajectory of charge carriers in the momentum space due to the spin-orbit contribution of a perfect crystal lattice to the corresponding band structure [3].

In a general case, local imperfections of the system, such as random distribution of donors or impurities, may lead to local enhancement or suppression of the spin-orbit coupling. Thus, charge carriers in the system propagate in an effective spin-orbit field that contains regular and random components. Such fluctuations significantly affect spin transport leading, for example, to strong modification of the spin relaxation as well as to spin Hall effect robust to impurity scattering [4, 5, 6]. A good example of systems with random spin-orbit field is graphene, in which the spatially fluctuating spin-orbit coupling may be due to ripples of the graphene plane, disorder, electron-phonon coupling in the substrate, the presence of adatoms, etc.

We will present results of our theoretical investigation of the spin Hall effect in graphene due to fluctuating Rashba field [7]. Using the Green function method and diagrammatic technique we have calculated the SHE conductivity of graphene in the situation when the Rashba interaction fluctuates around zero average value. The results show that potential scattering due to defects suppresses the spin Hall effect, but this suppression is not complete. The spin Hall conductivity in this case is generally not universal, but depends on the ratio of the total momentum and spin-flip relaxation rates. Thus, the behavior of spin Hall conductivity in graphene with fluctuating Rashba field is significantly different from that in the case of constant Rashba coupling[8].

[1] M. I. Dyakonov, V. I. Perel, ZhETF Pis. Red. **13**, 657 (1971).
[2] J. E. Hirsch, Phys. Rev. Lett. **83**, 1834 (1999).
[3] G. Vignale, J. Supercond. Nov. Magn. **23**, 3 (2010).
[4] M. M. Glazov, E. Ya. Sherman, V. K. Dugaev, Physica E **42**, 2157 (2010).
[5] V. K. Dugaev, M. Inglot, E. Ya. Sherman, J. Barnaś, Phys. Rev. B **82**, 121310(R) (2010).
[6] A. Dyrdał, J. Barnaś, Acta Phys. Pol. A **122**, 1016 (2012).
[7] A. Dyrdał, J. Barnaś, Phys. Rev. B **86**, 161410(R) (2012).
[8] A. Dyrdał, V. K. Dugaev, J. Barnaś, Phys. Rev. B **80**, 155444 (2009)

Temperature dependence and bipolar interference in graphene monolayer quantum rings

D. Smirnov[1], H. Schmidt[1], and R. J. Haug[1]

[1] *Institut für Festkörperphysik, Leibniz Universität Hannover, Germany*

We analyze the electronic properties of a topgated monolayer graphene ring. Micromechanical cleavage was used to place a flake on a Si/SiO2 substrate. The structuring and contacting was done via plasma etching and electron beam lithography. An additional gate was placed on top of one arm of the ring which allows us to control the charge carrier concentration locally and additionally to create a pnp- (npn-) junction inside the ring. The sample was measured in a He3 cryostat and is identified as single layer graphene via magnetotransport measurements.

We observe Aharonov Bohm (AB) effect by sweeping the magnetic field around 0 T. The period of the oscillations is approx. 16 mT which fits the size of the ring well. We also observe the AB-oscillations when a pnp-junction is created inside the ring. The period is independent of the existence of a pnp-junction and stays constant in all situations. We analyse the amplitude in dependence of the charge carrier concentration. The absolute amplitude is constant in the bipolar and unipolar region[1].

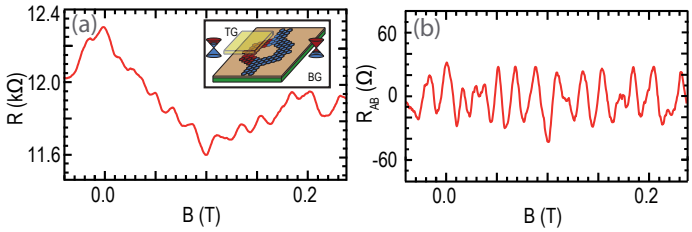

Figure 1: (a) shows the magnetotransport measurements in the range of 0 T with the weak localisation and AB oscillations. The Inset shows the schematic of the sample. (b) shows the oscillations with the background subtracted. A period of 16 mT can analysed and fits the geometry of the ring well.

We observe small AB amplitudes with visibilities of about $0.5 - 1\%$. This values are comparable to other ring experiments performed in graphene [2, 3, 4, 5]. To understand these small visibilities the temperature dependence of the AB oscillation was studied. The amplitude shows a fast decrease proportional to T^{-1} above 1 K and a slow decrease below 1 K. The origin of the slow decrease is not clear. Therefore the results are compared to the phase coherence length extracted from an analysis of the weak localization temperature dependence.

[1] D. Smirnov, H. Schmidt, and R. J. Haug, Appl. Phys. Lett. **100**, 203114 (2012).
[2] S. Russo, J. B. Oostinga, D. Wehenkel, H. B. Heersche, S. S. Sobhani, L. M. K. Vandersypen, and A. F. Morpurgo, Phys. Rev. B **77**, 085413 (2008).
[3] M. Huefner, F. Molitor, A. Jacobsen, A. Pioda, C. Stampfer, K. Ensslin, and T. Ihn, New J. Phys. **12**, 043054 (2010).
[4] J. S. Yoo, Y. W. Park, V. Skakalova, and S. Roth Appl. Phys. Lett. **96**, 143112 (2010).
[5] Y. Nam, J. S. Yoo, Y. W. Park, N. Lindvall, T. Bauch, and A. Yurgens, Carbon, **50**, 5562 (2012).

The electronic structure of graphene induced by substrate interaction

P. Dabrowski[1], W. Kozlowski[2], I. Wlasny[2], J. Slawinska[2], Z. Klusek[2], M. Kopciuszynski[3], R. Zdyb[3], M. Jalochowski[3], J.M. Baranowski[1,4], and W. Strupinski[1]

[1] *Institute of Electronic Materials Technology, Wolczynska 133, Warsaw, 01-919, Poland*
[2] *Department of Solid States Physics, Faculty of Physics and Applied Informatics, University of Lodz, Pomorska 149/153, Lodz, 90-236, Poland*
[3] *Institute of Physics, M. Curie-Skłodowska University, Place M. Curie-Skłodowskiej 1, Lublin 20-031, Poland*
[4] *Faculty of Physics, University of Warsaw, Hoza 69, Warsaw, 00-681, Poland*

Monolayer graphene (MG) is a new two-dimensional allotrope of carbon, which possesses unique electronic properties due to massless Dirac fermion character of charge carriers, which derives from the conical dispersion relation close to the Dirac point. It has been shown that this type of dispersion relation leads to the occurrence of quantum Hall effect, ballistic transport of electrons, electronic spin transport, micron scale coherence length and Klein tunneling and scattering.

However, it has been demonstrated that the presence of different adsorbates and substituting atoms leads to the significant modification of the electronic properties of this material. In particular, graphene conical dispersion relation can be also modified by the charge carrier transfer from the substrate, which is exhibited by shift of Fermi level relative to the Dirac point [1].

We present studies of graphene deposited on different substrates using Scanning tunneling microscopy/spectroscopy (STM/STS), atomic force microscopy (AFM), low energy electron diffraction (LEED), Angle Resolved X-ray Photoelectron Spectroscopy (ARXPS) and Angle Resolved Photoelectron Spectroscopy (ARPES). Samples were prepared by both CVD growth, where propane gas was used as a carbon precursor [2], and mechanical exfoliation. Our results recorded on the mono- and bilayer of graphene deposited SiO_2, SiC, TiO_2, and metallic substrates like Cu(111) and Cu foils clearly show that substrate significantly modifies graphene electronic structure and changes its corrugation. Depending on substrate, the Fermi level shift downwards or upwards relative to the Dirac point, which means that either holes or electrons are donated to the graphene. It is worth pointing out that these changes are also visible for non-conducting or semi-conducting substrates and can be changed locally in nanoscale. Our findings were confirmed by Density Functional Theory (DFT) calculations.

This work is supported by the National Science Centre under the postdoctoral research project DEC-2012/04/S/ST3/00186
This work is supported by the National Centre for Research and Development under the project GRAFMET/GRAF-TECH/NCBiR/01/32/2012

[1] G. Giovannetti, Phys. Rev. Lett. **101**, 026803 (2008).
[2] W. Strupinski, K. Grodecki, A. Wysmolek, R. Stepniewski, T. Szkopek, P. E. Gaskell, A. Grüneis, D. Haberer, R. Bozek, J. Krupka, J. M. Baranowski, Nano Lett. **11**, 1786 (2011)

Graphene on GaAs

Pauline Simonet[1], Clemens Rössler[1], Tobias Krähenmann[1], Christian Reichl[1], Werner Wegscheider[1], Klaus Ensslin[1] and Thomas Ihn[1]

[1] *Solid State Physics Laboratory, ETH Zurich, Switzerland*

We combine graphene nanostructures with high quality AlGaAs/GaAs two-dimensional electron systems (2DESs). The graphene flakes are placed in the region of interest using the transfer technique developed for boron nitride/graphene heterostructures [1]. We demonstrate that graphene can gate and be gated by the GaAs 2DES. Thus, a quantum point contact (QPC) is defined. Figure 1 a) is an atomic force micrograph of the graphene flake, which has been etched in the shape of two side-gates on the GaAs surface. The distance between the two graphene gates is 300nm. Figure 1 b) shows the differential conductance in the GaAs 2DES as a function of voltages applied to the graphene gates. Steps in the conductance occur until pinch-off, indicating the formation of discrete subbands between the gates.

Combining these two materials will allow us to use the GaAs 2DES to detect where localized states appear in graphene etched nanostructures. Moreover, graphene can simultaneously form top gates and very sensitive charge detectors, because nanoribbons are governed by Coulomb blockade [2, 3]. Graphene sensing gates can then be used for probing excitations in the quantum Hall regime in the GaAs.

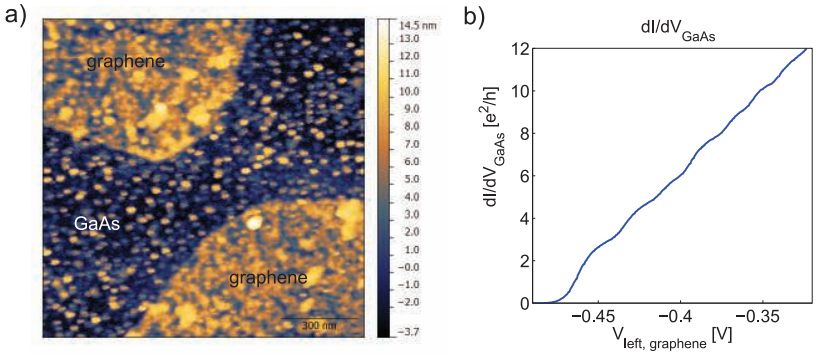

Figure 1: a) Scanning force microscope image of contacted and etched graphene gates (bright areas) defining a quantum point contact in the GaAs 2DES underneath. The dark area is the GaAs surface. Bright dots are grains of resist left from the processing. b) Differential conductance through the graphene defined QPC as a function of the two graphene gate voltages ($V_{\mathrm{right}} = 0.59 + 2.89\,V_{\mathrm{left}}$). A contact resistance of $R_{\mathrm{C}} = 970\,\Omega$ has been subtracted. The presence of localizations in the GaAs QPC causes deviations from the expected values of conductance plateaux.

[1] C.R. Dean, A.F. Young, I. Meric, C. Lee, L. Wang, S. Sorgenfrei, K. Watanabe, T. Taniguchi, P. Kim, K.L. Shepard and J. Hone, Nature Nanotechnology, **5**, pp. 722726, 2010

[2] F. Molitor, C. Stampfer, J. Güttinger, A. Jacobsen, T. Ihn and K. Ensslin, Semiconductor Science and Technology, **25**, 034002, 2010

[3] S. Schnez, J. Güttinger, M. Hüfner, C. Stampfer, K. Ensslin and T. Ihn, Physical Review B, **82**, 165445, 2010

Superconducting Graphene Nanodevices in the Ballistic Transport Regime

Joel I-Jan Wang [1, 2], Yu-An Chen[2], Kenji Watanabe[3], Takashi Taniguchi[3], Pablo Jarillo-Herrero[2]

[1] *Harvard School of Engineering and Applied Sciences, Cambridge, MA 02138, USA*
[2] *Department of Physics, Massachusetts Institute of Technology, Cambridge, MA 02139 USA*
[3] *National Institute for Materials Science, Namiki 1-1, Tsukuba, Ibaraki 305-0044, Japan*

Superconductivity carried by Dirac fermions can be realized through induced superconductivity in graphene [1]. Observation of novel phenomena anticipated by theories [2] calls for superconducting graphene devices with low disorder so that the transport is ballistic.

Current fabrication procedures to make graphene devices with low disorder, such as devices on suspension or ultra-flat substrates, all call for certain kinds of annealing to remove organic residues derived from the fabrication process [3],[4]. Applying these methods to superconducting devices is challenging since the transparency at the graphene/superconductor interface may be compromised.

Here we present the fabrication and characterization of superconducting graphene nanodevices with its 2-dimensional electron gases (2DEGs) encapsulated in hexagonal boron nitride (hBN) flakes. The ultra flatness and lack of dangling bond in the boron nitride substrate reduces the disorder in graphene, while the top hBN layer protects the graphene from contamination during nanofabrication. We believe that this kind of device will open the door for the study of ballistic Dirac fermions in the superconducting regime.

[1] H. B. Heersche *et al*., "Bipolar supercurrent in graphene," *Nature*, vol. 446, pp. 56-59, Mar. 2007.
[2] C. W. J. Beenakker, "Colloquium: Andreev reflection and Klein tunneling in graphene," *Rev. Mod. Phys*., vol. 80, pp. 1337-1354, 2008.
[3] Kirill I. Bolotin *et al*., "Observation of the fractional quantum Hall effect in graphene," *Nature*, vol. 462, pp. 196–199, Nov. 2009.
[4] T. Taychatanapat *et al*., "Quantum Hall effect and Landau level crossing of Dirac fermions in trilayer graphene," *Nature Physics*, vol. 7, pp. 621-625, 2011.

TuP26

Magnetoresistance of disordered graphene at high temperatures

P. S. Alekseev [1], A. P. Dmitriev [1], I. V. Gornyi [1,2] , and V. Yu. Kachorovskii [1]

[1] *Ioffe Physical-Technical Institute, 194021 St. Petersburg, Russia*
[2] *Institut fur Nanotechnologie, Karlsruhe Institute of Technology, 76021 Karlsruhe, Germany*

In graphene, the key parameter determining magnetotransport properties, a product of the cyclotron frequency and scattering time, $\omega_c \tau_q$, depends not only on magnetic field, but also on electron energy. As a result, a strong magnetoresistance arises already at the semiclassical level within the Drude-Boltzmann approach. Furthermore, for the same reason, quantum (separated Landau levels) and classical (overlapping Landau levels) regimes may coexist in the same sample at a fixed magnetic field, giving rise to an additional contribution to magnetoresistance.

We have theoretically studied magnetoresistance of graphene, focusing on the disorder-dominated transport regime with short-range impurities [1]. For short short-range impurities, the scattering time is inversely proportional to the energy: $\tau_q \sim \varepsilon^{-1}$, which gives the square-root magnetoresistance. We have calculated the conductivity tensor within the self-consistent Born approximation for graphene [2] for the case of relatively high temperature, when Shubnikov-de Haas oscillations are suppressed by thermal averaging. We demonstrate that both at very low and at very high magnetic field the longitudinal resistivity depends on magnetic field as a square root: $[\rho_{xx}(H) - \rho_{xx}(0)]/\rho_{xx}(0) = C\sqrt{H}$, where C is a temperature-dependent factor, different in the low- and strong-field limits. The cases $T >> \mu$ and $T << \mu$ were examined in details (here T is the temperature and μ is the chemical potential of carriers in graphene). We also predict a non-monotonic dependence of the Hall coefficient both on magnetic field and on the electron concentration. Finally, we discuss the case of screened charged impurities, where we also predict a square-root low-field dependence of magnetoresistance.

The experimental evidence of square-root MR in monolayer grapheme was reported recently in paper [3].

[1] P. S. Alekseev, A. P. Dmitriev, I. V. Gornyi, and V. Yu. Kachorovskii arXiv 1210.6081v1 [cond-mat.dis-nn].
[2] N. H. Shon and T. Ando, Journ. of the Phys. Soc. of Japan **67**, 2421 (1998).
[3] G. Yu. Vasileva, P. S. Alekseev, Yu. L. Ivanov, Yu. B. Vasilev, D. Smirnov, H. Schmidt, R. J. Haug, F. Gouider, and G. Nachtwei, Pis'ma v ZhETP **96**, 519 (2012) [JETP Letters **96**, 471 (2012)].

Effects of charged impurity clusters on the conductivity of supported graphene

N. Sule[1], K. J. Willis[1,2], S. C. Hagness[1], and I. Knezevic[1]

[1] *University of Wisconsin-Madison, Madison, WI 53706, USA*
[2] *AWR Corporation, 11520 North Port Washington Road, Mequon, WI 53092, USA*

Charged impurities are likely to be introduced into graphene samples by typical fabrication and processing techniques, and can persist even after annealing [1]. Such impurities are likely to produce electron-hole puddles with an average size of 20 nm [2]. These electron-hole puddles point towards a clustered impurity distribution, as opposed to a uniform random distribution. It has also been shown that spatially correlated impurities affect the conductivity of graphene [3, 4]. Therefore, a reliable and quantitative determination of the effects of such impurities on carrier transport in graphene supported on SiO_2 is important for the development of graphene-based applications. We have combined particle-based transport simulations, using the ensemble Monte Carlo (EMC) method, with numerical long-range and short-range field solvers, using the finite-difference time-domain (FDTD) technique and molecular dynamics (MD), respectively, in order to simulate the formation of electron-hole puddles and study the effect of charged impurity distributions on the conductivity of graphene supported on SiO_2. The coupled EMC-FDTD-MD algorithm has been used to calculate the high-frequency conductivity of bulk silicon [5, 6] in very good agreement with experimental data.

We simulate a structure consisting of a monolayer of graphene on top of an SiO_2 substrate. Clusters of impurity ions are present at and near the interface between graphene and the substrate. The charged impurity clusters are stochastically initialized using a correlation length parameter to define the average size and distribution of the clusters. By simulating carrier dynamics without any external fields, we have calculated the steady-state electron and hole density distributions for a uniform random, as well as a clustered impurity distribution. The average size of the electron-hole puddles, which is calculated using the full width at half maximum of the normalized spatial auto-correlation functions of the density distributions, are about 4 nm and 20 nm for the uniform random and clustered impurity distributions, respectively. We show that impurity clusters between the sizes of 30 and 40 nm are responsible for producing electron-hole puddles quantitatively similar to those seen in experiments [2]. We also calculated the conductivity in graphene as a function of the carrier density, for impurity-free, as well as for uniform random and clustered impurity distributions, with an impurity density of 10^{11}–10^{12} cm^{-2} and an average cluster size of 36 nm. We show that, for impurity densities greater than 10^{11} cm^{-2}, the distribution of impurities (random or clustered) significantly affects both the sublinearity and the slope of the linear region in the carrier-density dependence of conductivity. By turning off/on specific terms in the MD to elucidate the effect of short-range carrier-carrier and carrier-ion interactions, we find that the sublinearity in conductivity as a function of the carrier-density is due to direct and exchange carrier-carrier interactions limiting transport. Moreover, the slope of the linear region is strongly dependent on the short-range carrier-ion Coulomb interaction, and therefore on the density and distribution of the impurities.

In conclusion, we quantitatively show that clustered impurities, as well as the resulting short-range carrier-ion, and carrier-carrier interactions, play an important role in determining the room-temperature conductivity of supported graphene.

[1] L. Yung-Chang, L. Chun-Chieh, Y. Chao-Huei, J. Chuanhong, S. Kazu, and C. Po-Wen, Nano Lett. **12**, 414–419 (2012).
[2] A. Deshpande, W. Bao, Z. Zhao, C. N. Lau, and B. J. LeRoy, Phys. Rev. B **83**, 155409 (2011).
[3] J. Yan, and M. S. Fuhrer, Phys. Rev. Lett. **107**, 206601 (2011).
[4] Q. Li, E. H. Hwang, E. Rossi, and S. D. Sarma, Phys. Rev. Lett. **107**, 156601 (2011).
[5] K. J. Willis, S. C. Hagness, and I. Knezevic, Appl. Phys. Lett. **96**, 6 (2010).
[6] K. J. Willis, S. C. Hagness, and I. Knezevic, J. Appl. Phys. **110** 063714 (2011).

Manipulating Dirac cones in Graphene by periodic ac fields

A. Gómez-Leon[1], P. Delplace[2], and G. Platero[1]

[1] *Instituto de Ciencia de Materiales, CSIC, Cantoblanco, Madrid E-28049, Spain*
[2] *Département de Physique Théorique, Université de Genève, CH-1211 Genève, Switzerland*

In the last years, the search for topological effects in condensed matter systems has become a prior task. Graphene, because of its striking band structure, is an excellent platform to explore two-dimensional relativistic physics and topological phases. Topological transitions between semi-metallic and insulator phases are predicted to occur when the two inequivalent Dirac cones merge[1, 2] . The merging is achieved by introducing anisotropy in the honeycomb lattice, usually by mechanical means. However, the difficulties to properly control mechanically the anisotropy motivate the search of new methods, more controllable and non- destructive. We propose a theoretical model of graphene driven by an AC electric field, and show that such a driving allows for the manipulation of the Dirac cones in a high frequency limit. Their merging leads to rich diagrams with different semi-metallic and insulating phases topologically distinct. Furthermore, AC field-induced charge localization in selective spatial directions is found to occur at the transition between two insulating or two semi-metallic phases. In addition, we demonstrate that for low frequency driving, non-linear polarization breaks time reversal and particle-hole symmetry, allowing for new topological phases[3].

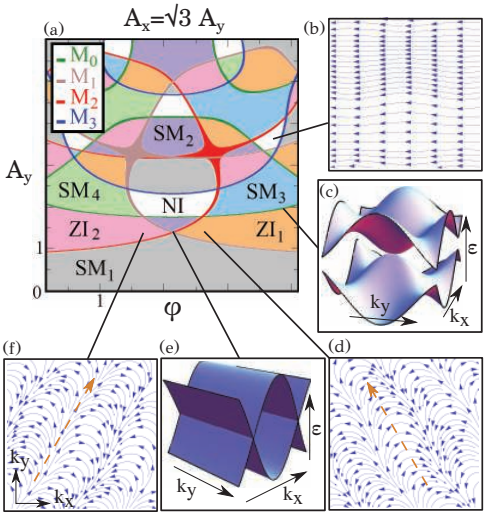

Figure 1:

Fig.1: (a) Phase diagram of graphene under a high frequency electric field elliptically polarized. Several insulating (I) or semi-metallic (SM) phases are found when tuning the phase shift between the x and y field components and the amplitude of the field in the y direction. The topological phase transitions between the I and SM phases can occur only at one of the four time-reversal symmetric points of the Brillouin zone where a pair of Dirac point is created/annihilated (M0 – M3). At such a transition the dispersion relation is linear in one direction but quadratic in the other one (c). In addition, certain insulating phases are found to be topologically nontrivial, (b) and (d), and host zero energy edge states protected by chiral symmetry (ZI1 and ZI2). The transition between two insulating or SM phases is characterized by a flat dispersion relation in one direction whereas it reminds linear in the other direction (e).

*References

[1] G. Montambaux et al., Eur. Phys. J. B, 72, 4, 509-520 (2009).

[2] L. Tarruell et al., Nature, 483, 302–305 (2012).

[3] A. Gómez-León, P. Delplace and G. Platero , submitted.

Ballistic transport in graphene *p-n* junctions

S. Morikawa [1], S. Masubuchi [1,2], M. Onuki [1], K. Watanabe [3], T. Taniguchi [3] and T. Machida [1,2,4]

[1] *Institute of Industrial Science, University of Tokyo, Tokyo, Japan*
[2] *Institute for Nano Quantum Information Electronics, University of Tokyo, Tokyo, Japan*
[3] *National Institute for Material Science, Tsukuba, Japan*
[4] *PRESTO-JST, Saitama, Japan*

P-N junctions in graphene promise to be a platform for investigating peculiar transport phenomena of Dirac fermions such as Klein tunneling and negative refraction. In order to observe these phenomena, we need graphene *p-n* junctions in which the charge carrier travels ballistically. However, in the conventional graphene *p-n* junctions, the interaction between graphene and substrate material degraded the charge carrier mobility. In this work, we fabricated high-mobility graphene *p-n* junctions by sandwiching graphene between two hexagonal boron-nitride (h-BN) crystals. The resistivity peak as a function of back-gate bias voltage was narrow ($\delta V_{BG}^{FWHM} \sim 1$ V), demonstrating high quality of our device. By tuning the global back gate (V_{BG}) and local top gate (V_{TG}), we formed *p-p*' and *p-n* junctions [Fig. 1]. When *p-p* junction was formed ($V_{TG} = 0$ V), characteristic peak structures were emerged in bend resistance $R_{CD,AB}$ plot [Fig. 2]. The positions of the peaks were well fitted by the curves with constant cyclotron radius R_c. This result indicates that the peak structures were caused by the charge carriers focused onto the voltage probe C from A by the ballistic carrier trajectory shown in Fig. 1. When the top gate voltage V_{TG} was varied, we observed the shift of the positions of focusing signals. We will discuss this result in terms of the change of the electron wave's refractive index at the *p-n* junctions.

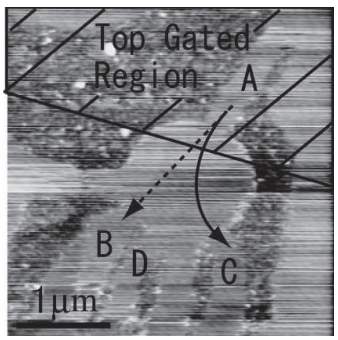

Fig. 1: AFM image of the representative device before transferring the top BN. The top gated region subsequently deposited is also depicted. The solid and dotted arrows indicate a ballistic carrier trajectory and a current direction, respectively.

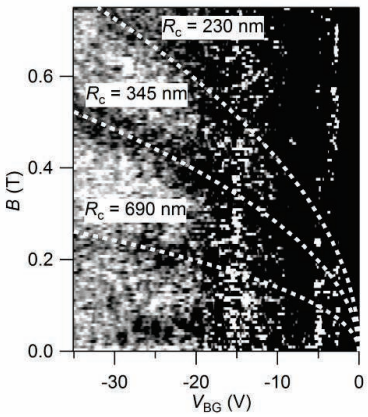

Fig. 2: Gray scale plot of bend resistance $R_{CD,AB}$ as a function of V_{BG} and B with V_{TG} = 0 V. The white dotted curves correspond to cyclotron radius R_c = 230, 345, 690 nm (top to bottom), suggesting the focusing of carriers onto the voltage probe C shown in Fig. 1.

Superfluid-insulator transitions of collective helical modes in the zero quantum Hall state of bilayer graphene

Victoria Mazo[1], Chia-Wei Huang[1], Herbert A. Fertig[2], Samuel Carr[3] and Efrat Shimshoni[1]

[1] Bar Ilan University, Israel
[2] Indiana University, USA
[3] University of Kent, UK

We derive an effective field-theoretical model for the one-dimensional collective modes associated with domain walls in a quantum Hall ferromagnetic state, as realized in bilayer graphene systems at zero filling subject to a kink-like perpendicular electric field. In particular, it is demonstrated that two pairs of collective helical modes are formed at opposite sides of the kink, each pair consisting of modes with identical helicities. The coupling between modes implies a description in terms of anisotropic quantum spin-ladders, whose parameters are tunable by varying the magnetic and electric fields. We show that this system possesses a rich phase diagram, which due to the helical nature of the modes implies a diversity of charge conduction properties. Most notably, we find that the helical ladders may undergo a transition from a superfluid to an insulating phase, manifested by a jump in the two-terminal conductance as well as the drag trans-conductance.

Strong suppression of conductance in dual-gated h-BN/bilayer graphene/h-BN device

M. Arai [1], S. Masubuchi [1,2], K. Watanabe [3], T. Taniguchi [3] and T. Machida [1,2,4]

[1] *Institute of Industrial Science, University of Tokyo, Japan*
[2] *Institute for Nano Quantum Information Electronics, University of Tokyo, Japan*
[3] *National Institute for Materials Science, Japan*
[4] *PRESTO, Japan Science and Technology Agency, Japan*

Bilayer graphene (BLG) has been receiving much attention for the application of graphene-based nano devices. Since the band gap of BLG could be opened by applying perpendicular electric field with a dual-gated (DG) structure, this material could be used for fabrication of various types of gate-defined nano structures such as a quantum point contact or a quantum dot. However, the low temperature transport characteristics of DG-BLG devices have not exhibited strong suppression of conductance [1]. It is believed that the hopping transport between localized states due to the impurities in SiO_2 substrate is dominant at low temperature. In this study, instead of SiO_2 substrate we use h-BN, which is atomically flat and impurity free, for substrate and top gate dielectric material in the DG-BLG device.

We fabricate the DG-BLG device, showed in the inset of Fig. 1, using the dry transfer method. This system enables independent control of charge density and perpendicular electric field amplitude. Fig. 1 shows the sheet resistance R_{sheet} measured as a function of top-gate voltages V_{TG} at various back gate voltages V_{BG}. The resistance peaks correspond to the charge neutrally point (CNP). As increasing V_{TG} and V_{BG} to opposite direction, perpendicular electric field D increases. R_{sheet} at the CNP increases exponentially with D due to the induced band gap and reaches to 10 MΩ at $D \sim 0.85$ V/nm. We measure the temperature dependence of the conductivity at the CNP. The conductivity of our h-BN-based device is 2 orders of magnitude smaller than that of the SiO_2-based device at 4 K [1] (Fig. 2). Thus our study reveals that the h-BN-based DG-BLG devices have significant advantages for fabricating the gate defined nano electronics devices.

[1] T. Taychatanapat, *et. al.*, Phys. Rev. Lett. **105**, 166601 (2010).

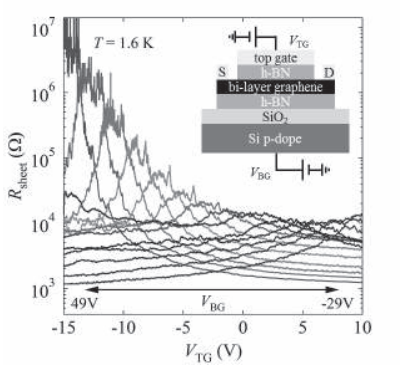

Fig. 1 R_{sheet} of DG-BLG at various V_{TG} and V_{BG}. Inset is the illustration of the device.

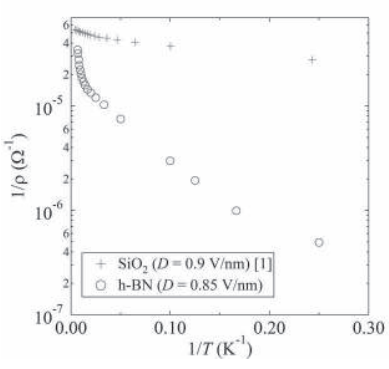

Fig. 2 Temperature dependence of the conductivity in h-BN- and SiO_2-based [1] devices.

Spontaneous electric polarization of the graphene lattice

S. A. Mikhailov

Institute of Physics, University of Augsburg, D-86135 Augsburg, Germany

Taking into account electron-electron interaction of π-electrons in intrinsic graphene we show that the hexagonal graphene lattice should be spontaneously electrically polarized, i.e. the ground state of graphene is ferroelectric.

The spectrum of π-electrons in graphene is usually described within the single-particle tight-binding approximation. The spontaneous-polarization effect resulting from electron-electron interaction is not taken into account in this approach. The tight-binding theory was first proposed and originally used for three-dimensional graphite [1] for which the ferroelectricity described above is not the case. While being perfectly correct for three-dimensional crystals, the tight-binding approach thus turns out to be not working for two-dimensional materials like graphene. Theoretical results which have been obtained for graphene so far and which are based on the single-particle tight-binding spectrum may thus need to be reconsidered.

The same conclusions are valid for bilayer graphene, boron nitride and other two-dimensional crystals.

This work was supported by Deutsche Forschungsgemeinschaft.

[1] P. R. Wallace, Phys. Rev. **71,** 622 (1947).

Single electron counting of spin-polarized current through a quantum dot

Masakazu Yamagishi [1], Narii Watase [1], Masayuki Hashisaka [1], Koji Muraki [2], and Toshimasa Fujisawa [1]

[1] *Department of Physics, Tokyo Institute of Technology, Tokyo, Japan.*
[2] *NTT Basic Research Laboratories, NTT Corporation, Atsugi, Japan.*

Spin dependent transport in non-magnetic semiconductor nanostructures can be used to manipulate both charge and spin degrees of freedom in electronic transport. Detection or generation of single electron spins would be an ultimate device to handle single electron spins. Here we demonstrate single-electron counting of spin-filtered and unfiltered current associated with Zeeman sublevels of an orbital in a quantum dot (QD). Fully spin-polarized current is detected when a spin-up Zeeman sublevel is located in the transport window. When both Zeeman sublevels contribute the transport, however, spin-down current is found to be always smaller than the spin-up current. This partially spin-polarized current can be explained with exchange enhanced spin splitting in the nearby low-density regions.

By adjusting some voltages on fine surface gates of an AlGaAs/GaAs device shown in Fig. 1(a), a QD with electron number N (= 1 – 5) is attached to a quantum point contact (QPC) working as a charge sensor. Application of in-plane field B (= 3 – 9 T) gives Zeeman splitting E_z for each well-separated orbital state. Extremely small current through the QD driven by a bias voltage V_b (= -2 – 2 mV) is detected by the single-electron counting scheme with a bandwidth of a few kHz [1]. The average dwell times in the empty state with (N – 1) electrons and the occupied state with N electrons determine the incoming rate Γ_{in} and the outgoing rate Γ_{out}, respectively. As shown in Fig. 1(c), their gate-voltage dependences show clear transition from spin-filtered transport for up-spins and unfiltered transport. Clear step-like dependences ensure high selectivity for spin-filtering. Importantly, step heights in the incoming rate are unequal, indicating spin-dependent rates $\Gamma_{in,\downarrow} < \Gamma_{in,\uparrow}$. Suppressed outgoing rate for unfiltered case ($\Gamma_{out,mix} < \Gamma_{out,\uparrow}$) also suggests the same tendency $\Gamma_{out,\downarrow} < \Gamma_{out,\uparrow}$. In contrast to the linear B dependence of Zeeman splitting, the ratio $\Gamma_{in,\downarrow}/\Gamma_{in,\uparrow}$ has no or weak dependence on B, as shown in the lower panel of Fig. 1(d), as well as on tunneling rates and electron number (tested for N = 1, 3, and 5). This spin-dependent tunneling rate could be attributed to the exchange enhanced spin splitting in the nearby low-density regions, as often discussed with the so-called 0.7 anomaly in the conductance of a QPC [2].

[1] T. Fujisawa et al., Science 312, 1634 (2006).
[2] K. J. Thomas et al., Phys. Rev. B 58, 4846 (1998).

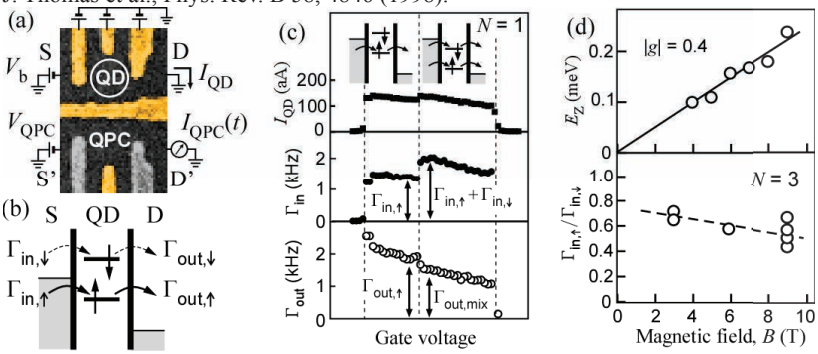

Fig. 1 (a) Schematic setup. (b) Energy diagram for spin-filtered transport. (c) Current, incoming and outgoing tunnel rates. (d) Zeeman energy and the ratio of incoming rates.

Wave function engineering in quantum dot-ring nanostructures

Elżbieta Zipper,* Marcin Kurpas, and Maciej M. Maśka
Instytut Fizyki, Uniwersytet Śląski,
ul. Uniwersytecka 4, 40-007 Katowice

Quantum structures which can be steered from the outside are highly relevant to new technologies in which the control and manipulations of electron spin and wave functions play an important role. We consider quantum nanostructures composed of a semiconductor quantum dot surrounded by a quantum ring (dot-ring nanostructure). The properties of such nanostructures can be strongly modified by changing the shape and the height of the barrier separating the structure and/or the relative position of the minima of the confining potential.

The manipulation of these parameters by, e.g., electrical gating leads to the change of the shape and the radial distribution of wave functions which strongly influence many properties. We show that such wave function engineering can alter [1]:

a) the relaxation time of nanostructure used as spin qubit or memory device by orders of magnitude,

b) the cross-section for intraband infrared or microwave absorption from large to negligible,

c) the transport properties of a single nanostructure and of an array of dot-ring nanostructures from highly conducting to insulating.

[1] E. Zipper, M. Kurpas, and M. M. Maśka, New. J. Phys **14**, 093029 (2012).

Electrical control of single-electron spin using spin-orbit effects in quantum dots

M. A. Rodriguez-Moreno[1], L. Meza-Montes[2], and A. D. Hernandez[1]

[1] *Centro de Investigaciones en Dispositivos Semiconductores, BUAP, Mexico*
[2] *Instituto de Fisica, BUAP, Mexico*

Coherent electrical control of quantum spin states has been experimentally demonstrated in nanolitographic quantum dots, showing the realization of qubits in these systems [1, 2]. Electrically-based spin manipulation and spin-orbit (SO) effects in general has been studied in semiconductor nanostructures [3]. The coupling between spin and orbital degrees of freedom induced by SO can readily be exploited by combining a static magnetic field and a time-dependent electric field. The so-called electric dipole spin resonance (EDSR) based on the SO interaction in quantum dots was theoretically analyzed within a pertubative framework [4].

In previous works we have determined stationary states and dynamical localization in double quantum dots [5]. Here we present a detailed study of the EDSR dynamics. A numerical approach is used in order to solve the time-dependent Schrödinger equation. This allows us to follow the evolution of a single-electron spin confined in a quantum dot. SO is taken into account by including the Rashba and linear Dresselhaus terms into the Hamiltonian of the system. Rabi oscillations are observed and their dependence on different parameters is studied. Comparison with theoretical results shows qualitative agreement, within the limits of the perturbative approximations.

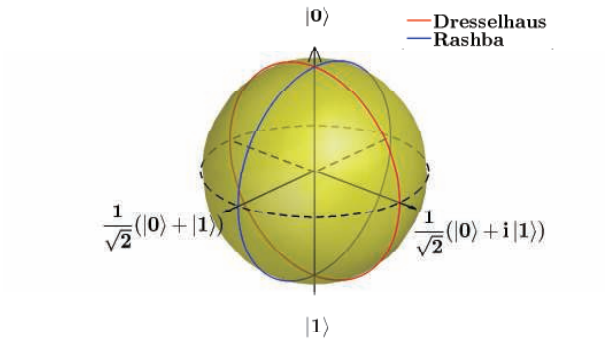

Figure 1: Spin evolution on the Bloch sphere for different SO Hamiltonians. A reference frame rotating about the z axis at the Larmor frequency of the system is used.

[1] F. H. L. Koppens, C. Buizert, K. J. Tielrooij, I. T. Vink, K. C. Nowack, T. Meunier, L. P. Kouwenhoven, and L. M. K. Vandersypen, Nature **442**, 766 (2006).
[2] K. C. Nowack, F. H. L Koppens, Y. V. Nazarov,, and L. M. K. Vandersypen, Science **318**, 1148092 (2007).
[3] E. I. Rashba and AI. L. Efros, Phys. Rev. Lett. **91**, 126405 (2003).
[4] V. N. Golovach, M. Borhani, and D. Loss, Phys. Rev. B **74**, 165319 (2006).
[5] L. Meza-Montes, Arezky H. Rodríguez, and Sergio E. Ulloa, Physica E **40**, 1226 (2008); L. Meza-Montes, Carlos F. Destefani, and Sergio E. Ulloa, Phys. Rev. B **78**, 205307 (2008).

Single photon emission from an InAs quantum dot in a GaAs nanowire grown on Si substrate

Jinkwan Kwoen [1], Katsuyuki Watanabe [2], Yasutomo Ota [2], Satoshi Iwamoto [1, 2] and Yasuhiko Arakawa [1, 2]

[1] *Institute of Industrial Science,* [2] *Institute for Nano Quantum Information Electronics, The University of Tokyo, 4-6-1 Komaba, Meguro-ku, Tokyo 153-8505, Japan*

Single quantum dots (QDs) in nanowire (NW) structures generate bright single photons in highly controlled manners. Especially, those which are fabricated solely from III-V semiconductors using top-down or bottom-up approaches have shown their distinguished properties as non-classical light sources [1, 2]. Further advantages of these emitters could be obtained by direct growth of them on Si substrate [3], which opens a promising avenue toward facile integration of such emitters into future 'on-silicon' quantum optical circuits. In this study, we report for the first time single photon generation from an InAs QD in a GaAs NW that was directly grown on a Si substrate.

Figure 1 shows a schematic of our QD-in-NW. The structure is based on a lateral core-shell heterostructure, composed of a GaAs NW core, an InAs QD layer, and a GaAs/AlGaAs/GaAs capping shell. The AlGaAs layer is expected to suppress non-radiative surface carrier recombination processes [3]. The QD-in-NWs were grown on 3-inch Si(111) wafer using a solid-source molecular beam epitaxy system under a self-catalyzed vapor-liquid-solid growth condition. Figure 2 shows an image of a typical NW containing QDs. The structures have a length of ~750 nm and a diameter of ~130 nm, on average. QDs are expected to be grown on the sidewall of the NWs [4].

We characterized optical properties of a grown QD-in-NW by micro photoluminescence (PL) measurements at 10K. An emission spectrum from the sample is shown in the inset of Fig. 3. We observed bright discrete emission lines from the QD. Intensity auto-correlation was measured for the emission line denoted as X using a conventional Hanbury-Brown-Twiss setup with a pair of silicon avalanche photodiodes, and is plotted in Fig. 3. The estimated time-origin value for the normalized second-order coherence function, $g^{(2)}(0)$, is 0.18 (< 0.5), which clearly demonstrates single photon generation from the QD-in-NW on Si.

[1] J. Claudon, *et. al.*, Nat photon **4**, 174 (2010) [2] M. Heiss, *et. al.*, Nat. Mater. doi:10.1038/nmat3557 (2013) [3] J. Kwoen, *et. al.*, ISCS2013 (2013) (*submitted*) [4] X. Yan, *et. al.*, Nano Lett., **11**, 3941 (2011)

This work was supported by the Special Coordination Funds for Promoting Science and Technology. This work was also supported by the Japan Society for the Promotion of Science through its "Funding Program for World Leading Innovation R&D on Science and Technology Program".

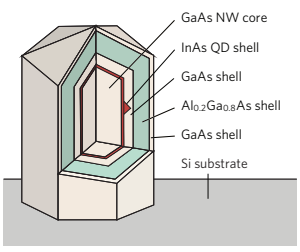

Figure 1: Schematic of the investigated QD-in-NW structure.

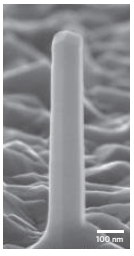

Figure 2: Scanning electron micrograph of a typical GaAs NW containing an InAs QD.

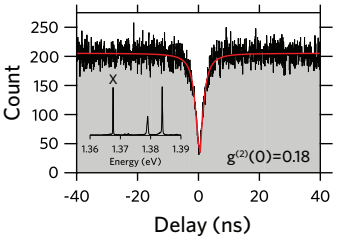

Figure 3: Measured auto-correlation histogram. Single photon generation ($g^{(2)}(0)<0.5$) from a single QD-in-NW grown on Si is clearly demonstrated. The inset shows a PL spectrum of the QD.

Large modulation of electronic states in InAs quantum dots by electric-double-layer gating

K. Shibata [1], H.T. Yuan [2], Y. Iwasa[2,3] and K. Hirakawa [1,4]

[1]*INQIE and IIS, University of Tokyo, 4-6-1 Komaba, Meguro-ku, Tokyo 153-8505, Japan*
[2]*QPEC and Department of Applied Physics, University of Tokyo, Tokyo, 113-8656, Japan*
[3]*Correlated Electron Research Group, RIKEN, Wako 351-0198, Japan*
[4]*CREST-JST, 4-1-8 Honcho, Kawaguchi, Saitama 332-0012, Japan*

Electrical manipulation and read-out of quantum mechanical states in zero-dimensional (0D) nanostructures by nanogap metal electrodes is expected to bring about great innovation in information-communication technology and have been intensively studied [1]. However, in these 0D nanostructures, the electrical tunability of the quantum states is rather limited due to the screening of the gate electric field by the nanogap metal electrodes. Electric-double-layer (EDL) gating with ionic liquids as gate dielectrics is powerful in tuning the Fermi energy in solids [2]. The EDL formed at liquid/solid interfaces (Fig. 1), which functions as a huge capacitance, can accumulate or deplete charge carriers over a large range. However, EDL gating has not been applied to 0D nanostructures yet.

In this work, we demonstrate a new way of electric field gating which realizes wide-range electrical tunability of 0D quantum states by adopting liquid-gated EDL transistor structures on single self-assembled InAs quantum dots (QDs) coupled to nanogap metal electrodes (Fig. 1). The transport characteristics are dramatically modulated by a small EDL-gate voltage, V_{EDL}, applied between the EDL-gate electrode and the QD (Fig. 2(a)-2(c)). The energy level spacing between *s*- and *p*-orbitals, $\Delta E_{s\text{-}p}$, was modulated from $\Delta E_{s\text{-}p}$ ~22 meV (V_{EDL} = -0.5 V) to ~10 meV (V_{EDL} = 0.1 V). The charging energy and the electron g-factor were also modulated in a wide range. The efficiency of gating is 10-100 times higher in EDL gating than that in the conventional solid-gating techniques (Fig. 2(d)). The EDL gating on QDs provides not only high tunability of electronic states but also good compatibility with optical manipulation of single electron charge/spin states [3], which is essential for their application to quantum information processing.

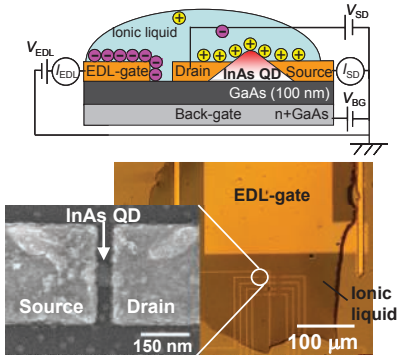

Fig. 1: Schematic illustration (upper) and the microscope images (lower) of QD-EDL transistors.

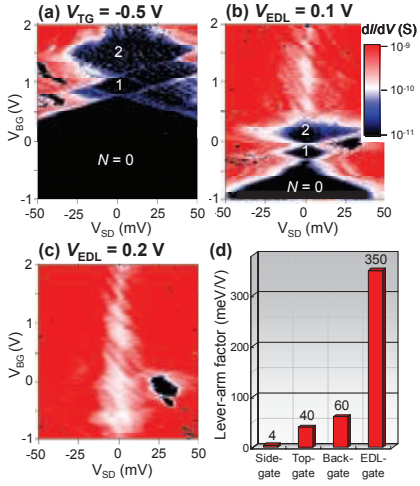

Fig. 2(a)-(c) Coulomb stability diagrams for different EDL-gate voltages. (d) Comparison of the gating efficiency with various methods.

[1] D. L. Klein et al., Nature **389**, 699 (1997).
[2] K. Ueno et al., Nature Mater. **7**, 855 (2008).
[3] K. Shibata et al., Phys. Rev. Lett. **109**, 077401 (2012).

Optically induced exciton generation in quantum dots via adiabatic rapid passage: influence of phonons and detuning

S. Lüker[1], K. Gawarecki[2], M. Glässl[3], D. E. Reiter[1], A. Grodecka-Grad[4], V. M. Axt[3], P. Machnikowski[2] and T. Kuhn[1]

[1] *Institut für Festkörpertheorie, Universität Münster, Wilhelm-Klemm-Strasse 10, 48149 Münster, Germany*
[2] *Institute of Physics, Wroclaw University of Technology, 50-370 Wroclaw, Poland*
[3] *Theoretische Physik III, Universität Bayreuth, 95440 Bayreuth, Germany*
[4] *QUANTOP, Danish National Research Foundation Center for Quantum Optics, Niels Bohr Institute, University of Copenhagen, 2100 Copenhagen Ø, Denmark*

The optical control of quantum dots (QDs) with chirped (frequency-swept) laser pulses, denoted as adiabatic rapid passage (ARP), provides a powerful tool to excite a QD. Recent experiments have demonstrated that a robust occupation of the exciton state is possible using ARP [1, 2]. In a chirped laser pulse the instantaneous frequency of the light field changes with time. Due to this, the laser field is shifted through resonance with the exciton transition energy. This leads to an anti-crossing in the dressed state eigenenergies of the light-matter Hamiltonian. The population inversion is achieved when the system evolves adiabatically along this anti-crossing.

We have recently shown that the coupling to phonons reduces the fidelity of the ARP process [3]. We found that there is only a minor impact of phonons at low temperatures and positive chirps. In contrast, for negative chirps or at higher temperatures the adiabatic evolutuion is strongly affected by interactions with the phonon bath. We model the quantum dot for our calculations in the strong confinement limit as a two level system, consisting of the ground state and the exciton state, which is coupled to longitudinal acoustic phonons via the deformation potential mechanism. The evolution of the system is calculated using a fourth order correlation expansion.

Usually in ARP, the central frequency of the laser pulse, which coincides with the frequency at the pulse maximum, is in resonance with the transition energy. We analyze, how the state preparation fidelity is affected when the central frequency is detuned, i.e., the central frequency at the pulse maximum is not in resonance with the transition energy. Without phonons the population inversion can still be achieved, if the detuning is not too strong and the resonance is passed during the pulse. Again at low temperatures for positive chirps, where the coupling to phonons is very weak, the adiabatic evolution is robust against moderate detunings. For negative chirps on the other hand it is possible to compensate the phonon impact on the carrier dynamics by detuning the central frequency, resulting in an improved efficiency of the ARP process.

[1] C.-M. Simon *et al.*, Phys. Rev. Lett. **106**, 166801 (2011).
[2] Y. Wu *et al.*, Phys. Rev. Lett. **106**, 067401 (2011).
[3] S. Lüker *et al.*, Phys. Rev. B **85**, 121302(R) (2012).

Pauli blocking dynamics in optically excited quantum dots: A picosecond excitation-correlation spectroscopic study

Richarj Mondal[1], Bhavtosh Bansal[1], A. Mandal,[2] S. Chakrabarti,[2] and Bipul Pal[1]

[1] *Indian Institute of Science Education and Research Kolkata, Nadia 741252, WB, India*
[2] *Indian Institute of Technology Bombay, Mumbai 400076, India*

Pauli's exclusion principle is the cornerstone in the physics of the many fermions in finite systems. The phenomenon of Pauli blocking, i.e., the physical manifestation of the exclusion principle is of course responsible for stability of matter. It is also important in specific processes of interest in fields ranging from nuclear physics, cold atomic gases, to semiconductor devices. We have studied Pauli blocking through the time-resolved dynamics of carrier redistribution between the discrete energy states in the self-assembled InAs/GaAs QDs through a novel variant of the picosecond excitation-correlation (EC) spectroscopy [1,2].

A train of pulses of 100 fs duration were split into two beams of equal fluence. The arrival of the pulses onto the sample from one of the beams was controllably delayed with respect to the corresponding pulses from the other beam and the steady-state PL was measured as a function of this delay. Since the number of photons incident on the sample is independent of the delay, this technique specifically probes the time-resolved dynamics of the nonlinear PL. We have observed that while the ground state EC response is always snubbed when the two excitation beams are temporally nearly coincident, the excited state response can either be enhanced or reduced, depending on the excitation power. This is a direct consequence of the exclusion principle. The time evolution of this response was studied for the first three levels in a QD ensemble. The observations were quantitatively reproduced using a minimal theoretical model, which does not use the rate equations, but combines carrier loss kinetics with principle of detailed balance and the exclusion principle.

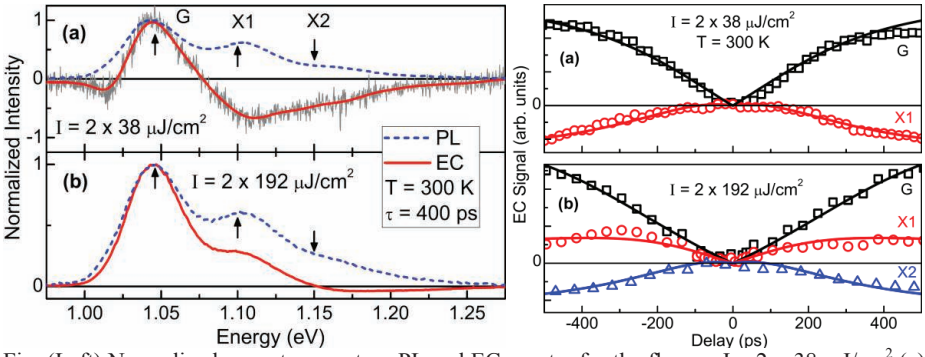

Fig: (Left) Normalized room temperature PL and EC spectra for the fluence I = 2 × 38 mJ/cm^2 (a) and 2 ×192 mJ/cm^2 (b). Note that the sign of the EC signal for the X1 state changes from negative to positive between (a) and (b). (Right) Delay dependence of the EC signal measured at energies indicated by arrows in Fig. (a) and (b) (Left). The solid lines are fits to the data by the model. Note that the definition of EC signal EC (τ, hν) =PL_{12} (τ, hν) − PL_{12} (τ=0, hν), where τ is the delay and hν is the photon energy, is opposite to that in refs [1-2].

[1] H. Hirori, K. Matsuda, Y. Miyauchi, S. Maruyama, at al., Phys. Rev. Lett. **97**, 257401 (2006).
[2] T. Kazimierczuk, M. Goryca, M. Koperski, A. Golnik, et al., Phys. Rev. B **81**, 155313 (2010).

Resonant excitonic effects in the density of states of InP nanowires

M. De Luca [1], S. Birindelli [1], A. Zilli [1], A. Polimeni [1], M. Capizzi [1], F. Mura [2], H. A. Fonseka [3], H. H. Tan [3] and C. Jagadish [3]

[1] *Dipartimento di Fisica, Sapienza Università di Roma, Italy*
[2] *Dipartimento di Scienze di Base e Applicate per l'Ingegneria, Sapienza Università di Roma, Italy*
[3] *Department of Electronic Materials Engineering, Research School of Physics and Engineering, The Australian National University, Canberra, Australia*

Semiconductor nanowires (NWs) are promising building blocks for next generation nanoscale devices [1]. The interest for these nanostructures stems from their exciting electronic properties and the possibility of controlling their synthesis. Indeed, the peculiar formation process of NWs, which involves vapor–liquid–solid mechanisms, enables switching from zincblende (ZB) to wurtzite (WZ) crystal phases, depending on growth conditions [2]. The presence of a WZ phase in the lattice structures of III-(As,P) semiconductors, notoriously stable in the ZB form as bulk, is one of the most surprising findings in these NWs and may lead to phase-modulated nano-WZ/ZB-structures along the wire axis.

Changes in the crystal phase create striking effects on the band-structure of InP NWs [3]. We use photoluminescence (PL) excitation spectroscopy (PLE) to investigate the density of states (DOS) of WZ InP NWs [see scanning electron-microscope, SEM, images in Fig. 1 (a)], whose PL spectrum [dashed line in Fig. 1 (b)] is characterized by sharp lines related to the free exciton and crystal defects.

The NW DOS, as it results from PLE (blue, solid line), exhibits several resonances (*A, B,* and *C*). We find an energy difference between WZ (resonance *A*) and ZB (1.42 eV, not shown) band-gaps equal to 70 meV. The selection rules due to the crystal symmetry and the polarization degree (ρ, red solid line) of the absorbed light, as determined from polarization-resolved PLE, allows us to nicely associate those resonances to the transitions sketched in the inset. In particular, transition *A* shows a polarization degree (ρ~0.85) remarkably higher than that of transitions *B* and *C*, consistently with the symmetry of the involved critical points. The deep minima that ρ exhibits at the energies of the excitonic resonances *A, B,* and *C* can be ascribed to a mixing of valence bands with different symmetries driven by the excitonic interaction. ZB InP nanowires have also been studied for comparison, and we will provide a clear picture of the DOS of these technologically relevant nanostructures.

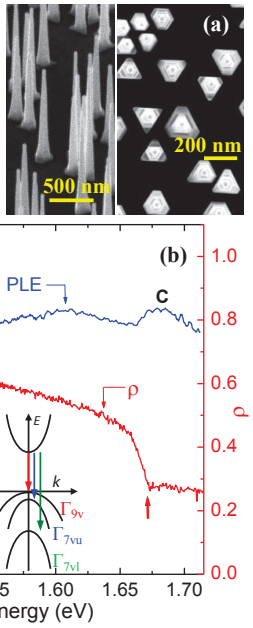

Fig. 1 (a) Side-view (left panel) and top-view (right panel) SEM images of WZ InP NWs. **(b)** PL (dashed line) and PLE (blue solid line, obtained by keeping the PL detection energy fixed at E_{det}, downward pointing arrow) spectra recorded in the same sample. The inset sketches the band diagram at the Γ point of WZ InP and the pertinent valence bands involved in transitions *A*, *B*, and *C*. At these energies, the polarization degree ρ (red solid line) shows deep minima (up-pointing arrows).

[1] P. Yang *et al.*, Nano Lett. **10**, 1529 (2010).
[2] S. Paiman *et al.*, J. Phys. D: Appl. Phys. **43**, 445402 (2010).
[3] E. G.. Gadret *et al.*, Phys. Rev. B **82**, 125327 (2010).

Observation of Purcell effect with a site-controlled pyramidal quantum dot coupled to a photonic crystal cavity mode

C. Jarlov[1], L. Ferrier[1], M. Calic[1], P. Gallo[1], V. Belykh[2], A. Rudra[1], B. Dwir[1] , N.N. Sibeldin[2] and E. Kapon[1]

[1]*Laboratory of Physics of Nanostructures, Ecole Polytechnique Fédérale de Lausanne, CH1015 Lausanne*
[2]*P. N. Lebedev Physical Institute, Russian Academy of Sciences, Moscow, Russia*

Cavity quantum electrodynamics (cQED) experiments with quantum dots (QD) and micro-cavities have been used to study quantum effects that can be useful for the field of quantum information processing. Especially the development of high-efficiency single photon emitters requires the control of QD radiative properties. In cQED experiments, the spontaneous emission rate of QDs is modified when QDs couple to a cavity mode through the Purcell effect[1]. We demonstrate the increase of the emission rate of a single site-controlled QD located at the centre of an L3 cavity where the electric field of the fundamental mode is maximum (Fig 1 (a)), ensuring an optimal overlap between the field distribution and the QD. Precise positioning of our QDs during the fabrication process allows for a position error of less than 50nm[2]. We first performed polarization resolved photoluminescence (PL) and power dependence measurements of the ground state features of the single pyramidal QD coupled to the cavity mode (Q=2000) (Fig. 1-(d)) in the off-resonant and resonant configurations to identify the QD features and the coupling to the cavity mode. Figure 1-(b) and (c) show time-resolved PL measurements of the QD in the off-resonant and resonant cases. The biexciton's lifetime is drastically decreased when resonant with the cavity mode. A model based on a four-level rate equation model is used to fit the decay rates and retrieve the lifetime of the biexciton. An increase by a factor of 7 of the spontaneous emission rate of the biexciton is achieved.

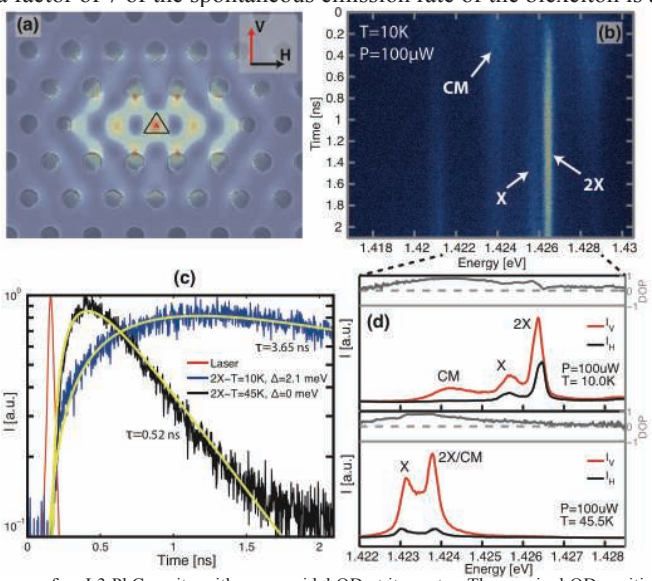

Fig. 1- (a) SEM image of an L3 PhC cavity with a pyramidal QD at its center. The nominal QD position is indicated by the red triangle. The field distribution of the fundamental mode of the cavity is superimposed on the image (FDTD simulations). (b) Time resolved image of the ground state feature of the QD coupled to the cavity. At T=10K, the 2X feature is detuned by 2.1meV from the cavity mode. (c) Temporal evolution of the 2X luminescence for an off-resonant (blue) and resonant cavity mode (black). (d) PL linearly resolved in polarization of the QD ground state features along the directions perpendicular (V) and parallel (H) to the cavity axis. Both the resonant case (bottom) and off-resonant case (top) are shown.

[1] D. G. Gevaux et al., Appl. Phys. Lett.. **88**, 13 131101 (2006).
[2] M. Calic et al., Phys. Rev Lett.. **106**, 22 7402 (2011).

Raman and AFM Profiling of Quantum Dot Multilayers

Evgeniya Sheremet [1], Raul D. Rodriguez [1], Dmitry Dmitriev [2], Alexander Toropov [2], Alexander Milekhin [2] and Dietrich R.T. Zahn [1]

[1] *Semiconductor Physics, Chemnitz University of Technology, D-09107 Chemnitz, Germany*
[2] *Institute of Semiconductor Physics, Novosibirsk, Russia*

InAs/AlGaAs quantum dots (QDs) are of a great interest for optoelectronic applications since they have interband transition energies in the visible spectral range. InAs/AlAs and InAs/$Al_{0.75}Ga_{0.25}As$ modulated QD structures were prepared by molecular beam epitaxy in the Stranski-Krastanov growth mode on (001)-oriented GaAs substrates. The structures contain five blocks separated by GaAs layers and each consisting of ten InAs QD layers with periods of 50 and 100 nm in Al(Ga)As matrices. The cleaved (110)-oriented edges of the samples were studied by atomic force microscopy (AFM) and Raman spectroscopy. AFM images correlate with transmission electron microscopy results and allow individual QD layers due to partial oxidation of the AlAs or AlGaAs matrices to be resolved (Fig.1). Raman spectroscopy from a cleaved surface allows profiling the Raman intensity of phonon modes. For a better access to the spatial changes in the phonon spectra, the samples were wedged at an angle of 5 – 7 degree with respect to the sample surface which allowed us to resolve Al(Ga)As matrices and intermediate GaAs layers (Fig.1).

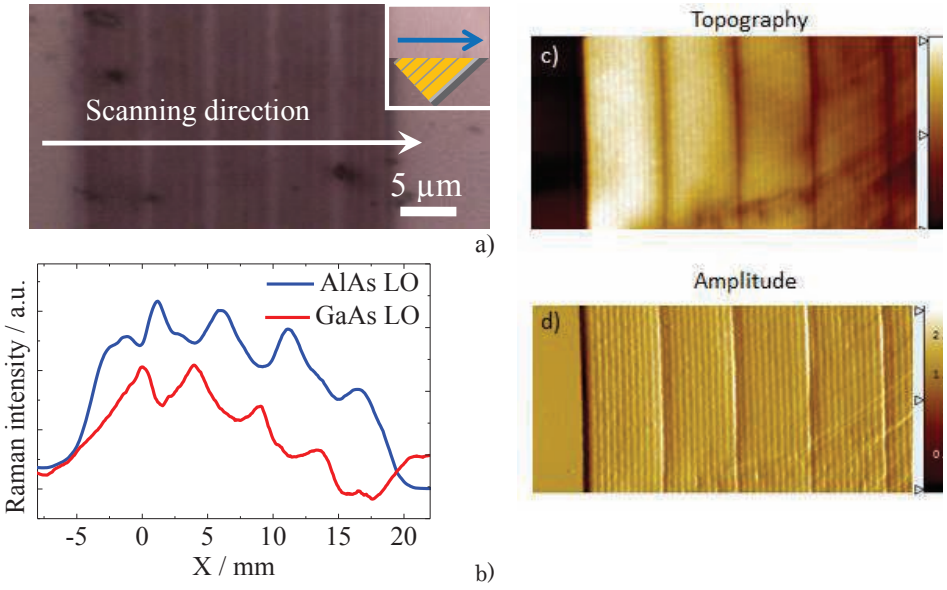

Fig. 1. Raman and AFM profiles obtained on the wedge and (110)-edge of InAs/AlAs QD structure. a) optical microscopy view of the wedged sample. The inset shows the scanning direction in the side view. b) Modulation of Raman signal intensity in the wedged sample demonstrating resolution of individual blocks. c) and d) Topography and amplitude AFM images, respectively, of a cleaved InAs/AlAs QD structure.

This work was supported by the DFG project ZA146/22-1 and DFG Research Unit 1713.

Research on the new mechanism of a spatial separation of a spin density in a two-electron quantum dot

J. Pawłowski, S. Bednarek

Faculty of Physics and Applied Computer Science,
AGH University of Science and Technology, Kraków, Poland

Among the several possible physical implementations of a quantum bit, the most promising is its location on the spin of an electron confined within a semiconductor nanodevice. The majority of previous implementations require using strong external magnetic fields in order to separate the energy levels of electrons with different spin orientations. This poses a significant technical difficulty for the construction of a quantum computer. It would be much better if we were able to avoid using a magnetic field. Single-qubit operations on an electron spin can also be performed without a magnetic field. We have proposed and simulated the operation of such a nanodevice in our previous work [1].

The most difficult issue to solve, however, is the intentional spin setup in the beginning without the use of a magnetic field. In the current project, is scheduled to research the possibilities to carry out such a process. Our preliminary research has shown that this is possible. As a structure of the system, we propose a double gate-defined quantum dot system with a tuned interdot barrier. The barrier height is low at the beginning of the system evolution. We shall put two electrons in a potential well. We assume that, in the beginning, the system will be in singlet state, which is the ground state for a double-electron system and may be generated e.g. by thermalisation [2, 3]. It turns out that if a spin-orbit interaction with a periodic variable coupling constant appears in a quantum dot, a pair of electrons can enter the triplet state. For this purpose, we use the Rashba interaction [4, 5], whose amplitude can be controlled with variable voltage applied to electrodes [6, 7, 8]. When the electrons enter a state of balanced linear combination of singlet and triplet state, we interrupt the spin-orbit coupling constant oscillation. The transition between singlet and triplet states will be disturbed. If we then lift the potential barrier inside the well, we can spatially separate both electrons. If we select the time of barrier formation properly, electrons with specific spins will go in both separated regions. In the left side, one with a spin up and in the right, one with a spin down.

If we manage to solve the issue of initializing the spin without a magnetic field, we may be able to build a quantum computer operating on electron spins, controlled only by local voltages and requiring no external fields. The research would provide an insight at some very interesting properties of double-electron systems in semiconductor nanostructures, with particular emphasis on their spin degrees of freedom.

[1] S. Bednarek, J. Pawłowski, and A. Skubis, Appl. Phys. Lett. **100**, 203103 (2012).
[2] J. R. Petta, A. C. Johnson, J. M. Taylor, E. A. Laird, A. Yacoby, M. D. Lukin, C. M. Marcus, M. P. Hanson, A. C. Gossard, Science **309**, 2180 (2005).
[3] H. Bluhm, S. Foletti, I. Neder, M. Rudner, D. Mahalu, V. Umansky and A. Yacoby, Nat. Phys. **7**, 109 (2011).
[4] L. S. Levitov and E. I. Rashba, Phys. Rev. B **67**, 115324 (2003).
[5] M. V. Entin and L. I. Magarill, Europhys. Lett. **68**, 853 (2004).
[6] D. Grundler, Phys. Rev. Lett. **84**, 6074 (2000).
[7] J. Nitta, T. Akazaki, H. Takayanagi, and T. Enoki, Phys. Rev. Lett. **78**, 1335 (1997).
[8] V. I. Litvinov, Appl. Phys. Lett. **89**, 222108 (2006).

Hole spin relaxation in InAs and GaAs quantum dots: the role of Dresselhaus spin-orbit interaction

Juan I. Climente [1], **Carlos Segarra**[1] **and Josep Planelles**[1]

[1]Dept. de Química Física i Analítica, Universitat Jaume I, Castelló, Spain

Currently, there are ongoing efforts to use the spin of holes confined in quantum dots for quantum information devices.[1] Understanding and controlling the hole spin relaxation is a requisite for further progress, but the underlying mechanism is still under debate. Different theoretical studies have *assumed* different dominating spin-orbit terms,[2-5] but a full comparison is missing.

Here we present a unified description of spin-orbit induced hole spin relaxation in quantum dots. Using k·p theory, we compare the relaxation due to k-linear, k-quadratic (Luttinger Hamiltonian) and k-cubic (Dresselhaus) spin-orbit terms. We show that cubic Dresselhaus spin-orbit interaction dominates over k-quadratic heavy hole-light hole mixing in gated quantum dots, while both mechanisms have comparable contributions in self-assembled dots.

Our systematic study reconciles seemingly contradictory results of previous theoretical works[2,3], sheds light on some experimental open questions, and reveals new effects resulting from the concurrence of different spin-orbit mechanisms. All in all, the dependence of hole spin relaxation on quantum confinement is drastically different from that of electrons. [6]

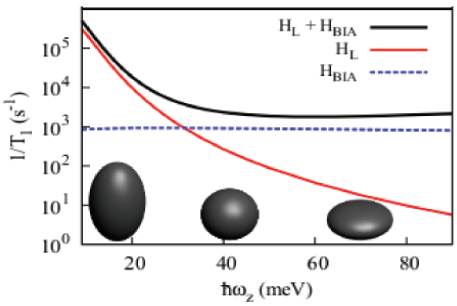

Figure: Hole spin relaxation rate vs vertical confinement for different spin admixture terms. H_L: Luttinger Hamiltonian; H_{BIA}: Bulk inversion asymmetry Hamiltonian.

[1] B. Gerardot et al. Nature **451**, 441 (2008); K. De Greve et al. Nature Phys. **7**, 872 (2011).
[2] L. M. Woods, T. L. Reinecke, and R. Kotlyar, Phys. Rev. B **69**, 125330 (2004)
[3] C. Lü, J. L. Cheng, and M. W. Wu, Phys. Rev. B **71**, 075308 (2005)
[4] D. Bulaev, and D. Loss, Phys. Rev. Lett **95**, 076805 (2005); M. Trif, P. Simon, and D. Loss, Phys. Rev. Lett. **103**, 106601 (2009).
[5] K. Roszak, V. M. Axt, T. Kuhn, and P. Machnikowski, Phys. Rev. B **76**, 195324 (2007); E. Tsitsishvili, R. v. Baltz, and H. Kalt, Phys. Rev. B **72**, 155333 (2005).
[6] J. I. Climente, C. Segarra, and J. Planelles, arXiv: 1301.4381

In-plane radiative recombination channel of a dark exciton in self-assembled quantum dots

T. Smoleński[1], T. Kazimierczuk[1], M. Goryca[1], T. Jakubczyk[1], Ł. Kłopotowski[2], Ł. Cywiński[2], P. Wojnar[2], A. Golnik[1], and P. Kossacki[1]

[1] *Institute of Experimental Physics, Faculty of Physics, University of Warsaw, Poland*
[2] *Institute of Physics, Polish Academy of Sciences, Warsaw, Poland*

Neutral exciton in a self-assembled quantum dot (QD) usually consists of the electron and the heavy hole with total angular momentum projections on the growth axis equal respectively to $\pm 1/2$ and $\pm 3/2$. Due to the isotropic electron-hole exchange interaction, the excitonic states are split in energy into two pairs: *bright excitons* (X_b) and *dark excitons* (X_d). Typically, the dark excitons are considered optically inactive as the spin of the electron and the heavy hole are combined into total spin 2. Thus, the dark exciton persists in QD relatively long time and might affect the performance of QD devices. The decay rate of the dark exciton is widely believed to be determined by a spin-flip process turning a dark exciton into a bright one [1, 2]. However, such a process is inefficient for the low temperatures as it requires absorption of energy from the phonon bath equal to (isotropic) electron-hole exchange constant δ_0.

In this study we demonstrate a clear evidence for a different, *radiative recombination channel* of dark excitons in self-assembled QDs. This channel is due to a light hole admixture in the excitonic ground state. The dipole moment of this transition is oriented along the growth axis. Therefore, X_d photoluminescence (PL) is emitted only in the direction perpendicular to the growth axis. We have confirmed this prediction by a direct measurement of a CdTe/ZnTe QD PL spectra from a cleaved edge of the sample. In such a geometry emission at the energy corresponding to the dark exciton was indeed observed for a sufficiently low excitation power (Fig. 1(a)). We emphasize that X_d emission line is almost fully linearly polarized along the growth axis (Fig. 1(b)), which shows that X_d PL *cannot be detected using typical setup geometry* (i.e., when detection is perpendicular to the sample surface). Importantly, a strong correlation between the dark exciton lifetime and the in-plane hole g-factor enabled us to show that the radiative recombination is the dominant decay channel of the dark excitons in CdTe/ZnTe QDs [3].

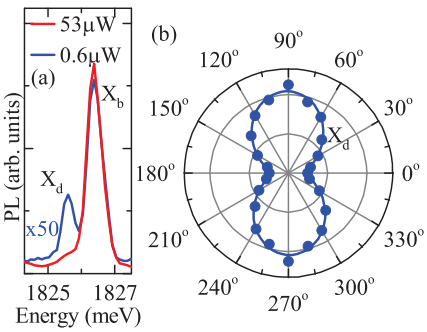

Figure 1: (a) PL spectra of a neutral exciton measured from the cleaved edge of the sample under CW excitation. (b) Polar plot presenting the polarization of the dark exciton emission (the 90° and 270° directions are along the QD growth axis).

We underline that X_d radiative recombination demonstrated in our work is not specific for CdTe/ZnTe QDs and should be present in all QDs exhibiting heavy-light hole mixing. Moreover, the dominance of this recombination channel over other X_d decay mechanisms opens a new possibility of a direct optical control of the dark exciton state.

[1] O. Labeau *et al.*, Phys. Rev. Lett. **90**, 257404 (2003).
[2] J. Johansen *et al.*, Phys. Rev. B **81**, 081304(R) (2010).
[3] T. Smoleński *et al.*, Phys. Rev. B **86**, 241305(R) (2012).

TuP46

Carrier trapping and phonon-assisted relaxation in non-uniform quantum dashes

P. Kaczmarkiewicz[1], P. Machnikowski[1], T. Kuhn[2]

[1] *Institute of Physics, Wrocław University of Technology, 50-370 Wrocław, Poland*
[2] *Institut für Festkörpertheorie, Universität Münster, D-48149 Münster, Germany*

We study theoretically phonon-assisted relaxation processes in highly elongated quantum dots, also referred to as quantum dashes (QDashes) [1]. Such a system is often characterized by the presence of shape irregularities, which can provide an additional confinement in the system [2]. This additional trapping within the QDash not only strongly influences its electronic and optical properties [3], but also phonon-induced carrier relaxation. We study the influence of the morphology of the widening of the structure on the phonon-mediated relaxation process and identify the possible relaxation bottlenecks in the system. The presence of the QDash widening strongly influences the phonon relaxation rates and can lead to both, their enhancement as well as decline, depending on the exact shape geometry of the widened section of a QDash. We show that a sufficiently large width fluctuation can even lead to the formation of a bottleneck for the relaxation to the exciton ground state. The appearance of this bottleneck is a direct result of the increase in the energy separation between the ground state and the excited states.

It has been shown that QDashes have several advantages over other nanostructures, especially in telecommunication applications, where InP structures are now commonly used in high performance lasers and optical amplifiers operating at 1.55 μm [1]. The morphology of some of the InAs QDash structures suggests that variations in their width may lead to the appearance of additional trapping within the volume of a QDash. The influence of the presence of such an additional trapping center on the optical properties of the system has already been studied [2, 3]. On the other hand the influence of such structure irregularities on phonon-mediated relaxation has not yet been investigated. The phonon relaxation of carrier confined in QDashes is important from the point of view of possible applications (eg. lasers, optical amplifiers). Understanding of the phonon-assisted relaxation and therefore carrier dynamics can be of particular interest for a broad range of optical devices.

We base our modeling of the electron-hole system on a single-band effective mass and envelope wave function description. For modeling of the carrier envelope wave functions we use a variational method and follow the adiabatic approximation [4]. Coulomb correlations are included within the configuration-interaction scheme. In our modeling we consider the case of a single exciton confined in a QDash. We take into account phonon couplings via deformation potential and piezoelectric interaction. The relaxation rates are calculated within the Fermi golden rule.

[1] J. P. Reithmaier, G. Eisenstein, A. Forchel, *Proc. IEEE* **95**, 1779 (2007).
[2] A. Musiał, P. Kaczmarkiewicz, G. Sęk, P. Podemski, P. Machnikowski, J. Misiewicz, S. Hein, S. Hoefling, A. Forchel, *Phys. Rev. B* **85**, 035314 (2012).
[3] P. Kaczmarkiewicz, P. Machnikowski, *Semicond. Sci. Technol.* **27**, 105012 (2012).
[4] A. Wójs, P. Hawrylak, S. Fafard, L. Jacak, *Phys. Rev. B* **54**, 5604 (1996).

Spectral jitter of single CdSe/ZnS nanoparticles: Where is the charge?

D. Braam[1], A. Mölleken[1], G. M. Prinz[1], M. Geller[1] and A. Lorke[1]

[1] *Fakultät für Physik and CENIDE, Universität Duisburg-Essen, Lotharstraße 1, 47057 Duisburg, Germany*

Blinking and spectral jitter are both limiting the optical properties of semiconductor nanoparticles. They are generally attributed to a charge diffusion in the vicinity of the nanoparticle [1]. However, the position of this meandering charge is under strong debate. We use here time-resolved μ-photoluminescence (PL) of single CdSe/ZnS nanoparticles in combination with a simple model to locate the diffusing charge and find that it is trapped in the ligand layer.

PL spectra were taken at room temperature and fitted to a Lorenzian function to obtain both the emission peak energy and the corresponding linewidth (FWHM), two quantities which are correlated: A shift in the emission line to lower energies (a redshift) is accompanied by a broadening of the linewidth (see fig. 1 left inset). This is attributed to the Stark shift, by which the electric field of an outside charge carrier influences the nanoparticle's electronic structure and shifts the emission energy to the red. Due to the quadratic nature of the Stark effect, a perturbation at strong fields is more effective than at small fields, thus inducing a stronger broadening at higher field strengths.

Plotting the redshift over the FWHM, a superlinear correlation becomes apparent (see fig. 1). Employing a simple charge carrier model, the appropriate fit yields a mean position fluctuation of $\delta r = 0.8\,\mathrm{nm}$. Furthermore, it is possible to determine the distance between charge carrier and nanoparticle core. We find that most of the data lies in the range between 3 and 5 nm (see fig. 1 right inset). Because the particles consist of about 2 nm core, 1 nm shell and 2 nm ligands, we conclude that the diffusing charge carrier is predominantly located within the ligand layer.

Measurements of nanoparticles under the influence of photooxidation support these findings.

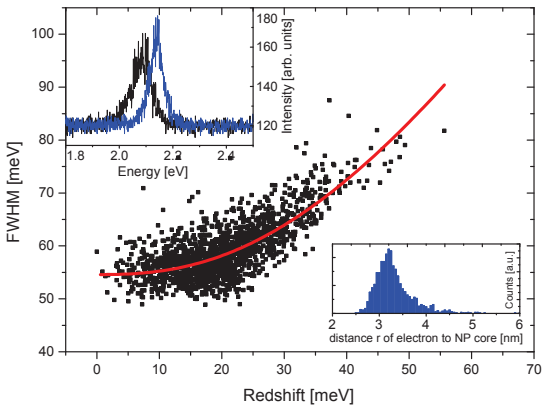

Figure 1: Linewidth over redshift showing a superlinear behaviour. The insets show exemplarily two representative spectra (left) and the spatial distribution of the diffusing charge with respect to the NP core (right).

[1] S. A. Empedocles, M. G. Bawendi, Science **278**, 2114 (1997).

Magnetic-Field Control of Photon Echo from the Electron-Trion System

L. Langer,[1] S.V. Poltavtsev,[1,2] I. A. Yugova,[1,2] D. R. Yakovlev,[1,3] G. Karczewski,[4] T. Wojtowicz,[4] J. Kossut,[4] I. A. Akimov,[1,3] and M. Bayer[1]

[1] *Experimentelle Physik 2, Technische Universität Dortmund, 44221 Dortmund, Germany*
[2] *Spin Optics Laboratory, St. Petersburg State University, 198504 St. Petersburg, Russia*
[3] *A.F. Ioffe Physical-Technical Institute, 194021 St. Petersburg, Russia*
[4] *Institute of Physics, Polish Academy of Sciences, PL-02668 Warsaw, Poland*

Coherent optical phenomena in atomic ensembles and other systems with discrete energy level structure attract a lot of attention for realization of optical quantum memories. One of these phenomena is the photon echo where in the classical picture an intense optical pulse results in rephasing and retrieval of the macroscopic medium's polarization, which was created before by another optical pulse. Currently experimental realizations of quantum light-matter interfaces are based on alkali atoms or strongly isolated impurity centers like rare earth ion crystals. Semiconductor nanostructures have not been considered mainly due to their large decoherence rates and their complex energy level structure. However, compared to isolated atoms the fundamental optical excitation in semiconductors, the exciton, has a large dipole moment, which allows fast operation (below 1ps). Moreover recent developments in optical control of charged excitations in semiconductors nanostructures (trions) open new possibilities in which the long-lived electron spin in the system's ground state can be used as single qubit.

In this work we develop the novel and simple approach to control the photon echo amplitude by application of a transverse magnetic field [1]. For demonstrational purposes we use the electron-trion system in a CdTe semiconductor quantum well where the neutral and charged (trion) excitons are spectrally well separated. Exploiting the Larmor precession of electron spins about the transverse magnetic field we demonstrate transfer of coherence between optically accessible and inaccessible pairs of states. As the result the photon echo signal exhibits oscillatory behavior, which depends sensitively on the polarization configuration of the exciting and refocusing pulses. The echo amplitude can be fully tuned from the maximum down to zero depending on the time delay between the two pulses and the magnetic field strength. The results are explained in terms of the optical Bloch equations accounting for the spin level structure of electrons and trions.

[1] L. Langer, S.V. Poltavtsev, I. A. Yugova, D. R. Yakovlev, G. Karczewski, T. Wojtowicz, J. Kossut, I. A. Akimov, and M. Bayer, "Magnetic-Field Control of Photon Echo from the Electron-Trion System in a CdTe Quantum Well: Shuffling Coherence between Optically Accessible and Inaccessible States", Phys. Rev. Lett. **109**, 157403 (2012).

Fiber-based bidirectional photon detection from a single quantum dot

H. Sasakura [1], X. Liu[2], S. Odashima[2], H. Kumano[2], I. Suemune[2], and S. Muto [3]

[1] *Creative Research Institution, Hokkaido University, Sapporo 001-0021, Japan*
[2] *Reserch Institute for Electronic Science, Hokkaido University, Sapporo 001-0021, Japan*
[3] *Depertment of Applied Physics, Hokkaido University, Sapporo 060-8268, Japan*

Semiconductor quantum dots (QDs) are attractive nanoscale structures for solid-state nonclassical light sources and are expected to play key roles in a quantum information network[1]. Above all, single QDs fabricated by epitaxial growth can serve as stable and bright photon emitters. From a scientific and engineering viewpoint, the long-term stability is one of the most important properties for a fiber-based nanoscale photon emitter. However, the precise positioning, solid maintenance of geometry, and highly accurate nanofabrication are required for the efficient coupling between the nanoscale emitters and optical fibers. This study reports a fiber-based bidirectional solid-state single-photon emitter based on epitaxially grown InAs QDs using single-mode-fibers (SMFs). The placing the solid-state single-photon sources and the SMFs in direct contact is useful from a practical perspective because it offers robust stability and does not require an opto-mechanical alignment. Moreover, this simple structure facilitates the low-cost fabrication of photon emitters and the sufficient stability of the output photon number from a scientific viewpoint.

To extract the emitted photons in both directions, we used flake forms of the epitaxial InAs QD on GaAs layers. The detailed growth conditions and overall optical characteristics are presented in Ref. [1]. The flakes having diameter and thickness of 1--20 μm were obtained by simply scratching the surface with an ordinary diamond cutter. These flakes were directly attached to the edge face of an FC/PC SMF patch cable (Corning, SMF-28) by electrostatic forces. To mechanically fix the flakes and effectively extract the generated photons into two SMFs, the edge face of another SMF patch cable was directly connected to the opposite side of the flakes using an conventional FC/PC-FC/PC joint. The FC/PC-FC/PC joint part with its embedded flakes was set in a liquid ^{4}He reservoir at 4.2 K. To spatially separate the emissions that traveled in the SMF in the direction opposite to that of the excitation laser, a wavelength division multiplexing module was used.

For the autocorrelation measurements, the output of each SMF is filtered with a 0.5-nm-wide band-pass filter to select the emissions originating from a InAs QD. The emission was then sent to an SSPD. The single count rate of the *X* line at each SSPD was ~5 kHz with an excitation power of 1.4 W/cm^2. A histogram of the normalized coincidence counts with time bins of 244 ps and an integration time of 8.5 h is shown in Fig. 1. The data exhibits the well-known antibunching dip at a zero time delay and is fit with the second-order correlation function. At zero delay, the function gives $g^{(2)}(0)=0.35$, suggesting that the single InAs QD emits nonclassical light.

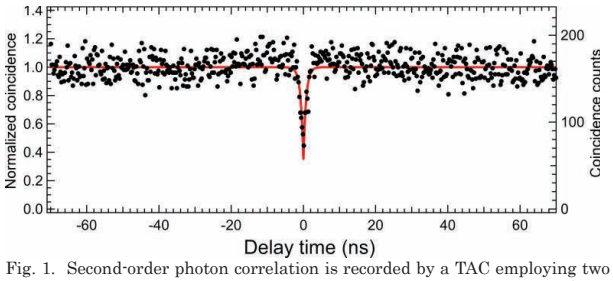

Fig. 1. Second-order photon correlation is recorded by a TAC employing two SSPDs. Normalized histograms of the autocorrelation measurement (solid circles) at an excitation power of 1.4 W/cm^2. Excitation wavelength is 830 nm and the time bins are 244 ps. The integration time and count rates are 8.5 h and ~10 kHz, respectively. The solid (red) line is fit, indicating a dip in the correlation function of $g^{(2)}(0)=0.35$.

[1] H. Sasakura, S. Kayamori, S. Adachi, and S. Muto, J. Appl. Phys. **102**, 013515 (2007).
[2] H. Sasakura, X. Liu, S. Odashima, H. Kumano, S. Muto, and I. Suemune, arXiv:1210.3123v2.

Confinement of Excitons in Strain-engineered InAs/InGaAs/GaAs Metamorphic Quantum Dots

Shaukat A. Khattak[1, 2], Manus Hayne[1], Luca Seravalli[3], GiovannaTrevisi[3] and Paola Frigeri[3]

[1]*Department of Physics, Lancaster University, Lancaster LAI 4YB, UK*
[2]*Department of Physics, Abdul Wali Khan University Mardan, Pakistan*
[3]*CNR-IMEM Institute, Parco delle Scienze 37a, I-43100 Parma, Italy*

Lasers based on self-assembled quantum dots (QDs) emitting at 1.3 μm are commercially available, but producing longer wavelength devices has proven challenging. In both cases strain-engineered InAs/$In_xGa_{1-x}As$/GaAs metamorphic structures are exploited, with the InGaAs layers above and below the QDs called upper and lower confining layers (CLs).

The emission wavelength may be controlled by changing two independent parameters of the relaxed $In_xGa_{1-x}As$ lower CL [1]. (1) Changing x results in modifications of the band discontinuities between the QDs and CLs and also affects the QD-CL mismatch f that determines the QD strain. (2) Changing the lower CL thickness, d, only affects f [1].

By this method it should be possible to optimize the confinement of exciton whilst also extending the wavelength to 1.55 μm: emission as long as 1.59 μm in similar metamorphic nanostructures has been reported [2]. Measuring the emission wavelength is straightforward, but how about the confinement? Here we do this by studying exciton properties (Bohr radius, a_B and reduced mass, μ) using low temperature magneto-photoluminescence [3].

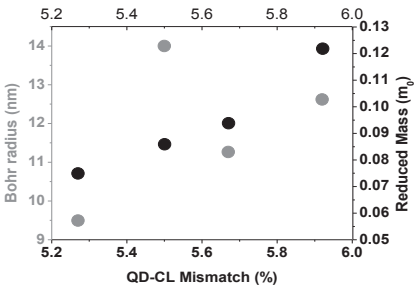

Figure 1

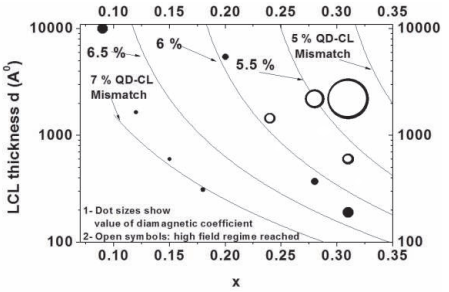

Figure 2

We have studied eleven InAs/$In_xGa_{1-x}As$/GaAs QD samples at 2 K and in magnetic fields up to 17 T (with another 15 in progress). AFM measurements confirm that the dot morphology is independent of both d and x. [1] Fig. 1 shows that reduced mass of exciton, μ increases with increasing mismatch for samples where the mismatch is low, but there is no clear trend in a_B with mismatch. Fig. 2 shows that diamagnetic coefficient, Γ, decreases with increasing mismatch for all samples, consistent with trend in μ ($\Gamma \propto a_B^2/\mu$). For samples where the QD-CL mismatch is low (5 to 6%), the high-field regime (where the magnetic length is $<a_B/\sqrt{2}$) is reached, but not when it is high ($\gtrsim$ 6%) implying that a_B < 9 nm. For samples where x is same (0.31), Γ decreases with decreasing d. Similarly for the samples where the d is same (600 Å), Γ decreases with decreasing x. Irrespective of x, when d is small ($\leq$ 370 Å) the high-field regime is not reached, and when x is low ($\leq$ 0.2) the high field regime is not reached irrespective of d.

[1] L. Seravalli et al, J. Appl. Phys. **101**, 024313 (2007) ; L. Seravalli et al, ibid **108**, 064324 (2010).
[2] L. Seravalli et al, Appl. Phys. Lett. **92**, 213104 (2008).
[3] M. Hayne and B. Bansal, Luminescence **27**, 179 (2012).

Electronic properties of a quantum wire with magnetic impurities

Tomasz Kwapiński

Institute of Physics, M. Curie-Skłodowska University,
20-031 Lublin, Poland, EU
e-mail: tomasz.kwapinski@umcs.pl

The conductance and density of states (DOS) of a quantum wire which is tunnel coupled to the underlying substrate are investigated theoretically using the retarded Green's function method. The wire is composed of periodically placed magnetic and non-magnetic impurities (see Fig. 1), and is modelled by a tight-binding Hamiltonian within the mean-field approximation.

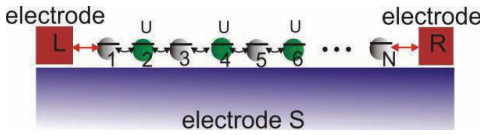

Fig. 1 Schematic view of a quantum wire consisting of N sites and coupled with the left (L), right (R) and surface (S) electron reservoirs. The wire is composed of interacting (magnetic) and noninteracting sites. In the above sketch the periodicity of impurities is m = 2.

It is shown that for a wire with periodically placed impurities a number of energy gaps in the DOS structure are observed. These gaps arise from the Coulomb correlations of the magnetic sites, U. For the case of non-periodic distributions of impurities or for vanishing U the DOS gaps of the system disappear.

Additionally, the quantum wire DOS as well as the conductance along the wire are studied for two different kinds of substrate: in one model the substrate's electronic wavefunctions are taken to be completely localized (an insulator surface) while in another model the substrate electronic wavefunctions are taken to be delocalized (a metal surface). It is interesting that for a substrate with localized electrons all energy gaps disappear with the wire-substrate coupling which is a signature of a metal-insulator transition. However, for the substrate with delocalized electrons the energy gaps survive and become somewhat wider. The conductance through the system also strongly depends on whether or not the substrate electrons are localized.

TuP52

Conductance instabilities in a quasi-1D quantum wire

Sanjeev Kumar[1], Kalarikad Thomas[1], Luke Smith[3], Michael Pepper[1,2], Ian Farrer[3], David Ritchie[3], Geraint Jones[3] and Jonathan Griffiths[3]

[1] *London Centre for Nanotechnology, University College London, 17-19 Gordon Street, London WC1H 0AH, UK*
[2] *Department of Electrical and Electronic Engineering, University College London, Torrington Place, London WC1E 7JE, UK*
[3] *Cavendish Laboratory, Madingley Road, Cambridge CB3 OHE, UK*

Recent theoretical work shows the possibility of forming a Wigner lattice in quasi one-dimensional (1D) quantum wires with low densities when the interaction among the electrons is strong [1]. This happens due to the fact that potential energy dominates the kinetic energy at low densities [1]. A quasi-1D wire is realised by electrostatically confining a two-dimensional electron gas (2DEG) between a pair of surface split-gates. Such ballistic 1D wires exhibit quantised conductance in units of $2e^2/h$. Transport measurement in 1D wires have largely been conducted, and understood, in the regime where electrons are strongly confined. For weak confinement strengths, as the density increases the Coulomb repulsion between electrons increases until it overcomes the confinement potential, whereupon the ground state distorts, which can lead to the bifurcation of the electronic system [2,3].

We present transport measurements of weakly confined quantum wires defined in a 2DEG by top-gated split-gate devices. In the previous work, weakening the confinement potential led to the formation of two rows, marked by a jump in conductance from zero to $4e^2/h$. We have investigated this regime of weaker confinement in great detail and observed intermediate jumps in quantised conductance from $2e^2/h$ to $6e^2/h$ and $4e^2/h$ to $8e^2/h$. Differential conductance and greyscale plots indicate the adjacent subband trajectories approach each other and there is anti-crossing or locking of the subbands. These observations may be an indication that multiple rows could also be formed in weakly confined wires. Such instabilities in 1D conductance in particular at low concentration give further insight in understanding Wigner lattice formation in quasi-1D wires.

[1] J. Meyer and K. A. Matveev, J. Phys.: Condens. Matter. **21,** 023203 (2009).
[2] W. K. Hew et al., Phys. Rev. Lett.**102**, 056804 (2009).
[3] L. W. Smith et al., Phys. Rev. B **80**, 041306(R) (2009).

Transport properties of Au nanoparticle-VO_2 nanowire assembly

Gil-Ho Kim[1], **Youngreal Kwak**[1], **Ji-Won Byon**[2], **Jeong Min Baik**[2], **Kyung Soo Yi**[3†]

[1] *School of Electronic and Electrical Engineer., Sungkyunkwan Univ., Suwon 440-746, Korea*
[2] *School of Mechanical and Advanced Materials Engineer., UNIST, Ulsan 689-805, Korea*
[3] *Department of Physics, Pusan National Univ., Busan 609-735, Korea*

We present electrical transport analysis for Au nanoparticle (NPs)-VO_2 nanowire (NW) assembly fabricated using ac dielectrophoresis (DEP) experiments. [1] Gold NPs of 10 nm radius are placed on the surface of VO_2 [100] NW of 210 nm x 120 nm rectangular cross section and 4 μm length. (See Fig. 1.) The number of Au NPs on the VO_2 NW surface is manipulated by varying duration, frequency, and bias voltage of the DEP processes.

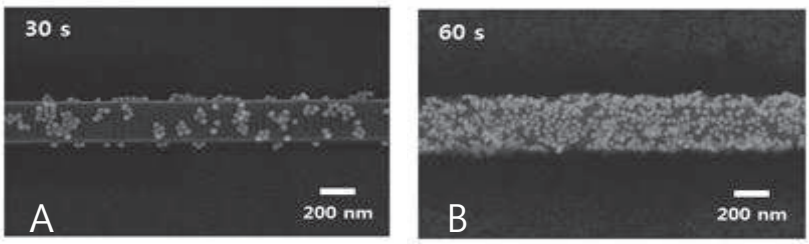

Figure 1 SEM images of DEP processed Au NP-VO_2 NW assemblies manipulated at 1 MHz and 2.5 V. DEP duration t = 30 s and surface density of Au NPs of 3.51×10^{10} cm^{-2} (panel A), and t = 60 s and Au NPs of 1.68×10^{11} cm^{-2} (panel B).

Under an external electrical bias, the nonlinear symmetric I-V characteristic, a signature of space-charge-limited transport, is observed and conductance oscillations prevail at 150 K. The current-voltage characteristic and channel conductance of an assembly with Ti/Au electrodes are illustrated in Fig. 2, respectively. We understand that the attached Au NPs act as dopant material providing mobile carriers to the semiconducting VO_2 NW forming a thin electron accumulation layer around the NW and that the carrier conduction occurs through the nanobelt around the insulating core of the VO_2 NW. The cross sectional area of the NW contributing to charge conduction is much reduced from the physical cross section of the NW. Observed plateau structures in the I-V curve and the oscillations in the corresponding channel conductance are analyzed with respect to quantum confinement-induced 2D subband structure of the nanobelt. [2] KSY acknowledges a partial support by a two-year grant from the PNU Research Foundation.

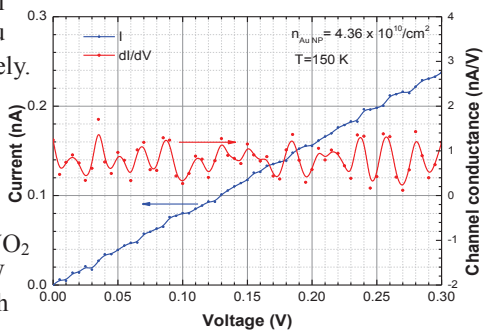

Figure 2 I-V characteristic and the corresponding channel conductance behavior as a function of source-drain voltage for the VO_2 NW at 150 K. The surface concentration of Au NPs was 4.36 x 10^{10} /cm^2.

[1] D. Cheon, S. Kumar, Gil-Ho Kim, Appl. Phys. Lett. **96**, 013101 (2010).
[2] K. S. Yi, K. Trivedi, H.C. Floresca, H. Yuk, W. Hu, M. Kim, Nano Lett. **11**, 5465 (2011).

† Corresponding author: ksyi@pusan.ac.kr

TuP54

Relation between structural properties and electron transport in Si nanowires

Enrique Montes[1], Konstantinos Gkionis[1], Ivan Rungger[2], Stefano Sanvito[2] and Udo Schwingenschlögl[1]

[1] *PSE Division, KAUST, Thuwal 23955-6900, Saudi Arabia*
[2] *School of Physics and CRANN, Trinity College, Dublin 2, Ireland*

One-dimensional medium-sized nano-structured systems such as nanowires are believed to be the most important building blocks for the next generation of electronic devices, due to the possibility to control the dimensionality, potentially affecting its physical properties. In particular, Silicon nanowires are attractive candidates due to their compatibility and ideal interface with the existing Si technology.

The electronic properties of Silicon nanowires can be modified by varying their diameter or by passivating the surface with different chemical species. Theoretical studies on the electronic properties of this systems have shown that the electronic structure depends on the growth orientation and the diameter. The band gap is strongly anisotropic and follows the order $E_g^{\langle 100\rangle} > E_g^{\langle 111\rangle} > E_g^{\langle 110\rangle}$ for wires of comparable diameter. Additionally, the gap strongly depends on the diameter. Bulk-Si has an indirect band gap, and Silicon nanowires have a direct gap. This property enables the use as optically active materials for photonics applications.

We investigate Silicon nanowire systems with different diameters. The electronic properties are modeled with density functional theory with the SIESTA package [1]. Electron transport calculations are performed using the non-equilibrium Green function approach as implemented in the SMEAGOL package [2], which is interfaced with SIESTA. We adopt different configurations: First we consider the leads as pure nanowires, obtaining a semi-infinite system, then we investigate the transport using metallic leads, Au$\langle 111\rangle$ and Fe$\langle 111\rangle$ electrodes are considered. Using density functional theory we relax the system and obtain the optimal configuration of the wire in contact with the metal electrodes. The distance between nanowire and metal and the nanowire length are optimized. For Au-electrodes we investigate how the symmetry of the orientations of the nanowires affects the transport properties by using transmission and complex band structure calculations. The results show a high symmetry of the $\langle 110\rangle$ growth orientation, as illustrated by a wave function isosurface plot.

For Fe-electrodes we analyze the transport considering different mutual alignments between the magnetization vectors of the electrodes. The magneto-resistance is calculated for the different orientations, showing a clear relationship between the symmetry of the wave function and the magnetic properties.

[1] D. Sánchez-Portal, P. Ordejón, E. Artacho, and J. M. Soler, Int. J. Quantum Chem. **65**, 453 (1997).
[2] A. R. Rocha, V. M. Garcí-Suarez, S. W. Báiley, C. J. Lambert, J. Ferrer, and S. Sanvito, Nat. Mater. **4**, 335 (2005).

Crystal structure and optical characterization of radial heterostructured GaAs/AlGaAs/GaAs nanowires

F.E.G.Guimarães, R. A. Caface, H.Arakaki, C.A. de Souza, and Yu.A.Pusep

Instituto de Fisica de São Carlos, Universidade de São Paulo, 13560-970 Sao Carlos, SP, Brazil

Structural and optical properties of heterostructured GaAs/AlGaAs/GaAs core/inner shell/outer shell NWs are studied. Transmittance electron microscopy, CW and time-resolved photoluminescence as well as Raman scattering measurements unambiguously manifest to the presence of segments crystallized in zinc-blende and wurtzite phases, which spread to the shells. The effect of in-built electric field is to energetically separate optical transitions due to recombination of spatially separated electron-hole pairs. Four observed photoluminescence lines are assigned to the radiative recombination of photoexcited electrons confined in the center of the GaAs core and at the heteroboundary between the outer GaAs shell and the inner AlGaAs one with the holes localized at the heteroboundary between the core and the inner AlGaAs shell; both recombinations take place in zinc-blende and wurtzite phases. One additional photoluminescence line is attributed to the spatially indirect recombination between the electrons in zinc-blende and the holes in wurtzite phases. Band gap of the wurtzite phase and the band offsets between the zinc-blend and wurtzite structures are determined. A simple model, based on representation of the valence band structure using two levels, accounts well for the observed temperature dependence of the integrated photoluminescence intensities. The proposed double shell structure with tunneling transparent inner shell sets conditions for easy control of the emission energy of the heterostructured nanowires. In addition, time-resolved photoluminescence was employed to study electron-hole dynamics in radial heterostructured GaAs/AlGaAs/GaAs core/inner shell/outer shell nanowires. It was found that impurity random potential produces a red shift of the decay time maximum with respect to the photoluminescence peak energy. The results of this study are partially published in [1].

[1] F.E.G.Guimarães, R. A. Caface, H.Arakaki, C.A. de Souza, and Yu.A.Pusep, J.Appl.Phys. **113**, 064315 (2013).

The growth and micro-Raman characterization of GaN nanorods

P. Kamyczek[1], Z. R. Zytkiewicz[2], E. Placzek-Popko[1], E. Zielony[1], M. Sobanska[2], A. Reszka[2], K. Klosek[2]

[1]*Institute of Physics, Wroclaw University of Technology, Wybrzeze Wyspianskiego 27, 50-370 Wroclaw, Poland*
[2]*Institute of Physics, Polish Academy of Sciences, Al. Lotnikow 32/46, 02-668 Warsaw, Poland*

Micro-Raman spectroscopy was used to study strain in GaN nanorods grown by plasma-assisted molecular beam epitaxy on Si(111) substrates. The growth comprised of a substrate deoxidation, exposure to a nitrogen flux and self-organized growth of nanorods under nitrogen-rich conditions, without catalyst. The morphology of the samples was characterized by high resolution scanning electron microscopy. The GaN nanorods were ~350 nm long with diameter of ~25nm, homogenously distributed, oriented along c-axis, perpendicularly to the substrate. Two types of nanorods grown at Ga source temperature T_{Ga} ~820°C and 800°C were studied. The nanorods in the sample A exhibit partial coalescence whereas in the sample B an ensemble of separated nanorods was formed. Micro-Raman spectroscopy was carried out with the use of Jobin–Yvon's T64000 system equipped with a CCD camera. 514.5 nm line of Ar^{2+} laser was used as an excitation source. Raman spectra show Si related signal at ~521cm^{-1} and E^{2high} GaN mode at 568cm^{-1}. The intensity of the mode is, as expected, higher for the sample A. Comparison of the Raman signals with bulk Si and GaN let us conclude that substrate and nanorods are strain free. A slight red-shift of the E^{2high} mode for higher laser powers (568 cm^{-1} at 4mW down to 567.4 cm^{-1} at 90mW) is associated with local increase of temperature upon laser illumination. The temperature of the samples was estimated using Stokes'/anti-Stokes' intensity ratio of the Si related signal**.**

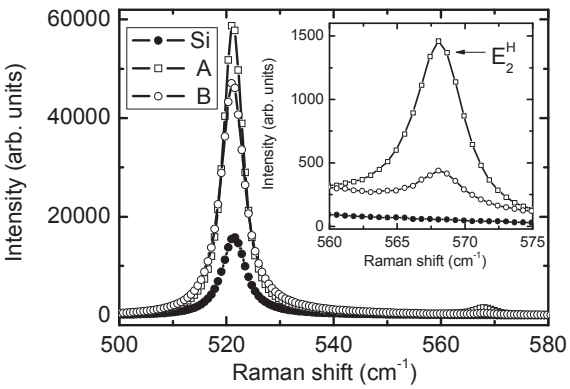

[1] P. Kamyczek, Z. R. Zytkiewicz, E. Placzek-Popko, E. Zielony, M. Sobanska, A. Reszka, K. Klosek, *The growth and micro-Raman characterization of GaN nanorods* – accepted for publication in *Sensor Letters*.

First-Principles Study of Doped GaAs nanowires

M. Galicka, R. Buczko, P. Kacman
Institute of Physics PAS, al. Lotników 32/46, 02-668 Warsaw, Poland

The problem of doping of nanowires (NWs) has become recently one of the major challenges to the growers of one-dimensional III-V semiconductor structures. GaAs NWs are considered as one of the most interesting structures for nanoelectronics and nanophotonics. Their potential application in novel electronic devices requires, however, controllable p-type and n-type conductivity. The specific growth conditions for NWs, their crystal structure and orientation of their side facets may lead to different incorporation behavior than known for planar layers.

To study theoretically the problem of doping the NWs, we consider GaAs wires, in which one cation/anion is substituted by a dopant atom. We consider several elements, which are usually used to obtain p- or n-type conductivity in GaAs, i.e., Si, Be and Sn. We study also the distribution of Au and O atoms, which can be unintentionally incorporated during the growth of these wires. Since the III-V semiconductor NWs can grow in both, zinc-blende (ZB) and wurtzite (WZ) structures, we check whether the crystal structure of the wire has an impact on the doping level and the distribution of impurities in GaAs NWs and, most important, on the electronic properties of the doped nanowires. The studied ZB NWs are oriented along (111) axis and WZ NWs along (0001) axis. These growth directions were shown to be the most energetically preferred for GaAs nanowires [1]. Using ab initio methods based on the density functional theory we have calculated the segregation energies for the studied impurities. The segregation energy is defined as the energy difference between the NW with a dopant in a given site and with this impurity situated in the center of the wire.

The calculations have shown that the distribution of impurities in the wires depends crucially on the crystal structure [2]. In NWs of ZB structure the segregation for the studied dopants is high, suggesting that the most common impurities should accumulate at the side surfaces of such wires – for Au, O and Be the lowest energy has been obtained when the dopants substitute the atom with extra dangling bond, at the corner of the wire's cross-section. This result is analogous to the result obtained before for ZB (Ga,Mn)As NWs [3]. Also Sn should be trapped in the outer shell of the wire, but at the subsurface, still in the vicinity of the surface atom with additional dangling bond. The energies of ZB GaAs NWs with the impurity in these positions are lower than in the core of the wire by ca 0.4 eV for beryllium, but by even 1.5-3 eV for gold and oxygen. For gold and oxygen in WZ wires the results are similar to those obtained for ZB structure but with lower, however still high, segregation. In contrast, all other studied impurities distribute much more homogeneously across the WZ wire and Be even prefers to substitute the Ga ion at the center of the wire.

Thus, our calculations suggest that growth conditions leading to WZ structure should be chosen in order to avoid accumulation of impurity atoms at the surface during the growth of doped III–V wires and that using Be seems to be the best choice for effective p-type doping of GaAs NWs. On the other hand, the results show segregation of Au atoms to lateral surfaces, in perfect agreement with the experimental observation [4]. According to our results the same should be also observed for oxygen. Finally, the formation energies for Si in GaAs NWs, calculated for various sets of chemical potentials suggest that the energy needed for substituting the anion and the cation, and thus the type of conductivity obtained by Si-doping, can be also different in ZB and WZ wires.

The research leading to these results has received funding from Foundation for Polish Science and Ministry of Higher Education (Poland) Grant IP 2011013671. All computations were carried out in the Informatics Center Tricity Academic Computer Net (CI TASK) in Gdansk.

References

[1] M. Bukala, M. Galicka, R. Buczko and P. Kacman Physica E **42**, 795 (2010)

[2] M. Galicka, R. Buczko and P. Kacman, arXiv:1302.0702 [cond-mat.mtrl-sci]

[3] M. Galicka, R. Buczko and P. Kacman, Nano Lett. **11**, 3319 (2011)

[4] D. E. Perea, *et al.* Nano Lett. **6**, 181 (2006).

TuP58

Electrical characteristics of N_2 plasma treatments on SnO_2 nanowires FET

Yong-Hee Choi[1,2*], Junhong Na[1], Jae-Sung Kim[1], Jong Mok Shin[1] and Gyu Tae Kim[1]

[1]School of Electrical Engineering, Korea University, Seoul, 136-701, Korea
[2]Process Development Team, Semiconductor R&D Center, Samsung Electronics Co. Ltd., Hwasung, 445-701, Korea

SnO_2 (tin oxide) are widely used in various research fields such as thin film transistors (TFTs) and sensors because of high electron mobility, flexibility and transparency. However, generally a large electrical hysteresis is often observed with voltage sweeps. To improve the device reliabilities of SnO_2 nanowires FETs, the N_2 plasma were treated. The N_2 plasma treatment on SnO_2 nanowires FET led to positive shift(4V) of Vth with a decrease of the hysteresis width on transfer characteristics. Despite the advantage of the reduction of hysteresis, the On-Off current ratio was significantly decreased and the degradation of the devices was observed with time. The threshold voltage shifted to the positive direction and the overall current was decreased. Furthermore, the hysteresis widths significantly increased. Passivation process was carried out with PMMA coating to prevent unnecessary changes of electrical properties after N_2 plasma treatment. The deterioration of the electrical properties is estimated by the recombination between oxygen vacancies on the surface of NWs and oxygen molecules in an ambient environment.

[1] E. Comini, G. Faglia, G. Sberveglieri, Z. Pan and Z. L. Wang, Appl. Phys. Lett. Res **18**, 1869 (2002).
[2] T. Lim, S. Lee, M. Suh and S. Ju, Electrochemical and Solid-State Lett. **14**, H218 (2011).
[3] . J. Na, J. Huh, S. C. Park, D. Kim, D. W. Kim, J. W. Lee, I. S. Hwang, J. H. Lee, J. S. Ha and G. T. Kim, Nanotechnology **21**, 485201 (2010).

In-plane oriented InAs nanowire formation by selective area molecular beam epitaxy on GaAs (211)B substrates

Masashi Akabori, Tatsuya Murakami, Syoji Yamada
Japan Advanced Institute of Science and Technology (JAIST), Nomi, Ishikawa, Japan

III-V compound semiconductor nanowires (NWs) have received much attention as base components of nanodevices. Especially, InAs NWs are very promising to realize high-performance electronic and spintronic nanodevices because of their high electron mobility and large spin-splitting. For the nanodevice applications, it is desirable that the NWs are synthesized with controlling their positions as well as orientations. Catalyst-free selective area epitaxy on partially masked (111)B substrates is one of the suitable methods to synthesize vertically-oriented InAs NWs [1]. However, in-plane-oriented NWs are more suitable for the nanodevice fabrication by using conventional lithography. To this end, selective area molecular beam epitaxy (SA-MBE) on (110) has been carried out [2]. However, since there are two <111>B directions in (110) plane, there is a difficulty in the orientation control. In this paper, we demonstrate in-plane oriented InAs NW formation by SA-MBE on GaAs (211)B substrates. Since (211)B has one <111>B direction in plane, it can be more suitable for in-plane oriented NW formation than (110).

We coated n-type GaAs (211)B substrates with hydrogen slisesquioxane (HSQ), and patterned them with a hole array by using electron-beam lithography and reactive ion etching. The initial opening holes were designed with a triangular shape. We treated the substrates by H_2SO_4 and de-ionized water followed by loading them into a conventional solid-source MBE system. The beam equivalent pressures of In and As were fixed to $1.0x10^{-7}$ and $1.0x10^{-6}$ Torr, respectively. The substrates were heated up to 590°C once under As ambient for the thermal cleaning, and then they were cooled down to 510°C for the growth. The growth time was fixed to 3 hours.

Figure 1 shows a scanning electron microscope (SEM) image of InAs NWs grown on (211)B. Almost all InAs growth started from the opening holes, and a few polycrystalline deposition on HSQ mask area was observed. Therefore, SA-MBE under the growth condition was almost succeeded. We can see three in-plane oriented NWs and one out-of-plane oriented NW in the image, which are <111>B oriented. The yield of in-plane oriented NW formation is roughly estimated to be ~15 %, which is almost similar to that on (110) [2]. Figures 2(a) and 2(b) show an atomic force microscope (AFM) image and a current image taken by a conductive AFM cantilever, respectively. Since current flowing through InAs NW and n-GaAs substrate was confirmed, the InAs NWs are conductive without any intentional doping.

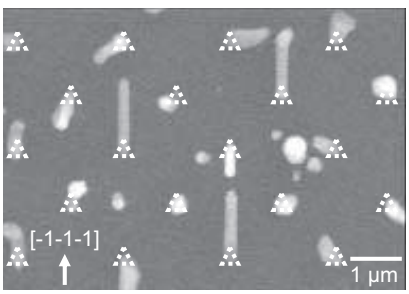

Fig. 1 Top-view of InAs SA-MBE on a GaAs (211)B substrate. Triangular marks represent position of initial opening holes.

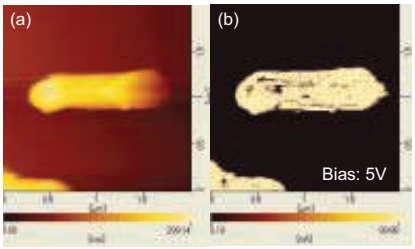

Fig. 2 AFM image (a) and current image (b) of InAs NWs.

[1] M. Akabori *et al.*, J. Crystal Growth, **311**, 3183 (2009).
[2] M. Akabori *et al.*, J. Crystal Growth, **345**, 22 (2012).

Interesting spatial inhomogeneities in n- and p-doped InAs nanowires grown by gold-seeded molecular beam epitaxy

C. Rolland[1], P. Caroff[1,2], X. Wallart[1] and R. Leturcq[1]

[1] *Institute of Electronics, Microelectronics and Nanotechnology, CNRS - UMR 8520, Departement ISEN, Avenue Poincaré, F-59652 Villeneuve d'Ascq, France*
[2] *Department of Electronic Materials Engineering, Research School of Physics and Engineering, The Australian National University, Canberra, ACT 0200, Australia*

A cornerstone for the realization of devices using semiconductor nanowires (NWs) is to control the impurity doping. We investigate the carrier concentration along intentionally doped InAs NWs using transport measurements in NW field effect transistors (NWFETs). We studied both n- (Si) and p- (Be) doped InAs NWs grown by molecular beam epitaxy (MBE) using gold as seed particles.

In Si-doped NWs, we observe non-uniform carrier concentration along the NW, with an electron density that decreases linearly from the base of the NW towards its tip, in contrast to what has been reported for Si-doped InAs NWs grown by metalorganic vapor phase epitaxy (MOVPE) [1]. Similar inhomogeneous doping incorporation was reported for different semiconductor materials [2, 3, 4]. Additionally it was observed that the sidewall morphology of gold-free InAs NWs is drastically affected by Si-doping [5]. Interestingly we do not observe any significant tapering or sidewall nanofaceting on our nanowires, and diffusion of dopants seems to be the most relevant mechanism, as already reported in P-doped Si NWs [6, 7]. We have also grown NWs starting with an undoped section and finishing with a doped section, which allows achieving non-tapered nanowires with an homogeneous controlled carrier concentration.

p-doping of InAs NWs is usually a challenge due to the surface pinning of the Fermi level in the conduction band [8, 9, 10, 11]. We demonstrate that Be-doping of InAs NWs using MBE also leads to an inhomogeneous carrier concentration, as observed for Si-doping. However, due to the surface pinning effect, the p-doped InAs NWs show much more complex characteristics. By acting on the Be concentration we investigate different regimes where $p-n$ junctions are formed between the p-doped NW and the n-doped surface. These junctions can be sharp enough in order to produce the characteristics of tunnel diodes. We thus show a simple way to create functional junctions whithout the need of an additonal controlled n-doped segment along these NWs.

[1] G. Zhang *et al.*, J. Phys. Chem. C **115**, 2923 (2011).
[2] E. Tutuc *et al.*, Appl. Phys. Lett. **89**, 263101 (2006).
[3] G. Imamura *et al.*, Nano Lett. **8**, 2620 (2008).
[4] J. Dufouleur *et al.*, Nano Lett. **10**, 1734 (2010).
[5] H. Ghoneim *et al.*, Nanotechnology **23** 505708 (2012).
[6] J. E. Allen, D. E. Perea, E. R. Hemesath and L. J. Lauhon, Adv. Mat. **21**, 3067 (2009).
[7] E. Koren, N. Berkovitch and Y. Rosenwaks, Nano Lett. **10**, 1163 (2010).
[8] Q. Hang, F. Wang, W. E. Buhro and D. B. Janes, Appl. Phys. Lett. **90**, 062108 (2007).
[9] H.-Y. Li *et al.*, Nano Lett. **7**, 1144 (2007).
[10] A. C. Ford *et al.*, Nano Lett. **10**, 509 (2010).
[11] B. S. Sørensen *et al.*, Appl. Phys. Lett. **92**, 012119 (2008).

Anisotropy and thermoelectric properties pure and Sn- doped Bi nanowires

A. Nikolaeva[1,2], L. Konopko[1,2], A. Tsurkan[1], and E. Istrate[1]

[1] *D. Ghitu Institute of Electronic Engineering and Nanotechnologies, Academy of Sciences, Academiei str. 3/3, MD-2028 Chisinau, Republic of Moldova*
[2] *International Laboratory of High Magnetic Fields and Low Temperatures, Wroclaw, Poland*

We study the thermoelectric properties of bismuth and Sn –doped Bi nanowires with different crystallographic orientations along the wire axis. Measurements of the resistance and thermopower wires with different wire diameters have been carried out over a wide range temperature (1.5 – 300K) and magnetic field (0-14 T).

Electron transport in semimetal wires has been actively studied recently [1–3] due to the fact that there was predicted considerable, almost an order of magnitude, increase of thermoelectric figure of merit in *Bi* on transition to semiconductor state with a narrow gap. In particular, this can be achieved by means of dimensional quantization of energy spectrum of carriers [2]. Taking into account that de Broglie wavelength in *Bi* ≈ 60–80 nm, one should expect manifestation of this effect at rather high temperatures (≈ 100 K), which is most important for practical applications.

For manifestation of dimensional quantization effect an important role is played by crystallographic orientation of samples.

One of the aim this work is to obtain nanowires with high anisotropy of the thermopower, high structural perfection, which can be used to create anisotropic thermal generators with low current consumption.

For the first time, anisotropies of resistance and thermopower of glass-insulated wires of pure and tin-doped bismuth are studied both in the absence of magnetic field and in magnetic field. The wires with diameters from 100 nm to 5 μm are fabricated by liquid phase casting [4, 5]. The wires with C_3 orientation along the axis are fabricated by zone recrystallization with seed. The anisotropy of magnetoresistance is studied using the method of angular diagrams of rotation of the transverse magnetoresistance. As shown, the magnetic field leads to an increase in the thermopower in absolute value.

Of particular significance result is the fact that thermopower anisotropy in Bi-0.05at.%Sn wires is $\Delta\alpha \approx 100$ μV/K at 250-300 K that is in two times more than in pure bismuth. With elastic strain it reaches the value $\Delta\alpha = 150–170$ μV/K, which is important in terms of practical use of single-crystal glass-coated Bi-0.05at.%Sn wires as anisotropic thermoelectric power generators.

This work was supported by STCU# 5373.

[1] L.D. Hicks, M.S.Dresselhaus, Phys.Rev.B, **47**, 16631 (1993).
[2] Yu-Mong Lin, X. Sun, and M.S. Dresselhaus, Phys. Rev. B **62**, 4610 (2000).
[3] I. Chowdhury et al., Nature Nanotech. **4**, 235 (2009).
[4] N.B. Brand, D.V. Gitsu, A.A. Nikolaeva, and Ya.G. Ponomarev, J. Exp. Teor. Phys. **72**, 2332 (1977).
[5] D. Gitsu, L. Konopko, A. Nikolaeva, and T. Huber, J. Appl. Phys. Lett. **86**, 10210 (2005).

Imaging Integer and Fractional Quantum Hall Edge States

Nikola Pascher[1], Clemens Rössler[1], Thomas Ihn[1] , Klaus Ensslin[1], Christian Reichl[1] and Werner Wegscheider[1]

[1]*Solid State Physics Laboratory, ETH Zurich, 8093 Zurich, Switzerland*

We present scanning gate microscopy (SGM) measurements on a quantum point contact (QPC) patterned on top of a high-mobility two-dimensional electron gas (2DEG) in a GaAs-AlGaAs heterostructure. The measurements are carried out at a temperature of 100 mK in a strong perpendicular magnetic field. A local potential perturbation induced by the voltage-biased tip of the microscope is used to probe the underlying 2DEG [1]. The tip acts as a movable gate. Depending on its position, quantum Hall edge channels can be selectively transmitted or reflected [2, 3]. Thus, as a function of tip-position stripes of constant filling factors are resolved. Even filling factors appear as very pronounced plateaus in the maps of the conductance as a function of tip position, as seen in fig. 1a). Odd filling factors can be seen as smaller stripes. At very high magnetic fields we can observe very distinct signatures of fractional filling factors 1b), c), d).

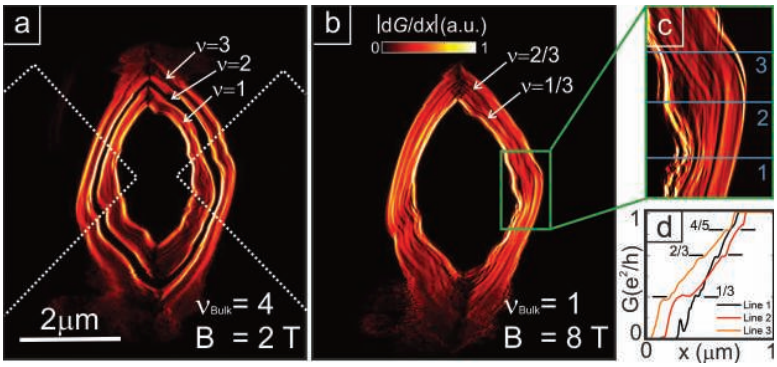

Figure 1: a) SGM image taken at a filling factor of 4 in the bulk. Plateaus at values of 3, 2 and 1 e^2/h can be observed. Dashed lines show the outline of the QPC. b) Same image at a filling factor of 1 in the bulk. Black stripes show filling factors of 1/3 and 2/3. c) Zoom at the position of the green frame in b). Especially in d) clear plateuas at filling factors 1/3, 2/3 and 4/5 are visible.

The measurements give a direct measure for the real space behavior and distribution of quantum Hall edge channels. Putting our results into a theoretical framework we can draw conclusions about the alternating compressible and incompressible stripes, which are formed in the quantum Hall regime [4]. The measurements show the fragile nature of fractional quantum Hall effect edge states and their behavior in the local potential landscape.

[1] N. Paradiso, S. Heun, S. Roddaro, L. Sorba, F. Beltram, G. Biasiol, L.N. Pfeiffer and K.W. West, PRL **108**, 246801 (2012).
[2] B. I. Halperin, PRB **25**, 2185 (1982).
[3] M. Büttiker, PRB **41**, 7906 (1988).
[4] D. B. Chklovskii, B. I. Shklovskii and L. I. Glazman, PRB **46**, 4026 (1992).

Even-denominator ν = ½ Fractional Quantum Hall Effect in GaAs 2D Hole Systems

Yang Liu[1], S. Hasdemir[1], A.L. Graninger[1], M. Shayegan[1], L.N. Pfeiffer[1], K.W. West[1], K.W. Baldwin[1] and R. Winkler[2]

[1]*Department of Electrical Engineering, Princeton University, Princeton, New Jersey, USA*
[2]*Department of Physics, Northern Illinois University, Dekalb, Illinois, USA*

When electrons at sufficiently high density are confined to a high-quality *wide* GaAs quantum-well, they occupy two electric subbands and possess a bilayer-like charge distribution. Under appropriate conditions, the additional layer and/or subband degree of freedom stabilizes a special fractional quantum Hall state (FQHS) at the *even-denominator* Landau level filling factor ν = ½ [1,2]. This state is generally believed to be the two-component Halperin (331) state, a FQHS with strong inter-layer and intra-layer correlations. Although the ν = ½ state was discovered over 20 only years ago, its observation has been only reported in high quality GaAs electron systems [1-5].

Here we report the first observation of the ν = ½ FQHS in GaAs *hole* systems. Figure 1 shows the longitudinal and Hall resistances measured in a symmetric 35-nm-wide GaAs quantum well at density p = 1.44 x 10^{11} cm^{-2}. At filling factor ν = 1/2, we observe a strong minimum in R_{xx} and a clear plateau in R_{xy} quantized at $2h/e^2$. As a function of density, we observe an evolution of the ν = ½ FQHS which is qualitatively similar to that of the electron systems: the FQHS is only observed at intermediate densities; the system becomes metallic at low densities, and insulating at very high densities [2,3]. However, we also observe an unexpectedly strong ν = ½ FQHS which is unique to 2D hole systems.

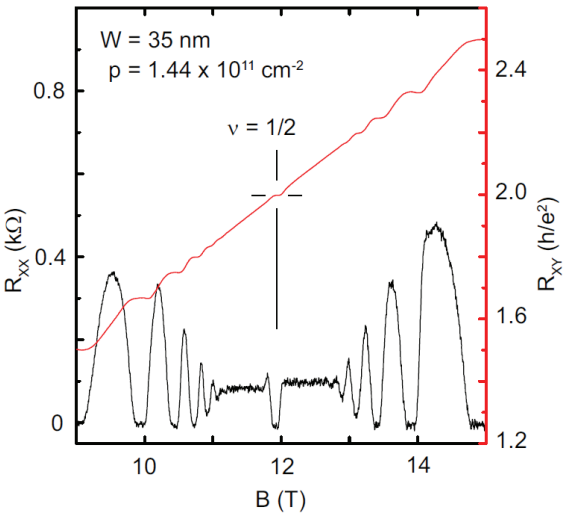

Fig. 1. Longitudinal (R_{xx}) and Hall (R_{xy}) resistances taken from a 2D hole system in a symmetric 35-nm-wide GaAs quantum well.

We discuss the results of our study, carried out as a function of both density and quantum well width, in light of the very complex and rich band structure of GaAs 2D holes.

[1] Y.W. Suen, L.W. Engel, M.B. Santos, M. Shayegan, and D. Tsui, Phys. Rev. Lett. **68**, 1379 (1992).
[2] Y.W. Suen, H.C. Manoharan, X. Ying, M.B. Santos, M. Shayegan, Phys. Rev. Lett.**72**, 3405 (1994).
[3] H.C. Manoharan, Y.W. Suen, M.B. Santos, M. Shayegan, Phys. Rev. Lett. **77**, 1813 (1996).
[4] D. Luhman, W. Pan, D.C. Tsui, L.N. Pfeiffer, K.W. West and K.W. Baldwin, Phys. Rev. Lett. **101**, 266804 (2008).
[5] J. Shabani, T. Gokman, and M. Shayegan, Phys. Rev. Lett. **103**, 046805 (2009).

Anomalous electric transport induced by dynamic nuclear polarization in the vicinity of ν=2/3 quantum Hall state

S. Tsuda[1], D. Terasawa[2], S. Mitani[1], Minh Hai N.[1], A. Fukuda[2], and A. Sawada[3]

[1] *Graduate School of Science, Kyoto University, Kyoto, 606-8501 Japan*
[2]*Department of Physics, Hyogo College of Medicine, Nishinomiya, 663-8501 Japan*
[3]*Research Center for Low Temp. and Mat.Sciences, Kyoto University, Kyoto, 606-8502 Japan*

Quantum Hall effects at filling factor ν = 2/3 is known to show a huge magnetoresistance R_{xx} [1] accompanying with hysteresis due to the degeneracy between different spin states, spin polarized (SP) state and spin unpolarized (SU) state. The Hyperfine coupling of electron spins and nuclear spins in the host material dynamically changes the nuclear spin polarization, and the R_{xx} proportionally changes the value with regard to the dynamical nuclear spin polarization (DNP) [2]. We report that the increased resistance state, which is induced by a large current (~60 nA), shows the temperature dependence that is indicative of the Anderson insulator as the underlying cause [3]. Here we present the experimental results of the electric transport measurement before and after DNP that is induced at the points different from the exact ν = 2/3 point.

The sample that we use in this study is GaAs/AlGaAs heterojunctions grown by molecular beam epitaxy in NTT basic research laboratories. The sample has two conducting layers, however we use only one layer (monolayer experiment). The low temperature mobility is approximately 2 x 10^6 cm^2/Vs. Figure 1 shows the R_{xx} and R_{xy} before and after DNP as a function of the inverse of ν (1/ν). The values before DNP are obtained by the fast sweep of the density with regard to the constant magnetic field B = 7.1 T and the measuring current I_m of 5 nA. The values after DNP are obtained after 3000 s DNP at 1/ν=1.55 (indicated by a dash-and-dot line) with the nuclear spin pumping current I_p of 60 nA and I_m of 5 nA by sweeping 1/ν toward the increasing direction. This sweep is done before the DNP is relaxed to equilibrium, and is confirmed that there is only a small hysteresis between the directions of the sweeps. R_{xx} before DNP has three minima corresponding to ν=2/3 SU state, ν=2/3 SP state, and ν=3/5 state, respectively. We find that R_{xx} after DNP changes its I_m dependence for 1/ν < 1.5 and for 1/ν > 1.5. We also notice that R_{xy} after DNP deviates upward for 1/ν > 1.5 from the quantized value of $3h/(2e^2)$, where h denotes Planck's constant and e denotes the elementary charge, and makes another plateau. Interestingly, this deviation in R_{xy} becomes opposite and I_m dependence of R_{xx} changes its behavior when the position of DNP is 1/ν < 1.5 (not shown here). We further show the DNP time dependence of R_{xx} and R_{xy} and discuss the relation with regard to the amount of B_N and the SU-SP transition point in the conference.

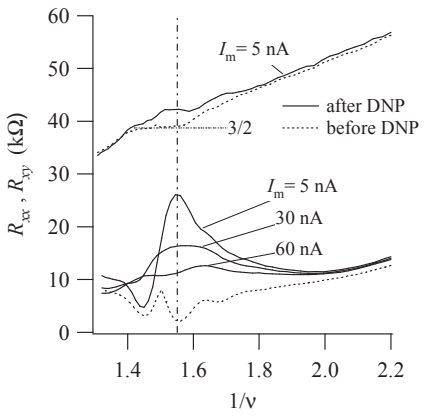

Figure 1 R_{xx} and R_{xy} before DNP and after DNP as a function of 1/ν. Note that the measurement method is different between before and after DNP (see text).

[1] S. Kronmüller, *et al*., Phys. Rev. Lett., **81** 2526 (1998)
[2] K. Hashimoto, *et al*., Phys. Rev. Lett., **88**, 176601 (2002).
[3] S. Tsuda, *et al*., to be presented in EP2DS-20.

Probing energy relaxation in quantum Hall edge states utilizing quantum point contacts

T. Otsuka[1,2*], Y. Sugihara[1*], J. Yoneda[1], T. Nakajima[1,2] and S. Tarucha[1,2]

[1] *Department of Applied Physics, University of Tokyo, Bunkyo-ku, Tokyo 113-8656, Japan*
[2] *RIKEN Advanced Science Institute, RIKEN, 2-1 Hirosawa, Wako, Saitama 351-0198, Japan*

Quantum Hall edge states attract strong interests in basic science and application to quantum electronics because of their long coherence lengths in solids and well defined chiralities. For the application of quantum Hall edge states, it is important to investigate the local electronic properties in microscopic way. Recently, experiments probing the local electronic states and energy relaxation in quantum Hall edge states utilizing quantum dots as local probes have been reported [1]. In our experiment, we measured the local electronic states with a different kind of probe: quantum point contacts (QPCs). With this local probe, we investigated the spatial change of the electronic states and evaluated energy relaxation lengths. By comparing the results with previous experiments, we have checked the validity of our method. We applied this method to probe energy relaxation around a specific energy dissipation point called as a hotspot in quantum Hall regimes which is formed near a gate by applying large bias across the gate and creating hot electrons.

Figure (a) shows a schematic of the device structure. Five QPCs connected to a mesa were fabricated on a GaAs/AlGaAs heterostructure wafer. Non-equilibrium energy distribution in the edge channels, which induced the energy relaxation, was generated by using QPC_1 and the change of the local electronic states was monitored by QPC_n with different propagation lengths d. First, we measured the energy relaxation only with energy exchange between edge channels. We set the conductance through QPC_1 to e^2/h and created the distribution with two Fermi levels (μ_0 and μ_1) with $\mu_1 - \mu_0 = eV_1$ in the outer edge channel and measured the voltage V_n at QPC_n. The observed change of the signal (dV_n/dV_1) as a function of d is shown in Fig. (b). We observed decay of dV_n/dV_1. From the fitting, the relaxation length was evaluated as 3 ± 1 μm. We did same measurement in the case of the energy relaxation with electron tunneling between edge channels. The obtained relaxation length was > 30 μm. These results are consistent with previous reports [1, 2, 3] and show the validity of our method. We applied this method to probing energy relaxation around a hotspot created by hot electrons. We observed relaxation length of 2 ± 1 μm and this implies the possible relaxation mechanism is the energy exchange without electron tunneling.

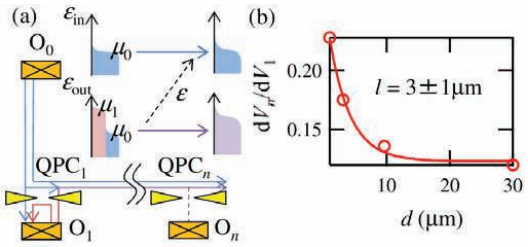

Figure: (a) Schematic of the device structure. We prepared five QPCs to initialize (QPC_1) and probe local electronic states ($QPCn$, n = 2, 3, ···, 5) in the quantum Hall edge states. (b) dV_n/dV_1 as a function of d. The solid line is the result of fitting.

[1] H. le Sueur *et al*., Phys. Rev. Lett. 105, 056803 (2010).
[2] G. Müller *et al*., Phys. Rev. B 45, 3932 (1992),
[3] S. Komiyama *et al*., Phys. Rev. B 45, 11085 (1992).

* These authors contribute equally to this work.

Theory of the integer quantum Hall transition broadening due to the electron-phonon interaction

A. A. Greshnov and Y. M. Beltukov

Ioffe Physical-Technical Institute RAS, St. Petersburg, Russia

Although the integer quantum Hall effect has been studied intensively during the last three decades and general picture behind the phenomenon seems to be clear, a real quantitative approach suitable for description of the magnetotransport at given temperature is still lacking. As contrasted with the weak localization, one has to be satisfied with the only essential conclusion of the so-called scaling theory of the integer quantum Hall effect [1] that widths of the transitions between the adjacent plateaus scale with the temperature as $\Delta B \propto T^k$, with the exponent k to be found from something else. However, specific shape of the magnetotransport curves contains rich information about the system, especially on interaction and type of disorder [2], and it would be worth not to miss it.

It is not easy to decide which type of the interaction, electron-electron or electron-phonon, governs broadening of the quantum Hall transitions by disturbing coherence of the electron-impurity system. Here we focus on the electron-phonon interaction which has been addressed in a number of papers [3]-[5], however, without no specific magnetotransport curves being calculated. In order to describe conductivity of a quantum Hall system at finite temperatures we consider a network of random resistors $R_{\alpha\beta} = e^2/(T\Gamma_{\alpha\beta})$ connecting the nodes (α, β) associated with the one-electron states in a random potential, $\Psi_\alpha(\mathbf{r})$, which are localized according to $\xi \propto |E - E_n|^{-\nu}$ with $\nu \approx 2.3$ [1]. Here $\Gamma_{\alpha\beta}$ is the effective transition rate between the one-electron states with emission or absorption of a phonon. It accumulates statistics of the electrons and phonons and the quantum-mechanical rate $w_{\alpha\beta}$ which can be evaluated numerically as shown in Fig.1(a). On the other hand, temperature dependence of the averaged transition rate for the pair of states, which lie near the Fermi level and overlap in space, can be estimated as $\overline{w_{\alpha\beta}} \propto T^3$. Using this approximation and estimation for a number of the mutually overlapping states, $m \propto T\xi^2$, it is straightforward to estimate the longitudinal conductivity σ_{xx} [6], which becomes of the order of e^2/h as $\xi \propto T^{-1}$ leading to a simple relationship $k = \frac{1}{\nu} \approx 0.42$, in agreement with the numerical results shown in Fig. 1(c) and recent experimental data [7].

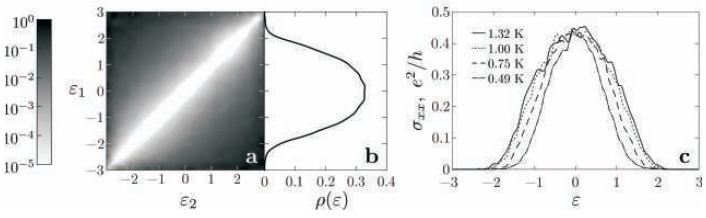

Figure 1: Electron-phonon transition probabilities (a), density of states (b), and longitudinal conductivity for various temperatures (c) are shown as functions of the energy.

[1] B. Huckestein, Rev. Mod. Phys. **67**, 357 (1995).
[2] A.A. Greshnov, G.G. Zegrya, E.N. Kolesnikova, JETP **107**, 491 (2008).
[3] D.G. Polyakov, B.I. Shklovskii, Phys. Rev. Lett. **73**, 1150 (1994).
[4] H.L. Zhao, S. Feng, Phys. Rev. Lett. **70**, 4134 (1993).
[5] T. Brandes, L. Schweitzer, B. Kramer, Phys. Rev. Lett. **72**, 3582 (1994).
[6] A.A. Greshnov, Y.M. Beltukov, Semiconductors (in press).
[7] W. Li et al, Phys. Rev. Lett. **102**, 216801 (2009).

Fractional Quantum Hall Effect in a Diluted Magnetic Semiconductor

C. Betthausen[1], C. Preis[1], P. Giudici[1], V. Kolkovsky[2], M. Wiater[2], G. Karczewski[2], B. Piot[3], J. Kunc[3], M. Potemski[3], T. Wojtowicz[2], and D. Weiss1[1]

[1]*Department of Experimental and Applied Physics, Regensburg University, 93040 Regensburg, Germany.* [2]Institute of Physics, Polish Academy of Sciences, 02668 Warsaw, Poland [3]*Laboratoire National des Champs Magnetiques Intenses, CNRS-UJF-UPS-INSA, 38042 Grenoble, France*

Since the discovery of the fractional Quantum Hall effect (FQHE) nearly 30 years ago experimental research was concentrated on investigating fractional states in nonmagnetic materials. Typically GaAs-based systems have been studied where the small Zeeman energy E_Z causes several fractional Quantum Hall (FQH) ground states to be spin unpolarized. More recently, the FQHE was reported in a CdTe quantum well (QW) [1] - a systems exhibiting spin-polarized fractional ground states due to their much larger g-factors compared to GaAs.

Magnetic manganese ions can easily be incorporated into CdTe based quantum structures, hence making this material system ideally suited for the search of fractional states in a Diluted Magnetic Semiconductor (DMS). $Cd_{1-x}Mn_xTe$ is one of the most thoroughly investigated members of the class with all its spin dependent properties being strongly enhanced due to spin exchange interaction between mobile carriers and localized magnetic moments (s-d exchange). Therefore, the Zeeman splitting of electronic states can not only be gigantic but may also be engineered both in magnitude, sign and field dependence.

Here we report on the observation of FQH states in the lowest Landau level (LL) of a 2DEG formed in two high quality 30 nm wide $Cd_{1-x}Mn_xTe$ quantum wells with 0.24% and 0.30% of Mn concentration and densities of $n_s = 3.9510^{11}/cm^2$ and $2.7710^{11}/cm^2$, respectively. Standard magnetotransport experiments were performed up to 34 T in a tilted magnetic field and at temperatures between 15 mK and 1 K. Due to the presence of Mn impurities the Zeeman energy is extremely high at low magnetic fields and is *reduced* when increasing the external field. We have designed our sample by adjusting the Mn concentration such that the Zeeman splitting vanishes at about 13.5 T. This gave us the unique opportunity to investigate spin effects in QH states emerging at these fields. By measuring activation energies at tilted magnetic fields we obtained the dependence on Zeeman energy of the excitation gaps at filling factors $\nu = 4/3$, 5/3, 7/5 and 8/5. By analyzing the excitation gap as a function of an in-plane magnetic field we demonstrate that exchange interaction between the Mn spins and the electrons crucially affects the properties, e.g., the spin polarization, of FQH ground states. This provides a recipe to tune the spin-splitting and hence the spin-polarization in a wide range, thus offering a novel means to manipulate fractional states. Using a simple model within the framework of Composite Fermions (CFs) [2] we extracted CF masses m_{CF} and g-factors in the vicinity of $\nu = 3/2$. A quantitative comparison between model and experiment considering deviations coming from disorder effects or LL broadening will be discussed[3].

[1] B. A. Piot et al., Phys. Rev. B **82**, 081307 (2010)
[2] J. K. Jain, Phys. Rev. Lett. **63**, 199 (1989)
[3] C. R. Dean et al., Phys. Rev. Lett. **100**, 146803 (2008); R. R. Du et al., Phys. Rev. Lett. **70**, 2944 (1993)

Local detection of nuclear spin resonance in a quantum-Hall-related system

K. Hashimoto [1,2], T. Tomimatsu [2], K. Sato[1], and Y. Hirayama [1,2,3]

[1] *Department of Physics, Tohoku University, Sendai, 980-8578, Japan*
[2] *JST-ERATO Nuclear Spin Electronics Project, Sendai 980-8578, Japan*
[3] *WPI-Advanced Institute for Materials Research, Tohoku University, Sendai 980-8577, Japan*

In quantum Hall (QH) related systems [1], strong interaction between a two-dimensional electron gas (2DEG) and nuclear spins provokes current-induced nuclear spin polarization. Resulting polarized nuclear spins are expected to be inhomogenously distributed due to correlation with the electron spins. We performed local detection of the resistively-detected nuclear spin resonance (NSR) using scanning gate microscopy technique.

The bottom panel shows an atomic force microscopy (AFM) profile taken along a line across a Hall bar which contains a 20-nm $GaAs/Al_{0.3}Ga_{0.7}As$ quantum well. Nuclear spins of the host materials are polarized within the Hall bar using the current-induced nuclear spin polarization in the QH effect breakdown [2], which was induced by applying a large source-drain current I_{sd} = 370 nA at a filling factor $\nu \sim 1$. During the AFM measurement, we applied a radio frequency (RF) bias voltage to the AFM tip with measuring the longitudinal resistance R_{xx}. We found clear drops in R_{xx} at the fundamental NSR frequency of ^{75}As nuclei $f = f_{75As}$ as well as a subharmonic frequency $f = f_{75As}/2$. The observed reduction in R_{xx} (ΔR_{xx}) is plotted in the upper panel as a function of the corresponding position depicted in the AFM profile (bottom panel). The f_{75As}-detected ΔR_{xx} (upper curve) contains a back ground of about 30 Ω at the positions well away from the Hall bar and it gradually increases toward to the Hall bar. In contrast, the $f_{75As}/2$-detected ΔR_{xx} (lower curve) sharply increases near the edges of the Hall bar from a zero back ground. We speculate that the application of the RF bias to the tip leads to two different NSRs. The key NSR is locally induced by the RF electric field beneath the tip [3]. Another occurs even at a distance from the tip due to an unintentional RF magnetic field which spreads over the sample, e.g., from the bias line connected to the tip. The former may arise at both $f = f_{75As}$ and $f_{75As}/2$ due to an electron-spin-mediated NSR [4], while the latter arises only at $f = f_{75As}$ as same as the conventional magnetic NSR. Thus, the $f_{75As}/2$ detection allows us to probe the nuclear spins, polarized within the Hall bar, at a higher resolution without the back ground.

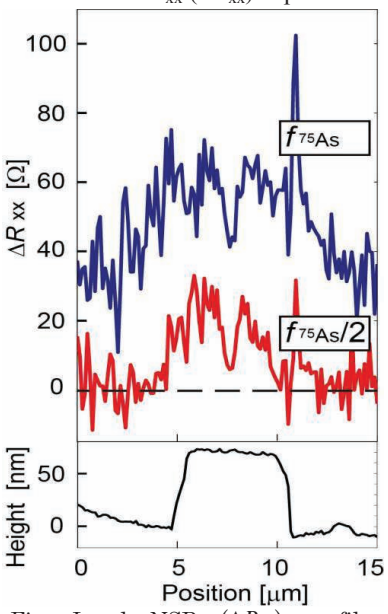

Fig. Local NSR (ΔR_{xx}) profiles measured with applying a RF voltage to the local gate at $f = f_{75As}$ (upper curve) and $f_{75As}/2$ (lower curve) along a line across the Hall bar (See AFM profile in bottom panel); temperature T = 160 mK, static magnetic field B = 8 T; the dashed line: $\Delta R_{xx} = 0$.

Authors are grateful to K. Muraki for supplying the high quality wafers and to S. Goshima and S. Ninomiya for experimental supports.

[1] Y. Hirayama *et al*., Semicond. Sci. Technol. **24**, 023001 (2009). [2] M. Kawamura *et al*., APL. **90**, 022102 (2007). [3] A possible mechanism is argued for the electric NSR observed at a fractional QH system in N. Kumada *et al*., PRL. **101**, 137602 (2008). [4] S. Watanabe *et al*., Physica E **42**, 999 (2010).

Theory of Spin Orbit Effects in Two-Dimensional Electron Gases

Saadi Lamari

Departement de Physique and LESIMS, Faculte des Sciences,
Université Ferhat Abbas I , El Bez, Route d'Alger, Setif 19000 DZ
Algeria

Following the seminal paper of Datta and Das in 1990 [1] where a new kind of device called the spin polarized field effect transistor (spin FET) was introduced for the first time, and in which current flow between source and drain is spin dependent, the study of spin-orbit effects in semiconductor research both by experimentalists and theoreticians has grown tremendously in the last few years thus giving rise to the emerging field of spintronics where the new nano-devices exploit the spin degree of freedom on a large scale. In their original proposal, using a simple model capturing the essential physics Datta and Das show that provided a phenomenological constant α called the Rashba parameter can be tuned by a gate voltage Vg, spin related current modulation follows and a thorough understanding of this parameter was therefore more than necessary.

The experimental as well as the theoretical study of this parameter turned out to be less obvious than first thought due mainly to its sensitivity to many variables such as doping concentration, 2D electron density, non-parabolicity, heterostructure design etc …

In the present contribution and as a follow up to our previous work [2], for heterostructures made of semiconductors with wide to medium size gaps we investigate with the help of our electronic structure calculation codes the relative importance of the main spin orbit mechanisms known as Rashba and Dresselhaus. We also monitor their variations with the applied gate voltage and pay particular attention to their interesting interference effects.

Moreover, we study in detail the influence of the heterostructure design and pay special attention to steps in either the confining potential or the bulk band structure parameters such as the effective mass. Furthermore, in an effort to gain more control on spin orbit importance in heterostructures, we also explore the intricate effects of the interfaces and the barriers and how these together combine to yield the well width dependence of the spin orbit splitting. In addition, particular attention is paid to the effect of tunneling that we monitor as a function of the applied gate voltage.

[1] S. Datta and B. Das, Appl. Phys. Lett. 56, 665 (1990)
[2] S. Lamari, Phys. Rev. B 75 , 155302 (2007)

Spin relaxation in 2D systems with boundaries

V.A. Slipko [1,2*] and Y.V. Pershin [1]

[1]Department of Physics and Astronomy, University of South Carolina, Columbia, SC USA
[2]Department of Physics and Technology, V.N. Karazin Kharkiv National University, Kharkiv, Ukraine
*Email: slipko@univer.kharkov.ua

The D'yakonov-Perel' spin relaxation mechanism in two-dimensional (2D) systems has attracted wide attention because of its fundamental importance for the field of spintronics. However, while all previous studies of D'yakonov-Perel' spin relaxation have been focused on infinite semiconductor systems, the influence of the sample boundaries (actually existing in any experimental system or device) on spin relaxation has received much less attention. As we discuss below, the sample boundaries can dramatically change the character of spin relaxation, result in an incomplete spin relaxation and spin echo effects.

Specifically, we have found [1] that a homogeneous spin polarization in one-dimensional structures of finite length in the presence of Bychkov-Rashba spin-orbit coupling decays spontaneously toward a persistent spin helix. Such a strikingly different and simple method enables us to generate robust spin structures whose properties can be tuned by the strength of the spin-orbit interaction and/or the structure's length. These results can be generalized for the two-dimensional case predicting the formation of a persistent spin helix in two-dimensional channels from homogeneous spin polarization. Our analysis of the formation of a spin helical state is based on an approach mapping spin drift-diffusion equations into a heat equation for a complex field.

Next, let us consider the problem of D'yakonov-Perel' spin relaxation in two-dimensional circles with Rashba spin-orbit interaction [2]. One may think that in small systems the spin relaxation is incomplete as the spin precession angle across the system is small. However, in such a situation, the different effect plays a role: the noncommutativity of spin rotations. Because of this effect, the electron spin precession angle can largely exceed the maximum rotation angle allowed by naive geometrical considerations.

In Ref. [2] we report an exact solution for the problem of electron spin relaxation. Our analysis shows that the spin relaxation in finite-size regions involves three stages and is described by multiple spin relaxation times (see Fig. 1). It is important that the longest spin relaxation time increases with the decrease in system radius but always remains finite. Therefore, at long times, the spin polarization in small 2D systems always decays exponentially with a size-dependent rate. This prediction is supported by results of Monte Carlo simulations.

Finally, we note that an additional insight on spin polarization dynamics might be obtained beyond the traditional drift-diffusion equations approach. In particular, the use of a more general spin kinetic equation [3] allows obtaining novel features of spin polarization on shorter length and time scales. For example, it is found that a propagating spin-polarization profile reflects from a system boundary and returns back to its initial position similarly to the reflectance of sound waves from an obstacle. In addition, there exists an interesting transformation [3] mapping 1D spin kinetic equation into the Klein-Gordon equation with an imaginary mass. This result establishes a novel connection between semiconductor spintronics and relativistic quantum mechanics.

References

[1] V.A. Slipko et al., Phys. Rev. B **83**, 193302 (2011).
[2] V.A. Slipko et al., Phys. Rev. B **84**, 075331 (2011).
[3] V.A. Slipko et al., Phys. Rev. B **84**, 155306 (2011).

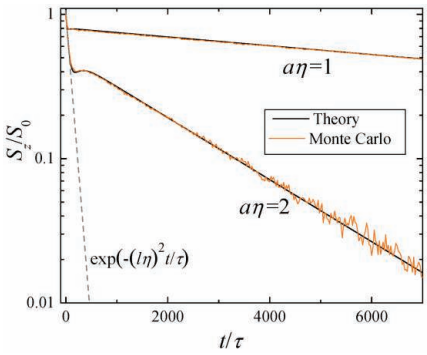

Figure 1: *Time dependence of spin polarization in the center of a 2D circle of radius a (η is the spin rotation angle per unit length).*

Intrinsic phase separation in magnetically doped 2DES

T. Andrearczyk[1,2], Hanna Terletska,[2] T. Wojtowicz[1], G. Karczewski[1] ,T. Dietl[1], V. Dobrosavljević[2], Dragana Popović[2], J. Jaroszynski[2]

[1]*Institute of Physics, Polish Academy of Sciences, Warszawa PL 02-668, Poland;*
[2]*National High Magnetic Field Laboratory, Tallahassee FL 32310, USA;*
E-mail: jaroszy@magnet.fsu.edu

There is growing evidence that phase separation is responsible for several striking effects, such as colossal magnetoresistance (CMR) around metal-insulator transition (MIT) in bulk manganites and similar complex magnetic materials. At the same time, the apparent metal-insulator transition (MIT) in two-dimensional electron systems (2DES) remains one of the most challenging problems of condensed matter physics. Several recent theoretical studies suggest the existence of an intermediate region near the 2D MIT, where the competition between distinct ground states results in their phase separation. Thus particularly intriguing are properties of magnetically doped 2DES in semiconductor heterostructures with their relatively simple electronic and crystal structure. They make it possible to study both magnetism and reduced dimensionality effects near the MIT in one sample with electron density tuned externally.

We report [1] on magnetotransport in 2D modulation doped (Cd,Mn)Te:I diluted magnetic quantum well (QW). This MBE grown sample contains a 10 nm wide $Cd_{0.985}Mn_{0.015}Te$ in which the 2DES is confined by $Cd_{0.8}Mg_{0.2}Te$ barriers. A 10 nm thick layer of the front barrier residing 20 nm away from the QW is doped with iodine donors up to $n_I \approx 10^{18}$ cm^{-3}. A front metal gate controls electron density from 1.4 to 4.2 $\times 10^{11}$ cm^{-2}.

We observe anomalous transport around metal-insulator boundary. Resistivity shows very strong temperature and magnetic field dependence, as in other CMR materials. However, resistivity depends unusually weak on electron density, as figure on the right shows.

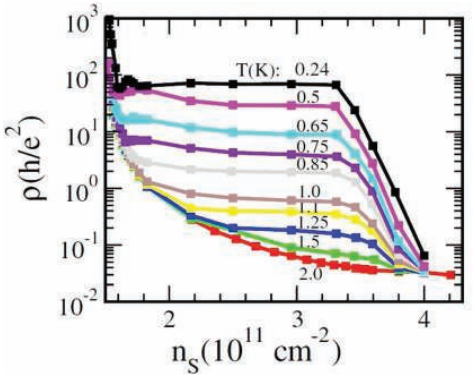

Resistivity of (Cd,Mn)Te heterostructure as a function of electron density at different temperatures shows strikingly weak density dependence.

We suggest, that observed phenomena reflect nanoscale phase separation of the electron fluid and the emergence of ferromagnetic clusters in an intermediate density regime. Our results suggest that the clustering around the MIT is ubiquitous not only in CMR manganites and underdoped cuprates but also in disordered semiconductors. This picture is in striking agreement with recent dynamical mean-field theory calculations. [2]

National Science Centre (Poland) and National Science Foundation (USA) supported the research under grants DEC-2012/06/A/ST3/00247 and DMR-1157490, respectively.

References

[1] J. Jaroszynski et al., Phys. Rev. B 76, 045322 (2007).
[2] H. Terletska and V. Dobrosavljević; Phys. Rev. Lett. 106, 186402 (2011)

TuP72

Comparison of non-local and three-terminal detection of spin accumulation in (Ga,Mn)As/GaAs spin Esaki diode devices

J. Shiogai[1], M. Ciorga[2], M. Kohda[1], M. Utz[2], D. Schuh[2], D. Bougeard[2], T. Nojima[3], J. Nitta[1], and D. Weiss[2]

[1]*Department of Materials Science, Tohoku University, Sendai, Japan*
[2]*Institute for Experimental and Applied Physics, University of Regensburg, Regensburg, Germany*
[3]*Institute for Materials Research, Tohoku University, Sendai, Japan*

Electrical detection of spin accumulation generated by spin injection in ferromagnet/non-magnetic semiconductor heterojunctions is typically realized by four-terminal (4T) measurement in non-local (NL) configuration, *i.e.*, with spin injector and detector circuits separated from each other. An alternative method of spin detection involves three-terminal (3T) measurement (see e.g. [1]) in which both spin injection and detection are performed with a single ferromagnetic contact. The 3T-method is particularly useful in cases when no NL signal can be observed. This technique was successfully employed for many materials, especially Si and Ge [2, 3]. There has been, however, a lot of controversies related to this method, mainly because the amplitude of the measured signal often exceeds by orders of magnitude the prediction of the standard spin drift-diffusion model of the spin injection. In the present work we compare 3T and NL spin signals observed in spin injection devices with (Ga,Mn)As/GaAs spin Esaki diode structures [4].

A spin injection sample is patterned into a 50-μm-wide mesa from a wafer consisting of 50 nm (Ga,Mn)As, 2.2 nm (Al,Ga)As, 8.0 nm n^{++}-GaAs, 15 nm $n^{++} \rightarrow n^{+}$-GaAs, 0.2 μm n^{+}-GaAs, and 0.8 μm n-GaAs grown on semi-insulating GaAs substrate. Ferromagnetic spin injecting and detecting contacts were defined by electron beam lithography, wet chemical etching, and Au / Ti evaporation.

When the external magnetic field is swept along the contacts, spin-valve effect and tunneling anisotropic magnetoresistance (TAMR) effect are observed in NL and 3T voltage, respectively. Out-of-plane field sweeps result in clear Hanle-type depolarization of the spin signal observed in both configurations, thus allowing their direct comparison. We particularly focus on the signal's dependence on bias voltage/current applied to the injector. With increasing bias the NL-signal drops monotonically as spin injection efficiency is lower for higher bias voltages [4]. The 3T signal, on the other hand, increases with increasing bias up to the voltage corresponding to the Esaki dip in the current-voltage characteristic, reaches maximum and decreases upon further increase of the bias. While comparable at low bias, the 3T signal is at the maximum by a factor of ~100 larger than the NL one. A behavior of the 3T-Hanle signal will be discussed in terms of spin accumulation in localized states [1] and also taking into account the effect of electric field on the sensitivity of the spin detection [5].

[1] M. Tran *et al*., Phys Rev. Lett. **102**, 036601 (2009)
[2] S. P. Dash *et al*., Nature **462**, 491 (2009)
[3] H. Saito *et al*., Solid State Comm. **151**, 1159 (2011).
[4] M. Ciorga *et al.*, Phys. Rev. B **79**, 165321 (2009)
[5] A. N. Chantis and D. L. Smith, Phys. Rev. B **78**, 235317 (2008)

Contact geometry dependent spin-valve signal from spin injection devices with (Ga,Mn)As/GaAs spin Esaki diode contacts

Mariusz Ciorga, Martin Utz, Dieter Schuh, Dominique Bougeard, and Dieter Weiss

Institute for Experimental and Applied Physics, University of Regensburg, Regensburg, Germany

Generation of a spin accumulation in non-magnetic semiconductors by means of electrical spin injection and its subsequent electrical detection is one of the key issues in semiconductor spintronics. One of the basic experimental methods used to study spin injection is measurement of the non-local spin valve (NLSV) effect. In such measurement one monitors non-local voltage at the detector contact, resulting from spin injection at the nearby injector, while sweeping magnetic field along the magnetic easy axis of the both contacts. As a result of switching between parallel (P) and antiparallel (AP) alignment of magnetizations in the contacts, one observes a switching in the non-local voltage leading to a typical spin valve signal [1]. From the amplitude of the NLSV one can extract such important parameters as spin injection efficiency or spin diffusion length.

We previously reported on realization of an all-semiconductor GaAs-based scheme for a spin injection/detection with (Ga,Mn)As/GaAs spin Esaki diodes as spin injecting/detecting contacts [2]. From our experiments it became clear that a switching observed in NLSV signal was not caused by a typical mechanism described above but it originated from vanishing of a total spin signal in a certain range of magnetic field instead.

Here we present the results of systematic study of the switching behavior in NLSV signal from such devices. We investigated a dependence of the signal on the geometry of the contacts, i.e., their crystallographic direction, as well as their dimensions. For contacts oriented along [110] we typically observed the antiparallel-parallel (AP–P) switching in NLSV signal, even for the same width of injector and detector contacts [3]. Situation was different however for contacts along [010] direction, geometry used also in experiments described in [2]. Typical results for this geometry are shown in Fig.1. As one can see there exists always a range of magnetic field where spin signal is equal zero. For the case of injector and detector contacts of equal widths (the top panel in Fig.1.) the existence of this "zero spin signal" is a sole origin of the SV-like feature observed in measurements. AP–P switching is observed additionally when one of the contacts is very narrow (bottom panel of Fig.1.) We discuss the observed behavior of the NLSV signal in terms of magnetic anisotropy of narrow (Ga,Mn)As stripes and resulting variation of the angle between direction of injected spins, detector's magnetization and the external magnetic field.

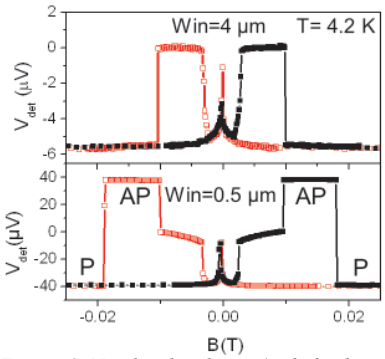

Figure 1 Non-local voltage (with background removed) measured at 4 μm wide detector for different injector widths. All contacts were 50 μm long, oriented along [010] direction.

The work was supported by German Science Foundation (DFG) through the project SFB689.

[1] F. J. Jedema et al., Nature **410**, 345, (2001)
[2] M. Ciorga et al., Phys. Rev. B **79**, 5321(2009)
[3] M. Ciorga et al., AIP Adv. **1**, 022113 (2011)

Spin dynamics in p-doped semiconductor nanostructures subject to a magnetic field tilted from the Voigt geometry

K. Korzekwa[1,2], M. Kugler[3], C. Gradl[3], S. Furthmeier[3], M. Griesbeck[3], M. Hirmer[3], D. Schuh[3], W. Wegscheider[4], C. Schüller[3], T. Korn[3], T. Kuhn[5], P. Machnikowski[2]

[1] *Department of Physics, Imperial College London, London SW7 2AZ, United Kingdom*
[2] *Institute of Physics, Wrocław University of Technology, 50-370 Wrocław, Poland*
[3] *Institut für Experimentelle und Angewandte Physik, Universität Regensburg, 93040 Regensburg, Germany*
[4] *Solid State Physics Laboratory, ETH Zurich, 8093 Zurich, Switzerland*
[5] *Institut für Festkörpertheorie, Universität Münster, 48149 Münster, Germany*

Spintronics, with its possible applications like spin memory or semiconductor spin-based quantum computer, is a very promising branch of nanoscience. However, for the control and readout of spin states one has to maximize their life times. Extended life times observed in semiconductor nanostructures, especially for hole spin states (for which reduced hyperfine interaction makes the spin decoherence slower), seem very promising. Thus, the understanding of the properties of spins in confined semiconductor systems is crucial.

We present a description of the time-resolved Kerr rotation and resonant spin amplification (RSA) experiments on an ensemble of independent holes in a semiconductor nanostructure (e.g., confined in a quantum dot or trapped in a quantum well). We extend our former model [1] to describe spin dynamics in a magnetic field tilted from the Voigt geometry. We study the microscopic evolution of spin polarization and obtain an analytical formula for the Kerr signal. We show that the signal consists of two parts: one depending on hole and the other on trion dynamical variables, each containing damped oscillation and decay terms (due to radiative recombination and hole decoherence). This gives us the insight into effective T_1 and T_2 times and their dependence on the magnetic field tilt angle. We also analytically describe the RSA signal in the limit of small tilt angles, when trion spin dynamics does not differ much from the one in the Voigt configuration, but hole spin dynamics is substantially changed due to the strong anisotropy of the hole g-factor. Specifically we show that the RSA signal is nontrivially affected by the equilibrium spin polarization and that the RSA peaks can get inverted in the tilted field.

In our theoretical approach we treat the pump pulse perturbatively (low-power limit) and use a generic Markovian description of the hole and trion dephasing [2]. To obtain the expression for the RSA signal we find the stationary point of the spin polarization transformation corresponding to one repetition of the pulsed laser (pumping, precession and decoherence). We simplify our expressions by assuming that the trion radiative decay rate is much larger then the hole dephasing rates (which is consistent with the experimental conditions). We include also the inhomogenous broadening of the hole g-factors and model it with the normal distribution. The Kerr and RSA response calculated in this way show good agreement with the experimental results.

[1] M. Kugler, K. Korzekwa, P. Machnikowski, C. Gradl, S. Furthmeier, M. Griesbeck, M. Hirmer, D. Schuh, W. Wegscheider, T. Kuhn, C. Schüller, T. Korn, Phys. Rev. B **84**, 085327 (2011).
[2] P. Machnikowski, T. Kuhn, Phys. Rev. B **81**, 115306 (2010).

Spin Orbit Effects in the 2DEG of Semiconductor Quantum Wells

Saadi Lamari

Departement de Physique and LESIMS, Faculte des Sciences,
Université Ferhat Abbas I , El Bez, Route d'Alger, Setif 19000 DZ
Algeria

Following the seminal paper of Datta and Das in 1990 [1] where a new kind of device called the spin polarized field effect transistor (spin FET) was introduced for the first time, and in which current flow between source and drain is spin dependent, the study of spin-orbit effects in semiconductor research both by experimentalists and theoreticians has grown tremendously in the last few years thus giving rise to the emerging field of spintronics where the new nano-devices exploit the spin degree of freedom on a large scale. In their original proposal, using a simple model capturing the essential physics Datta and Das show that provided a phenomenological constant α called the Rashba parameter can be tuned by a gate voltage Vg, spin related current modulation follows and a thorough understanding of this parameter was therefore more than necessary.

The experimental as well as the theoretical study of this parameter turned out to be less obvious than first thought due mainly to its sensitivity to many variables such as doping concentration, 2D electron density, non-parabolicity, heterostructure design etc …

In the present contribution and as a follow up to our previous work [2], for heterostructures made of semiconductors with wide to medium size gaps we investigate with the help of our electronic structure calculation codes the relative importance of the main spin orbit mechanisms known as Rashba and Dresselhaus. We also monitor their variations with the applied gate voltage and pay particular attention to their interesting interference effects.

Moreover, we study in detail the influence of the heterostructure design and pay special attention to steps in either the confining potential or the bulk band structure parameters such as the effective mass. Furthermore, in an effort to gain more control on spin orbit importance in heterostructures, we also explore the intricate effects of the interfaces and the barriers and how these together combine to yield the well width dependence of the spin orbit splitting. In addition, particular attention is paid to the effect of tunneling that we monitor as a function of the applied gate voltage.

[1] S. Datta and B. Das, Appl. Phys. Lett. 56, 665 (1990)
[2] S. Lamari, Phys. Rev. B 75 , 155302 (2007)

Modulation of the Spin Conductance in a Magnetic Superlattice

Nammee Kim [1,2], Jinwoo Kim [2] and Heesang Kim [1,2]

[1] *Department of Physics, Soongsil University, Seoul 156-743, Korea*
[2] *Institute for Integrative Basic Science, Soongsil University, Seoul 156-743, Korea*

We study the spin miniband structure and the ballistic spin-polarized transport of a magnetic superlattice [1], formed by inhomogeneous magnetic field in a semiconductor nanowire. Based on the transfer matrix theory and Bloch's theorem, we calculate the energy dispersion having spin-minibands and spin-minigaps due to Bloch periodicity and spin-dependent ballistic conductance [2] for various geometrical and physical parameters. Results show that full spin-polarization in the ballistic conductance of the system occurs clearly for each spin, and that the fully spin-polarized range for each spin can be enhanced by modulation of geometrical and physical parameters. For a spin device application of a magnetic superlattice, we also investigate the optimal condition to get a fully spin-polarized current with sizable ballistic conductance. We obtain such a condition by analyzing energy miniband dispersion and a spin dependent transmission probability for each channel. From the results, we propose an optimized aspect ratio of size parameters of a quasi-one dimensional magnetic superlattice as a spin filter to generate currents having simultaneous full spin-polarization and sizable ballistic conductance.

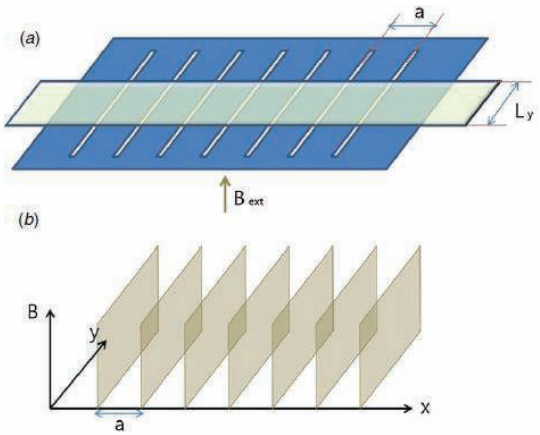

Figure 1. (*a*) Schematic diagram of the spin filter. A quasi-one-dimensional wire is placed on the top of a gridded superconducting mask. *a* is the grid spacing, i.e. the lattice constant and L_y is the width of the wire. External magnetic field is applied. (*b*) Periodic magnetic field profile, applied to the wire.

[1] I. S. Ibrahim and F. M. Peeters, Phys. Rev. B 52, 17321 (1995).
[2] J. L. Cardoso, P. Pereyra, and A. Anzaldo-Meneses, Phys. Rev. B 63, 153301 (2001).

Universal Conductance Fluctuation in Quasi-1D Wires of Epitaxial Bi_2Se_3

Sadashige Matsuo [1], Tomohiro Koyama[1], Kensaku Chida[1], Masaki Nagata[1], Daichi Chiba[1], Kensuke Kobayashi[1,2], Teruo Ono[1], Keith Slevin[2], Tomi Ohtsuki[3], Cui-zu Chang[4], Ke He[4], Xu-cun Ma[4] and Qi-kun Xue[4]

[1] *Institute for Chemical Research, Kyoto University, Uji, Kyoto 611-0011, Japan*
[2] *Department of Physics, Osaka University, Toyonaka, Osaka 560-0043, Japan*
[3] *Department of Physics, Sophia University, Chiyoda-ku,Tokyo 102-8554, Japan*
[4] *Institute of Physics, Chinese Academy of Sciences, Beijing 100190, China*

Bi_2Se_3 is a well-known excellent thermoelectric material and is recently invoking renewed interest as a typical example of a three-dimensional topological insulator. Although a few groups have already reported the conductance fluctuation in this material, its origin is still controversial [1,2].

Here we report the universal conductance fluctuation (UCF) in quasi-1D wires fabricated from epitaxial Bi_2Se_3 thin film. Our purpose is to quantitatively investigate the conductance fluctuation systematically.

We fabricated and measured the quasi-1D wires with the same width but with different lengths. In Fig.1, the typical experimental result of the magnetoresistance in quai-1D wire is shown. We checked the fluctuation in magnetoresistance is reproducible; therefore the fluctuation is intrinsic properties of the wire sample. We extracted the component of the conductance fluctuation, and then we investigated the scaling relationship between the size of the conductance fluctuation and the characteristic lengths such as the coherence length, the thermal diffusion length, and the wire length. Prior to this analysis, we analyzed the weak antilocalization phenomenon, namely the resistance dip structure near 0 T as shown in Fig. 1, and deduced the coherence lengths in each wire samples.

We found that the conductance fluctuation can be well explained as the universal conductance fluctuation.

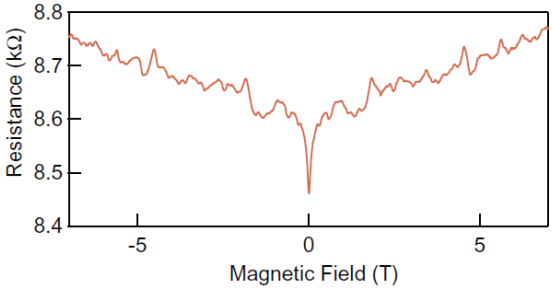

FIG. 1. Typical result of the magnetoresistance of our quasi-1D wire. There are two features; the dip due to the weak antilocalization and the fluctuation.

[1] J. G. Checkelsky, *et al.*, Phys. Rev. Lett. **103**, 246601 (2009)..
[2] S. Matsuo, *et al.*, Phys. Rev. B **85** 075440 (2012).

Electron transport signatures of bulk band inversion in $Pb_{1-x}Sn_xSe$ topological crystalline insulators

K. Dybko, M. Szot, Z. Tkaczyk, A. Szczerbakow and T. Story

Institute of Physics, Polish Academy of Sciences, Al. Lotników 32/46, 02-668 Warsaw, Poland

Topological insulators are a new class of quantum materials in which time-reversal symmetry and relativistic (spin-orbit) effects and inverted band structure result in electronic metallic states on the surface of bulk crystals. These states exhibit Dirac-like energy dispersion across bulk band-gap and are topologically protected against disorder. Theoretical proposals show that topological insulator states can also be induced in new materials by specific crystalline symmetries [1]. The first material that has been theoretically identified as topological crystalline insulator is SnTe [2]. In subsequent research it has been demonstrated that $Pb_{1-x}Sn_xSe$ and $Pb_{1-x}Sn_xTe$ solid solutions exhibiting inverted band structure belong to the same class of topological crystalline insulators family [3,4,5].

Here we report on electric and thermoelectric transport characteristics of topological crystalline insulator samples made of bulk $Pb_{1-x}Sn_xSe$ monocrystals grown by self-selective vapour growth with composition (x) ranging from 0.19 to 0.30. A set of measurements of resistivity as well as Hall, Seebeck and transverse Nernst-Ettingshausen effects were performed for each sample. The PbSe sample served us as a trivial insulator (non-topological) reference. All the samples are highly degenerate with electron concentration on the order $10^{18}cm^{-3}$. Even though the resistivity, Hall and Seebeck coefficients display some broad features in the vicinity of band inversion temperature, its the precise determination requires detailed model of band structure parameters over whole range of compositions. Likely, it occurred that Nernst-Ettingshausen coefficient changes sign, while passing through point where bulk bands interchange their order. The transition temperature obtained this way agrees well with that determined from angle resolved photoemission spectroscopy studies [3]. Furthermore, the non-topological reference sample does not exhibit such a sing change. Consequently, we propose transverse Nernst-Ettingshausen coefficient to be a good experimental signature of transition to topological crystalline insulator state.

Work supported in part by the European Regional Development Fund through the Innovative Economy grant (POIG.01.01.02-00-108/09), and the Polish National Science Centre Grant No. 2011/03/B/ST3/02659.

[1] L. Fu, *Phys. Rev. Lett.* **106**, 106802 (2011).
[2] T.H. Hsieh, H. Lin, J. Liu, W. Duan, A. Bansil and L. Fu, *Nature Commun.* **3**, 982 (2012).
[3] P. Dziawa, B. J. Kowalski, K. Dybko, R. Buczko, A. Szczerbakow, M. Szot, E. Łusakowska, T. Balasubramanian, B. M.Wojek, M. H. Berntsen, O. Tjernberg and T. Story, *Nature Materials*, **11**, 1023 (2012).
[4] Y. Tanaka, Zhi Ren, T. Sato, K. Nakayama, S. Souma, T. Takahashi, Kouji Segawa and Yoichi Ando, *Nature Physics*, **8**, 800 (2012).
[5] Su-Yang Xu, Chang Liu, N. Alidoust, M. Neupane, D. Qian, I. Belopolski, J. D. Denlinger, Y. J. Wang, H. Lin, L. A. Wray, G. Landolt, B. Slomski, J. H. Dil, A. Marcinkova, E. Morosan, Q.Gibson, R. Sankar, F. C. Chou, R. J. Cava, A. Bansil, and M. Z. Hasan, *Nature Comm.* **3**, 1192 (2012).

Observation of 3D massless fermions in a zinc-blende semiconductor at the point of a topological transition

M. Orlita[1,2], D. M. Basko[3], M. Zholudev[4,5], F. Teppe[4], W. Knap[4], V. Gavrilenko[5], N. Mikhailov[6], S. Dvoretskii[6], P. Neugebauer[7], C. Faugeras[1], A.-L. Barra[1], G. Martinez[1], and M. Potemski[1]

[1] *Laboratoire National des Champs Magnétiques Intenses, CNRS, Grenoble, France*
[2] *Charles University, Faculty of Mathematics and Physics, Praha, Czech Republic*
[3] *Université Grenoble 1/CNRS, LPMMC UMR 5493, Grenoble, France*
[4] *Laboratoire Charles Coulomb,CNRS & Université Montpellier II, Montpellier, France*
[5] *Institute for Physics of Microstructures, RAS, Nizhny Novgorod, Russia*
[6] *A.V. Rzhanov Institute of Semiconductor Physics, RAS, Novosibirsk, Russia*
[7] *Institut für Physikalische Chemie, Universität Stuttgart, Stuttgart, Germany*

A spectacular analogy between ultra-relativistic particles in quantum electrodynamic and electrons in some solid-state systems has been demonstrated both in one dimension (carbon nanotubes [1]) and in two dimensions (graphene [2, 3]). However, a three-dimensional (3D) solid-state system whose electrons would mimic massless particles (in which such an analogy would be even closer) appeared to be missing up to now. In the present work, we fabricate and characterize a zinc-blend semiconductor, HgCdTe, at the point of a topological transition. The presence of 3D massless electrons with the velocity about 10^6 m.s^{-1} in this material is clearly manifested (i) by infrared absorption which increases strictly linearly with the photon frequency, and (ii) in a magnetic field B, by a $\sqrt{B}$ dependence of inter-Landau-level resonances, see Fig. 1.

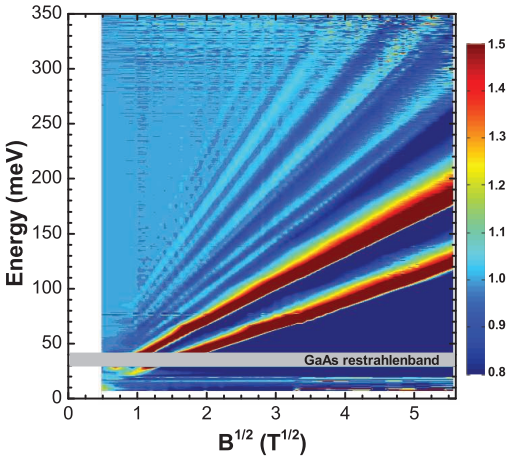

Figure 1: Relative change of absorbance of a thin layer of $Hg_{0.83}Cd_{0.17}Te$, grown by MBE method on a GaAs semi-insulation substrate, plotted as a false color-map. All the observed inter-Landau level resonances clearly follow the characteristic follow the $\sqrt{B}$-dependence, which is typical of massless particles.

[1] J.-C. Charlier, X. Blase, and S. Roche, Rev. Mod. Phys. **79**, 677 (2007).
[2] K. S. Novoselov *et al.*, Nature **438**, 197 (2005).
[3] Y. B. Zhang *et al.*, Nature **438**, 201 (2005).

Weak antilocalization in HgTe quantum wells with inverted and normal energy spectra

Alexander V. Germanenko[1], Grigori M. Minkov[1,2], Andrey A. Sherstobitov[1,2], Olga E. Rut[1], Sergey A. Dvoretski[3], and Nikolai N. Mikhailov[3]

[1] *Institute of Natural Sciences, Ural Federal University, 620000 Ekaterinburg, Russia*
[2] *Institute of Metal Physics RAS, 620990 Ekaterinburg, Russia*
[3] *Institute of Semiconductor Physics RAS, 630090 Novosibirsk, Russia*

The energy spectrum of carriers in single CdTe/HgTe/CdTe quantum well depends drastically on the quantum well width (d) [1]. When thickness is small, $d < d_c \simeq 6.5$ nm, the energy spectrum is characterized by normal band ordering (NBO). It is analogous to that in conventional narrow-gap semiconductors; the highest valence subband at $k = 0$ is formed from the heavy hole Γ_8 states, while the lowest electron subband is formed both from the Γ_6 states and light hole Γ_8 states. For thicker HgTe layer, $d > d_c$, the quantum well is in inverted-band-ordering (IBO) regime; the lowest electron subband is formed from the heavy hole Γ_8 states, whereas the Γ_6 states sink into the valence band.

We present the results of experimental study of the magnetoconductivity of 2D electron gas caused by suppression of the interference quantum correction to the conductivity in HgTe single quantum well heterostructure both with inverted ($d \simeq 9.0$ nm) and with normal ($d \simeq 5$ nm) energy spectrum. Analyzing the shape of the magnetoconductivity curves on the gated Hall bars we obtain the temperature and conductivity dependences of the phase and spin relaxation times (τ_ϕ and τ_s, respectively) over the wide conductivity range, $\sigma = (3 - 130)\, G_0$, where $G_0 = e^2/\pi h$. We have found that the temperature dependences of τ_ϕ and τ_s demonstrate reasonable behavior independently of whether the quantum well is in IBO or NBO regime. The spin relaxation time is constant in the temperature as it should be for the degenerate electron gas. The T dependence of the phase relaxation time is close to $1/T$ that corresponds to inelasticity of electron-electron interaction as the main mechanism of the phase relaxation.

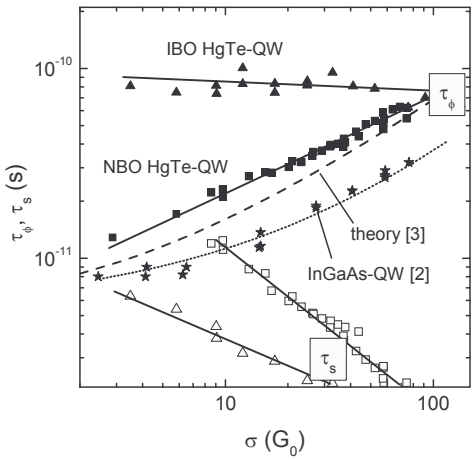

The key result of the report is the conductivity dependence of τ_ϕ shown in the figure. In the quantum well with NBO, it is analogous to that observed in conventional A_3B_5 based 2D system [2] and accords well with theoretical prediction [3]. In the quantum well in the IBO regime, the τ_ϕ value remains practically independent of the conductivity, indicating that the electron interference and/or dephasing processes in the 2D electron systems with inverted band ordering differs significantly from that in conventional systems.

[1] A. Bernevig, T. L. Hughes, and S.-C. Zhang, Science **314**, 1757 (2006).
[2] G. M. Minkov, A. V. Germanenko, and I. V. Gornyi, Phys. Rev. B **70**, 245423 (2004).
[3] G. Zala, B. N. Narozhny, and I. L. Aleiner, Phys. Rev. B **64**, 214204 (2001).

Quantum Magnetotransport in the HgTe Double Quantum Well with Inverted Energy Spectrum

M.V. Yakunin [1], A.V. Suslov [2], S.M. Podgornykh [1], A.P. Savelyev [1], S.A. Dvoretsky [3], and N.N. Mikhailov [3]

[1] *Institute of Metal Physics, Ekaterinburg 620990, Russia*
[2] *National High Magnetic Field Laboratory, Tallahassee, Florida 32310, USA*
[3] *Institute of Semiconductor Physics, Novosibirsk 630090, Russia*

The energy spectrum of the HgTe quantum well wider than 6.3 nm radically differs from a traditional one as it is inverted, thus both its valence and conduction subbands are of the Γ_8 nature. This results in a strong nonparabolicities, large spin splittings [1], strong manifestations of the spin polarization effects [2], overlaps of the conduction and valence subbands *etc.* The question arises: how would manifest such an unusual combination of properties in a double quantum well (DQW) made of HgTe layers? Existence of an additional degree of freedom connected with the possibility for an electron to reside in one of the two interconnected layers is known to result in a formation of new correlation states of the electronic system. Then, how would manifest here the addition of one more degree of freedom – a well pronounced spin degree? And further, how would manifest the inverted energy band structure of HgTe in the DQW? The interest to this subject is still enhanced by the prediction that a special kind of topological insulator may be created in the HgTe DQW.

We present the first experimental study of the DQW system created on the basis of 2D HgTe layers with inverted energy spectrum. The quantum magnetotransport (Fig. 1) reveals a dramatic overlap of the conduction and valence bands, much stronger than in any known single quantum well, which manifests in a pronounced *N*-shaped and double-*N*-shaped Hall magnetoresistance (MR) with multiple quantum features superimposed upon it. In the quantum Hall range of fields, the Hall MR reveals a reentrant behavior between electronic and hole conductivities and a zero resistivity state. The latter appears when the Fermi level enters the gap between the lowest electron and the highest hole Landau levels, while the whole experimental picture is much influenced by the nonmonotonous course of the valence band levels with field connected with its lateral maxima.

[1] M.V. Yakunin, S.M. Podgornykh, N.N. Mikhailov, S.A. Dvoretsky, Physica E **42**, 948 (2010).
[2] M.V. Yakunin, A.V. Suslov, S.M. Podgornykh, N.N. Mikhailov, S.A. Dvoretsky, Phys. Rev. B **85**, 245321 (2012).

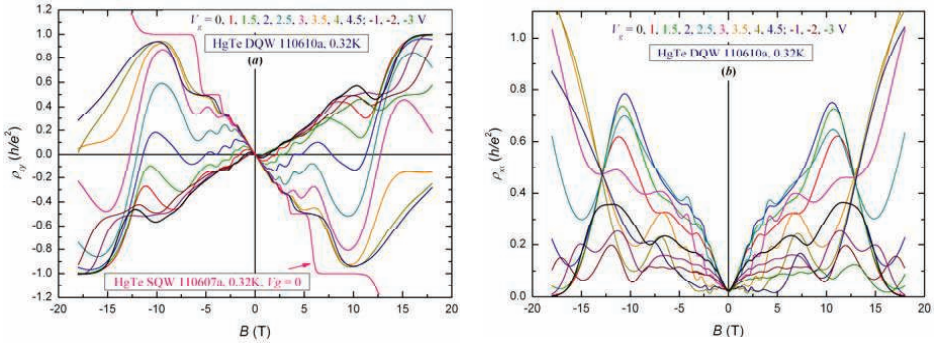

Fig. 1. DQW (a) Hall and (b) longitudinal magnetoresistivities at different gate voltages as compared to a similar single QW [in (a)].

Weak anti-localization in 2D Dirac fermions in CdHgTe/HgTe/CdHgTe quantum well

D. A. Kozlov[1], Z. D. Kvon[1,2], N. N. Mikhailov[1], S. A. Dvoretskiy[1]

[1] *A. V. Rzhanov Institute of semiconductor Physics, 630090, Novosibirsk, Russia*
[2] *Novosibisk State University, 630090, Novosibirsk, Russia*

Weak localization in a system of gapless two-dimensional Dirac fermions in HgTe quantum wells with thickness $d = 6.6$ nm, which corresponds to the transition from a normal to an inverted spectrum and linear energy dispersion law for both electrons and holes, has been investigated experimentally. The experimental samples studied were 6.6 nm $Cd_{0.7}Hg_{0.3}Te$/HgTe/$Cd_{0.7}Hg_{0.3}Te$ QW grown by molecular beam epitaxy on a (013) CdTe/ZnTe/GaAs substrate. The magnetotransport measurements were carried out on hundred μm-sized hallbars. Samples were covered by SiO_2 + Si_3N_4 insulator with total thickness of 300 nm and metallic Ti-Au gate. The main results of the work are following:

1. Magnetotransport measurements were carried out in the temperature range of 0.2-10 K in magnetic fields of up to 1 T. Typical dependence $\rho_{xx}(V_g)$ is a smooth curve with a single maximum which corresponds Fermi energy crossing the Dirac point (fig. 1, left). The maximum value of $\rho_{xx}^{\max}(V_g)$ at $T = 4$ K is $8 - 16$ kOhm (vary for different samples) and curve $\rho_{xx}(V_g)$ is symmetric in the region of ± 0.4 V from the maximum. Such behavior corresponds system of gapless Dirac fermions better then in [1].

2. We investigated quantum corrections to the conductivity for Dirac electrons, holes and for the carriers directly in the Dirac point. A negative logarithmic correction to the conductivity of the system has been observed both at the Dirac point and in the vicinity of this point (fig. 1, middle).

3. The anomalous magnetoresistance of two-dimensional Dirac fermions is positive (fig. 1, right). This indicates that weak localization in the system of two-dimensional Dirac fermions occurs owing to localization and interaction effects in the presence of rapid spin relaxation.

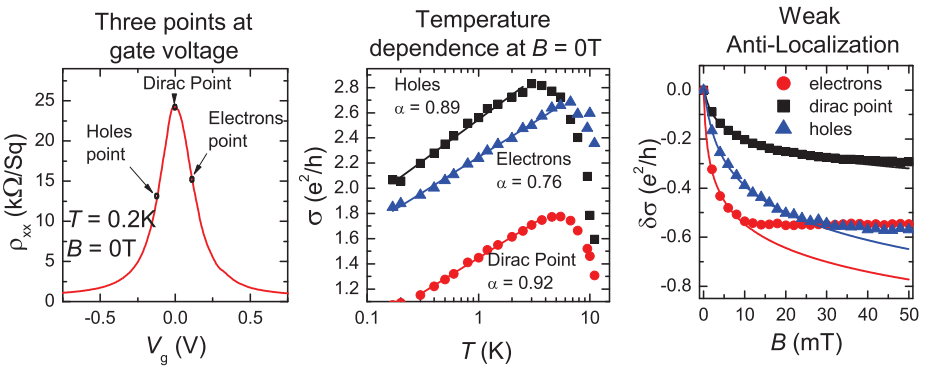

Figure 1: Gate voltage dependence, temperature dependencies and magnetic field dependencies of the resistivity.

[1] B. Büttner *et al.*, Nature Phys **7**, 418 (2011).
[2] D. A. Kozlov *et al.*, JETP Letters, **96** (11), 730 (2012).

Two-dimensional semimetal in a wide HgTe quantum well: magnetotransport and energy spectrum

Grigory M. Minkov[1,2], Alexander V. Germanenko[1], Andrey A. Sherstobitov[1,2], Olga E. Rut[1], Sergey A. Dvoretski[3], and Nikolai N. Mikhailov[3]

[1] *Institute of Natural Sciences, Ural Federal University, 620000 Ekaterinburg, Russia*
[2] *Institute of Metal Physics RAS, 620990 Ekaterinburg, Russia*
[3] *Institute of Semiconductor Physics RAS, 630090 Novosibirsk, Russia*

Two-dimensional (2D) systems based on gapless semiconductors such as HgTe represent unique object. A great variety of two-dimensional electron and hole systems based on this materials can be realized depending on the quantum well width and content of cadmium in $Hg_{1-x}Cd_xTe$ barriers. The energy spectrum and transport phenomena of 2D carriers in HgTe based structures were studied intensively last decade both experimentally and theoretically. The experimental data on the energy distance between the different 2D subbands at zero quasimomentum are in satisfactory agreement with the theory. Electron energy spectrum, electron effective mass and their dependence on the quantum well width are in agreement with the calculation results also. As regards to the experimental data on the valence band energy spectrum, namely the value of bands overlapping, effective masses at $k = 0$ and at large quasimomentum (k), they are discrepant. In this report, we present the results of experimental study of the transport properties of the heterostructure with the 20 nm HgTe quantum well. The measurements were performed over wide range of electron and hole densities including the vicinity of the charge neutrality point. Simultaneous analysis of the gate voltage, V_g, dependences of the positions of the minima oscillations in ρ_{xx} (Fig.1a), periods of Shubnikov-de Haas oscillations and Hall densities (Fig.1b), holes effective mass found from temperature dependence of the oscillations allows us to reconstruct the valence band energy spectrum at $k > 8 \times 10^5$ cm^{-1}, which is plotted in Fig.1c. Already, these results show radical difference from $E(k)$ dependence calculated in framework of three-bands kP-method. The energy spectrum at $k < 8 \times 10^5$ cm^{-1} can be estimated from the analysis of electron (electron-like) and hole densities found from the magnetic field dependences of ρ_{xx} and ρ_{xy} (Fig.1d) at different V_g. These data are presented in Fig.1c also. Thus, the experimental E-vs-k dependence drastically differs from the calculated one. Accordance with other experimental data is discussed.

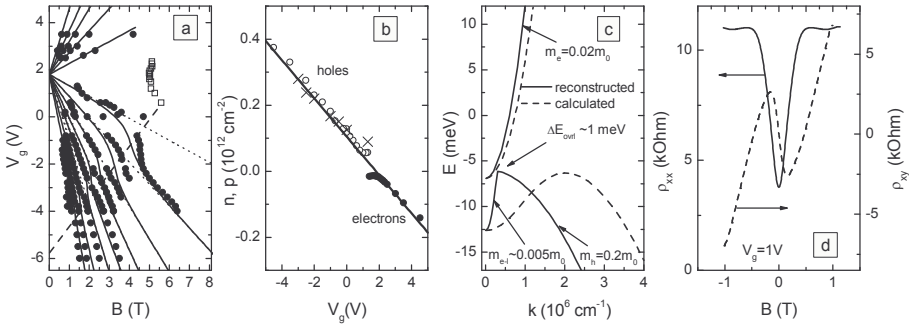

This work has been supported in part by the RFBR (Grant Nos. 11-02-12126, and 12-02-00098).

2DEG resistance asymmetry caused by an effective spin injection in a parallel magnetic field

D. I. Golosov[1], I. Shlimak[1], A. Butenko[1], K.-J. Friedland[2], and S. V. Kravchenko[3]

[1] *Jack and Pearl Resnick Institute of Advanced Technology, Department of Physics, Bar-Ilan University, Ramat-Gan 52900, Israel*

[2] *Paul-Drude Institut für Festkörperelektronik, Hausvogteiplatz 5-7, 10117, Berlin, Germany*

[3] *Physics Department, Northeastern University, Boston, MA 02115, U.S.A.*

Longitudinal resistivity in strong parallel magnetic fields up to B = 14 Tesla was measured in Si-MOSFET with a narrow slot (90nm) in the upper metallic gate that allows to apply different gate voltage across the slot and, therefore, to control the electron density n_1 and n_2 in the two parts of the sample independently. The experimental scheme allows to pass through the source-drain channel relatively large DC current ($I_{\rm DC}$), while the measuring the dynamic resistance. It is found that the sample resistance is asymmetric with respect to the direction of DC current. The asymmetry increases with increase of magnetic field (Fig. 1), DC current, and difference between n_1 and n_2.

These observations can be understood in terms of spin drift-diffusion picture: the degree of spin polarisation is different in the two parts of the sample, implying different magnitudes of spin current away from the slot. The carriers therefore must leave the excess spin (of the appropriate sign) in the region around the slot, leading to *s*pin accumulation (or depletion). The rate of this novel effective spin injection is proportional to I_{DC} and changes sign at $I_{DC} = 0$. Due to the positive parallel-field magnetoresistance of 2DEG, the ensuing magnetisation change around the slot gives rise to an asymmetric correction, $\Delta R = R(I_{DC}, H) - R(0, H)$, in the measured resistance.

We further observe that the value of $R(I_{\rm DC})$ saturates at large $I_{\rm DC}$; possible origins of this effect are discussed. Preliminary results were reported in Ref. [1].

[1] I. Shlimak *et al.*, Solid State Phenomena **190**, 129 (2012).

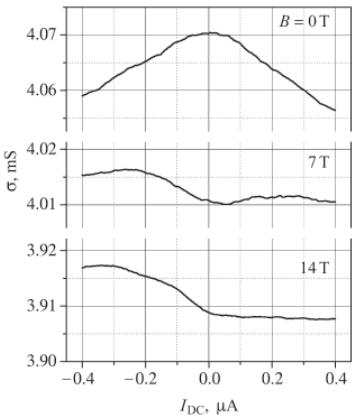

Figure 1: Sample conductance as a function of DC current at $B = 0$, 7, and 14 T. Electron densities in the two parts of the sample are $n_1 = 0.9 \cdot 10^{12}\text{cm}^{-2}$ and $n_2 = 2.5 \cdot 10^{12}\text{cm}^{-2}$, and temperature $T = 0.3$K

Influence of spin polarisation on resistivity of a two-dimensional electron gas in Si MOSFET at metallic densities

I. Shlimak[1], A. Butenko[1], D. I. Golosov[1], K.-J. Friedland[2], and S. V. Kravchenko[3]

[1] *Jack and Pearl Resnick Institute of Advanced Technology, Department of Physics, Bar-Ilan University, Ramat-Gan 52900, Israel*

[2] *Paul-Drude Institut für Festkörperelektronik, Hausvogteiplatz 5-7, 10117, Berlin, Germany*

[3] *Physics Department, Northeastern University, Boston, MA 02115, U.S.A.*

Positive magnetoresistance (PMR) of a silicon MOSFET in parallel magnetic fields B has been measured at high electron densities $n \gg n_c$ where n_c is the critical density of the metal-insulator transition (MIT). It turns out that the normalised PMR curves, $R(B)/R(0)$, merge together when the field is scaled according to $B/B_c(n)$ where B_c is the field in which electrons become fully spin polarised. The values of B_c in Fig. 1 have been calculated from the simple equality between the Zeeman splitting energy and the Fermi energy taking into account the experimentally measured dependence of the spin susceptibility on the electron density. This extends the range of validity of the scaling all the way to a deeply metallic regime far away from MIT. The subsequent analysis of PMR for low $n \gtrsim n_c$ demonstrated that the merging of the initial parts of curves can bee achieved only with taking into account the temperature dependence of B_c (hence introducing a renormalised value, B_c^*, in Fig. 1). It is also shown that the shape of the PMR curves at strong magnetic fields is affected by a crossover from a purely two-dimensional (2D) electron transport to a regime where out-of-plane carrier motion becomes important (quasi-three-dimensional regime)[1].

[1] I. Shlimak *et al.*, Europhys. Lett. **97**, 37002 (2012).

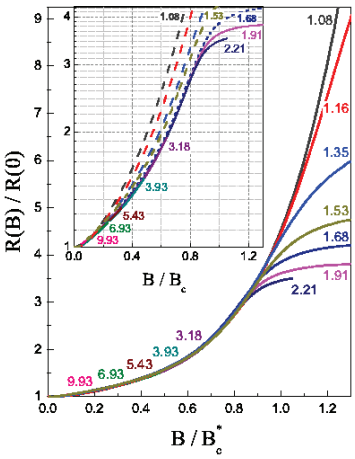

Figure 1: Normalised magnetoresistance $R(B)/R(0)$ scaled as a function of B/B_c (inset) and as a function of B/B_c^* (main panel). Values of n are in units of 10^{11}cm^{-2}; for $n \geq 2.21\text{cm}^{-2}$, the position of each value marks the end of the corresponding curve.

TuP86

Modelling of *bcc* multicomponent low dimensional structures composed of transition metals and metalloids

A. Go [1]

[1] *Faculty of Physics, University of Białystok, Lipowa 41, 15-424 Białystok, Poland*

Bcc multicomponent alloys composed of transition metals and metalloids are interesting from both applied and basic physics. Their ordering processes result in formation of a large class of alloys, some of them having quite extreme characteristics such as large negative magnetoresistance in Fe_2VAl and quenched $Co_2Cr_{0.6}Fe_{0.4}Al$, semi-magnetic properties in NiMnSb, or semiconductor-like temperature dependence of the resistivity in Fe_2VAl [1 and references therein]. These properties are reflected in the electronic structure of the alloys. On the other hand, it is well known, that a shape and a size of a structure strongly influences on its electronic and magnetic properties. The aim of the study is to show how these geometrical features change electronic densities of states of the b*cc* multicomponent alloys composed of transition metals and metalloids. Additionally transition from surface to bulk magnetic properties is analyzed.

Band structure calculations of the investigated alloys are carried out within the framework of generalized gradient approximation using FP-LAPW method.

[1] K. Perzyńska, K. Szymański, M. Biernacka, A. Go, W. Olszewski, D. Oleszak, K. Rećko, J. Waliszewski, P. Zaleski, L. Dobrzyński, J.Phys.Soc.Japan **81** 064715 (2012).

Light-induced dissipationless electron transport in quantum wells

O. V. Kibis

Department of Applied and Theoretical Physics, Novosibirsk State Technical University, Novosibirsk 630073, Russia

It is well known that the strong interaction between a solid and a monochromatic electromagnetic field with a frequency ω_0 can open energy gaps $\Delta\varepsilon$ within electron energy bands of the solid due to the dynamical Stark effect [1,2]. These gaps $\Delta\varepsilon$ are opened in the resonant points of $\boldsymbol{k}$ space (i.e., at electron wave vectors $\boldsymbol{k}$ satisfying the condition of "the photon energy $\hbar\omega_0$ is equal to the energy interval between electron bands"). If the electron energy spectrum of the solid is symmetric, $\varepsilon(\boldsymbol{k}) = \varepsilon(-\boldsymbol{k})$, the resonant points — and, correspondingly, the gaps $\Delta\varepsilon$ — are positioned symmetrically in the $\boldsymbol{k}$ space with respect to band edges [see Fig.1(a)]. Though the light-induced gap opening has been known for a long time [1,2], its theory was developed exclusively for solids with such a symmetric electron energy spectrum. It follows from the fundamentals of quantum mechanics that the asymmetric energy spectrum of electrons, $\varepsilon(\boldsymbol{k}) \neq \varepsilon(-\boldsymbol{k})$, can exist in systems with broken time-reversal symmetry. Particularly, it takes place in nanostructures in the presence of a magnetic field. For definiteness, let us consider an asymmetric quantum well (QW) confining electrons in the plane (x,y), which is exposed to an in-plane magnetic field H_y directed along the y axis. It is well-known that the electron energy spectrum of the QW consists of a set of subbands which are shifted along the k_x axis with respect to each other by the wave vector $\Delta k_x \propto H_y$ [3]. This diamagnetic shifting, which is schematically pictured in Fig. 1(b), leads to the asymmetric energy spectrum of electrons, $\varepsilon(k_x) \neq \varepsilon(-k_x)$, in the QW. As a consequence of this asymmetry, resonant points of the intersubband electron-photon interaction are positioned asymmetrically in the $\boldsymbol{k}$ space with respect to subband edges. Correspondingly, the photon-induced energy gaps $\Delta\varepsilon$ are positioned asymmetrically within the subbands. The remarkable feature of such an asymmetrically gapped energy spectrum is the nondissipative flowing of electron gas. For instance, let an electron gas fills states under the Fermi level μ [see Fig. 1(b)]. It is easy to show that the electric current along the x axis, produced by the electron gas, is $j_x \propto \Delta\varepsilon$. Since this nonzero current is associated to the ground state of the electron system, it flows without dissipation. Thus, the photon-dressed electron system with broken time-reversal symmetry can demonstrate the superconductor-like behavior. The theory of this novel quantum phenomenon is developed in the recent papers [4,5] and will be presented in the given talk.

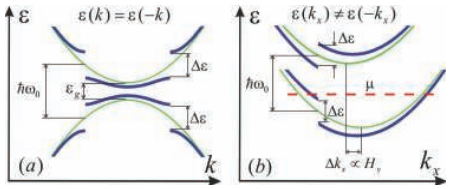

FIG. 1: Energy spectrum of free electrons (thin lines) and electrons dressed by an electromagnetic field with the frequency ω_0 (solid lines): (a) conductivity band and valence band in a bulk semiconductor with the band gap ε_g [2]; (b) first two electron subbands in an asymmetric quantum well exposed to an in-plane magnetic field H_y [5].

The work was partially supported by the Seventh European Framework Program (project FP7- 316432) and the RFBR (projects 13-02-90600 and 13-02-92600).

[1] V. M. Galitskii, S. P. Goreslavskii, and V. F. Elesin, Sov. Phys. JETP **30**, 117 (1970).
[2] S. P. Goreslavskii and V. F. Elesin, JETP Lett. **10**, 316 (1969).
[3] T. Ando, A. B. Fowler, and F. Stern, Rev. Mod. Phys. **54**, 437 (1982).
[4] O. V. Kibis, Phys. Rev. Lett. **107**, 106802 (2011).
[5] O. V. Kibis, Phys. Rev. B **86**, 155108 (2012).

Microwave polarization dependence of magnetoresistance oscillations of 2DES

Jesus Inarrea

Escuela Politécnica Superior, Universidad Carlos III, Leganes, Madrid, Spain

We solve analytically the time dependent Schrodinger equation of a two-dimensional quantum oscillator subjected to a time-varying force. As a direct application, we analyzed a two-dimensional electron system under a static and uniform magnetic field and microwave radiation. The obtained formalism is applied to the case of linearly polarized microwave induced resistance oscillations measured in a two-dimensional electron gas. We use the obtained formalism to study the role of the polarization angle on the radiation-induced magnetoresistance. We consider different regimes, from the radiation electric field parallel to the current (0^0) to perpendicular to it (90^0). We obtain, in agreement with recently measured experimental results [1], that magnetoresistance (R_{xx}) is sensitive to the orientation of the radiation electric field and that it is damped from the parallel to the current configuration to perpendicular to it (see Fig. 1). This is in clear contradiction with previous experimental and theoretical evidence. Here we present a novel theoretical approach based in the sample quality and shape, trying to reconcile both scenarios.

[1] A. N. Ramanayaka et al., Phys. Rev. B, 85, 205315 (2012).

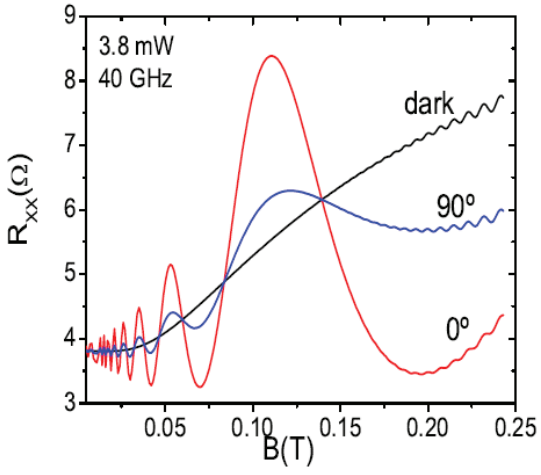

Figure 1

Influence of surface states on quantum and transport lifetimes in high-quality undoped heterostructures

D. Q. Wang[1], J. C. H. Chen[1], O. Klochan[1], K. Das Gupta[2], D. Reuter[3], A. D. Wieck[3], D. A. Ritchie[2], and A. R. Hamilton[1]

[1] *School of Physics, University of New South Wales, Sydney NSW 2052, Australia*
[2] *Cavendish Laboratory, J. J. Thomson Avenue, Cambridge, CB3 OHE, United Kingdom*
[3] *Angewandte Festkörperphysik, Ruhr-Universität Bochum, D-44780 Bochum, Germany*

While extremely high mobility 2D systems have been realized in modulation-doped heterostructures, remote ionized impurities, which can act as an additional source of disorder causing both Coulomb scattering and long-range fluctuation of the potential landscape, are ineluctably introduced to the system[1]. Therefore, the presence of these ionized impurities is the predominant factor limiting the transport and stability of shallow modulation-doped heterostructures[2, 3]. Undoped heterostructures, on the other hand, are expected to have fewer ionized impurities owing to the absence of intentional doping, which makes shallow undoped hereostructures more desirable than modulation-doped ones for nanostructures with fine lithographic configurations. However, there still exists unavoidable surface charge, which may affect the carriers in a manner similarly to remote ionized impurity scattering, adding unwanted disorder to undoped devices. We present a comparison between experimental and theoretical values of transport τ_t and quantum τ_q scattering lifetimes in high-quality undoped AlGaAs/GaAs heterostructures. We obtain excellent agreement between the experimental and modeled scattering times using three scattering processes: background impurity (BI) scattering, interface roughness (IR) scattering, and remote ionized impurity scattering from surface charge (SC). We show that despite the high mobility ($\mu_{peak} = 5.6 \times 10^6 cm^2 V^{-1} s^{-1}$), the quantum lifetime τ_q is significantly reduced by small-angle scattering from remote surface charge. We further show that in shallow undoped heterostructures scattering from surface charge will be a limiting factor for both transport and quantum lifetimes.

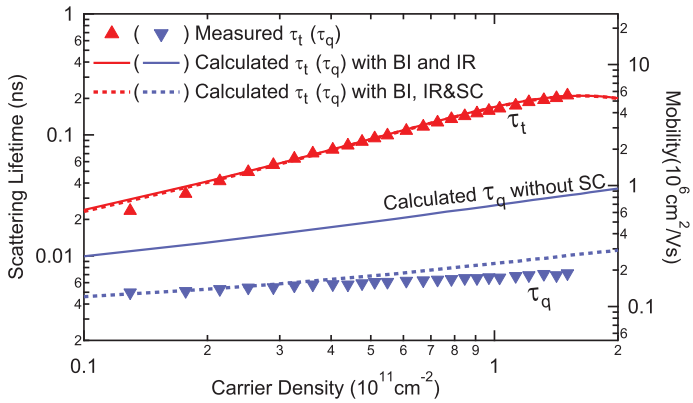

[1] B.E. Kane, L.N. Pfeiffer, K.W. West, and C.K. Harnett, Appl. Phys. Lett. **63**, 2132 (1993).
[2] D. Laroche, S. Das Sarma, G. Gervais, M.P. Lilly, and J.L. Reno, Appl. Phys. Lett. **96**, 162112 (2010).
[3] A.M. See, B.C. Scannell *et al.*, Phys. Rev. Lett. **108**, 196807 (2012).

Direct band structure measurements of a buried δ-layer

Jill A. Miwa[1], Philip Hofmann[1], Michelle Y. Simmons[2] and Justin W. Wells[3]

[1] *Department of Physics and Astronomy, Interdisciplinary Nanoscience Center (iNANO), Aarhus University, 8000 Aarhus C, Denmark.*
[2] *Centre of Excellence for Quantum Computation and Communication Technology, School of Physics, University of New South Wales, Sydney, NSW 2052, Australia.*
[3] *Department of Physics, Norwegian University of Science and Technology (NTNU), N-7491 Trondheim, Norway.*

We directly measure the band structure of a buried two dimensional electron gas (2DEG) using angle resolved photoemission spectroscopy [1]. The buried 2DEG is formed several nanometers beneath the surface of p-type silicon (001), because of a dense δ-layer of phosphorus n-type dopants which are placed there. Although the δ-layer is deeply buried, relative to the photoelectron mean free path, photoemission is still possible at very low kinetic energies, or when a resonant enhancement is invoked.

Here we present direct measurements of the band structure of the buried 2DEG using angle resolved photoemission spectroscopy (ARPES). Our measurements confirm the layer to be metallic and give direct access to the Fermi level position, as well as facilitating a direct comparison with calculations. In addition, we report the dependence of the band structure on properties such as dopant confinement and temperature, and discuss the resonant enhancement mechanism which facilitates such measurements.

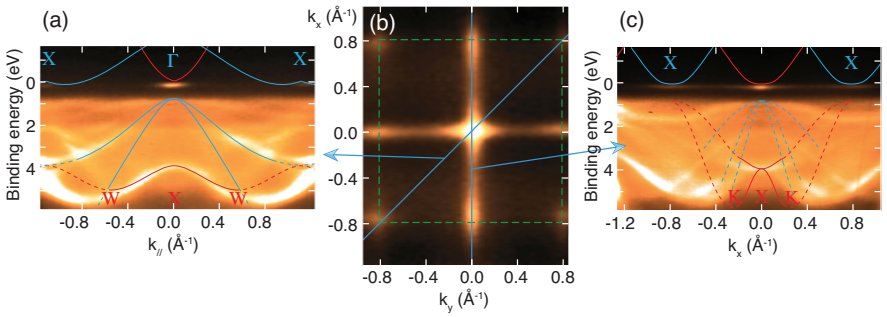

Figure 1: Measured band structure **a,c** and Fermi surface **b** of δ-doped Si(001), with band structure calculations from Ref. [2] overlaid. *Adapted from Ref. [1].*

[1] Jill A. Miwa, Philip Hofmann, Michelle Y. Simmons and Justin W. Wells. Phys. Rev. Lett. *(accepted)*, arxiv.org/abs/1210.7113
[2] M. Rohlfing, P. Krüger, and J. Pollmann. Phys. Rev. B, **48**:17791, 1993.

Theory of radiation-induced zero resistance states in 2D systems

Ivan A. Dmitriev[1,2]

[1] *Institute for Theoretical Condensed Matter physics, Karlsruhe Institute of Technology, 76128 Karlsruhe, Germany*
[2] *Ioffe Physical Technical Institute, 194021 St. Petersburg, Russia*

Illumination of 2D electron systems by radiation detuned from a multiple of the cyclotron frequency can lead to vanishing dissipative resistance that is associated with an electrical instability and spontaneous formation of domains [1, 2, 3, 4, 5]. Such zero resistance states (ZRS) were initially discovered in high-mobility semiconductor 2D systems [2, 3], and, more recently, in 2D electron liquid on the surface of liquid He [4, 5]. ZRS should also be observable in graphene. We develop a model of the domain state in such nonequilibrium radiation-driven 2D system [6]. The analytical solution enables us to build the phase diagram incorporating continuous and discontinuous transitions between the uniform and domain states in a biased finite-size system. We calculate the residual negative resistance in the domain state and discuss the bias-induced transverse instability of the simplest domain configurations. We also study dynamics of the domain formation in 2D electron system on surface of liquid He [7], where the associated charge transfer can be monitored as image charges in a properly designed system of electrostatic gates [5].

[1] I. A. Dmitriev, A. D. Mirlin, D. G. Polyakov, and M. A. Zudov, Rev. Mod. Phys. **84**, 1709 (2012).
[2] R. G. Mani, J. H. Smet, K. von Klitzing, V. Narayanamurti, W. B. Johnson, and V. Umansky, Nature (London) **420**, 646 (2002).
[3] M. A. Zudov, R. R. Du, L. N. Pfeiffer, and K. W. West, Phys. Rev. Lett. **90**, 046807 (2003).
[4] D. Konstantinov and K. Kono, Phys. Rev. Lett. **105**, 226801 (2010).
[5] D. Konstantinov, A. Chepelianskii, and K. Kono, J. Phys. Soc. Jpn. **81**, 093601 (2012).
[6] I. A. Dmitriev, M. Khodas, A. D. Mirlin, and D. G. Polyakov, in preparation.
[7] A. D. Chepelianskii and I. A. Dmitriev, in preparation.

TuP92

Effect of electron-electron interactions on the magnetoresistivity of a weakly-screened, low-density, two-dimensional electron liquid

I. Karakurt[1] **and A.J. Dahm**[2]

[1] *Department of Physics, Işık University, Şile, Istanbul 34980, Turkey*
[2] *Department of Physics, Case Western Reserve University, Cleveland, OH 44106-7079, USA*

We study the strength of electron-electron interactions using magneto-resistivity measurements of two dimensional non-degenerate electrons on helium. Magneto-resistivity of electrons were measured as a function of a magnetic field transverse to the two-dimensional electron layer. With our ability to achieve very low densities we were able to study the effect of electron-electron interactions on magneto-resistivity in the classical regime and at intermediate fields. We observe a crossover from strongly-interacting electron (Drude) regime to independent-electron regime where the data are qualitatively described by self-consistent Born approximation (SCBA) at finite fields. Our data confirm the theory of Lea and Dykman [1-3], and show that electron-electron interactions are important to very low densities. We also find that the SCBA magnetoresistance is density dependent, which in turn suggests that SCBA theory is incomplete.

[1] M.I. Dykman and M.J. Lea and P. Fozooni and J. Frost, Phys. Rev. Lett., 70, 395 (1993).
[2] M.J. Lea and M.I. Dykman, Philos. Mag. B, 69, 1059 (1994).
[3] C.Fang-Yen and M.I. Dykman and M.J. Lea, Phys. Rev. B, 55, 16249 (1997).

Microscopic theory for the Doppler velocimetry of spin propagation in semiconductor quantum wells

M. Q. Weng and M. W. Wu

Hefei National Laboratory for Physical Sciences at Microscale and Department of Physics, University of Science and Technology of China, Hefei, Anhui, 230026, China

We provide a microscopic theory for the Doppler velocimetry of spin propagation in the presence of spatial inhomogeneity, driving electric field and the spin orbit coupling in the (001) GaAs quantum wells in a wide range of temperature regime based on the kinetic spin Bloch equation. It is analytically shown that when the spin-orbit coupling is weak enough and only the elastic scattering is important, the spin density wave with wave vector q envolves as

$$\begin{aligned} S_z(x,t) &= S_z(q,0)\exp[-(Dq^2+1/\tau_s)t]/2 \\ &\quad\times\left\{e^{-2Dqq_0t}\cos[qx-v_d(q+q_0')t]+e^{2Dqq_0t}\cos[qx-v_d(q-q_0')t]\right\}. \quad (1) \end{aligned}$$

Here D, τ_s and v_d are the spin diffusion coefficient, spin relaxation time of the spin density wave and the drift velocity under the electric field E, respectively. q_0 and q_0' are determined by the spin-orbit coupling. Therefore under an applied electric field, the spin density wave gains a time-dependent phase shift $\phi(t)$. Without the spin-orbit coupling ($q_0 = q_0' = 0$), $\phi(t) = v_d q t$ which is equivalent to a normal Doppler shift in optical measurements. Without the applied electric field ($v_d = 0$) the amplitude of the spin density wave decays biexponentially with fast and slow rates $Dq^2 + 1/\tau_s \pm 2Dqq_0$. Due to the joint effect of spin-orbit coupling and the applied electric field, the phase shift behaves differently at the early and the later stages. At the early stage, the fast and slow modes share the same weights, therefore the phase shifts are the same with or without the spin-orbit coupling. While at the later stage, the phase shift becomes $\phi(t) = v_d(q - q_0)t$ and deviates from the normal Doppler one as the the slow mode becomes dominating mode. The crossover time from the early normal Doppler behavior to the anomalous one at the later stage is about $t_c \sim 1/(4D|qq_0|)$, which is inversely proportional to the spin diffusion coefficient, wave vector of the spin density wave and the spin-orbit coupling strength. In the high temperature regime, the crossover time becomes large as a result of the decreased spin diffusion coefficient. The analytical results capture all the quantitative features of the experimental results, while the full numerical calculations agree quantitatively well with the experimental data obtained from the Doppler velocimetry of spin propagation [1]. We further predict that the coherent spin precession, originally thought to be broken down at high temperature, is robust up to the room temperature for narrow quantum wells. We point out that one has to carry out the experiments longer to see the effect of the coherent spin precession at higher temperature due to the larger crossover time [2].

We also study the ambipolar transport of the spin density wave in (111) GaAs quantum well. Due to the smaller hole diffusion coefficient and enhanced hole spin relaxation time in (111) quantum well near the cancellation gate voltage [3], both hole and electron spin could be important. In some cases hole spin could even surpass the electron spin. This is quite different from the case in (001) quantum well, where hole spin quickly diminishes.

[1] L. Yang, J. D. Koralek, J. Orenstein, D. R. Tibbetts, J. L. Reno, and M. P. Lilly, Nat. Phys. **8**, 153 (2012).
[2] M. Q. Weng and M. W. Wu, Phys. Rev. B **86**, 205307 (2012).
[3] L. Wang and M. W. Wu, Phys. Rev. B **85**, 235308 (2012).

TuP94

Terahertz Induced Magnetoresistance Oscillations of a High_Density and High_Mobility Two_Dimensional Electron Gas

Z. D. Kvon [1,2], D. A. Kozlov [1,2] S. N. Danilov [3], C. Zoth [3], P. Vierling[3], S. Stachel[3], V. V. Bel'kov [3], and S.D.Ganichev [3]

[1] *Institute of Semiconductor Physics, Siberian Branch, Russian Academy of Sciences, pr. Akademika Lavrent'eva 13, Novosibirsk, 630090 Russia*

[2] *Novosibirsk State University, ul. Pirogova 2, Novosibirsk, 630090 Russia*

[3] *Terahertz Center, University of Regensburg, D 93040 Regensburg, Germany*

One of the remarkable phenomena discovered in two dimensional electron systems in the past decade is the phenomenon of microwave induced magnetoresistance oscillations which under certain conditions exhibit zero-resistance states [1]. Until recently, the great majority of works in this direction have been devoted to experiments in the microwave range (1–250 GHz), although the question of existence of these oscillations in the terahertz range is of undoubted interest. It is noteworthy that such investigations are hindered by a drastic decrease in the oscillation amplitude with an increase in the radiation frequency. Thus, investigation of the terahertz response of a 2DEG, especially at frequencies of about 1 THz, remains currently topical. In this work, we present the results of studying the terahertz response of a 2DEG to irradiation at a frequency of 0.7 and 1.63 THz. We measured the terahertz response (photoresistance and photovoltage) of the above structures at wavelengths of 432 and 184 μm in magnetic fields of up to 3 T. The experimental samples were Hall bars with a width of 50 μm and a distance between the voltage contacts of 350 μm fabricated on the basis of GaAs 13 nm quantum well with a high density (N_s = (0.8–1.0) × 10^{12} cm^{-2}) and high mobility (μ = (1.5–2) × 10^6 cm^2/Vs) two-dimensional electron gas (2DEG). The side barriers of the well were formed by an AlAs/GaAs superlattice, which made it possible to produce a high mobility 2DEG with a high electron density in the well. A molecular laser with an optical pumping by a CO_2 laser was used as a terahertz source. The terahertz radiation power was about 80 and 5 mW at the 184 and 432 μm lines, respectively. Photoresistance was measured with the use of a standard Lock-in detection at a modulation frequency of 200–270 Hz and the dc bias current across the sample I = (10–40) μA. The current source was disconnected to measure photovoltage. The main results are as follows:

1. The most interesting result is the observation of terahertz induced magnetoresistance oscillations (TIRO) of a high mobility 2DEG with the period corresponding cyclotron resonance harmonics These oscillations are observed only under of 0.7 THz radiation and its amplitude strongly growth as the temperature decreases from 10 K to 1.9 K. At 1.9 K oscillations with harmonics number up to 9 were clearly observed.

2. Study of the influence of random potential character on TIRO manifests the strong influence of its microscopic structure of this potential: screening of its long range part leads to the significant increasing of TIRO amplitude.

3. Under 1.63 THz radiation only the second and third harmonics were observed in photovoltage signal and there was no observable photoresistance oscillations.

[1]. I. A. Dmitriev, A. D. Mirlin, D. G. Polyakov, and M. A. Zudov, Rev. Mod. Phys. **84**, 1709 (2012).

Conductance matrix in silicon nanosandwiches

N.T. Bagraev, E.Yu. Danilovskii, D.S. Gets, L.E. Klyachkin , A.M. Malyarenko

Ioffe Physical Technical Institute of the Russian Academy of Sciences, St. Petersburg, Russia

The quantum conductance studies are the subject of a considerable amount of researches that is caused by applying to quantum computing phenomena [1]. The Landauer-Buttiker formalism (LBF) is well-known to be a powerful tool for the analysis of the quantum conductance revealed by measuring the transport characteristics of multi-terminal devices [2]. Within frameworks of the LBF approach, the total current in such systems is presented in the matrix form as $\boldsymbol{I} = \boldsymbol{GV}$, where $\boldsymbol{I}$ and $\boldsymbol{V}$ are column vectors for the probe currents and voltages, whereas $\boldsymbol{G}$ is an $N \times N$ - conductance matrix and N is the number of probes.

Here we present the developments of the conductance matrix to study the spin-dependent transport in the eight-terminal device that was prepared by using the silicon nanosandwich which is the high mobility p-type silicon quantum well (Si-QW), 2 nm, confined by the δ-barriers heavily doped with boron on the *n*-type Si (100) surface. These silicon nanosandwiches performed within frameworks of the Hall geometry of leads have been shown to be interested in the studies of the ballistic and mesoscopic transport, because the boron centers inside the δ-barriers appeared to be the impurity dipoles formed by the negative-U reconstruction of the shallow boron acceptors along the <111> crystallographic axis, $2B^0 \rightarrow B^+ + B^-$ [3]. Moreover, the dipole negative-U centers of boron have been found to be electrically ordered thereby forming the topological edge states in the Si-QW that are vertically separated, with the variations of both the sheet density of 2D holes and Rashba spin-orbital interaction by biasing the top gate voltage.

In order to identify the conductance matrix, we measured the values of voltages $U_{i,j}$ between all probes at different directions of the highly-stabilized current $I_{i,j}$, where i,j – indexes of probes. Then, the data obtained were used to solve the system of the linear algebraic equations based on the Kirchhoff's circuit laws for each from the eight terminals. Thus, the conductance matrix $\boldsymbol{G}$ was achieved taking account of the instrument and statistical accuracy of every element $G_{i,j}$, which are able to demonstrate the quantum conductance of the silicon nanosandwich in units of e^2/h.

The longitudinal, $G_{xx} = 4e^2/h$, and transversal, $G_{xy} = e^2/h$, conductance of the silicon nanosandwiches that were registered at extremely low value of the stabilized source-drain current, 0.25 nA, has been found to indicate the exhibition of the Quantum Spin Hall effect [4]. These results are discussed in the LBF terms applied to the topological edge states that are vertically separated being belonged to different δ–barriers.

The conductance matrix allows the verification of the top-gate bias dependence on the conductance matrix element $G_{i,j}$ separately. Besides, the multi-current experiment becomes to be performed using four terminals as current probes, while another four terminals are voltage probes. This area appears to be very perspective also to analyze the local coherent transport in the asymmetrical 2D-topological insulators and superconductors.

[1] S. Das Sarma, M. Freedman, C. Nayak, Phys. Rev. Lett. **94**, 166802 (2005).
[2] M. Buttiker, Phys. Rev. Lett. **57**, 1761 (1986).
[3] N.T.Bagraev, N.G.Galkin, W.Gehlhoff, L.E.Klyachkin, A.M.Malyarenko, J. Phys. Condens. Matter. **20**, 164202 (2008).
[4] N. T. Bagraev, E. Yu. Danilovskii, L. E. Klyachkin, A. M. Malyarenko, V. A. Mashkov, Semiconductors **46**, 75 (2012).

TuP96

Fractional quantum conductance in silicon nanosandwiches

N.T. Bagraev, E.Yu. Danilovsky, D.S. Gets, L.E. Klyachkin, A.A. Kudryavtsev, A.M. Malyarenko

Ioffe Physical-Technical Institute, 194021, St. Petersburg, Russia

We present the findings for the fractional quantum conductance of holes that is caused by the edge channels in the silicon nanosandwiches prepared within frameworks of the Hall geometry. These nanosandwiches represent the ultra-narrow *p*-type silicon quantum well (Si-QW), 2 nm, confined by the δ-barriers heavily doped with boron on the *n*-type Si (100) surface [1]. The edge channels in the Si-QW plane are revealed by measuring the longitudinal quantum conductance staircase, G_{xx}, as a function of the voltage applied to the Hall contacts, U_{xy}. It should be noted that the important condition to register quantum conductance staircase is to stabilize the drain-source current in the range of 0.1 ÷ 10 nA.

In addition to the standard plateaus, $2(e^2/h)\cdot N$, the quantum conductance staircase appears to reveal the additional plateaus at the values of $7/4\cdot(e^2/h)$, $3\cdot(e^2/h)$, and $15/4\cdot(e^2/h)$; where N denotes the number of the filled one-dimensional hole subbands. This fractional quantum conductance seems to result from the ferromagnetic exchange interaction between localized and propagating holes that gives rise to the high degree the spin polarization [2]. These findings became possible owing to the small effective mass, $<6\cdot10^{-4}\ m_0$, of the heavily holes that was controlled by studying the temperature dependences of the de Haas – van Alphen oscillations in low sheet density Si-QW [3]. Besides, the effective mass values appear to be in a good agreement with both the cyclotron resonance data and the estimations from the period of the Aharonov-Casher oscillations [1].

The G_{xx} fractional values revealed by tuning the U_{xy} voltage appear to evidence that the only closely adjacent helical channels to the sample's edge make dominating contribution in the quantum conductance as distinguished from the internal channels. The variations of the U_{xy} voltage seem to effect on the degree of the spin polarization in the edge channels. Besides, the edge channels are able to exhibit either ballistic and superconducting properties or their combination [4]. Here, the dipole centers of boron in the δ-barriers confining the Si-QW appear to result in the formation of helical edge channels along the [011] axis.

Finally, the quantum conductance staircase of holes shows the maximum value of the conductance in the edge ballistic channels, $G_{max}=4(e^2/h)$, that appears to be caused by the multiple Andreev reflections in the case of their superconducting properties.

[1] N.T.Bagraev, N.G.Galkin, W.Gehlhoff, L.E.Klyachkin, A.M.Malyarenko, J. Phys. Condens. Matter. **20**, 164202 (2008).
[2] I.A.Shelykh, Galkin, N.T.Bagraev, Phys. Rev. B **74**, 1 (2006).
[3] N.T.Bagraev, E.S.Brilinskaya, D.S.Gets, L.E.Klyachkin, A.M.Malyarenko, V.V.Romanov, Semiconductors **45**, 1447 (2011).
[4] N.T.Bagraev, E.Yu.Danilovskii, L.E.Klyachkin, A.M.Malyarenko, V.A.Mashkov, Semiconductors **46**, 75 (2012).

Electrical control of coupling characteristics in vertically-stacked double-quantum-point-contact

S. Ichinokura[1], T. Hatano[2], K. Nagase[2], W. Izumida[1] and Y. Hirayama[1,2,3]

[1] *Department of Physics, Tohoku University, Aoba, Sendai, Japan*
[2] *ERATO Nuclear Spin Electronics Project, Aoba, Sendai, Japan*
[3] *WPI-AIMR, Aoba, Sendai, Japan*

A coupled double quantum-point-contact (D-QPC) has received much interest as fundamental quantum nanostructure where charge and spin interactions play an important role. Here, we fabricated vertically-stacked D-QPC starting from bilayer (20-nm GaAs/2.2-nm $Al_{0.33}Ga_{0.67}As$/20-nm GaAs) quantum well. As schematically shown in Fig. 1, the fabricated D-QPC has a pair of split Schottky gates and a fine center gate. Si-doped GaAs substrate operates as a back gate. In this D-QPC, we can control electron density independently in the upper and lower QPCs by using biases applied to the center and back gates. The bias applied to the split Schottky gates is used to constrict the one-dimensional (1D) channel.

The fabricated two split gates originally have some asymmetry in depletion spreading probably arising from a difference in etching depth and surface condition before Ti/Au gate deposition. We can thus realize asymmetrically confined D-QPC when equal biases are applied to the two split gates. Figure 2(a) shows transport characteristics obtained for such a condition. To clarify the 1D-subband diagram, transconductance data are grey-plotted as a function of V_{bg} and V_{sgR}=V_{sgL}=V_{sg}, where V_{bg}, V_{sgR} and V_{sgL} are voltages applied to back gate, right split gate, and left split-gate, respectively. Asymmetric alignment between upper and lower QPC results in anti-crossing behavior of 1D subbands, manifested by checker-board type behavior reflecting 1D-subband diagram schematically shown in the inset of Fig. 2(a). On the other hand, the original asymmetry can be cured by applying an asymmetric bias between V_{sgR} and V_{sgL}. Figure 2(b) shows transconductance behavior observed in such a symmetric condition. The obtained characteristics agree with the 1D-subband configuration (inset of Fig. 2(b)) expected for the center-aligned D-QPC, in which anti-crossing occurs only between the subbands of same symmetry. These results indicate successful control of coupling characteristics by electrical means. Although coupling control was reported by using a parallel magnetic field [1], electrical control provides additional freedom to tune QPC coupling in zero and a constant magnetic field, and is helpful to use D-QPC devices for various purposes.

We would like to thank K. Muraki (NTT) for supplying us high-quality wafers.

[1] K. J. Thomas *et al.*, Phys. Rev. B59, 19 (1999).

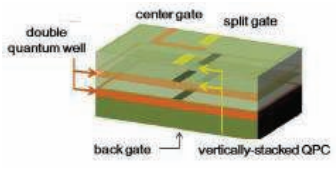

Fig. 1 Schematic diagram of the fabricated D-QPC.

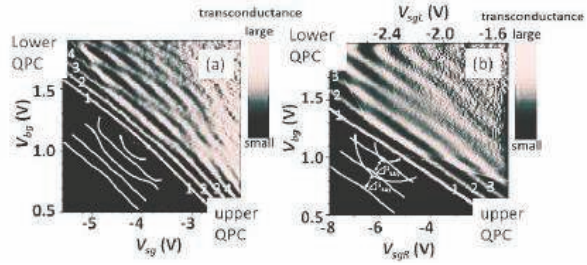

Fig. 2 (a) Grey-plot of transconductance of asymmetrically confined D-QPC, where upper and lower QPCs are staggered. (b) Grey–plot of transconductance of symmetrically confined D-QPC, where the center of upper and lower QPCs is aligned.

Fractional conductance oscillations in the charged two-terminal semiconductor quantum ring

T. Chwiej and B. Szafran

AGH University of Science and Technology,
Faculty of Physics and Computer Science,
al. Mickiewicza 30, 30-059 Kraków, Poland

We study the single electron transport through the two-dimensional quantum ring which additionally confines one or two electrons in the Aharonov-Bohm regime. For that purpose we simulate the many-particle wave-packet for a few hundreds of picoseconds by solving the time dependent Schrödinger equation in which the interparticle correlations arising due to electrostatic interaction are taken into account exactly. For an ideal quantum ring we have found that the conductance oscillates depending on magnetic field strength with a period $\Phi = \Phi_0/N$, where $\Phi_0 = h/e$ is the magnetic flux quantum and N is the total number of electrons forming the transient few-particle system in the ring. This fractional periodicity is noticeable if the subsystem of $(N-1)$ electrons originally confined in the ring, i.e. spatially separated from the incoming electron, is in the ground state. This finding is consistent with the fractional conductance oscillations measured by Keyser et al. [1] and also with previously predicted fractional oscillations of persistent currents in the closed quantum rings [2]. The amplitude of these oscillations strongly depends on the ring channels widths since an uneven injection of electron wave packet to both arms of the ring driven by magnetic (Lorentz) force effectively suppresses the quantum interference at its output[3]. We also analyze the conductance oscillations for the ring with disorder in confinement potential which even for $N = 1$ may lead to a fractional periodicity ($\Phi = \Phi_0/2$) due to Altshuler-Aronov-Spivak effect [4]. In that case, the contribution to the conductance oscillations from mods oscillationg with period $\Phi = \Phi_0/N$ are distinctly diminished[5].

[1] U. F. Keyser, C. Fühner, S. Borck, R. J. Haug, M. Bichler, G. Abstreiter, W. Wegscheider, Phys. Rev. Lett. **90**, 196601 (2003).
[2] T. Chwiej, B. Szafran, Phys. Rev. B **78**, 245306 (2008).
[3] T. Chwiej, K. Kutorasiński, Phys. Rev. B **81**, 165321 (2010).
[4] A.G. Aronov, Y.V. Sharvin, Rev. Mod. Phys. **59**, 755 (1987).
[5] D.-I. Chang,G. L. Khym, K. Kang, Y. Chung, H.-J. Lee, M. Seo, M. Heiblum, D. Mahalu, V. Umansky, Nat. Phys. **4**, 205 (2008)

Thermoelectric Power of the $LaAlO_3/SrTiO_3$ Heterostructure

A. Jost[1], V.K. Guduru[1], S. Wenderich[2], G. Koster[2], M. Huijben[2], M.K. Kruize[2], G. Rijnders[2], A. Brinkman[2], H. Hilgenkamp[2], A. McCollam[1], U. Zeitler[1], J.C. Maan[1]

[1] *High Field Magnet Laboratory, IMM, Radboud University Nijmegen, NL*
[2] *MESA+ Institute for Nanotechnology, University of Twente, Enschede, NL*

We present a complete set of magneto-resistance (MR), Hall-effect (HE), Seebeck-effect (SE) and Nernst-Ettingshausen-effect (NE) measurements in a temperature-range from 4.2 K up to 250 K and magnetic fields up to 16 T on $LaAlO_3/SrTiO_3$. This only recently discovered system[1] has generated great interest in the recent years[2]. In particular, the heterostructure made of $LaAlO_3/SrTiO_3$ got much attention due to a variety of different properties such as superconductivity[3] and magnetism[4].
From our data we can distinguish three different regions (figure 1a): The longitudinal resistance (R_{xx}) in region I is weakly decreasing with temperature and shows a small negative magneto-resistance (MR) (not shown). In region II, R_{xx} is decreasing faster and shows a strong non-quadratic MR. At even higher temperatures the resistance is increasing again with a small quadratic MR, marking region III. The Hall-effect (not shown) is small and linear in region I and III and becomes big and non-linear in region II.
The thermopower (S_{xx}) (figure 1a) shows a weak negativ magnetic-field dependence in region I (figure 1b). In region II S_{xx} is increasing with temperature and shows a strong non-linear decrease with magnetic field. In region III S_{xx} shows first a plateau at exactly the same temperature as the minimum in R_{xx} and is increasing further to higher temperatures with a weak and negativ field dependence. The Nernst-effect (figure 1b) is small and linear in regions I and III and bigger and strongly non-linear in region II.
We tentatively interprete this behavior as a result of two different electron-like charge carriers with different mobilities[5], of which one experiences a magnetic, Kondo-like freeze-out.

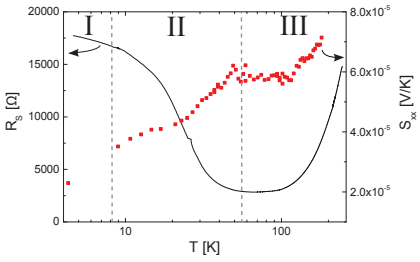

(a) Temperature dependence of sheet-resistance (black line) and Thermopower S_{xx} (red dots)

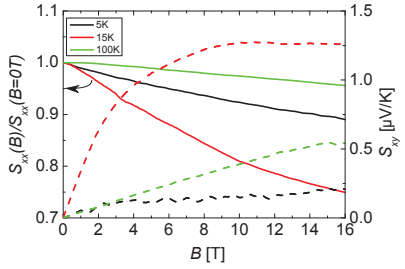

(b) Field dependence of Thermopower S_{xx}(solid lines) and Nernst-effect S_{xy} (dashed lines) at 5 K, 15 K and 100 K

[1] A. Othomo and H.Y. Hwang, Nature **427**, 423 (2004).
[2] H.Y. Hwang *et al.*, Nature Mater. **11**, 103 (2012).
[3] N. Reyren *et al.*, Science **317**, 1607 (2007).
[4] A. Brinkmann *et al.*, Nature Mater. **6**, 493 (2007).
[5] V.K. Guduru *et al.*, APL **102**, 051604 (2013).

$k \cdot p$ subband structure of the $LaAlO_3/SrTiO_3$ interface

L. W. van Heeringen[1], G. de Wijs, A. McCollam, J. C. Maan and A. Fasolino

Institute for Molecules and Materials, Radboud University Nijmegen, The Netherlands
[1] *l.vanheeringen@science.ru.nl*

A high-mobility electron gas at the $SrTiO_3/LaAlO_3$ interface [1] showing multisubband Shubnikov-de Haas oscillations with a few meV subband separation has been observed [2]. We analyze these results by calculating the subband structure in the 6-band $\boldsymbol{k}\cdot\boldsymbol{p}$ envelope function approach with an electric field confining the electron gas in the $SrTiO_3$ at the interface. By fitting to DFT band structure calculations we determine the 5 relevant parameters: 3 effective mass parameters for the t_{2g} conduction band edge (d_{xy}, d_{yz} and d_{zx}) of $SrTiO_3$, the spin-orbit coupling and the low temperature tetragonal distortion. The electric field strength F is treated as a variable since we do not incorporate lattice and electron screening in our model. This model leads to anisotropic non-parabolic bands as in Fig. 1. Similar band structures result from tight binding calculations in the 'low density regime'[3].

This model allows a direct comparison to the frequency of the quantum oscillations observed in high magnetic fields through quasiclassical quantization for a given density. Our results are in good agreement with the experiments for an electric field strength $F = 0.1$ meV/Å and a density of 7.1×10^{12} cm^{-2}.

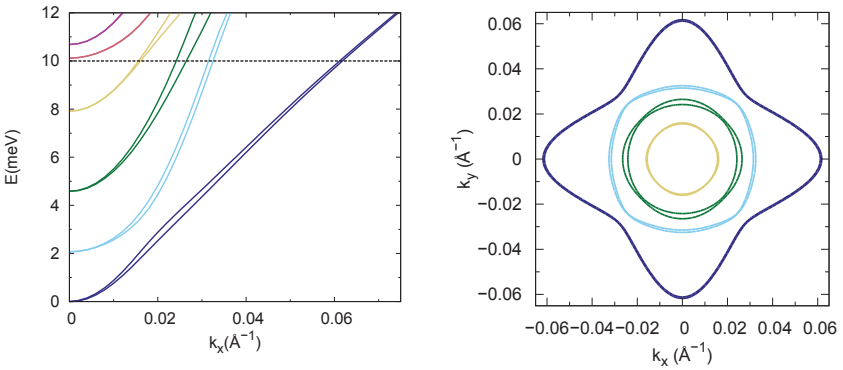

Figure 1: Left: $SrTiO_3$ subbands in an electric field of $F = 0.1$meV/Å. The small spin splittings are due to the asymmetric well in presence of spin-orbit coupling. Right: corresponding equal energy contours at $E = 10$ meV. Note the highly non-parabolic and anisotropic nature of the subbands.

[1] A. Ohtomo, H. Hwang, Nature, **427**, 204 (2006).
[2] A. McCollam, S. Wenderich, M. K. Kruize, V. K. Guduru, H. J. A. Molegraaf, M. Huijben, G. Koster, D. H. A. Blank, G. Rijnders, A. Brinkman, H. Hilgenkamp, U. Zeitler, J. C. Maan, *arXiv:1207.7003* (2012).
[3] G. Khalsa, A. H. MacDonald, Phys. Rev. B, **86**, 125121 (2012).

High mobility 2D electrons in undoped InN epitaxial layers grown on N-polarity GaN buffer

L.H. Dmowski [1], M. Baj [2], L. Kończewicz [3], A. Kwiatkowski [2], J. Przybytek [2], T. Suski [1], X. Q. Wang [4]

[1] *Institute of High Pressure Physics "Unipress", 01-142 Warsaw, Poland*
[2] *Faculty of Physics, Institute of Experimental Physics, University of Warsaw, Poland*
[3] *Laboratoire Charles Coulomb, CC074, Universite Montpellier 2, Pl. E. Bataillon, F-34095 Montpellier, France*
[4] *State Key Laboratory of Artificial Microstructure and Mesoscopic Physics, School of Physics, Peking University, Beijing 100871, China*

It was established that in epitaxial InN films beside bulk electrons there is always a thin (~10 nm) low-mobility electron accumulation layer on the InN surface. In this paper we report on another 2D electron channel with high mobility, existing in undoped InN samples. We measured Shubnikov de Haas (SdH) oscillations at 1.5 – 4 K as well as conductivity tensor σ_{xx} and σ_{xy} as a function of magnetic field for T between 4 K and 300 K. We observed two sets of SdH oscillations giving evidence of two high mobility electron contributions (Figure 1). The SdH measurements performed at tilted magnetic field revealed that one of them was of 2D character. Basing on magnetic field dependences of σ_{xx} and σ_{xy} tensor, we performed mobility spectrum analysis [1] (it is an established method to determine the contributions to the conductivity and corresponding mobilities in multicarrier semiconductor systems). The obtained mobility spectrum $\sigma(\mu)$ exhibited three peaks corresponding to different electron contributions to the conductivity: low mobility one which we attributed to the surface electrons and two high mobility contributions (Figure 2). To distinguish which one corresponds to 2D electrons we calculated electron concentrations of each contribution expressed both in cm^{-2} and cm^{-3}. Comparison of these values with the ones obtained from the period of SdH oscillations allowed to associate the peaks to the proper conductivity channels. Magnetic field dependences of σ_{xx} and σ_{xy} measured as a function of temperature allowed to observe evolution of the 2D mobility spectrum versus the 3D one with increasing temperature. In conclusion we suggest that 2D high mobility electrons originate from the InN/GaN interface.

[1] S. Kiatgamolchai, M. Myronov, O. A. Mironov, V. G. Kantser, E. H. C. Parker, and T. E. Whall, Phys. Rev. E 66, 036705 (2002)

Figure 1

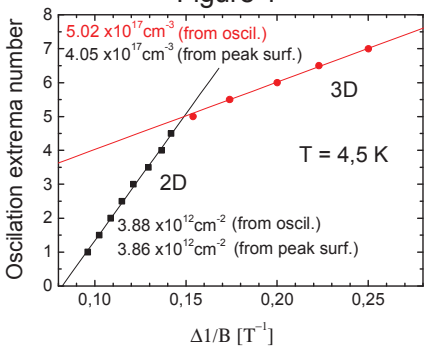

Figure 2

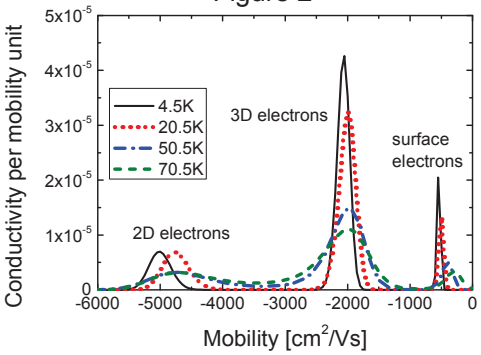

Effects of Bias cooling and illumination on undoped GaAs/AlGaAs Heterostructures

W.Y.Mak[1], F.Sfigakis[1], H.E.Beere[1], I. Farrer[1], K. Das Gupta[2] and D.A.Ritchie[1]

[1] *Cavendish Laboratory, University of Cambridge, Cambridge CB3 0HE, United Kingdom*
[2] *Indian Institute of Technology Bombay, Mumbai 400076, India*

Bias cooling and illumination are two common techniques used in experiments on semiconductor devices. Bias cooling can reduce random telegraph signals (charge noise) in mesoscopic devices whereas illumination is generally used to increase carrier density. Extensive studies (e.g.[1, 2, 3]) have been carried out of these two techniques in doped GaAs/AlGaAs heterostructures. However, with the exception of [4], there has been no reported studies of bias cooling and illumination on undoped devices [5, 6] .

To investigate this, bias cooling and illumination was carried out on a set of 2D samples made on three undoped GaAs/AlGaAs heterostructures where the 2DEG was 60nm, 110nm, and 160nm below the surface. In the illumination experiment, there is a slight improvement in the density-mobility relation in the samples after illumination with a red LED at 10mA (data points). This can be modelled (solid lines) by a decrease in the ionised background impurity level, and is in agreement with [4]. In the bias cooling experiment, the density-mobility relation was mostly unaffected (data points). However, for certain combinations of voltages and insulators, mobility could be decreased or increased. It is possible to model (solid lines) the change in the density-mobility relation by only varying the term corresponding to the overall tilt of the bandstructure in the crystal (N_{depl}).

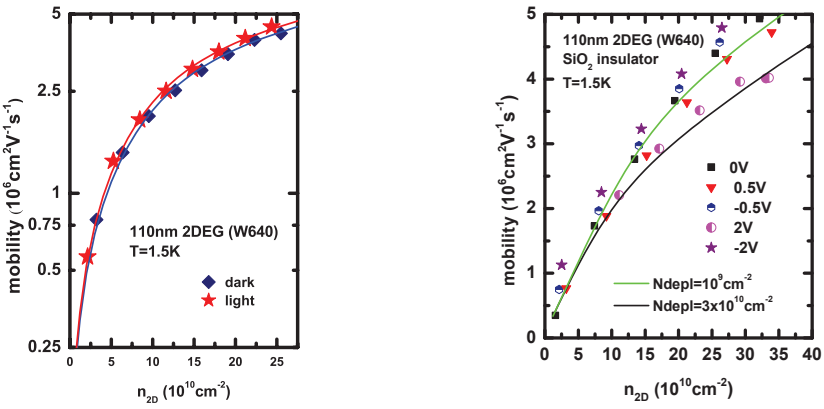

(a) (b)

Figure 1: Effects of (a) illumination and (b) bias cooldown on the density-mobility relation of 110nm deep undoped 2DEGs.

[1] A. Kastalsky and J.C.M. Hwang. Solid State Commun., **51** 317 322 (1984).
[2] P.T. Coleridge. Semicond Sci Tech, **12** 22 (1996).
[3] M. Pioro-Ladriere *et al.* Phys. Rev. B, **72** 15331(2005).
[4] T.Saku *et al.* Jpn. J. Appl. Phys., **37** L765 (1998).
[5] R.H.Harrell *et al.* Appl. Phys. Lett., **74** 2328 (1999).
[6] W.Mak et al., Appl. Phys. Lett. **97**, 242107 (2010).

Two-electron states localized by charged acceptors in GaAs/GaAlAs quantum wells in ultra-quantum regime of magnetic fields

M. Kubisa [1], K. Ryczko [1], I. Bisotto [2], C. Chaubet [3], A. Raymond [3] and W. Zawadzki [4]

[1] *Institute of Physics, Wroclaw University of Technology, 50-370 Wroclaw, Poland*
[2] *LNCMI, UPR 3228, CNRS-INSA-UJF-UPS, BP166, 38042 Grenoble, France*
[3] *L2C UMR 5221, CNRS-Universite Montpellier 2, Place E. Bataillon, 34090 Montpellier, France*
[4] *Institute of Physics, Polish Academy of Sciences, 02668 Warsaw, Poland*

We demonstrate both theoretically and experimentally that a negatively charged acceptor located inside or near a two-dimensional (2D) quantum well can localize more than one conduction electron. The phenomenon occurs in a strong magnetic field normal to the 2D plane. The energy and wave function of two conduction electrons trapped by an acceptor are calculated variationally as functions of the magnetic field and impurity position. In calculations we use a realistic model for the potential in doped quantum wells (QWs) and include the effect of screening by mobile carriers. The investigated two-electron state is analogous to the well-known state of D^- center composed of two electrons and a positively charged donor. However, in contrast to the donor case, the electron pair is localized by the acceptor, but not bound. The theory is compared with magneto-transport measurements on n-type GaAs/GaAlAs QWs, additionally doped in the well with beryllium. In such structures, a dramatic increase of resistance is observed at high currents and strong magnetic fields (corresponding to the filling factor $\nu<1$), as shown in Fig.1. This effect was called the "magnetic boil-off" and was interpreted as a result of electron transitions from the delocalized (conductive) states to the localized (nonconductive) states on acceptors caused by the Hall electric field [1]. A detailed analysis of the resistance data at intermediate currents ($\approx 1\ \mu$A) reveals a two-step character of the boil-off process. We attribute the first resistivity step, which appears at lower magnetic fields (and thus at smaller Hall voltages), to a localization of electrons into single-particle states. The second resistivity step. which arises when all acceptors are occupied by electrons, is assigned to the formation of two-particle localized states. Our model explains well both the magnetic field and current dependences of the boil-off effect. We also show that the electric fields necessary to localize electrons are consistent with the measured Hall voltage, although an intrinsic inhomogeneity of the Hall field (see for example [2]) prevents a detailed comparison with the theory.

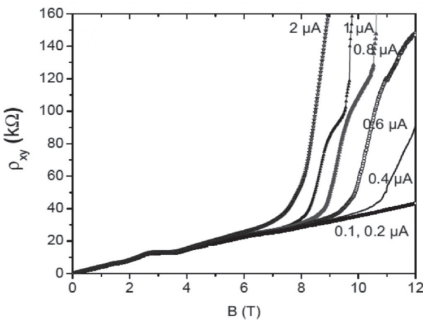

FIG. 1. Transport characteristics of sample 35A55 measured for high currents in dc experiments. The sharp increase of ρ_{xy} observed in the ultra-quantum limit of magnetic fields is caused by a localization of conduction electrons by negatively charged acceptors.

[1] I. Bisotto et al., Phys. Rev. B **86**, 085321 (2012).
[2] P. F. Fontein et al., Phys. Rev. B **43**, 12090 (1991).

TuP104

Phase evolution in the spin-incoherent Luttinger liquid

Hiroyuki Tamura, Toshiyuki Kobayashi and Tatsushi Akazaki

NTT Basic Research Laboratories, NTT Corporation, Atsugi, Kanagawa 243-0198, Japan

Electronic transport in non-interacting one-dimensional conductors reveals the quantized conductance in multiples of the universal quantum $2e^2/h$ in the ballistic regime. In experiments, so-called 0.7 structure appears as a quasi-plateau in the conductance at very low electron density in the wire. One of the possible mechanisms is a formation of the Wigner crystal at intermediate temperature $J \ll T \ll E_F$ where J is the exchange constant [1]. This state is called the spin-incoherent Luttinger liquid (SILL) where the electron spins have no correlation but the charge modes are in the ground states.

To examine how the transmission phase evolves in the SILL, we consider a model Hamiltonian $H = H_{2D} + H_{1D} + H_T$ where H_{2D} is the Hamiltonian for the two-dimensional (2D) electron gas, H_{1D} is the Hamiltonian for the one-dimensional (1D) wire, and H_T is the Hamiltonian for the tunnel region between 2D and 1D regions [2]. The tunnel region consists of two different paths forming a closed loop where the phase evolution due to the wavenumber k and Aharanov-Bohm flux ϕ in the magnetic field produces a small oscillating component in the transmission probability which can be simulated by the expression $T(k) = 1 - T_0 \cos(|k|L - \phi)$ where $0 < T_0 < 1$ and L is the length of tunnel path. While the spectral function of the noninteracting Fermi liquid in 1D is simply given by $A_{1D}(k, \epsilon) = 2\pi\delta(\epsilon - \epsilon_k)$, the low-energy spectral density for a finite spin-incoherent wire in zero magnetic field has been obtained by the expression $A_{1D}(k, u) \propto e^{-k^2u^2/2}/(5 + 4\cos ka)$ [3] where u represents the fluctuation of electron position and a is the mean spacing of electrons.

The conductance is calculated using the standard tunneling current formula as functions of k_F and ϕ for the normal Fermi liquid and the SILL in 1D. For the normal Fermi liquid, the oscillation shows an ordinary k_F dependence of $\cos(k_F L - \phi)$. For the SILL, the oscillation behaves quite differently due to the peculiar spectral function. For the SILL with large u, the Wigner crystal is formed but electrons are still fluctuating largely around their original position. The spectral function has a single peak at $k \sim 0$ and then the oscillation becomes only weakly dependent on k_F. For the SILL with small u, electrons can fluctuate only a small amount around their original position due to the strong repulsive interaction and a "stiff Wigner crystal" is formed. In this case, the spectral function has large peaks near $k \sim \pm 2k_F$ and then the oscillation shows $2k_F$ dependence as $\cos(2k_F L - \phi)$. In the recent experiment, $k_F \to 2k_F$ shift of the transmission phase in the 0.7 structure has been observed in parallel QPCs [4] and we consider it as an evidence of the Wigner crystallization in the SILL.

[1] K.A. Matveev, Phys. Rev. Lett. **92**, 106801 (2004); Phys. Rev. B **70**, 245319 (2004).
[2] S.A. Grigera, A.J. Schofield, S. Rabello, and Q. Si, Phys. Rev. B **69**, 245109 (2004); M. Trushin and A.L. Chudnovskiy, Euro. Phys. Lett. **82**, 17008 (2008).
[3] G. A. Fiete, J. Qian, Y. Tserkovnyak, and B. I. Halperin, Phys. Rev. B **72**, 045315 (2005).
[4] T. Kobayashi, S. Tsuruta, S. Sasaki, H. Tamura, and T. Akazaki (to be published).

Optical characterization of GaAsSb/GaAs type-II quantum well with an adjacent InAs quantum-dot layer composite structures

H. P. Hsu[1,*], J. D. Wu[2], Y. J. Lin[2], Y. S. Huang[2], Y. R. Lin[3] and H. H. Lin[3]

[1] *Department of Electronic Engineering, Ming Chi University of Technology, Taishan, Taipei 243, Taiwan*
[2] *Department of Electronic Engineering, National Taiwan University of Science and Technol ogy, Taipei, 106, Taiwan*
[3] *Department of Electrical Engineering and Graduate Institute of Electronics Engineering, National Taiwan University, Taipei 106, Taiwan*

Due to the type-II band alignment, the electron and hole in a GaAsSb/GaAs strained quantum well (QW) are spatially separated. This configuration leads to the fundamental transition energy of QW being lower than the band gaps of the barrier and well. This is a great advantage in application to long wavelength lasers [1]. However, the spatial separation of the electron and hole wavefunctions results in a low optical matrix element which leads to high threshold current density in GaAsSb/GaAs QW 1asers. One way to increase the matrix element is to enhance the confinement of the active medium. A composite structure consisting of a GaAsSb/GaAs QW and an adjacent InAs/GaAs self-assembled quantum dots (QDs) has been proposed to improve the performance of the type-II laser diodes [2]. In this composite structure, GaAsSb QW and a GaAs spacer layer were grown beneath InAs QDs. Since the strain exerted by InAs QDs on their bottom is tensile below the dots and compressive under the edge of the dots, the band diagram of the GaAs spacer and GaAsSb QW are modulated to form potential wells in the growth plane. As a result, both electrons and holes are trapped in the potential wells induced InAs QDs. Along the growth direction, the type-II GaAsSb/GaAs heterostructure provides the confinement of the third dimension.

In this work, a detailed optical characterization of this composite structure was carried out by using by using surface photovoltage spectroscopy (SPS) and photoluminescence (PL) techniques. The room temperature SPS spectra exhibit the features originated from QDs, QW, wetting layer and GaAs cap-layer/barrier. The low-temperature PL band of the modulated potential wells in GaAsSb QW, resulting from the tensile strain exerted by the InAs QD stressor, showing a giant redshift as compared with the GaAsSb QW control sample at low excitation level. At higher temperature, the thermalization of carriers in QDs enhances the fluctuation of the potential wells, which provides extra quantum confinement for the carriers and enhances the luminescence intensity. This effect can be used to improve the performance of type-II GaAsSb/GaAs QW lasers.

[1] N. N. Ledentsov, M. Grundmann, F. Heinrichsdorff, D. Bimberg, V. M. Ustinov, A. E. Zhukov, M. V. Maximov, Zh. I. Alferov, and J. A. Lott, IEEE J. Sel. Top. Quantum Electron. 6, 439 (2000).
[2] Y. R. Lin, H. H. Lin, and J. H. Chu, Electron. Lett. 45, 682 (2009).

TuP106

Properties of excitonic states in MOCVD-grown Zn(Cd)Se/ZnMgSSe quantum wells with spreaded heterointerfaces

A. F. Adiyatullin [1, 2], S. V. Shevtsov [1, 2] A. N. Minnullin [2] and V. S. Krivobok [1, 2]

[1] *Lebedev Physical Institute of Russian Academy of Sciences, Moscow, Russia*
[2] *Moscow Institute of Physics and Technology, Dolgoprudny, Moscow Region, Russia*

ZnSe is considered as a promising material for achieving Bose-Einstein condensate of exciton polaritons in microcavities with embedded quantum wells (QWs). This material allows to reach strong coupling mode at room temperatures [1] and exhibits several mechanisms of polariton relaxation. Particularly, polariton-phonon scattering can be further enhanced due to low LO phonon energy. The influence of a real heterointerface on these processes may be of crucial importance for an efficient control of polariton relaxation and thus deserves a detailed study.

Structures with 1 and 2 Zn(Cd)Se/ZnMgSSe QWs were grown by MOCVD on GaAs substrates in a hydrogen atmosphere at 85 Torr and 450–460 °C. Due to high growth temperature spreading of the QW heterointerfaces was observed, however, their lateral homogeneity remained high. In the samples with two QWs, the bottom QW was held at the high growth temperature longer than the top one, resulting in different degree of interface blurring for these QWs. This allows us to study the optical properties of two QWs with different interface spreading in the same sample.

The structure of exciton states in all QWs is well described in the framework of a strained Zn(Cd)Se layer thicker than the exciton Bohr radius. The different extent of QWs blurring leads to the energy shift between emission spectra of two QWs. The doublet structure dominating in the PL spectra is determined by the radiative recombination of free excitons (X) and excitons localized on neutral donors (D^0X). The spectral distance between maxima of X and D^0X lines is higher for QWs with blurred interfaces. This is related to the change in the decay of the wavefunction near interfaces for localized and delocalized exciton states [2].

The exciton-phonon coupling is enhanced for the QWs with spreaded interfaces. The most likely reason for this is the different degree of localization of electrons and holes near the interface, which enhances the exciton–phonon interaction via the Fröhlich mechanism.

A bi-exponential PL decay with the quenching times ~ 40 ps and ~ 400 ps is observed for each QW. The short time is caused by trapping of excitons by charged donors D^+. The slowly decreasing part is related to the radiative recombination of X and D^0X with no charged centers nearby. The interface spreading apparently leads to the increase of concentration of charged defects, which results in the decrease of the PL quenching time in blurred QWs.

Under additional below-barrier illumination with photon energy 1.9 eV the following phenomena in PL spectra are observed: (1) drastic decrease of PL quantum yield; (2) D^0X line disappearance; (3) change of X line width. Absorption of this illumination causes electrons to escape from QWs, leading to the growth of the number of ionized donors D^+ and to the decrease of the number of neutral donors D^0. A huge time constant (~1 s) of the phenomena points to charge redistribution between QWs and the substrate, which is considered to be a primary reason of PL lines narrowing due to lowering of the contribution of electron-exciton scattering. Other mechanisms that could affect PL line widths may be an increase in level of fluctuations of QW potential or a change of exciton-phonon interaction constant, both induced by a raise of the number of charged impurities.

[1] K. Sebald et al., Appl. Phys. Lett. **100**, 161104 (2012).
[2] A. F. Adiyatullin et al., J. Exp. Theor. Phys. **115**, 885 (2012).

Shot noise of a quantum point contact on a two-dimensional hole gas

Y. Nishihara[1,2], K. Chida[1,2], T. Arakawa[1,2], S. Matsuo[1,2], T. Tanaka[1,2], K. Kobayashi[2], T. Ono[1], Y. Komijani[3], T. Ihn[3], K. Ensslin[3], D. Reuter[4] and A. D. Wieck[4]

[1] *Institute for Chemical Research, Kyoto University*
[2] *Graduate School of Science, Osaka University*
[3] *Solid State Physics Laboratory, ETH*
[4] *Angewandte Festkörperphysik, Ruhr-Universität Bochum*

Current fluctuation (current noise) is a powerful probe to address details of the fundamental transport properties beyond the conductance. Especially the shot noise, the nonequilibrium current noise, is sensitive to quantum statistics, scattering, and many-body effects [1]. Shot noise measurement at a quantum point contact (QPC) fabricated on two-dimensional electron gas (2DEG) have been performed already by many groups [2,3], where the shot noise suppression below the Poisson value was observed as theoretically predicted. Compared to such conventional QPCs, a QPC fabricated on two-dimensional hole gas (2DHG) has not been fully investigated so far. As holes in 2DHG have larger effective mass and stronger spin-orbit interaction than electrons in 2DEG, it is very interesting to investigate the similarity and dissimilarity between the electron QPC and the hole QPC [4-6].

Here we present shot noise measurements on a hole QPC. To the best of our knowledge, shot noise of hole QPCs has not been explored so far.

The experiment was performed on a QPC fabricated by local anodic oxidation lithography (Fig. 1) on a p-doped GaAs/AlGaAs heterostructure. Conductance and shot noise were measured in a dilution refrigerator with a resonant circuit and a home-made cryogenic amplifier [7].

The QPC shows a clearly quantized plateau at $2e^2/h$ tuned via adjusting a side gate bias voltage below 1 K [5]. In addition, we can see the extra plateau at $0.7(2e^2/h)$, so called 0.7 structures, which remains visible above 1 K. We obtain the Fano factor determined from the shot noise. The Fano factor measured in 1.5 K is observed to be close to zero on a quantized conductance plateau, whose behavior is similar to that of the QPC on 2DEG. However, the shot noise measured at 0.6 and 0.3 K around the 0.7 structure unexpectedly exhibits a peak structure around zero bias, which is reminiscent of the zero-bias conductance anomaly.

[1] Y. M. Blanter and M. Büttiker, Phys. Rep. **336**, 1 (2000).
[2] M. Reznikov *et al*., Phys. Rev. Lett. **75**, 3340 (1995).
[3] A. Kumar *et al*., Phys. Rev. Lett. **76**, 2778 (1996).
[4] R. Danneau *et al*., Phys. Rev. Lett. **100**, 016403 (2008).
[5] Y. Komijani *et al*., Europhys. Lett. **91**, 67010 (2010).
[6] Y. Komijani *et al*., arXiv 1301.3992 (2013).
[7] Y. Nishihara *et al*., Appl. Phys. Lett. **100**, 203111 (2012).

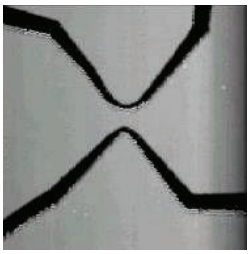

Fig. 1 Photo image of the QPC fabricated by the AFM oxidation technique. The width of the QPC is 200 nm.

TuP108

Spin splitting and effective masses in p-type GaAs two dimensional hole gases

Fabrizio Nichele[1], Atindra Nath Pal[1], Thomas Ihn[1] , Klaus Ensslin[1], Christian Reichl[1] and Werner Wegscheider[1]

[1]*Solid State Physics Laboratory, ETH Zurich, 8093 Zurich, Switzerland*

We present magnetotransport measurements of two-dimensional hole gases (2DHG) embedded in carbon doped p-type GaAs/AlGaAs hetorostructures grown on [100] oriented substrates. A pronounced beating pattern in the Shubnikov-de Haas (SdH) oscillations (see Fig. 1(a)) proves the presence of strong spin-orbit interaction in the 2DHG. With the use of a global top gate we can tune the hole density from 0.8×10^{15} m^{-2} to 3.0×10^{15} m^{-2} and observe a corresponding change in the spin-orbit interaction induced spin-splitting.

It is possible to distinguish various peaks in the Fourier spectrum of the data (see Fig. 1(b)). Two of them are identified as originating from spin-split subbands at frequencies $f_1 = n_1 \times h/e$ and $f_2 = n_2 \times h/e$. Other prominent peaks are also observed at frequencies $f_1 + f_2$ and $f_2 - f_1$, as reported by others [1, 5]. Here we associate them with magneto intersubband (MIS) [3] oscillations resuling from spin-split subbands. In contrast to the case where two size-quantized subbands are occupied, spin-split subbands have significantly different effective masses. The resulting MIS oscillations have a peculiar temperature dependence.

We further estimated the effective masses of heavy-light holes (HLH) and heavy-heavy holes (HHH) by measuring the temperature dependence of the SdH oscillations similarly to Ref. [1]. In previous work [1, 2] a linear dependence of the effective mass on the perpendicular magnetic field was observed. The high quality of the 2DHG in our samples allows us two resolve SdH oscillations at lower magnetic field. In the limit of low magnetic field our results suggest that the effective masses are independent of the field and a deviation occurs only outside the validity range of the model in use. While the LHH mass is independent of Fermi energy, the HHH mass has a strong Fermi energy dependence, suggesting a SOI-induced non parabolicity of the valence band [4].

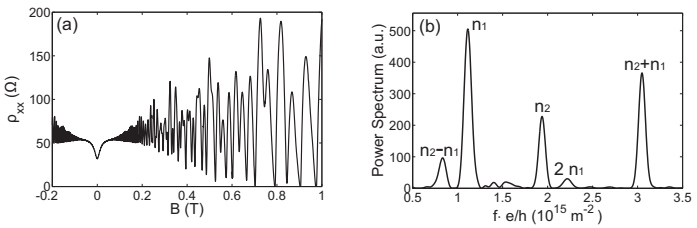

Figure 1: a) Longitudinal resistivity measured in a Hall bar geometry at a density of $n = 3.0 \times 10^{15}$ m^{-2}. b) Power spectrum of the data in a) plotted as a function of $1/B$.

[1] B. Habib, E. Tutuc, S. Melinte, M. Shayegan, D. Wasserman, S.A. Lyon, PRB **69**, 125312 (2004).
[2] J. Eisenstein and H. Stormer, PRL **53**, 27 (1984).
[3] M. Raikh and T. Shahbazyan, PRB, **49**, 8 (1994).
[4] R. Winkler, *Spin-Orbit Coupling Effects in 2D Electron and Hole Systems*, (Springer, 2003).
[5] B.Grbic, R. Leturcq, T. Ihn, K. Ensslin, D. Reuter, A.D. Wieck, PRB **77**, 11 (2004).

Thermodynamic and transport properties of interacting electrons in two dimensions with diagonal and off-diagonal disorder

Prabuddha B. Chakraborty,[1,2,*] Krzysztof Byczuk,[3] and Dieter Vollhardt[2]

[1] *Indian Statistical Institute, Chennai Centre, SETS Campus, MGR Knowledge City, Taramani, Chennai 600113, India*
[2] *Theoretical Physics III, Center for Electronic Correlations and Magnetism, Institute of Physics, University of Augsburg, D-86135, Augsburg, Germany*
[3] *Institute of Theoretical Physics, Faculty of Physics, University of Warsaw, ul. Hoża 69, 00-681, Warszawa, Poland*

We present numerical results on transport and thermodynamic properties of a two-dimensional electron system in the presence of both Coulomb repulsion and disorder potential, none of which can be considered weak. The numerical method used is quantum Monte Carlo simulations on a $d = 2$ square lattice. We investigate disorder potential with different symmetries like diagonal (site) disorder and off-diagonal (bond) disorder. The common features and salient differences in the physics of interacting electrons in low dimensions when the disorder symmetries are different will be stressed in this talk. In particular, evidence of universality in the value of the critical conductivity at the quantum critical point between a metallic and a localized state for the site disordered system will be highlighted, and comparisons will be made to the corresponding case of bond disorder. Interesting magnetic properties of the system at different regimes of interaction and disorder strength will also be discussed.

* Electronic address: prabuddha@isichennai.res.in

TuP110

Dimensionality crossover in pumping: from one to two-dimensional systems

T. Kaur [1], L. Arrachea[2] and N. Sandler [1,3]

[1]Department of Physics and Astronomy, Ohio University, Athens, OH - USA
[2] Departamento de Física, Univ. Nac. de Bs. As., Bs. As., Argentina
[3]Dahlem Center for Complex Quantum Systems, Freie Universität, Berlin, Germany.

The generation of a net charge current in the absence of explicit bias, a phenomenon known as pumping, is a fascinating mechanism of relevance for transport devices. After the first proposal of charge transfer via pumping [1], the technique was analyzed in detail by studying several mesoscopic models and also shown to work in real experimental settings by Switkes [2] with periodic time-dependent voltages applied to quantum dots. Soon after, the application of a periodic perturbation to pump dc charge or spin currents was achieved in various other experimental settings including carbon nanotubes as well as semiconducting and superconducting structures and different pumping techniques.

While most of the theoretical studies have focused on descriptions of mesoscopic models in the adiabatic regime (low driving frequencies), few works have addressed the role of confinement and geometry of samples and contacts in the pumped current at and away from adiabatic and linear conditions.

To understand the role of confinement and geometry, we have undertaken a detailed analysis of the properties of non-equilibrium zero-bias currents produced by two external out-of-phase time-dependent harmonic potentials through systems with varying dimensionality. To this end we use the non-equilibrium Keldysh formalism, based on Green's functions, to solve tight-binding models for one-, quasi-one (ribbons) and two-dimensional systems with square and honeycomb lattice connectivity. Realistic experimental settings are modeled by including the effect of confining barriers and metallic reservoirs (represented by square lattices) with mismatched lattice constants. We obtain a full description of DC currents and current spectral functions for different model parameter values describing adiabatic, non-adiabatic, linear and non-linear regimes.

We present also the results of a study on the stationary (equilibrium) conductance for different geometries of the model that allows identifying features due to confinement and lattice mismatch. Furthermore, for the adiabatic regime, we propose an extension of the concept of stationary conductance in terms of a transmission matrix to non-equilibrium systems. This non-equilibrium transmission matrix displays features that describe the crossover between equilibrium and non-equilibrium regimes.

For quasi-one dimensional systems with mismatched lattices, we review the role played by the contact and system geometry on the properties of the pumped current [3].

[1] D. J. Thouless, Phys. Rev. B **27,** 6083, (1983).
[2] M. Switkes et al., Science **283**, 1905 (1999).
[3] T. Kaur, L. Arrachea and N. Sandler. Submitted for publication; arXiv:1203.3952A.

Fractal dynamics in chaotic quantum transport

V. Kotimäki[1], E. Räsänen[2,3], H. Hennig[3] and E. J. Heller[3]

[1] *NSC, Department of Physics, University of Jyväskylä, FI-40014 Jyväskylä, Finland*
[2] *Department of Physics, Tampere University of Technology, FI-33101 Tampere, Finland*
[3] *Physics Department, Harvard University, Cambridge, Massachusetts 02138, USA*

Fractal patterns can be commonly observed in nature, e.g., in snowflakes, fern leaves, coastlines, and also in the fluctuations of human-generated time series as in heartbeats [1] and music [2, 3]. Remarkably, these self-affine structures have also been found in magnetoconductance of chaotic, e.g., stadium-shaped nanostructures [4].

So far, quantum mechanical transport simulations on realistic chaotic cavities have been beyond the computational capabilities. Here, we have carried out such calculations in real space and real time for a two-dimensional stadium cavity [5]. Our results show that the conductance of the system as a function of magnetic field has a distinctive fractal scaling. Moreover, the estimated fractal dimension qualitatively agrees with the experimental data [4]. We show that the detrended fluctuation analysis (DFA), a widely used method in time-series analysis, is a powerful tool in the fractal analysis of the magnetoconductance.

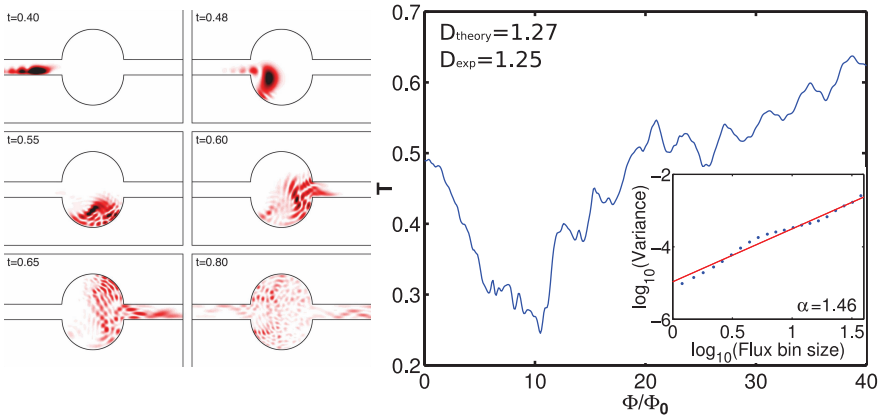

Figure 1: Left: Density snapshots of the electron transport through the stadium nanostructure. Right: Transmission coefficient as a function of magnetic flux through the stadium at $t = 1.4$. Inset: Determination of the scaling exponent α obtained with DFA.

[1] A. L. Goldberger *et al.*, PNAS **99**, 2466 (2002).
[2] R. F. Voss *et al.*, Nature **258**, 317 (1975).
[3] H. Hennig *et al.*, PLoS ONE **6**, e26457 (2011).
[4] A. S. Sachrajda *et al.*, Phys. Rev. Lett. **80**, 1948 (1998).
[5] V. Kotimäki *et al.*, Submitted to PRL, arXiv:1210.3815.

Wave excitations of drifting two-dimensional electron gas under strong inelastic scattering

V. A. Kochelap[1], V. V. Korotyeyev[1], and L. Varani[2]

[1] *Institute for Semiconductor Physics, Pr. Nauki 41, Kiev 03028, Ukraine*
[2] *Institut d'Électronique du Sud, CNRS UMR 5214, University Montpellier 2 France*

We have analyzed low-temperature behavior of two-dimensional electron gas in polar heterostructures subjected to a high electric field. When the optical phonon emission is the fastest relaxation process, we have found existence of collective wave-like excitations of the electrons. These wave-like excitations are periodic in time oscillations of the electrons in both real and momentum spaces. The excitation spectra are of multi-branch character with considerable spatial dispersion (see Figure). There are one acoustic-type and a number of optical-type branches of the spectra. Their small damping is caused by quasi-elastic scattering of the electrons and formation of relevant space charge. Also there exist waves with zero frequency and finite spatial periods - the standing waves. The found excitations of the electron gas can be interpreted as synchronous in time and real space manifestation of well-known optical-phonon-transient-time-resonance.

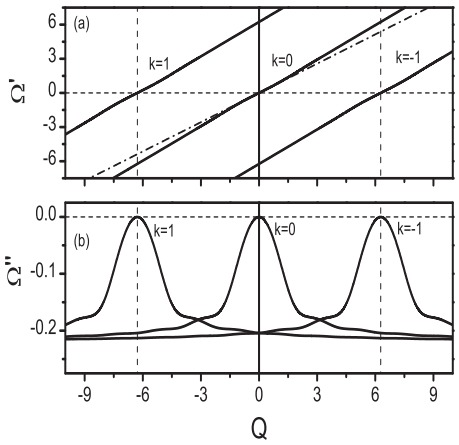

Figure 1: Real (a) and imaginary (b) parts of the dimensionless frequency as functions of the dimensionless wavevector for three branches of the dispersion relation at an electric field corresponding to the streaming regime. Dash-dotted line is for $\Omega' = V_{dr}Q$, V_{dr} is the drift velocity of the electrons. The vertical dashed lines mark wavevectors equal to $Q = \pm 2\pi$. Note that the vertical scales in (a) and (b) are very different.

Estimates of parameters of the excitations for two polar heterostructures, GaN/AlGaN and ZnO/MgZnO, have shown that excitation frequencies are in THz-frequency range, while standing wave periods are in sub-micrometer region. As an example, for AlGaN/GaN heterostructures at T = 50..100 K, the results shown in the Figure correspond to an applied field $\approx 14\,kV/cm$; the frequency of the lowest optical-like branches at $q \to 0$ is found to be $1.5 \times 10^{13} s^{-1}$, its damping equals $6 \times 10^{11} s^{-1}$. Undamped standing waves are realized for a wavevector equal to $\pm 9.4 \times 10^5 cm^{-1}$.

Shot noise of CdTe/CdMgTe Quantum Point Contact

J. Wróbel[1,2], M. Czapkiewicz[1], P. Nowicki[1], V. Kolkovsky[1], T. Wojciechowski[1], M. Wiater[1], and T. Wojtowicz[1]

[1]*Institute of Physics, Polish Academy of Sciences, al Lotników 32/46, 02-668 Warszawa, Poland*
[2]*Department of Mathematics and Natural Sciences, Rzeszów University, al. Rejtana 16A, 35-959 Rzeszów, Poland*

Shot noise, a non-equilibrium current fluctuations in electronic devices, occurs due to the discreteness of electric charge and stochastic nature of electron transmission processes. As it is well known, the noise spectroscopy of low-dimensional nanostructures provides a unique information on carrier statistics, their mutual correlations, quasi-particle charges, dephasing mechanisms, and others. For example, a suppression of the noise relative to that predicted by theory for spin degenerate transport is observed in GaAs/AlGaAs Quantum Point Contacts (QPCs) near so-called "0.7 anomaly" (for conductance $G \approx 0.7$ in $G_0 = 2e^2/h$ units) [1]. Observed results are well accounted for within a model in which the twofold degeneracy of one-dimensional channel is lifted by the electron-electron correlation effects [2].

Recently we have reported on fabrication and low temperature magneto-transport measurements of QPCs patterned from a novel two-dimensional electron system — CdTe/CdMgTe modulation doped heterostructure [3]. It is expected that the correlation effects in CdTe are more important, as compared to GaAs, since the effective mass is larger and the dielectric constant is smaller. Indeed, we have provided evidence for a spontaneous formation of a quasi bound state in short and nominally symmetric QPCs, which appearance is caused by stronger *e-e* interaction. One of the arguments relied on the observation of a plateau-like feature at $G \approx 0.25\, G_0$. Calculations suggest [4], that if a weakly bound state is present in the constriction, its local density of states follows Fermi energy when gate voltage V_g is changed and the pinning of the resonant level leads to the appearance of an additional "kink" on G vs V_g curve. Such "0.25-anomaly" was measured before only for rather long (0.4 to 1.0 μm) GaAs quantum wires [5].

In this work we report, for the first time, on shot noise signatures related to the "0.25-anomaly", measured for CdTe/CdMgTe QPC at $T = 0.3$ K. We find a *suppression* of Schottky noise around the anomalous conductance plateau. That gives an experimental evidence that near the 0.25 feature electrons are transported by two non-degenerate one-dimensional channels, each with a different transmission coefficient. This agrees with the previous results obtained for "0.7" plateau. Therefore we suggest, that the weakly bound state, formed within the constriction, is at least partially spin polarized and that the exchange energy plays an important role in its formation.

The research was partially supported by National Science Centre (Poland) under the grant DEC-2012/06/A/ST3/00247.

[1] P. Roche, J. Ségala, D. C. Glattli, J. T. Nicholls, M. Pepper, A. C. Graham, K. J. Thomas, M. Y. Simmons, and D. A. Ritchie, Phys. Rev. Lett. **93**, 116602 (2004).
[2] A. Lassl, P. Schlagheck, and K. Richter, Phys. Rev. B **75**, 045346 (2007).
[3] M. Czapkiewicz, V. Kolkovsky, P. Nowicki, M. Wiater, T. Wojciechowski, T. Wojtowicz, and J. Wróbel, Phys. Rev. B **86**, 165415 (2012).
[4] S. Ihnatsenka, I. V. Zozoulenko, and M. Willander, Phys. Rev. B **75**, 235307 (2007).
[5] S. M. Cronenwett, H. J. Lynch, D. Goldhaber-Gordon, L. P. Kouwenhoven, C. M. Marcus, K. Hirose, N. S. Wingreen, and V. Umansky, Phys. Rev. Lett. **88**, 226805 (2002).

Using the Coupled Cluster Singles and Doubles method to calculate many electron effects in 2D semiconductor structures

C. J. Wesslén[1], E. Lindroth[1]

[1] *Department of Physics, Stockholm University, AlbaNova, S-106 91 Stockholm, Sweden*

The coupled cluster (CC) method has been shown to be a powerful tool when calculating many-body effects in nuclear, atomic and molecular physics. As other methods used in these areas of physics, the CC method can also be applied to atom-like 2D semiconductor structures. We have implemented the Coupled Cluster Singles and Double (CCSD) method and applied it to a 2D harmonic oscillator quantum dot to investigate the electronic many-body properties [1]. The implementation has proven to be accurate in comparison to previous Full Configuration Interaction and Quantum Monte Carlo calculations for up to twelve electrons and relative interaction strengths of up to at least $\lambda = 2$. Methods for extrapolating onto larger basis-sets have also been presented to enable more accurate results at a low cost.

We are capable of modeling systems of cylindrical symmetry, such as 2D dots, rings and concentric rings using a numerical B-spline basis. The exact shape of the radial potential can be chosen freely, so that hard walls, harmonic oscillators and Gaussian curves are all viable options to match the required system properties. In our early atempts, the program has been used to study concentric rings such as those conceived experimentally by Mano *et al.* [2]. For this we have used the material parameters for GaAs with the radial potential modeled using two superposed Gaussian curves. In Figure 1 the probability density of such a system, containing four electrons, can be seen. This configuration is completely spin polarized and contains one single electron in the outer ring, and the others in the inner. The program is currently being used to further study several interesting properties of this system, including correlation effect when shifting the inner/outer ring placements and interactions with external magnetic fields.

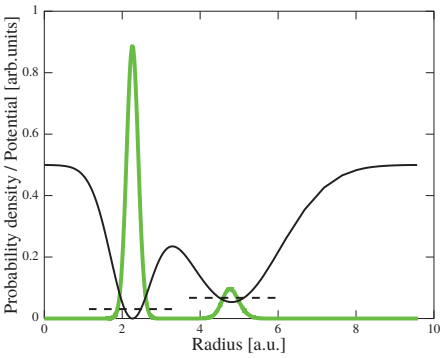

Figure 1: The probability density for concentric quantum rings. The black solid line indicates the shape of the potential in the radial dimension. The two dashed lines represent the energy levels of the states in the inner and outer ring in scale with the potential. Finally the green line is the normalized electron density for the four electrons.

[1] E. Waltersson, C. J. Wesslén, E. Lindroth, Phys. Rev. B **87**, 035112 (2013).
[2] T. Mano *et al.*, Nano Letters **5**, 425 (2005).

Electric-field control of penetration of quantum-mechanical current density under semi-infinite potential barrier at the interference of the electron waves in semiconductor 2D nanostructures

V.A.Petrov [1] , A. V. Nikitin[1]

[1] *Institute of Radio Engineering and Electronics, Russian Academy of Sciences, Moscow, 125009, Russia*

The influence of a constant transverse (along z – axis; z-axis being the axis of the quantization) electric field with strength F on penetration of quantum-mechanical current density $ej_x(x, z)$ (e being an electron charge) under semi-infinite potential barrier in height V at the interference of the electron waves in semiconductor 2D nanostructures have been theoretically studied. We have considered a situation when in 2D nanostructure at the left, from region 1 ($x < 0$, QW_1) the electronic wave of unit amplitude with energy $E_x < V$ on such barrier in region 2 ($x > 0$, QW_2) falls. We have shown, that in a situation when the electron wave falls on the first quantum-confined electron subband in QW_1 and longitudinal energy E_x of the particle less than energy of the bottom of the second subband in this reg. 1 and reflection of the electron wave probably only on the same first subband the quantum-mechanical current density $ej_x(x, z)$ in reg. 2 equal to zero. However, if energy of the particle in reg. 1 is more than energy of the bottom of the second quantum-confined electron subband in QW_1 a situation because of the interference of the reflected waves cardinally varies. The possibility of the exist of the reflected wave on the second subband on $x \rightarrow -\infty$ results to the situation, when under a barrier the quantum-mechanical current density $ej_x(x, z) \neq 0$ (penetration of quantum-mechanical current density) and its amplitude exponentially dumped at $x \rightarrow \infty$. Thus under a barrier there are two zones of distribution of the $ej_x(x, z)$: the zone (2), in which $ej_x(x, z)$ it is directed in a positive direction of the x- axis and zone (1), in which $ej_x(x, z)$ has a return direction. On zone (1) there is an outflow of a charge from under a barrier. Distinction of potentials $U_1(z)$ and $U_2(z)$ localizing a particle along the z-axis in regions 1 ($x < 0$) and 2 ($x > 0$) respectively provide nonorthogonality of the transverse wave functions in these regions. It results to confuse of the electron subbands in different regions and to appearance of the electronic interference effects. Certainly, the complete probability current density (or the complete quantum-mechanical current density) along the x-axis $J_x = \int j_x(x, z)\, dz$ has no coordinate dependence from x. As is known [1], at falling of the free electron with energy E_x (the x-axis is the direction of propagation of the electron wave) on a rectangular potential wall in height V_0 ($x > 0$) under condition of $E_x < V_0$ the quantum-mechanical current density $ej_x(x, z)$ in the reg. 2 is equal to zero, because of the real exponent of the wave function. Certainly, in this case exists exponentially dumped penetration of wave function of the particle into this region at $x > 0$.

We have calculated effect of penetration of a $ej_x(x, z)$ in the reg. 2 for the 2D nanostructure with parameters GaAs. Width of the structure is 300Å, $F = 7 \cdot 10^5$ V/cm.

[1] L. D. Landau and E. M. Lifschitz, Quantum Mechanics (Non – Relativistic Theory), Pergamon Press, Oxford, 1977.

TuP116

Mechanism of giant microwave response of two-dimensional electron system near the second harmonic of the cyclotron resonance

A.A. Zabolotnykh[1,2] and V.A. Volkov[2,1]

[1] *Moscow Institute of Physics and Technology, Moscow Region 141700, Russia*
[2] *V.A. Kotelnikov Institute of Radio-engineering and Electronics of RAS, Moscow 125009, Russia*

Remarkable features of microwave (MW) response of high-mobility two-dimensional electron systems (2DESs) at low temperature in magnetic field B have excited much interest the last few years, for review see [1]. Recently in ultraclean 2DESs new phenomenon has been revealed [2, 3, 4, 5]: colossal narrow photoresistivity spike was observed when MW radiation frequency Ω is near the second cyclotron resonance harmonic $2\omega_c$, where $\omega_c = |eB/mc|$, m is electron effective mass. It is significant to note that all 2DESs where the spike occurs show giant negative magnetoresistance in the absence of MW radiation. The origin of the spike is not clear.

We propose an explanation of the spike appearance in terms of classical approach to the description of 2DES. Our explanation is based on the parametric resonance (PR) phenomenon of electron motion caused by spatial inhomogeneous electric field of MW pumping. Such an inhomogeneous field appears due to metal contacts to 2DES near which the incident MW radiation is strongly modified [6]. One can understand the occurrence of PR by an analogy with swings which length varies periodically with frequency Ω. The fundamental mode of PR emerges at double eigenfrequency of the swings. In 2DES in magnetic field one can consider ω_c as eigenfrequency and therefore PR arises at $\Omega \approx 2\omega_c$.

We describe motion 2D electrons with the hydrodynamic velocity $\mathbf{V}$ which depends on coordinates and time and obeys the Euler equation. This equation contains the nonlinear term $(\mathbf{V}, \nabla)\mathbf{V}$ which is significant to our approach. One can examine the term as nonlinear local and instantaneous Doppler shift and this is the term which causes PR. We show that nonlinear correction to velocity $\mathbf{V}$ can grow exponentially over time, i.e. PR realizes, provided the gradient of electric field acting on 2D electrons exceeds threshold value.

We also discuss the spatial structure of the electric field acting on electrons as compared to the electric field of the incident MW radiation. The former field can be much greater as against the latter via the presence of metal contacts and as well as via nonlocal effects. Nonlocal effects emerge due to inhomogeneity of electric field of MW pumping on the electron cyclotron radius R_c scale, where $R_c = v_F/\omega_c$, v_F is the Fermi velocity.

Thereby we show that instability can arise in 2DES provided the gradient of MW electric field acting 2D electrons is greater than the threshold value which likely occurs at $\Omega \approx 2\omega_c$. Instability leads to heating of 2DES which destroys negative magnetoresistance state. This in turn leads to the sharp photoresistivity spike observed in experiments [2, 3, 4, 5].

[1] I.A.Dmitriev, A.D. Mirlin, D.G. Polyakov, and M.A. Zudov, Rev. Mod. Phys., **84**, 1709 (2012).
[2] Ya. Dai, R.R. Du, L.N. Pfeiffer, and K.W. West, Phys. Rev. Lett. **105**, 246802 (2010).
[3] Ya. Dai, K. Stone, I. Knez, C. Zhang, R.R. Du, C. Yang, L.N. Pfeiffer, and K.W. West, Phys. Rev. B **84**, 241303(R) (2011).
[4] A.T. Hatke, M.A. Zudov, L.N. Pfeiffer, and K.W. West, Phys. Rev. B **83**, 121301(R) (2011).
[5] A.T. Hatke, M.A. Zudov, L.N. Pfeiffer, and K.W. West, Phys. Rev. B **83**, 201301(R) (2011).
[6] S.A. Mikhailov and N.A. Savostianova, Phys. Rev. B **74**, 045325 (2006).

Investigation of the effective mass in $GaAs_{1-y}N_y$

Faina Lomakina[1,2], Oleksiy Drachenko[1], Harald Schneider[1], Amalia Patanè[3], Mark Hopkinson[4], and Manfred Helm[1,2]

[1] *Institute of Ion Beam Physics and Material Research, Helmholtz-Zentrum Dresden-Rossendorf, 01314 Dresden, Germany*
[2] *Technische Universität Dresden, 01062 Dresden, Germany*
[3] *The University of Nottingham, Nottingham NG7 2RD, United Kingdom*
[4] *University of Sheffield, Sheffield S3 3JD, United Kingdom*

Dilute nitride semiconductors (DNS), such as $GaAs_{1-y}N_y$, with a nitrogen content y of a few percent or even less, have recently attracted considerable interest due to the giant bowing effect. That, in turn, offers the possibility to tailor the band structure of new devices, like LEDs, lasers, solar cells, and infrared photodetectors by varying the nitrogen content [1]. Determining proper values of the effective mass (EM) of DNS is a topic of interest because of the inconsistency of previous results (e.g. [2, 3]). To clarify the conflict we study a series of GaAsN samples ($y = 0\% - 1\%$) by cyclotron resonance (CR) spectroscopy, Fourier transform infrared spectroscopy and photoluminescence spectroscopy in magnetic fields in order to deduce the EM via the CR frequency, plasma frequency and the diamagnetic shift, respectively. So far, we are able to show that the discrepancies of

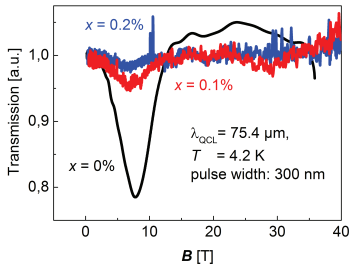

Figure 1: Determination of the EM by CR spectroscopy.

former publications are most likely caused by the particular choice of the experimental technique. Probably the most direct and reliable method is the CR spectroscopy, which has rarely been used due to the low electron mobility in GaAsN. Figure 1 illustrates that the CR does not significantly change with different N contents and thus the EM. Our magneto-PL spectroscopy results exhibit a huge increase of the EM with the N content ($m^*_{0\%} = 0.07m_e, m^*_{0.1\%} = 0.23m_e, m^*_{0.2\%} = 0.41m_e$) which is even bigger than in previous publications and in contrast to the CR result. The investigation of the diamagnetic shift of the electron to carbon impurity transition is a common technique (e.g.[2]) for the EM determination and is dominated by the identification of the slope s of ΔE. Our experiment shows a strong dependence of this value on the magnetic field region of interest. In our opinion, this method is not accurate enough for the EM determination.

[1] A. Erol, Dilute III-V Nitride Semiconductors and Material Systems, Springer-Verlag Berlin Heidelberg(2008).
[2] F. Masia et. al., Appl. Phys. Lett. **82**, 4474 (2003).
[3] Y. J. Wang et. al., Appl. Phys. Lett. **82**, 4453 (2003).

Magnetic focusing affected by an in-plane magnetic field in an InGaAs two-dimensional electron gas

Takanori Okayasu, Mokoto Kohda, and Junsaku Nitta

Graduate School of Engineering, Tohoku University, Sendai 980-8579, Japan

An InGaAs based quantum point contact generates a spin polarized current without magnetic fields and magnetic materials [1,2], which is a promising candidate for future spintronic devices. In order to apply the spin functional devices, we need to evaluate the spin polarization under the finite bias condition. Magnetic focusing in semiconductor nanostructures is an attracting method because it enables us to evaluate the spin polarization in a transport measurement [3]. However, magnetic focusing of an InGaAs based nanostructure is still challenging due to relatively short mean free path in comparison with a GaAs system. In this work, we demonstrate magnetic focusing in an $In_{0.7}Ga_{0.3}As/In_{0.53}Ga_{0.47}As$ two dimensional electron gas (2DEG) by using two narrow constrictions (NCs), which contain about twenty channels. By applying a perpendicular magnetic field to the 2DEG plane, electron orbital motion from the emitter NC is modulated due to the Lorentz force and focused to the collector NC, which results in the peak resistance in the collector bias.

A wafer consists of an $In_{0.53}Ga_{0.47}As/In_{0.7}Ga_{0.3}As/In_{0.53}Ga_{0.47}As$ structure and was processed into two parallel NCs with Hall bar structure as shown in an inset of Fig. 2. Both NCs and Hall bar were covered with an Al_2O_3 gate insulator (100 nm) and a Cr/Au (20 nm/150 nm) top gate electrode to modulate the electron mean free path. Magnetotransport measurements were performed at 1.7 K. By applying the positive top gate bias V_{tg}, the induced electrons are occupied not only in the first subband but also in the second subband, which induces the different electron momentum at the Fermi energy.

The in-plane magnetic field dependence of the focusing peak under $V_{tg} = 4.0$ V is shown in Fig. 1. Two resistance peaks are observed around -0.3 T and -0.2 T, which corresponds to the first subband and second subband momentum. However, momentum difference between spin up and down was not detected. This is probably due to the many conductance channels in NCs and low electron mobility of InGaAs 2DEG. In addition, when an in-plane magnetic field is applied, two peaks are shifted to opposite directions. The magnetic field at the resistance peak of the first subband is shown in Fig. 2 as a function of in-plane magnetic fields. In order to understand this peak shift, we consider the diamagnetic effect [4], which increases the subband energy difference ΔE under the in-plane magnetic field. The calculated magnetic field is shown as a blue line in Fig. 2, which is similar dependence to the experimental result. As a result, we can detect the subband energies and their energy shifts by using the transverse magnetic focusing in the InGaAs 2DEG.

[1] P. Debray *et al.*, Nat. Nanotech. **4**, 759 (2009). [2] M. Kohda *et al.*, Nat. Commun. **3**, 1082 (2012). [3] R. M. Potok *et al.*, PRL **89**, 266602 (2002). [4] W. Beinvogl *et al.*, PRB **14**, 4274 (1976).

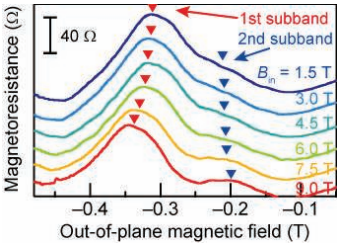

Figure 1: In-plane magnetic field dependence of focusing peaks.

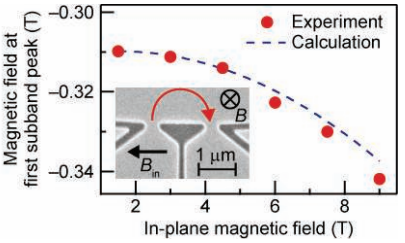

Figure 2: Experimental and calculated results. Inset: SEM image of the device.

Morphology and charging of heteropolar SiC/AlN and SiC/GaN interfaces

Małgorzata Sznajder[1] **and Jacek A. Majewski**[2]

[1] *Institute of Physics, University of Rzeszów, ul. Rejtana 16a, 35-310 Rzeszów, Poland*
[2] *Faculty of Physics, University of Warsaw, ul. Hoża 69, 00-681 Warszawa, Poland*

Thin nitride films on silicon carbide substrate constitute many technologically important devices [1,2], where the nitride/SiC interface plays particularly important role. In spite of intensive experimental efforts [e.g., 3], the microscopic physics of these intriguing interfaces is mostly unknown. The heterovalent character of these interfaces, in addition to the piezo- and pyroelectric character of the junction materials, leads to polarization charges and very strong electric fields that could in turn cause changes in atomistic details of the interfaces.

In this work, we present first-principles studies for 4H-SiC/wz-AlN, 3C-SiC(111)/wz-AlN, 4H-SiC/wz-GaN, and 3C-SiC/wz-GaN interfaces in the framework of the density functional theory. We have calculated the atomistic details of the interfaces, their formation enthalpies, valence band offsets (VBO's), induced interface charges, and electric fields. The theoretical studies of the similar interfaces have been reported previously for some cubic structures [4]. In the present calculations we employed the supercells with up to 136 atoms, and performed precise calculations for hexagonal systems employing the SIESTA code.

In heteropolar SiC/nitride systems, the abrupt interfaces contain 'oversaturated' or 'under saturated ' tetrahedral bonds with more than 2 or less than 2 electrons per bond, respectively. This bond heteropolarity leads to a macroscopically charged interface that is typically energetically unstable and undergoes various reconstructions to roughly restore charge neutrality. For example, the simplest atomic reconstructions leading to the neutral interfaces are those with one mixed layer (e.g., N/C, Ga/Si or Al/Si).

Our calculations show that the preferred bonding configurations of the reconstructed interfaces are found to be Si-N and Ga-C. The calculated valence band discontinuities for SiC/AlN and SiC/GaN heterostructures lie in the range of 1.5 - 2.3 eV and 0.4 - 1.4 eV, respectively, depending on the atomistic details of the reconstruction, and compare reasonably well with available experimental data. The SiC/AlN heterostructures are predicted to be of type I, whereas SiC/GaN heterostructures can be of type I or II, depending on the orientation and chemical composition of the interface. The polarization induced interface charges are of the order of 4.8 x 10^{12}cm^{-2} and 0.7 x 10^{12} cm^{-2} in SiC/AlN and SiC/GaN junctions, respectively. Comparing the interface charges in the junctions with hexagonal 4H-SiC and cubic 3C-SiC heterostructures, we conclude that the spontaneous polarization in bulk 4H-SiC is negligible in comparison to the one in AlN and GaN.

The present studies shed light on the physics of heteropolar SiC/nitride interfaces and provide microscopic knowledge of interface morphology together with theoretical predictions of important parameters of the junctions. They constitute also the basis for reliable modeling of important phenomena in these junctions such as the charge and spin transport across the interface and the thermal boundary resistance effect.

[1] A. V. Sampath, *et al*., Appl. Phys. Lett. **101**, 093506 (2012).
[2] Y. Huang, *et al*., Appl. Phys. Lett. **86**, 122102 (2005).
[3] S. W. King, R. F. Davis, and R. J. Nemanich, Surf. Sci. **602**, 405 (2008); M. Losurdo, *et al*., Appl. Phys. Lett. **86**, 021920 (2005).
[4] M. Städele, J.A. Majewski, and P. Vogl, Phys. Rev. B **56**, 6911 (1997); P. Ferrara, N. Binggeli, and A. Baldereschi, Phys. Rev. B **55**, R7418 (1997).

TuP120

Imaging electrons in graphene nanostructures

Sagar Bhandari, Estelle Kalfon-Cohen, David Bell, Robert M. Westervelt

School of Engineering and Applied Sciences, Harvard University, Cambridge, MA 02138
Email: sbhandar@fas.harvard.edu

Graphene has great promise for quantum devices with atomic dimensions [1, 2]. Research has developed novel techniques to make atomic-scale structures in graphene, understand their stability, and their electronic behaviour. We present methods to fabricate suspended graphene nanostructures using the electron beam of a high-resolution transmission electron microscope, and we describe the implementation of a scanning capacitance probe operating at liquid helium temperatures that is designed to probe electron motion in these devices. The capacitive probe senses electrons using a cooled charge amplifier [3]. We have achieved a low noise figure for this technique, which show great promise as a tool to study the electronic behaviour of nanoscale devices.

Supported by DoE DE-FG02-07ER46422.

[1] A.K. Geim and K.S. Novoselov, Nature Materials **6**, 183 (2007).
[2] Melinda Y. Han, Barbaros Ozyilmaz, Yuanbo Zhang, and Philip Kim, Phys. Rev. Lett. **98**, 206805 (2007).
[3] G.A. Steele, R.C. Ashoori, L.N. Pfeiffer and K.W. West, Phys. Rev. Lett. **95**, 136804 (2005).

Photocurrent studies of GaAs/AlGaAs coupled quantum well solar cells

T. Noda [1], M. Jo [1], T. Mano [1], T. Kawazu [1] and H. Sakaki [1,2]

[1] *National Institute for Materials Science, Tsukuba, Ibaraki, 305-0047, Japan*
[2] *Toyota Technological Institute, Nagoya 468-8511, Japan*

Intermediate band (IB) solar cells have attracted considerable interests because of their potential for improvement of energy conversion efficiency [1]. In this type of solar cell, an IB formed between the conduction and valence bands of the host semiconductor plays a key role. To realize an IB, the coupling of neighboring states is necessary. So far, we have studied current-voltage (*I-V*) characteristics of a solar cell in which coupled multiple quantum wells (MQWs) are embedded, and found a substantial decrease in the photocurrent (PC) at low bias voltages [2]. This reduction of PC is explained by the suppression of carrier escape processes and resultant carrier accumulation in the well, which could cause a band bending in a MQW structure. In this work, we study in detail photocurrent spectra of a coupled MQW solar cell at various bias voltages and discuss the results in connection with *I-V* characteristics.

A sample having *pin* structure was grown on n-type GaAs(100) by molecular beam epitaxy. The MQW layer consisting of 10 periods of 4 nm GaAs well and 3 nm AlGaAs barrier were embedded in the middle part of a 1-μm thick *i*-AlGaAs layer. Structural details were reported in ref. [3]. The sample was processed into a mesa-shaped diode with an area of about 6.6×10^{-7} m^2. PC measurements were done at 10 K by using a monochromator and a halogen lamp.

Figure 1 shows PC spectra at different bias voltages. For large negative biases ($V < \sim1$ V), a series of peaks are clearly seen, reflecting the localization of electron wavefunction under high electric fields. As the bias increases to the forward direction, the peak structure is smeared due to the delocalization of electron. In addition, as V is raised, the PC decreases as a result of carrier confinement in the MQW. The inset plots the PC as a function of bias voltage (*I-V* curve) under 720-nm excitation. The PC remains constant at $V < -1$ V since almost all carriers escape out of the MQW before recombination. Then, as electric fields decreases, the PC drops off owing to the carrier confinement. Interestingly, the disappearance of peak structure in the PC spectra becomes noticeable at $V = -1$ V, which implies that the band for the MQW region is rather flat at an early stage of the carrier confinement. As discussed in Ref. 3, the accumulation of carriers in a *coupled* structure causes the partial screening of the electric field inside, which leads to the formation of relatively flat band. The combination of PC and *I-V* studies will provide fruitful information on important features of IB solar cells.

[1] A. Luque and A. Marti, Phys. Rev. Lett. **78**, 5014 (1997). [2] T. Noda, et al. Phys. Status Solidi C **8**, 349 (2011). [3] T. Noda, et al. Jpn. J. Apply. Phys. **51**, 10ND07 (2012).

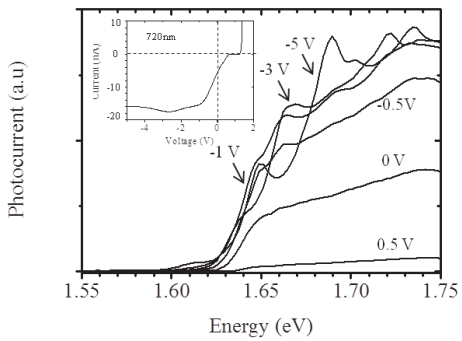

Fig.1 Photocurrent spectra at different bias voltages. The power of light was ~1 μW. Inset: current-voltage characteristic at 10 K.

TuP122

Structural properties of GaAsBi layers grown on GaAs by molecular beam epitaxy

J. Puustinen[1], A. Schramm[1], P. Laukkanen[2], L. Juhola[1], M. Wu[3], E. Luna[3], M. Laitinen[4], T. Sajavaara[4] and M. Guina[1]

[1] *Optoelectronics Research Centre, Tampere University of Technology, P.O. Box 692, FI-33101 Tampere, Finland*
[2] *Department of Physics and Astronomy, University of Turku, FI-20014 Turku, Finland*
[3] *Paul-Drude Institut für Festkörperelektronik, Hausvogteiplatz 5-7, 10117 Berlin, Germany*
[4] *Department of Physics, P.O.Box 35, FI-40014 University of Jyväskylä, Finland*

The semiconductor alloy $GaAs_{1-x}Bi_x$ has recently attracted attention due to its potential applications in optoelectronics. Adding small amounts of Bi to the GaAs lattice leads to a large reduction of the band gap, allowing access to important wavelengths in the infrared region. Due to the tendency of Bi to surface segregate, successful incorporation of Bi in the GaAs lattice requires nonconventional growth conditions, such as growth temperatures below 400°C and precise control of As beam equivalent pressure, which are nonoptimal in terms of quality of the host material [1, 2]. In particular, low growth temperatures are known to lead to formation of various defects in GaAs [3]; the defect formation mechanisms are expected to be even more complicated in the case of GaAsBi. In attempt to reduce the defects one can use annealing that is a common method to improve the quality of semiconductor materials.

Here, we summarize our recent studies concerning the effects of thermal annealing on the properties of GaAsBi materials grown at different temperatures. $GaAs_{1-x}Bi_x$ bulk layers with Bi composition x of ~1.2-1.5% were grown on GaAs by solid-source molecular beam epitaxy at temperatures of 220-315°C. Samples were subsequently annealed ex-situ in a rapid thermal annealing (RTA) oven at temperatures between 500°C and 800°C using a GaAs proximity cap, and characterized with X-Ray diffraction, Rutherford backscattering spectroscopy and transmission electron microscopy.

The lattice constant of GaAsBi samples grown at the lower temperatures (220-270°C) decreased significantly towards the GaAs lattice with post-growth annealing, while the samples grown at higher temperatures did not exhibit this behavior. Similar GaAs samples exhibited smaller changes with annealing due to diffusion of excess As. We relate this behavior to the formation of clusters with high Bi content in lower-temperature grown GaAsBi samples.

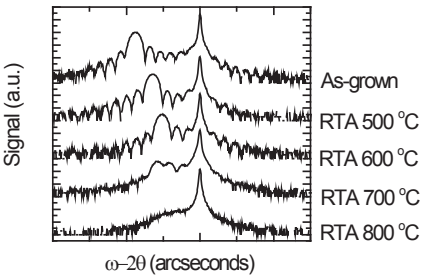

Fig 1: XRD spectra of a GaAsBi sample grown at 220°C and annealed at various temperatures.

[1] S. Tixier, M. Adamcyk, T. Tiedje, S. Francoeur, A. Mascarenhas, P. Wei and F. Schiettekatte, Appl. Phys. Lett. **82**, 2245 (2003)
[2] R. B. Lewis, M. Masnadi-Shirazi and T. Tiedje, Appl. Phys. Lett. **101**, 082112 (2012)
[3] X. Liu, A. Prasad, J. Nishio, E. R. Weber, Z. Liliental-Weber and W. Walukiewicz, Appl. Phys. Lett. **67**, 279 (1995)

Annealing induced modulation of joule heating based metal-insulator transition point of VO_2 nanobeams for smart nanodevice applications

S. Rathi[1], Jinhyung Park[1], Inyeal Lee[1], Min Jin Kim[2], Jeong Min Baik[2], Kyung Soo Yi[3] and Gil-Ho Kim[1]

[1]*Department of Electronic and Electrical Engineering and Sungkyunkwan Advanced Institute of Nanotechnology (SAINT), Sungkyunkwan University, Suwon 440-746, Korea*
[2]*School of Mechanical and Advanced Materials Engineering, Ulsan National Institute of Science and Technology (UNIST), Ulsan 689-805, Korea*
[3]*Department of Physics, Pusan National University, Busan 609-735, Republic of Korea*

Of all correlated transition metal oxides, vanadium dioxide (VO_2), transition temperature (T_{IMT}), at which transition from insulator to metal phase (IMT) occurs, is closest to room-temperature (67 ^oC), which makes this material interesting for potential technological applications including sensors and memristors.[1]
Joule heating based transition is one of the simple and common method to induce IMT in VO_2 nanobeams (NBs).[2] However, the voltage at which Insulator to Metal Transition (V_{IMT}) occurs is susceptible to processing and fabricating conditions, though its accurate determination and control is at the heart of devices like sensors and switches based on VO_2.

In this work, the effect of annealing conditions on VO_2 NBs having average width of 300 nm, have been studied through voltage and temperature induced hysteretic plots, Fig.1. Our analysis shows that annealing conditions have a profound impact on the V_{IMT} values through a simultaneous variation in both NBs conductivity and T_{IMT} values. The results obtained were also confirmed by a mathematical model. These variations in V_{IMT} and T_{IMT} are possibly due to oxygen deficiency induced monoclinic lattice defect and doping behavior of oxygen vacancies in the resulting nonstoichiometric VO_2 NBs. These finding can be very useful for device engineers who can not only control V_{IMT} point, albeit at the cost of minor trade-off (variation in conductivity and T_{IMT} point), but can also scale down voltage supply for prospective low-voltage sensors applications.

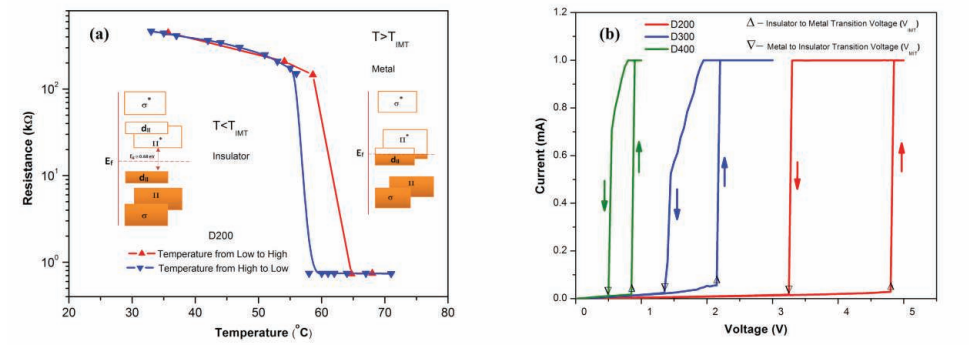

Fig. 1. (a) Temperature hysteretic plot of VO_2 NB, annealed at 200 ^oC, 1 minute in Argon ambient. [inset showing energy band diagrams in insulating and metallic phase], **(b)** Variation in V_{IMT} point of VO_2 nanobeams following Rapid Thermal Annealing (RTA) at 200 ^oC (D200), 300 ^oC (D300), 400 ^oC (D400) in Argon ambient for 1 minute, with compliance set at 1.0 mA to avoid thermal breakdown.

[1] Z. Yang, C. Ko, and S. Ramanathan, Annu. *Rev. Mater. Res.* **41**, 337 (2011).
[2] J. W. Byon, *et al. Jour. Phy. Chem. C.* **116**, 226 (2012).

TuP124

A single-photon 'click' detector for microwave light

N. J. Lambert[1], M. Edwards[1], A. A. Esmail[1], F. Pollock[2], B. W. Lovett[3], A. J. Ferguson[1]

[1] *Microelectronics Group, Cavendish Laboratory, J. J. Thomson Avenue, Cambridge, CB3 0HE, UK*

[2] *Clarendon Laboratory, Parks Road Oxford, OX1 3PU, UK*

[3] *School of Engineering & Physical Sciences, Heriot-Watt University, Edinburgh, EH14 4AS, UK*

We demonstrate a single-photon click detector in the frequency range 30 GHz to 50 GHz. The device is based on a superconducting double dot, with readout via quantum capacitance measurement. We show that the detector threshold can be tuned, and establish its linearity.

Single photon detection at visible and IR frequencies is a well-established technology, but the task becomes more difficult as the photon energy decreases. Microwave photons have energies 10000 times lower than those detected by silicon avalanche photodiodes and single photon detection at these energies would be of considerable interest, for example in the quantum information applications of circuit quantum electrodynamics[1]. Whilst the Hanbury-Brown – Twiss effect has been observed for microwave frequencies[2], this is the first time a click detector has been demonstrated for photons at these energies.

We have fabricated a superconducting double quantum dot, with two Al islands connected via Josephson junctions to each other, and tunnel junctions to normal leads. The energetics of a normal double dot is characterized entirely by the charging energy (E_c) of the islands. In our superconducting device the superconducting gap (Δ) and the Josephson energy act as additional energy scales, breaking the symmetry between even and odd parity charge states. For a sufficiently low value of E_c / Δ odd parity states, which involve quasiparticles, are energetically unfavourable.

To probe the state of our device, we use r.f. reflectometry. In particular, we measure the quantum capacitance of the system [3]. We can distinguish even parity and odd parity states with a signal to noise ratio of ~4 and a bandwidth of 100kHz.

By the application of a magnetic field, the ratio between E_c and Δ can be changed. We tune the device so that a quasiparticle state is energetically accessible by absorption of a single non-equilibrium microwave photon. This change in parity is readily measurable, and so we can detect the absorption of the photon.

Single shot time domain measurements taken at the (2,0)/(0,2) degeneracy show stochastic switching between the (2,0) and (1,1) states. We attribute this to the absorption of background microwave photons by the device. We demonstrate the device operating as a 'click' detector of photons by applying microwaves in the 30-50GHz range. The photon count is linear with applied microwave power, and by changing the applied magnetic field, we can change the detection threshold.

[1] D. Bozyigit *et al*. Nature Physics **7**, 154–158 (2011)
[2] Y.-F. Chen *et al*. Phys. Rev. Lett. 107, 217401 (2011)
[3] K. D. Petersson *et al.* Nano Letters **10**, 2789-2793 (2010).

Quantum Multiplexer: A novel device architecture for low-temperature measurements

H. Al-Taie[1,2], L. W. Smith[1], J. P. Griffiths[1], H. Beere[1], G. A. C. Jones[1], D. A. Ritchie[1], C. G. Smith[1] and M. J. Kelly[1,2]

[1] *Cavendish Laboratory, Department of Physics, University of Cambridge, J. J. Thomson Avenue, Cambridge, CB3 0HE, United Kingdom*

[2] *Centre for Advanced Photonics and Electronics, Electrical Engineering Division, Department of Engineering, University of Cambridge, 9 J. J. Thomson Avenue, Cambridge, CB3 0FA, United Kingdom*

Low-temperature semiconductor device physics is an area of intense research with a wide range of applications. However, research into this field suffers from limitations set by the small number of electrical contacts available on a single chip. The result is that only a few devices can be fabricated on a single chip, thus limiting the device or circuit complexity. Because of this, current research continues to be a slow, costly and time-consuming procedure where fabrication and measurement of several chips is necessary in order to study statistical variations of electrical characteristics and yield.

We present a novel low-temperature device architecture which significantly increases the number of electrical contacts locally available on a single chip, without the modification of existing fabrication or experimental setups. The 'Quantum Multiplexer' allows contact to a much larger number of mesoscopic devices on a single chip, as well as the design of more complex nano-scale circuits.

We demonstrate the applicability of the multiplexer to devices based on GaAs/AlGaAs heterostructures by presenting conductance measurements of 256 quasi-one-dimensional quantum wires formed by split-gate devices with common source-drain contacts on a single chip using only 19 electrical contacts. Yang *et al.* presented initial results [1-3] of statistical studies of split-gate characterisation, however, these measurements required many different chips to be tested on different cool downs. The advantage of our measurements is that they are conducted in a single cool down using common source-drain contacts, therefore eliminating variations in ohmic-contact resistance between devices. This provides a more comprehensive study of intrinsic yield and reproducibility through detailed statistical analysis of electrical characteristics such as one-dimensional channel definition, channel pinch-off and the '0.7 structure'.

The multiplexer makes a whole series of further, some intrinsically new, statistical investigations of both quantum phenomena and device fabrication/manufacturability possible. An incomplete list of possibilities include statistical studies of zero-dimensional quantum dots, parallel charge pumps, low-temperature shift registers and device analysis for quantum computing applications.

[1] Q.-Z. Yang, G. A. C. Jones, M. J. Kelly, H. Beere and I. Farrer, Semicond. Sci. and Technol. 21 558-64 (2006).

[2] Q.-Z. Yang, G. A. C. Jones, M. J. Kelly, H. Beere, and I. Farrer, Semicond. Sci. and Technol. 23 055018: 7pp (2008).

[3] Q.-Z. Yang, M. J. Kelly, H. Beere, I. Farrer and G. A. C. Jones, Appl. Phys. Lett. 94 033502 (2009).

Towards nano-structure circuits using split gates

L. W. Smith[1], H. Al-Taie[1,2], B. Xu[1], J. P. Griffiths[1], H. E. Beere[1], G. A. C. Jones[1], D. A. Ritchie[1], C. G. Smith[1], and M. J. Kelly[1,2]

[1] *Cavendish Laboratory, J. J. Thomson Avenue, Cambridge, CB3 0HE, United Kingdom*
[2] *Centre for Advanced Photonics and Electronics, Department of Engineering, University of Cambridge, 9 J. J. Thomson Avenue, Cambridge, CB3 0FA, United Kingdom*

It is hard to underestimate the importance of the simple split-gate in the world of mesoscopic devices. It was using split gates that the conductance through a one-dimensional (1D) constriction was first shown to be quantised in units of $2e^2/h$. Since then, split gates fabricated on GaAs heterostructures have been ubiquitous in 1D physics, facilitating a vast amount of research on quantum phenomena.

It has recently been demonstrated that split gates can be used as an electrical means of generating a spin-polarized current, which has potential application in the emerging field of 'spintronics', where information is transferred in a circuit using the spin state of electrons [1, 2]. However, in order for split gates to be used in larger, more complex circuits, the scalability of this technology must be considered; it should be shown that electrical characteristics are highly consistent from device to device.

We have fabricated 256 lithographically-defined split gates on a single chip, by developing a novel device layout which enables selective contact to each split gate individually. Our split-gate yield was better than 94%, and we measured more than 600 nominally-identical devices fabricated on two different GaAs/AlGaAs wafers. We compare the conductance through the split gates before and after thermal cycling, as well as before and after illumination, and show how the quality of the conductance quantisation is affected by carrier density and mobility, impurity scattering, background-potential variations, and split-gate roughness. This is the first real test of the reproducibility of the electrical characteristics of a large number of split gates, inspired by initial work by Yang *et al.* [3], which was limited in the number of split gates that could be measured on a single cool down. We will also present statistical variations in the occurrence of the '0.25 feature', which appears at $0.25 \times (2e^2/h)$ when a large dc bias is applied across the split gate [4]. The 0.25 feature has the characteristics of being spin polarised, and as such has potential as an electrically-controlled spin injector in spintronic applications [2].

Our array of split-gate devices is a powerful tool. It tests the quality of the underlying GaAs wafer, since it is possible to determine the probability of encountering an impurity in the 1D channel, and hence an estimate of the impurity density. In addition, a systematic study of statical variations in the occurrence of conductance anomalies – such as the 0.7 structure and zero bias anomaly – can be performed for the first time. This will be instructive, since a definitive explanation for these conductance anomalies remains to be given.

[1] P. Debray, S. M. S Rahman, J. Wan, R. S. Newrock, M. Cahay, A. T. Ngo, S. E. Ulloa, S. T. Herbert, M. Muhammad, and M. Johnson, Nature Nanotech. **4**, 759 (2009).
[2] T.-M. Chen, M. Pepper, I. Farrer, G. A. C. Jones, and D. A. Ritchie, Phys. Rev. Lett. **109**, 177202 (2012).
[3] Q.-Z. Yang, M. J. Kelly, I. Farrer, H. E. Beere, and G. A. C. Jones, Appl. Phys. Lett. **94**, 033502 (2009).
[4] T.-M. Chen, A. C. Graham, M. Pepper, I. Farrer, and D. A. Ritchie, , Appl. Phys. Lett. **93**, 032102 (2008).

Manipulation of circular polarization in a three-dimensional chiral photonic crystal

S. Takahashi [1], A. Tandaechanurat [1], R. Igusa [2], Y. Ota [1], J. Tatebayashi [1], S. Iwamoto [1,2] and Y. Arakawa [1,2]

[1] *NanoQuine, University of Tokyo,* [2] *IIS, University of Tokyo, 4-6-1 Komaba, Meguro-ku, Tokyo 153-8505, Japan*

Optical activity, which consists of optical rotation and circular dichroism in the basis of the circular polarization, can occur when light passes through a structure without mirror and spatial inversion symmetry, such as helices or chiral molecules. Artificial optically active photonic media are effective tools for manipulating the polarization of photons, which could be useful in several applications including spin-photon interfaces in quantum information processing [1]. Quasi-two-dimensional chiral systems made from metals, dielectrics, or semiconductors exhibit starkly modified electric fields at the material interface, and show large degrees of optical rotation [2]. Three-dimensional (3D) helical structures are expected to further enhance the optical activity, although their fabrication at the optical wavelength scale is still challenging, especially for semiconductor materials. So far, such 3D helical structures have been realized using, for instance, a liquid crystal [3], a polymer [4], and a metamaterial [5] and studied only in terms of the circular dichroism.

In this study, we demonstrate for the first time a GaAs-based 3D chiral photonic crystal based on a rotationally-stacked woodpile structure, and successfully manipulate the circular polarization using both kinds of optical activity. The structure of the sample belonging to a spatial group with 4_1 screw operation was fabricated by a micro-manipulation technique [6] (see Fig.1).

We characterized both the optical rotation and the circular dichroism by measuring the polarization of laser light transmitted along the helical axis. Figure 2 shows the wavelength dependences of polarization rotation angles and of ellipticities for linearly polarized light after transmission. Both sets of experimental data show good agreement with finite-difference time-domain calculation results, and suggest large optical activity in our structure. Further experiments on input azimuth angular dependences of the polarization rotation angle resulted in sinusoidal oscillations of output polarization rotation angle, together with some offset. This offset reaches -45° at 1300nm, demonstrating a large genuine optical rotation angle [2]. A reciprocal optical activity was confirmed in the same structure by illuminating the laser light from the backside, further validating the manifestation of the large optical activity.

[1] K. D. Greve *et al.*, Nature **491**, 421 (2012), W. B. Gao *et al.*, Nature **491**, 426 (2012). [2] K. Konishi *et al.*, Opt. Exp. **16**, 7189 (2008). [3] H. Coles and S. Morris, Nat. Photo. **4**, 676 (2010). [4] M. Thiel *et al.*, Opt. Lett. **32**, 2547 (2007). [5] Y. Zhao *et al.*, Nat. Comm. **3**, 870 (2012). [6] A. Tandaechanurat *et al.*, Nat. Photo. **5**, 91 (2010). Acknowledgement: This work was supported by the Project for Developing Innovation Systems of MEXT and JSPS through its FIRST Program.

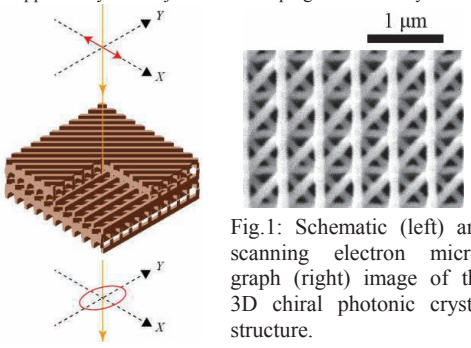

Fig.1: Schematic (left) and scanning electron micro-graph (right) image of the 3D chiral photonic crystal structure.

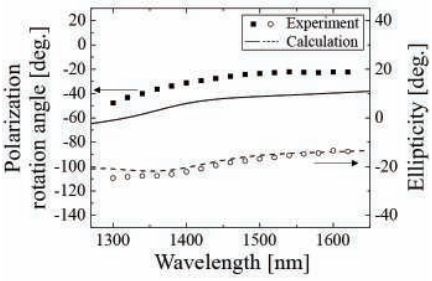

Fig.2: Wavelength dependence of optical activity in the structure shown in Fig.1.

SAXS domain structure characterization of a GaAs-GaSe multilayer film using irradiation wavelengths near absorption edges

Michael E. Boiko, Michael D. Sharkov, Andrei M. Boiko and Alexander V. Bobyl

[1] *Ioffe Physico-Technical Institute, St. Petersburg, Russia*

An effective approach to studying substance domain structure is provided by the technique of small-angle x-ray scattering (SAXS). This experimental method allows one to estimate sizes and shape of homogeneous fragments of the sample (domains, grains, clusters, pores, etc.) as well as determine spatial features of superstructures (e.g. superlattice interplanar distances and layer widths). A special role in multiphase specimen characterization is played by SAXS data sets measured at wavelength values close to absorption edges concerned to the atoms constituting the sample substance. Comparing such SAXS spectra one can get a way to relate separate results of SAXS analysis to sample components with a certain chemical composition.

A multi-layered GaAs-GaSe film was subject to SAXS measurements at three wavelength values: 1.54 Å (the Cu K_α line magnitude), 1.043 Å (slightly shorter than the As K edge), 0.979 Å (unsubstantially shorter than the Se K edge). The SAXS spectrum obtained with the help of the Cu K_α wavelength beam is represented at Fig. 1.

The SAXS spectrum measured at the Cu K_α beam wavelength happened to contain a wide Bragg peak that could correspond to different values of superstructure spatial parameters (from 15 nm up to 30 nm). Nevertheless, the SAXS curve obtained with the help of the beam harder than the As K edge included a Bragg peak explicitly corresponding to the spatial parameter value of about 15 nm. Thus, this meaning might be related to the specimen components without As atoms (e.g. GaSe domains forming a regular net along the film surface).

In turn, the SAXS data set measured using the beam with energy higher than the Se K edge included a Bragg peak reflecting the spatial parameter magnitude about 25 nm. This one, therefore, must be related to the sample components consisting of atoms but Se, i.e. with GaAs chemical composition. Thus, the size value of 15 nm has been connected with the GaSe compound while the GaAs composition has been stated to correspond to the value of 25 nm.

It is argued that the alleged film of solid solution GaAs/Se splits into multilayers of GaAs and GaSe. Density waves at SEM photos corresponded to packs of such sublayers.

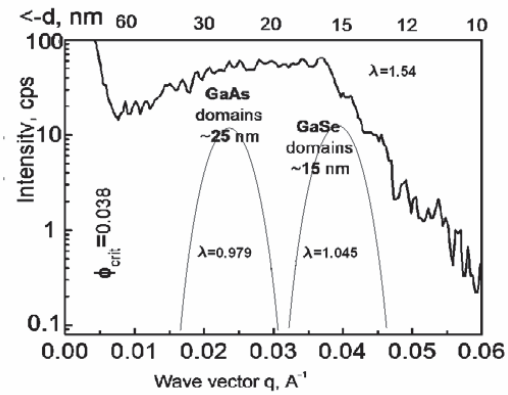

Fig. 1. SAXS data registered for the GaAs-GaSe multilayer film at the Cu K_α beam wavelength.

Electric and thermoelectric properties of CdTe/PbTe epitaxial nanocomposite

M. Szot, K. Dybko, P. Dziawa, L. Kowalczyk, V. Domukhovski, B. Taliashvili, A. Reszka, B. J. Kowalski, P. Dłużewski, M. Wiater, T. Wojtowicz, T. Story

Institute of Physics, Polish Academy of Sciences, Al. Lotników 32/46, 02-668 Warsaw, Poland

The nanostructuring of thermoelectric materials is known to improve their thermoelectric efficiency described by the figure of merit parameter $Z=S^2\sigma/\kappa$, where S is Seebeck coefficient (thermopower), σ and κ are electrical and thermal conductivities, respectively. The decrease of κ due to the resonantly enhanced phonon scattering on nano-grain crystal boundaries and the increase of S due to increased the electron density of states at the Fermi level are two key effects leading to the improvement of thermolelectric properties of nanostructured material. Here we examine the electrical and thermoelctrical properties of the novel layered nano-material composed of wide bandgap, zinc-blende CdTe anti-dots embedded in a narrow bandgap, rock-salt PbTe thermoelectric matrix [1]. The investigated nanocomposite was prepared by the two-stage technological procedure i.e. high vacuum annealing of properly designed CdTe/PbTe multilayer grown on GaAs substrate by molecular beam epitaxy. The method exploit the fact that due to the difference in their crystal structure, the constituent materials of nanocomposite are in practice immiscible at room temperature. In contrast to the other growth techniques the procedure presented here allows to govern the distribution of CdTe anti-dots and their sizes (from 5 to 30 nm) in nanocomposite by controlling the film thicknesses in initial multilayer. The Hall effect measurements performed in temperature range 4÷300 K showed that both n- and p-type conductivity can be obtained in these nanocomposites with carrier concentration up to 6×10^{18} cm^{-3}. Very good crystal quality of the nanocomposite was confirmed by the observation of the Shubnikov-de Hass oscillations at low temperatures. The carrier mobility depends on temperature in non-monotonic way. Moreover, in the case of samples containing only a few layers of CdTe antidots, the relatively sharp maximum at about 100 K with peak value up to 3500 cm^2/Vs is observed. This behavior will be discussed within the model involving the electron scattering on CdTe nano-grain boundaries. In turn, the measurements of Seebeck coefficient show linear dependence in studied range of temperatures with value of about 250 μV/K at 300 K for samples containing smallest CdTe anti-dots. This thermopower is over 20 % higher than expected for reference bulk thermoelectric PbTe crystals with corresponding electron concentration. We interpreted this finding as a result of enhanced density of states for electrons in PbTe crystalline matrix. Our interpretation is corroborated by fact, that for samples containing bigger CdTe anti-dots we observe no thermopower enhancement.

Work supported within the European Regional Development Fund, through the Innovative Economy grant (POIG.01.01.02-00-108/09).

[1] M. Szot*, K. Dybko, P. Dziawa, L. Kowalczyk, E. Smajek, V. Domukhovski, B. Taliashvili, P. Dłużewski, A. Reszka, B. J. Kowalski, M. Wiater, T. Wojtowicz, T. Story, Cryst. Growth Des., **11**, 4794 (2011)

TuP130

A semiconductor-like InN?

Kuang-I Lin [1], I-Cheng Su [2], Jenn-Shyong Hwang [2] and Shangjr Gwo [3]

[1] *Department of Electrical Engineering, National Chung Hsing University, Taichung, Taiwan*
[2] *Department of Physics, National Cheng Kung University, Tainan, Taiwan*
[3] *Department of Physics, National Tsing Hua University, Hsinchu, Taiwan*

There are considerable discrepancies between the reported theoretical data of the crystal-field splitting from 17 to 301 meV and the spin-orbit splitting from 1 to 13 meV of InN [1,2], which have played a very important role in elucidating the band structure of semiconductors and in investigating the control of spin relaxation rate for spintronics [3]. A few papers on photoreflectance (PR) or electroreflectance study in InN have been reported [4,5], and only the band gap has been characterized. A metal-semiconductor transition behavior in Ga- or Al-doped ZnO at low temperatures has been demonstrated, which is a candidate for transparent conducting oxides [6]. Recently, temperature-dependent electrical resistivity in InN films and InN nanowires with side lengths larger than 80 nm also shows similar behavior as observed in doped ZnO [7,8]. This makes it possible to measure PR spectra of InN at low temperatures due to the semiconductor-like properties.

Two native n-type InN samples are studied. The InN-1 sample is grown by metal organic chemical vapor deposition. The InN-2 sample is grown by plasma-assisted molecular beam epitaxy. Room-temperature Raman spectra and temperature-dependent PR and photoluminescence (PL) spectra are utilized to investigate the crystalline quality, electron concentrations, electronic band structures, and optical properties of the InN films. The electron concentrations are estimated to be 1.44×10^{19} and 0.58×10^{19} cm^{-3} at room temperature for InN-1 and InN-2, respectively, according to the PL peak positions considering the Burstein-Moss effect. For InN-2, PR feature is not detectable until the temperature is below about 100 K. This result can be attributed to a transition from a metal-like conductor (above 100 K) to a semiconductor caused by free electrons cooling down to trap states at such low temperatures. This observation is well consistent with Refs. [7,8]. The energy level of the trap has been reported around 52 meV below the conduction band minimum [7]. For InN-1, no PR signal is observed even at 15 K. The presence of high concentration of free carriers prevents efficient electromodulation. The temperature-dependent PL lineshapes are also different for InN-1 and InN-2. Based on the PR results and the appropriate Hamiltonian, the values of crystal-field splitting and spin-orbit splitting in InN are experimentally determined, for the first time, as 24.2 and 17.4 meV, respectively, at 30 K for example.

[1] L.C. de Carvalho, A. Schleife, F. Fuchs, F. Bechstedt, Appl. Phys. Lett. **97**, 232101 (2010).
[2] I. Vurgaftman, J.R. Meyer, J. Appl. Phys. **94**, 3675 (2003).
[3] Z.W. Jia, W.Z. Shen, H. Ogawa, Q.X. Guo, Appl. Phys. Lett. **89**, 232107 (2006).
[4] R. Kudrawiec, T. Suski, J. Serafińczuk, J. Misiewicz, D. Muto, Y. Nanishi, Appl. Phys. Lett. **93**, 131917 (2008).
[5] J.-W. Yoon, S.S. Kim, H. Cheong, H.-C. Seo, S.-Y. Kwon, H.-J. Kim, Y. Shin, E. Yoon, Y.-S. Park, Semicond. Sci. Technol. **20**, 1068 (2005).
[6] V. Bhosle, A. Tiwari, J. Narayan, Appl. Phys. Lett. **88**, 032106 (2006).
[7] G.R. Mutta, J.M. Routoure, B. Guillet, L. Méchin, J. Grandal, S. Martin-Horcajo, T. Brazzini, F. Calle, M.A. Sánchez-García, P. Marie, P. Ruterana, Appl. Phys. Lett. **98**, 252104 (2011).
[8] C. Blömers, J.G. Lu, L. Huang, C. Witte, D. Grützmacher, H. Lüth, T. Schäpers, Nano Lett. **12**, 2768 (2012).

Coulomb blockade in 2DEG potential fluctuations revealed by SGM

H. Sellier [1], P. Liu [1], B. Hackens [2], F. Martins [2], X. Wallart [3], L. Desplanque [3], V. Bayot [1,2], and S. Huant [1]

[1] *Institut Néel, CNRS & Université Joseph Fourier, BP 166, F-38042 Grenoble*
[2] *IMCN/NAPS, UCLouvain, 2 chemin du cyclotron, B-1348 Louvain-la-Neuve*
[3] *IEMN, UMR CNRS 8520, UST Lille, BP 60069, F-59652 Villeneuve d'Ascq*

Semiconductor heterostructures with remote doping create two-dimensional electron gases (2DEGs) with ballistic transport over several microns at low temperatures thanks to the absence of impurity in the conduction channel. The random distribution of ionized dopants in the barrier, a few tens of nanometers from the 2DEG, is however a source of long-range potential fluctuations. This disorder potential controls the transition to the insulating state at low electron density by breaking the 2DEG into several electron puddles. This behavior has been extensively studied by global transport experiments using planar gates that control electron density over the entire sample. Local microscopic investigation of the disorder potential is a much more difficult task because the 2DEG is buried deep below the surface. Scanning capacitance microscopy [1] has been employed to study large un-patterned 2DEGs and scanning gate microscopy (SGM) [2] has been developed for nanoscale devices.

Here, we present new results on SGM experiments that reveal detailed features of the disorder potential in a low density InGaAs/InAlAs 2DEG etched into 200 nm wide wires. SGM images at 4.2 K reveal the presence of discrete spots where the conductance is strongly affected by the negative potential perturbation induced by the tip of the microscope. These very sensitive spots correspond to the hills of the electrostatic potential that become barriers for transport. In addition, we found that the conductance of these spots does not decrease continuously when the tip bias is getting more negative, but shows periodic oscillations which are typical of Coulomb blockade. These single electron charging effects can be explained by the presence of localized states with low capacitance when the potential landscape presents two barriers in series. Similar Coulomb blockade oscillations have been observed by SGM in epitaxial nanowires [3] and graphene [4], but surprisingly have not been reported for 2DEGs where only charge traps in the barriers have been observed [5].

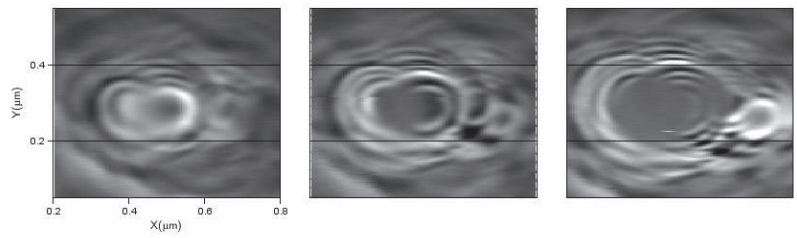

Figure : SGM images recorded above a 200 nm wide horizontal wire (between the two lines) for tip voltages equal to -2.2, -2.5, -2.8 V (from left to right). Several sets of concentric circles appear in the transconductance signal dI/dV_{tip} due to Coulomb blockade in the 2DEG potential fluctuations.

[1] S. Chakraborty *et al.*, Phys. Rev. B **69**, 073308 (2004)
[2] M. Topinka *et al.*, Nature **410**, 183 (2001)
[3] A. Bleszinski *et al.*, Nano Lett. **7**, 2559 (2007)
[4] S. Schnez *et al.*, Phys. Rev. B **82**, 165445 (2010)
[5] A. Pioda *et al.*, Phys. Rev. B **75** 045433 (2007)

Tunable Charge Detectors for Semiconductor Quantum Circuits

Clemens Rössler, Tobias Krähenmann, Stephan Baer, Thomas Ihn, Klaus Ensslin, Christian Reichl, and Werner Wegscheider

Solid State Physics Laboratory, ETH Zurich, 8093 Zurich, Switzerland

Nanostructures defined in high-mobility two-dimensional electron systems offer a unique way of controlling the microscopic details of the investigated device. Quantum point contacts play a key role in these investigations, since they are not only a research topic themselves, but turn out to serve as convenient and powerful detectors for their electrostatic environment. We investigate how the sensitivity of charge detectors can be further improved by reducing screening, increasing the capacitive coupling between charge and detector and by tuning the quantum point contacts' confinement potential into the shape of a localized state [1]. An example is depicted in figure 1. If the detector channel (shaded region in figure 1a)) is defined far away from a small gap in-between the bottom gates, typical quantized conductance is observed (figure 1b)). Pushing the detector channel closer to the gapped region (figure 1c)) gives rise to additional resonances due to the formation of a localized state (figure 1d)). Finally, we demonstrate how such a localized state can be employed for fast and well-resolved charge detection of a large quantum dot in the quantum Hall regime.

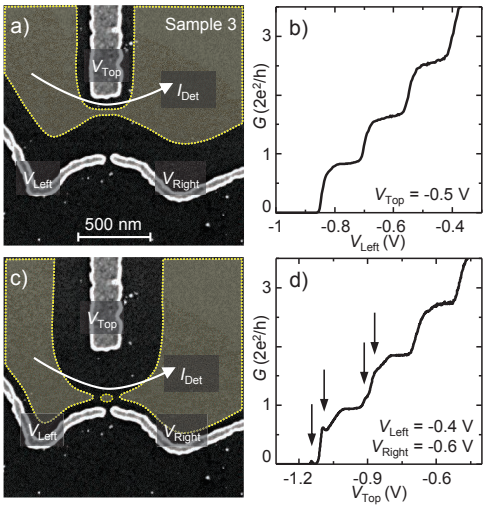

Figure 1: a) Scanning electron micrograph. Applying more negative voltages to the bottom gates shifts the conducting channel (shaded area) upwards. b) Linear conductance of the channel, plotted as a function of V_{Left} while $V_{\mathrm{Right}} = V_{\mathrm{Left}} - 0.2\,\mathrm{V}$. The expected conductance quantization is observed. c) Applying more negative voltage to the top gate shifts the channel downwards, enabling a localization to form at the gap between the left and right gate. d) Linear conductance as a function of V_{Top}. Multiple charging events of a localized state are observed (arrows).

[1] Clemens Rössler et al., arXiv:1209.4447.

Hole hyperfine interaction: valence band orbital composition and its effect on hole spin qubit dephasing

E. A. Chekhovich[1], M. M. Glazov[2,3], A. B. Krysa[4], M. Hopkinson[4], P. Senellart[5], A. Lemaître[5], M. S. Skolnick[1] and A. I. Tartakovskii[1]

[1] *Department of Physics and Astronomy, University of Sheffield, Sheffield S3 7RH, UK*
[2] *Ioffe Physical-Technical Institute of RAS, St Petersburg 194021, Russia*
[3] *Spin Optics Laboratory, St Petersburg State University, St Petersburg 198504, Russia*
[4] *Department of Electronic and Electrical Engineering, University of Sheffield, S1 3JD, UK*
[5] *Laboratoire de Photonique et de Nanostructures, Route de Nozay,Marcoussis, France*

Decoherence caused by nuclear field fluctuations is a fundamental obstacle to the realization of quantum information processing using single electron spins. Alternative proposals have been made to use spin qubits based on valence band holes having weaker hyperfine coupling. However, it was demonstrated recently both theoretically [1, 2] and experimentally [3, 4] that the hole hyperfine interaction is not negligible, although a consistent picture of the mechanism controlling the magnitude of the hole-nuclear coupling is still lacking. We address this problem by performing isotope selective measurement of the valence band hyperfine coupling in InGaAs/GaAs, InP/GaInP and GaAs/AlGaAs quantum dots [5], enabled by recent progress in nuclear magnetic resonance in nanostructures [6]. Contrary to existing models [1, 2] we find that the hole hyperfine constant along the growth direction of the structure (normalized by the electron hyperfine constant) has opposite signs for different isotopes and ranges from −15% to +15%. We attribute such changes in hole hyperfine constants to the competing positive contributions of *p*-symmetry atomic orbitals and the negative contributions of *d*-orbitals. Furthermore, we find that the *d*-symmetry contribution leads to a new mechanism for hole-nuclear spin flips which may play a major role in hole spin decoherence.

Material \ *C/A* (%)	In	Ga	As	P
InGaAs/GaAs	-15.0±3.5	-5.0±4.5	+9.0±2.0	-
GaAs/AlGaAs	-	-7.5±3.0	+16.0±3.5	-
InP/GaInP	-12.5±3.0	-		+18.0±8.0

The measured hole hyperfine constants (*C*) normalized by electron hyperfine constants (*A*) are shown in the Table for four different chemical elements (In, Ga, As, P) in three different quantum dot systems. The opposite signs of *C* for cations and anions cannot be explained by existing theories [1, 2]. Such discrepancy is due to inadequate description of the valence band states, which were assumed to be constructed of *p*-symmetry orbitals only. We show that this controversy can be resolved when the contribution of the cationic *d*-shells (*3d* for Ga and *4d* for In) into the valence band states is considered. Furthermore, previous conclusion that pure heavy holes are immune to hole-nuclear spin flips [1, 2] is shown to arise from the same oversimplified assumption about the orbital composition of the valence band.

.

[1] J. Fischer, W. A. Coish, D. V. Bulaev, D. Loss, Phys. Rev. B **78**, 155329 (2008).
[2] C. Testelin, *et al*, Phys. Rev. Lett. **102**, 146601 (2009).
[3] P. Fallahi, S. T. Yilmaz, A. Imamoglu, Phys. Rev. Lett. **105,** 257402 (2010).
[4] E. A. Chekhovich *et al*, Phys. Rev. Lett. **106**, 027402 (2011).
[5] E. A. Chekhovich *et al*, Nature Physics **9**, 74 (2013).
[6] E. A. Chekhovich *et al*, Nature Nanotechnology **7**, 646 (2012).

TuP134

On-chip Photon-assisted detection of the noise of a Quantum Point Contact

P. Roulleau [(1)], Y. Jompol [(1)], Th. Jullien [(1)], I. Farrer[(2)] , D.A. Ritchie[(2)], and D.C. Glattli[(1)]

[1] *Nanoelectronics Group, Service de Physique de l'Etat Condensé, CEA Saclay, F-91191 Gif-sur-Yvette, France*

[2] *Cavendish Laboratory, University of Cambridge, J.J. Thomson Avenue, Cambridge CB3 0HE, UK*

We describe the first experimental realization of on-chip detection of the noise of a Quantum Point Contact (QPC) (emitter) using an additional capacitive-coupled QPC (detector). Here, the QPC emitter is dc biased and emits a wide band quantum shot noise which, due to the capacitive coupling, will generate electron-hole pairs in the detector line. The detection is based on the following mechanism: when a QPC is submitted to a time dependent drain-source voltage, electron-hole pairs are generated. Their partitioning at the QPC generates a current noise called photon-assisted shot noise (PASN). Alternatively to shot noise, electron-hole pairs also generate a photon-current. We report photo-current and PASN measurements in excellent agreement with theoretical predictions. In particular, this approach enables us to detect fluctuations up to several tens of GHz and could be extended to THz by improving the geometry or replacing QPCs by Carbone nanotubes.

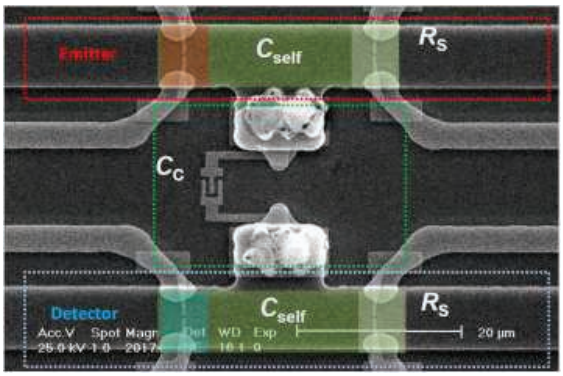

Figure: Scanning electron microscope view of the sample. Two lines defined by wet etching of the mesa are coupled via a coupling capacitance C_C. On the upper line are patterned two QPCs in serie: in red the QPC emitter, and in white a serie resistor tuned on a plateau (therefore noiseless). On the lower line, the QPC detector is colored in blue.

[1] Y. Jompol, Th. Jullien, P. Roulleau, I. Farrer, D.A. Ritchie, and D.C. Glattli (*in preparation*)

4 July (Thursday)

17.00 – 19.00

Poster sessions 3

EP2DS – MSS Joint session

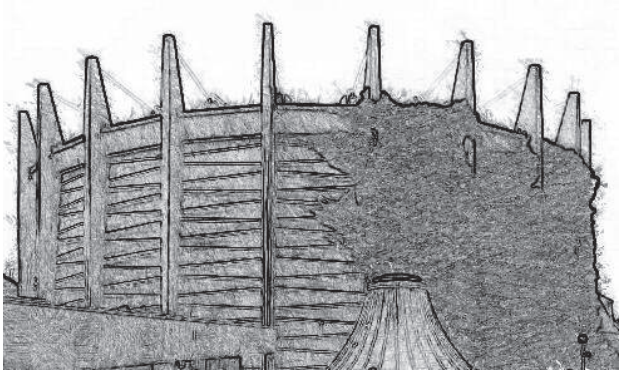

Rotunda of
The Racławicka Panorama

Pseudo-magnetic field and resonant transport in strained graphene ribbons

Diana A. Gradinar[1], Marcin Mucha-Kruczynski[1,2], Henning Schomerus[1], and Vladimir I. Fal'ko[1]

[1] *Department of Physics, Lancaster University, LA1 4YB Lancaster, United Kingdom*
[2] *Department of Physics, University of Bath, Claverton Down, Bath, BA2 7AY, United Kingdom*

In graphene, inhomogeneous strain affects electrons in a manner similar to that of a valley-antisymmetric magnetic field [1, 2, 3, 4]. In suspended graphene membranes, inhomogeneous strain may be expected near the clamped contacts [5], and here we show how the pseudo-magnetic Landau Level formation can be manifested in the transport characteristics.

As a model we study an armchair graphene ribbon (GR) suspended from two metallic contacts and show that the conductance of an armchair GR subject to 5% inhomogeneous deformations exhibits resonances which we trace (a) to standing waves in the middle of the suspended ribbon and (b) to the peculiar $n = 0$ LL for Dirac electrons in an effective pseudo-magnetic field.

[1] V. M. Pereira, A. H. Castro Neto, and N. M. R. Peres, Phys. Rev. B **80**, 045401 (2009).
[2] F. Guinea, M. I. Katsnelson, and A K. Geim, Nat. Phys. **6**, 30-33 (2010).
[3] M. A. H. Vozmediano, M. I. Katsnelson, and F. Guinea, Phys. Rep. 496, 109 (2010).
[4] D. Rainis, F. Taddei, M. Polini, G. Leon, F. Guinea, and V. I. Fal'ko, Phys. Rev. B **83**, 165403 (2011).
[5] M. Mucha-Kruczynski and V. I. Fal'ko, Solid State Comm. **152**, 1442 (2012).

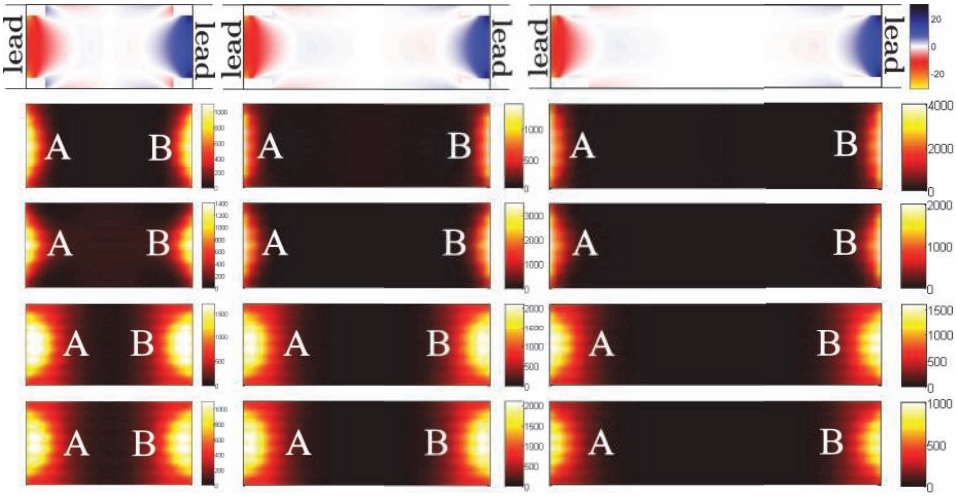

Figure 1: Top row: Distribution of the pseudo-magnetic fields (measured in Tesla) for electrons in the K valley, for ribbons of $W = 40$nm and aspect ratios $W/L = 0.5$, 0.33 and 0.25 arranged from left to right. All other rows: Distribution of the LDOS at fixed energies corresponding to the four peaks at the DP, linked to the $n = 0$ LL. The profiles also show the sublattice favored by the fields at the two ends.

Magnetotransport of the ^{4}He-Adsorbed Bilayer Graphene

A. Fukuda [1], D. Terasawa [1], Y. Ohno [2] and K. Matsumoto [2]

[1] *Department of Physics, Hyogo College of Medicine, Nishinomiya 663-8501, Japan*
[2] *The Institute of the Scientific and Industrial Research, Osaka Univ., Ibaraki 567-0047, Japan*

Graphene, a two-dimensional (2D) sheet of carbon, is a promising material not only for investigating a basic physics about relativistic electrodynamics with massless Dirac fermions but also for opening up a realization of various electric devices such as the FET. On the other hand, graphene has another fascinating property where the 2D electron system is easily accessible from outside. Therefore, electron transport is sensitively modified by the adsorption or chemical adjunction of various kinds of molecules [1]. Thus it is challenging to investigate the affection of the adsorption of an inert gas on graphene, which may be considered to be the least in effect [2]. It is noteworthy that the various quantum phases of 2D ^{4}He film on graphite has been elaborately studied for a long period [3].

In this study, we carry out the magnetotransport measurements of ^{4}He-adsorbed bilayer graphene at the temperature of 7 K and the magnetic field up to 7 T. The bilayer graphene is prepared by the micromechanical cleavage technique mounted on the top of the 300 nm-thick SiO_2 on n^+-Si wafer. A Ti/Au contact leads are attached to graphene sheets by using electron-beam lithography. A mobility of the sample is about 2,500 cm^2/Vs at room temperature and number of layers is confirmed by the Raman spectroscopy. The magnetresistance R_{xx} is measured by the standard low frequency Lock-in technique with the current of 37.7 Hz and 50 nA. Helium 4 gas is introduced at low temperature to the well-annealed graphene into the sample cell. Grafoil sheet having 1.2 m^2 effective area is placed inside the cell to regulate the adsorption layers of ^{4}He. Figure 1 shows the R_{xx} change ΔR_{xx} from the pristine graphene as a function of gate voltage V_g and magnetic field B to 1/10 layers and one layer for ^{4}He-adsorbed graphene. The overall magnitudes of ΔR_{xx} for one layer are larger than the one for 1/10 layer. Signs of ΔR_{xx} clearly depend on the V_g for most B, reflected the R_{xx} oscillations in the pristine graphene. In the conference, we discuss the effects of the adsorption of the inert gas to magnetotransport and its origins in detail.

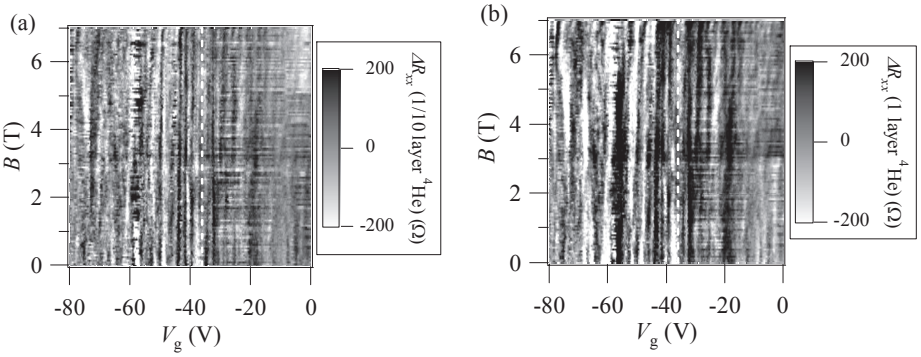

Fig. 1 Image plot of magnetoresistance change ΔR_{xx} as a function of gate voltage V_g and magnetic field B for (a) 1/10 layer and (b) one layer ^{4}He adsorbed graphene, respectively. Dashed lines indicate charge neutral points.

[1] F. Schedin *et al*. Nature Mat. **6**, 652 (2007).
[2] M. C. Gordillo *et al*., Phys. Rev. Lett. **102**, 085303 (2009).
[3] D. S. Greywall *et al*., Phys. Rev. Lett. **67**, 3535 (1991).

Microscopic theory of ultrafast dynamics of carriers photoexcited by THz and near-infrared linearly-polarized laser pulses in graphene

B. Y. Sun and M. W. Wu*

Hefei National Laboratory for Physical Sciences at Microscale and Department of Physics, University of Science and Technology of China, Hefei, Anhui, 230026, China
Email: mwwu@ustc.edu.cn

We investigate the dynamics of photoexcited carriers and nonequilibrium phonons in graphene by solving the microscopic kinetic Bloch equations with the relevant scatterings (including the Coulomb scattering with dynamic screening) explicitly included. Under the gauge invariant approach, both the drift and pump terms are included naturally. We look into the dynamics of carriers photoexcited by the linear polarized laser pulses with the pump-photon energy in both near-infrared and THz regimes. When the pump-photon energy is high enough, the influence of the drift term is shown to be negligible. Moreover, the anisotropic photoexcited electrons tend to be isotropic under the scattering and an isotropic hot-electron Fermi distribution is established before the end of the pulse investigated here. However, in the case with low pump-phonon energy, the drift term is important and leads to a net momentum transfer from the electric field to electrons. Together with the dominant Coulomb scattering, a drifted Fermi distribution different from the one established under static electric field is found to be established in several hundred femtoseconds. Besides, we also show that the temporal evolution of the differential transmission (DT) measured by Hale et al. [1] can be well fitted with our microscopic calculation. We further show that the Auger process investigated in the literature which involves only the diagonal terms of density matrices, is forbidden by the dynamic screening. However, we propose an Auger process involving the interband coherence and show that it contributes to the dynamics of carriers when the pump-photon energy is low. In contrast, it is shown that the rotation-wave approximation widely accepted in semiconductor optics fails when the pump energy is low. The negative DT is further studied by fitting the temporal evolution of DT measured by Sun et al. [2]. Our results support their suggestion that their negative DT comes from the weakening of the Pauli blocking due to the heating of the electrons by the pump pulse. In addition, the anisotropical momentum-resolved hot-phonon temperatures due to the linearly polarized light are also investigated, with the underlying physics revealed.

[1] P. J. Hale, S. M. Hornett, J. Moger, D. W. Horsell, and E. Hendry, Phys. Rev. B **83**, 121404(R) (2011).
[2] D. Sun, Z.-K. Wu, C. Divin, X. Li, C. Berger, W. A. de Heer, P. N. First, and T. B. Norris, Phys. Rev. Lett. **101**, 157402 (2008).
[3] B. Y. Sun, Y. Zhou, and M. W. Wu, Phys. Rev. B **85**, 125413 (2012).
[4] B. Y. Sun and M. W. Wu, arXiv:1302.3677.

Plasmon guiding in graphene demonstrated by time-resolved electrical measurements

N. Kumada[1], R. Dubourget[1], S. Tanabe[1], H. Hibino[1], K. Sasaki[1], M. Hashisaka[2], H. Kamata[2], K. Muraki[1], and T. Fujisawa[2]

[1]*NTT Basic Research Laboratories, NTT Corporation, Atsugi, Japan*
[2]*Department of Physics, Tokyo Institute of Technology, Ookayama, Tokyo, Japan*

Plasmons, which are collective charge oscillations, in graphene have attracted recent interest owing to tunable properties by chemical or electrostatic doping. Here, we demonstrate gate-controlled plasmon guiding in graphene by time-resolved electrical measurements. The guiding is based on local tuning of the carrier density, through which transport properties of the system can be changed.

The sample used was fabricated from graphene grown on SiC. It has three separated top gates; the side two gates (guiding gates) and the center gate (channel gate) serve to define the channel for the plasmon transport and change the properties of guided plasmons, respectively (Fig. 1**a**). All measurements were performed at 1.5 K. For the time-resolved electrical measurement [1], pulsed plasmons at gigahertz frequencies are generated in graphene by applying a voltage step to the injection gate. The plasmons are detected as the time-dependent current through three detector Ohmic contacts: D1 is connected to the channel, while D2 and D3 are separated from the channel by a guiding gate. When the guiding gate bias ($|V_{\rm gg} - V_{\rm CNP}|$: $V_{\rm CNP}$ is the bias at the charge neutrality point) is large, largest signal appears in the detector D2, which is closest to the injector (dashed line in Figs. 1**b** and **c**). As $|V_{\rm gg} - V_{\rm CNP}|$ is decreased, the plasmon signal through D1 increases, while that through D2 decreases and almost disappears at $V_{\rm gg} = V_{\rm CNP}$ (solid line in Figs. 1**b** and **c**). This indicates that plasmons are guided in the channel; 84% of injected plasmons are transmitted to D1 when $V_{\rm gg} = V_{\rm CNP}$ (Fig. 1**d**).

[1] N. Kumada *et al.*, Nature Commun. **4**, 1363 (2013).

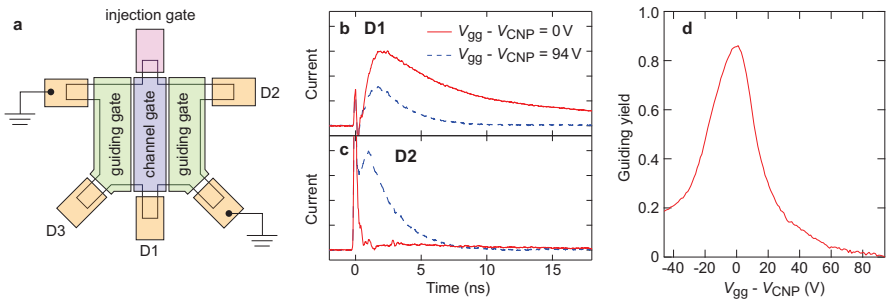

Figure 1: **a**, Schematic illustration of the sample structure with side guiding gates and a center channel gate. The width of the channel gate is 50 μm. **b** and **c**, Current as a function of time detected through the Ohmic contacts D1 and D2, respectively, for the guiding gate bias $V_{\rm gg} - V_{\rm CNP} = 94$ V (solid line) and 0 V (dashed line). The sharp peak at $t = 0$ is due to crosstalk, while the broad peak with time delay is plasmon signal. The channel gate bias is fixed at $V_{\rm cg} - V_{\rm CNP} = 94$ V. **d** Guiding yield as a function of $V_{\rm gg} - V_{\rm CNP}$.

Electron spin relaxation in bilayer graphene

L. Wang and M. W. Wu*

Hefei National Laboratory for Physical Sciences at Microscale and Department of Physics, University of Science and Technology of China, Hefei, Anhui, 230026, China
Email: mwwu@ustc.edu.cn

We investigate the electron spin relaxation due to the D'yakonov-Perel' mechanism in bilayer graphene with only the lowest conduction band being relevant. The spin-orbit coupling $\mathbf{\Omega}^{\mu}(\mathbf{k})$ is constructed from the symmetry group analysis with the parameters obtained by fitting to the numerical calculation according to the latest report by Konschuh *et al.* [1] from first principles. Its three components can be written as $\mathbf{\Omega}_x^{\mu}(\mathbf{k}) = \alpha_1(k)\sin\theta_{\mathbf{k}} + \mu[\alpha_2(k)\sin 2\theta_{\mathbf{k}} + \alpha_3(k)\sin 4\theta_{\mathbf{k}}]$, $\mathbf{\Omega}_y^{\mu}(\mathbf{k}) = -\alpha_1(k)\cos\theta_{\mathbf{k}} + \mu[\alpha_2(k) \times\cos 2\theta_{\mathbf{k}} - \alpha_3(k)\cos 4\theta_{\mathbf{k}}]$ and $\mathbf{\Omega}_z^{\mu}(\mathbf{k}) = \mu\beta_1(k) + \beta_2(k)\cos 3\theta_{\mathbf{k}}$, with μ standing for the two va lleys. The leading term of the out-of-component $\mathbf{\Omega}_z^{\mu}(\mathbf{k})$ shows a Zeeman-like term with opposite effective magnetic fields in the two valleys. This Zeeman-like term opens a spin relaxation channel in the presence of intervalley scattering. The intervalley electron-phonon scattering, which has not been reported in the previous literature, strongly suppresses the in-plane spin relaxation time at high temperature whereas the intervalley short-range scattering plays an important role in the in-plane spin relaxation especially at low temperature. A marked nonmonotonic temperature dependence of the in-plane spin relaxation time with a minimum of several hundred picoseconds is predicted in the absence of short-range scatterers. This minimum is comparable to the experimental data. The nonmonotonic behavior originates from the crossover between the weak and strong intervalley electron-phonon scattering. Moreover, a peak in the electron density dependence of the in-plane spin relaxation time at low temperature is predicted. We also find a rapid decrease in the in-plane spin relaxation time with increasing initial spin polarization at low temperature, which is opposite to the situation in both semiconductors and single-layer graphene. A strong anisotropy between the out-of- and in-plane spin relaxations at high temperature is also revealed. Detailed comparisons of the temperature and electron density dependences of the spin relaxation with the existing experiments of Han and Kawakami [2], Avsar *et al.* [3] and Yang *et al.* [4] are reported. Our result is comparable to the experimental data at high temperature in the absence of short-range scattering, indicating that the intervalley electron-phonon scattering plays an important role in the in-plane spin relaxation at high temperature. As for low temperature, with the inclusion of the short-range scattering, the spin relaxation time from our calculation agrees fairly well with the experimental data.

[1] S. Konschuh, M. Gmitra, D. Kochan, and J. Fabian, Phys. Rev. B **85**, 115423 (2012).
[2] W. Han and R. K. Kawakami, Phys. Rev. Lett. **107**, 047207 (2011).
[3] A. Avsar, T.-Y. Yang, S. Bae, J. Balakrishnan, F. Volmer, M. Jaiswal, Z. Yi, S. R. Ali, G. Güntherodt, B. H. Hong, B. Beschoten, and B. Özyilmaz, Nano Lett. **11**, 2363 (2011).
[4] T.-Y. Yang, J. Balakrishnan, F. Volmer, A. Avsar, M. Jaiswal, J. Samm, S. R. Ali, A. Pachoud, M. Zeng, M. Popinciuc, G. Güntherodt, B. Beschoten, and B. Özyilmaz, Phys. Rev. Lett. **107**, 047206 (2011).
[5] L. Wang and M. W. Wu, arXiv:1302.5880.

Super-Zitterbewegung oscillations in monolayer graphene

Tomasz M. Rusin[1] and Wlodek Zawadzki[2]
[1] *Orange Customer Service sp. z o. o., ul. Twarda 18, 00-105 Warsaw, Poland*
[2] *Institute of Physics, Polish Academy of Sciences, Al. Lotników 32/46, 02-688 Warsaw, Poland*
(Dated: February 24, 2013)

We consider the Zitterbewegung (ZB, trembling motion) in monolayer graphene in the presence of a monochromatic electric wave. In analogy to the Bloch oscillations in the presence of an electric wave [1] we call the considered effect the Super-Zitterbewegung (SZB). Within the dipole approximation the average velocities of delta-like and Gaussian wave packets are calculated as functions of time. The oscillating electric field gives rise to several new effects. First, for nonzero wave there appear two or more oscillating components of the motion, as compared to simple ZB [2]. For low field intensities the additional components have smaller amplitude than ZB, while for large fields they dominate. Second, in the presence of electric wave the motion of the packet exists in two directions. Third, the decay times of Gaussian wave packets in the presence of the wave are much longer than in the field-free case.

We start our analysis assuming weak intensity of the electric field E_0 and the wave frequency ω_D to be smaller than the ZB inter-band frequency $w_Z = 2u|k|$, where $u \simeq 1\times10^6$ m/s and $\boldsymbol{k}$ is the wave vector. The time-dependent Schrodinger equation is solved numerically and the average packet velocity is calculated for delta-like and Gaussian wave packets. Frequencies of ZB and of the satellite related to the external field vary with the field intensity. To find the resulting frequencies we used the Rotating Wave Approximation (RWA). The calculated frequencies are:

$$\omega_\pm = \omega_D \pm \sqrt{(\omega_D - \omega_Z)^2 + \left(\frac{eE_0 u}{\hbar\omega_D}\right)^2}. \qquad (1)$$

Figure 1 compares the numerical results with $\omega_\pm$ obtained in Eq. (1) for $\omega_D = 2\times10^{15}s^{-1}$ and $\omega_Z = 2.31\times10^{15}s^{-1}$ for delta-like packet. The upper line describes ZB-related frequency, while the lower one the satellite frequency. If the driving frequency ω_D is larger than ω_Z the resulting frequency modes are reversed. For the delta-like packet the oscillatory motion has a permanent character in time. For larger electric fields, or for large differences between ω_D and ω_Z, a multi-frequency motion appears suggesting that we deal with nonlinear wave phenomena. In that case the amplitude of ZB is comparable or smaller than that of the satellites.

For the Gaussian wave packets similar calculations give the motion decaying in time, but the decay times are more than order of magnitude longer than that for the simple ZB motion. We also calculated a time-dependent polarization of graphene $\boldsymbol{P}(t) \propto \langle\psi(t)|\boldsymbol{r}|\psi(t)\rangle$, which is, on one hand, proportional to the oscillations of position operator and, on the other hand, it can be measured in the time-dependent spectroscopy. The dependence of the mode frequencies on the externally controlled parameters ω_D and E_0 should allow one to measure more precisely the ZB frequency ω_Z.

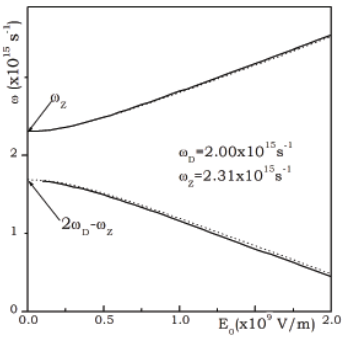

FIG. 1: Frequencies of the two calculated motion components delta-like wave packet in monolayer graphene in the presence of an electric wave versus the wave amplitude. Upper line: ZB-like component; lower line: satellite. Solid lines: the exact results, dotted lines: approximations given by Eq. (1).

[1] E. Haller, R. Hart, M. J. Mark, J. G. Danzl, L. Reichsollner and H. C. Nagerl, Phys. Rev. Lett. **104**, 200403 (2010), arXiv:1001.1206.

[2] T. M. Rusin and W. Zawadzki, Phys. Rev. B **76**, 195439 (2007), arXiv:cond-mat/0702425.

Thermal infrared emission from large area graphene

C. Adlem, T. Poole, N. H. Mahlmeister, L. M. Lawton, I. J. Luxmoore, and G. R. Nash

Functional Materials Group, College of Engineering, Mathematics and Physical Sciences, University of Exeter, Exeter, EX4 4QF, U.K.

Thermal infrared emission has been used extensively over the last few years as a means of probing the electronic structure of graphene transistor devices under bias [1,2]. In such devices, the thermal infrared emission is not spatially uniform and a maximum in emission (a "hotspot") occurs at the place in the sample corresponding to the minimum in conductivity at the Dirac point.

So far, these studies have been confined to relatively small (tens of microns) samples fabricated using exfoliated graphene. In this paper we describe measurements made on large area (3mm x 3mm) devices fabricated from graphene grown by chemical vapour deposition and then transferred onto SiO_2/Si wafers. We have investigated the spatial characteristics of the thermal infrared emission, mapped using a scanning detector, as a function of current through the device, current direction and also of frequency. At relatively low frequencies a peak in emission occurs, as shown in Figure 1, the position of which can be altered by the application of a bias applied between the source and gate contacts, or by reversal of the current direction. We believe that this peak in emission is due to Joule heating at the Dirac point, as has been seen in smaller exfoliated devices, and the magnitude of the emission demonstrates a dependence on the current squared (electrical measurements made on the same device show a peak in device resistance as a function of applied gate bias). At high frequencies (up to 100kHz) a more complex spatial characteristic is observed, which we believe is due to the manifestation of mechanisms other than Joule heating. These are the currently the subject of further investigation.

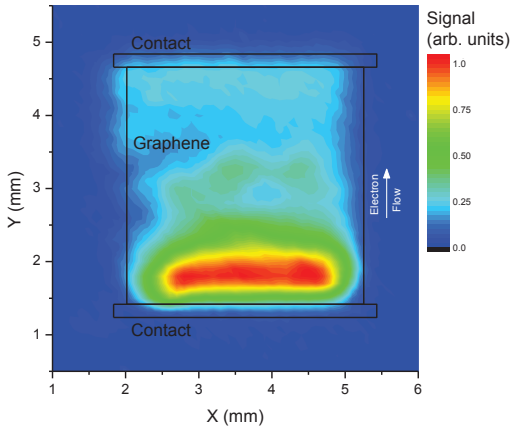

Figure 1: Thermal infrared emission mapped with the electron current going from bottom to top. Measurements were performed with the device under vacuum, and driven with a 1kHz square waveform (50% duty cycle) with a peak injection current of 20mA, and at room temperature.

[1] M. Freitag, H.-Ying Chiu, M. Steiner, V. Perebeinos and P. Avouris, Nature Nanotech. **5**, 497 (2010).
[2] M.-Ho Bae, S. Islam, V. E. Dorgan, and E. Pop, ACS Nano **5**, 7936 (2011).

Graphene in periodic deformation fields

V. K. Dugaev[1,2] and M. I. Katsnelson[3]

[1] *Department of Physics, Rzeszów University of Technology, 35-959 Rzeszów, Poland*
[2] *Department of Physics and CFIF, Instituto Superior Técnico, TU Lisbon, 1049-001 Lisbon, Portugal*
[3] *Radboud University Nijmegen, Institute for Molecules and Materials, 6525 Al. Nijmegen, The Netherlands*

Electronic properties of graphene can be strongly affected by deformations generating certain scalar and vector gauge fields. Such fields act on electrons as effective pseudo-electric and pseudo-magnetic fields, which can have enermously high magnitude [1]. For example, the pseudo-magnetic field is estimated to reach up to 300 T. It gives us an additional tool for very effective manipulation of electrons in graphene by the strains (strain engineering). Especially important is using periodic deformations creating periodic pseudo-electric and magnetic fields, which do not necessarily break the periodicity of the lattice. As a result, we can obtain a substantially modified electronic structure of graphene. One of the existing possibilties is related to creation of a standing strain wave in graphene.

Here we present the results of our theoretical calculations of the effect of periodic scalar and vector potentials generated by periodic deformations of the graphene crystal lattice, on the electron energy spectrum [2]. It is found that the periodic fields do not create the gap in the Dirac point but they change substantially the velocity of electrons near the Dirac point, and the resulting electron energy spectrum can be strongly anisotropic.

We also discuss the effect of screening of the periodic scalar potential. For this purpose we calculated the dielectric function as a function of the wave length of the scalar potential. This calculation shows that the periodic scalar field can be in fact strongly suppressed by the screening, so that only the pseudo-magnetic periodic field is of importance. The screening is relevant at nonzero chemical potential and is due only to the presence of free electrons and holes, which means that virtual transitions associated with electron polarization are not important.

Self-consisting consideration of the screening, which in its turn is depending on the electron spectrum (electron velocity), leads to rather nontrivial renormalization of the electron velocity. We solved the renormalization group equations for velocity components and found their asymptotic isotropization behavior and an increase of velocity with the renormalization parameter.

By using the dependence of electron velocity on the periodic field we also studied the variation of the plasmon spectra in graphene. We found that the spectrum of plasmon excitations can be also effectively controlled by the periodic strain field. Namely, the plasmon velocity in its linear part can be effectively manipulated by the periodic strain.

This work is supported by National Science Center in Poland as a research project for years 2011 – 2014.

[1] M. I. Katsnelson. Graphene: Carbon in Two Dimensions (Cambridge Univ. Press, 2012).
[2] V. K. Dugaev, M. I. Katsnelson. Phys. Rev. B **86**, 115405 (2012).

Quantum magnetooscillations in the ac conductivity of disordered graphene

U. Briskot [1,2], I. A. Dmitriev [1,2,3], and A. D. Mirlin [1,2,4]

[1] Institut für Nanotechnologie, Karlsruhe Institute of Technology, Germany
[2] Institut für Theorie der Kondensierten Materie, Karlsruhe Institute of Technology, Germany
[3] Ioffe Physical Technical Institute, Russia
[4] Petersburg Nuclear Physics Institute, Russia

We present the results of calculations of the dynamic magnetoconductivity $\sigma(\omega)$ of disordered graphene [1] and make connections to recent experiments [2]. Analytic expressions for $\sigma(\omega)$ are obtained in various parametric regimes ranging from the quasiclassical Drude limit corresponding to strongly overlapping Landau levels (LLs) to the extreme quantum limit where the conductivity is determined by the optical selection rules of the clean graphene.
The nonequidistant LL spectrum of graphene renders its transport characteristics quantitatively different from conventional 2D electron systems with parabolic spectrum. Since the magnetooscillations in the semiclassical density of states are anharmonic and are described by a quasi-continuum of cyclotron frequencies, both the ac Shubnikov-de Haas oscillations and the quantum corrections to $\sigma(\omega)$ that survive to higher temperatures manifest a slow beating on top of fast oscillations with the local energy-dependent cyclotron frequency. Correspondingly, both types of quantum oscillations possess nodes at characteristic frequencies. In the quantum regime of separated LLs, we study both the cyclotron-resonance transitions, which have a rich spectrum due to the nonequidistant spectrum of LLs, and the disorder-induced transitions violating the clean selection rules of graphene. The strongest disorder-induced transitions can be identified in recent magnetotransmission experiments [2]. We also compare the temperature- and chemical potential-dependence of $\sigma(\omega)$ in various frequency ranges: from the dc limit (allowing intra-LL transitions only) to the universal high-frequency limit (where the Landau quantization provides a small B-dependent correction to the universal value of the interband conductivity of the clean graphene).
The obtained results also form a basis for future studies of nonequilibrium magnetotransport phenomena [3] in graphene driven by strong ac and dc fields.

[1] U. Briskot, I. A. Dmitriev, and A. D. Mirlin, arXiv:1301.7246 (2013).
[2] M. Orlita, C. Faugeras, R. Grill, A. Wysmolek, W. Strupinski, C. Berger, W. A. de Heer, G. Martinez, and M. Potemski, Phys. Rev. Lett. 107, 216603 (2011).
[3] I.A. Dmitriev, A.D. Mirlin, D.G. Polyakov, and M.A. Zudov, Rev. Mod. Phys. 84, 1709–1763 (2012).

High Temperature Superfluidity in Double Bilayer Graphene

D. Neilson[1], A. Perali[1], and A.R. Hamilton[2]

[1]*Università di Camerino, Camerino 62032, Italy*
[2]*School of Physics, University of New South Wales, Sydney 2052, Australia*

We show that by employing atomically thin crystals such as a pair of adjacent bilayer graphene sheets, equilibrium superfluidity of electron-hole pairs should be achievable for the first time. The transition temperatures calculated with screening are well above liquid helium temperatures. Because the sample parameters needed for the device have already been attained in similar graphene devices, our work suggests a new route towards realizing high-temperature superfluidity in existing quality graphene samples.

Our proposed system consists of a pair of parallel bilayer graphene sheets (Fig. 1(a)). The lower bilayer sheet is an electron bilayer and the upper bilayer sheet is a hole bilayer. The two bilayer sheets are separated by a hBN insulating barrier of width D_B to prevent tunneling between the sheets and recombination. There are separate electrical contacts to the two bilayers. By tuning a bias V_{BB} between the bilayers, and biases V_{TG} and V_{BG} on top and bottom metal gates, a wide range of carrier densities can be achieved. Because the bilayers have quadratic energy bands, the regions of strong correlations are readily accessible. We discuss bilayer graphene since it has been well characterized but a number of other such crystals are possible.[1]

Figure 1(b) shows $\Delta_{\max}$, the maximum of the $T = 0$ gap calculated with screening included. Densities are restricted to $n > n_{min}$ so that E_F lies in the quadratic energy band range. For each D_B, above a critical density n_c the gap is so small that in realistic disordered systems it is unlikely there would be pairing. However at $n = n_c$ a discontinuous jump in $\Delta_{\max}$ occurs to much higher energies. Reference [2] reported a similar jump for two monolayer Graphene but only at an inaccessible $r_s > 2.35$. For smaller D_B, the superfluidity persists to higher n_c and higher temperatures. For comparison, $\Delta_{\max}$ calculated without screening is shown for $D_B = 0.5$ nm. For $n > n_c$, it is screening that suppresses the superfluidity. At low densities the effect of screening on $\Delta_{\max}$ is progressively reduced because of large Fermi surface smearing.

[1] K.S. Novoselov,*et al.*, P.N.A.S. **1**02, 10451 (2005).
[2] Yu.E. Lozovik, S.L Ogarkov, and A.A. Sokolik, Phys. Rev. B **8**6, 045429 (2012).

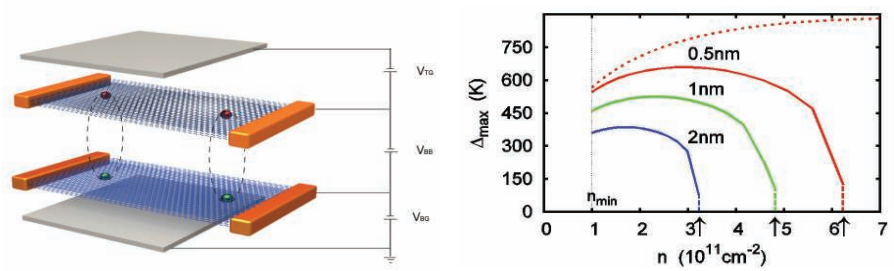

Figure 1: (a) Spatially separated electron-hole system with electrons in one graphene bilayer sheet separated by a hBN dielectric barrier of thickness D_B from holes in a second graphene bilayer sheet. Top and bottom metal gates control the densities. (b) $\Delta_{\max}$ calculated with screening for barrier thicknesses D_B as labeled. At density n_c (arrows), $\Delta_{\max}$ drops discontinuously to sub-mK energies. Dotted red line is $\Delta_{\max}$ for $D_B = 0.5$ nm calculated without screening.

Spin-orbit coupling enhancement in graphene due to hydrogenation

M. Gmitra[1], D. Kochan[1], and J. Fabian[1]

[1] *Institute for Theoretical Physics, University of Regensburg, 93040 Regensburg, Germany*

Spin-orbit coupling is an essential ingredient for magnetoanisotropies, spin relaxation, as well as for recently emerged topological quantum spin Hall phenomena. The intricate history of spin-orbit coupling in graphene have brought revival investigations of its essentials [1]. It has now been established that spin-orbit coupling of the itinerant electrons in graphene comes from hybridized $2p_z$ and $3d$ orbitals forming π bands [1, 2]. The coupling splits the bands at the K point of about 24 μeV [1]. Our first-principles and tight-binding analyses [3] show that the intrinsic spin-orbit coupling in bilayer, trilayer and multilayers of graphene – all the way to graphite – have the same origin derived from the physics of graphene. When graphene is placed in a transverse external electric field, mixing of the $\sigma - \pi$ states is allowed and bands are further split by the Rashba effect. The calculated splitting is about 10 μeV in field of 1 V/nm [1].

When hydrogen is absorbed on graphene, it covalently bonds to a carbon atom and modifies the trigonal sp^2 structure towards the tetragonal sp^3 one. The $\sigma - \pi$ mixing is responsible for the enhancement of the intrinsic spin-orbit coupling as reported in buckled graphene [1]. In the talk we will present first principles calculations of the spin-orbit coupling effects in hydrogenated graphene structures, for varying hydrogen coverage densities, using the linearized augmented plane wave method as implemented in FLEUR code [4]. The covalent bond between the hydrogen and carbon atoms locally deforms the graphene sheet, giving rise to an overlap between the Dirac and sigma electrons and a giant enhancement (from roughly 0.01 to 1 meV) of the local spin-orbit interaction. Based on group theoretical principles we derive effective tight-binding Hamiltonian models and identify dominant contributions to the spin-orbit coupling that comes from breaking of pseudospin inversion symmetry. The calculated spin-orbit coupling induced splittings on the band structure and the emerging spin patterns of the electronic states well agree with first-principles calculations.

This work is supported by the DFG SPP 1285, SFB 689, and GRK 1570.

[1] M. Gmitra, S. Konschuh, C. Ertler, C. Ambrosch-Draxl, and J. Fabian , Phys. Rev. B **80**, 235431 (2009).
[2] S. Konschuh, M. Gmitra, and J. Fabian, Phys. Rev. B **82**, 245412 (2010).
[3] S. Konschuh, M. Gmitra, D. Kochan, and J. Fabian, Phys. Rev. B **85**, 115423 (2012).
[4] FLEUR code, http://www.flapw.de

Superlattice Effects on Electronic- and Transport Properties of Graphene Nanoribbons

F. Tkatschenko[1], V. Krueckl[1] and K. Richter[1]

[1] University of Regensburg , Germany

Keywords: superlattice, graphene, Bloch-oscillations

As recently discoverded by various groups[1,2] the electronic properties of two dimensional systems such as graphene show interesting characteristics in presence of superlattices, including the emergence of extra Dirac points accompanied by an anisotropic velocity renormalization. Other interesting effects are Bloch-oscillations in presence of resonant Zener tunneling[3] giving rise to a negative differential conductance in the current voltage characteristics.
We focus on a scalar superlattice system extended by a constant mass term which opens a gap between the valance and conduction band in the miniband structure. Analytical calculations within the effective Dirac model show that it is possible to tune the energy gap by variation of the superlattice amplitude. By additional numerical calculations based on the tight-binding model we confirm the analytical results. The method allows us to design the electronic structure of the systems.

References:
[1] L. Brey and H. Fertig, Phys. Rev. Lett. 103 (046809)
[2] M. Barbier, P. Vasilopoulos, and F. Peeters, Phys. Rev. B 81(075438)
[3] V. Krueckl and K. Richter, Phys. Rev. B 85 (115433)

The electronic properties of graphene quantum dots in a strong magnetic field

Paweł Potasz[1], Devrim Güçlü[2], Błażej Jaworowski[1], and Paweł Hawrylak[3]

[1] *Institute of Physics, Wrocław University of Technology, PL-50-370 Wrocław, Poland*
[2] *Department of Physics, Izmir Institute of Technology, IZTECH, TR35430, Izmir, Turkey*
[3] *Quantum Theory Group, Security and Disruptive Technology, Emerging Technologies Division, National Research Council of Canada, Ottawa, Canada and Department of Physics, University of Ottawa, Ottawa, Canada*

Electronic properties of graphene quantum dots (GQD) in an external magnetic field are investigated [1, 2, 3, 4, 5]. Single particle properties are studied using tight-binding approximation with magnetic field included via Peierls substitution [6]. Electron-electron interactions are treated via Hartree-Fock and configuration interaction method (tb-HF-CI)[7, 8, 9]. Recent theoretical works were focused on detail analysis of single particle energy spectra of graphene quantum dots with variety of shapes and edge termination [5, 10, 11]. In this work, we present new theoretical results regarding single particle and many-body effects in triangular GQDs with zigzag edges (TGQD) that exhibit a shell of degenerate states at the Fermi level, in the middle of a size dependent energy gap [12]. We show numerically and prove semi-analytically that the degenerate shell is immune to the magnetic field. Next, we study the formation of the states of the $n = 0$ Landau level ($0LL$) close to the Fermi level as a function of increasing magnetic field. At higher magnetic field the $0LL$ states become energetically degenerate with the zero-energy shell. We analyze electronic interactions between electrons from the degenerate shell and electrons from $0LL$ states. We study the ground state and total spin of TGQD as a function of the magnetic field. We show that electrons from the zero-energy shell are spin polarized and act on electrons from $0LL$ as effective magnetic field due to exchange interaction flipping their spins. This allows us to derive an approximate single particle phase diagram with electrons from the zero-energy shell included in an effective g^*-factor.

[1] A. H. Castro Neto, F. Guinea, N. M. R. Peres, K. S. Novoselov, A. K. Geim, Rev. Mod. Phys. **81**, 109 (2009).
[2] Z. Z. Zhang, K. Chang, and F. M. Peeters, Phys. Rev. B **77**, 235411 (2008).
[3] S. Schnez, F. Molitor, C. Stampfer, J. Gttinger, I Shorubalko, T. Ihn, and K. Ensslin, Appl. Phys. Lett. **94**, 012107 (2009).
[4] D. A. Bahamon, A. L. C. Pereira, and P. A. Schulz, Phys. Rev. B **79**, 125414 (2009).
[5] M. Wimmer and A. R. Akhmerov, and F. Guinea, Phys. Rev. B **82**, 045409 (2010).
[6] R. E. Peierls, Z. Phys. **80**, 763 (1933).
[7] A. D. Güçlü, P. Potasz, O. Voznyy, M. Korkusinski, P. Hawrylak, Phys. Rev. Lett. **103**, 246805 (2009).
[8] P. Potasz, A. D. Güçlü, O. Voznyy, J. A. Folk, P. Hawrylak, Phys. Rev. B **83**, 174441 (2011).
[9] P. Potasz, A. D. Güçlü, A. Wójs, P. Hawrylak, Phys. Rev. B **85**, 075431 (2012).
[10] M. Zarenia, A. Chaves, G. A. Farias, and F. M. Peeters, Phys. Rev. B **84**, 245403 (2011).
[11] I. Romanovsky, C. Yannouleas, and U. Landman, Phys. Rev. B **83**, 045421 (2011).
[12] P. Potasz, A. D. Güçlü, P. Hawrylak, Phys. Rev. B **81**, 033403 (2010).

Electron-electron and finite state interactions in optical properties of colloidal graphene quantum dots

Isil Ozfidan[1,2], Marek Korkusinski[1], Alev Devrim Guclu[1,3], and Pawel Hawrylak[1,2]

[1] *Quantum Theory Group, Security and Disruptive Technologies, National Research Council of Canada, Ottawa, Canada*
[2] *Physics Department, University of Ottawa, Ottawa, Canada*
[3] *Department of Physics, Izmir Institute of Technology, IZTECH, TR35430, Izmir, Turkey*

The electronic, optical and magnetic properties of graphene can be modified by engineering lateral size, shape, and edge [1-4]. Here we present new results describing the role of electron-electron and final state interactions in the optical properties of small colloidal graphene quantum dots (GQD)[1] with a well-defined structure, shown in Fig.1. Building on our previous work [2-4] we describe the single-particle energy spectra of P_z carbon orbitals using the tight-binding model. All direct and exchange two-body Coulomb matrix elements are computed using Slater P_z orbitals for on-site and nearest and next nearest neighbors and approximated for farther neighbors. All Coulomb matrix elements are screened by a dielectric constant of external medium controlling the ratio of Coulomb interactions to the tunneling matrix element. For a given GQD with a defined shape, size, edge, and dielectric constant we start with the tight-binding calculation of single-particle states followed by a fully self-consistent Hartree-Fock treatment. We construct a HF phase diagram of the GQD as a function of the interaction strength V relative to the tunneling matrix element t. We find a semiconducting state originating from the semi-metallic ground state of bulk graphene, followed by a Mott-insulating state with decreasing screening. The ground state wavefunction and energy is improved by inclusion of a limited number of pair excitations using CI+Lanczos technique. For a semiconducting GQD ground state the singlet and triplet optical spectra, shown in Fig.1, are obtained by creating quasi-electron-hole pair excitations from the HF state and solving the Bethe-Salpeter equation. The bandgap renormalization and excitonic effects are analyzed as a function of GQD size, shape, and edge and compared with experiments on colloidal graphene quantum dots [1].

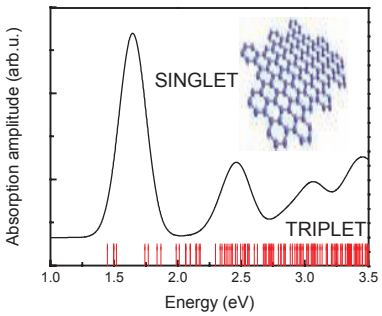

Fig. 1. Singlet and triplet exciton and absorption spectrum of a graphene quantum dot. Inset shows a schematic picture of the dot used in the calculation.

[1] M. L. Mueller, X. Yan, J. A. McGuire, and L.-S. Li, Nano Letters **10**, 2679 (2010); X. Yan, B. Li, and L.-S. Li, Acct. Chem. Research, DOI : 10.1021/ar300137p (2012).
[2] P. Potasz, A. D. Guclu, and P. Hawrylak, Phys. Rev. B **81,** 033403 (2010); O. Voznyy, A.D. Guclu, P. Potasz, and P. Hawrylak, Phys. Rev. B **83.** 165417 (2011).
[3] A. D. Guclu, P. Potasz, and P. Hawrylak, Phys. Rev. B **82,** 155445 (2010).
[4] A. D. Guclu, P. Potasz, O. Voznyy, M. Korkusinski, and P. Hawrylak, Phys. Rev. Lett. **103,** 246805 (2009); A. D. Guclu and P. Hawrylak, Phys. Rev. B **87,** 035425 (2013).

Excitons in Armchair Graphene Nanoribbons

I.Naghmouchi[2], S. Jaziri[1,2]
[1] Laboratoire de Physique de la Matière condensée, Faculté des Sciences de Tunis, Tunisia.
[2]Laboratoire de Physique des Matériaux, Faculté des Sciences de Bizerte, 7021 Jarzouna, Tunisia.

Keywords: graphene, armchair nanoribbon, exciton

Graphene armchair ribbons have several special properties that are well suited for optic applications, when a gap exists in the energy spectrum. The energy gap arising in a graphene nanoribbon makes it possible to generate excitons by optical excitation or electron-hole injection. Confined excitons strongly affect optical properties of the system. We have investigated, using effective mass approach, excitonic properties of armchair graphene nanoribbons when the electrons and holes of occupy only the lowest conduction and valence subbands. We find that excitonic properties, binding energy and oscillator strength depend sensitively on the width of the ribbon. we have performed a detailed first-principles study of the effects of self-energy and electron-hole interaction in the optical response. Because of reduced dimensionality, excitonic effects are dominant in the optical spectrum. In addition, dark excitons are found, and this is also of importance to the photophysics of these materials.

Momentum alignment of photoexcited carriers in graphene

M. E. Portnoi[1] **and R. R. Hartmann**[2]

[1] *School of Physics, University of Exeter, Stocker Road, Exeter EX4 4QL, UK*
[2] *Physics Department, De La Salle University, 2401 Taft Avenue, 1004 Manila, Philippines*

A linearly polarized excitation is shown to create a strongly anisotropic distribution of photoexcited carriers in graphene (Fig.1a), where the momenta of photoexcited carriers are aligned preferentially normal to the polarization plane. This hitherto overlooked effect offers an experimental tool to generate highly directional photoexcited carriers which could assist in the investigation of "direction-dependent" phenomena in graphene-based nanostructures. The depolarization of hot photoluminescence (HPL) has been used with great success to study relaxation processes in conventional 2D systems [1, 2]. In such systems the alignment is due to the spin-orbit interaction for photoexcited holes [3], whereas in graphene, it is due to the pseudo-spin. Namely, the ratio of the two components of the spinor-like graphene wave function depends on momentum which influences the optical transition selection rules [4]. By comparing the depolarization of HPL from successive phonon replicas, the mechanisms of phonon-assisted relaxation of minority carriers in graphene can be studied by simple optical polarization measurements in contrast to a more sophisticated method based on intraband THz absorption, which is used to study carrier-carrier relaxation of the majority carriers [5]. Furthermore, studying the depolarization of HPL in a magnetic field (the Hanle effect) allows one to obtain momentum relaxation times of hot electrons. The effect of momentum alignment in graphene provides a contact-free method of characterizing energy and momentum relaxation. Our analysis of momentum alignment in the high frequency regime shows that a linearly polarized excitation allows the spatial separation of carriers belonging to different valleys (see Fig.1b), therefore opening the door to an optical means of controlling valley polarization (optovalleytronics) and valley-based quantum computing in graphene.

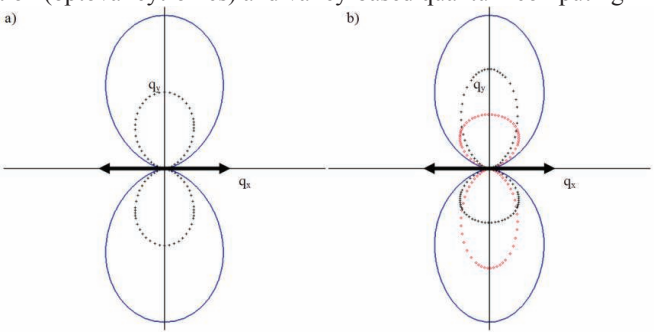

Fig. 1: The polar plots of the distribution function of photoexcited carriers: a) for an excitation energy $h\nu << \gamma$, where $\gamma \approx 3\,\mathrm{eV}$ is the hopping parameter; b) for an excitation energy $h\nu = 0.6\gamma$. The bold arrows show the polarization vector of the excitation and the dotted lines show the separate contributions from each valley.

[1] D. N. Mirlin and V. I. Perel, Semicond. Sci. Technol. **7**, 1221 (1992).
[2] D. S. Kainth, M. N. Khalid, and H. P. Hughes, Solid State Commun. **122**, 351 (2002).
[3] I. A. Merkulov, V. I. Perel, and M. E. Portnoi, Sov. Phys. JETP **72**, 669 (1991).
[4] R. R. Hartmann and M. E. Portnoi, Optoelectronic Properties of Carbon-based Nanostructures: Steering electrons in graphene by electromagnetic fields (LAP LAMBERT Academic Publishing, Saarbrücken, 2011).
[5] K. J. Tielrooij et.al., Nature Physics, DOI:10.1038/nphys2564 (2013).

Zero-energy states in graphene

M. E. Portnoi[1], C. A. Downing[1], R. R. Hartmann[1,2] and N. J. Robinson[1,3]

[1] *School of Physics, University of Exeter, Stocker Road, Exeter EX4 4QL, UK*
[2] *Physics Department, De La Salle University, 2401 Taft Avenue, 1004 Manila, Philippines*
[3] *Rudolf Peierls Centre for Theoretical Physics, University of Oxford, Oxford OX1 3NP, UK*

The current interest in zero-energy states in condensed matter systems with linear quasi-particle dispersion is mostly driven by the on-going search for Majorana fermions in topological insulators. We argue that zero-energy states in graphene, which exist independently of the sign of the confinement potential but are not self-adjoint, also provide a diverse range of interesting problems with important practical implications. For example, there is a widespread belief that electrostatic confinement of graphene charge carriers, which resemble massless Dirac fermions, is impossible as a result of the Klein paradox. We show that full confinement is indeed possible for zero-energy states in pristine graphene. We present exact analytical solutions for the zero-energy modes of two-dimensional massless Dirac fermions confined within a smooth one-dimensional potential given by hyperbolic secant [1], which provides a reasonable fit for the potential profiles of existing top-gated graphene structures [2,3]. A simple relationship between the characteristic strength and the number of confined modes within this model potential is found.

A numerical method for finding the number of fully confined zero-energy modes in any smooth potential, decaying at large distances faster than the Coulomb potential, has also been developed and used to evaluate the conductivity of a channel formed by a more realistic top-gate potential [4]. The long-range behavior of the potential defines the threshold condition for confinement, with power-decaying potentials demonstrating the absence of threshold in the potential strength for the appearance of at least one bound state which is different from exponentially-decaying and square well models. An experimental setup is proposed for the observation of confined electronic guided modes.

We also show that full confinement is possible for zero-energy states in electrostatically-defined quantum dots and rings with smooth potential profiles. The necessary condition for confinement is a non-zero value of angular momentum, i.e. the confined states are vortices. Analytic solutions are found for a class of model potentials [5]. These exact solutions allow us to draw conclusions on general requirements for the potential to support fully confined states, including a critical value of the potential strength and spatial extent. The implications of fully-confined zero-energy states for STM measurements and minimal conductivity are discussed.

We demonstrate that the excitonic insulator gap predicted some time ago [6] and revisited recently by several theory groups [7,8] cannot exist in back-gated graphene samples as confirmed by experiments [9]. A qualitatively different picture based on Bose-Einstein condensation of zero-energy electron-hole vortices (excitons) is proposed to explain the Fermi velocity renormalization in gated graphene structures which is observed instead of the gap.

[1] R. R. Hartmann, N. J. Robinson, and M. E. Portnoi, Phys. Rev. B **81**, 245431 (2010).
[2] A. F. Young and P. Kim, Nature Physics **5**, 222 (2009).
[3] J. R. Williams et al., Nature Nanotechnology **6**, 222 (2011).
[4] D. A. Stone, C. A. Downing, and M. E. Portnoi, Phys. Rev. B **86**, 075464 (2012).
[5] C. A. Downing, D. A. Stone, and M. E. Portnoi, Phys. Rev. B **84**, 155437 (2011).
[6] D. V. Khveshchenko, Phys. Rev. Lett. **87**, 246802 (2001).
[7] J. E. Drut and T. A. Lähde, Phys. Rev. Lett. **102**, 026802 (2009).
[8] T. Stroucken, J. H. Grönqvist, and S. W. Koch, Phys. Rev. B **84**, 205445 (2011).
[9] A. S. Mayorov et al., Nano Letters **12**, 4629 (2012).

Paramagnetic and fluorescent manganese-doped PbS nanocrystals

Lyudmila Turyanska[1], Fabrizio Moro[2], Andrew N. Knott[1], Michael W. Fay[3], Tracey D. Bradshaw[4] and Amalia Patanè[1]

[1] School of Physics and Astronomy, The University of Nottingham, NG7 2RD, UK,
[2] School of Chemistry, The University of Manchester, M13 9PL, UK
[3] Nottingham Nanotechnology and Nanoscience Centre, NG7 2RD, UK
[4] School of Pharmacy, The University of Nottingham, NG7 2RD, UK

The controlled incorporation of dopant impurities in a single colloidal nanocrystal (Quantum dot, QD) is a challenging field of research with potential for numerous applications in nanotechnology. Of particular interest is the incorporation of 3d transition metal ions (Mn, Co, etc) whose d-shell electronic configurations imprint the nanocrystal with unique magnetic and optical properties [1]. Here we report the successful synthesis in aqueous solution of colloidal manganese-doped PbS nanocrystals. Our "one pot" synthesis approach produces nanoparticles that combine within one structure, paramagnetic properties of transition metals (see EPR spectra in Fig. 1a) with efficient/tuneable photoluminescence (PL) emission in the near-infrared (NIR) wavelength range (850-1200 nm) (Fig. 1b). Interestingly, the formation of alloyed (PbMn)S nanocrystals also leads to a thermal energy shift of the QD PL emission, which decreases with increasing Mn-content thus leading to a temperature independent emission for Mn-contents of about 10% (see inset in Fig. 1b).

These new functional nanoparticles are of fundamental and technological interest. The solubility of PbS:Mn nanoparticles in physiological solvents and their dual functionality, i.e. NIR luminescence and paramagnetism, open up exciting prospects for future exploitation of these nanocrystals as imaging labels for combined fluorescence and magnetic resonance imaging (MRI). Although chelated Mn-complexes can be employed as contrast agents in MRI, a Mn-doped nanocrystal will be less susceptible to chemical alterations (i.e. less toxic). Thus these nanocrystals will offer unique combined functionalities and imaging opportunities.

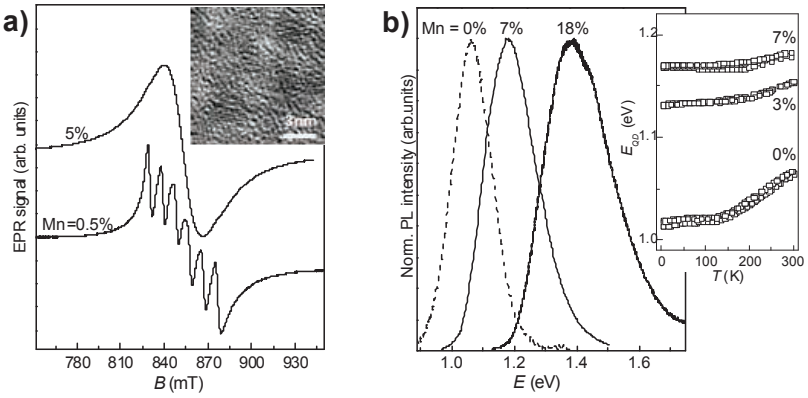

Figure 1 (a) Room temperature K-band EPR spectra for (PbMn)S QDs. Six resonances are observed for samples with Mn < 3% due to hyperfine interaction between the *d*-electrons and the nuclear Mn spins. Inset: HR TEM image of (PbMn)S with 10% Mn. (b) Room temperature photoluminescence (PL) spectra of PbS (dashed line) and (PbMn)S QDs and temperature dependence of the PL peak position (Inset).

[1] S. T. Ochsenbein and D. R. Gamelin, Nature Nanotechnology 6, 112 (2011).

Orbital Lamb Shift of the pseudo-zero-mode Landau Levels in Bilayer and Trilayer Graphene

K. Shizuya

Yukawa Institute for Theoretical Physics, Kyoto University, Japan

Graphene supports massless Dirac fermions that lead to its unique and promising electronic properties. Recently interest appears to center on bilayers and few layers of graphene, where the added layers make the physics and applications of graphene richer, with, e.g., a tunable band gap in bilayer graphene [1].

A notable signal of Dirac fermions is the fact that graphene, in a magnetic field, supports a special set of zero-energy Landau levels. Bilayer graphene, in particular, has eight such zero-energy levels, with an extra twofold degeneracy [1] in Landau orbitals $n = 0$ and 1. This orbital degeneracy is a consequence of topology and the added layer, and is a feature intrinsic to few-layer graphene. In real samples these zero-energy levels evolve into (nearly degenerate) pseudo-zero-mode (PZM) levels, or broken-symmetry states, as explored theoretically and experimentally.

The interplay of orbital degeneracy and Coulomb interactions brings about a new realm of quantum phenomena in graphene few-layers. At EP2DS-20, I would like to report my recent study [2] on this subject. I point out the following:

(1) The orbital degeneracy of the PZM levels in few-layer graphene is lifted by Coulombic quantum fluctuations of the valence band (the Dirac sea). This is a many-body quantum phenomenon analogous to the Lamb shift in the hydrogen atom (i.e., the $2P_{1/2}$ *vs* $2S_{1/2}$ splitting due to vacuum fluctuations).

(2) This "orbital" Lamb shift has been unnoticed in earlier approaches. It is a vacuum effect but is intimately correlated with the Coulomb interaction acting among the PZM levels, and it essentially governs the structure and spectrum of the PZM sector of few layers. It is shown for both bilayers and *ABC*-stacked trilayers how these "Lamb-shifted" orbital modes, with filling, get mixed via the interaction; see Fig. 1.

(3) Experimental signatures for the orbital Lamb shift come from the interaction-enhanced spin or valley or orbital gaps observed via quantized conductance within the lowest Landau level of few-layer graphene. Clear evidence for the $\nu = 0$ gap, in particular, is the $\nu = 0$ insulating state, which, normally, is first observed as a nontrivial feature within the lowest Landau level in bilayers [3] and trilayers [4].

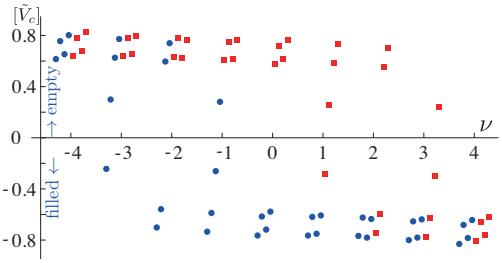

Fig.1 Spectra of the PZM octet at each integer filling factor $\nu \in [-4, 4]$. Each level is specified by spin, valley and orbital ($n = 0, 1$). Band gaps are enhanced by Coulomb exchange interactions.

[1] E. McCann and V. I. Fal'ko, Phys. Rev. Lett. **96**, 086805 (2006).
[2] K. Shizuya, Phys. Rev. B **86**, 045431 (2012); Phys. Rev. B **87**, 085413 (2013).
[3] B. E. Feldman, *et al.*, Nat. Phys. **5**, 889 (2009); R. T. Weitz, *et al.*, Science **330**, 812 (2010).
[4] W. Bao, *et al.*, Phys. Rev. Lett. **105**, 246601 (2010); Nat. Phys. **7**, 948 (2011).

Quantum Transport Phenomena in Molecular Dirac Fermion Systems

N. Tajima,[1, 2] T. Yamauchi,[1] M. Suda,[3] Y. Kawasugi,[4] H. M. Yamamoto,[2, 3, 5] R. Kato,[2] Y. Nishio[1] and K. Kajita[1]

[1] *Department of Physics, Toho University, Miyama 2-2-1, Funabashi, Chiba 274-8510, Japan.*
[2] *RIKEN, Wako, Saitama, 351-0198 Japan.*
[3] *Institute for Molecular Science, Okazaki, Aichi, 444-8585 Japan.*
[4] *Graduate School of Engineering Science, Osaka University, Toyonaka 560-8531, Japan.*
[5] *JST-PRESTO, Kawaguchi, Saitama, 332-0012 Japan.*

First bulk (multilayer) two-dimensional (2D) zero-gap state with massless Dirac particles was realized in an organic conductor α-$(BEDT\text{-}TTF)_2I_3$ under pressure [1-3]. We have succeeded in detecting the zero-mode Landau level and its spin-split levels in this system probed by inter-layer magnetoresistance [3]. The Shubnikov-de Haas oscillations (SdHO) or the quantum Hall effect (QHE), however, have not been observed yet because Fermi level always locates at the Dirac point. Moreover, the multilayered structure makes control of Fermi level by the field-effect-transistor method much more difficult than in the case of graphene. In this work, we made a breakthrough in the detection of SdHO and QHE in this multilayered massless Dirac fermion system.

According to our investigation of the Hall effect in this system, the carrier density at low temperature is only 10^8 cm^{-2}/sheet [2]. Yet, the carriers are not localized but mobile with high mobilities. Thus, by fixing a crystal on a substrate weakly negatively charged by contact electrification, the effects of hole doping can be detected in the transport. Indeed, we succeeded in detecting the hole doping effects on the magnetoresistance and the Hall effect by fixing a crystal onto a polyethylene naphthalate (PEN) substrate. The detection of SdHO originated from the Dirac particles strongly indicates that the carrier doping was successful. The most impressive phenomenon is the QHE plateaux for ν=4, 6, 10, 14 and 18. Those steps are essence of 2D Dirac fermion systems. Moreover, we reveal that the Coulomb interaction plays an important role to the present Dirac particles.

[1] S. Katayama, et al., J. Phys. Soc. Jpn. **75**, 054705 (2006).
[2] N. Tajima, et al., EPL **80**, 47002 (2007).
[3] N. Tajima, et al., Phys. Rev. Lett. **102**, 176403 (2009).

Spin-orbit vs. Zitterbewegung in 2D Kane and Dirac-like semiconductors

P. E. Kunavin, E. L. Rumyantsev

Institute of Natural Sciences, Ural Federal University, 620000 Ekaterinburg, Russia

The effect of Zitterbewegung being of great theoretical interest in recent years [1, 2] is considered within second quantized method in intrinsic 2D Kane semiconductors with normal and inverted band ordering. The 2D Dirac-like Hamiltonian was subjected to the same transformation in order to verify the proposed approach. It was shown in this "classical" situation that the unambiguous expression for single particle position operator can be obtained if we define it in accordance with the expression for spin-orbit (SO) term induced by linear potential (constant force): $\hat{V} = -F \cdot \hat{x}$. This particular SO term so as general expression (coinciding with classical one as it must be) were obtained within the same approximation as was used during investigation of Zitterbewegung effect, namely, the vacuum (Dirac sea, filled valence band) was considered to be stable under application of external potential. The obtained expression for position operator in momentum representation contains curl-like terms which contrary to considered by Dirac gradient terms cannot be excluded by the redefinition of Eigen functions phases [3]. In Kane problem the expressions for position operators of electron, light (LH) and heavy holes (HH) were obtained along the same way of derivation within the same approximation neglecting electron-hole pair-production. It was shown that as the introduced position operators in Kane problem demonstrates non local behavior as in classical paper [4], the interconnected with them SO terms are in general also non-local. It is shown that along with common expressions for SO terms of the second order of parameter Pk/E_g (P - Kane velocity) the additional "topological" terms of the zeroth order in this parameter emerges in proposed approach. Their arising is due to the degeneracy between LH and HH for direct ordering, or to the degeneracy between electron band and HH in the inverted case at the Γ point. This fact is confirmed while considering Dirac problem where the same type of terms are obtained in "graphene case" at $E_g = 0$ (Dirac point). Contrary to Dirac problem where symmetry between electron and hole SO terms exists, in Kane problem the SO terms for electrons and LH demonstrate different behavior.

[1] W. Zawadzki, T. M. Rusin, J.Phys.: Condens. Matter, **23**, 143201 (2011).
[2] R. Winkler, U. Zulicke, J. Bolte, Phys. Rev. B. **75**, 205314 (2007).
[3] P. Dirac, The principles of Quantum Mechanics, Oxford: Clarendon, 1958.
[4] T. D. Newton, E. P. Wigner, Rev. of Mod. Phys. **21**, 400 (1949).

Pumping in graphene: ribbons: transport in adiabatic and non-adiabatic regimes.

T. Kaur [1], L. Arrachea [2] and N. Sandler[1,3]

[1] *Department of Physics and Astronomy, Ohio University, Athens, OH - USA*
[2] *Departamento de Fisica, Universidad Nacional de Buenos Aires, Bs. As. Argentina*
[3] *Dahlem Center for Complex Quantum Systems, Freie Universität, Berlin - Germany*

The interest in the development of devices at the nano-scale has intensified the search for mechanisms that provide control of transport properties while reducing effects of heat dissipation and contact resistance. Charge pumping, in which dc currents are generated in open-quantum systems by applying time-dependent potentials, may achieve these goals. Since the theoretical proposal by Thouless [1], the application of a periodic perturbation to pump dc charge or spin current was achieved in various experimental settings. Most of these works focused on the adiabatic regime (low driving), in configurations with two or more periodically changing parameters that yield dc currents proportional to the driving frequency.

New insights into pumping have appeared from studies of models of two-dimensional graphene systems. The solution of a two-parameter pumping model in the adiabatic regime, based on the Dirac Hamiltonian, showed an enhanced pumped current (as compared with semiconductor materials), which was attributed to the unusual persistence of evanescent modes in the presence of Dirac points [2]. Green's function methods were used to analyze the effects of resonant tunneling in a similar configuration, showing the persistence of anomalous behavior in this regime [3].

Among the extraordinary properties of graphene, there are those arising from confinement effects with significant consequences for the conductance of finite samples.

With the purpose to understand the effect of boundaries and geometry in realistic experimental settings, we have analyzed the properties of non-equilibrium zero-bias currents through graphene nanoribbons using a tight-binding Hamiltonian and the Keldysh non-equilibrium formalism.

Using a numerical implementation with two local single-harmonic time-dependent potentials, we provide detailed analysis of transport through armchair and zigzag ribbons, attached to metallic leads (modeled by semi-infinite square lattice contacts, as a function of chemical potential of the leads and pumping parameters. The model fully describes adiabatic and non-adiabatic regimes and the crossover between both for finite size ribbons. Furthermore, it provides a detailed account of the contribution of evanescent modes to the current, which it is shown to strongly depend on the aspect ratio of the ribbon.

Most importantly, the analysis of different boundaries and contact geometries reveals the fundamental role played by space inversion symmetry in the value of the pumped current that can vanish for appropriate setups [4].

[1] D. J. Thouless, Phys. Rev. B **27**, 6083, (1983).
[2] E. Prada, P. San-Jose, and H. Schomerus, Phys. Rev. B **80**, 245414 (2009).
[3] E. Grichuk and E. Manykin, Europhys. Lett. **92**, 47010 (2010).
[4] T. Kaur, L. Arrachea and N. Sandler. Submitted for publication; arXiv:1203.3952

Magnetotransport properties of epitaxial graphene grown on SiC

M. Gryglas-Borysiewicz[1], A. Kwiatkowski[1], J. Przybytek[1], S. Butun[2], E. Ozbay[2], W. Strupiński[3], R. Stępniewski[1], M. Baj[1]

[1] *Institute of Experimental Physics, Faculty of Physics, University of Warsaw, ul. Hoża 69, 00-681 Warsaw, Poland*
[2] *Nanotechnology Research Center (NANOTAM), Bilkent University, Turkey*
[3] *Institute of Electronic Materials Technology, ul. Wólczyńska 133, 01-919 Warsaw, Poland*

We performed magnetotransport studies of the graphene layers grown on semi-insulating SiC by CVD method [1]. Two kinds of samples were studied: samples grown on (000-1) SiC and on (0001) SiC. The samples were processed by means of optical lithography into large hall bars (263μm x 526μm) with Ti/Au metallization for ohmic contacts. Resistivity tensor was measured in Oxford Instruments VTI system in temperatures ranging from room temperature down to 1.5 K and magnetic fields up to 12T, with additional illumination of the samples at low temperatures.

We have observed significant differences in the electrical properties for the two polarities. The samples grown on the silicon (0001) polarity showed quantum oscillations of the resistivity tensor. They had electron conductivity with Hall mobility of the order of 1000 $cm^2/V{\cdot}s$ and Hall concentration of about $3{\cdot}10^{12}$ cm^{-2}. The samples prepared on carbon–terminated SiC were n-type but with significant contribution of holes evidenced by mobility spectrum analysis [2] with large effective Hall concentration of $3{\cdot}10^{13}$ cm^{-2} and Hall mobility a few times lower than in silicon-polarity samples. No oscillations were registered for that group of samples. We have observed that the samples grown on Si-terminated SiC were very sensitive to external environment (making FLG a potentially sensing material), to thermal cycles and exposure to light. In particular, they showed changes of the order of a few % after each 4 K – room temperature thermal cycle while those grown on C-terminated SiC were stable (samples were kept under He atmosphere at all times). Looking for the possible explanation we performed subsequent experiments with illumination of the samples at low temperatures. The behaviour of the samples grown on Si-polarity SiC was influenced by light whereas the other samples showed no such sensitivity. This diverse sensitivity of FLG to thermal cycles and light is discussed in this report.

References:
[1] W. Strupiński, K. Grodecki, A. Wysmołek, R. Stepniewski, T. Szkopek, P. E. Gaskell, A. Grüneis, D. Haberer, R. Bozek, J. Krupka, and J. M. Baranowski, Nano Lett., **11** (4),1786 (2011)
[2] M. Gryglas-Borysiewicz, B. Jouault, J. Tworzydło, S. Lewinska, W. Strupinski and J.M. Baranowski, Acta Phys. Pol. A **116,** 838 (2009)

Magnetotransport study of the energy band in bilayer graphene

G. Yu. Vasileva[1,2,3], D. Smirnov[1], Yu. B. Vasilyev[1,2], P. S. Alekseev[2], Yu. L. Ivanov[2], A. P. Dmitriev[2], V. Yu. Kachorovskii[2] , H. Schmidt[1], A. Heine[1], and R. J. Haug[1]

[1] *Institut für Festkörperphysik, Universität Hannover, Hannover, 30167 Germany*
[2] *Ioffe Physical Technical Institute, St. Petersburg, 194021 Russia*
[3] *St. Petersburg State Polytechnical University, St. Petersburg, 195251 Russia*

Bilayer graphene has a parabolic band structure with a zero gap. When an electric field is applied perpendicular to the layer a gap between the valence and conduction bands appears and increases with increasing voltage. The gap has a complex structure that resembles the shape of a Mexican hat (inset of Fig.1). The size of the gap was evaluated in numerous optical absorption measurements and temperature studies of conductivity.

One consequence of such a band structure is the simultaneous coexistence of electrons and holes, when the Fermi level is placed inside the Mexican hat. The Fermi surface in this case has the shape of a ring. The external side of the ring contains states of the major types of carriers and the inner side corresponds to the different type of carriers. Due to this structure one can expect to see features in the magnetoresistance. Up to now no magnetoresistance research have been done when all particles reside inside the Mexican hat. We demonstrate that, in the regime when the Fermi energy E_F is smaller than the Mexican hat depth E_H the magnetoresistance is positive (Fig.1.) and perfectly fitted with the two-carrier Drude model. It allows us to develop a new approach to probe parameters of electrons and holes in bilayer graphene. We deduce the carrier densities and scattering times for electrons and holes separately. Moreover positive magnetoresistance method using a top-gate structure permit to determine the parameters of the Mexican hat.

Part of this work was supported by RFBR and Russian Academy of science.

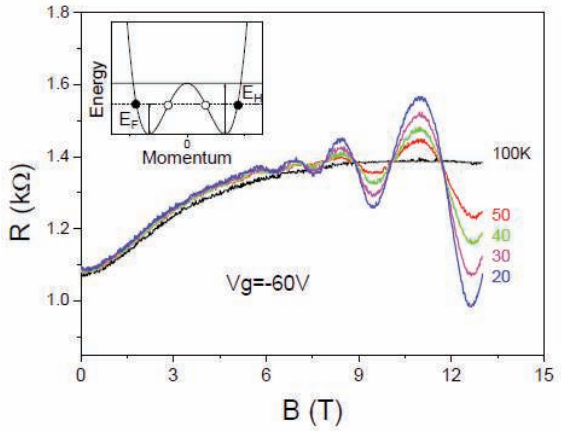

Fig.1. Longitudinal resistance R as a function of magnetic field B at gate bias V_g = -60V and for various temperatures. Inset: "Mexican-hat" dispersion of a biased bilayer graphene near the bottom of the conduction band.

Electrooptical properties of diluted GaAsN on GaAs grown by APMOVPE

P. Kamyczek[1], P. Bieganski[1], E. Placzek-Popko[1], E. Zielony[1], L. Gelczuk[2], B. Sciana[2], D. Pucicki[2], D. Radziewicz[2], M. Tlaczala[2], K. Kopalko[3], M. Dabrowska-Szata[2]

[1]Institute of Physics, Wroclaw University of Technology, Wybrzeze Wyspianskiego 27, 50-370 Wroclaw, Poland
[2]Faculty of Microsystem Electronics and Photonics, Wroclaw University of Technology, Janiszewskiego 11/17, 50-372, Wroclaw, Poland
[3]Institute of Physics, Polish Academy of Science, Al. Lotnikow 32/46, 02-668 Warsaw, Poland

In this paper we report on the optical and electrical studies of single $GaAs_{1-x}N_x$ epitaxial layers grown on GaAs substrates by means of atmospheric pressure metal organic vapour phase epitaxy (APMOVPE). Three kinds of samples with 1,2 %, 1,6 % and 2,7 % nitrogen (N42, N48, N44) content were studied. Optical properties of the layers were investigated with the use of room temperature transmittance and reflectance measurements. Subsequently Schottky Au-$GaAs_{1-x}N_x$ contacts were processed and characterized by current-voltage (*I-V*) and capacitance-voltage (*C-V*) measurements within 80 – 480 K temperature range. From the *I-V* and *C-V* characteristics the ideality factor, series resistance and built-in potential were determined. Obtained diodes can be used for further studies on defects with the use of DLTS method.

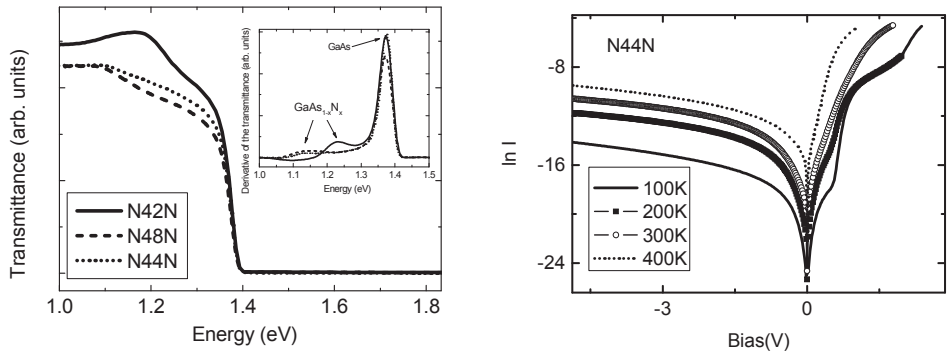

[1] P. Kamyczek, P. Bieganski, E. Placzek-Popko, E. Zielony, L. Gelczuk, B. Sciana, D. Pucicki, D. Radziewicz, M. Tlaczala, K. Kopalko, M. Dabrowska-Szata, *Electrooptical properties of diluted GaAsN on GaAs grown by APMOVPE* - accepted for publication in Optica Applicata.

Effect of structural disorder on quantum oscillations in graphite

B. C. Camargo [1], Y. Kopelevich [1] M. A. Cotta [1], S. B. Hubbard [2], A. Usher [2], W. Böhlmann [3] and P. Esquinazi [3]

[1] *Instituto de Fisica "Gleb Wataghin", Universidade Estadual de Campinas, Unicamp 13083-970, Campinas, Sao Paulo (Brazil)*
[2] *School of Physics, University of Exeter, Stocker Road, Exeter EX4 4QL (UK)*
[3] *Division of Superconductivity and Magnetism, Institute for Experimental Physics II, University of Leipzig, Linnestrasse 5, D-04103 Leipzig (Germany);*

We studied effects of structural disorder on Shubnikov de Haas (SdH) and de Haas van Alphen (dHvA) quantum oscillations measured in single crystalline and highly oriented pyrolitic graphite samples down to temperature T = 30 mK and magnetic field up to B = 14 T. The measurements were performed on samples with different mosaicity characterized by means of x-ray difraction, transmission electron microscopy (TEM) and surface roughness measurements. The obtained results revealed a correlation between the occurrence of quantum oscillations and the sample structural disorder. Namely, dHvA and SdH effects are most attenuated in disordered samples that possess a pronounced surface roughness. We also demonstrate that the presence of sharp interfaces in graphite due to stacking disorder can enhance de amplitude of the quantum oscillations.

Electronic, Magnetic and Transport Properties of Graphene Ribbons Terminated by Nanotubes

M. A. Akhukov, Shengjun Yuan, M. I. Katsnelson and A. Fasolino[1]

Institute for Molecules and Materials, Radboud University Nijmegen, The Netherlands.
[1] *a.fasolino@science.ru.nl*

By a combination of density functional (DFT) calculations and large-scale tight-binding (TB) simulations of transport properties we study the electronic and magnetic properties of graphene nanoribbons with edges rolled to form nanotubes[1], an edge structure with low formation energy[2]. We show that, besides protecting the edges from contamination and reconstructions, nanotubes at the edges may lead to magnetism and are not detrimental for the electronic mobility despite the row of sp^3 hybridized atoms at the nanoribbon-nanotube junction.

Edges with armchair nanotubes present magnetic moments localized either in the tube or the ribbon and metallic or half-metallic character, depending on the symmetry of the junction (see Figure1). These properties have potential for spin valve and spin filter devices with advantages over other proposed systems.

Edges with zigzag nanotubes are either metallic or semiconducting without affecting the intrinsic mobility of the ribbon. By varying the type and size of the nanotubes and ribbons offers the possibility to tailor the magnetic and transport properties, making these systems very promising for applications.

Figure 1: Structure and spin density for symmetric (left) and asymmetric (right) of nanoribbon edges terminated by armchair nanotubes. The localization of magnetization depends on the nanoribbon-nanotube junction.

[1] M. A. Akhukov, Shengjun Yuan, A. Fasolino and M.I. Katsnelson N. J. Phys. **14**, 123012 (2012)

[2] V. V. Ivanovskaya, A. Zobelli, P. Wagner, M. I. Heggie, P. R. Briddon, M.J. Rayson and C. P. Ewels Phys. Rev. Lett. **107**, 065502 (2011).

Dissipationless drag effect in double-layer graphene systems

B. Tanatar[1]

[1] *Department of Physics, Bilkent University, Bilkent, 06800, Ankara, Turkey*

We consider a double-layer graphene system in the superconducting state. Assuming that each layer has a background flow which varies little and that the dynamics of the superconductor near $T = 0$ is the same as that of a normal fluid, we obtain the dispersion relations for the collective modes in the presence of background flow. Decomposing the background flow into two parts, the center-of-mass flow and counterflow, we focus on the properties of the counterflow. We first find an estimate of the change in the zero-point energy ΔE^0 due to counterflow for a unit area of double layers making use of the collective mode dispersions. Combining this with the free energy F of the system and taking the partial derivatives with respect to background velocities in the layers, we determine the current densities which reveal the fact that current in one layer does not only depend on the velocity in the same layer but also on the velocity of the other layer. This is the drag effect and we calculate the drag coefficient for the double-layer graphene system. We compare our results with those in semiconductor double-layer electron systems.[1, 2, 3]

[1] J.-M. Duan, Phys. Rev. Lett. **70**, 3991 (1993).
[2] J.-M. Duan and S. Yip, Phys. Rev. Lett. **70**, 3647 (1993).
[3] B. Tanatar and A. K. Das, Phys. Rev. B **54**, 13827 (1996).

Effect of Dielectric Environment on Carrier Mobility in Graphene Double Layer

Kazuhiro Hosono, Katsunori Wakabayashi

International Center for Materials Nanoarchitectonics, National Institute for Materials Science, Namiki 1-1, Tsukuba 305-0044, Japan

One of recent progresses in nanoscience is the successful graphene device fabrication. Especially, graphene double layer structure (GDLS), where a structure of two graphene single layer embedded in three different relative dielectrics (ϵ_1, ϵ_2, and ϵ_3 in Fig. 1), has rich physics and possibility of real device application. In first experiment of GDLS, Al_2O_3 were used as inner dielectrics [1]. Another promising internal dielectric is h-BN [2], which has atomically smooth surface due to similar lattice constant of graphite, a large electronic band gap, and it can control internal layer number.

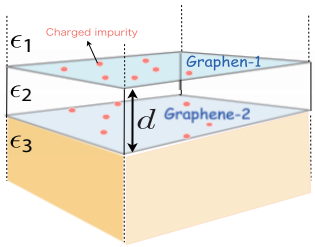

Figure 1: Schematic illustration of our target. A graphene double layer structure (separation distance d) in emerged in a three layered dielectric medium ϵ_1, ϵ_2, and ϵ_3. Red circles represents the random charged impurities.

This experimental progress demands to reveal the carrier transport properties on GDLS from theoretical calculation. Our main question is how the carrier mobility on GDLS depends on both the inner layer thickness d and background dielectrics, ϵ_1, ϵ_2, and ϵ_3. This question will be essential for next graphene based device application with including dielectric engineering [3, 4]. To answer this question, we have theoretically evaluated carrier mobility due to charged impurity on GDLS, by using Boltzmann transport theory and static screening effect on graphene [5]. Coulomb scattering potential due to charged impurity were introduced by mirror effect as first pointed out in Ref [6].

We will show the inner layer thickness d dependence of carrier mobility in several patterns of dielectric constants (e.g., h-BN, Al_2O_3, HfO_2), and discuss the condition that enhances carrier mobility as function of inner layer thickness. Our results offer a simple and practical design strategy to improve the impurity limited mobility in graphene double layer structures.

[1] S. Kim *et al.*, Physical Review B **83**, 161401 (2011). S. Kim *et al.*, Physical Review Letters **108**, 116404 (2012).
[2] L.A. Ponomarenko *et al.*, Nature Physics **7**, 958 (2011).
[3] D. Jena and A. Konar, Physical Review Letters **98**, 136805 (2007).
[4] C. Jang *et al.*, Physical Review Letters **101**, 146805 (2008). A. Newaz *et al.*, Nature Commun **3**, 734 (2012).
[5] T. Ando, Journal of Physics Society Japan **75** (2006).
[6] M. Kumagai and T. Takagahara, Physical Review B **40** (1989).

ThP30

Multiple Auger processes in Graphene

M. Richter [1], M. Städter [1], U. Starke [2] and D. Schmeißer [1]

[1] *Brandenburg University of Technology Cottbus, Applied Physics and Sensors, K.-Wachsmann-Allee 17, 03046 Cottbus, Germany*
[2] *Max-Planck-Institut für Festkörperforschung, Heisenbergstraße 1, 70569 Stuttgart, Germany*

Resonant decay processes of graphene systems have been studied by resonant photoemission (resPES) and X-ray absorption spectroscopy (XAS). The π*-resonance is sensitive for structural details (defects, substrate distance and screening) and is used to identify the degree of localization of the lowest unoccupied states in the conduction band.

The influence of the substrate and interlayer coupling manifests itself in the appearance of different multiple Auger decays at the π*-resonance. Its appearance and spectral intensity is a measure for the magnitude of perturbation of the π-cloud in graphene.

In HOPG, as a reference system for many layer graphene with strong layer interaction, we find remarkable difference in the profile of the Auger decay between π* and σ*–band, which we attribute to an additional multiple-Auger in the π-system with a three-hole (3h) final state [1]. For graphene flakes the 3h decay is replaced by a characteristic Auger-gain (-4h) and Auger-loss (+4h) process at the π*-resonance.

A prerequisite for the appearance of this decay mechanism is the existence of localized excitonic states, which cause the appearance of the multiple Auger decay. We can distinguish between inter-layer (3h) and intra-layer excitons (±4h).

Through monolayer graphene – metal substrate interaction this characteristic Auger decay vanishes. Instead we observe a characteristic pre-edge structure at 284.5eV photon energy in the total electron yield XAS spectra [2].

We will show that the pre-edge peak reported for graphene on metal substrates is not due to doping but due to a low energy Auger decay.

In consequence it is necessary to avoid metallic substrates in order to study the pristine free carrier properties of graphene.

[1] M. Richter, D. Friedrich, D. Schmeißer, Physica E (2013), accepted.
[2] M. Richter, I. Paloumpa, D. Friedrich, D. Schmeißer, ECS Trans. (2013), accepted.

Spin Conductance of Diffusive Graphene Nanoribbons

Jan Bundesmann[1], Ming-Hao Liu[1], Inanc Adagideli[2] and Klaus Richter[1]

[1] Institute for Theoretical Physics, University of Regensburg, D-93040 Regensburg, Germany
[2] Faculty of Engineering and Natural Sciences, Sabanci University, Orhanli-Tuzla, Istanbul, Turkey

We investigate spin transport in diffusive graphene nanoribbons with both clean zigzag and rough edges. Along the edges long range disorder causes the local doping to come close to the charge neutrality point at certain regions. In this work, we focus on a model where such regions have localized magnetic moments, similar to the well known magnetic edge of smooth zigzag graphene nanoribbons. This random edge magnetization can polarize charge currents and cause sample to sample fluctuations of the spin currents that follow universal predictions from the Dorokhov-Mello-Pereyra-Kumar equations (Fig. 1). In the present work, we show that although the average spin conductance G_S of these ribbons vanishes, an applied transverse in-plane electric field a finite average spin conductance can be observed (Fig. 2). Similar effect can also be achieved by aligning the edge magnetic moments e.g. by applying an external magnetic field.

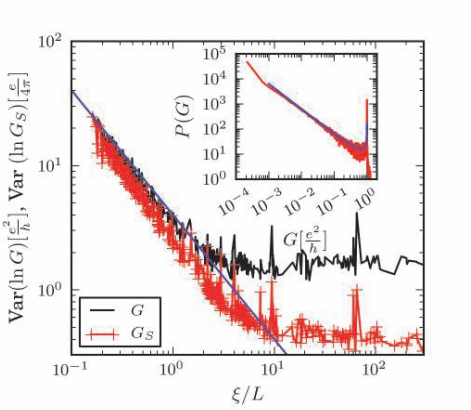

Fig. 1: Var [ln G] (black) and Var [ln G_S] (red) as a function of ξ / L for various ribbons of length L and localization length ξ. According to DMPK equations the eigenvalues of the conductance matrix exhibit a log-normal distribution with ⟨ln G⟩ = 2 Var [ln G] = L / 2 ξ (blue curve). While ⟨G_S⟩ = 0, also Var [ln G_S] is determined by the single parameter ξ / L.

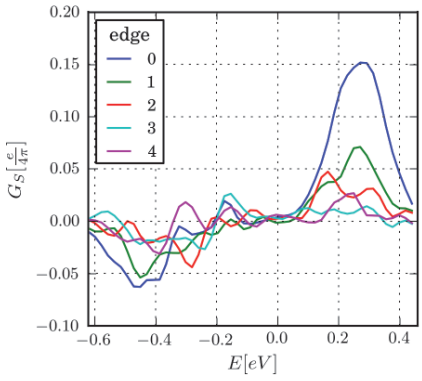

Fig. 2:Average spin transmission of nanoribbons under the influence of a transverse in-plane electric field. The potential difference leads to a maximum spin conductance at Fermi energies V_{dis}-t' and -V_{dis}, where t' is the next-nearest neighbor hopping The edge indices indicate the roughness fromx 0 for a perfectly clean zz edge, to 4 for an edge with approximately 8% defects.

Electron-pseudophonon interaction and inelastic scattering in suspended graphene

Nojoon Myoung[1], Kyungchul Seo[1], and Gukhyung Ihm[1]

[1] *Department of Physics, Chungnam National University, Daejeon 305-764, Korea*

The suspended graphene sheet has been one of the systems with strain effects on electronic properties of graphene due to the high flexibility[1]. When a graphene sheet is clamped at two parallel leads as illustrated in Fig. 1(a), the deformation of the sheet is induced by applying an electric field which can influence on quantum transport. Especially, it has been reported that a uniform effective vector potential can be induced by considering the elastic deformation[2]. In this study, we show that a time-periodic strain of the suspended graphene produces inelastic scattering of electrons as a consequence of an interaction between electrons and pseudophonons.

We consider the effective vector potential induced by the time-periodic strain is given as

$$\vec{A}(\vec{r},t) = \frac{\beta h_0^2}{6a_0L^2}\left[\theta\left(x+\frac{L}{2}\right)-\theta\left(x-\frac{L}{2}\right)\right]\cos\omega t, \tag{1}$$

where $\beta = C\left(\partial \ln t/\partial \ln a_0\right) \approx 2$ with $C \sim 1$, $t \approx 3\,eV$, $a_0 \approx 1.4\mathring{A}$, $h_0 = \left(4h_0/L^2\right)\left(x^2 - L^2/4\right)$ is the vertical deformation, L is the length of the suspended region, and ω is the frequency of the time-periodic strain. By using Floquet scattering theory, eigenstates of the system is given as

$$\Psi(\vec{r},t) = e^{ik_y y}\sum_{n,m=-\infty}^{+\infty} c_m e^{ik_x^m x} J_{n-m}(\chi)\, e^{-i(E-n\hbar\omega)t}, \tag{2}$$

where $k_x^m = \sqrt{\left[\left(E+m\hbar\omega\right)/\left(\hbar v_F\right)\right]^2 - \left[k_y + \left(n\omega\right)/\left(v_F\Lambda\right)\right]^2}$ with $\Lambda = \psi^\dagger\sigma_y\psi$ and $J_{n-m}(\chi)$ is the Bessel function of the first kind with $\chi = \left[\left(ev_F\beta\Lambda\right)/\left(6a_0\hbar\omega\right)\right]\left(h_0/L\right)^2$. Electrons can be scattered from pseudophonons by gaining or losing both energy and momentum quanta; $n\hbar\omega$ and $\left(n\hbar\omega\right)/\left(v_F\Lambda\right)$, as shown in Fig. 1(b). The strength of the electron-pseudophonon scattering is determined by $J_{n-m}(\chi)$.

Our main finding in this study is that the electron-pseudophonon interaction depends on the incident angle of electron since $J_{n-m}(\chi)$ has the angle-dependence. The angle-dependent feature of the electron-pseudophonon interaction allows normally incident electrons to propagate through suspended region without any inelastic scattering despite of the existence of the strain.

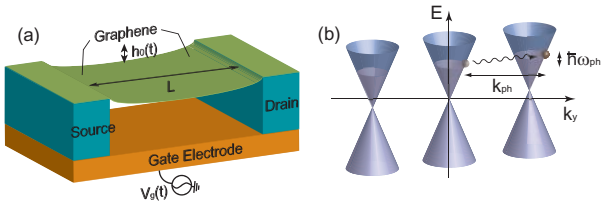

Figure 1: (a) Schematic view of the system. (b) Graphitic diagram of inelastic scattering as a result of the electron-pseudophonon interaction.

[1] C. Lee, X. Wei, J. W. Kysar, J. Hone, Science **321**, 385 (2008).
[2] M. M. Fogler, G. Guinea, M. I. Katsnelson, Phys. Rev. Lett. **101**, 226804 (2008).

Dynamics of Dirac Electrons in a Photon Cavity

L. Hesse[1], K. Richter[1], and X. Chen[2]

[1] *Institute for Theoretical Physics, University of Regensburg, D-93040 Regensburg, Germany*

[2] *Department of Physics, Shanghai University, Shanghai 200444, Peoples Republic of China*

We consider low energy excitations of monolayer graphene embedded in an optical cavity and exposed to an perpendicular constant magnetic field. The influence of an additional radiation field can yield resonant cyclotron transitions of the Dirac fermions of graphene which can be studied within techniques known from cavity quantum electrodynamics. The coupling of cavity photons with condensed matter has been realized in the context of electron gases[1, 2] and very recently also proposed for graphene[3, 4] and opens a new field of interesting issues concerning fundamental and applied aspects. We consider for realistic tight-binding models of graphene the influence of edge effects, such as inter-valley scattering, in this context. In addition to that we plan to extend the theory describing light-matter coupling in closed graphene cavity systems to graphene nanoribbons coupled to such a photon cavity in order to investigate transport properties.

[1] D. Hagenmüller, S. De Liberato and C. Ciuti, Phys. Rev. B **81**, 235303 (2010).
[2] G. Scalari, C. Maissen, D. Turčinková, D. Hagenmüller, S. De Liberato, C. Ciuti, C. Reichl, D. Schuh, W. Wegscheider, M. Beck, and J. Faist, Science **335**, 1323 (2012).
[3] D. Hagenmüller and C. Ciuti, Phys. Rev. Lett. **109**, 267403 (2012).
[4] L. Chirolli, Marco Polini, V. Giovannetti and A. H. MacDonald, Phys. Rev. Lett. **109**, 267404 (2012).

Doping effect in graphene deposited on metals - scanning tunneling spectroscopy and density functional theory studies

Z. Klusek[1], P. Dabrowski[2], I. Wlasny[1], W. Kozlowski[1], P.J. Kowalczyk[1], I. Zasada[1], J. Slawinska[1], W. Strupinski[2], J.M. Baranowski[2]

[1]Department of Solid States Physics, Faculty of Physics and Applied Informatics, University of Lodz, Pomorska 149/153, Lodz 90-236, Poland
[2] Institute of Electronic Materials Technology, Wolczynska 133, Warsaw 01-919, Poland

It is obvious that graphene electronics devices require metallic contacts. However, metal/graphene interaction is still not fully understood and demands experimental and theoretical studies. Particularly, it has been proved theoretically using density functional theory (DFT) and van der Waals density functional (vdW-DF) calculations that the unique conical dispersion relation around K/K' points in graphene is preserved on (111) surfaces of Al, Cu, Ag, Pt, and Au. However, this is accompanied with the change of position of the Dirac point (E_D) relative to the Fermi level (E_F) due to the presence of substrate (doping effect).

We describe influence of different substrates on graphene physical properties and focus on understanding of the metal-graphene contacts. Particularly, we will show detailed scanning tunneling microscopy/spectroscopy (STM/STS) and Raman spectroscopy (RS) studies of graphene interactions with Au(111) and Cu(111) substrates [1-3]. The obtained experimental results will be discussed in the frame of density functional theory (DFT) calculations. The representative results obtained for graphene/gold system are presented in Fig.1.

This work is supported by the National Science Centre under project DEC-2012/05/B/ST5/00354.

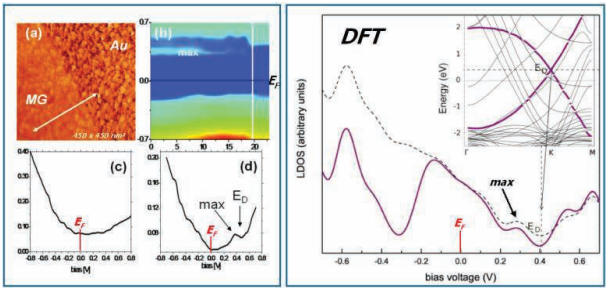

Fig.1. (a) 450 x 450-nm STM topography showing the details of graphene and Au borderline. (b) LDOS(*E*, line) map recorded on graphene/Au interface along arrow shown in panel (a). (d) The example of the LDOS profile recorded on Au region. (d) The example of the LDOS profile recorded on the graphene/Au region. Right panel shows DFT calculation of LDOS function using DFT method.

[1] Z. Klusek, P. Dabrowski, P. Kowalczyk, W. Kozlowski, W. Olejniczak, P. Blake, M. Szybowicz, T. Runka, Appl. Phys. Lett. **95**, 113114 (2009).
[2] J. Slawinska, P. Dabrowski, I. Zasada, Phys. Rev. B **83**, 245429 (2011).
[3] J. Slawinska, P. Dabrowski, I. Wlasny, Z. Klusek, I. Zasada, Phys. Rev. B **85**, 235430 (2012).

Mixing of Edge States at a Bipolar Graphene Junction

Hennrik Schmidt[1,2], Johannes Rode[1], Christopher Belke[1], Dmitri Smirnov[1], and Rolf J. Haug[1]

[1] *Institut für Festkörperphysik, Leibniz Universität Hannover, Germany*
[2] *Graphene Research Center, National University of Singapore*

The unique nature of single layer graphene makes it possible to continuously tune the charge carrier concentration and also the carrier type from electrons to holes in this truly two-dimensional system. This can be used to create regions of different doping or polarity in the sample, for example with the use of local gates [1] or chemical doping [2]. We use an Atomic Force Microscope to change the doping level of a monolayer graphene sheet in a defined region while conserving the unique transport properties as well as mobilities in the order of 10^4 cm^2(Vs)$^{-1}$. Using a global backgate voltage, the resulting system of areas with different charge carrier densities is then tuned into different states, i.e. a unipolar n-n/p-p or a bipolar p-n junction. At low temperatures, edge channel transport is studied in a perpendicular magnetic field in which, due to the different filling factors, the edge channels equilibrate at the junction. The longitudinal resistance measured across it shows the expected quantized resistance values for the unipolar case, depending on the direction of edge channels and therefore the magnetic field. In the p-n case (0.2 V$\leq V_{BG} \leq$ 5.5 V), the edge states in the two areas are counterpropagating. While for B=4 T and T=1.5 K the difference in the longitudinal resistances also shows the expected quantized value, it decreases for higher magnetic fields, suggesting a suppression of edge-channel mixing at the p-n interface [3].

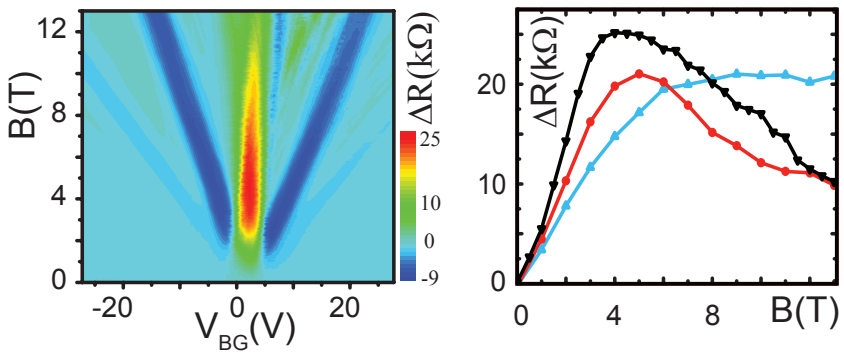

Figure 1: Left: The difference of longitudinal resistances before and after edge state equilibration as a function of backgate voltage and magnetic field at T =1.5 K. Right: This difference in the p-n regime at V_{BG}= 2.5 V and T =1.5 K (black), 125 K (red), and 270 K (cyan), as a function of magnetic field.

[1] J. R. Williams, L. DiCarlo, and C. M. Marcus, Science **317** 638 (2007).
[2] T. Lohmann, K. von Klitzing, and J. H. Smet, Nano Lett. **9**,1973 (2009).
[3] H. Schmidt, J. Rode, C. Belke, D. Smirnov, and R. J. Haug, arXiv:**1212.2824** (2012).

ThP36

Resistive switching in reduced graphene oxide

M. Rogala[1,2], P.J. Kowalczyk[1], W. Kozłowski[1], L. Lipińska[3], J. Jagiełło[3], K. Librant[3], P. Dąbrowski[3], J.M. Baranowski[3], K. Szot[2] and Z. Klusek[1]

[1]*Department of Solid States Physics, Faculty of Physics and Applied Informatics, University of Lodz, Pomorska 149/153, 90-236 Lodz, Poland*
[2]*Peter Grünberg Institut and JARA-FIT, Forschungszentrum Jülich, 52425 Jülich, Germany*
[3]*Institute of Electronic Materials Technology, Wolczynska 133, 01-919 Warsaw, Poland*

A resistive switching (RS) mechanism relays on electrically inducted reversible changes of the material resistivity between two distinguishable states of low (ON) and high (OFF) resistance. It was mainly studied in metal oxides [1], however, recently it turned out that the RS can be also observed in graphene oxide (GO) [2]. This discovery seems to be of high importance due to potential application of the GO in flexible and transparent electronics in particular in a novel resistive random-access memory modules. Interestingly, the origin of the switching phenomena in GO is not fully recognized up to date.

In our presentation we show that the RS can be observed not only in GO but also in reduced GO (rGO). We used here the rGO produced by oxidation-reduction method. The starting material - expandable graphite from Asbury Carbons was oxidised using modified Hummers method followed by the chemical reduction using simultaneously two inorganic compounds in the presence of sodium deoxycholan. The reduction process used here was found to prevent the agglomeration of carbon flakes. Obtained in such a way noncovalently functionalised rGO was deposited from water solution on p-doped silicon wafer using drop cast method which resulted in the resistivity rGO layer at the level of 300 Ωcm^2.

We conducted our experiments both in macro- and nanoscale. For macroscale measurements various metals were used as an electrode material. Electrodes were contacted to the rGO layer, which gave us the opportunity to record I(V) characteristics. The measurements were conducted in air at room temperature (RT) and also for a sample rinsed in liquid nitrogen and with a droplet of water in electrode contact area. The nanoscale measurements were conducted in air and at RT using atomic force microscope (AFM) with conducting platinum coated tip. All the measurements showed presence of the RS, however, there are clear differences dependent on the electrodes material, temperature and environment in which the experiment was carried out. What is more, we show that in rGO both unipolar and bipolar RS is possible.

This work is supported by the National Science Centre under the project DEC-2012/05/B/ST5/00354.

[1] K. Szot, M. Rogala, W. Speier, Z. Klusek, A. Besmehn, R. Waser, Nanotech. **22**, 254001 (2011).
[2] C.L. He, F. Zhuge, X.F. Zhou, M. Li, G.C. Zhou, Y. W. Liu, J.Z. Wang, B. Chen, W.J. Su, Z.P. Liu, Y.H. Wu, P. Cui, and R.-W. Li, Appl. Phys. Lett. **95**, 232101 (2009).

Electron transport properties of the fluorocarbon chain bridging two graphene leads

Małgorzata Wawrzyniak-Adamczewska, Tomasz Kostyrko

Faculty of Physics, A. Mickiewicz University, ul. Umultowska 85, 61-614 Poznań, Poland

Inspired by the experiment showing realization of the stable free-standing carbon atomic chains connected to graphene flakes [1], as well as by the theoretical electron transport studies in such systems [2, 3, 4], the numerical analysis of the electronic properties of the fluorocarbon chain bridging two graphene leads is presented and discussed. Such a system may be possibly realized during the fluorine-passivation process of the graphene-chain-graphene junction. The role of the type of the graphene edges, the length and parity of the formed chain, as well as the range of the fluorine passivation is examined. The electronic properties such as partial and local density of states, the transmission function and the current-voltage characteristics is studied within density functional approach using SIESTA package [5]. The *ab initio* results are then compared to tight-binding model ones.

[1] C. H. Jin, H. P. Lan, L. M. Peng, K. Suenaga and S. Iijima, Phys. Rev. Lett. **102**, 205501 (2009).
[2] Wei Chen, A. V. Andreev, Phys. Rev. B, **80**, 085410 (2009).
[3] J. A. Fürst, M. Brandbyge, A.-P. Jauho, EPL **91** 37002 (2010).
[4] S. K. Ambavale, A. C. Sharma, phys. stat. sol. b **249**, 107-112 (2012).
[5] Ordejón P., Artacho E., and Soler J. M., Phys. Rev. B, **53** (1996) 10441; Soler J. M., Artacho E., Gale J. D., Garcia A., Junquera J., Ordejón P. and Sanchez-Portal D., J. Phys. Cond. Mat., **14** (2002) 2745; Brandbyge M, Mozos J. L., Ordejón P., Taylor J. and Stokbro K., Phys. Rev. B, **65** (2002) 165401.

ThP38

Electron-electron interaction in graphene quantum dots

Błażej Jaworowski[1], Paweł Potasz[1], and Devrim Güçlü[2]

[1] *Institute of Physics, Wrocław University of Technology, PL-50-370 Wrocław, Poland*
[2] *Department of Physics, Izmir Institute of Technology, IZTECH, TR35430, Izmir, Turkey*

We investigate electron-electron interaction effects in graphene quantum dots using variational and diffusion quantum Monte Carlo (QMC) tehniques. Following the recent isolation of a single graphene layer, both experimental and theoretical research on graphene structures has increased exponentially due to their unique physical properties and promising potential for technological applications, especially in nanoscale electronics [1, 2, 3]. Recent theoretical work based on tight-binding and configuration interaction approach has shown that many-body correlation effects due to electron-electron interactions can play an important role in the electronic and magnetic properties in graphene quantum dots [4, 5, 6]. In this work, we build accurate many-body trial wave functions using tight-binding and density functional theory molecular orbitals multiplied by a Jastrow factor [7, 8]. Once the trial wave function is optimized, we perform diffusion Monte Carlo calculations to obtain fixed-node solutions, which allow us to investigate electronic and magnetic structure of small graphene quantum dots of various sizes and shapes.

[1] K. S. Novoselov, A. K. Geim, S. V. Morozov, D. Jiang, M. I. Katsnelson, I. V. Grigorieva, S. V. Dubonos, A. A. Firsov, Nature **438**, 197-200 (2005).
[2] A. K. Geim, K. S. Novoselov, Nature Materials **6**, 183 - 191 (2007).
[3] A. H. Castro Neto, F. Guinea, N. M. R. Peres, K. S. Novoselov, A. K. Geim, Rev. Mod. Phys. **81**, 109 (2009).
[4] A. D. Güçlü, P. Potasz, O. Voznyy, M. Korkusinski, P. Hawrylak, Phys. Rev. Lett. **103**, 246805 (2009).
[5] P. Potasz, A. D. Güçlü, O. Voznyy, J. A. Folk, P. Hawrylak, Phys. Rev. B **83**, 174441 (2011).
[6] P. Potasz, A. D. Güçlü, A. Wójs, P. Hawrylak, Phys. Rev. B **85**, 075431 (2012).
[7] D. M. Ceperley, Rev. Mod. Phys. **67**, 279 (1995).
[8] W. M. C. Foulkes, L. Mitas, R. J. Needs, and G. Rajagopal, Rev. Mod. Phys. **73**, 33 (2001).

Fast and robust preparation of excitons and biexcitons in a quantum dot even at strong carrier-phonon coupling

M. Glässl[1], A. M. Barth[1,], M. D. Croitoru[1,], A. Vagov[1,], and V. M. Axt [1]

[1] *Institut für Theoretische Physik III, Universität Bayreuth, 95440 Bayreuth, Germany*

Realizing a high-quality, on-demand and robust exciton or biexciton preparation in semiconductor quantum dots is of great importance for many quantum dot based devices such as single or entangled photon sources. While a perfect initiation of the quantum dot to both states can in principle be realized via resonant Rabi flopping, these schemes suffer from a high sensitivity on the dipole moments and the pulse intensity. A robust preparation can be achieved using protocols with frequency swept pulses, that rely on adiabatic rapid passage (ARP). However, the degree of exciton inversion realized in recent ARP-based experiments [1, 2] stayed below the ideal case and theoretical works gave compelling evidence that this reduction can be attributed to acoustic phonons [3, 4, 5].

Here, we present protocols that combine the simplicity of Rabi flopping with the robustness of ARP-based protocols and give the discussion of phonon influences a completely different perspective by demonstrating how one can highly benefit from the otherwise undesired carrier-phonon coupling. Using a numerically exact real-time path-integral approach [6] it is demonstrated how the exciton and the biexciton state of a strongly confined quantum dot can be prepared with high fidelity by applying a strong laser pulse that is circularly polarized and tuned above the exciton resonance for exciton preparation and chosen linearly polarized and in resonance with the exciton transition for biexciton preparation (cf. Fig. 1). Our protocols make active use of the phonon-induced relaxation towards photon dressed dressed states in laser driven quantum dots [7]. The presented schemes result in a fast preparation on a timescale of 10 pico-seconds and perform the better the stronger the carrier phonon coupling is. Thus, they allow for an almost ideal state preparation even in situations with strong system-environment interaction that are usually thought of as making control protocols impossible.

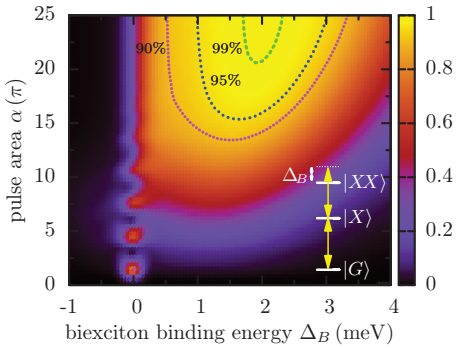

Figure 1: Final biexciton occupation C_{XX} after a Gaussian pulse of 15 ps FWHM at $T = 4$ K as a function of the biexciton binding energy Δ_B and the pulse area α. The laser frequency is chosen in resonance with the ground state to exciton transition and thus, for finite Δ_B, off-resonant to the exciton to biexciton transition (cf. inset). Contour lines show where certain values of C_{XX} are reached.

[1] C. M. Simon et al., Phys. Rev. Lett. **106**, 166801 (2011).
[2] Y. Wu et al., Phys. Rev. Lett., **106**, 067401 (2011).
[3] S. Lüker et al., Phys. Rev. B, **85**, 121302(R) (2012).
[4] K. Gawarecki et al., Phys. Rev. B, **86**, 235301 (2012).
[5] M. Glässl et al., Phys. Rev. B, **87**, 085303 (2013).
[6] A. Vagov et al., Phys. Rev. B, **83**, 094303 (2011).
[7] M. Glässl et al., Phys. Rev. B, **84**, 195311 (2011).

Fano resonances in L3 photonic crystal slab cavities

J.P. Vasco[1,2], P.T. Valentim[1,2], H. Vinck-Posada[3], and P.S.S. Guimarães[1,2]

[1] *Departamento de Física, Universidade Federal de Minas Gerais, Belo Horizonte MG, Brazil.*

[2] *DISSE-INCT de Nanodispositivos Semicondutores, Brazil.*

[3] *Departamento de Física, Facultad de Ciencias, Universidad Nacional de Colombia - Sede Bogotá, Bogotá, Colombia.*

In the last two decades, semiconductor optics has been focused on building high efficiency and low loss devices for optoelectronic applications. The control of the dissipation channels is fundamental for this purpose and thus constitutes an important and active area of intense research. Semiconductor systems which present a spatially periodic dielectric function, known as photonic crystals, are optimal candidates for this purpose. Particularly, photonic crystal slab cavities show an interesting phenomena called Fano resonances, which are produced by the electromagnetic interference between the bounded states of the cavity and the external or scattering states through a dissipation channel, which is created by the finite thickness of the crystal. Therefore, changes of the lineshape of the Fano resonances reflect changes in the dissipation physical conditions. In this work we investigate the Fano resonances in two dimensional slab photonic crystal cavities of the type L3. These photonic crystals are fabricated on membranes of a semiconductor patterned with a periodic array of air holes. The actual cavity consists of three (L3) holes missing along one of the lines of the pattern. We calculate the Fano interference lines in the reflectivity through the scattering matrix method, with a defective periodic pattern described by a plane wave basis. The electric field inside and outside the structure is analyzed for a better understanding of the interference phenomenon. We find that the Fano lineshape can be tuned in a controllable way through the polarization of the incident field, which changes the effective phase between the two contributions to the interference. We show that for some polarizations angles the symmetry of the Fano resonance is reversed. A comparison with experimental data [1] on the reflectivity of photonic crystal cavities is also presented.

[1] P.T. Valentim, J.P. Vasco *et al.*, submitted for publication.

Type-II GaSb/GaAs quantum rings: charging mechanisms and the bimolecular recombination approximation

Peter D. Hodgson,[1] Robert J. Young,[1] Mazliana Ahmad Kamarudin,[1,2] Peter J.Carrington,[1] Anthony Krier,[1] Qian D. Zhuang,[1] Erwin P. Smakman,[3] Paul M. Koenraad[3] and Manus Hayne[1]

[1] *Department of Physics, Lancaster University, Lancaster LA1 4YB, UK*

[2] *Department of Physics, Universiti Putra Malaysia, 43400 UPM Serdang, Selangor Darul Ehsan, Malaysia*

[3] *Department of Applied Physics, Eindhoven University of Technology, The Netherlands*

Type-II GaSb/GaAs self-assembled quantum dots (QDs) and quantum rings (QRs) have numerous potential applications including memories, solar cells and lasers. Blueshifts of QD emission energy, E, with increasing laser power, P, in photoluminescence (PL) measurements have been widely reported. This characteristic behavior has been attributed to either band bending effects [1] or capacitive charging of QD/QRs [2]. However, without careful analysis, it can be difficult to discern between the two mechanisms. Our results show that analyses based on the assumption that $P \propto I \propto n^2$, where $I \propto n^2$ is the bimolecular recombination approximation (BMRA), are flawed.

We studied the QR PL energy shift of eleven different samples. The observation of sub-peaks in Sample A [3], which correspond to ground state recombination of discretely-charged ring states, allowed us to conclusively show that capacitive charging dominates the blueshift and that the simplistic capacitor model describes our data. Furthermore, simple estimates show that the energy shift due to capacitive charging is an order of magnitude larger than that of band bending. Thus we confidently expect the laser power induced blueshift in all of our samples to be dominated by capacitive charging.

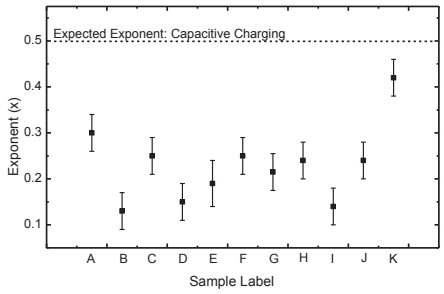

Exponents extracted by plotting log(ΔE) vs log(I) for each QR sample.

As Sample A is unique in showing charge quantized sub-peaks, a more general method using log(ΔE) vs log(I) was employed. This method uses emission intensity, I, as an indicator of carrier density rather than P, avoiding assumptions related to QR capture cross-section. Also, a log-log analysis enables the determination of the exponent, x, in $\Delta E \propto I^x$ without the need for *a priori* assumptions of x. It can be seen from the figure that all values are consistently lower than the 0.5 value expected for capacitive charging. This result illustrates that it is not possible to infer QD/QR occupancy, n, through the commonly used $I \propto n^2$ relationship, i.e. the BMRA breaks down when applied to type-II QD/QRs. This result has important consequences for the performance of type-II QD/QR devices; indicating benefits for the wavelength stability and emission intensity of lasers, but may also point to reduced efficiency in solar cells.

[1] D. Alonso-Álvarez et al., Appl. Phys. Lett. 91, 263103 (2007).
[2] B. Bansal et al., Phys. Rev. B 80, 205317 (2009).
[3] R. Young et. al., Appl. Phys. Lett. **100**, 082104 (2012).

Optically-induced charge depletion in type-II GaSb/GaAs quantum dots and rings

Peter D. Hodgson,[1] Robert J. Young,[1] Qian D. Zhuang,[1] Mazliana Ahmad Kamarudin,[1,2] and Manus Hayne[1]

[1] *Department of Physics, Lancaster University, Lancaster LA1 4YB, UK*

[2] *Department of Physics, Universiti Putra Malaysia, 43400 UPM Serdang, Selangor Darul Ehsan, Malaysia*

There are many potential applications of type-II GaSb/GaAs self-assembled quantum dots (QDs) and quantum rings (QRs) including memories, solar cells and lasers. Blueshifts of the QD/QR emission energy, E, with increasing laser power, P, are commonly observed in photoluminescence measurements and result from capacitive charging [1]. However, at temperatures below 100 K, *redshifts* with increasing laser power have been observed and attributed to optically-induced charge depletion (OICD) [2]. OICD is caused by the interaction of photogenerated carriers with carbon acceptors in the sample. Here we report the remarkable observation of OICD at low temperatures (<20 K) in the wetting layer (WL), followed by the emergence of OICD above room temperature in the QD/QRs.

The sample was grown by molecular beam epitaxy on a (100) GaAs substrate and contains both GaSb QDs and QRs [3]. PL measurements were carried out at temperatures, T, of 2 to 400 K and laser power densities, P, of 10^{-1} to 10^{4} mWcm^{-2}. The magnitude of the OICD redshift in the WL *decreases* with increasing temperature [Fig. (a)]. In contrast, OICD is only seen in the QD/QRs at temperatures above 300 K [Fig (b)], and the magnitude of the redshift *increases* with increasing temperature. A simple rate equation model was created to replicate the OICD behavior seen in our data. It can be seen in Fig (c) that this model is successful in replicating the general behavior of OICD in the QD/QRs.

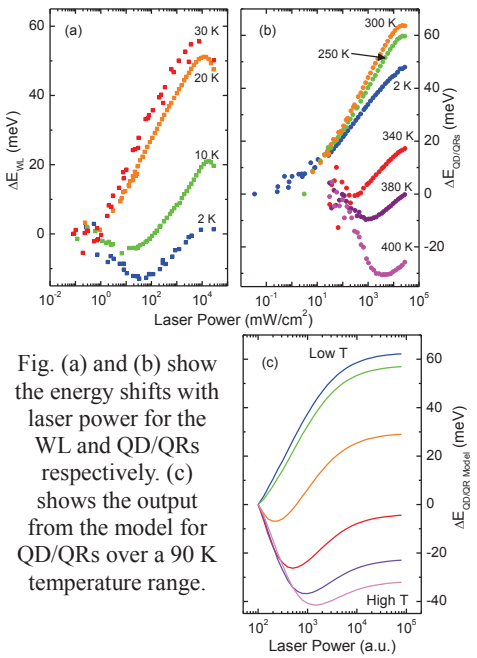

Fig. (a) and (b) show the energy shifts with laser power for the WL and QD/QRs respectively. (c) shows the output from the model for QD/QRs over a 90 K temperature range.

Our results indicate that the acceptor holes occupy the WL at T<20 K and migrate into the QD/QRs at T>300 K. The preferential occupation of QRs at T>300 K is promising for the implementation of GaSb/GaAs QRs in devices operating at room temperature. We tentatively suggest that highly strained QDs may account for the acceptor states at intermediate temperatures, with the majority of the PL emission in this sample arising from the less strained QRs.

[1] P. D. Hodgson et al., *'Type-II GaSb/GaAs quantum rings: charging mechanisms & the bimolecular recombination approximation'*, abstract submitted to MSS-16.

[2] M. Hayne et al., Phys. Rev. B 70, 081302(R) (2004).

[3] M. Ahmad Kamarudin et. al., Phys. Rev. B 83, 115311 (2011)

Quantum Simulations in Quantum Dots Arrays

Pierre Barthelemy[1], **Lieven Vandersypen**[1]

[1] *Quantum Transport, Kavli Institute of Nanoscience, TU Delft, The Netherlands*

Arrays of laterally-defined quantum dots in semiconductor heterostructure offer a unique platform for quantum simulations of the Hubbard model[1, 2]. Indeed, placing such a device in a dilution refrigerator would bring the system to a temperature low enough to observe the influence of spin exchange onto the electron wavefunctions. So far, the main issue to reach this goal has been the strong disorder in the (doped) semiconductor heterostructures.

By using capacitance spectroscopy techniques[3], we propose to measure the density of states in a quantum dot lattice defined by placing a surface grid-shaped gate above a 2D electron gas (2DEG). The use of capacitive measurement schemes allows to strongly decrease the influence of disorder: first, is allows the use of undoped systems, thereby removing the dominant contribution to the disorder. But the vicinity of the back electrode of these capacitive systems to the 2DEG strongly screens the remaining disorder. Our calculations showed that onsite fluctuations should fall below 10-20μeV, low enough to efficiently simulate Hubbard physics with hopping energies of the order of 100μeV. We present in this contribution the advances made in our group towards towards the fabrication and measurement of the density of states in capacitive quantum dots arrays.

[1] T. Byrnes, N.Y. Kim, K. Kusudo and Y. Yamamoto, Phys. Rev. B, **78**, 075320 (2008).
[2] A. Singha, *et al.*, Science**332**, 1176-1179 (2011).
[3] R.C. Ashoori, J.A. Lebens, N.P. Bigelow and R.H. Silsbee, Phys. Rev. B, **48**, 4616-4628 (1993).

Coupling between surface plasmon polaritons and proximal InGaAs quantum dots in Au-GaAs plasmonic nanostructures

G. Bracher, K. Schraml, J. Wierzbowski, N. Coca Lopez, M. Blauth, M. Bichler, K. Müller, M. Kaniber and J. J. Finley

[1]*Walter Schottky Institut, Am Coulombwall 4a, 85748 Garching, Germany*

Improving fabrication techniques now facilitate the routine fabrication of nanometer scale metallic structures, opening the way to use surface plasmon polaritons (SPPs) to guide, confine and manipulate light over lengthscales far below the diffraction limit and enhance the strength of the light-matter interaction. However, when proximal quantum emitters are brought close to such metallic nanostructures, competing radiative and non-radiative processes often complicate understanding of the precise nature of the light-matter coupling. Moreover, imaging of SPPs is non-trivial, typically calling for near field optical techniques. Here, we present investigations of lithographically defined rectangular SPP waveguides [1] and directional couplers on GaAs into which a sparse array of InGaAs quantum dot (QD) emitters is grown 25±2 nm beneath the surface [2]. Our results allow us to elucidate how the optical properties (radiative dynamics and luminescence yield) of the QDs are influenced by the proximity to the Au-GaAs interface and, furthermore, demonstrate that the QD emission can be used to directly image surface plasmon polaritons. In time resolved measurements, a highly local $\sim 1.5\times$ enhancement of the spontaneous emission decay rate is observed close to the plasmonic nanostructures with a commensurate increase of the emission intensity of dots excited by propagating plasmons. Whilst such spatially resolved spectroscopy clearly indicates the presence of a unidirectional energy transfer mechanism from the propagating SPP modes to the dots, it also facilitates imaging of the propagating SPPs modes. For passive structures that do not contain dots we measure SPP propagation lengths ranging between 13.4 ± 1.5 µm and 27.5 ± 1.7 µm for waveguide widths of 2 µm and 5 µm, respectively [1]. In contrast, for active structures containing QDs we observe an exponential decay of the intensity of the QD emission along the waveguide with a decay length of ~5 µm, indicative of the existence of a different mode, which couples efficiently to the QDs. The local emission from QDs was used to test the operation of a plasmonic beam splitter [3] consisting of two parallel waveguides with evanescent coupling over a well-defined interaction length – L (fig 1a). By exciting plasmons in the left hand input port of the waveguide, the intensity of the QD PL in the left and right hand output ports was monitored as a function of L. Figure 1b shows the typical QD emission intensity recorded as a function of the interaction length, showing excellent agreement with the results of FDTD simulations.

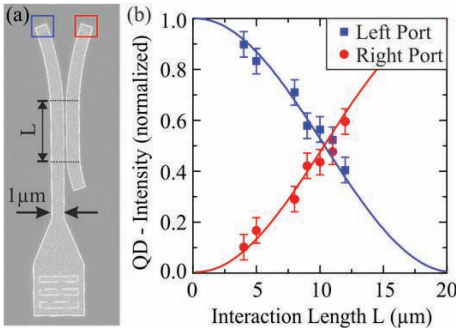

Fig. 1: (a) SEM image of a typical plasmonic beamsplitters on GaAs - Inset: Spatially resolved image of the QD emission showing the plasmonic beamsplitters (b) Splitting ratios of directional couplers: Relative intensities (scatter plot) of the two stripes plotted as a function of their interaction length. Solid lines indicate corresponding simulations of the system.

[1] Bracher et al., J. Appl. Phys. 110, 123106 (2011)
[2] Bracher et al., Proc. of SPIE 8269, 826920-1 (2012)
[3] Wahsheh et al., Optics Comm. 282,4622-4626 (2009)

All electrical control of quantum gates for single heavy hole spin qubits in the presence of nuclear spins

P. Szumniak and S. Bednarek

AGH University of Science and Technology, Faculty of Physics and Applied Computer Science,
al. Mickiewicza 30, 30-059 Kraków, Poland

Recently the spin state of the hole emerged as an alternative and very promising candidate for the realization of a qubit in semiconductor solid state systems. Its main advantage over the electron spin is the fact that the hole is less sensitive to the interaction with the nuclear spin of the surrounding material. Since the hole is described by a p-type orbital in many semiconductors, its wave function vanishes at the nuclear site and thus the contact hyperfine interaction between hole spin and nuclear spin is canceled. Even though holes still experience interaction with nuclear spins with dipolar character, it is about ten times weaker than the contact interaction for electrons [1, 2, 3]. Consequently, the coherence time of the spin state of the hole is longer than for the electron spin. The coherence time also depends on the heavy hole (HH)-light hole (LH) mixing. For pure HH states, the coherence time of the hole reaches its maximum because the interaction between hole spin and nuclear spins has an Ising type character [1, 2].

We propose a set of the nanodevices [4] which can act as Pauli X, Y , Z quantum gates and as a gate that acts similar as a Hadamard gate (i.e. it creates a balanced superposition of basis states but with an additional phase factor) on the heavy hole spin qubit. The proposed devices exploit the self-focusing effect of the hole wave function[5] which allows for guiding the hole along a given path in the form of a stable soliton-like wave packet[6]. Thanks to the presence of the Dresselhaus spin orbit coupling, the motion of the hole along a certain direction is equivalent to the application of an effective magnetic field which induces in turn a coherent rotation of the heavy hole spin[7]. The hole motion and consequently the quantum logic operation is initialized and controlled only by weak static voltages applied to the electrodes which cover the nanodevice.

In our calculations the interaction between hole spin and nuclear spin bath of the CdTe host material is considered within the quasi static approximation (QSA)[8] - hole spin experiences effective random nuclear magnetic field with non-homogeneous Gaussian distribution[2]. Such an interaction leads to a dephasing of the hole spin qubit (i.e. decay of the Rabi oscillations). The effect of the valence band mixing as well as an influence of the width of the nuclear spin distribution on the hole spin dynamic will be discussed.

[1] J. Fischer, W. A. Coish, D. V. Bulaev, and D. Loss, Phys. Rev. B **78**, 155329 (2008).
[2] C. Testelin, F. Bernardot, B. Eble, and M. Chamarro, Phys. Rev. B **79**, 195440 (2009).
[3] E. A. Chekhovich, A. B. Krysa, M. S. Skolnick, and A. I. Tartakovskii, Phys. Rev. Lett. **106**, 027402 (2011).
[4] P. Szumniak, S. Bednarek, S. Pawłowski, and B. Partoens, ArXiv (2013).
[5] S. Bednarek, B. Szafran, and K. Lis, Phys. Rev. B **72**, 075319 (2005).
[6] S. Bednarek, B. Szafran, R. J. Dudek, and K. Lis , Phys. Rev. Lett. **100**, 126805 (2008).
[7] P. Szumniak, S. Bednarek, B. Partoens, and F. M. Peeters, Phys. Rev. Lett. **109**, 107201 (2012).
[8] I. A. Merkulov, Al. L. Efros, and M. Rosen Phys. Rev. B **65**, 205309 (2002).

Exotic quantum couplings in optically active quantum dot molecules

P.L. Ardelt, K. Müller, A. Bechtold, G. Abstreiter and J.J. Finley

Walter Schottky Institut and Physik Department, Technische Universität München, Am Coulombwall 4a, 85748 Garching, Germany

We report detailed magneto-optical investigations of electron tunnelling and Coulomb quantum couplings of excitonic transitions in electrically tunable quantum dot (QD) molecules. Single molecule photocurrent (PC) absorption, photoluminescence (PL) emission and PL-excitation spectroscopy are combined to carefully map the entire spectrum of spatially *direct* ($e + h$ in same dot) and *indirect* ($e + h$ in different dots) excitonic transitions of a single molecule. Comparison with simulation allows us to obtain a full and consistent picture of the conduction and valence band orbital structure [1].

From PC-measurements we firmly identify the spatially direct neutral exciton transition with both e and h localized in the upper dot (X^0_{ud}). By tracking the electric field dependence of X^0_{ud}, we clearly observe the expected anticrossings arising from tunnel couplings between different electronic orbital states of the QD-molecule [2,3] (fig 1). In addition, a number of *unexpected* anticrossings are observed in PC spectroscopy and shown to arise from Coulomb mediated coupling of excitonic transitions, involving entirely *different* single particle orbitals. By examining the evolution of the tunnel and Coulomb mediated couplings with magnetic field applied in Faraday geometry, we extract new information about the orbital structure of excited hole states in the QD-molecule.

By performing ultrafast optical pump-probe spectroscopy in the PC-regime we obtain new information about ultrafast carrier and spin dynamics in the system. Close to quantum couplings we observe a strong reduction of the electron tunneling time. The results obtained elucidate the roles of ultrafast (<5ps) elastic and inelastic intra-molecular electron tunneling and allow us to directly extract the exciton - acoustic phonon coupling in the system [4]. The ability to electrically switch the system into a regime with ultrafast inter-dot tunneling enables us to optically initialize a single hole spin on timescales only limited by the width of the initializing laser pulse (<5ps) with a purity of >96% (only limited by noise). By monitoring the time evolution of a single coherent hole spin in lateral magnetic fields using optically polarized ultrafast laser pulses we observe coherent Larmor precession of a single hole spin with no observable loss of coherence within the hole lifetime [5].

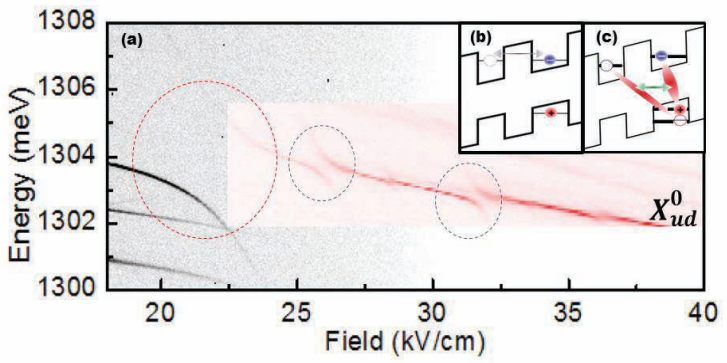

Fig.1 – (a)Typical electric field dependent PL (blue coding) and PC (red coding) spectra showing X^0_{ud} and couplings arising from tunnel and Coulomb couplings at F = 22.5 kV/cm and F=26.1kV/cm. Inset: Schematic representation of tunnel (b) and Coulomb (c) mediated couplings.

References

[1] K. Müller et al., Phys Rev. B **84**, 081302 (2011)

[2] H. J. Krenner et al. Phys Rev Lett **94**, 057402 (2005) and Phys Rev Lett **97**, 076403 (2006)

[3] M. Scheibner et al. Nature Physics **4**, 291 (2008)

[4] K. Müller *et al.*, Phys. Rev. Lett., **108**, 197402 (2012)

[5] K. Müller *et al.*, Phys. Rev. B, **85**, 241306(R) (2012)

The evolution of spatial coherence in double quantum dots under the influence of phonons

Paweł Karwat, Paweł Machnikowski

Institute of Physics, Wrocław University of Technology, 50-370 Wrocław, Poland

The experimental evidence of collective effects in the emission from quantum dot (QD) samples suggests that such systems cannot be treated as ensembles of independent emitters [1]. The enhanced, "superradiant" emission from the ground state of a QD ensemble has been successfully modeled [2] under assumption that the QDs are coupled not only by long-range dipole interactions but also by short range ones (e.g. due to tunneling). This model accounted for the experimentally observed system evolution as a function of the number of QDs and detection energy with respect to the maximum of the ensemble photoluminescence. However, the striking difference between the time-resolved ensemble emission under quasi-resonant excitation (optical transition to higher confined shells, leading to a collective enhancement of emission) and non-resonant excitation (transition to wetting layer or bulk states with no enhancement of emission observed) has not been discussed.

In this presentation, we make the first step towards understanding of this dependence on the excitation conditions. As the collective emission requires that a spatially delocalized superposition of exciton states in various dots exists in the system, the most likely explanation of the observed facts is that spatial coherence is preserved during exciton relaxation between confined shells but lost upon trapping from wetting layer or bulk states. Therefore, we study the evolution of the spatial coherence during relaxation between delocalized exciton states in the simplest case of a double quantum dot (DQD) coupled to acoustic phonons. We investigate under what conditions (alignment of energy levels, coupling, inter-dot distance) the spatial coherence is preserved during the relaxation between these states in a DQD system. In addition, we study the effect of thermalization of occupations and dephasing on the collective emission.

Our description of the system kinetics is based on a few-level description of two coupled QDs and a Markovian Lindblad equation for carrier-phonon dynamics with transition rates derived from standard carrier-phonon couplings. Using this model, we show that no coherence can appear in the ground state manifold for uncoupled QDs in the absence of degeneracy of the intraband transition energies. However, either degeneracy or coupling between the dots can lead to coherence transfer, similar to the exciton-biexciton case [3]. Thus, the interplay of the coupling strength and energy degeneracy is crucial not only for the appearance of collective emission itself [3,4] but also for the coherence transfer during relaxation that is needed for the appearance of a "superradiant" superposition in the ground state.

[1] M. Scheibner, T. Schmidt, L. Worschech, A. Forchel, G. Bacher, T. Passow, D. Hommel, *Nature Phys.* **3**, 106 (2007).

[2] M. Kozub, Ł. Pawicki, P. Machnikowski, *Phys. Rev. B* **86**, 121305(R) (2012).

[3] P. Karwat, A. Sitek, P. Machnikowski, *Phys. Rev. B* **84**, 195315 (2011).

[4] A. Sitek, P. Machnikowski, *Phys. Rev. B* **75**, 035328 (2007).

ThP48

Exciton dynamics in InAs/$In_{0.53}Ga_{0.23}Al_{0.24}As$/InP quantum dashes

W. Rudno-Rudziński[1], Ł. Dusanowski[1], M. Syperek[1], G. Sęk[1], J. Misiewicz[1], A. Somers[2], R. Schwertberger[2], J. P. Reithmeier[2, 3], S. Höfling[2] and A. Forchel[2]

[1] *Institute of Physics, Wroclaw University of Technology, Wybrzeże Wyspiańskiego 27, 50-370 Wrocław, Poland*
[2] *Technische Physik, Universität Würzburg, Am Hubland, D-97074 Würzburg, Germany*
[3] *Currently at Institute of Nanostructure Technologies and Analytics, Universität Kassel, Heinrich-Plett-Str. 40, 34132 Kassel, Germany*

In this work there are presented the results of photoluminescence (PL) and time-resolved photoluminescence (TRPL) measurements on InAs/$In_{0.53}Ga_{0.23}Al_{0.24}As$ strongly elongated quantum dots called quantum dashes (QDashes), grown by molecular beam epitaxy on (001) InP substrate. The experiments have been performed at low temperature (5 K), both on the ensemble and single dashes. In the case of the emission from the ensemble, a series of structures has been investigated with different cross-sectional dimensions: height and base width changing from 3x12 nm to 5x20 nm, leading to a pronounced spectral shift of PL emission peak from 1.4 to 1.65 μm, due to the increase in their volume. The TRPL experiments use a mode-locked Ti:Sapphire laser with 76 MHz train of 150 fs wide excitation pulses and exploit a time correlated single photon counting technique, thanks to the application of very fast (50 ps) and low dark count (<10 s^{-1}) superconducting single photon detectors with a significant detectivity and quantum efficiency in NIR.

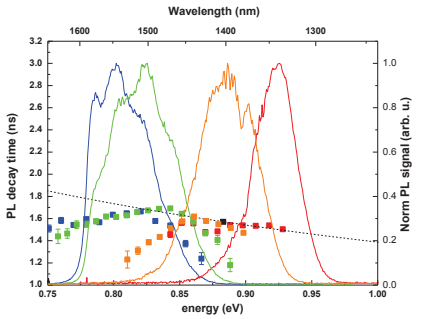

Fig. 1 PL spectra and PL decay time dispersion.

For each of the structures the ensemble PL decay time dispersion vs photon emission wavelength has been recorded. The results are shown in Fig. 1. It shows the PL decay time increase from ~1.5 up to ~1.67 ns with increasing emission wavelength (from ~1.33 to 1.5 μm), which is consistent with the tendency for a strong confinement regime (dotted line). However, for longer wavelengths, the PL decay time starts to decrease. This is interpreted as a transition to the intermediate regime, where Coulomb correlation becomes more important and the transition oscillator strength should depend linearly on the exciton coherent volume, and thus also on the QDash size. The shift occurs for slightly different wavelengths due to the fact that the energy structure of dashes depends not only on their size, but on the strain as well, which very between structures.

Single dash PL measurements were performed on a sample emitting at 1.45 μm, with submicron mesas, to assure small enough probed area to resolve the individual emission lines. Several lines attributed to the emission from excitons and exciton complexes were visible for very low excitation powers. The TRPL spectra revealed two main groups of lines, with lifetimes differing by a factor of two, as is expected for strongly confined excitons and biexcitons. The emissions with longer decay times showed non-exponential behavior, with the maxima of the emission shifting to longer times for higher excitation powers and long rise times, agreeing with the decay constants for the emissions with shorter times, having monoexponential decay for any excitation power. Such a behavior is also consistent with biexciton/exciton cascade. The temperature evolution of the decay curves for excitonic lines was also investigated, showing that they regain exponential behavior at higher temperatures.

Exciton fine structure splitting and biexciton binding energy in InAs/InGaAlAs/InP quantum dashes

P. Mrowiński[1], A. Musiał[1], G. Sęk[1], J. Misiewicz[1], S. Hein[2], S. Höfling[2], A. Forchel[2]

[1]*Institute of Physics, Wrocław University of Technology, PL-50-370 Wrocław, Poland*
[2]*Technische Physik, Physikalisches Institut, Universität Würzburg & Am Hubland, D-97074 Würzburg, Germany*

The fine structure splitting (FSS) of exciton and binding energy (ΔE_{XX}) of biexciton in quasi-zero-dimensional systems are crucial parameters for developing a new kind of quantum-electrodynamics-based devices, as sources of single photons or entangled photon pairs with defined polarization. In view of applications it is beneficial to control both of them. Quantum-dot-like structures in the InAs/InP material system can potentially be considered due to their easily tunable emission wavelength covering well the telecommunication range, and far beyond. However up to now, any comprehensive study of both the FSS and ΔE_{XX} has not been reported.

Hereby, we present systematic investigation of molecular-beam-epitaxy-grown InAs/InGaAlAs/InP quantum dashes (QDashes) which are characterized by strongly elongated geometry and long-wavelength emission between 1.2 and 1.6 μm, depending on their cross-sectional size. We performed a high resolution microphotoluminescence experiment on small submicron mesas etched on the sample surface, in order to focus on the properties of strictly single emission lines. Preliminary identification of exciton and biexciton emission from a single QDash relies on excitation power dependent series compared with a rate equation model [1]. In this work we try to establish a reliable statistics of both the FSS and ΔE_{XX} values, their spectral/size dispersions and find out which system properties determine them primarily. There belong here such effects as Coulomb correlations, electron-electron and electron-hole exchange interactions, but also the regime of quantum confinement and the strain conditions. Some trends have been shown for small and symmetric InAs quantum dots in AlAs and GaAs matrices [2-4], but also for slightly anisotropic InAs/GaAs QDs, suggesting basically a decrease of both FSS and ΔE_{XX} for very small dots. Here, the physical situation is more complex due to the strong elongation of the investigated structures and the probable existence of the local carrier/exciton trapping on the dash size fluctuations [5]. For most of the dashes we obtained a very small values of FFS, significantly below 100 μeV, in agreement with the localization picture, however, we observed also sporadically values in a range of 100-300 μeV, which suggests an impact of anisotropic exchange interactions for the asymmetrically extended states of the dashes without a confining traps. Additionally, the increasing trend of biexciton binding energy with exciton's energy up to 3.7 meV is contrary to the previous reports for GaAs-based structures [2-4], which supposedly means a different origin of emission, namely lower energy lines come from fluctuations in larger QDashes, whereas higher energy emission is from the excitons localized within the entire QDash volume. Our study shows that the shape anisotropy and confinement regime are actually the factors driving the single dash properties in these nanostructures.

References:

[1] G. Sęk, A. Musiał, P. Podemski, and J. Misiewicz, Journal of Applied Physics **108**, 033507 (2010).
[2] D. Sarkar, H.P. van der Meulen, J.M. Calleja, J.M. Becker, R.J. Haug, and K. Pierz, Journal of Applied Physics **100**, 023109 (2006).
[3] S. Rodt, A. Schliwa, K. Pötschke, F. Guffarth, and D. Bimberg, Physical Review B **71**, 155325 (2005).
[4] U.W. Pohl, R. Seguin, S. Rodt, A. Schliwa, K. Pötschke, and D. Bimberg, Physica E: Low-dimensional Systems and Nanostructures **35**, 285 (2006).
[5] A. Musiał, P. Kaczmarkiewicz, G. Sęk, P. Podemski, P. Machnikowski, J. Misiewicz, S. Hein, S. Höfling, and A. Forchel, Physical Review B **85**, 035314 (2012).

Temperature dependent emission linewidth and the exciton dephasing in large and asymmetric III-V semiconductor quantum nanostructures

Anna Musiał[1], Grzegorz Sęk[1], Aleksander Maryński[1], Michał Kozub[1], Jan Misiewicz[1], Andreas Löffler[2], Sebastian Hein[2], Sven Höfling[2], Stephan Reitzenstein[2,3], Johann P. Reithmaier[2,4], Martin Kamp[2] and Alfred Forchel[2]

[1] *Institute of Physics, Wrocław University of Technology, Poland*
[2] *W. C. Röntgen-Center for Complex Material Systems, University of Würzburg, Germany*
[3] *Institute for Solid State Physics, Technische Universität Berlin, Germany*
[4] *Institute of Nanostructure Technology and Analytics, University of Kassel, Germany*

Optical properties of epitaxially grown burried semiconductor nanostructures can be strongly influenced by the surrounding solid state matrix and the interaction with it reduces the coherence of the carrier excitations. The dephasing of an exciton becomes a crucial issue whenever applications are considered and this is why the identification of the dephasing mechanisms and ways to control and minimize them are of high importance. On the search for quantum systems being more robust against decoherence, large nano-objects have been predicted to be advantageous due to their weakened confining potential and resulting larger wave function extension [1-3].

To probe the exciton dephasing in two groups of large and asymmetric nanostructures microphotoluminescence has been measured on patterned samples, and the thermal evolution of the full width at half maximum (FWHM) of single emission lines has been analyzed, which has not been carried out for this kind of structures so far.

At first, lowly strained $In_{0.3}Ga_{0.7}As/GaAs$ and slightly elongated QDs (lateral aspect ratio - LAR ~ 2) with typical geometry of (20 x 50 x 5 nm^3) and shallow confining potential (approx. 30 meV) have been investigated. Low temperature FWHM varies in the range of 200 - 500 μeV, and is limited by spectral diffusion while no phonon-related spectral features can be resolved. Strong influence of Coulomb interactions with carriers/excitons in the wetting layer on emission from those dots has already been proven [4] and can lead to large values of FWHM at 5 K. Spectral diffusion effects originate mostly from the fluctuating charges trapped on the mesa sidewalls what has been evidenced by studying the emission for different mesa sizes. With increasing temperature the FWHM of single emission line is almost constant up to 30-40 K and then increases strongly, which we relate to the thermally enhanced interaction with the acoustic phonons and the increased contribution of the so called phonon sidebands to the emission spectral line. In the case of smaller mesas, the FWHM increase starts at lower temperatures and is faster.

An analogical study has been carried out for strongly elongated (LAR exceeding 5) exhibiting deeper confinement quantum dashes (approx. 20 x 150 x 3 nm^3) in the InAs/InP system. The initial FWHM value for those structures is lower (50 - 200 μeV) and the abrupt increase starts at higher temperatures around 60 K in agreement with expected size-related trends. Results for QDs with different height show that enhanced size in the strongest confinement direction causes lower sensitivity of FWHM to temperature changes in the high temperature limit.

[1] L. Besombes et. al., Phys. Rev. B **63**, 155307 (2001).
[2] E. Peter et. al., Phys. Rev. B **69**, 041307 (2004).
[3] P. Borri et. al., Phys. Rev. B **71**, 115328 (2005).
[4] Ł. Dusanowski et. al., J. Appl. Phys. **111**, 063522 (2012).

Optical properties of quantum-dot-like InAs nanostructures grown by molecular beam epitaxy on InP substrate

A. Maryński[1], G. Sęk[1], A. Musiał[1], J. Andrzejewski[1], J. Misiewicz[1], C. Gilfert[2] and J. P. Reithmaier[2]

[1] *Institute of Physics, Wrocław University of Technology, Wybrzeże Wyspiańskiego 27, 50-370 Wrocław, Poland*
[2] *Technische Physik, Institute of Nanostructure Technology and Analytics, CINSaT, University of Kassel, Heinrich Plett-Str. 40, D-34132, Kassel, Germany*

We present our recent work on the optical properties of InAs quantum-dot-like structures grown on InP substrate. In this material system and typically used growth conditions of molecular beam epitaxy (MBE) there are favorably formed strongly elongated structures called quantum dashes with lateral aspect ratio exceeding 5. They have widely been investigated and exploiting their intrinsic properties as e.g. high surface density or broad gain function there have been demonstrated improved performances in several laser device applications in telecommunication range especially [1]. However, there are application-relevant cases where a more symmetric and smaller quantum dot like objects could be indispensable, as they can offer higher gain due to increased ensemble homogeneity, lower threshold current, a possibility of unpolarized emission and higher characteristic temperature T_0 related to stronger confining potential in smaller nanostructures.

Within this communication we investigate almost symmetrical nanostructures of the abovementioned material system achieved by using As_2 instead of As_4 in the MBE growth process [2,3]. We used photoluminescence measurements combined with theoretical 8-band k·p modeling [4] to obtain the information on the electronic structure and the shape anisotropy of these dots. Polarization-resolved photoluminescence experiment was performed to measure the emission from an ensemble of QDs for two perpendicular linear polarization directions (according to the expected structure elongation axis), from both the surface and edge of the sample. This allowed us to obtain the respective degrees of polarization (DOP), which can directly be related to the structure geometry [4]. The obtained DOP from the surface is approx. 0.2, which is significantly less than for the strongly elongated dashes and gives the expected lateral aspect ratio of only about 2, in agreement with previous structural data [3]. This has further been confirmed by the DOP values for both the sample edges. Values of 0.8 and 0.38 were obtained for edges parallel and perpendicular to the object elongation axis. Also, the calculated separation of the energy levels is in the range of 10-50 meV, confirming the quasi-zero-dimensional character of these dots.

Additionally, we have studied the emission properties of these structures on the single dot level and detected several exciton and biexciton lines, identified based on rate equation modeling. The obtained exciton to biexciton lifetime ratio is of about 2, which is clear fingerprint of strong confinement regime.

[1] J. P. Reithmaier, G. Eisenstein, and A. Forchel, *Proc. of IEEE* **95**, 1779 (2007);
[2] C. Gilfert, V. Ivanov, N. Oehl, M. Yacob and J. P. Reithmaier, *Appl. Phys. Lett.* **98**, 201102 (2011);
[3] C. Gilfert, E.-M. Pavelescu and J. P. Reithmaier, Appl. Phys. Lett. 96, 191903 (2010);
[4] A. Musiał, P. Podemski, G. Sęk, P. Kaczmarkiewicz, J. Andrzejewski, P. Machnikowski, J. Misiewicz, S. Hein, A. Somers, S. Höfling, J. P. Reithmaier and A. Forchel, Semicond. Sci. Technol. 27, 105022 (2012).

Andreev spin-polarized tunneling through a quantum dot interacting with phonons

K. Bocian and W. Rudziński

Faculty of Physics, Adam Mickiewicz University, ul. Umultowska 85, 61-614 Poznań, Poland

Using the nonequlibrium Green-function technique we study theoretically spin-polarized transport due to Andreev reflection (AR) in a hybrid ferromagnet-quantum dot-superconductor junction based on a single-level quantum dot interacting with a local phonon mode. Phonon spectra have been calculated for arbitrary Coulomb correlations on the dot. The phonon-assisted AR phenomenon is analyzed within the Green function approach based on the dot correlators including both hole and electron contributions. Thus, it is shown that the phonon emission satellites in density of states spectrum calculated for the Andreev transmission may appear on both sides of the main resonance peaks corresponding to the quantum dot energy levels. The effect of the intradot Coulomb correlations on behavior of the conductance is shown for phonon-assisted AR transmission in the linear regime of bias voltage as well as in the nonequilibrium situation. In particular it is shown that the Franck-Condon blockade gives rise to a suppression of the transmission through the Andreev bound states in the linear bias voltage regime and may lead to a significant enhancement of the phonon resonances. In nonequilibrium situation, an effect of competition between intradot Coulomb correlations and the phonon field on the resonances in the differential conductance is discussed. An influence of the vibrational modes on the matching condition for the perfect AR phenomenon is analyzed as well. The numerical results obtained by means of different approximations of the Green-function correlators for the dot interacting with a local phonon mode are compared and discussed in detail.

Nonlinear transport through interacting quantum dots with superconducting leads in the weak coupling regime

S. Ratz[1], **and M. Grifoni**[1]

[1] *Institute for Theoretical Physics, University of Regensburg, D-93040 Regensburg, Germany*

We present a nonequilibrium real-time diagrammatic transport theory for the systematic investigation of the quasiparticle and Josephson currents through a hybrid superconductor-quantum dot system in the weak coupling regime. In details, our device consists of an interacting quantum dot coupled to two biased spin-singlet superconducting leads. Such systems have received great attention in the last decade, since they provide a wide platform for studying fundamental issues like superconducting proximity effects and the Coulomb blockade [1, 2].

To describe the transport dynamics, we derive a completely general equation of motion for the reduced density matrix including all the contributions of a perturbation expansion in the tunneling Hamiltonian. Within these investigations, already in fourth order we can identify the contributions of the nonlocal time evolution kernel to the quasiparticle and DC Josephson transport. To clarify the difference between quasiparticle cotunneling and phase-coherent two-particle Andreev tunneling in fourth order, we first choose a single-level Anderson impurity model for the interacting quantum dot. In particular, one can give a clear explanation for subgap features due to proximity effects, which are also important when we finally compare our theoretical results for a carbon nanotube quantum dot with recent experimental observations.

[1] S. de Franceschi, L. Kouwenhoven, C. Schönenberger, and W. Wernsdorfer, Nature Nanotech. **5**, 703-711 (2010).

[2] K. Grove-Rasmussen, H. I. Jorgensen, B. M. Andersen, J. Paaske, T. S. Jespersen, J. Nygard, K. Flensberg, and P. E. Lindelof, Phys. Rev. B **79**, 134518 (2009).

Blue-Shifted Photoluminescence of MEHPPV Nanoparticles Fabricated by a Novel Visible-Laser Solution-Droplet Processing

Akihiro Tomioka [1], Kouhei Takada [1] and Masato Kawabata [1]

[1] *Osaka Electro-Communication University, 18-8 Hatucho, Neyagawa, Osaka 572-8530, Japan*

Liquid-phase laser processing, where the laser-irradiated target material is immersed in water for cooling, has been reported as a promising processing technique for thermally fragile organic materials. Although nanometer-sized particles have been reported to be obtained with the liquid-phase laser processing, the physical property did not change because quantum-mechanical size effect does not exhibit itself in the zero-radius Frenkel excitons. In the present study, we step further to use solution droplets as a target material, where organic molecules are dispersed in an organic solvent and, therefore, expected to easily alter the conformation and the energy upon laser irradiation [1]. Small volume organic solvent is quickly evaporated upon laser irradiation, letting the bare organic molecule placed in water and rapidly cooled. To prevent the chemical decomposition of the target π-conjugated molecule, the specimen was resonantly irradiated by a ns-pulse green laser, not by a conventional UV laser.

When the solid state spin-coat film of MEH-PPV was used as a irradiation target immersed in water, resulting MEH-PPV particles showed similar photoluminescence (PL) like the PL of the spin-coat film and PL of the chloroform solution, including the 0-1, 0-2, 0-3 vibrational transitions: this indicates that the energy levels were not modified from the spin-coat film. In comparison, when tiny droplets of MEH-PPV chloroform solution (orange color) were suspended in water, laser irradiation gave rise to yellow MEH-PPV particles which showed 550 nm and 530 nm PL (type B), blue-shifted from the spin-coat film PL 580 nm (type A), suggesting a successful phase transition of MEH-PPV polymer conformation. When these yellow MEH-PPV particles were dissolved in chloroform and irradiated again by a green laser, the resulting particles showed the identical type B PL. The unidirectional phase transition from type A to type B suggests that the type B ground state has lower energy than type A, which is consistent with the blue-shifted PL of type B, providing that the excited state energy is similar between the two states. Thermal annealing up to 200^{o}C of type A state did not give rise to type B state, which indicates that the activation potential between the two states is higher than the thermal energy at 200^{o}C, and that only the proposed solution-phase laser processing enables the system to cross over this potential.

[1] K. Takada, A. Tomioka, J. Phys.: Conf. Ser. **358**, 112012 (2012).

Lowered Melting Point of Polyvinyl Pyrrolidone Bound 1D Ag Nanowires

Akihiro Tomioka [1], Kenji Ozasa [1] and Masato Kawabata [1]

[1] *Osaka Electro-Communication University, 18-8 Hatucho, Neyagawa, Osaka 572-8530, Japan*

Ag nanowires draw an increasing attention as a material with superior electrical conductance: with adequate printing on a transparent glass or plastic film, they bring about a semitransparent electrode, which has a demanding need in touch panel devices in "smart phones" and portable "tablets".

Ag nanowires were grown by an energy-conserving solution process in the present study via polyol-assisted scheme: ethylene glycol (EG) served both as reducing agent and as solvent. EG enabled the chemical reaction performed up to its boiling point (195^{o}C). We utilized Au nanoparticles as crystallization seeds, based on the fact that Ag and Au have similar crystal lattice spacing. Polyvinyl pyrrolidone (PVP), reported to attach Ag crystal in a facet-selective manner and thereby to act as structural directing agent, was used to facilitate the preferential formation of 1D Ag nanowires on Au nanoparticle seed (purple color appearance). The elongation of 1D Ag nanowires was easily ascertained by the color change to turbid gray (greenish or yellowish, depending on the nanowire length). The elongation time was dramatically shortened above 160^{o}C, indicating that PVP serves as catalyst to facilitate the elongation of nanowires. Thermal energy at 160^{o}C should be equal to the activation energy of PVP binding to Ag nanowire side face.

The resulting Ag nanowires were centrifuged and resuspended in 2-propanol twice in order to wash out the reagents, and deposited on Si wafers. Morphology of Ag nanowires was observed by SEM, before and after successive heat treatment at 200^{o}C, 230^{o}C, 250^{o}C, 270^{o}C and 300^{o}C. As deposited, Ag nanowires showed straight profile over 5μm, with sharp well-defined edges. Some of the nanowires, or only portions of single nanowire, became spherical (droplet-like) and the ratio was increased monotonically with increasing temperature. All the nanowires became spherical at 300^{o}C, indicating that the melting point (MP) was 200^{o}C - 300^{o}C, greatly lowered from 962^{o}C of the bulk Ag MP.

Even Ag nanowires with similar diameter (60-70 nm) preserved the same variation of the MP, suggesting that nanowire diameter did not govern the MP. The lower MP is not due to the Ag-Si eutectic because Si wafer has a naturally formed SiO_2 surface layer (~3 nm thick) which inhibits Si atom incorporation into Ag nanowires. For example, Au (MP 1064^{o}C) and Si (MP 1414^{o}C) forms eutectic whose MP can be as low as 370^{o}C, and Ag-Si eutectic also shows similar MP: this is not the case with Ag nanowires on stable oxide.

Possible origin may be PVP polymers tightly bound to the nanowire surface: catalytic behavior of PVP suggests a large binding energy of PVP, which will modulate the surface energy of Ag nanowires. Flexible C-C single-bond PVP backbone may induce a structural variation among tightly bound PVP's, leading to surface energy variation along a nanowire and among different nanowires.

In-plane Raman scattering by acoustic phonons in InAs/AlAs and Ge/Si quantum dot superlattices

Alexander G. Milekhin [1,2], Nikolay A. Yeryukov [1], Alexander I. Toropov [1], Alexander I. Nikiforov [1] and Dietrich R. T. Zahn [3]

[1] *A.V. Rzhanov Institute of Semiconductor Physics, pr. Lavrentieva 13, 630090, Novosibirsk, Russia*
[2] *Novosibirsk State University, Pirogov str. 2, 630090, Novosibirsk, Russia*
[2] *Semiconductor Physics, Chemnitz University of Technology, D- 09107 Chemnitz, Germany*

We present the results of micro-Raman scattering study of acoustic phonons of InAs/AlAs and Ge/Si quantum dot superlattices grown by molecular beam epitaxy in the Stranski-Krastanow growth mode on (001)-oriented GaAs and Si substrates, respectively. InAs/AlAs structures are composed of 20 periods of InAs QD layers with a nominal thickness of 2.8 monolayers separated by 6, 8, 10, and 13 nm of AlAs. The Ge/Si nanostructure consists of 10 Ge and Si layers with nominal thicknesses of 1.4 and 30 nm, respectively.

The micro-Raman scattering experiments were performed using a micro-Raman setup with the 514.5 nm line of an Ar^+ laser. The laser light with a spot size of 1 μm was focused either on a planar sample surface or a cleaved (110)-oriented sample edge.

Raman scattering from the planar surface and the cleaved (110)-oriented edge of the nanostructures was investigated. All possible doublets of folded longitudinal acoustic (FLA) phonons and a number of doublets of FLA phonons (up to 12th order) were observed in the Raman spectra of InAs/AlAs and Ge/Si nanostructures, respectively, measured in the z(x,x)-z scattering geometry (Fig.1). The energy positions of the FLA doublets are well described by the elastic continuum model of Rytov. The in-plane Raman scattering spectra measured in the y'(x',x')-y' geometry reveal the changing energy positions and intensities of the FLA doublet components which are consistent with changing the effective wave vector in the nanostructures induced by the momentum transfer of the light. The Raman selection rules for the FLA phonons with different symmetries in the both type of nanostructures are discussed.

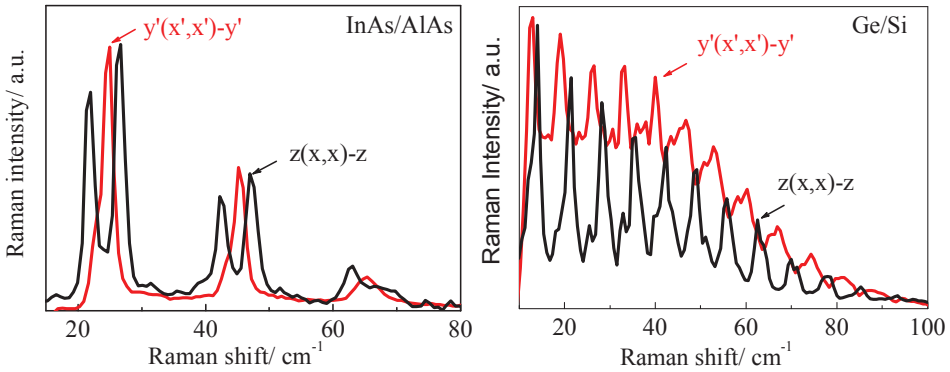

Fig.1 Raman spectra of InAs/AlAs and Ge/Si quantum dot superlattices measured in backscattering from the (100) and (110) planes (black and red curves, respectively).

Transconductance spectroscopy on self-assembled dots: Beyond the ensemble average

D. Zhou[1], A. Beckel[1], A. Kurzmann[1], A. D. Wieck[2], D. Reuter[2,3], M. Geller[1], and A. Lorke[1]

[1] *Faculty of Physics and CENIDE, University of Duisburg-Essen, Lotharstraße 1, 47057 Duisburg, Germany*

[2] *Chair for Applied Solid State Physics, Ruhr-Universität Bochum, Universitätsstraße 150, 44780 Bochum, Germany*

[3] *Department Physik, Universität Paderborn, 33098 Paderborn, Germany*

We have recently developed a so-called transconductance spectroscopy (TCS), which is an all-electrical preparation and probing method for non-equilibrium (excited) states in an ensemble of self-assembled quantum dots (QDs) [1,2]. We demonstrate here the scalability of the measurement technique down to about 100 QDs with the future vision of an all-electrical single dot measurement; a necessary requirement for preparation and control of quantum states in self-assembled QDs for quantum information processing.

The device is a high electron mobility transistor (HEMT) with an embedded layer of InAs QDs, separated by a tunneling barrier from a two-dimensional electron gas (2DEG). The 2DEG is used as a sensitive charge detector as well as a reservoir for electrons in the QD states. This device offers time-resolved charge detection via a transconductance measurement as well as ideal scaling properties. Therefore, electron beam lithography has been used to define a gated channel containing only $\sim$ 100 QDs, see Fig. 1(a). The equilibrium TCS of the present device shows enhanced energy resolutions in Fig. 1(b) with clear signatures of the s- and p-shell for the displayed blue line. Reducing gate pulse amplitude and source drain voltage further increases the resolution, allowing us to observe reproducible, sharp peaks that can be attributed to the many-particle states for smaller subsets within the QD ensemble, see red line in Fig. 1(b).

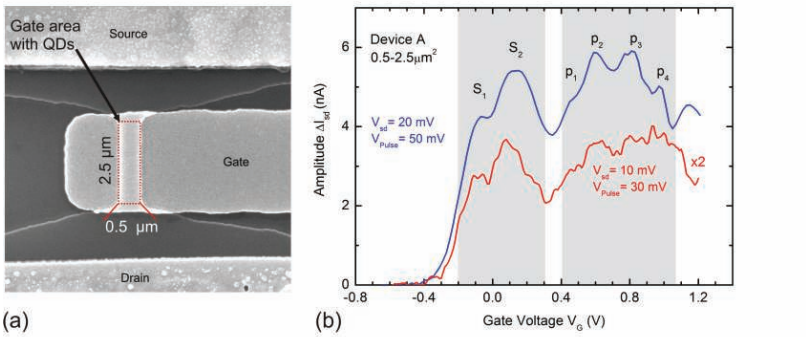

Figure 1: (a) HEMT device containing $\sim$100 QDs in the active gate region. (b) Transconductance spectroscopy of the device in (a), where the inhomogeneous broadening splits up into discrete lines of QD sub-ensembles.

[1] B. Marquardt et al., Nature Commun. **2**, 209 (2011).
[2] B. Marquardt et al., Appl. Phys. Lett. **95**, 22113, (2009).

ThP58

On the importance of in plane coupling within the ensemble of InAs/InGaAlAs/InP quantum dashes

K. Ryczko, G. Sęk and J. Misiewicz

Institute of Physics, Wroclaw University of Technology, 50-370 Wroclaw, Poland

Semiconductor quantum dashes can be fabricated in the InAs-InP material system by molecular epitaxy. They have been proven to be advantageous when employed as the active region of infrared photonic devices, especially when considering telecommunication and data communication applications, and have been demonstrated to be application relevant in lasers and optical amplifiers, as high gain, tunable or polarization insensitive emitters especially at fiber-based optoelectronics relevant wavelengths [1]. Furthermore, preliminary work on single quantum dashes [2-4] and their perspectives as emitters in quantum-electrodynamics-based experiments has recently been performed revealing possibility of realizing single photon sources at the telecommunication wavelengths. In all the cases, the electronic structure is discussed in the picture of independent dashes in spite of normally very high surface of these structures (even more than 10^{11} cm^{-2}) making the average in plane distances significantly smaller than the dash characteristic sizes. This makes possible an existence of finite and even efficient carrier tunneling between the dashes, which could significantly affect both the ensemble properties in the laser active region, as well as the subtle properties of single dashes, properties of which can appear to be dependent on that quantum mechanical coupling.

In this work, we discuss the electronic structure of the system composed of coupled InAs quantum-wire-like structures (the confinement in the longest dimension is neglected for simplicity) separated laterally by a thin barrier InGaAlAs barrier lattice matched to InP substrate. The respective confined states energy levels and the carrier probability densities are calculated within the k·p theory for different cross-sectional shapes and sizes of the dashes, and in function of the lateral distance between them. The results are confronted with the existing data on the optical transitions in such structures [5,6]. Eventually, it has been concluded that for realistic system parameters (geometry and spatial in-plane separation) the obtained direct coupling is indeed negligible and most of the applications the dashes can be considered individually and any carrier transfer is rather indirect, via e.g. the wetting layer states.

[1] J. P. Reithmaier, G. Eisenstein, and A. Forchel, Proc. of IEEE 95, 1779 (2007).
[2] G. Sęk, P. Podemski, A. Musiał, J. Misiewicz, S. Hein, S. Höfling, A. Forchel. J. Appl. Phys. 105(2009)086104.
[3] T. Mensing, L. Worschech, R. Schwertberger, J. P. Reithmaier, A. Forchel. Appl. Phys. Lett. 82(2003)2799.
[4] N. Chauvin, P. Nedel, C. Seassal, B. Ben Bakir, X. Letartre, M. Gendry, A. Fiore, P. Viktorovitch. Phys. Rev. B 80(2009)045315.
[5] W. Rudno-Rudzinski, R. Kudrawiec, P. Podemski, G. Sęk, J. Misiewicz, A. Somers, R. Schwertberger, J. P. Reithmaier, A. Forchel, *Appl. Phys. Lett.* 89, 031908-1-3 (2006).
[6] G. Sęk, P. Podemski, R. Kudrawiec, J. Misiewicz, A. Somers, S. Hein, S. Höfling, J. P. Reithmaier, A. Forchel, Proc. SPIE 6481, 64810F (2007).

Biexciton-exciton radiative cascade in single InAs/InGaAlAs/InP quantum dashes emitting near 1.55 μm

Ł. Dusanowski[1], W. Rudno-Rudziński[1], M. Syperek[1], G. Sęk[1], J. Misiewicz[1]
S. Hein[2], S. Höfling[2] and A. Forchel[2]
[1]*Institute of Physics, Wrocław University of Technology, Wybrzeże Wyspiańskiego 27, 50-370 Wrocław, Poland*
[2] *Technische Physik, Physikalisches Institut & Wilhelm-Conrad-Röntgen-Research Center for Complex Material Systems, University of Würzburg, Am Hubland, D-97074 Würzburg, Germany*

At the cross point between quantum information processing and fiber-based optical communication technologies there emerges the necessity of developing new devices, with specific requirements. Especially interesting could be a true single photon source or a quantum repeater operating in the spectral range near 1.55 μm, allowing the transport of quantum coded information over long distances. It has been well established that a self-assembled semiconductor quantum dot (QD), thanks to its properties, can constitute the key element of the above mentioned devices [1]. However, it is still a challenge to achieve single photon QD emission at 1.55 μm. In this respect the real alternative can be a self-assembled InAs/InGaAlAs quantum dash (QDash) grown on InP substrate. Although some of the emission properties of single QDashes have already been studied [2], the exciton and biexciton dynamics and the characteristic time of the biexciton-exciton cascade evolution in such structures are still unknown.

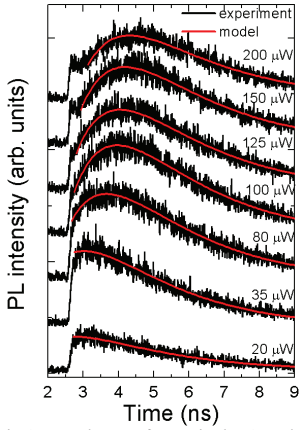

Fig.1. PL decays from single QDash at excitation powers ranging from 20 to 200 μW (black solid line) and modeled X recombination decay in XX-X radiative cascade (red solid line) assuming τ_X=2.4 ns τ_{XX}=1.2 ns.

In this work we present experimental and theoretical studies focused on the exciton (X) and bi-exciton (XX) kinetics in single, self-assembled InAs/$In_{0.53}Ga_{0.23}Al_{0.24}As$ QDashes. The X and XX kinetics have been measured in the time-resolved micro-PL (TRμPL) experiment at T=4.2 K, utilizing the time-correlated single photon counting technique. The key element of the setup was fast (50 ps) and low dark count (<10 c/s) superconducting NbN single photon detector. The analysis of the TRμPL traces allows determining the X and XX decay time constants of 2.4±0.2 ns, and 1.2±0.2 ns, respectively. It shows clearly, that in spite of a high QDash spatial asymmetry, which should lead to the weakening of the confinement regime, the X to XX lifetimes ratio can be very similar to that observed for QD structures being in the strong confinement limit. In order to obtain more insight into the X-XX cascade emission process, the excitation power dependent TRμPL experiment has also been performed. The time evolution of the X emission demonstrates characteristic slowdown of its initial relaxation with the excitation power density. This process is controlled either via the relaxation from QDash higher confined states or the internal XX-X cascade relaxation. The latter one has been confirmed by applying the two level rate equation model, which directly reproduced the experimental data (see Fig. 1).

[1] S. M. Ulrich et al., Phys. Rev. Lett. **98**, 043906 (2007).
[2] N. Chauvin et al., Phys. Rev. B **80**,0 45315 (2009).

Type II heterostructures based on narrow-gap InAs-rich compounds

K. Moiseev [1], E. Ivanov [1], M. Motyka [2], F. Janiak [2], J. Misiewicz [2]

[1] *Ioffe Institute, Politekhnicheskaya 26, 194021 St Petersburg, Russia*
[2] *Institute of Physics, Wrocław University of Technology, Wybrzeze Wyspianskiego 27, 50-370 Wrocław, Poland*

Type II heterostructures in InAs-based solid solution systems have been intensively studied in recent years as promising candidates for the design of optoelectronic devices operating in the mid-infrared spectral range (3-5 μm). Asymmetric band-offsets at the type II heterointerface leads to formation of potential barriers for both electrons and holes simultaneously. Strong accumulation and effective confinement of the spatially separated electrons and holes in self-consistent quantum wells near the heteroboundary result in unusual optical and electrical properties of the heterostructures. Due to carriers' quantization interface (tunneling-assisted) radiative transitions exhibited high-temperature performance. However, there is a very important parameter, which must be taken into account in designing the laser structures based on narrow-gap compounds, is the spin-orbit splitting in the valence band. The resonance between the split-off valence bands and the energy of the emitted photons results in a significant increase of the Auger recombination rate and enhanced intervalence band absorption, which deteriorates the luminescent characteristics of the infrared emitters operating at the 3-5 μm.

We present temperature and compositional dependences of photoluminescence (PL) and photoreflectance (PR) spectra connected to the energy gap and the spin-orbit split off transition in $InGa_xAsSb_y/Ga_{0.84}In_{0.16}As_{0.22}Sb_{0.78}/InAs$ heterostructures [1]. The spin-orbit splitting compositional dependence for the GaInAsSb alloys system has been recognized as a nonlinear with the negative bowing parameter $C(\Delta_0)$=-0.25 eV. There are two points of the quaternary alloy compositions ($InGa_{0.03}AsSb_{0.06}$ and $InGa_{0.93}AsSb_{0.87}$) for which a resonance condition ($E_0 = \Delta_0$) can be realized at 77 K.

The quaternary solid solutions in the Ga-In-As-Sb and In-As-Sb-P systems can form type II heterojunctions with both staggered and broken-gap alignment. It was established that InAsSbP/InAs heterostructure is a type II staggered heterojunction in the whole composition range of the pseudomorphic InAsSbP epilayer. Intense interface electroluminescence in the type II staggered p-InAs/p-InAsSbP heterojunction was observed at T=300 K [2]. Transition from staggered to broken-gap alignment in type II heterostructures formed by the quaternary GaInAsSb alloys was demonstrated [3]. Suppression of the non-radiative recombination and enhancement of the interface luminescence was demonstrated in a type II broken-gap InAs/Ga(In)AsSb heterojunction [4].

This work was performed in framework of the programs of General Physics Division of RAS and was in part supported by Russian Basic Researches Foundation (grant #11-02-00234). In addition, M.M. would like to also acknowledge the Ministry of Science and Higher Education for financial support from the Iuventus Plus program.

[1] M. Motyka, F. Janiak, G. Sęk, J. Misiewicz, K.D. Moiseev, Appl. Phys. Lett. **100**, 211906 (2012).
[2] M.M. Grigoryev, P.A. Alekseev, E.V. Ivanov, K.D. Moiseev, Semicond. **47**, 28 (2013).
[3] M.P. Mikhailova, K.D. Moiseev, T.I. Voronina, T.S. Lagunova, Yu.P. Yakovlev, Semicond. **41**, 161 (2007).
[4] K.D. Moiseev, A. Krier, M.P. Mikhailova, Yu.P. Yakovlev, J. Phys. D: Appl. Phys. **35**, 631 (2002).

Integration of single site-controlled InAs quanum dots, fabricated by nanoimprint lithography and molecular beam epitaxy, into optical micropillar cavities

A. Schramm*[,1], J. Tommila[1], T. V. Hakkarainen[1], E. Heinonen[2], M. Dumitrescu[1], and M. Guina[1]

[1] *Optoelectronics Research Centre, Tampere University of Technology, P.O. Box 692, FIN-33101, Tampere, Finland*
[2] *Center of Microscopy and Nanotechnology, University of Oulu, P.O. Box 7150, FIN-90014, Oulu, Finland*

Single, coherently strained InAs quantum dots (QDs) are promising candidates for building blocks in novel information processing applications. The optical properties of QDs, e.g. the widely tunable wavelength range, the narrow emission linewidth, the ability to emit single photons on demand and the tuning of carrier spins in QDs show great promises for novel devices. In order to use the advantageous optical opportunities for single QD devices it would be beneficial to have control over the lateral position of individual QDs. This can be achieved by defining the nucleation sites by patterning substrates prior the QD deposition.

Here we present our recent developments in deterministic integration of single site-controlled InAs QDs into optical micropillar cavities (inset in Fig. 1(b)). We used a combination of UV-nanoimprint lithography (NIL) and molecular beam epitaxy (MBE) for creating large arrays of widely spaced QDs [1-3]. Figure 1(a) shows a scanning electron microscopy (SEM) image of single site-controlled QDs with a period of 2.5 μm. Figure 2(b) shows exciton emission spectra (red curve) tuned into resonance with the cavity mode (blue curve) via changing the temperature. We observed the crossing of the exciton and the cavity mode and an increase in the PL intensity as an indication of QD-cavity coupling.

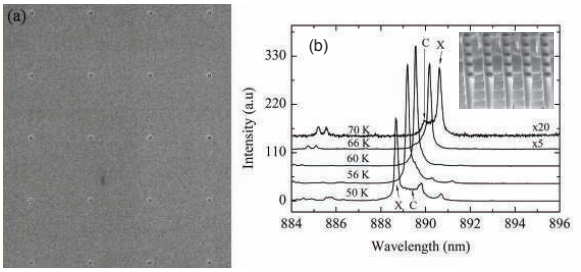

Fig. 1(a) shows single site-controlled InAs QDs with a period of 2.5 μm. (b) Temperature dependent micro-PL spectra of a single site-controlled QD embedded in an optical micropillar cavity. Exciton and cavity mode are denoted by X and C, respectively. The inset shows a SEM image of micropillars with diameters of 1 μm.

[1] J. Tommila, A. Tukiainen, J. Viheriälä, A. Schramm, T. V. Hakkarainen, A. Aho, P. Stenberg, M. Dumitrescu, and M. Guina, J. Crystal Growth 323, 183 (2010).
[2] A. Schramm, J. Tommila, C. Strelow, T. V. Hakkarainen, A. Tukiainen, M. Dumitrescu, A. Mews, T. Kipp, and M. Guina, Nanotechnology 23, 175701 (2012).
[3] J. Tommila, Ch. Strelow, A. Schramm, T. V. Hakkarainen, M. Dumitrescu, T. Kipp and M. Guina, Nanoscale Res. Lett. 7, 313 (2012).

*andreas.schramm@tut.fi

High-Q resonance peak observed from metal-embedded InAs/GaAs quantum dot nano-cavity

N. Ishihra[1], R. Takemoto[1], N. A. Jahan[1], H. Nakajima[1], M. Jo[2], T. Mano[2], H. Kumano[1], I. Suemune[1]

[1] Research Institute for Electronic Science, Hokkaido University, Sapporo 001-0021 Japan
[2] Photonic Materials Unit, National Institute for Materials Science, Tsukuba 305-0047 Japan

Interactions of semiconductor nanostructures with optical microcavites are one of the present most active research areas. Distributed Bragg reflector (DBR) microcavity pillars and photonic crystal nanocavities have been extensively studied. Metal-embedded structures have attractive features to tightly confine optical fields to nano-area and have been actively studied for nano-lasers, nano-cavities, and plasmonic effects. However, the resonance Q values reported have remained low due to the optical absorption associated with metals.

In this paper, we demonstrate the observation of high-Q cavity resonance mode from semiconductor pillar embedded with metal (SPEM) shown in Fig. 1. In this structure photo-excitation and photon extraction is limited to the surface area and efficient optical coupling is possible (recently we observed the photon collection efficiency of ~20%). One of the prepared structures is shown in Fig. 2. The silver (Ag) surface and the interface with the GaAs nanostructure is covered with SiO_2. The GaAs nanostructure includes InAs quantum dots (QDs) inside. One of the observed photoluminescence (PL) spectra is shown in the inset of Fig. 3. The temperature dependence of the PL peak is compared with that of GaAs energy gap by energy-shifting the well-known Varshni equation. The extremely weak temperature dependence demonstrates that this is the cavity resonance mode feeded from InAs QD emission. The observed Q value of ~7000 is the largest ever reported with the SPEM structures. This explores the high new possibilities for electrons interact with highly confined photonic fields in nano-PEM structures.

This work was supported in part by the SCOPE from the MIAC and Nano-macro materials, devices and systems alliance.

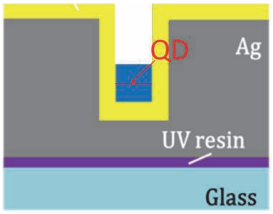

Fig. 1. Schematic of SPEM structure with InAs/GaAs QDs.

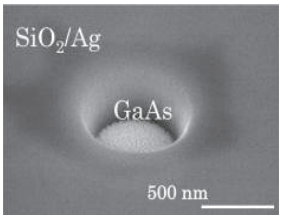

Fig. 2. One of fabricated structures observed with SEM.

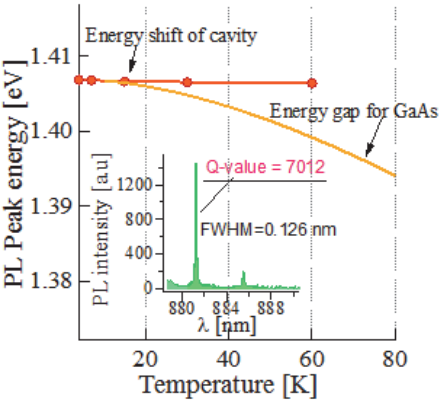

Fig. 3. Temperature dependence of PL peak energy. The observed peak (red) is much less temperature dependent. GaAs energy gap energy-shifted with the Varshni relation is shown in comparison (orange line).

Type II InSb quantum dots in narrow-gap InAs(Sb,P) matrix: structural, electrical and luminescent properties

Ya. Parkhomenko, V. Romanov, P. Dement'ev, N. Nevedomsky, N. Bert, E. Ivanov, K. Moiseev

Ioffe Institute, Politekhnicheskaya 26, 194021 St Petersburg, Russia

We report on study of structural, transport and optical properties of narrow-gap type II heterostructures with InSb quantum dots (QDs) inserted into the InAs-based matrix. The samples with InSb QDs were grown on the (100)-orientated surface by both liquid phase epitaxy and metal-organic vapour phase epitaxy. The self-assembled InSb QDs were obtained under Stranski-Krastanow growth mode. The high density ($2*10^{10}$ cm^{-2}) uniform QDs with dimensions of 3 nm in height and 14 nm in diameter were found to be dislocation-free without any extended defects. Structural parameters of the InSb QDs such as size, shape and internal strain will be demonstrated and discussed. Technological conditions, where transition between two mechanisms of QDs formation (Volmer-Weber and Stranski-Krastanow) can be realised, will be considered.

Use of the multicomponent In-As-Sb-P solid solutions lattice-matched with InAs substrate as matrix layers leads to a considerable change of the surface chemistry of a matrix material and allows controlling size distribution and sheet density of the InSb QDs deposed. High-resolution TEM cross-section images of the free-standing InSb QDs and ones buried into the InAs(Sb,P) matrix were obtained for the first time.

Local I-V characteristics of the single InSb QD situated on the InAs-rich surface were studied by scanning probe microscopy at room temperature to investigate tunnelling carrier transport through the confined states. Intense positive and negative electroluminescence (EL) for the mesa-diode heterostructures with the InSb QDs was found in the spectral range 3-4 μm at temperatures 77-300 K. Evolution of the EL spectra in dependence on applied external bias was observed. The energy band diagram of the InSb/InAs(Sb,P) heterostructure with a type II quantum dot at the heterointerface will be proposed.

This work was performed in framework of the programs of General Physics Division of RAS and was in part supported by Russian Basic Researches Foundation (grant #11-02-00234).

ThP64

Hyperfine interaction induced dephasing of coupled spin qubits in semiconductor double quantum dots

Jo-Tzu Hung[1], Łukasz Cywiński[2] Xuedong Hu[1], and S. Das Sarma[3]

[1] *Department of Physics, University at Buffalo, SUNY, Buffalo, New York 14260-1500, USA*

[2] *Institute of Physics, Polish Academy of Sciences, al. Lotników 32/46, PL 02-668 Warszawa, Poland*

[3] *Condensed Matter Theory Center, Department of Physics, University of Maryland, College Park, MD 20742-4111, USA*

We investigate theoretically the hyperfine (hf) induced dephasing of two-electron-spin states in a double quantum dot (DQD) with a finite singlet-triplet splitting J. In particular, we derive an effective pure dephasing Hamiltonian, which is valid when the hf-induced mixing is suppressed due to the relatively large J and the external magnetic field. Using both a quantum theory based on resummation of ring diagrams [1] and semiclassical methods, we identify the dominant dephasing processes in regimes defined by values of the external magnetic field, singlet-triplet splitting J, and inhomogeneity in the total effective magnetic field. We address both free induction and Hahn echo decay of superposition of singlet and unpolarized triplet states (both cases are relevant for S-T_0 qubits realized in DQDs), and we also study hf-induced exchange gate errors for two single-spin qubits. Theoretical results relevant for recent experiments in GaAs [3] and InGaAs [4], as well as predictions for silicon-based quantum dots are presented [2].

For the S-T_0 qubit we find that in the absence of a magnetic field gradient across the DQD, inhomogeneous broadening for an S-T_0 qubit is significantly suppressed relative to a single spin qubit, with the most significant source of inhomogeneous broadening being the term proportional to the square of the fluctuations of the longitudinal Overhauser field difference between the dots. Another important decoherence channel is due to the dressing of the singlet state by the polarized triplets due to transverse Overhauser fields. Throughout a wide range of parameters, these two terms compete for the role of the dominant source of decoherence, leading to a non-monotonic dependence of the T_2 dephasing time on J. On the other hand, in the presence of the field gradient the two-spin eigenstates are now superpositions of the S and T_0 states, and there is a finite electron spin polarization in each of the two quantum dots. Random longitudinal Overhauser field difference can now cause dephasing between the two-spin eigenstates, in analogy to inhomogeneous broadening in a single spin qubit - the S-T_0 encoding acquires more of a single-spin-qubit decoherence characteristics as the singlet-triplet mixing increases. This increased hf-induced dephasing is the price that one has to pay for having two-axis control (with the x axis rotations provided by the field gradient) over the S-T_0 qubit.

[1] Ł. Cywiński, W.M. Witzel, and S. Das Sarma, Phys. Rev. Lett. **102**, 057601 (2009); Phys. Rev. B **79**, 245314 (2009).

[2] J.-T. Hung, Ł. Cywiński, X. Hu, and S. Das Sarma, preprint arXiv:1304.6711.

[3] O.E. Dial, M.D. Shulman, S.P. Harvey, H. Bluhm, V. Umansky, and A. Yacoby, Phys. Rev. Lett. **110**, 146804 (2013).

[4] K.M. Weiss, J.M. Elzerman, Y.L. Delley, J. Miguel-Sanchez, and A. Imamoğlu, Phys. Rev. Lett. **109**, 107401 (2012)

Direct measurement of the valley splitting in a few-electron silicon quantum dot using charge sensor source-drain bias spectroscopy

Kosuke Horibe [1], Tetsuo Kodera [1,2,3] and Shunri Oda [1]

[1] *Quantum Nanoelectronics Research Center, Tokyo Institute of Technology*
[2] *Institute for Nano Quantum Information Electronics, the University of Tokyo*
[3] *PRESTO, Japan Science and Technology Agency (JST)*

One of the important topics for silicon based qubits is the investigation of the valley degeneracy [1], such as the valley splitting and physics of electron transition between the different valleys. In this work, we measured directly the valley splitting in a few-electron silicon QD using charge sensor source-drain bias spectroscopy at 300 mK.

We fabricated a double QD (DQD) and a charge sensor (CS) QD in a metal-oxide-semiconductor structure on a non-doped silicon-on-insulator substrate (Figure 1(a)). Few-electron occupancy states in the DQD are detected by measuring the transconductance dI_{CS}/dV_{SG2} of the CS (Figure 1(b)). Figure 1(d) shows the plot of dI_{CS}/dV_{SG2} as functions of the side gate voltage V_{SG2} and the source-drain bias voltage V_{DCS} on the CS. We observed two transition lines between the (0, 1) region and the (0, 2) region; the left and right lines in the Fig. 1(d) correspond to the lower and higher energy Γ valley on the conduction band in the right QD of the DQD in Fig. 1(a), respectively. When V_{DCS} is higher than 3.5 mV, the right side line appears because of the increase in the excitation rate Γ_3 of electrons from the lower energy valley to the higher energy valley (Figure 1(c)). This excitation is ascribed to the dissipated energy generated by the electrons which transport through the CS. We obtained the valley splitting $E_{VS} \approx 0.33$ meV.

This work was financially supported by KAKENHI (22246040, 24102703), JST-PRESTO, Yazaki Memorial Foundation for Science and Technology, and Project for Developing Innovation Systems of the Ministry of Education, Culture, Sports, Science and Technology (MEXT) and Global COE Program, "Photonics Integration-Core Electronics", MEXT, Japan.

[1] M. A. Eriksson *et al.*, Quantum Inf. Process. **3**, 133 (2004).

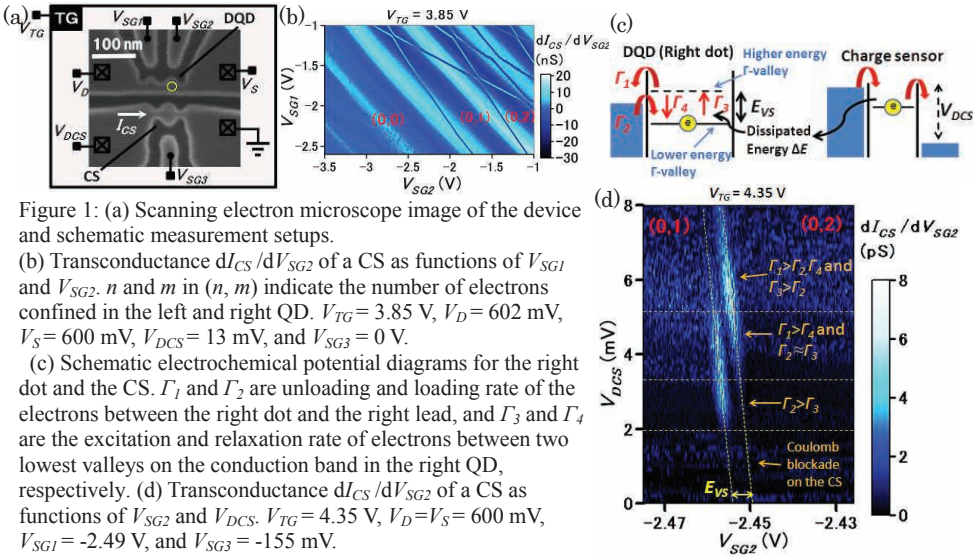

Figure 1: (a) Scanning electron microscope image of the device and schematic measurement setups.
(b) Transconductance dI_{CS}/dV_{SG2} of a CS as functions of V_{SG1} and V_{SG2}. n and m in (n, m) indicate the number of electrons confined in the left and right QD. $V_{TG} = 3.85$ V, $V_D = 602$ mV, $V_S = 600$ mV, $V_{DCS} = 13$ mV, and $V_{SG3} = 0$ V.
(c) Schematic electrochemical potential diagrams for the right dot and the CS. Γ_1 and Γ_2 are unloading and loading rate of the electrons between the right dot and the right lead, and Γ_3 and Γ_4 are the excitation and relaxation rate of electrons between two lowest valleys on the conduction band in the right QD, respectively. (d) Transconductance dI_{CS}/dV_{SG2} of a CS as functions of V_{SG2} and V_{DCS}. $V_{TG} = 4.35$ V, $V_D = V_S = 600$ mV, $V_{SG1} = -2.49$ V, and $V_{SG3} = -155$ mV.

Single Hole Transistor in a Conventional Silicon Metal-Oxide-Semiconductor Structure

R. Li[1], F. E. Hudson[2,3], A. S. Dzurak[2,3], and A. R. Hamilton[1]

[1] *School of Physics, University of New South Wales, Sydney NSW 2052, Australia*
[2] *Australian National Fabrication Facility, University of New South Wales, Sydney NSW 2052, Australia*
[3] *Centre of Excellence for Quantum Computation and Communication Technology, School of Electrical Engineering and Telecommunications, University of New South Wales, Sydney NSW 2052, Australia*

Over the past 15 years much effort has gone into the development and study of electron quantum dots as artificial atoms, ultra-sensitive electrometers, and quantum bits for quantum information applications. To operate as a spin qubit requires a long spin coherence time T_2, which in GaAs and standard Si is limited by the hyperfine interaction between the electron spin and nuclei in the host crystal. Recently hole quantum dots have attracted significant interest since the strong spin-orbit coupling allows all electrical spin manipulation, while the hyperfine interaction is significantly reduced by the lack of overlap between the p-wave hole orbitals and the nuclear spins, promising longer T_2 times [1]. However to date there have been few studies of holes in gate defined quantum dots [2, 3].

In this work, we report the first study of a planar silicon metal-oxide-semiconductor based single hole transistor. The device was fabricated using standard silicon processing techniques on a silicon substrate with a 5.9 nm gate-oxide. Electron beam lithography was used to define multilayer gates separated by AlO_X [4], shown schematically in Fig.1 (a). The $\sim 40 \times 40$ nm^2 dot is formed underneath plunger gate P1. Fig. 1 (b) shows the conductance as a function of gate bias on P1 taken in a dilution fridge, with clear Coulomb Blockade oscillations demonstrating the operation of the single hole transistor. Fig. 1 (c) shows the Coulomb diamonds obtained in source-drain bias spectroscopy measurements. As V_{P1} is made more positive the diamonds open up and the charging energy increases to ∼10 meV, suggesting that we are approaching the last few holes in the dot. Excited states could be resolved, which confirms that the device is in the few hole regime. A second hole dot could be induced by changing the bias on gate P2, with the charge stability diagram showing coupling between the two dots.

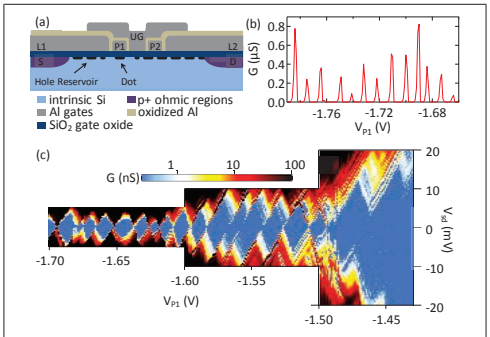

Figure 1: (a) Schematic cross section of the device, showing the hole dot under gate P1. (b) Conductance trace shows periodic Coulomb blockade oscillations. (c) Source-drain biasing shows Coulomb diamonds down to the last few holes, with excited states visible.

[1] G. Burkard, Nat. Mater. **7**, 100 (2008).
[2] F. A. Zwanenburg *et al.*, Nano Lett. **9**, 1071 (2009).
[3] O. Klochan *et al.* Appl. Phys. Lett. **96**, 092103 (2010).
[4] S. J. Angus *et al.* Nano Letters **7**, 2051 (2007).

Few-electron silicon single and double quantum dots fabricated in a metal-oxide-semiconductor structure

Tetsuo Kodera [1,2,3], Kosuke Horibe [1], Yasuhiko Arakawa [2,4] and Shunri Oda [1]

[1] *Quantum Nanoelectronics Research Center, Tokyo Institute of Technology*
[2] *Institute for Nano Quantum Information Electronics, the University of Tokyo*
[3] *PRESTO, Japan Science and Technology Agency (JST)*
[4] *Institute of Industrial Science, the University of Tokyo*

Confining a single electron in a quantum dot (QD) is important for realizing electron spin qubits. However, it is still challenging for silicon because of the relatively large effective mass m^* of electrons and their small tunneling rates in silicon. We successfully realize confining a single electron in a lithographically-defined silicon QD.

We fabricate silicon QD devices in a metal-oxide-semiconductor (MOS) structure on a silicon-on-insulator substrate. Figure 1(a) and (b) show scanning electron microscope (SEM) images of single QD (SQD) and double QD (DQD) devices. Charge sensors, SCS and DSC, are fabricated near SQD and DQD, respectively. By applying a top gate voltage V_{TG} to the poly-Si top gate (TG) (not shown) formed on the SiO_2 gate insulator, a two dimensional electron gas (2DEG) is induced in the SOI layer near the Si/SiO_2 interface.

Changes in number of electrons in SQD and DQD are detected by measuring abrupt changes in the current I_{SCS} and I_{DCS} which flow through SCS and DCS as shown in Fig.1 (c) and (d), respectively. In lower left region of Fig. 1(c) and (d), there are no lines of transition of electrons in the QDs, which indicates that we successfully obtain the pinch-off of both SQD and DQD devices.

This work was financially supported by KAKENHI (22246040, 24102703), JST-PRESTO, Yazaki Memorial Foundation for Science and Technology, and Project for Developing Innovation Systems of the Ministry of Education, Culture, Sports, Science and Technology (MEXT).

[1] G. Yamahata, T. Kodera, H. O. H. Churchill, K. Uchida, C. M. Marcus, and S. Oda Phys. Rev. B **86**, 115322 (2012).
[2] K. Horibe, T. Kodera, T. Kambara, K. Uchida, and S. Oda, J. Appl. Phys. **111**, 093715 (2012).

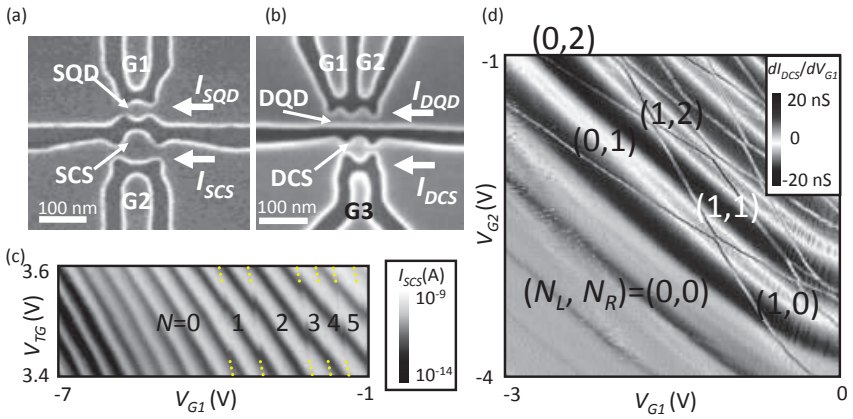

Figure 1 (a,b) SEM images of SQD and DQD devices before formation of top gate. (c) Current I_{SCS} through a charge sensor in the plane of V_{TG} and V_{G1}. The number of electron N in SQD is indicated. (d) Contour plot of dI_{DCS}/dV_{G1} as functions of V_{G1} and V_{G2}. The number of electron (N_L, N_R) in each QD of DQD is indicated.

Time resolved study of magnetic fluctuations in CdTe/ZnTe quantum dots containing a few Mn^{2+} ions.

Maciej Koperski [1], Mateusz Goryca [1], Filip Malinowski [1], Tomasz Smoleński [1], Andrzej Golnik [1], Piotr Wojnar [2] and Piotr Kossacki [1]

[1] *Institute of Experimental Physics, Faculty of Physics, University of Warsaw, Poland*
[2] *Institute of Physics, Polish Academy of Sciences, Warsaw, Poland*

CdTe/ZnTe quantum dots doped with Mn^{2+} ions have been shown to be an interesting system to study various spin related phenomena. For example, in extremely diluted case with only one Mn^{2+} ion in the dot, the possibility to optically write and read-out the spin state of the magnetic impurity has been demonstrated [1,2]. For quantum dots with higher concentration of Mn^{2+} ions (about 50 ions or more per dot) the time resolved measurements revealed the formation of magnetic polaron [3].

Here we explore the system of a quantum dot containing a few magnetic ions. In nonmagnetic quantum dots the recombination of neutral exciton gives rise to a single sharp line in the photoluminescence (PL) spectrum, which spectral width equals to about 300μeV. In the presence of a single Mn^{2+} ion in the dot the anisotropy of the heavy hole and exchange interaction with the Mn^{2+} spin causes the sixfold splitting of the neutral exciton PL line. In the case of dots with a few Mn^{2+} ions, the individual PL lines, which correspond to different spin states of Mn^{2+} ions cannot be spectrally resolved. The neutral exciton recombination forms a broad feature with the width of about 2 meV (*figure **(a)***). The PL signal monitored at different values of emission energy corresponds to different averaged spin projections of Mn^{2+} system on the growth axis, parallel to the direction of exciton (heavy hole) anisotropy. We employ the time-resolved single photon correlation technique to study the magnetization fluctuations of the Mn^{2+} spin system at different values of external magnetic field.

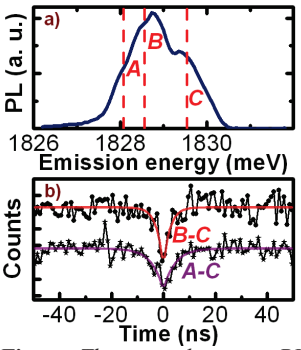

Figure. *The neutral exciton PL line of a quantum dot containing a few Mn^{2+} ions (a) and the exemplary correlation functions measured for 3 chosen values of emission energy (b).*

The samples were grown by MBE technique. The PL measurements were done in μPL setup equipped with seven avalanche photodiodes, which detected photons dispersed by the spectrometer. Therefore we could simultaneously, under the same experimental conditions, measure the correlations between photons emitted at 7 different wavelengths corresponding to 7 configurations of Mn^{2+} ions spins.

The characteristic time of the magnetization fluctuations derived from antibunching in the correlation functions was determined as a function of energetic distance between the diodes. We have established that this time increases with the greater energetic mismatch between analyzed states (*figure **(b)***). For a given energy difference the application of external magnetic field causes the slowdown of the magnetization dynamics. At the field of 4T the reconfiguration times were an order of magnitude larger than those obtained without the external magnetic field.

[1] C. Le Gall, *et al.*, Phys. Rev. Lett. **102**, 127402 (2009).
[2] M. Goryca, *et al.*, Phys. Rev. Lett. **103**, 087401 (2009).
[3] Ł. Kłopotowski, *et al.*, Phys. Rev. B **83**, 081306(R) (2011).

Kondo Correlations in Optical Spectrum of Electrons Confined in Quantum Dots Doped with Single Mn Spin

Udson C. Mendes [1,2], Marek J. Korkusinski [1], Anna H. Trojnar [1,3], and Pawel Hawrylak [1,3]

[1] *Quantum Theory Group, Security and Disruptive Technologies, National Research Council, Ottawa, Canada*
[2] *Institute of Physics "Gleb Wataghin", State University of Campinas, Campinas-SP, Brazil*
[3] *Department of Physics, University of Ottawa, Ottawa, Canada*

Kondo effect is one of the non-perturbative effects in condensed matter physics. Most theory of Kondo effect describes non-interacting electrons occupying states directly interacting with a magnetic impurity (MI) while those electrons of the Fermi sea that do not interact with the MI are neglected. Recent fabrication of quantum dots (QDs) doped with single magnetic Mn impurity and with controlled number of electrons opens the opportunity to investigate analogs of Kondo effect in finite interacting electron system.

In parabolic quantum dots doped with a single Mn ion in its centre only electrons that occupy zero angular momentum orbitals are directly coupled with Mn spin and those electrons in orbitals with finite angular momentum are not coupled with Mn spin. Therefore, these QDs are perfect candidates to investigate both the role of electron-electron interactions (e-e) and the role of electrons in angular momentum channels that are not directly coupled with Mn spin on the Kondo-like physics.

We present here a microscopic model of N-interacting electrons confined in a CdTe QD doped with a single Mn impurity. The Hamiltonian is composed of a kinetic energy, e-e Coulomb interactions, and electron-Mn exchange interaction (e-Mn). The e-Mn contact exchange interaction is described by a Heisenberg Hamiltonian [1]. The QD electron single particle states are treated in the effective-mass approximation as states of a two-dimensional harmonic oscillator. The Hamiltonian matrix is constructed in the space of N electron configurations and M states of the MI. Using exact diagonalization techniques we calculate the eigenvalues and eigenvectors of our many-body Hamiltonian.

Here we show our results for a QD containing up to six electrons and Mn in the QD centre as function of a number of confined shells and e-e interaction. We observe that by changing the number of shells one can tune exchange interaction between electrons and Mn, from ferromagnetic to antiferromagnetic or zero. More importantly, we find an effective e-e mediated interaction between spins of electrons in finite angular momentum orbitals with spins of Mn ions. This indirect exchange interaction modifies Kondo interactions in the interacting electrons system.

To extract Kondo correlations in interacting electron system, we add an exciton to N electrons plus Mn, and calculate its photoluminescence spectrum (PL) as described in Ref. [2]. Here we present the PL spectrum for the X^{3-} +Mn complex, i.e, four electrons and a hole in the initial state of the emission, for a QD containing three shells. We show how indirect exchange interaction between electrons and Mn can be detected in PL spectrum.

[1] F. Qu and P. Hawrylak, Phys. Rev. Lett. **95**, 217206 (2005).
[2] A. Wojs and P. Hawrylak, Phys. Rev. B **55**, 13066 (1997).

ThP70

Signatures of exciton spin relaxation in photoluminescence spectra of semimagnetic quantum dots

Ł. Kłopotowski[1], V. Voliotis[2], Ł. Cywiński[1], P. Wojnar[1], M. Szymura[1], K. Fronc[1], T. Kazimierczuk[3], A. Golnik[3], R. Grousson[2], G. Karczewski[1], and T. Wojtowicz[1]

[1] *Institute of Physics, Polish Academy of Sciences, Warsaw, Poland*
[2] *Institut des NanoSciences de Paris, Université Pierre et Marie Curie, CNRS, France*
[3] *Faculty of Physics, University of Warsaw, Warsaw, Poland*

In this report, we present experimental and theoretical investigations of photoluminescence (PL) spectra of $Cd_{1-x}Mn_xTe$ quantum dots (QDs). We show that reaching thermal equilibrium in the system of the Mn ions and the exciton involves an intermediate stage, in which the exciton spin is relaxed, while the Mn ion spins are not. This stage gives rise to a specific, asymmetric PL lineshape. We develop a theoretical model for the PL spectrum, compare its results with the experiment, and find excellent agreement.

Semimagnetic QDs are an ideal system for investigations of semiconductor magnetism on the nanoscale. In particular, the dot magnetization can be formed without an external magnetic field, purely as a result of the exchange field that the exciton inposes on the Mn ions. From the point of view of potential applications, it is important to establish and tailor the formation dynamics of this magnetization. It has been shown[1, 2] that its development is accompanied by a redshift of the exciton transition energy. Indeed, the driving force for the ordering of the paramagnetic Mn spins is minimization of the exchange interaction between the exciton and the Mn ions. Magnetization formation is thus directly linked to establishing of the thermal equilibrium in this system. Moreover, it was shown [2] that the exciton spin relaxation occurs before the equilibrium is reached.

In this work, we show that the PL line shape is a tool sensitive to the degree of equilibration in the exciton – Mn ion system. In time-resolved PL measurements we directly demonstrate the transition between the relaxation stages: from a totally unrelaxed system, via exciton spin relaxation, to establishing of full equilibrium and forming the magnetization. We show that the equilibration dynamics critically depends on the concentration of Mn ions x. We study a set of samples with x ranging from 1% to 20%. We investigate PL spectra dependence on magnetic field and temperature and pinpoint features related to particular stages of magnetization formation. In particular, we find that exciton spin relaxation leads to a characteristically asymmetric PL spectrum and its narrowing by a factor reaching 2 and dependent on magnetic field and temperature.

The number of Mn ions in the studied dots ranges from about 20 to a few hundred. We thus model the PL lineshape treating the Mn ion spin as a classical variable. It allows us to develop analytical expressions for the PL spectra at each of the relaxation stages. Fitting of the model spectra allows us to extract from the PL measurements the exciton localization volume and the number and temperature of the Mn ions.

[1] J. Seufert *et al.*, Phys. Rev. Lett. **88**, 027402 (2001).
[2] Ł. Kłopotowski *et al.*, Phys. Rev. B **83**, 081306 (2011).

Scaling of the Kondo zero bias peak in a hole quantum dot at finite temperature

O. Klochan[1], A. Micolich[1], A. Hamilton[1], D. Reuter[2], A. Wieck[2], F. Reininghaus[3], M. Pletyukhov[3], H. Schoeller[3]

[1] *School of Physics, University of New South Wales, Sydney NSW 2052, Australia*
[2] *Angewandte Festkörperphysik, Ruhr-Universität Bochum, D-44780 Bochum, Germany*
[3] *Institut für Theorie der Statistischen Physik and JARA - Fundamentals of Future Information Technology, RWTH Aachen, 52056 Aachen, Germany*

The Kondo effect is a classic example of the importance of electron-electron interactions in solids, and has been extensively studied in quantum dots [1]. The strength of these interactions is characterized by a single parameter - the Kondo temperature T_K. The usual method for measuring T_K in a quantum dot is to study the temperature dependence of the conductance and compare to theory with T_K as a fitting parameter [2]. Recently a much simpler technique has become available based on analyzing the differential conductance G′ as a function of source-drain bias $V_{SD,}$ rather then temperature T [3]. The theory provided numerical results for the bias dependence of G′ in the limit of T=0, and in recent experiments has been used to extract values of T_K and compare to the values obtained from the temperature dependence of the conductance [4]. However this theory is only valid for T=0, i.e. $T/T_K \approx 0$.

In this work we extend the study of the Kondo effect at finite bias to the regime where $T/T_K>0$. The sample used here is a spin-3/2 hole quantum dot in a GaAs/AlGaAs heterostructure [5]. We scale the zero bias conductance peak as a function of V_{SD} and compare to theory in the limit of T=0 and at finite T as shown in Fig.1. We observe deviations between our experimental data (circles) and the T=0 theory (blue dashed line, top x-axis). These deviations can be eliminated by using newly available finite T theory (solid red line, bottom x-axis). Our analysis shows that even though T/T_K is small in our experiments, there are significant deviations from the T=0 theory [6].

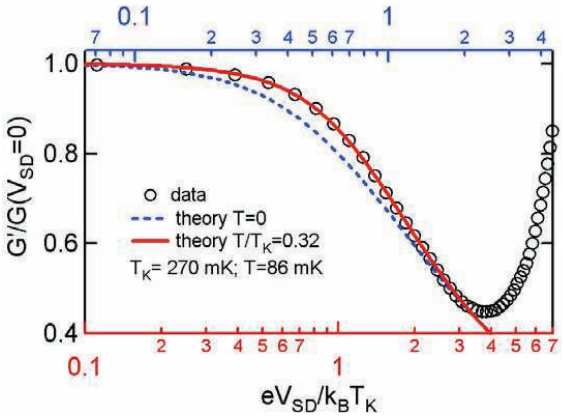

Figure 1. The excess Kondo conductance $G'/G(V_{SD}=0)$ through the dot as a function of scaled bias eV_{SD}/k_BT_K. T_K is used as a fitting parameter to scale experimental data (circles) to theoretical calculations for T=0 (blue dashed line) and T >0 (red solid line).

[1] L. Kouwenhoven and L. Glazman, Physics world 33 (2001).
[2] D. Goldhaber-Gordon *at el.*, Phys. Rev. Lett. **81**, 5225 (1998).
[3] M. Pletyukhov, H. Schoeller, Phys. Rev. Lett. **108**, 260601 (2012).
[4] A.V. Kretinin *at el.*, Phys. Rev. B **84**, 245316 (2011).
[5] O. Klochan *at el.*, Phys. Rev. Lett. **107**, 076805 (2011).
[6] O. Klochan *at el.*, submitted to Phys. Rev. B (2013).

Kondo effect of a quantum dot in the mixed valence regime

Alexander W. Heine[1], Daniel Tutuc[1], Rok Žitko[2], and Rolf J. Haug[1]

[1] *Institut für Festkörperphysik, Leibniz Universität Hannover, D-30167 Hannover, Germany*

[2] *Department of Theoretical Physics, Institut "Jožef Stefan", SI-1001 Ljubljana, Slovenia*

Quantum dots are high versatile and tunable devices and therefore give rise to the observation of many quantum effects in an controllable environment. Their investigation as magnetic impurities yielded the realization of an artificial Kondo system[1, 2, 3]. The Kondo effect describes the spin entanglement of a many-electron system, where a single localized spin on the quantum dot is screened by the delocalized electrons in the leads. A new ground state is formed with the binding energy T_K, the Kondo temperature.

We investigate the fingerprint of the Kondo effect, the so-called zero bias anomaly, in the regime of high tunnel coupling, where the coupling strength is comparable to the charging energy of the dot. Thus we enter the so-called mixed valence regime[1].

The sample consists of a two-dimensional electron system 37 nm below the surface. Using local anodic oxidation with an atomic force microscope a quantum dot with a diameter of about 150 nm is created[4]. Its energy level and tunnel coupling to the gates are controlled by three in-plane gates. Standard lock-in technique is used to perform transport measurements in a ^{3}He/^{4}He dilution refrigerator with a base temperature of about 20 mK.

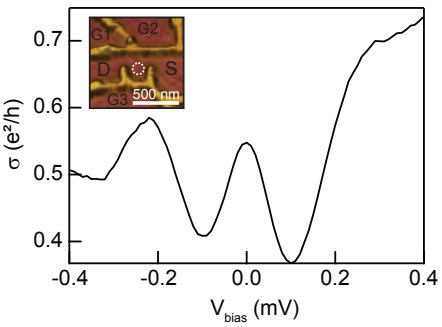

Figure 1: Differential conductance of the quantum dot as function of bias at $T = 20$ mK. Inset: AFM image of the sample.

The quantum dot is tuned into the mixed valence regime and the differential conductance is measured as function of bias and temperature. After subtraction of the background induced by broad Coulomb peaks we extract the Kondo temperature by analyzing the temperature dependence. Hence we fit results of numerical renormalization group calculations to the measurement data. The obtained Kondo temperatures are compared to values determined by investigating the width of the zero bias anomaly.

[1] D. Goldhaber-Gordon, J. Gres, M. A. Kastner, H. Shtrikman, D. Mahalu, and U. Meirav, Phys. Rev. Lett. **81**, 5225 (1998).
[2] S. M. Cronenwett, T. H. Oosterkamp, and L. P. Kouwenhoven, Science **281**, 540 (1998).
[3] J. Schmid, J. Weis, K. Eberl, and K. v. Klitzing, Phys. Rev. Lett. **84**, 5824 (2000).
[4] D. Tutuc, B. Popescu, D. Schuh, W. Wegscheider, and R. J. Haug, Phys. Rev. B **83**, 241308 (2011).

Resistive read-out of nuclear spin signals from a single quantum dot under the Kondo effect regime

Minoru Kawamura [1], Daniel Gottwald [1], Keiji Ono [1], Tomoki Machida [2, 3] and Kimitoshi Kono [1]

[1] *RIKEN, Japan*
[2] *Institute of Industrial Science, University of Tokyo, Japan*
[3] *Institute for Nano Quantum Information Electronics, University of Tokyo, Japan*

We study dynamic polarization and resistive detection of nuclear spins in a single quantum dot (QD) under the Kondo effect regime. We find that the differential conductance dI/dV_{sd} spectra of the QD exhibit remarkable hysteresis under the Kondo effect regime in magnetic fields when the bias voltage V_{sd} is scanned in the positive and negative directions (Fig. 1a). We also find that dI/dV_{sd} increases slowly under a fixed V_{sd} where the hysteresis is observed. Relevance of nuclear spins to the hysteresis and the slow increase in dI/dV_{sd} is unambiguously confirmed by the detection of nuclear magnetic resonance signals by monitoring dI/dV_{sd} under the irradiation of rf-magnetic fields. We attribute the origin of the hysteresis to the dynamic nuclear spin polarization (DNP) in the QD. Because the DNP develops during the scans of V_{sd} in the dI/dV_{sd}-V_{sd} measurement, the resultant difference in the effective magnetic field causes the hysteresis in the dI/dV_{sd}-V_{sd} curves.

Impact of the newly developed technique for the dynamic polarization and resistive detection of nuclear spins is further emphasized by the following nuclear spin relaxation rate $1/T_1$ measurement. Because $1/T_1$ is enhanced by the electron spin fluctuation, electron spin dynamics in the QD can be studied through the $1/T_1$ measurement. We find that the value of $1/T_1$ suppressed at around $V_{sd} = 0$ μV increases steeply with increasing V_{sd}, suggesting a bias-voltage-driven crossover from a spin-fixed state to a spin-fluctuating state (Fig. 1b). The crossover is one of unique features of the non-equilibrium Kondo effect under a magnetic field and is directly observed for the first time in the present study [1].

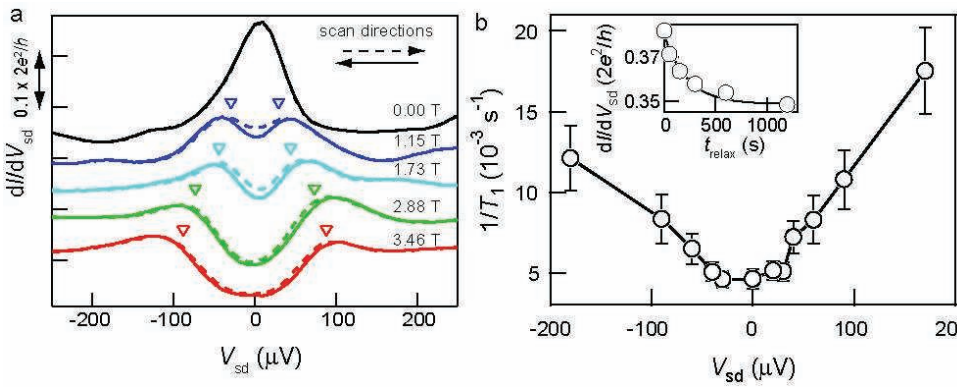

FIG. 1: (a) Differential conductance spectra of a QD under Kondo effect regime under variou magnetic fields.The curves are offset for clarity. (b) Bias voltage dependence of nuclear spi relaxation rate at $B = 2.88$ T. Inset shows a representative nuclear spin relaxation curve.

[1] M. Kawamura, D. Gottwald, K.Ono, T. Machida, and K. Kono, Phys.Rev. B **87**, 081303(R), 2013.

How to directly measure Kondo cloud's length

J. Park[1], S.-S. Lee[1], Y. Oreg[2], and H.-S. Sim[1]

[1] *Department of Physics, Korea Advanced Institute of Science and Technology, Daejeon 305-701, Korea*

[2] *Department of Condensed Matter Physics, Weizmann Institute of Science, Rehovot 76100, Israel*

The Kondo effect in a quantum dot has been intensively studied over the last decade. Tunability of a quantum dot has enabled to clarify the various aspects of the Kondo effects. Although the Kondo effect is well known, its spatial features still remain to be addressed. The Kondo singlet between the impurity spin and a conduction electron is formed over an extended conduction electron region, called the screening cloud. The size of Kondo screening cloud is $\xi_K = \hbar v_F / T_K$, where T_K is the Kondo temperature and v_F is the Fermi velocity. There have been several proposals for ways to detect the cloud, but no one has experimentally deteted it yet.

We theoretically propose how to directly detect the size ξ_K of the Kondo cloud, based on the intution that a change of conduction electrons inside the Kondo cloud will affect the Kondo effect [1]. We consider a quantum dot at $x = 0$ coupled to two semi-infinite wires with tunneling amplitude t_{WD} (Figure 1). Gate voltages V_g are applied to the wires beyond distance L from the dot (in $|x| > L$). We find that when $L \gg \xi_K$, V_g negligibly affects the cloud. However, when $L \ll \xi_K$, the Kondo temperature T_K is sensitive to V_g. By measuring the conductance or T_K with varing L or t_{WD}, one can detect the crossover and hence ξ_K. We analyze the system using the poor man scaling, the numerical renormalization group study, and the Fermi liquid theory.

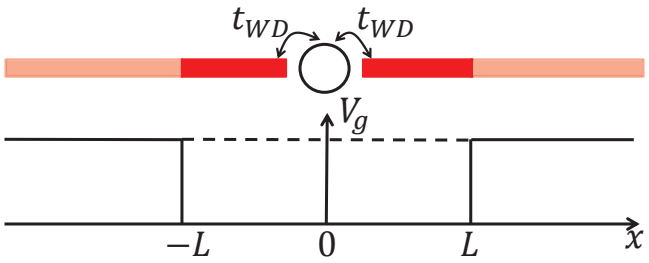

Figure 1: A quantum dot couples to quantum wires along $\hat{x}$ axis, with electron tunneling amplitude t_{WD}. Gate voltage V_g is applied over distance L from the dot (in $|x| > L$). The Kondo effect becomes sensitive to V_g, as L decreases below the cloud size.

[1] Jinhong Park, S.-S. B. Lee, Yuval Oreg, and H.-S. Sim, arXiv:1210.6138.

The effect of charged quantum dots on the mobility of a two-dimensional electron gas: How strong is Coulomb scattering?

A. Kurzmann[1], A. Beckel[1], S. Wisotzki[1], D. Reuter[2,3], A. D. Wieck[2], M. Geller[1] and A. Lorke[1]

[1] *Faculty of Physics and CeNIDE, University of Duisburg-Essen, Lotharstr. 1, 47057 Duisburg, Germany*

[2] *Chair of Applied Solid State Physics, Ruhr-Universität Bochum, Universitätsstr. 150, 44780 Bochum, Germany*

[3] *Department Physik, Universität Paderborn, 33098 Paderborn, Germany*

An electrical read-out of spin and charge states of self-assembled quantum dots (QDs) can be realized by a nearby two-dimensional electron gas (2DEG) [1], where the coupling mechanisms determine the strength of the detection signal. Therefore, we have investigated the coupling mechanisms between a layer of charged QDs and the 2DEG with single electron resolution [3] using Transconductance Spectroscopy (TCS) [2]. We are able to separate all contributions to the change in conductance by the charged electrons and find, surprisingly, that the influence of the charged QDs as Coulomb scatterers on the mobility is negligible for a 2DEG that is separated by a 30 nm barrier to the charged QDs.

The device is a high electron mobility transistor (HEMT) with an embedded layer of InAs QDs, separated by a 30 nm thick tunneling barrier from the 2DEG. By applying a suitable gate voltage we can charge the s- and p-shell with electrons (see Fig. 1, red line). Using Hall measurements, the influence of both mobility and charge carrier concentration on the 2DEG conductivity can be determined. They have almost equal contributions [3]. The overall change in mobility $\Delta\mu$ (see Fig. 1, black line) is on one hand caused by a decrease of the charge carrier density $\Delta\mu_n$ (see Fig. 1, blue line) by depletion of the 2DEG when the QDs are charged. On the other hand, the mobility decreases as a result of Coulomb scattering, induced by potential fluctuations by the charged QDs $\Delta\mu_{QD}$ (see Fig. 1, green line). The results in Fig. 1 show that the effect of the charged QDs as Coulomb scatters on the mobility is negligible, in very good agreement with calculations using the Stern-Howard-model.

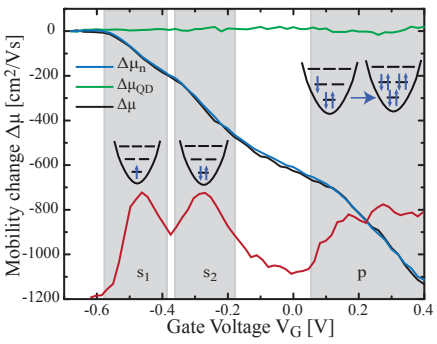

Figure 1: Measured overall change in mobility in the 2DEG $\Delta\mu$ due to Coulomb scattering by the charged QDs $\Delta\mu_{QD}$ and the change in charge carrier concentration $\Delta\mu_n$.

These results are of great interest for future devices. The read-out signal in a QD-HEMT device is almost independent of the distance between QDs and 2DEG for such devices; it will be only influenced by the ratio between the distance QD-2DEG and QD-Gate (the lever arm), as every electron loaded into the QDs is either "screened" by charge depletion on the gate or in the 2DEG.

[1] B. Marquardt et al., Nat. Commun. **2**, 209 (2011).
[2] B. Marquardt et al., Appl. Phys. Lett. **95**, 022113 (2009).
[3] B. Marquardt et al., Appl. Phys. Lett. **99**, 223510 (2011).

Phonon effects on the measurement of two-spin states in a double quantum dot

Łukasz Marcinowski, Katarzyna Roszak, Paweł Machnikowski

Institute of Physics, Wrocław University of Technology, 50-370 Wrocław, Poland

Gate-defined double quantum dots (DQD) coupled to a quantum point contact (QPC) are proposed as a single shot measurement device of the spin configurations of two electrons confined in DQD[1-3]. The measurement is performed by monitoring QPC current which depends on the configurations of the charges in DQD due to Coulomb interaction between a DQD electrons and a QPC tunneling barrier. The access to a spin-configuration information is possible because transitions between different charge states are allowed for anti-symmetric spin configuration(singlet) and forbidden for symmetric configuration(triplet)[3]. Since in a lack of DQD-QPC interaction QPC current is Poissonian and DQD-QPC interaction depends on the charge distribution of the electrons in DQD, the QPC current fluctuations will be changed for a spin-singlet configuration in DQD as a consequence of transitions between different charge states. On the other hand there is a transfer of energy between QPC current and DQD electrons allowing the transitions between the singlet states. This leads to a different current noise characteristics for the singlet and triplet states. Furthermore readout of the information is not instantaneous since it is gradually inferred from the current fluctuations.

In this work we investigate phonon impact on the singlet-triplet measurement in a realistic model. We model a gate-defined lateral DQD formed on a GaAs/AlGaAs quantum well in the low temperature regime which is typical for spin experiments performed on such dots[4]. The electron-phonon interaction which is unavoidable in a solid state environment will suppress excitation to doubly occupied spin-singlet states in such systems. Hence, the fluctuations of the charge distribution are also suppressed and it will hinder distinguishability between the QPC current noise for the spin-singlet and spin-triplet states. The analysis of this effect allows us to find limitations for the applicability of the QPC current noise measurement of the DQD two-electron spin system.

[1] A.C. Johnson, J.R. Petta, J.M. Taylor, A. Yacoby, M.D. Lukin, C.M. Marcus, M.P. Hanson, and A.C. Gossard, Nature **435**, 925 (2005).
[2] T. M. Stace and S. D. Barrett, Phys. Rev. Lett. **92**, 136802 (2004).
[3] S. D. Barrett and T. M. Stace, Phys. Rev. B **73**, 075324 (2006).
[4] M. C. Rogge, B. Harke, C. Fricke, F. Hohls, M. Reinwald, W. Wegscheider and R. J. Haug, Phys. Rev. B **72**, 233402 (2005).

Oscillatory persistent currents in quantum dots

A.A. Vasilchenko

Kuban State Technological University, Moskovskaya 2, 350072 Krasnodar, Russia

The system of Kohn-Sham equations for quantum dots in strong magnetic field with the number of spin-polarized electrons N from 3 to 40 was solved numerically. Many-body effects are taken approximately into account by the use of local exchange energy.

The calculations have been performed for different sets of the angular moment of electrons. We found that the dependence of the total angular moment M on magnetic field represents a series of a plateau. Change of the angular momentum of the electrons leads to a jump in the persistent current.

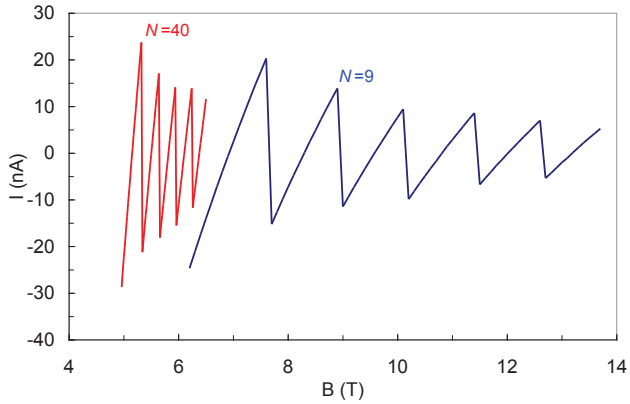

FIG. 1. The persistent current versus the magnetic field in quantum dots with N =9 and N =40 electrons.

The results of calculations for GaAs quantum dots are shown in Fig. 1. Persistent current has an oscillatory form with almost linear segments. The period of oscillations of persistent current is well described by the formula

$$\Delta B = 2B_1/(N+1),$$

where B_1 corresponds to the middle of the plateau with $M = N(N\text{-}1)/2+N$.

Different segments correspond to different value of M which increases as the magnetic field increases. The oscillation period decreases slightly as the magnetic field increases. The amplitude of the oscillations decreases due to the fact that for large M diamagnetic current compensates paramagnetic one.

This work was supported by Ministry of Education and Science of the Russian Federation.

ThP78

Characteristics of Majorana modes in cylindric wires

L. Serra[1,2], **J. S. Lim**[1], **and R. López**[1,2]

[1] *Institut de Física Interdisciplinària i Sistemes Complexos IFISC (CSIC-UIB), E-07122 Palma de Mallorca, Spain*
[2] *Departament de Física, Universitat de les Illes Balears, E-07122 Palma de Mallorca, Spain*

We report theoretical calculations of Majorana modes in semiconductor wires with cylindrical symmetry. Peculiar features like topological phases hosting two different Majorana modes on the same edge, as well as characteristic spatial distributions of the densities are found. The modelling is done assuming a space continuum approach, as opposed to tight-binding chains, and emphasis is placed on the role of the orbital effects induced by the magnetic field and on the mixing mechanism induced by spin-orbit coupling. We discuss results for finite cylinders, where the two oppossite edges interfere, as well as for semi-infinite wires where Majorana modes, if present, are not disturbed by finite size effects. The Majorana physics in cylinders is compared with that of planar structures we have previously investigated in Refs. [1, 2, 3].

[1] J. S. Lim, L. Serra, R. López, and R. Aguado, Phys. Rev. B **86**, 121103 (2012).
[2] J. S. Lim, R. López, and L. Serra, New Journal of Physics **14**, 083020 (2012).
[3] L. Serra, Phys. Rev. B **87**, 075440 (2013).

Measurements of *g* factors in GaSb/InAs core/shell nanowire hole quantum dots

Bahram Ganjipour*, B. Mattias Borg, Lars-Erik Wernersson, Lars Samuelson, H. Q. Xu and Claes Thelander

Division of Solid State Physics/ The Nanometer Structure Consortium, Lund University, Box 118, S-221 00 Lund, Sweden

**Corresponding author e-mail: bahram.ganjipour@ftf.lth.se*

Hole spins confined within quantum dots have emerged as promising candidates for spin-based quantum information processing.[1, 2] The strong spin-orbit interaction in bulk two-dimensional hole systems lead to a significant reduction in spin relaxation times. In addition, recent studies have reported[3] that the spin relaxation times of holes confined into quantum wells are also longer than in bulk. Another attractive property of GaSb is that it has the highest hole mobility among the III-V semiconductors.

In this work, hole quantum dots were realized using GaSb/InAs core/shell nanowires. The nanowires were grown from gold aerosol nanoparticles which were deposited on a GaAs (111) B substrates.[4] The nanowires were transferred from the growth substrates to highly doped Si substrates with a 100-nm-thick SiO_2 capping layer. Ti/Au contacts with a varying contact separation were defined to the GaSb nanowire segments of selected nanowires. The fabricated devices were characterized by low temperature (50 mK) transport measurements, where periodic conductance oscillations due to Coulomb blockade were observed in the measurements, with a charging energy of 5 meV. Detailed experiments at perpendicular magnetic field show Zeeman splitting in the GaSb hole quantum dots. The measurements show that quantum levels of the GaSb quantum dots have g factors with absolute value up to ~4. An energy gap of 150 μeV has also been deduced from an avoided level crossing between ground state and first excited state in such a GaSb nanowire quantum dot.

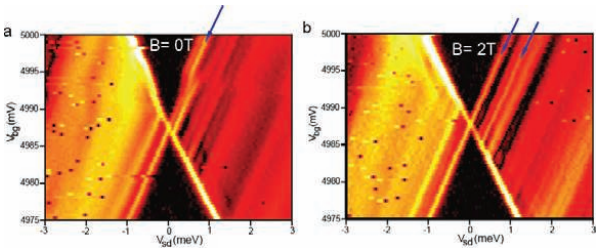

Figure1: Logarithmic differential conductance as a function of source-drain bias and gate voltages at different magnetic field of 0 and 2 T.

References

[1] D. Klauser, W. A. Coish, and Daniel Loss, Phys. Rev. B **78**, 205301 (2008).

[2] B. D. Gerardot, D. Brunner, P. A. Dalgarno, P. Öhberg, S. Seidl, M. Kroner, K. Karrai, N. G. Stoltz, P. M. Petroff, R. J. Warburto, Nature. **451**, 441 (2008).

[3] P. Schneider , J. Kainz, S. D. Ganichev, S. N. Danilov, U. Rössler, W. Wegscheider, D. Weiss, W. Prettl, V. V Bel'kov, M.M Glazov, L. E. Golub, D. Schuh., J. Appl. Phys. **96**, 420 (2004).

[4] M. Jeppsson**,** K. A. Dick**,** J. B. Wagner**,** P. Caroff**,** K. Deppert**,** L. Samuelson**,** L-E.Wernersson**,** Journal of Crystal Growth**. 310**, 4115 (2008)

Coherent Transport in GaAs/InAs Core/Shell Nanowires

F. Haas[1,2], P. Zellekens[1,2], Ö. Gül[1,2], T. Rieger[1,2], M. Lepsa[1,2], D. Grützmacher[1,2], H. Lüth[1,2] and Th. Schäpers[1,2]

[1] *Peter Grünberg Institute 9, Semiconductor Nanotechnology, Forschungszentrum Jülich, 52425 Jülich, Germany*

[2] *JARA – Fundamentals of Future Information Technologies*

Modern epitaxial growth technology of semiconductor nanowires allows the formation of complex axial and radial heterostructures and the combination of materials having large lattice mismatches. In this context, radial heterostructure nanowires made of a GaAs core and a surrounding InAs shell are a very interesting system [1, 2]. Here the low bandgap InAs shell forms a cylindrical tube-like conductor around the high bandgap GaAs core.

In this contribution, we present magneto-transport measurements of the GaAs/InAs core/shell nanowires at different temperatures in a magnetic field applied alongside the wire axis (see Fig. 1). Aharonov-Bohm Oscillations with h/e periodicity are found in the conductance of the wires (see Fig. 2). The appearance of the flux quantum period can be explained by one-dimensional transport through angular momentum states [3].

The oscillations are visible at temperatures up to 50 K, indicating a long phase coherence length (see Fig. 3). The GaAs/InAs core/shell heterostructures are therefore an excellent system for studying phase coherent transport effects in semiconductor nanowires.

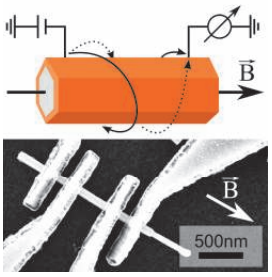

Fig. 1: Measurement setup of a core/shell wire.

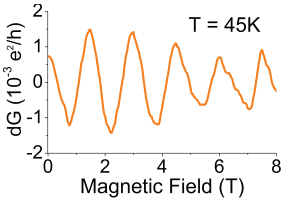

Fig. 2: Nanowire conductance without a slowly varying background.

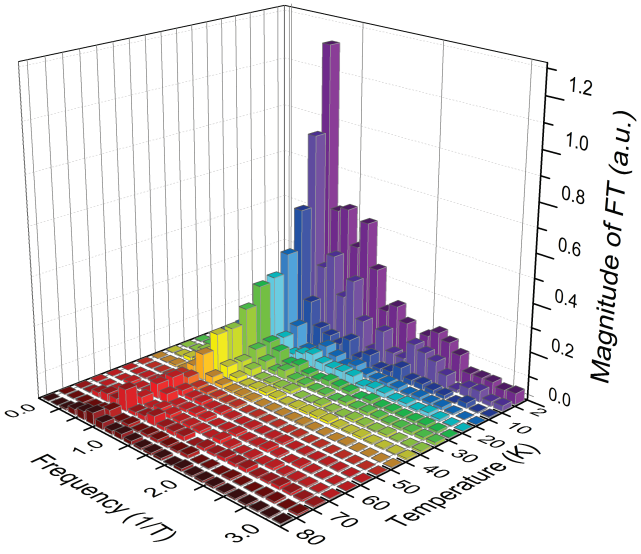

Fig. 3: Fourier transformation of the h/e magneto-conductance oscillations of a GaAs/InAs core/shell nanowire in an axially oriented magnetic field.

[1] F. Haas et al. (2013) Nanotechnology **24** 085603.
[2] T. Rieger et al. (2012) Nano Letters **12**(11) 5559.
[3] C. Blömers et al. (2013) Nanotechnology **24** 035203.

Spin current polarization at room temperature in a nanowire resonant tunneling diode

P. Wójcik[1*], J. Adamowski[1], B. J. Spisak[1], M. Wołoszyn[1]

[1] *Faculty of Physics and Applied Computer Science, AGH – University of Science and Technology,*
Al. Mickiewicza 30, 30-059 Kraków, Poland
[*] *e-mail: Pawel.Wojcik@fis.agh.edu.pl*

The operation of the magnetic resonant tunneling structures (RTS) as a spin filter has been demonstrated experimentally by Slobodskyy et. al [1]. In this type of nanostructures, the spin splitting of the quasi-bound state energy levels in the magnetic quantum well causes that the resonant tunneling conditions for spin up and spin down electrons are satisfied for different bias voltages, which leads to the spin polarization of the current. The spin filter effect in the magnetic RTS investigated to date is limited to very low temperatures and requires a strong magnetic field. These restrictions cause that recently more interest is focused on the application of the ferromagnetic RTS, especially these based on dilute magnetic semiconductors with the high Curie temperature, e.g. GaMnAs and GaMnN. Although the recent experiments reported that GaMnN exhibits the ferromagnetic properties at room temperature [2], the theoretical calculations show that the RTS based on GaMnN allows to achieve only 20 % spin polarization of the current at room temperature [3].

In the present report, we study the resonant tunneling structure embedded in a nanowire with ferromagnetic lead and quantum well made from DMS, e.g. GaMnN. The parallel and antiparallel magnetization of the lead and the quantum well is considered. Using the adiabatic approximation, we have shown that the resonant tunneling between the spin splitted subbands in the ferromagnetic lead and the quasi bound state in the quantum well leads to the full spin polarization of the current at low temperature for both the parallel and antiparallel magnetization of the magnetic layers. Calculations at room temperature show that for parallel magnetization the spin current polarization vanishes. On the other hand, the application of the nanostructure with the antiparallel magnetization of the magnetic regions reduces the spin current polarization to 70 % at room temperature. According to the best of our knowledge, this is the highest value of the spin polarization predicted at room temperature for the magnetic RTD.

[1] A. Slobodskyy, C. Gould, T. Slobodskyy, C.R. Becker, G. Schmidt, L.W. Molenkamp and A.-P. Jauho, *Phys. Rev. Lett.* **90**, 246601 (2003).
[2] A. Pearton, D. Norton, M. Ivill, A. Hebard, J. Zavada, W. Chen and Buyanova, *J. Electron. Mater.* **36**, 462 (2007).
[3] J. Wang, Y. Liu, H. Mao, Q. Zhao, *Appl. Phys. Lett.* **94**, 172501 (2009).

Observation of Direct Spin Injection from NiFe into an InAs Nanowire

Z. Cui, R. Perumal, T. Ishikura, and Kanji Yoh

Research Center for Integrated Quantum Electronics, Hokkaido University, N13, W8, Kita-ku, Sapporo, 060-8628 Japan

Among numerous spintronics device proposals, the spin field effect transistor due to Datta and Das [1] has attracted a lot of attention. Recently, control of the spin orbit (SO) interaction in semiconductor has been proposed to use the Rashba SO and Dresselhaus SO coupling to perform controlled rotations of electron spins, and Datta-Das type spin FET structure is shown to be effective in a condition when Rashba and Dresselhaus effect are matched known as Persistent Spin Helix (PSH) state [2]. However, the relaxation of the spin coherence along the channel is still one of the most important issues for the feasible operation. InAs nanowire is a good candidate for the spin device channel material because Rashba coefficient α and Dresselhaus coefficient β of InAs are both large and comparable. To apply this quasi-1 dimension material, it is necessary to quantify the spin transport properties and control fabrication processes of InAs nanowires grown along [110] directions.

Here we report the local spin injection measurements based on a single InAs nanowire grown by MBE, whose growth orientation is expected to be [110] according to Pd assistance growth mechanism [3]. As shown in Fig. 1, nanowires were dispersed onto an addressed highly doped p-type Si substrate with SiO_2 layer. All of the lithograph patterns were defined by electron beam (EB) lithography and Ti/Au were used as bonding pads, NiFe ferromagnetic electrodes were formed without annealing processes. The relative magnetoresistance (MR) characteristics in two different bias currents at 20K are shown in Fig.2. Assuming the spin diffusion length l_{sd} to be 290nm in an InAs nanowire measured separately [4] and the maximum theoretical l_{sd} to be 10μm [2e], the estimated spin injection efficiency ranged from 20% (l_{sd}=10μm) to 50% (l_{sd}=290nm). It suggests Pd-mediated-VLS-grown InAs nanowires to be a candidate of practical spintronics devices.

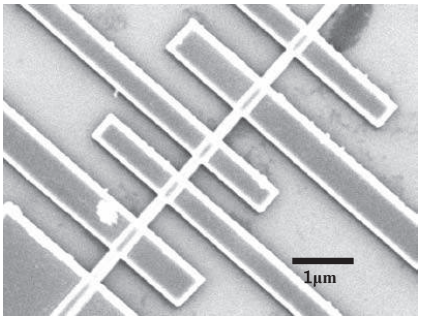

Fig.1 SEM image of spin injection device of an InAs nanowire with FeNi electrodes.

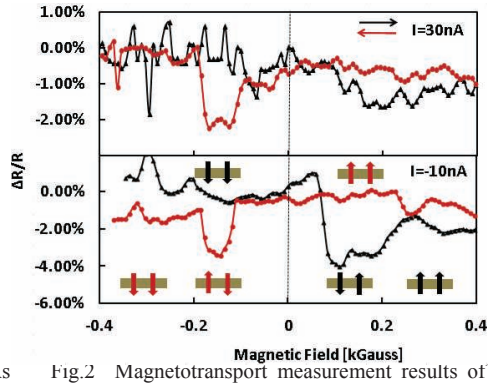

Fig.2 Magnetotransport measurement results of an InAs nanowire in local set-up.

[1] S. Datta and B. Das, Appl. Phys. Lett. **56**, 665 (1990).
[2] (a) J. Schliemann, et al, Phys. Rev. Lett. **90**,146801 (2003); (b) R. Winkler, Phys. Rev. B **69**, 045317 (2004) ; (c) M. Ohno and K. Yoh, Phys. Rev. B **75**, 241308 (2007); (d) M.Ohno and K. Yoh, Phys. Rev. B **77**, 045323 (2008); (e) Munekazu Ohno and Kanji Yoh, Physica E **40**, 1539-1541 (2008).
[3] Hongyi. Xu, et al., Nano Lett., **12 (11)**, pp 5744–5749 (2012); R.Perumal and K.Yoh, unpublished.
[4] Z. Cui, T. Ishikura, F. Jabeen, J.-C. Harmand, K. Yoh, J. Crystal Growth, in press.

Poster upgraded to oral presentation in Thursday *MSS* Session 4

Correlation of structural and optical properties of single core shell GaAs/AlAs nanowire in polarization-resolved and power-dependent photoluminescence

J. Jadczak [1,2], P. Plochocka [1], A. Mitioglu [1], D. K. Maude [1], G. L. J. A. Rikken [1] and Hadas Shtrikman [3]

[1] *Laboratoire National des Champs Magnétiques Intenses, CNRS-UJF-UPS-INSA, Toulouse*
[2] *Institute of Physics, Wrocław University of Technology, Wrocław, Poland*
[3] *Center for Submicron Research, Weizmann Institute of Science, Rehovot 76100, Israel*

Polarization-resolved micro-photoluminescence (μPL) of single core shell GaAs/AlAs nanowires (NWs) is used to probe their low temperature (T=5.5K) structural and optical properties. The NW was excited using a Ti: Sapphire laser tuned to 760 nm with powers in the range 0.5 to 15 μW. Under the low excitation power the dominant part of the spectrum is found below 1.519 eV, where shoulders at 1.496 eV and 1.507eV are distinguished as well as prominent emission lines centered at 1.510 eV and 1.516 eV (dashed white lines). Further increase of the power excitation causes the emergence of a new peak of stronger intensity at higher energy 1.529 eV. The low energy lines were identified with recombination of excitons bound to defect pairs. The emission at 1.516 eV and 1.529 eV was attributed to the recombination of exciton in purely ZB or WZ segments (the thickness of the insertions in the NW controls the energy of transitions between electrons confined in ZB sections and holes in WZ sections). In order to determine the crystal structures of the NW we determined it's orientation on the substrate and analyzed the emission polarization with setups shown in Fig.1(c-d). Results are shown in standard form of color maps of emission intensity as a function of polarization angle (Fig.1(a-b)). Using the Jones formalism, we found that the PL intensity is proportional to $I \sim \sin^2(2c-\alpha)$, where c is the position of $\lambda/2$ and α the NW orientation. It clearly shows the different selection rules for WZ and ZB sections; transition above 1.519 eV exhibits polarized emission perpendicular to NW axis, while lines observed below are more prominent for polarization parallel to NW axis.

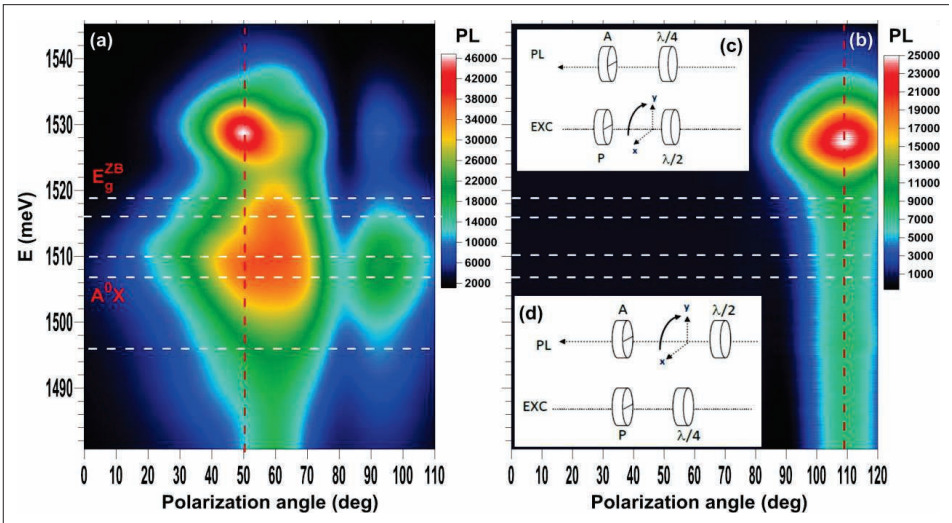

Figure 1: PL emission from a single core shell NW as a function of the polarization. (a) Rotating the linear polarization of the excitation (see c) to determine the orientation of the NW. (b) Rotating the linearly polarized detection (see d) to determine selection rules.

Self-Organization of Bi Bilayers in Nanowires

L. Konopko [1,2], T. Huber [3] and A. Nikolaeva [1,2]

[1] *Ghitu Institute of Electronic Engineering and Nanotechnologies, ASM, Chisinau, Moldova*

[2] *International Laboratory of High Magnetic Fields and Low Temperatures, Wroclaw, Poland*

[3] *Howard University, Department of Chemistry, Washington, DC 20059,USA*

In thin single-crystal Bi nanowires (d<80 nm) with the $(10\bar{1}1)$ orientation along the nanowire axis, in a transverse magnetic field, we have observed the self-organization of helical edge states of Bi(111) bilayers, which leads to series-connected conglomerates of Bi(111) bilayers; in a transverse magnetic field, each of them contains a closed conducting loop, which results in the appearance of Aharonov-Bohm (AB) oscillations.

The single nanowire samples were prepared by the high frequency liquid phase casting in a glass capillary using an improved Ulitovsky technique; they were cylindrical single-crystals with $(10\bar{1}1)$ orientation along the wire axis. In this orientation the trigonal axis C_3 is inclined to the wire axis at an angle of ~70°.

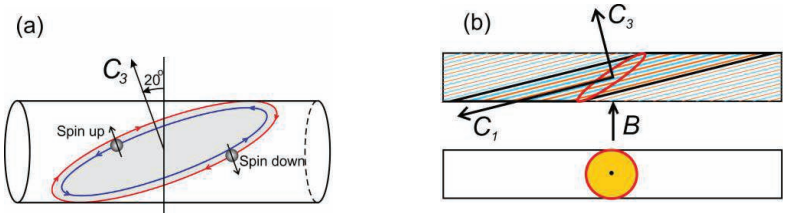

Fig. 1. (a): Location of Bi bilayer in nanowire.; (b): Sketch of the conglomerate of Bi bilayers.

Non monotonic changes in transverse magnetoresistance, which are equidistant in a direct magnetic field, were observed at low temperatures in a wide range of magnetic fields up to 14 T [1,2]. The period of oscillations depended on wire diameter d as for the case of longitudinal magnetoresistance; moreover, in a wide range of angles θ between the direction of applied magnetic field B and the C_3 wire axis (~50°) the period maintained a constant value. The amplitude of oscillations depended on angle θ and increased in intensity with increasing angle θ.

It was recently suggested that Bi(111) bilayers can exhibit the quantum spin Hall effect [3]. 2D single-bilayer has a pair of helical edge states carrying spin currents with opposite spins (Fig.1 (a)). In 45-nm nanowire, the self-organization of helical edge states leads to series-connected conglomerates of bilayers, each of which in a transverse magnetic field contains a closed conducting loop (see Fig.1 (b)), which results in the appearance of AB oscillations. The number of bilayers in the conglomerate decreases with increasing angle θ between the direction of applied magnetic field B and the C_3 axis, thus improving conditions for the occurrence of AB oscillations, which leads to the observed dependence of the amplitude of the AB oscillations on angle θ [1].

This work was supported by the STCU Grant # 5373.

[1] L. Konopko, T. Huber, A. Nikolaeva, J. Low Temp. Phys. **162**, 524 (2011).
[2] L. Konopko, T. Huber, A. Nikolaeva, J. Low Temp. Phys. DOI 10.1007/s10909-012-0850-x.
[3] S. Murakami, Phys. Rev. Lett. **97**, 236805 (2006).

Diffusion thermopower of quantum Hall systems measured in Hall-bar and Corbino geometry

Shuhei Kobayakawa, Akira Endo, Shingo Katsumoto, and Yasuhiro Iye

Institute for Solid State Physics, University of Tokyo, Kashiwa, Chiba 277-8581, Japan

It has been pointed out that the radial thermopower S_{rr}^{C} measured in the Corbino geometry is qualitatively different from the longitudinal thermopower S_{xx}^{H} in the Hall-bar geometry in the quantum Hall systems (QHS) [1, 2]. In terms of the conductivity and the thermoelectric conducitivity tensors, $\hat{\sigma}$ and $\hat{\epsilon}$, which relate the electric field $\boldsymbol{E}$ and the temperature gradient $\boldsymbol{\nabla} T$ to the current density $\boldsymbol{j}$ as $\boldsymbol{j} = \hat{\sigma}\boldsymbol{E} - \hat{\epsilon}\boldsymbol{\nabla} T$, the thermopowers are given as $S_{rr}^{\mathrm{C}} = \epsilon_{rr}/\sigma_{rr}$ and $S_{xx}^{\mathrm{H}} \simeq \epsilon_{yx}/\sigma_{yx}$, respectively, where we made use of the relation $\sigma_{xx} \ll |\sigma_{yx}|$ for the latter. The great majority of the thermopower measurements have been carried out on the Hall-bar samples thus far [3]. In the present paper, we report our measurement performed on both the Corbino and Hall-bar setups.

The thermopower generally contains contributions from two distinct mechanisms: diffusion and phonon drag. While the latter is known to be dominant in the GaAs/AlGaAs QHS [1, 3], it is the former that is expected to be more sensitive to the electronic properties of the systems. In order to detect the diffusion contribution selectively, we introduce the gradient only to the electron temperature T_{e} by employing the microwave heating technique. In the method, microwaves propagating through the coplanar waveguide (CPW) placed on the surface are absorbed by the electrons beneath the slots of the CPW and raise the T_{e} (Fig. 1 inset), thereby generating the gradient $\boldsymbol{\nabla} T_{\mathrm{e}}$ toward the large Ohmic contact designed as the low-temperature anchor of the device.

The Corbino thermopower S_{rr}^{C} thus measured is plotted in Fig. 2 along with the conductivity σ_{rr}. In the QH plateau regions, S_{rr}^{C} takes large positive (negative) values just below (above) integer fillings and inverts the sign at the center of the plateaus. This is in marked contrast to S_{xx}^{H}, which vanishes within the QH plateau regions. The behavior of S_{rr}^{C} is in agreement with the diffusion Corbino thermopower calculated in a recent theory [2] treating disorder within the self-consistent Born approximation.

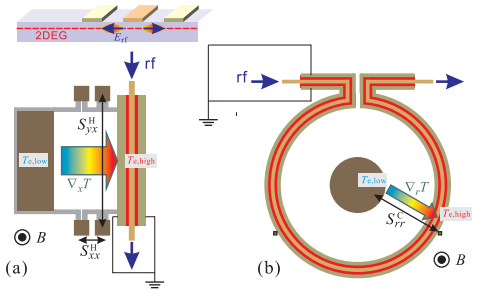

Fig. 1: Measurement devices in Hall-bar (a) and Corbino (b) setups. Upper inset depicts the close-up cross section of the heater section.

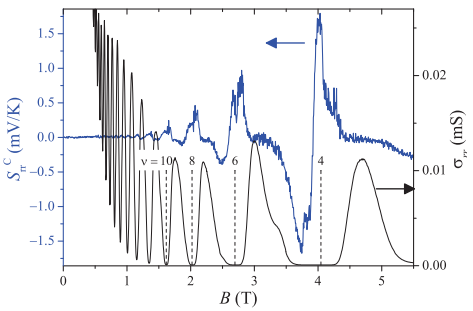

Fig. 2: Thermopower S_{rr}^{C} and conductivity σ_{rr} measured in the Corbino geometry.

[1] H. van Zalinge, R. W. van der Heijden, J. H. Wolter, Phys. Rev. B **67**, 165311 (2003).
[2] Y. Barlas, K. Yang, Phys. Rev. B **85**, 195107 (2012).
[3] R. Fletcher, Semicond. Sci. Technol. **14**, R1 (1999) and references therein.

Quantum Hall effect in $In_{0.75}Ga_{0.25}As/In_{0.75}Al_{0.25}As$ two-dimensional electron gas bilayer samples

S. Hidaka [1], H. Iwase [1], M. Akabori [1], S. Yamada [1], Y. Imanaka [2] T. Takamasu [2]

[1] *Center for Nano Materials and Technology (CNMT), Japan Advanced Institute of Science and Technology (JAIST) 1-1, Asahidai, Nomi, Ishikawa, 923-1292 Japan*
[2] *National Institute for Materials Science (NIMS) 3-13, Sakura, Tsukuba, Ibaraki, 305-0003 Japan*

We have recently fabricated $In_{0.75}Ga_{0.25}As/In_{0.75}Al_{0.25}As$ two-dimensional electron gas (2DEG) bilayer samples and found that the bilayer system could be a base material for new type spintronics devices [1] by using spin-orbit interaction still surviving. We have this time measured quantum Hall effects (QHEs) in those samples up to 23 Tesla and observed some curious plateau features similar to those in the fractional QHE.

The bilayer samples were made in the form of wide quantum wells (thickness w) modulation-doped from both the upper and lower sides. In the five samples with different ws (40, 60, 80, 100, 120 nm), sheet electron densities (n_ss) in the upper and lower 2DEGs are almost equal and they are typically 1 (2×10^{11}/cm^2) : 3 (6×10^{11}). So that, in this sense, the bilayer system is very asymmetric and especially under high magnetic field, the lower 2DEG could play a dominant role.

Figure 1 shows ρ_{xx} and ρ_{xy} in the w = 80 nm sample. As seen in the figure, not ν =3 plateau (ν, filling factor) but close fractional (ν = 4/3, 8/3, 10/3) plateaus seem to be observed. Similar curious behavior is confirmed also in the wide well sample (w = 120 nm) but not in the narrow well one (40 nm). The reason is not clear at present, since the interaction between the upper and lower 2DEGs is weak due to the relatively low n_s of the upper 2DEG. The behavior of ρ_{xy} in the latter sample is very normal and there is almost no fractional plateaus up to ν =2. This might suggests that the bilayer 2DEG in the w = 40 nm sample should be regarded as a monolayer 2DEG.

Fig. 1

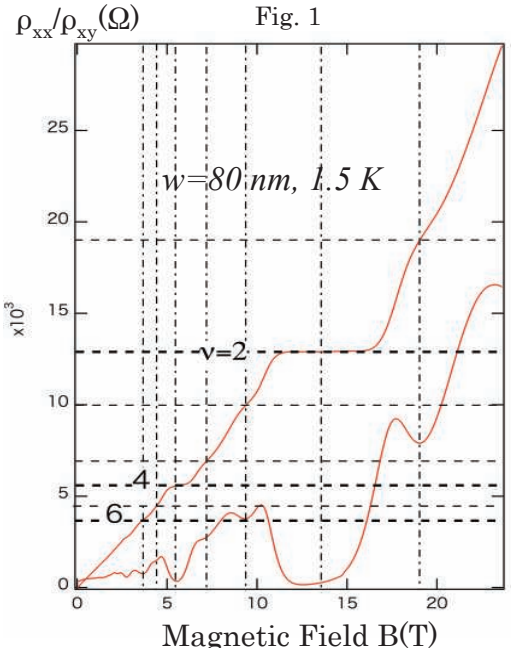

Reports on the fractional QHEs have seemed to be very rare [2] in the 2DEGs in InGaAs/InAlAs material system. We are thus planning to make even low temperature magneto-resistance measurements to resolve the fractional properties more precisely.

[1] M. Akabori, et al., J. Appl. Phys. **112**, 113711 (2012).
[2] P. Wei et al., Phys. Rev. B**32**, 7016 (1985).

ThP88

Coexistence of two different mechanism of dynamic nuclear polarization in a transition region between integer quantum Hall states

R. Moriya [1], S. Umezawa [1], S. Masubuchi [1,2], Y. Hashimoto [3], S. Katsumoto [2,3] and T. Machida [1,2]

[1] *Institute of Industrial Science, University of Tokyo, Tokyo 153-8505, Japan*
[2] *INQIE, University of Tokyo, Tokyo 153-8505, Japan*
[3] *The Institute for Solid State Physics, University of Tokyo, Chiba 277-8581, Japan*

In the quantum Hall states (QHS) of semiconductor two-dimensional electron gas, the hyperfine coupling between electron spin and nuclear spin has been utilized for polarizing and detecting the nuclear spins. Up to now, there have been two different processes to polarize nuclear spin; these are edge channel (EC) and bulk states (BS) of QHE. These two processes had been treated as independent method to control nuclear spins. However, since the nature of QHE, these two contributions can not be completely separated and could be coexisting depending on device geometry. We compared current induced dynamic nuclear polarization (DNP) in Hall bar device in longitudinal resistance (LR) and non-local resistance (NLR) configuration and revealed coexisting of EC and BS contribution.

The 2-dimentional electron gas (2DEG) in GaAs/AlGaAs is patterned into the Hall bar device. At the filling factor $\nu = 1.7$ of the QHS, the differential NRL R_{NL} and LR R_{xx} is measured under dc-current bias I_{SD} as shown in top panel of Fig. 1 and 2, respectively. We observed clear hysteresys between up and down sweep due to the polarization of nuclear spins. We determined the magnitude of DNP using pump-probe measurements where we pumped nuclear system with various I_{SD} for 200 second and probed the nuclear spin states at I_{SD}=0. The difference of R_{xx} at I_{SD}=0 before and after the pumping is derived as ΔR and obtained I_{SD} dependence of ΔR is plotted on the bottom panel of Fig. 1 and 2, respectively. The ΔR vs. I_{SD} can be viewed as a superposition of symmetric and asymmetric dependence on I_{SD}. We compared ΔR_{xx} and ΔR_{NL} with various contact configuration and external field direction. Results indicate that these asymmetric and symmetric contributions can be explained by the DNP induced by the EC and BS, respectively. And these two contributions coexist in Hall bar device.

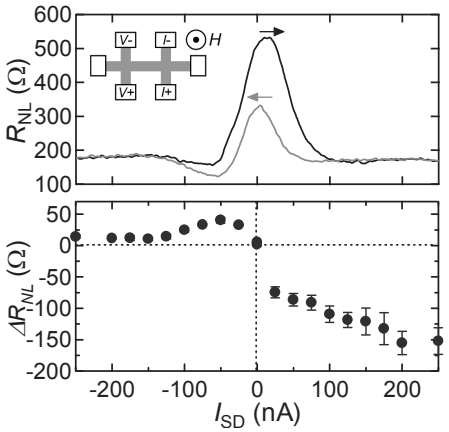

Fig. 1: I_{SD} dependence of R_{NL} and ΔR_{NL}.

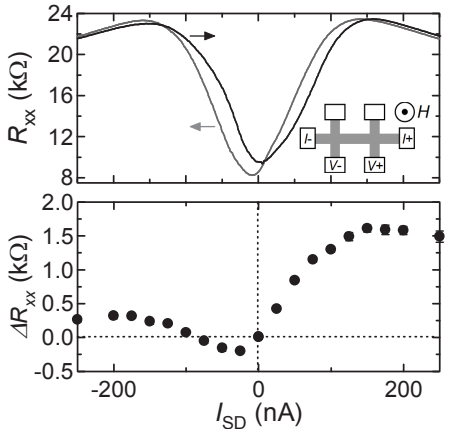

Fig. 2: I_{SD} dependence of R_{xx} and ΔR_{xx}.

Spin Polarization on a Plateau of a Half Conductance Quantum in a Quantum Point Contact

S. W. Kim, Y. Hashimoto, T. Nakamura, Y. Iye, and S. Katsumoto

Institute for Solid State Physics, The University of Tokyo
5-1-5 Kashiwanoha, Kashiwa, Chiba 277-8581, Japan

Perfect spin filtering in a quantum point contact (QPC) with strong spin-orbit interaction was claimed based on the conductance quantization with the unit of a half conductance quantum ($G_q/2 = e^2/h$) [1]. As a more sound experimental proof, we measured transport through a QPC terminated with a quantum dot (QD) spin detector [2]. However, in this setup, the spin current through the QPC is inevitably blocked by the QD resulting in difficulties both in the elimination of back action from the QD and in the application of the spin current to spintronics. Here we report measurement of spin polarization in the vicinity of such a QPC with a single-lead quantum dot (SLQD) spin detector [3]. In the present setup, the spin current through the QPC is mostly introduced to the electrodes at a minimal back action from the QD and can be used, e.g., as flying spin qubits.

Figure 1(a) explains the principle to measure the spin polarization, which is attained through the comparison of tunneling rates for the process of $N = 0 \rightarrow 2$, and that of $1 \rightarrow 3$. This can be intuitively understood with considering the case in which the polarization is one. In the former process, the tunneling of the second electron is blocked by the Pauli principle while it is not in the latter. In Fig.1(b), the white regions are Ti/Au gates on a two-dimensional electron gas (the dark gray region) in an $In_{0.11}Ga_{0.89}As$ quantum well. Electron tunneling rate from the target QPC (t-QPC) to the QD can be measured as the signal in remote charge detection with the detector QPC (d-QPC) locked to a square-wave modulation of the plunger gate voltage.

A clear half-conductance quantization in t-QPC at 100 mK is demonstrated in the inset of Fig.2. The main panel of Fig.2 shows the signal amplitudes in $N = 0 \rightarrow 2$, and $1 \rightarrow 3$ regions when t-QPC is on the first half-quantized plateau as a function of the period of gate-swing. Apparent difference in the two regions manifests the spin polarization. We have estimated the polarization as $P = 0.70 \pm 0.11$ from rate-equation analysis.

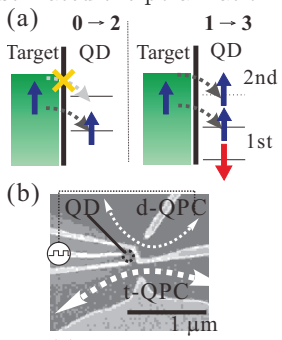

Fig.1. (a) Detection scheme of spin polarization by using two-electron tunneling processes to a side-coupled quantum dot and (b) the actual sample configuration.

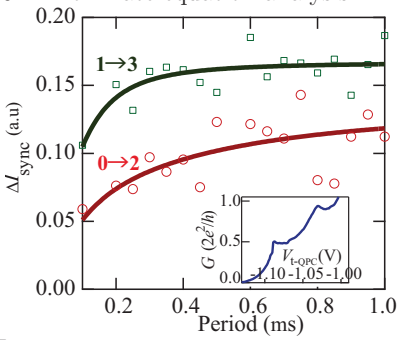

Figure 2. Tunneling signal amplitude in $N =$ $0 \rightarrow 2$ and $1 \rightarrow 3$ regions as a function of th period of the gate voltage modulation. The soli lines are obtained by the fitting.

[1] P. Debray, *et al.*, Nature Nanotechnology **4**, 759 (2009).
[2] S-W. Kim, *et al.*, J. Phys. Soc. Jpn **81**, 053709 (2012).
[3] J. M. Elzerman, *et al.*, Appl. Phys. Lett. **84**, 4617 (2004).

Current Frequency Dependence of the Resistance Enhancement in the ν = 2/3 Quantum Hall State

S. Tsuda [1], S. Mitani [1], Minh Hai N. [1], A. Fukuda [2], D. Terasawa [2] and A. Sawada [3]

[1] *Graduate School of Science, Kyoto University, Kyoto 606-8502, Japan*
[2] *Department of Physics, Hyogo College of Medicine, Nishinomiya 663-8501, Japan*
[2] *Research Center for Low Temp. and Mat. Sci., Kyoto University. Kyoto 606-8502, Japan*

The spin degree of freedom plays an important role in the fractional quantum Hall States (QHSs). It is responsible for a variety of phenomena such as phase transitions between different ground states and interactions of the electronic system with the nuclei. At the spin phase transition point in the ν = 2/3 QHS, an anomalous longitudinal resistance R_{xx} peak is observed. So far, the enhancement of the R_{xx} is explained by a domain structure of the two different spin phases of the ν = 2/3 QHS[1]. It is believed that when current passes across a domain boundary, electron spins flip-flop scatters nuclear spins causing dynamic nuclear spin polarization (DNP), then the spin polarization affects back the domain formation and increases the length of the domain boundaries. However, details of the domain structure and the mechanism of the R_{xx} enhancement are still unclear. One reason may be a difficulty of the ultra-low frequency measurements although there are several reports [2].

We investigate the DNP pumped by the large and ultra-low frequency electric current around the spin transition point in the ν = 2/3 fractional QHS in a GaAs/AlGaAs quantum well structure. We observe the time dependence of the magnetoresistance R_{xx} during the DNP in the wide range of frequencies of the pumping currents. In Figure 1, the time evolutions of the R_{xx} for the various pumping current frequencies are illustrated. The pumping current amplitude is 60 nA. We used the rectangular shape current to make the input power the same for all frequencies. We often change to 5nA and 37.7Hz sinusoidal current to measure the R_{xx} for a short moment. In Fig. 1, when frequencies are high (≥ 1.0 Hz), the R_{xx} monotonously increase for about several hundred seconds and saturate. At ultra-low frequencies (< 0.1 Hz), the R_{xx} decrease after the enhancement. The lower frequency we use, the smaller value the R_{xx} become. The R_{xx} also shows pulsation motion at ultra-low frequencies. These results suggest that the fluctuation of domain formation by AC current cause splits of the domains and the resistance enhancement at the ν = 2/3 QHS. In the conference, we discuss the dynamics of the nuclear spin and domain morphology.

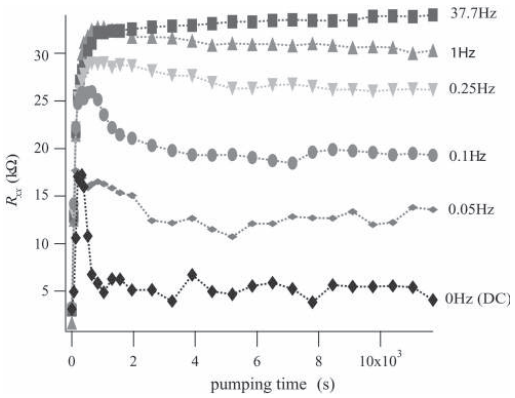

Figure 1 Time dependence of the R_{xx} during the DNP for various pumping frequencies. Pumping current has an amplitude of 60 nA with rectanguler shape. Detection is carried out with a sinusoidal current with 5 nA and 37.7 Hz.

[1] S. Kraus *et al.*, Phys. Rev. Lett. **89** (2002) 266801.
[2] J. H. Smet, *et al.*, Phys. Rev. Lett. **80**, (1998) 4538.

Possible Observation of Nuclear Superradiant Emission in Quantum Hall System

M. H. Fauzi [1], and Y. Hirayama [1,2,3]

[1] *Department of Physics, Tohoku University, Sendai 980-8578, Japan*
[2] *ERATO Nuclear Spin Electronics Project, Sendai 980-8578, Japan*
[3] *WPI-Advanced Institute for Materials Research, Tohoku University, Sendai 980-8577, Japan*

The recent interest in possible observation of a cooperative and self-organized radiation from nuclear spin ensemble mediated by the hyperfine coupling with the electron spins, in analogy with Dicke superradiance in quantum optics, has been very stimulating [1-2]. Here we demonstrate that the nuclear spin could exhibit superradiant emission in the quantum Hall regime only when the electronic system produces low energy excitation modes. The nuclear spin dynamic is detected by domain walls formed at the fractional filling factor ν = 2/3 quantum Hall ferromagnet [3]. The interaction between the nuclear- and electron spin could be tuned by altering the electron density via a gate biasing voltage. We show that when the non-equilibrium nuclear spin polarization (dynamically formed by current flow at the ν = 2/3 spin phase transition) was exposed to the filling factor ν = 1.1 quantum Hall states where Skyrmion phases were formed, we observed a sudden intense burst of the hyperfine field on the electron spin (red line curve in Fig. 1b) before finally got relaxed rapidly within 50 seconds. The intense burst was determined by the shift of the transition curve to a lower filling factor and the width was very narrow compared to the filling factor ν = 1.

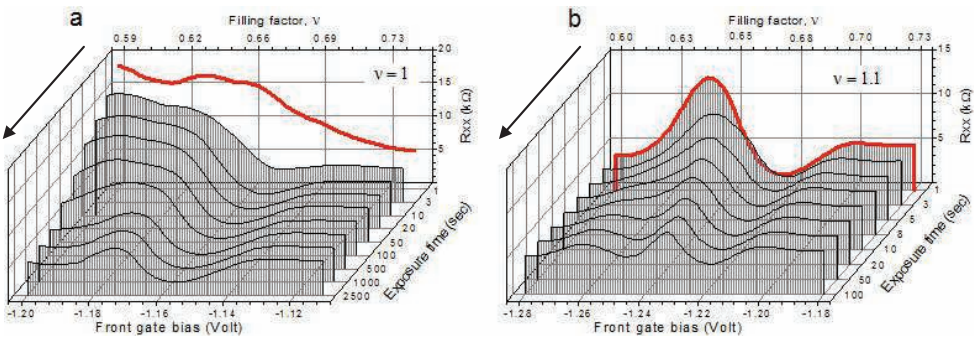

Figure 1: The evolution of spin phase transition curve of the filling factor ν = 2/3 after exposed to (a) the filling factor ν = 1 and (b) ν = 1.1 for a given interval of time. The nuclear spin dynamics was registered in the evolution of the transition curve towards its equilibrium (see the arrow direction). The first exposure transition curve is highlighted by the red line. We have to note that the bias condition changes slightly by thermal cycle.

We observed similar behavior with stronger intensity when the nuclear spin was exposed to a canted antiferromagnetic of the total filling factor ν = 2 bilayer quantum Hall state.

[1] E. M. Kessler. et.al. Phys. Rev. Lett. **104**, 143601 (2012).
[2] B.Urbaszek. et.al. Rev. Mod. Phys. 85, 79 (2013); M. J. A. Schuetz. et.al. Phys. Rev B. **86**, 085322 (2012).
[3] M. H. Fauzi et.al. *App. Phys. Lett*. **101**, 162105 (2012).

Detecting the energy spectrum of single electron emission in the quantum Hall regime

M. Kataoka [1], J. D. Fletcher [1], H. Howe [2], M. Pepper [2], P. See [1], S. P. Giblin [1], J. P. Griffiths [3], G. A. C. Jones [3], I. Farrer [3], D. A. Ritchie [3], and T. J. B. M. Janssen [1]

[1] *National Physical Laboratory, Hampton Road, Teddington, Middlesex TW11 0LW, UK*
[2] *London Centre for Nanotechnology, and Department of Electronic & Electrical Engineering, University College London, Torrington Place, London, WC1E 7JE, UK*
[3] *Cavendish Laboratory, University of Cambridge, J. J. Thomson Avenue, Cambridge CB3 0HE, UK*

The emission characteristics of a single-electron source [1,2] need to be understood if such device technologies [3,4] are to be used in quantum metrology and fermion quantum optics experiments. Particularly, when electrons are ejected at well above the Fermi energy [5], inelastic processes [6,7] can hamper the coherent transport of emitted electrons. Here, we investigate the emission characteristics of a tunable-barrier single-electron pump, using the energy-detection-barrier technique that has been developed in Ref. [7]. We place a tunnel barrier approximately 3 μm away from a single-electron pump [Fig. 1(a)]. In a perpendicular magnetic field B, the emitted electrons travel through edge states, well above the Fermi energy, before they reach the detector barrier. Depending on the barrier height relative to the electron energy, the electrons are transmitted through the barrier and appear as the collector current I_c, or are reflected by the barrier and appear as the side-contact current I_s. The calibration of detector barrier height is obtained by applying a bias across one of the pump gates. At very large magnetic field (B > 12 T), we find a sharp energy spectrum at E > 150 meV [Fig. 1(b)]. We find that the electron energy can be controlled linearly with the gate voltage on the exit barrier of the pump [Fig. 1(c)]. The inelastic scattering length is estimated to be over 40 μm. The second emission spectrum is observed when two electrons are pumped per cycle. At lower B, the phonon replica of spectrum lines are observed due to the emission of single/multiple LO phonon(s) per electron, resulting in a much shorter scattering length [Fig. 1(d) and (e)].

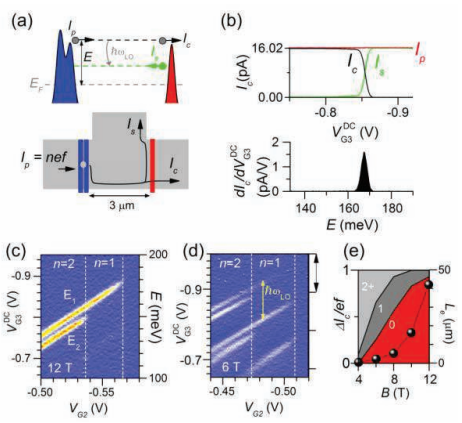

Fig. 1

[1] M. Moskalets and M. Büttiker, Phys. Rev. B **83**, 035316 (2011).
[2] F. Battista and P. Samuelsson, Phys. Rev. B **85**, 075428 (2011).
[3] G. Fève *et al*., Science **316**, 1169 (2007).
[4] M. D. Blumenthal *et al*., Nature Physics **3**, 343 (2007).
[5] C. Leicht *et al*., Semicond. Sci. Technol. **26**, 055010 (2011).
[6] M. Heiblum *et al*., Phys. Rev. Lett. **55**, 2200 (1985).
[7] D. Taubert *et al*., Phys. Rev. B **83**, 235404 (2011).

Electrically-detected ESR in silicon nanostructures inserted in microcavities

N.T. Bagraev[1], E.Yu. Danilovsky[1], W. Gehlhoff[2], D.S. Gets[1], L.E. Klyachkin[1], A.A. Kudryavtsev[1], R.V. Kuzmin[1], A.M. Malyarenko[1], V.A. Mashkov[3], V.V. Romanov[3]

[1]Ioffe Physical-Technical Institute, 194021, St.Petersburg, Russia
[2]Institut für Festkörperphysik, TU Berlin, D-10623 Berlin, Germany
[3]State Polytechnical University, 195251, St.Petersburg, Russia

We present the first findings of the new electrically detected electron spin resonance technique (EDESR), which reveal single point defects in the ultra-narrow silicon quantum wells (Si-QW) confined by the superconductor delta-barriers [1]. This technique allows the ESR identification without application of an external cavity as well as a high frequency source and recorder, with the measurements of the only response of the magnetoresistance caused by the microcavities embedded in the Si-QW plane. The ESR lines with the characteristic hf splitting of 4.1 mT that are related to the single phosphorus centers close to the p+-n junction area are observed. Besides, the spin-dependent scattering of 2-D holes is revealed by measuring the phosphorus line splitting that is to be evidence of the exchange interaction, which is similar to the effect of zero-field splitting in 1-D channels. The high sensitivity of the new EDESR technique is confirmed by measuring the NL8 spectrum that identifies residual oxygen thermodonors, TD+ - state, in the p-type Si-QW. This center of the orthorhombic symmetry has been also found by the ordinary EDESR method in the sandwich structure discussed here. The central lines in the EDESR spectrum are slightly different from the NL10 spectrum that is related to the neutral thermodonor containing a single hydrogen atom. Nevertheless, this EDESR spectrum appears to identify the hydrogen-related center in the p-type Si-QW, because its characteristic hf splitting, 23 MHz, corresponds to the hf hydrogen splitting. Different phases of the hf lines that result from the hydrogen-related center seem to result from the high spin polarization of holes in 1-D channels [2]. The 23 MHz hf splitting was also verified in the EDESR line with a g-value of 2.07 that seems to be related to the Fe^0 center. The high sensitivity of the EDESR technique allowed the studies in weak magnetic fields that are of importance for the measurements of the hf splitting for the centers inserted in Si-QWs, which are characterized by the large g-values such as the Fe^+ center and the trigonal erbium-related center. Since the measurements of magnetoresistance were performed without any light illumination and injection of carriers from the contacts, the EDESR effects appear to result from the spin-dependent scattering of spin-polarized holes from the single paramagnetic centers at the edge channels of the S–Si-QW–S sandwich structures. Therefore the resonant positive magnetoresistance data appear to be interpreted here in terms of the interference transitions in the diffusive transport of free holes, respectively, between the weak antilocalization regime ($\tau_S > \tau_\varphi > \tau_m$) in the region far from the ESR of a paramagnetic point defects located inside edge channels and the weak localization regime ($\tau_\varphi > \tau_S > \tau_m$) in the nearest region of the ESR of that defect.

[1] N.T. Bagraev et al., Physica C **468,** 840 (2008).
[2] N.T. Bagraev, et al., Journal of Modern Physics **2**, 256 (2011).

ThP94

Spin-resolved conductance quantization and evidence for zitterbewegung in InAs

Hauke Lehmann [1], Till Benter [1], Toru Matsuyama [1], and Ulrich Merkt [1]

[1] *Universität Hamburg, Institut für Angewandte Physik und Zentrum für Mikrostrukturforschung, Jungiusstraße 11, 20355 Hamburg, Germany*

Spintronics envisions to carry and process information by both, the charge and the spin of the electrons. To this aim reliable generation, manipulation and detection of spin-polarized currents are mandatory. All-electric and all-semiconductor devices would be favorable, and that in the same semiconductor in order to prevent interface scattering and conductivity mismatch. Most appropriate and promising materials are InAlAs/InGaAs hetereostructures with narrow InAs quantum wells. They provide two-dimensional electron gases with high electron mobility and strong spin-orbit interaction of the Rashba type [1, 2]. The intrinsic spin Hall effect spatially separates the spins in quasi one-dimensional InAs quantum wires [3]. However, the electron density has to be reduced to the limit where only the lowest one-dimensional subband is occupied as otherwise intersubband scattering obscures the spin Hall information. This limit can be achieved either by side-gate electrodes that constrict the wires locally or by a top-gate electrode that depletes the whole device homogeneously. We study two-staged double-Y-shaped spin-filter cascades. The first stage acts as a polarizer, the second stage as an analyzer [4]. A straight central wire connects the two stages and allows for tuning the lateral separation of the spin probability density at the entrance of the second filter via the spin precession length. The precession length depends on the top-gate voltage and the strength of an in-plane magnetic field.

This contribution reports on measurements of spin-resolved conductance plateaus of quantum wires and quantum point contacts that our spin filters are composed of. These nanostructures have been prepared separately on the same InAs heterostructures. At a temperature of 5 K all integer and all spin-resolved half-integer plateaus of the conductance in units of $2e^2/h$ are observed up to the highest occupied mode ($N = 16$). Subsequently, we present results on the quantized conductance through top-gated spin-filter cascades that prove quasi-ballistic charge transport in these rather complex devices. Oscillations of the conductances of the second filter's outputs with the strength of an in-plane magnetic field perpendicular to the central wire provide evidence for the so-called zitterbewegung [5, 6]. At the same time they substantiate the interpretation of the conductance imbalance at the second filter's outputs as the consequence of a spin polarization. The period of the oscillations $\Delta B \approx 1$ T and the dependence of their amplitude on the occupation of subbands agree with simple theories [7].

We aknowledge financial support of the Deutsche Forschungsgemeinschaft via grant DFG Me 916/11 and the Graduiertenkolleg 1286.

[1] A. Richter, M. Koch, T. Matsuyama, C. Heyn, and U. Merkt, Appl. Phys. Lett. **77**, 3227 (2000)
[2] D. Grundler, Phys. Rev. Lett. **84**, 6074 (2000)
[3] J. Sinova, D. Culcer, Q. Niu, N. A. Sinitsyn, T. Jungwirth, and A H. MacDonald, Phys. Rev. Lett. **92**, 126603 (2004)
[4] J. Jacob, H. Lehmann, U. Merkt, S. Mehl, and E. Hankiewicz, J. Appl. Phys. **112**, 013706 (2012).
[5] E. Schrödinger, Sitzungsberichte der Preußischen Akademie der Wissenschaft, Physikalisch-Mathematische Klasse **24**, 418 (1930)
[6] J. Schliemann, D. Loss, and R. M.Westervelt, Phys. Rev. Lett. **94**, 206801 (2005)
[7] P. Brusheim and H. Q. Xu, Catching the zitterbewegung, ArXiv (2008)

Influence of spin relaxation and Coulomb correlations on the dynamics of an open quantum dot

Benjamin Baxevanis and Daniela Pfannkuche

I. Institute for Theoretical Physics, University of Hamburg, Germany

Recent experimental advancement allowed for a time-resolved electron charging of quantum dots by a two-dimensional electron gas (2DEG) [1]. We have simulated the charging dynamics for a better understanding of the role of Coulomb interactions and relaxation processes on the time-dependent occupation probabilities of quantum dots.

The quantum dots are assumed to be initially empty and we calculate the time evolution as the gate voltage is instantly changed to enable electron tunneling from the 2DEG into the quantum dots. The charging of a single quantum dot in the sequential tunneling regime is determined by using a master equation for the occupation probabilities. To incorporate many-body effects, the eigenstates of a finite number of correlated electrons in the quantum dot obtained by the exact diagonalization method are taken into account. The electrons in the quantum dot can interact with phonons and nuclear spins which lead to two types of relaxation processes: 1. an orbital relaxation in the dot, which is instantaneous compared to the tunneling dynamics and 2. a spin relaxation with a time scale that can be in the order of the tunneling times. A detailed analysis of the time dependence reveals the complex interplay between Coulomb correlations and different spin-relaxation mechanisms.

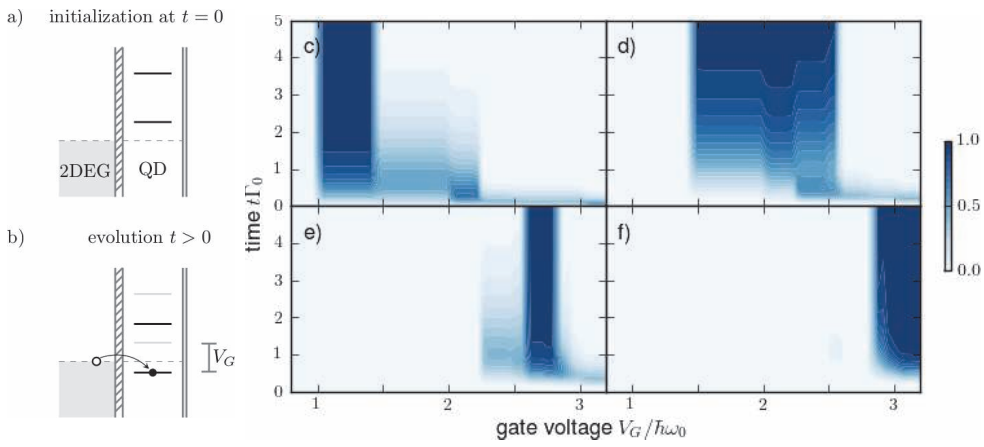

FIG. 1: An initially empty quantum dot coupled to a two-dimensional electron gas (a) is brought out of equilibrium by applying a gate voltage (b). The time-dependent occupation probability for one to four electrons (c-f) depending on the gate voltage reflects the distinct charging times from which the influence of electronic correlations and relaxation can be inferred.

[1] B. Marquardt, M. Geller, B. Baxevanis, D. Pfannkuche, A.D. Wieck, D. Reuter, and A. Lorke, *Nat. Commun.* **2**, 209 (2011)

Heating efficiency of the Mn spin system by photoexcited holes in type-II (Zn,Mn)Se/(Be,Mn)Te quantum wells

J. Debus[1], A. A. Maksimov[2], D. Dunker[1], I. I. Tartakovskii[2], E. V. Filatov[2], D. R. Yakovlev[1,3], A. Waag[4], and M. Bayer[1]

[1] *Experimentelle Physik 2, Technische Universität Dortmund, 44227 Dortmund, Germany*
[2] *Institute of Solid State Physics, RAS, 142432 Chernogolovka, Russia*
[3] *Ioffe Physical-Technical Institute, RAS, 194021 St. Petersburg, Russia*
[4] *Institute of Semiconductor Technology, Braunschweig Technical University, 38106 Braunschweig, Germany*

Diluted magnetic semiconductors (DMS) are regarded as model structures for applications in spin electronics, as they combine electronic semiconductor properties with a strong enhancement of spin-dependent phenomena. In this respect, the magnetic ions, incorporated into II-VI host material, play a key role, since their presence leads to a strong exchange interaction of their localized magnetic moments with the conduction-band electrons and/or valence-band holes giving rise to giant magneto-optical effects. A particular example is the excitonic giant Zeeman shift which can be used by optical techniques to obtain information about the spin system of magnetic Mn^{2+} ions and its coupling to free carriers and the phonon bath [1].

Spin-lattice relaxation of the excited Mn^{2+} ion system into its equilibrium with the phonon bath strongly depends on the Mn ion concentration. Its increase leads to the formation of Mn ion clusters providing fast spin relaxation, and spin diffusion from excited single Mn ions to such clusters, in turn, considerably accelerates the spin-lattice relaxation process of DMS on the whole [2]. While the spin-lattice relaxation dynamics have extensively been studied, an open question is the optical heating efficiency of the Mn spin system in DMS structures. The free carriers with excess kinetic energy (photoexcited or electrically injected) can heat (depolarize) the Mn spin system. There are two different ways for transferring energy and spin from hot carriers to the Mn spin system in DMS heterostructures. An indirect transfer arises from phonons emitted by the free carriers and absorbed by Mn ions. A direct way is due to fast carrier exchange scattering on the localized Mn spins and is characterized by very short transfer times in the picosecond range.

We trace the relationship between the lifetime of photoexcited holes and heating efficiency of the Mn spin system in the (Zn,Mn)Se layer of differently thick $Zn_{0.99}Mn_{0.01}Se$/ $Be_{0.93}Mn_{0.07}Te$ heterostructures under different levels of optical excitation power. The giant Zeeman shift of the exciton providing information about the temporal and spatial distribution of the Mn spin temperature is monitored by use of a time-resolved pump-probe reflectivity measurement. The spin and energy transfer efficiency from the photoexcited holes to the Mn system considerably depends on the thickness of the (Zn,Mn)Se layer. Hereby, the importance of multiple hole spin-flip processes for the Mn heating is demonstrated. The photoexcited hole lifetime in the (Zn,Mn)Se layer is very sensitive to the optical excitation power. This allows us to determine the characteristic time of spin and energy transfer from photoexcited holes to the Mn system to about 20 ps.

[1] J. Debus, A. A. Maksimov, D. Dunker, et al., Phys. Rev. B **82**, 085448 (2010).
[2] A. A. Maksimov, D. R. Yakovlev, J. Debus, et al., Phys. Rev. B **82**, 035211 (2010).

Magnetic order, magnon confinement and propagation in MnTe/ZnTe superlattices

Wojciech Szuszkiewicz [1]*, Bernard Hennion [2#], Sylvain Petit [2], Elżbieta Dynowska [1], Elżbieta Janik [1], Grzegorz Karczewski [1] and Tomasz Wojtowicz [1]

[1] *Institute of Physics PAS, Al. Lotników 32/46, 02-668 Warszawa, Poland*
[2] *Laboratoire Léon Brillouin, CEA-CNRS, CE Saclay, 91191 Gif-sur-Yvette, France*

MnTe with the zinc blende (ZB) structure, obtained with the use of non-equilibrium growth techniques, such as MBE, exhibit an antiferromagnetic (AF) order of type-III at low temperatures (Néel temperature of about 65 K). This kind of magnetic order persists also in MnTe layers in MnTe/ZnTe superlattices (SLs). Because of the distortion of the *fcc* lattice an energy-minimizing magnetic configuration with the unit cell doubling direction along the SL growth axis is realized in such structures. The presence of an interlayer exchange coupling has been reported for selected MnTe/ZnTe SLs previously [1,2] but details of this coupling and an anomalous temperature behavior of features observed by the neutron diffraction were not fully understood. The goal of the current research was to gain more information on the magnetic properties of various SLs mentioned above.

Several MBE-grown, MnTe/ZnTe short period SLs with various numbers of monolayers in magnetic and non-magnetic slabs were analyzed by elastic and inelastic neutron scattering. The first method demonstrated a magnetic coherence in selected SLs for a distance as high as 900 Å at low temperatures. The temperature behavior of spectra observed in our experiments was found to be quite different from that previously reported in the literature. Possible physical mechanisms responsible for observed magnetic correlation in AF-ordered MnTe layers of these SLs are discussed.

In our earlier studies we have determined the collective magnetic excitations (magnons) dispersion in quasi-bulk ZB-MnTe slab at low temperature (in AF-III phase) by inelastic neutron scattering [3]. In current research we have observed not only a long-range coherency between AF layers for ZnTe spacer thickness up to ~25 Å, but also the propagation of collective magnetic excitations (magnons) along the SL-stacking direction in short-period SLs. For large enough ZnTe spacers, on the other hand, the AF MnTe layers are no longer correlated and size quantization effects (confinement) for magnons take place. An experimental evidence of both effects was found in our inelastic neutron scattering measurements, performed with the use of thermal and cold neutron beams. A similarity of theoretically predicted and experimentally observed magnon spectra was also shown. To the best of our knowledge presented results constitute the first clear evidence of magnon propagation and magnon confinement in magnetic SLs that was demonstrated with the use of inelastic neutron scattering technique.

This work was partially supported by the research grant N N202 128639 from Ministry of Science and Higher Education (Poland) and by the European Union within the Neutron Muon Integrated Infrastructure Initiative under contract NMI3-II EC-GA 283883.

* Corresponding author. E-mail address: szusz@ifpan.edu.pl.
# Retired.

[1] J. Lin, J.J. Rhyne, J.K. Furdyna, T.M. Giebultowicz, J. Appl. Phys. **83**, 6554 (1998).
[2] L.E. Stumpe, J.J. Rhyne, H. Kaiser, S. Lee, et. al., J. Appl. Phys. **87**, 6460 (2000).
[3] B. Hennion, W. Szuszkiewicz, E. Dynowska, E. Janik, T. Wojtowicz, Phys. Rev. B **66**, 224426 (2003).

ThP98

Improvement in incomplete persistent spin helix by dynamical Mn-spin polarization in dilute magnetic semiconductors

Takuma Tsuchiya

Division of Applied Physics, Faculty of Engineering, Hokkaido University
Sapporo 060-8628, Japan

Magnetic and spin-related properties of semiconductors have attracted much attention in recent years, because of interests in the physics and spintronics device applications. One of the most important issues of this research field is spatial control of electron-spin polarization. For this purpose, we usually use electron-spin precession comes from spin-orbit effective magnetic fields, or the Rashba and Dresselhaus fields. This type of spin control, however, degrades spatial spin coherence through the Dyakonov-Perel spin relaxation mechanism. [1] For two-dimensional electrons in hetero-junctions and quantum wells grown in the [001] direction, it was found that the spin-coherence length is improved for electron transport along [110] or [1-10] under the persistent spin helix (PSH) condition, i.e., the coefficient α for the strength of the Rashba field proportional to the electron wavelength k, and β for the k-linear term of the Dresselhaus field are the same. [2,3] However, PSH is not really persistent, because of the inherent k^3-term of the Dresselhaus field.

Recently, we have proposed to use dilute magnetic semiconductors to improve the spatial electron-spin coherence. [4] Under electron-spin polarization, spins of Mn impurities are polarized by spin transfer comes from the s-d spin flip scattering. This induced Mn-spin polarization changes the electron-spin precession and improves the electron-spin coherence as a result. This method is expected to be valid even under the PSH condition.

In this study, we perform a numerical simulation for electron-spin transport in a 10 nm [001] $Cd_{0.99}Mn_{0.01}Te$ quantum well at 4.2 K. In this calculation, we take into account electron transport, by means of the Monte Carlo method, the spin transfer to Mn spins, and the electron-spin precession caused by the Mn-spin polarization and the Rashba and Dresselhaus fields. The direction of the electron transport is in [1-10], and the spins of electrons just injected from a ferromagnetic source-electrode are polarized along the z, or [001] axis. We assume that the electron injection starts at the time $t = 0$, and Mn-spins are not polarized for $t \le 0$. In figures below, we show numerical results for $\alpha = \beta$, or the PSH condition. As is shown in Fig. (a), the electron-spin coherence length is limited even under the PSH condition, when the Mn spins are not polarized. On the contrary, it is clear in Fig. (b) that the electron-spin coherence is much improved under sufficiently induced Mn-spin polarization at $t = 100$ ns.

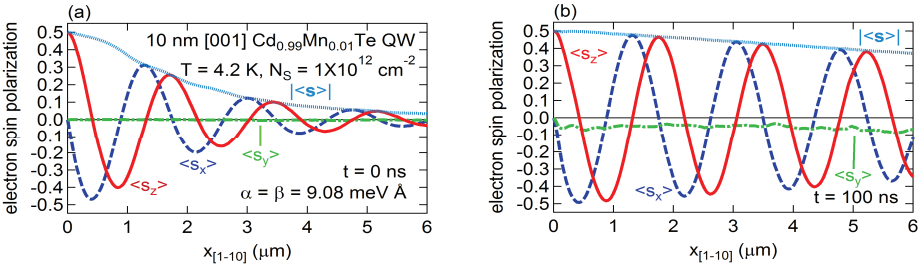

[1] M. I. Dyakonov and V. I. Perel, Sov. Phys. JETP **33**, 1053 (1971).
[2] B. A. Bernevig, J. Orenstein, and S. -C. Zhang, Phys. Rev. Lett. **97**, 236601 (2006).
[3] T. Tsuchiya, J. Phys.: Conf. Ser. **61**, 1191 (2007).
[4] T. Tsuchiya, J. Phys. Soc. Jpn. **81**, 094706 (2012).

Spin Supercurrent in the Canted Antiferromagnetic Phase

Yusuke Hama[1,2], George Tsitsishvili[3], and Zyun. F. Ezawa[2]

[1] *Department of Physics, The University of Tokyo, Tokyo 113-0033, Japan*
[2] *Nishina Center, RIKEN, Wako 351-0198, Japan*
[3] *Department of Physics, Tbilisi State University, Tbilisi 0128, Georgia*

Physics of the bilayer quantum Hall (QH) system is enormously rich owing to the intralayer and interlayer phase coherence controlled by the interplay between the spin and the layer (pseudospin) degrees of freedom. At the filling factor $\nu = 1$ there arises a unique phase, the spin-ferromagnet and pseudospin-ferromagnet phase, showing the intriguing phenomena such as the anomalous behavior of the Hall resistance reported in counterflow and drag experiments [1]. They are triggered by the supercurrent within each layer [2], which are played by the Goldstone mode describing a pseudospin wave.

On the other hand, at $\nu = 2$ the bilayer QH system has three phases, the spin-ferromagnet and pseudospin-singlet phase, the spin-singlet and pseudospin ferromagnet phase, and a canted antiferromagnetic phase (abridged as the CAF phase) [3], depending on the relative strength between the Zeeman gap and tunneling gap.

We have recently analyzed the full details of these Goldstone modes in each phase [4]. The CAF phase is most interesting, where one of the Goldstone modes become gapless, having a linear dispersion relation as the tunneling gap vanishes. It is an urgent and intriguing problem what kind of phase coherence this Goldstone mode develops.

In this research, we show that it is the entangled spin pseudospin phase coherence, and explore the associated phase coherent phenomena. We show that the supercurrent flows within the layer when there is inhomogeneity in the phase field. The Hall resistance is predicted to become anomalous precisely as in the $\nu = 1$ bilayer system in the counterflow and drag experiments. Furthermore, it is shown that the total current flowing the bilayer system is a supercurrent carrying pure spins in the counterflow geometry (Figure 1). All these phenomena occur only in imbalanced bilayer systems [4].

[1] M. Kellog et al., Phys. Rev. Lett. **88**, 126804 (2002); M. Kellog et al., Phys. Rev. Lett. **93**, 036801 (2004).
[2] Z. F. Ezawa et al., Phys. Rev. B **76**, 045307 (2007); Z. F. Ezawa et al., Eur. Phys. J. B (2012) **85**: 270.
[3] L. Zheng *et al.*, Phys. Rev. Lett. **78**, 2453 (1997); V. Pellegrini *et al.*, Phys. Rev. Lett. **78**, 310 (1997); V. S. Khrapai *et al.*, Phys. Rev. Lett. **84**, 725 (2000). J. Schliemann *et al.*, Phys. Rev. Lett. **84**, 4437 (2000).
[4] Y. Hama et al., Eur. Phys. J. B (2012) **85**: 368; Yusuke Hama et al., cond-mat/arXiv:1211.0384; Yusuke Hama et al., to appear in Prog. Theor. Exp. Phys.

Gate-controlled spin precession of drifting electrons in GaAs QW

Yoji Kunihashi[1], Haruki Sanada[1], Hideki Gotoh[1], Koji Onomitsu[1], Makoto Kohda[2], Junsaku Nitta[2], Tetsuomi Sogawa[1]

[1] *NTT Basic Research Laboratories, NTT Corporation, Atsugi, Japan*
[2] *Department of Materials Science, Tohoku University, Sendai, Japan*

We demonstrated gate-controlled spin dynamics during drift transport induced by photocurrent. We observed that the spatial frequency of spin precession depends strongly on the externally applied gate voltages and the transport directions. The experimental results enabled us to determine the tunable range of the Rashba spin-orbit interaction (SOI), which will provide important information as regards extending the spin transport length using the persistent spin helix mode [1].

The sample was a GaAs/AlGaAs-based high-electron-mobility transistor (HEMT), which contained two-dimensional electrons in a 25-nm-wide GaAs quantum well. We deposited a semi-transparent Au Schottky gate on the surface of a chip without touching the InSn ohmic contact formed in one corner of the chip (Fig. 1). A bias voltage applied between these two electrodes enabled us to tune both the electron density and the in-plane electric field simultaneously. The spin dynamics during transport was measured using spatially- and time-resolved Kerr rotation microscopy with a mode-locked Ti:sapphire laser. A circularly polarized pump light generated spin-polarized electrons at a fixed position on the sample; and a linearly polarized probe light, which can be scanned in the QW plane, was used to detect the magneto-optic Kerr effect. Since the Kerr rotation angle is proportional to the spin density at the probe position, we can obtain two-dimensional images of the spin distribution.

Figure 2 shows the gate-voltage dependence of the spatial spin propagation measured in the absence of external magnetic fields. The circularly polarized pump pulses injected electron spins at a certain position under the Schottky gate film, and the resultant photocurrent transported the electrons from the pump position toward the ohmic contact. The oscillations of the Kerr rotation, which lasted over a distance of 100 μm, are attributed to the spin precession induced by a spin-orbit effective magnetic field. When we increased the negative gate voltage from -2.6 to -4.0 V, the spatial frequency of the spin precession decreased. This change is explained by the gate modulation of the Rashba SOI. The demonstrated gate control of drifting spins realized by using a spin-obit effective magnetic field will provide a core technique for manipulating spins in semiconductor spintronics devices.

[1] J. Schliemann and D. Loss, Phys. Rev. B **68**, 165311 (2003).
This work was supported by JSPS KAKENHI (No. 24686004 and 23310097).

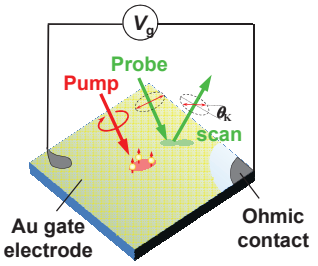

Fig. 1 Schematic image of sample structure and pump-probe measurement.

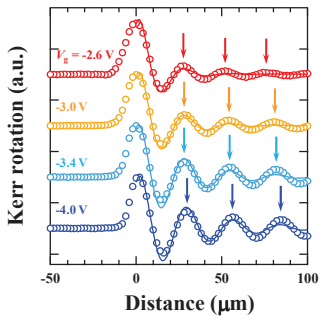

Fig. 2 Gate voltage dependence of space-resolved Kerr rotation (open circles). Solid lines indicate fitting result of empirical functions.

On the origin of ferromagnetism and weak spin interaction in $Zn_{1-x}Co_xO$

Sh. U. Yuldashev[1], H. C. Jeon[1], Y. H. Kwon[1], S. J. Lee[1†], T. W. Kang[1,2], G. Ihm[3] and Kh. T. Igamberdiev[1]

[1] *Quantum-functional Semiconductor Research Center, Dongguk Univ., Seoul 100-715, Korea*
[2] *Department of Physics, Dongguk Univ., Seoul 100-715, Korea*
[3] *Department of Physics, Chungnam National University, Daejeon, Korea*

The ZnO-based diluted magnetic semiconductor (DMS) is a promising candidate for realizing a ferromagnetic semiconductor with high Curie temperature. $Zn_{1-x}Co_xO$ with the Curie temperature higher than room temperature has become a model example for diluted magnetic oxides (DMOs)[1]. However, the magnetic properties of $Zn_{1-x}Co_xO$ reported so far by different research groups are quite contradictory. Some papers found that $Zn_{1-x}Co_xO$ is ferromagnetic at room temperature but the magnetic moment is much smaller than expected. On the other hand, there are also works that report on the absence of ferromagnetism in these materials. Here we present the results of experimental study of the weak ferromagnetism in $Zn_{1-x}Co_xO$. The temperature dependencies of magnetization and thermal diffusivity have been conducted. Diluted magnetic semiconductor $Zn_{1-x}Co_xO$ (x = 0.03) thin films were deposited on Si (100) substrates by using ultrasonic spray pyrolysis. Aqueous solutions of zinc acetate (0.5 mol/l) and cobalt acetate (0.5 mol/l) were used as sources of Zn and Co, respectively. The substrate temperature was set at 400 ^{0}C, and the thickness of $Zn_{0.97}Co_{0.03}O$ films were about 200 nm. The magnetization dependencies on the magnetic field, M(H) curve, and on the temperature, M(T) curve, were measured using a superconducting quantum interference device (SQUID) magnetometer. The thermal diffusivity measurements were made using photothermal method. The structural analysis of Co doped ZnO films were carried out by using an X-ray diffractometer (XRD, Rigaku mini flex).

The XRD pattern for $Zn_{0.97}Co_{0.03}O$ films grown on Si substrates show only peaks related to the wurtzite structure without any secondary phase up to the detection limit of the instrument. Magnetization M(H) measurements show a hysteresis loop which indicates an existence of ferromagnetism in $Zn_{0.97}Co_{0.03}O$. However, the magnetic moment per Co ion is much lower than expected. A comparison of M(T) measured at zero-field-cooled (ZFC) and field-cooled (FC) conditions shows a superparamagnetic like behavior and the blocking temperature is about 130K. Temperature dependence of the thermal diffusivity of $Zn_{0.97}Co_{0.03}O$ shows a pronounced lambda-shaped minimum at 130K, which indicates an existence of a second-order phase transition at this temperature. The low value of phase transition entropy shows that only a small part of Co ions is involved in ferromagnetic ordering. The weak ferromagnetism in $Zn_{0.97}Co_{0.03}O$ with a Curie temperature of 130 K is ascribed to an uncompensated magnetic moment of CoO nanoclusters with radii of about 1 nm existing at the surface[2,3].

This work was supported by the Korea Science and Engineering Foundation through the Quantum-functional Semiconductor Research Center at Dongguk University, and this work was also supported by the National Research Foundation of Korea (NRF) grant funded by the Korean government (MEST) (No.2012-00109, No.2012-0000217, No.2012R1A1A2005772)

[1] R. Janisch,; P. Gopal, and N. A. Spaldin, J. Phys. Condens. Mater. **17**, R657 (2005).
[2] S. H. Park and S. L. Chuang, J. Appl. Phys. **87** 353(2000).
[3] H.-J. Lee, C. Bordel, J. Karel, David W. Cooke, M. Charilaou, and F. Hellman, Phys. Rev. Lett. **110**, 087206 (2013)

† **Email:** leesj@dongguk.edu

Spin-flip Raman scattering of electron and heavy-hole in CdTe quantum well enabled by anisotropic exchange

J. Debus[1], V. F. Sapega[2,3], D. Dunker[1], D. R. Yakovlev[1,2], G. Karczewski[4], T. Wojtowicz[4], and M. Bayer[3]

[1]*Experimentelle Physik 2, Technische Universität Dortmund, 44227 Dortmund, Germany*
[2]*Ioffe Physical-Technical Institute, RAS, 194021 St. Petersburg, Russia*
[3]*Spin Optics Laboratory, St. Petersburg State University, 198504 St. Petersburg, Russia*
[4]*Institute of Physics, Polish Academy of Sciences, 02668 Warsaw, Poland*

The dynamics of carrier spins in low-dimensional semiconductor structures attract remarkable interest due to the possibilities of spin storage and transfer and related information processing. For spin electronic and quantum information applications, understanding of the fundamental interactions between confined carrier spins is essential, since these interactions may limit information handling due to spin relaxation. An essential interaction between two confined carrier spins is the exchange interaction arising from the carrier-carrier Coulomb interaction. The exchange interaction can be divided into isotropic and anisotropic contributions. While the isotropic exchange conserves the total spin of both carriers involved, the anisotropic one leads to spin relaxation. In that context, relaxation due to electron-hole exchange and due to exchange interaction between identically charged carriers need to be considered. The effect of anisotropic exchange interactions between an exciton and a resident electron or hole localized by potential fluctuations in a quantum well (QW) has not been addressed in detail yet.

We report on the experimental study of spin-flip Raman scattering (SFRS) in a $CdTe/Cd_{0.63}Mg_{0.37}Te$ QW [1]. The Raman scattering processes of the electron and heavy-hole spins are compared for resonant excitation of the neutral as well as positively and negatively charged excitons. We demonstrate that the spin-flip scattering of a single electron or hole in a neutral exciton becomes allowed when the exciton symmetry is reduced. As a result of the lifting of the angular momentum conservation, electrons and/or holes can mutually interact via anisotropic exchange. Also, a magnetic field tilted with respect to the QW growth axis can provide an electron- or a hole-SFRS process. The scattering via an acoustic phonon or isotropic exchange supports the symmetry-breaking in order to fulfill the required energy conservation. Variations in the resonant excitation energy and lattice temperature demonstrate that localization of resident electrons and holes controls the Raman process probability and is also responsible for symmetry reduction. We show that the intensity of the electron spin-flip scattering is strongly affected by the lifetime of the exciton complex and in tilted magnetic fields by the angular dependence of the anisotropic electron-hole exchange interaction.

[1] J. Debus, D. Dunker, V. F. Sapega, et al., arXiv:1301.3108 (2013).

Transport properties of thin Bi_2Se_3 flakes in the presence of defects and disorder

S. Dusari[1], P. Meixner[1], A. Mogilatenko[2], J. Sanchez-Barriga[3], L.V. Yashina[4], S. Valencia[3], A. Ünal[3], F. Kronast[3], O. Rader[3] and S. F. Fischer[1]

[1] *Novel Materials, Humboldt Universität zu Berlin, D-12489 Berlin*
[2] *Ferdinand Braun Institut, D-12489 Berlin*
[3] *Helmholtz-Zentrum Berlin für Materialien und Energie, D-12489 Berlin*
[4] *Department of Chemistry, Moscow State University, Russia*

Topological insulators (TIs) are an intriguing class of materials which have electrically insulating states in the bulk and robust conducting states along the edges [1, 2]. One critical issue is the effect of disorder and defects on the helical surface states. We investigate the effects of the controlled combination of dimensionality and designed defect and metallic impurity structures on the transport properties of Bi_2Se_3 TIs.

Here we report on single crystalline exfoliated Bi_2Se_3 flakes grown by Bridgeman technique. The exfoiliated flakes on a SiO_2 substrate are in the thickness range of 10 - 150 nm. Contacts for transport measurements are prepared by micro-laser lithography, followed by Cr/Au (10 nm/40 nm) sputtering and lift-off (Fig. 1 (a)). Samples are characterized using atomic force microscopy and energy-dispersive X-ray spectroscopy. Surface stability and composition are determined using photoemission electron microscopy. Transmission electron microscopy (TEM) analysis is used to identify the dislocation networks on the exfoiliated flakes (extreme case see Fig. 1(b)). Low temperature transport measurements show metallic behavior, and weak-antilocalization (WAL) (Fig. 1(c)) is observed in the virgin state of samples. The dependence of electrical resistivity and carrier concentration of surface and bulk carriers on the defect concentration is investigated.

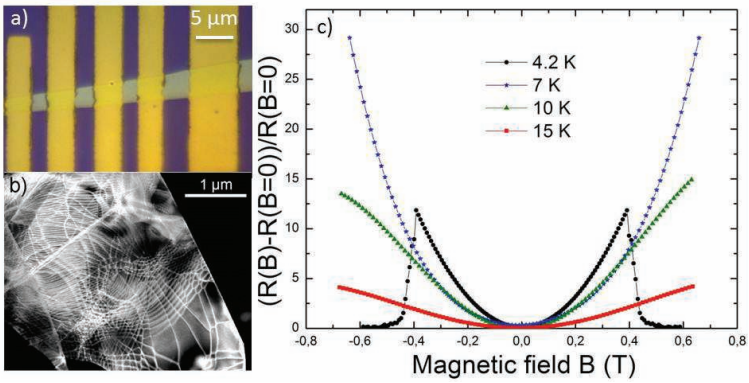

Figure 1: (a) Optical microscope image of a 70 nm thick Bi_2Se_3 device; (b) Annular dark-field TEM image of 20 nm thin exfoliated Bi_2Se_3 flakes, showing the presence of a complex dislocation net appearing after the exfoliation; (c) Magnetoresistance vs. magnetic field applied normally to layers of a Bi_2Se_3 sample at different temperatures. WAL behaviour is observed at 4.2 K.

[1] C. L. Kane, and E. J. Mele, Phys. Rev. Lett. **95**, 1357 (2005).
[2] M. Z. Hasan and J. E. Moore, Annu. Rev. Condens. Matter. **2**, 55-78 (2011).

Surface states of the topological crystalline insulator $Pb_{0.4}Sn_{0.6}Te$

S. Safaei, P. Kacman, R. Buczko
Institute of Physics PAS, al. Lotników 32/46, 02-668 Warsaw, Poland

Lately, it has been shown by angle-resolved photoelectron spectroscopy (ARPES) studies, that IV-VI substitutional alloys, $Pb_{(1-x)}Sn_xTe$ and $Pb_{(1-x)}Sn_xSe$ with Sn content x higher than a critical value, are topological crystalline insulators (TCIs) [1,2]. Very recently, spin-resolved photoelectron spectroscopy (SRPES) allowed the observation of chiral spin textures of (001) surface states in the TCI phase of these alloys [1, 3].

Here, using a tight-binding approach, we study theoretically the nature of surface states in $Pb_{(1-x)}Sn_xTe$. The Sn content x=0.6 assures the band inversion and, thus, the newly discovered TCI phase in the (Pb,Sn)Te material. In this rock-salt TCI, the surface states with nontrivial Dirac-like energy spectrum can form at any surface of the crystal. The number of Dirac points in the surface Brillouin zone corresponds to four L-points. At least two of these Dirac points are topologically protected only at crystal surfaces symmetric about any of {110} mirror planes. These are {n n m} surfaces. We study thus, apart from the (001)-oriented surface, the surface states for the two other surface families, {011} and {111}, in which the mirror symmetry of the crystal's rock-salt structure plays the same role.

For {n n m} surfaces the four L-points in the 3-dimensional Brillouin zone project to four different points in the 2-dimensional Brillouin zone, but only when n and m have the same parity (it means of course that they are both odd numbers). When the parities of n and m are different, the L-points are projected in pairs. In this case, two protected Dirac points appear on the mirror symmetry line in the vicinity of the L-projection. Only for (001) surface there are two such lines and four Dirac points are topologically protected. Indeed, our calculations show that while in (111) $Pb_{0.4}Sn_{0.6}Te$ four single topologically protected Dirac-cones should appear, for the (011) surface states the protection is lifted for two L points projections. In this case, instead of the Dirac points energy gaps for the surface states occur, due to the interaction between the two L valleys.

The spin polarization of metallic surface states in the TCI phase of $Pb_{0.4}Sn_{0.6}Te$ has been studied by calculating the in-plane spin texture along the constant-energy lines of the surface states. For all studied surfaces, (001), (011) and (111), chiral spin textures have been obtained. In the Figure this is shown for the (001) surface, as an example. The blue to yellow color coding indicates the contributions of the cation (yellow) and anion (blue) p orbitals to the wavefunctions.

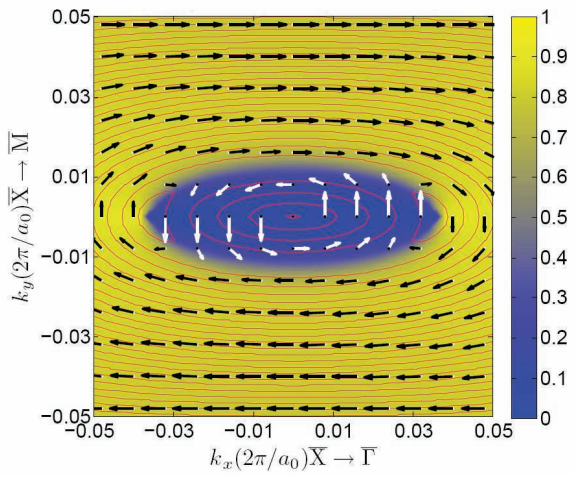

The research leading to these results has received funding from the European Community's 7th Framework Programme [FP7/2007-2013] under grant agreement n° 215368, the European Regional Development Fund through the Innovative Economy grant (POIG.01.01.02-00-108/09), and the Polish National Science Centre (NCN) Grant No. 2011/03/B/ST3/02659.

References

[1] Su-Yang Xu, *et al.* Nat. Commun. **3,** 1192 (2012)

[2] P. Dziawa, *et al.* Nat. Mater. **11**, 1023 (2012)

[3] B. Wojek, *et al.* arXiv:1212.1783 [cond-mat.mtrl-sci]

Inducing topological order in dirty wires: Majorana fermions from scattering

I. Adagideli[1], M. Wimmer [2], and A. Teker[1]

[1] *Faculty of Engineering and Natural Sciences, Sabanci University, Orhanli-Tuzla, Istanbul, Turkey*
[2] *Instituut-Lorentz, Universiteit Leiden, P.O. Box 9506, 2300 RA Leiden, The Netherlands*

We focus on inducing topological state from regular, or irregular scattering in (i) p-wave superconducting and (ii) proximity coupled Rashba wires [1]. We find that while disorder is detrimental to topological state in p-wave wires, we find that it can induce topological state in Rashba wires contrary to common expectations. We find that the total phase space area of the topological state is conserved for long disordered wires, and can be even increased in an appropriately engineered superlattice potential.

[1] I. Adagideli, M. Wimmer, A. Teker arXiv:1302.2612 (2013).

ThP106

Manifestation of the properties of a topological insulator in semiconducting $Bi_{1-x}Sb_x$ nanowires

A. Nikolaeva[1,2], L. Konopko[1,2], T. Huber[3], I. Popov[1], N. Kablukova[4]

[1] *D. Ghitu Institute of Electronic Engineering and Nanotechnologies, Academy of Sciences, Academiei str. 3/3, MD-2028 Chisinau, Republic of Moldova*
[2] *International Laboratory of High Magnetic Fields and Low Temperatures, Wroclaw, Poland*
[3] *Department of Chemistry, Howard University, 500 College St. N.W., DC 20059 Washington, U.S.A.*
[4] *Herzen State Pedagogical University, 6 Kazanskaya st., 191186, St. Petersburg, Russia*

This paper reports a series resistance and magnetoresistance measurements made on single crystal $Bi_{1-x}Sb$ nanowires in semiconductor region with diameters ranging from 100 nm to 1000 nm.

It is known that $Bi_{1-x}Sb_x$ alloys demonstrated the topological nature of surface state. The surface states of pure Bi and Sb have been intensively studied experimentally and theoretically [1-3]. The first 3D topological insulator to be identified experimentally was the semiconducting alloy $Bi_{1-x}Sb_x$, whose unusual surface bands were mapped in an angle-resolved photo emission spectroscopy (ARPES).

Single crystal $Bi_{1-x}Sb_x$ nanowires in glass cover are the most suitable object for studied of the influence dimensional and surface state on electron transport.

Individual monocrystalline Bi-17at%Sb nanowires in glass capillary with diameter 100nm – 3mkm were prepared by liquid phase casting, using the improved Ulitovsky methods [4, 5]. Multiple horizontal zone recrystallizations of the nanowires were used for the homogenization and to improve their structural perfection.

Measurement of the resistance have been carried out over a wide range of temperatures (2-300K) and magnetic field up to 14T. The temperature dependences of the zero-field resistivity and the longitudinal magneto- coefficient of the semiconductor $Bi_{1-x}Sb_x$ nanowires show the sensitive to wire diameter.

Analyses of the resistance dependences R(T) on the wire diameters indicates that at low temperatures in the thin Bi-17at%Sb wires a sharp deviation from exponential temperature behavior resistance R(T) characteristic of bulk semiconductor is observed. In order to explain the experimental results of R(T), we need to take the surface state into account. According to the this deviation correspond to a considerable influence of a metalized well conducting near surface layer formed from the surface states arising through a spin- orbital Rashba interaction in nanowires. We measure the field dependences resistance R(H) at 1.5- 4.2 K and observed quantum oscillations only in thin Bi-17at%Sb wires in longitudinal and transverse directions. This fact indicates a essential contribution of surface states in electron transport a semiconducting $Bi_{1-x}Sb_x$ nanowires.

This work was supported by STCU# 5373, by The Ministry of Education and Science of Russian Federation, project 14.B37.21.0891.

[1] L. Fu and C.L. Kane. Phys. Rev. B **6**, 045302 (2007).
[2] P. Hoffman, Prog. Surf. Sci. **81**, 191 (2006).
[3] M.Z. Hasan, C.L. Kane. Rev. Mod. Phys. **82**, 3045 (2010).
[4] N.B. Brand, D.V. Gitsu, A.A. Nikolaeva, and Ya.G. Ponomarev, J. Exp. Teor. Phys. **72**, 2332 (1977).
[5] A. Nikolaeva, L. Konopko, T. Huber, P. Bodiul, I. Popov. J. of Solid State Chem. **193**, 71 (2012).

Transport studies on ultrathin epitaxial Bi_2Se_3 Topological Insulator epilayers

Y. Arango [1], J. Kampmeier[1], T. Merzenich[1], C. Weyrich[1], G. Mussler [1], D. Grützmacher[1], and T. Schäpers [1]

[1] *Peter Grünberg Institut (PGI-9), Forschungszentrum Jülich, 52425 Jülich, Germany*

The so-called "*next generation*" of topological insulator (TI) materials including Bi_2Se_3, Bi_2Te_3 and Sb_2Te_3 became a rich playground for studying the exotic electronic structure predicted in 3D TI [1]. The surface state electronic transport is a key tool for exploring the predicted novel phenomena and feasible applications of TIs. Despite considerable advances, the suppression or at least decoupling of the residual bulk states from the surface states as well as the ability to tune the carrier density remains an experimental challenge. Thin film technology potentially offers pathways to achieve these goals, hence, in the present study molecular beam epitaxy (MBE), was employed to grow Bi_2Se_3 films on Si (111) substrates with thickness down to 10 nm [2]. Subsequently, Hall bar structure based devices in the micrometer scale have been fabricated and the respective transport studies reveal an n-type carrier concentration around 2.3 x 10^{13} cm^{-2}, typical for a significant bulk contribution of charge carriers next to the surface state transport. Nonetheless, the pronounced weak antilocalization (WAL) feature observed in Fig. 1 for conductance measurements, as well its angular dependence in Fig. 2 renders immunity to localization generally caused by the transport of non trivial metallic states in this material. The fitting of the WAL feature to the low field Hikami-Larkin-Nagaoka (HLN) model [3] indicates a mixing or coupling of bulk and surface states in a single transport channel. Moreover, the fit excludes any possible decoupling of the channels via the reduction in the phase coherence time as the temperature increases [4]. In order to reduce the effect of the high bulk electronic concentration in the Bi_2Se_3 thin films, an effective tuning of the carrier densities through the top-gate voltage is evaluated by testing $LaLuO_3$, and ZrO_2 as dielectric materials.

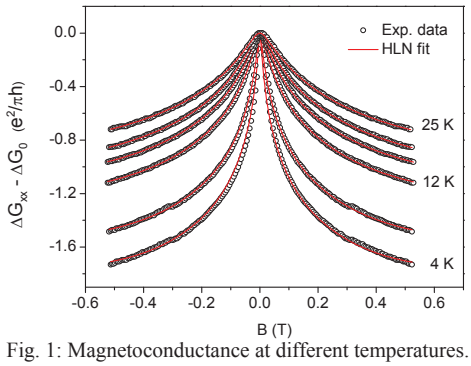

Fig. 1: Magnetoconductance at different temperatures. Fit to the HLN model (solid lines).

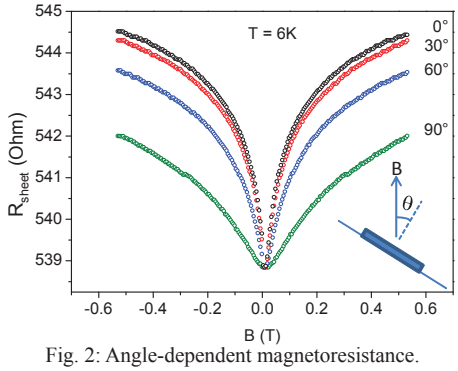

Fig. 2: Angle-dependent magnetoresistance. Inset: Angle definition in the experiment.

[1] L. Fu, C. L. Kane and E. J. Mele, Phys. Rev. Lett. **98**, 106803 (2007).
[2] J. Krumrain, G. Mussler, S. Borisova, T. Stoica, L. Plucinski, C. M. Schneider, and D. Grützmacher, J. Cryst. Growth **324**, 115 (2011).
[3] S. Hikami, A. I. Larkin, and Y. Nagaoka, Progress of Theoretical Physics **63**, 707 (1980).
[4] H. Steinberg, J. –B. Lalöe, V. Fatemi, J. S. Moodera, and P. Jarillo-Herrero, Phys. Rev. B **84**, 233101 (2011).

Transport on the surface of a topological insulator

V. Vargiamidis*, P. Vasilopoulos*, and Marcos R. S. Tavares**

*Department of Physics, Concordia University,
7141 Sherbrooke West, Montreal, Quebec, Canada H4B 1R6

**Centro de Ciéncias Naturais e Humanas, Universidade Federal do ABC,
Santo André, SP 09210-170, Brazil

We evaluate the dc and ac conductivities of a two-dimensional topological insulator including a mass term m_z in its Hamiltonian[1]. Starting with a Kubo formula we derive an expression for the dc Hall conductivity σ_{yx} valid for finite temperatures using the analytically derived eigenfunctions and eigenvalues. At zero temperature this expression gives the dc *half-quantum Hall conductivity*[1], $\sigma_{yx} = (m_z/|m_z|)(e^2/2h)$ *in the absence of a magnetic field*. Corrections due to scattering by impurities are taken into account. The longitudinal component σ_{xx} is evaluated as well. Further, we evaluate these conductivities for finite frequencies ω and show that in addition to a Drude term we have logarithmic, frequency-dependent corrections. We also evaluate the power absorption spectrum $P(\omega)$, pertinent to optical experiments, using the linear-response expression $P(\omega) = (E^2/2) \times \mathrm{Re}\{\sigma_{xx}(\omega) + \sigma_{yy}(\omega) + i\sigma_{yx}(\omega) - i\sigma_{xy}(\omega)\}$ with E the electric field of light. The sum $\sigma_{xx}(\omega) + \sigma_{yy}(\omega) = 2\sigma_{xx}(\omega)$ varies as $(E_F^2 - m_z^2)\tau / [\hbar E_F(1+\omega^2\tau^2)]$ whereas the real part of $i\sigma_{yx}(\omega)$ $(= - i\sigma_{xy}(\omega))$ surges upward at a frequency $\omega = 2|m_z|/\hbar$ and its imaginary part drops drastically, see Fig. 1(a). Accordingly, as shown in Fig. 1(b), $P(\omega)$ increases very sharply at this frequency.

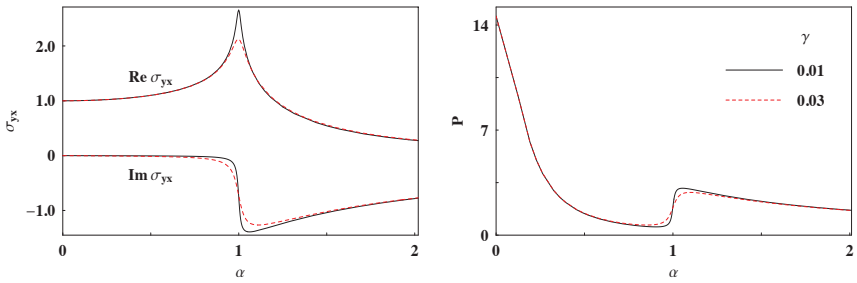

Fig. 1. Left panel. The real (upper) and imaginary (lower) part of $\sigma_{yx}(\omega)$ versus $\alpha = \hbar\omega/2|m_z|$ in units of $e^2/2h$. The solid (dashed) curves are for $\gamma = 0.01$ ($\gamma = 0.03$), $\gamma = \Gamma/2|m_z|$. Notice its dc limit $\sigma_{yx}(0) = e^2/2h$. Right panel. Power spectrum $P(\omega)$ vs α, in units of $E^2 e^2/2h$, for two values of γ with Γ the width of the energy levels, a relaxation time $\tau = 10^{-13}$ s, a Fermi level $E_F = 100$ meV, and $m_z = 0.2E_F$.

1. X.-L. Qi *et al*., Rev. Mod. Phys. **83**, 1057 (2011).

Magnetoresistance studies in GaAs/AlGaAs single quantum wells with different impurity densities

Eddy P. Rugeramigabo [1,2], Lina Bockhorn[1] and Rolf J. Haug[1]

[1] *Institut für Festkörperphysik, Abt. Nanostrukturen, Leibniz Universität Hannover*
[2] *QUEST Centre for Quantum Engineering and Space-Time Research, Leibniz Universität Hannover*

GaAs/AlGaAs heterostructures with GaAs single quantum wells have been grown using the molecular beam epitaxy (MBE) technique. The two dimensional electron gas (2DEG) in the quantum well is provided by Si δ-doping in AlAs/GaAs barriers on both side of the quantum well. The Si-doping is separated from the quantum well by 70 nm thick spacers. All grown samples have the same layer sequence but with different impurity densities in the quantum wells. For each sample, the quantum well has been intentionally doped with a different Si doping density. The quantum well of the reference sample has been left undoped, exhibiting only the unintentional background doping of the growth chamber.

Transport measurements have been performed on the samples for temperatures ranging from 0.4 K to 30 K. For the reference sample, we found a high electron mobility of 2 x 10^6 cm^2 V^{-1} s^{-1}. Upon doping, the electron mobility decreases to 5 x 10^4 cm^2 V^{-1} s^{-1} and 1 x 10^4 cm^2 V^{-1} s^{-1} for samples with additional doping of 5 x 10^{15} cm^{-3} and 4 x 10^{16} cm^{-3}, respectively. The electron mobilities show quite different temperature dependences.

All samples exhibit negative magnetoresistances at low magnetic fields and low temperatures. For increasing doping density weak localization [1,2] dominates more and more the magnetoresistance. In addition a parabolic magnetoresistance is observed where the curvature of this negative parabolic part of the magnetoresistance decreases with increasing doping density. This parabolic magnetoresistance is attributed to electron-electron interactions [3]. With increasing temperatures, the peak of the weak localization for the doped samples decreases continuously until it disappears. At the same time, the curvature of the negative parabolic magnetoresistance which has been decreasing with increasing temperature becomes positive. This behavior is in contrast to the temperature dependence of the magnetoresistance for the reference sample. In contrary to the doped samples, the curvature of the negative parabolic magnetoresistance decreases with increasing temperature, but it stays negative.

The differences in the magnetoresistance curves are analyzed in detail in order to study the direct influence of the impurity density on the magnetotransport in 2DEG systems.

[1] S. Hikami, A. I. Larkin, and Y. Nagaoka, Prog. Theor. Phys. **63**, 707 (1980)
[2] H.-P. Wittmann and A. Schmid, J. Low Temp. Phys. **69**, 131 (1987)
[3] M. A. Paalanen, D. C. Tsui and J. C. M. Hwang, Phys. Rev. Lett. **51**, 2226 (1983)

Bias controlled spin polarization in two dimensional electron and hole gases

V.O.Gordo [1], H.V.A. Galeti [2], L.K.S.Herval [1], Y. Galvão Gobato [1], M.J.S.P.Brasil [3], M. Henini [4], R.J.Airey[5]

[1] Physics Department, Federal University of São Carlos, São Carlos, Brazil
[2] Department of Eletrical Engineering, Federal University of São Carlos, São Carlos, Brazil
[3]Gleb Wataghin Physics Institute, UNICAMP, Campinas, Brazil
[4]School of Physics and Astronomy, University of Nottingham, Nottingham, U.K
[5]Department of Eletronic and Eletrical Engineering, University of Sheffield, Sheffield,U.K

Polarization-resolved magneto-luminescence and magneto-transport measurements have been performed on two-dimensional electron (2DEG) and hole gases (2DHG) in n-type resonant tunneling devices. By varying the applied bias and the laser intensity, it is possible to change significantly the concentration of electrons and holes through the device. Therefore, the optical emission from quantum well (QW) is bias controlled and can comprise neutral and charged excitons, also known as trions. The contact-layer optical emissions comprise indirect transitions from the two-dimensional electron- (2DEG) and hole- gases (2DHG) created next to the barriers. These 2D gases have voltage controlled g-factors and carrier densities. Under high magnetic fields, these 2D gases are usually strongly spin-polarized and can contribute to the polarization of the carriers in the QW by injecting preferentially polarized carriers at different applied biases. The QW circular polarization degree for charged and neutral excitons present higher values, up to -88% at 15T for low bias voltages. The 2DHG-e emission also presents a high negative circular polarization similar to the QW emission indicating that the spin polarization of carriers in the QW could be partially defined by the spin-polarization holes at the accumulation layer which tunnels into the QW. This spin injection seems to be very efficient at lower voltages. However, under higher voltages, other effects probably contribute to the spin polarization of carriers in the QW. Particularly, the 2DEG-h emission is observed after electron resonance and its polarization degree is higher than the QW polarization degree which indicates some spin polarization loss on the tunneling processes probably due to the efficient scattering processes in this voltage region.

[1] Y. Galvão Gobato et al , Appl. Phys. Lett **99**, 233507 (2011).
[2] V. O Gordo et al, Nanoscale Research Lett. **7**, 592 (2012).

Anomalous magnetoresistance in (110) quantum wells

L.E. Golub

Ioffe Physical-Technical Institute, Russian Academy of Sciences, St. Petersburg, Russia

After intensive study of spin-dependent phenomena in traditional two-dimensional systems in the last decade, the attention of semiconductor spintronic community is shifting now to specially designed structures where more subtle spin effects can be observed. One of the most interesting systems are symmetrical quantum wells (QWs) grown in [110] direction which have unusual spin properties due to absence of relaxation for spin component oriented along the growth direction. However, the symmetrically doped (110) QWs shown in Fig. 1 are symmetric only in average with the domains of the nonzero electric field produced by non-mirror symmetric impurity distributions in the doping layers equally remoted from the QW center. These electric fields result in a random spin-orbit coupling via the Rashba effect and, in turn, in a finite spin-relaxation time τ_s.

Electron spin properties can be probed in both optical and transport experiments, and one of the powerful tools for its study is measurements of the low-temperature resistance in classically-weak magnetic fields. It is well known that the magnetoresistance is caused by *weak localization* effect consisting in the interference of electron scattering paths. In this work we develop a theory for the low-field magnetoresistance in symmetrically doped (110) QWs. Analytical expressions for the magnetoconductivity are obtained with account for the spin relaxation processes in the random field of impurities. In Fig. 1 the magnetoconductivity is shown for different values of the spin relaxation rate. The magnetic field is given in units of the 'transport' field $B_{tr} = \hbar/(2el^2)$, where l is the electron mean free path. The minimum is present in the magnetoconductivity due to spin relaxation demonstrating antilocalization effect. Figure 1 demonstrates a shift of the minimum to the fields $B > B_{tr}$ at $\tau/\tau_s > 0.2$, where τ is the transport relaxation time. The dashed lines represent the results obtained in the 'diffusion' approximation where the traditional Hikami-Larkin-Nagaoka expression is valid. Comparison with the exact calculation shows that for $\tau/\tau_s \geq 0.1$ the diffusion approximation is inadequate even at low fields, and one should use exact expressions for fitting of the experimental data. To summarize, we demonstrated that the random spin-orbit coupling affects strongly the anomalous magnetoconductivity, and this can be observed in experiments.

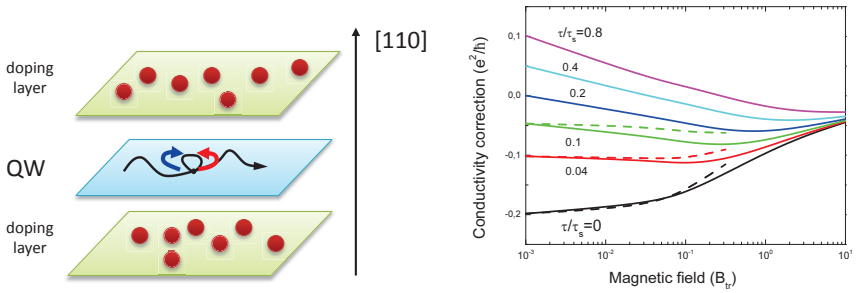

Figure 1: Left: Symmetrically doped (110) QW structure. Electrons propagating in the QW plane interfere due to the presence of self-intersecting paths. Non-mirror symmetric positions of impurities in the doping layers lead to spin relaxation. Right: Magnetoconductivity in symmetrically doped (110) QWs at different values of the spin relaxation time.

Effect of a tilted magnetic field on radiation-induced zero resistance states and resistance oscillations in a 2DEG

Jesus Inarrea [1], and Gloria Platero [2]

[1] *Escuela Politécnica Superior, Universidad Carlos III, Leganes, Madrid,28911, Spain*
[2] *Instituto de Ciencia de Materiales, CSIC, Cantoblanco, Madrid, 28049, Spain*

Recent experiments [1] show an unbalanced quenching of the radiation-induced resistance oscillations for increasing tilted magnetic field and tilt angle. Another effect is that this increasing field makes the zero resistance states to disappear. We present a theoretical model which explains these results based in a common physical mechanism. The theoretical framework is the microwave-driven electron orbits model [2]. According to the model the key point is that the parallel component of the tilted magnetic field, ($B\,sin(\theta)$), makes the electron confinement stronger in the z-direction (perpendicular to the 2DEG). As a result the interaction of radiation-driven electrons with acoustic phonons increases making much easier the release of radiation energy to the lattice. The main outcome of this is that the radiation-induced resistance oscillations are increasingly damped. The calculated results are in good agreement with experiments. The understanding of this behavior will allow to control the transport properties in a MW irradiated Hall bar.

[1] A. Bogan et al., Phys. Rev. B, 86, 235305 (2013).
[2] Jesus Inarrea et al., Phys. Rev. Lett., 94, 016806 (2005).

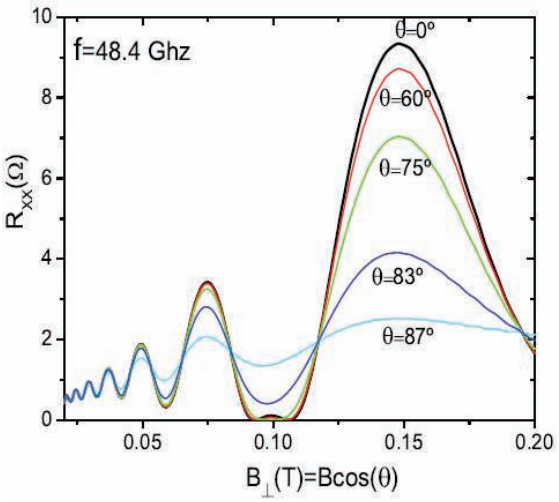

Figure 1

Self-sustained oscillations in coupled nanomechanical resonators

Marta Prada[1], and Daniela Pfannkuche[1]

[1] *I. Institut für Theoretische Physik, Universität Hamburg, Jungiusstr. 9, 20355 Hamburg, Germany*

We investigate theoretically the dynamics of a coupled nanomechanical oscillator consisting of moveable metallic grains integrated between two contacts (see Fig. 1). This double pendula structures in the nanoscale –also coined electron shuttles [1]– can be operated in radio frequencies (RF), possess a set of resonance frequencies, and reveal Coulomb blockade, even at room temperature [2]. Mechanically assisted charge transfer becomes possible as the mechanical motion of the shuttles is excited. This motion changes the capacitance of the islands, affecting the current through the system, which can in turn further excite the response in certain regions of the parameter space spanned by frequeny and intensity of the excitation. We explore these regions of parametric instabilities using a weak RF excitation and find self-sustained, greatly amplified oscillations in the response, suggesting a practical scheme for the realization of a vast nuber of future aplications in the nanoscale. In the absence of a DC bias, parametric instabilities induce spontaneous symmetry breaking with a subsequent observable direct current [3, 4]. The direction of the current is defined by the phase shift between parametrically excited mechanical oscillations and the RF signal [5].

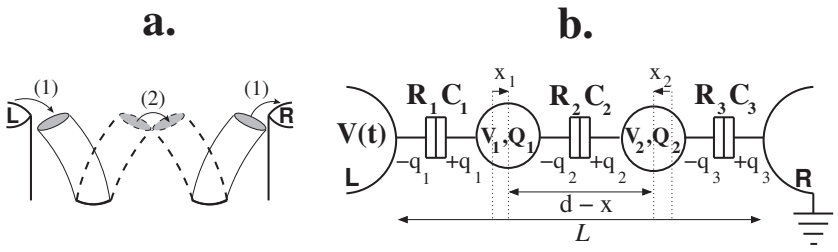

Figure 1: *a. The flexural mode which originates an efficient DC current has the center of mass at rest. b. Circuit representation: two metallic islands are capacitively coupled to each other and to both electrodes, L and R, which are connected to an external voltage source, $V(t)$. The islands are separated by a distance d in equilibrium, and their relative displacement is given by $x(t) = x_1 - x_2$. Their mutual capacitances C_i and the resistances R_i depend on this quantity, affecting the electrostatics of the device.*

[1] Y. L. Gorelik, A. Isacsson, M. V. Voinova, B. Kasemo, R. I. Shekhter, and M. Jonson , *Phys. Rev. Lett.* **80**, 4526–4529 (1998).
[2] C. Kim, M. Prada and R. H. Blick, *ACS Nano*, **6**, 651 (2012).
[3] C. Kim, J. Park, and R. H. Blick, *Phys. Rev. Lett.*, **105**, 067204 (2010).
[4] K.-H. Ahn, H. . Park, J. Wiersig, and J. Hong, *Phys. Rev. Lett.*, **97**, 216804–216807 (2006).
[5] M. Prada, and G. Platero, *Phys. Rev. B*, (2012).

Edge magnetoplasmons in strongly non-uniform magnetic field

I. A. Larkin[1], O. G. Balev[2]

[1]*Department of Physics, Minho University, Braga 4710-057, PORTUGAL*
[2]*Departamento de Física, Universidade Federal do Amazonas, 69077-000, BRAZIL*

We have theoretically studied two-dimensional electron gas (2DEG) placed in a strong laterally non-uniform magnetic field, which appears due to ferromagnetic film, see Fig 1. We have found, that in this case 2DEG experiences static charge redistribution that strongly depends on presence and configuration of the gates on the surface of a heterostructure [1].

Also, it is shown that lateral inhomogeneity of a strong magnetic field allows itself "magnetic gradient" or "magnetic-edge" magnetoplasmons due to complex lateral structure of magnetic field gradient. This mechanism is different from usual "density gradient" edge magnetoplasmons [2, 3]. We have investigated two families of different-chirality modes localized near the edge of the magnetic film. They are characterized by different direction of magnetoplasmon propagation that is determined by the sign of the gradient of magnetic field in the region where pertinent family of the modes is mainly localized.

Spectrum of plasmons is sensitive to preparation of a heterostructure surface. We have analyzed in detail influence of the electrostatic boundary conditions near the edge of metal gate in particular, due to ferromagnetic film. We have found, that gate always screens out long range Coulomb interaction and kernel of the integral equation that determine dispersion of magnetoplasmons remains finite. Therefore, contrary to the previous findings [2,3] none of the fundamental state has logarithmically large phase velocity at small wave vectors.

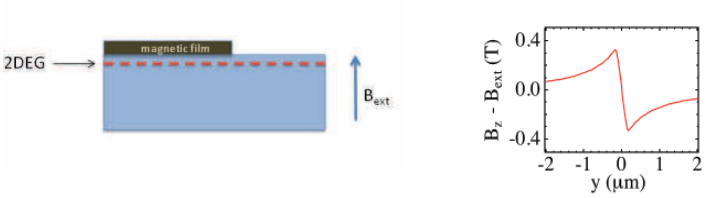

Fig. 1 Heterostructure layout and profile of the magnetic induction at the edge of the ferromagnetic film in perpendicular external field.

[1] I. A. Larkin, J. H. Davies, *Phys. Rev. B* **52**, 5535, (1995).
[2] I. L. Aleiner, L. I. Glazman *Phys. Rev. Lett.* **72,** 2935 (1994)
[3] O. G. Balev and P. Vasilopoulos, *Phys. Rev. Lett.* **81**, 1481 (1998)

Shubnikov - de Haas effect and spin-splitting in tilted magnetic fields in wide quantum well

Ivan Larkin[1], S. Ujevic[2], S. Wiedmann[3,4], N. C. Mamani[3], G. M. Gusev[4], A. K. Bakarov[5], and J. C. Portal[3,4,6]

[1]Department of Physics, Minho University, Braga 4710-057, PORTUGAL
[2]Departamento de Ciências Exatas - EEIMVR, Universidade Federal Fluminense, 27255-125, Volta Redonda, RJ, Brasil
[3]LNCMI-CNRS, UPR 3228, BP 166, 38042 Grenoble Cedex 9, France
[4]Instituto de Física da Universidade de São Paulo, CEP 05315-970, São Paulo, SP, Brazil
[5]Institute of Semiconductor Physics, Novosibirsk 630090, Russia
[6]Institut Universitaire de France, 75005 Paris, France

Bilayer two-dimensional electron system in double quantum wells demonstrated oscillations of the symmetric–antisymmetric energy gap in the presence of the in-plane magnetic field [1] which has been attributed to Aharonov-Bohm interference effect between cyclotron orbits in different layers [2]. The charge distribution in a wide single quantum well is more subtle than the one in the double quantum well. Here the Coulomb repulsion of the electrons in the well leads to a soft barrier inside the well, which in turn results in a bilayer electron system. Applying of the in-plane magnetic field can also lead to the charge redistribution inside of the well and distortion of the circular Fermi contour.

In the present work we have measured and calculated Shubnikov – de Haas effect in wide wells in the tilted magnetic field. We resolve spin-splitting that propotional to the total magnetic field.

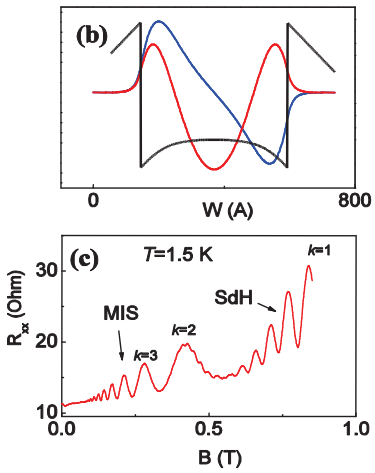

(b) Calculated confinement potential profile of our wide quantum wells and wave functions of electrons for the first two subbands.

(c) The magnetoresistance R_{xx} as a function of the magnetic field at T=1.5 K. Magnetoresistance exhibits MIS oscillations together with SdH oscillations.

[1] G. M. Gusev, C. A. Duarte, T. E. Lamas, A. K. Bakarov, and J. C. Portal, Phys. Rev. B **78**, 155320 (2008)
[2] V.M.Yakovenko, B.K.Cooper, Physica E **34**, 128 (2006); J. Hu and A. H. MacDonald, Phys. Rev. B **46**, 12554 (1992).

High-accuracy (0.1±0.2 nm) analysis of GaAs/$Al_xGa_{1-x}As$ layers using beam-exit cross-sectional polishing and selective etching

Alexander J. Robson [1], Ilya Grishin [1], Robert J. Young [1], Ana M. Sanchez [2], Oleg V. Kolosov [1] and Manus Hayne [1]

[1] *Department of Physics, Lancaster University, Lancaster, LA1 4YB, UK*
[2] *Department of Physics, University of Warwick, Coventry, CV4 7AL, UK*

Microscopy of semiconductor heterostructures on the sub-nm scale is presently only possible with techniques such as transmission electron microscopy (TEM), cross-sectional scanning tunneling microscopy and atom probe tomography which are expensive, of limited availability and require considerable expertise. We report a novel sample preparation technique, which, when combined with scanning probe microscopy (SPM), has the potential to provide easy access to high-resolution microscopy of semiconductor nanostructures [1].

A test structure with a variety of GaAs/$Al_xGa_{1-x}As$ layers (Fig. 1) was first prepared with beam-exit cross-sectional polishing (BEXP) [2], a modified form of cross-sectional Ar^+-ion polishing in which the Ar^+ beam impinges on the side of a sample and exits at the surface at a small angle. BEXP (i) enables cross-sections to be produced with roughness on the atomic scale close to the sample surface where nanostructures are located, and (ii) 'stretches' the vertical scale. The polished sample was then treated with a citric-acid/hydrogen peroxide selective chemical etch to introduce material-dependent topology on the polished surface so that the layer structure could be measured using tapping mode atomic force microscopy.

Fig. 1 compares composite images of the sample produced by this method with TEM. All layers are visible with both techniques (even at 1 nm thickness), with better contrast for $Al_xGa_{1-x}As$ layers that are thicker or have higher Al content, as might be expected. For a quantitative analysis SPM measurements were made using 750 nm scans at 512 samples per line. The thicknesses of 167 different layers were measured, and the results were compared with TEM. For layers <20 nm the difference between SPM and TEM was just 0.1±0.2 nm.

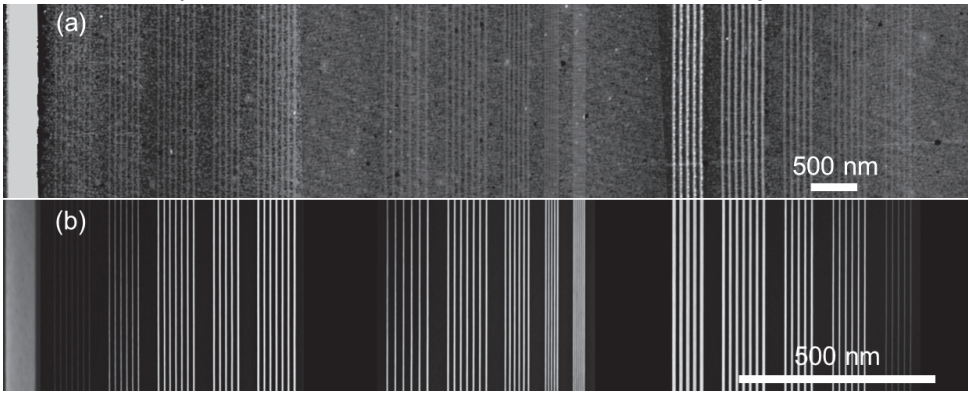

Fig. 1: Composite (a) BEXP-SPM and (b) TEM image of the GaAs/$Al_xGa_{1-x}As$ structure. From left to right: 75 nm AlAs barrier layer, 3 nm $Al_xGa_{1-x}As$ composition x varying layers (0.2 to 1), 3 nm AlAs layers with different GaAs spacing, and differing thickness AlAs and GaAs layers (from 8.5 to 1 nm). The scale bars are different due to the shallow angle of the BEXP cross-section.

[1] A. Robson *et al*., submitted to Appl. Mater. Interfaces.
[2] O.V. Kolosov, I. Grishin and R. Jones, Nanotechnology **22**, 185702 (2011).

Electron beam collimation and non-ohmic resistance addition in quasi-ballistic magnetic barriers

Tudor Chirila [1], Mihai Cerchez [1], Bernd Schüler[1] , Thomas Heinzel [1], Hans W. Schumacher[2], and Klaus Pierz[2]

[1] Condensed Matter Physics Laboratory, Heinrich-Heine-University Düsseldorf, Universitätsstr. 1, D- 40225, Düsseldorf, Germany.
[2] Physikalisch-Technische Bundesanstalt, Bundesallee 100, D-38116 Braunschweig, Germany.

Magnetic barriers (MBs) [1] are localized magnetic field structures that produce a magneto-resistance in two-dimensional electron gases (2DEGs) due to electron trajectories being deviated by the Lorentz force. They can be generated by the perpendicular component of the stray field under the edge of a ferromagnetic film magnetized along the electron transport direction. Their strength can be tuned by in plane magnetic fields which vary the magnetization of the film. In the open regime, MBs represent filters which transmit only a certain interval of angles of incidence. One would expect that all electrons get reflected at sufficiently strong MBs, which would lead to an infinite resistance. However, this magnetoresistance is limited by both scattering which helps electrons pass through the barrier and by $E \times B$ drift at the edges of the 2DEG. [2]

Here, we show theoretically and experimentally that MBs represent electron collimators, i.e., the selective transmission of certain angles of incidence transforms into a collimated beam of ejected electrons. This manifests itself in a non-ohmic addition of the resistance of two MBs in series. Two regimes can be distinguished: at open barriers, the electrons are emitted homogeneously along the barrier and move in a preferred direction. At closed barriers, a collimated electron beam is ejected at one edge of the Hall bar.

Devices feature a set of samples containing two MBs of opposite polarity in series, placed on top of a Hall bar etched into a GaAs/AlGaAs heterostructure. The size of the magnetic structure is comparable to the mean free path of the electrons, which places the structure in the quasi-ballistic regime [3]. The MB amplitude is tuned by an external magnetic field, and the electron density can be varied by a metallic top gate.

The collimated beam ejected from the first MB is probed by the second MB of opposite polarity acting as collector, which is located at various distances from the injecting MB. We find that the series resistance of the two barriers depends non-monotonously on the barrier spacing as well as on the magnetic barrier strength. Transmission resonances are found which can be explained semiclassically in terms of snake-orbit and cycloid trajectories that form in between the barriers and that get selectively occupied by the collimation effect. The maximum magneto-resistance is furthermore larger than twice the magneto-resistance of a single-barrier.

Simulations of the measurements based on the Landauer-Büttiker model in the semiclassical limit [4] with the experimentally determined parameters as input [3] reproduce the transmission functions and reveal the quasi-ballistic nature of the effects observed.

[1] M. L. Leadbeater et al, Phys. Rev. B **52**, R8629 (1995); F. G. Monzon et al., Appl. Phys. Lett. **71**, 3087 (1997).
[2] M. Cerchez et al., Phys. Rev B **75,** 035341 (2007).
[3] M. Cerchez and T. Heinzel, Appl. Phys. Lett. **98**, 232111 (2011).
[4] C. W. J. Beenakker and H. van Houten, Phys. Rev. Lett. **63**, 1857 (1989).

Universal behavior of the magnon gaps in doped quasi-2D antiferromagnets

M. Fidrysiak
Institute of Physics, Wroclaw University of Technology, 50-370 Wroclaw, Poland

Many cuprate compounds at low doping exhibit long-range antiferromagnetic (AF) order, e.g., $La_{2-x}Sr_xCuO_4$ (LSCO). In the Néel phase these materials can be effectively described as anisotropic quasi-2D Heisenberg antiferromagnets, where holes are represented by dipole fields linearly coupled to the background magnetization current. Small Dzyaloshinskii-Moriya (DM) and XY anisotropies are responsible for opening of the magnon gaps which in LSCO rapidly decrease with doping and close at the AF phase boundary $x_c \sim 0.02$.

Within the framework of the anisotropic quantum non-linear σ-model (QNLσM) we calculate doping dependence of the magnon gaps and obtain a good agreement with experiments on LSCO. It is shown that the reduction of the magnon gaps relative to their $x = 0$ value weakly depends on the anisotropies of the parent compound. Since the DM gap is highly sensitive to rare-earth element doping, this prediction could be tested on $La_{2-x-y}Eu_ySr_xCuO_4$ (LESCO) and $La_{2-x-y}Nd_ySr_xCuO_4$ (LNSCO).

Optical anisotropy in [0001] oriented $Al_xGa_{1-x}N$/AlN quantum wells under pressure

W. Bardyszewski and S. P. Łepkowski
Faculty of Physics, University of Warsaw, ul. Hoża 69, 00-681 Warszawa,Poland
Institute of High Pressure Physics, "Unipress", Polish Academy of Sciences, ul. Sokołowska 29/37, 01-142 Warszawa, Poland

Abstract. The question of possible switching of polarization of the emitted light from the wide gap nitride based quantum wells is very important in designing surface emitting devices. We investigate the influence of external pressure on optical anisotropy of GaN/ $Al_xGa_{1-x}N$ quantum wells (QWs) grown along the *c*-crystallographic direction on unstrained AlN substrates. Our theoretical study reveals that in the structures with properly chosen Al content in the QW layer a pressure-dependent switching of polarization of emitted light may occur. This switching of polarization primarily originates from reordering of the topmost valence subbands having different symmetries.
In the unstrained bulk GaN, the top subband is of Γ_9 character, leading to the emission of light with polarization perpendicular to the *c* axis whereas in the bulk AlN, due to the negative value of the crystal field splitting energy, the sequence of sub-bands is inverted with the topmost subband having Γ_7 symmetry favoring light emission with polarization parallel to the *c* axis. This inversion occurs also in AlGaN alloys at high enough concentration of Al. Using various material combinations such as AlGaN and GaN or AlN and AlGaN as barrier and quantum well materials gives a possibility to modify the symmetry properties of the top of the valence band states in a quantum well structure [1].
In the present study, we investigate the effect of the external hydrostatic pressure on the valence band structure and optical anisotropy of nitride QWs grown along the c-axis. To this end we have developed a model of optical transitions which fully takes into account (i) the influence of strain and the built-in electric fields on the conduction and valence band states in the QW and (ii) the excitonic effects which contribute significantly to the conditions for the reordering of corresponding optical transitions in emission and absorption spectra [2]. The optical spectra for different values of external pressure are obtained in two stages. First the effective one-particle Hamiltonian for the quantum well including the influence of strain and the electric field due to the spontaneous polarization and piezoelectric effect is diagonalized in order to obtain one-electron spectra in the valence and conduction subbands. In the second stage the optical spectra are obtained by solving the Bethe-Salpeter exciton equation in the envelope function representation using Landau orbitals basis set to describe the relative electron-hole motion [2].
We present the results of our calculations performed for narrow, 1.5nm wide $Al_xGa_{1-x}N$/AlN QWs with *x* equal to 0.7 and 0.8. The structures were assumed to be lattice matched to AlN substrates. We show that in the considered cases the difference in the exciton binding energies modifies the simple condition for polarization switching defined as the point of crossing of the valence subbands with different symmetry. We also present the evolution of theoretical absorption and photoluminescence spectra with pressure.

This work was supported by the Polish Ministry of Science and Higher Education, Project No. 2011/01/B/ST3/04353.

[1] R.G. Banal, M. Funato and Y. Kawakami, Phys. Rev. B79, 121308 (2009).
[2] W. Bardyszewski and S. P. Lepkowski, Phys. Rev. B85, 035318 (2012).

ThP120

High-index plasmon excitation in high electron mobility GaAs/AlGaAs heterostructures

M. Białek[1], K. Karpierz[1], M. Grynberg[1], M. Czapkiewicz[2], K. Fronc[2], J. Wróbel[2], V. Umansky[3], B. Piętka[1], and J. Łusakowski[1]

[1] *Faculty of Physics, University of Warsaw, ul. Hoża 69, 00-681 Warsaw, Poland*
[2] *Institute of Physics, PAS, al. Lotników 32/46, 02-668 Warsaw, Poland*
[3] *Weizmann Institute of Science, Rehovot 76100, Israel*

Excitation of plasmons with photons incident perpendicularly on a two-dimensional electron gas (2DEG) can be achieved only in an experimantal configuration which allows to fulfil the momentum and energy conservation laws. One of such a configuration can be realized with a metallic grid prepared on the sample surface [1]. Diffraction of the incident light on the grid allows to excite plasmons with a wavelength equal to the period of the grid and its subharmonics. In the case of a semiconductor electron plasma, typical frequency of the radiation falls within a THz band and the grid period is of the order of a micrometer.

A 2DEG of a high electron mobility allows to investigate details of the plasmon dispersion relation because of the possibility to observe low frequency plasmon modes and with high indexes. To this aim, a lithographically processed Hall bar with a Au grid-gate was prepared on a GaAs/AlGaAs heterostructure with a high electron mobility 2DEG. The lenght and width of the bar was equal to $L = 1.3$ mm and $w = 60$ μm, respectively. The period of the grid was equal to $l_0 = 4$ μm and the aspect ratio was 50%. The estimated Hall electron concentration and mobility was equal to, respectively, 2.7×10^{11} cm^{-2} and 6×10^5 cm$^2/Vs$. The samples were cooled down to 4 K and exposed to THz radiation in the range 0.10 - 0.66 THz generated by quasi-optical sources. The measured signal was a photovoltage created between the ohmic contacts of the Hall bar separated by 1.3 mm. The signal was measured with a lock-in technique as a function of the magnetic field and the electrical polarization of the grid-gate at a constant frequency of THz radiation. As a reference, experiments as a function of the magnetic field were carried out on another Hall bar which was not supplied with a grid-gate.

The photovoltage spectra measured as a function of the magnetic field showed up to 23 and 11 maxima in the case of not gated and gated sample, respectively. Dispersion relations derived from the experimental data were interpreted within a model of magnetoplasmon excitation in the Voigt configuration $\omega^2_{mp,j} = \omega_c^2 + \omega_p(jk_0)^2$ where $\omega_{mp}(B)$ is the magnetoplasmon frequency, ω_c is a cyclotron frequency and $\omega_p(jk_0)$ is the frequency of a plasmon with the k-vector equal to $jk_0 = 2\pi j/l_0$ at zero magnetic field; j is the index of the plasmon mode. We have obtained $\omega_p(k_0) = 150$ GHz and $k_0 = \pi/w$ in the case of not gated samples. We could also obtain the plasmon dispersion in case for gated and not gated sample which both fit to theoretical predictions [2]. We have permormed measurements on a Hall bar gated with a uniform gate and obtained the same result as on a grid-gated sample. The obtained results allowed to verify that in the case of a high-quality GaAs/AlGaAs heterostructure, high index plasmon modes in the Voigt geometry can be described within a non-local approximation neglecting retardation effects.

This work was partially supported by the Foundation for Polish Science grant POMOST /2010-1/8.

[1] E. Batke et al, Phys. Rev. B **34**, 6951 (1986).
[2] N. Okisu et al, Appl. Phys. Lett. **48**, 776 (1986).

Application of low-energy theories to describe the dynamics of doublons in the Bose-Hubbard model on a honeycomb lattice

Holger Niehus[1] and Daniela Pfannkuche[1]

[1] *I. Institute for Theoretical Physics, University of Hamburg, Jungiusstr. 9, D-20533 Hamburg, Germany*

Identifying the relevant processes for the dynamics of excitations far from equilibrium is one of the most challenging tasks in many particle physics. We approach this problem for a special class of excited states in the Bose-Hubbard model, so-called doublons, by means of effective low-energy models in conjunction with exact diagonalization.

In 2002 the superfluid to Mott-insulator transition has been observed for an ultra-cold Bose gas in an optical lattice and it was subsequently shown that theses systems can be used to simulate Hubbard models with precise control over the model parameters [1]. Furthermore, low-dimensional systems or unconventional geometries like the honeycomb geometry (best known from graphene) can be realized, the latter was shown recently [2]. With the additional ability to tailor particular initial states, this enables us to study many new effects of the Hubbard model in the absence of dissipation.

We are all familiar with composite objects created by attractive interactions, but in a periodic system and without a channel to dissipate energy, particles may be bound together also by repulsive forces. For the Bose-Hubbard model the existence of a band gap in conjunction with energy conservation prohibits the conversion of the interaction-energy of two particles on the same site – a doublon – to kinetic energy of the particles, rendering the direct decay impossible. This stability of doublons was recently observed experimentally for both ultra-cold bosons and fermions in optical lattices, where long lifetimes were measured in case of large repulsive interactions of the atoms [3, 4].

We use a method called Löwdin downfolding to derive effective low-energy models for the dynamics of doublons in two different environments. This perturbative approach is expected to be accurate in the limit of $t \ll U$. Using exact time evolution for small systems under periodic boundary conditions enables us to validate the quality of our effective models.

First we study the interaction of few doublons by creating two doubly occupied sites in an otherwise empty lattice. Its low-energy theory of third order in the hopping is recast to a doublon-doublon Hamiltonian capturing the essential dynamics. We show that all but second-order terms vanish. One is left with a next-neighbor hopping of the doublons and a strong next-neighbor interaction of the doublons, which prevents neighboring doublons from delocalizing completely. We also show that the application of this model to many doublons is limited and identify the mechanism responsible for it breaking down.

Complementary we study the influence of neighboring bosons on the dynamics of a single doublon in a unit filled lattice. We show that the dynamics of such systems may be described by a doublon-holon model. Here the doublon is no longer increasingly immobile for increasing U, but rather is able to delocalize in first order. Furthermore, we observe that the next-neighbor doublon-holon attraction is particularly weak and unable to bind them together.

[1] M. Greiner et al., Nature **415**, 39 (2002).
[2] P. Soltan-Panahi et al., Nature Physics **7**, 434 (2011).
[3] K. Winkler et al., Nature **441**, 853 (2006).
[4] N. Strohmaier et al., Phys. Rev. Lett. **104**, 080401 (2010).

ThP122

Current waveform synthesis by quantized single-electron pumping

F. Hohls, P. Mirovsky, L. Fricke, B. Kaestner, C. Leicht, K. Pierz, J. Melcher, and H.W. Schumacher

Physikalisch-Technische Bundesanstalt, Bundesallee 100, 38116 Braunschweig, Germany

Electrical quantum metrology links the electrical units to fundamental constants of nature, namely the charge of the electron e and Planck's constant h. The success of quantum metrology is documented by the plans of the General Conference on Weights and Measures to redefine the international system of units (SI) based on fundamental constants. In electrical quantum metrology the two effects which have been successfully applied for many years are the Josephson effect for the generation of quantized voltages and the quantum Hall effect for quantized resistance. Recently, semiconductor-based single-electron pumps (SEP) have become subject of intense studies as they might allow the realization of a quantum standard of the electrical base unit ampere [1,2]. When operated at a pumping frequency f such single-electron pumps generate quantized currents $I = ef$. These pumps have so far demonstrated output currents above 100 pA with ppm uncertainty [3], and promise lower uncertainties based on theoretical analysis [3,4].

Initially, all electrical quantum standards have been operated in dc mode only. Later, Josephson quantized ac voltage generation was realized based on switchable binary arrays and on pulse-driven arrays enabling arbitrary waveform synthesis. Additionally, studies of the ac quantum Hall effect have recently paved the way to a quantum standard of electrical capacitance [5]. However, the generation of quantized ac current waveforms based on frequency-modulated single-electron pumping has not been considered yet.

We will present the results of a proof-of-principle experiment on the generation of ac modulated quantized currents using a semiconductor-based single-parameter SEP [2] with frequency-modulated pumping frequency. These pumps are driven by a single high frequency signal and can be used over a wide frequency range which allows for a robust implementation of modulation schemes. ac-modulated quantized current waveforms are generated by sinusoidal and sawtooth modulation of the pumping frequency f. In our experiments kHz modulation frequencies and peak currents up to 100 pA are realized. The modulation frequency in our experiment was only limited by our current measurement bandwidth and thus our detection ability; generation of ac currents at MHz frequencies is possible. More advanced modulation schemes based on pulse-driven SEPs in combination with parallelization [6] could in the future enable arbitrary quantized current waveform synthesis with nA peak amplitude with applications in metrology and on-chip signal generation.

[1] M.D. Blumenthal et al., Nat. Phys. **3**, 343 (2007).
[2] B. Kaestner et al. Phys. Rev. B **77**, 153301 (2008); B. Kaestner et al. Appl. Phys. Lett. **92**, 192106 (2008); A. Fujiwara, K. Nishiguchi, Y. Ono, Appl. Phys. Lett. **92**, 042102 (2008).
[3] S. P. Giblin et al., Nature Commun. **3**, 930 (2012); B. Kaestner et al., Digest of *CPEM 14*, (2012).
[4] V. Kashcheyevs, B. Kaestner, Phys. Rev. Lett. **104**, 186805 (2010); F. Hohls, et al. Phys. Rev. Lett. **109**, 056802 (2012), and supplemental material.
[5] S. J. Schurr, F.-J. Ahlers, B. Kibble, Meas. Sci. Technol. **23**, 124009 (2012).
[6] P. Mirovsky et al. Appl. Phys. Lett. **97**, 252104 (2010).

Enhanced Kondo effect in two-dimensional helical electrons

A. Wong[1], K. Ingersent[1], M. Zarea[2,3], S. E. Ulloa[3,4], and N. Sandler[3,4]

[1] *Department of Physics, University of Florida, Gainesville, Florida, 32611, USA*
[2] *Department of Chemistry, Northwestern University, Evanston, Illinois, 60208, USA*
[3] *Department of Physics and Astronomy, and Nanoscale and Quantum Phenomena Institute, Ohio University, Athens, Ohio 45701, USA*
[4] *Dahlem Center for Complex Quantum Systems, Freie Universität, 14195 Berlin, Germany*

The effect of spin-orbit (SO) interactions in an electron system in the presence of a magnetic impurity in the Kondo regime has remained controversial for more than forty years [1]. Much of the difficulty in approaching the problem becomes evident when considering the Anderson Hamiltonian: the presence of SO interaction breaks the SU(2) spin symmetry considered essential for the Kondo effect. Recent works have addressed the issue with conflicting results: while some predict no essential change in the Kondo physics [2], there are indications that an exponential increase of the Kondo temperature could be achieved [3]. We address the question by analyzing the Kondo limit of an Anderson Hamiltonian for a 2DEG with Rashba SO interactions and a local spin ½ magnetic impurity. By means of an energy-dependent Schrieffer-Wolff transformation we obtain the effective Hamiltonian in the Kondo regime. As SO interactions inherently mix orbital and spin angular momenta, they preclude the use of spin as a good quantum number, which affects the resulting Kondo state. This is captured by the appearance of a Dzyaloshinsky-Moriya (DM) term in the Kondo Hamiltonian, which imparts a non-collinear magnetic interaction on the ground state.

In this paper, we present a study of this problem with numerical renormalization group (NRG) methods, revealing that the strength of the SO interactions determine two well defined regimes for Kondo physics. In agreement with previous studies, we find only minor changes in the Kondo temperature scale when the Rashba coupling is increased at *fixed Fermi energy*. However, for *fixed band filling*, increasing the SO coupling can move the Fermi energy near a Van Hove singularity in the effective density of states, leading to an exponential enhancement of the Kondo temperature. In this *helical* regime (where only one branch of the dispersion is accessible near the Fermi energy), static spin correlations confirm that the impurity couples to conduction channels of nonzero orbital angular momentum and convey an intrinsic spiral structure to the relative spin alignment of the reservoir electrons and the magnetic moment of the impurity.

[1] D. Gainon and A. J. Heeger, Phys. Rev. Lett. **22**, 1420 (1969).
[2] J. Malecki, J. Stat. Phys. **129**, 741 (2007); R. Zitko and J. Bonca, Phys. Rev. B **84**, 193411 (2011).
[3] M. Zarea, S. Ulloa and N. Sandler, Phys. Rev. Lett. **108**, 046601 (2012).

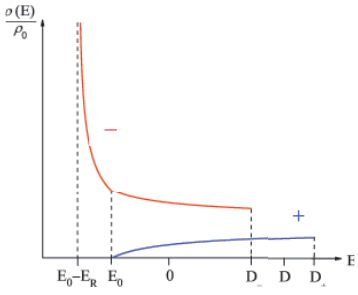

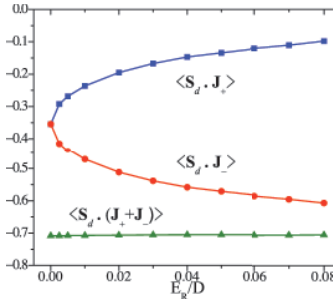

Fig. 1. Left panel: DOS for 2DEG in the presence of Rashba SOI. Red and blue curves indicate different chirality value (− or +). Notice Van Hove singularity of − channel near bottom of band at E_0-E_R. Right panel: Spin correlation amplitude per channel in Kondo in chiral regime.

Carriers mobility of 2DEG of AlGaN/GaN structure on bulk ammonothermal GaN substrate

Kruszewski P[1,2], Prystawko P[1,2] , Kasalynas I[3], Plesiewicz J[2], Dwiliński R[4], Zając M[4], Kucharski R[4], Leszczyński M [1,2]
[1] Institute of High Pressure Physics UNIPRESS, Warsaw, Poland
[2] TopGaN Sp.z o.o., Warsaw, Poland
[3] Center for Physical Science and Technology, Vilnius, Lithuania
[4]Ammono SA, Warsaw, Poland

Keywords: AlGaN/GaN HEMT structure, Ammonothermal method, MOVPE technique

It is rather well established that the performance of GaN-based High Electron Mobility Transistors (HEMT) is directly correlated with the type and quality of the substrate used for further epitaxial growth. Unwanted impurities, defects and high density of dislocations present in the HEMT structure can be a source of undesirable effects as parallel conduction or existence of effective scattering centers which can limit electron mobility in the channel of HEMT transistor. All of these parasitic effects can be significantly reduced when high quality, defect free and low dislocation density bulk GaN substrates for epitaxial growth are used.

In this study, we report on theoretical and experimental results obtained from electrical characterization of 2DEG (Two Dimensional Electron Gas) of AlGaN/GaN HEMT on bulk GaN substrate produced by ammonothermal method [1]. Such GaN substrate is characterized by an ultra high purity and dislocation density as low as 10^4 cm^{-2} [2]. The AlGaN layers grown by MOVPE (Metalorganic Chemical Vapour Phase Epitaxy) method reproduce this low dislocation density ensuring simultaneously high uniformity and smoothness of AlGaN/GaN interface such essential for high electron mobilities in the HEMT`s channel.

For our detail analysis, complementary Hall effect studies in the Van der Pauw configuration have been planned and successfully performed. A temperature dependent Hall effect measurements taken for different positions of the same epi-wafer have clearly shown that no parallel conduction in analyzed HEMT structure exists. Additionally, a slightly increase of the carrier concentration at liquid nitrogen has been observed suggesting stronger electron confinement in the quantum well in comparison with room temperature. These results have been also confirmed by Capacitance-Voltage measurements where no carriers freezing at low temperatures have been observed.

Finally, mobilities and concentrations of 2DEG obtained from Hall experiments are in range of 1500 cm^2/Vs (300K) , 8000 cm^2/Vs (77K) and $8x10^{12}$ cm^{-2} (for both, 77K and 300K), respectively and agree quite well with theoretical predictions calculated using one dimensional Poisson solver [3]. It is also worth to underline that Hall effect results were entirely independent on the position of analyzed sample clearly confirming high homogeneity and quality of grown HEMT structure.

Acknowledgements:
This work was supported by the PolHEMT Project under the Applied Research Programme of the National Centre for Research and Development, Contract no. PBS1/A3/9/2012 and NANOTEC Project "Nanostructured materials and RF-MEMS RFIC/MMIC technologies for highly adaptive and reliable RF systems", Contract no. 288531.

References:
[1] Dwilinski et al., J. Crystal Growth 310, 3911 (2008).
[2] R. Kucharski et al., Semicond. Sci. Technology 27, 024007 (2012).
[3] 1D Poisson solver website: www3.nd.edu/~gsnider/

Spin-Droplet State of an Interacting 2D Electron System

N. Teneh[1], A. Yu. Kuntsevich[2], V. M. Pudalov[2,3] and M. Reznikov[1]

[1] *Solid State Institute, Technion, Haifa 32000, Israel*
[2] *P.N. Lebedev Physical Institute, Moscow, 119991 Russia*
[3] *Moscow Institute of Physics and Technology, Moscow, 141700, Russia*

We report thermodynamic magnetization measurements of two-dimensional electrons in several high mobility Si metal-oxide-semiconductor field-effect transistors. We provide evidence for an easily polarizable electron state in a wide density range from insulating to deep into the metallic phase [1]. The temperature and magnetic field dependence of the magnetization is consistent with the formation of large-spin droplets in the insulating phase. These droplets melt in the metallic phase with increasing density and temperature, although they survive up to large densities.

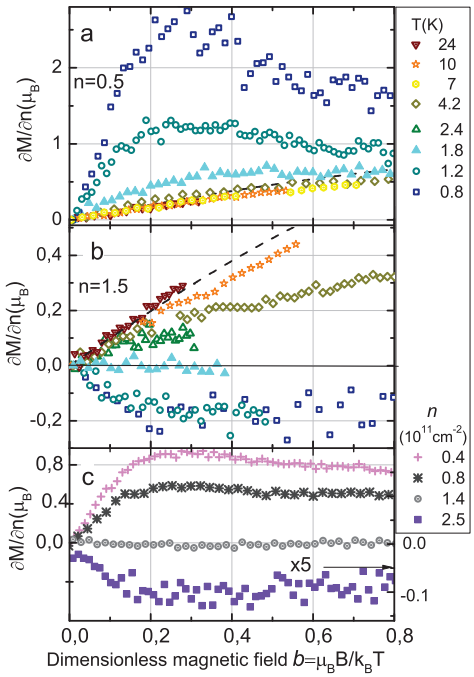

Figure 1: Panel (a): $\partial M/\partial n$ vs normalized magnetic field $b = \mu_B B/k_B T$ at $n = 0.5 \times 10^{11}\text{cm}^{-2}$ (insulating phase). We subtracted the diamagnetic contribution estimated from the high-temperature data, $\sim 0.04\mu_B$ per tesla [2]. Panel (b): the same as panel (a) at $n = 1.5\times10^{11}\text{cm}^{-2}$ (metallic phase); the subtracted diamagnetic contribution is $\approx 0.035\mu_B$ per tesla. Dashed lines in (a) and (b) show $\partial M/\partial n$ for localized spins 1/2. Panel (c) $\partial M/\partial n$ vs b at different densities at $T = 1.8$K. Note that $\partial M/\partial n(b)$ becomes nonlinear at the density and temperature independent b^*.

[1] N. Teneh, A. Yu. Kuntsevich, V. M. Pudalov, M. Reznikov, Phys. Rev. Lett. **109**, 226403 (2012).

[2] M. Reznikov, A. Yu. Kuntsevich, N. Teneh, V. M. Pudalov, JETP Lett. **92**, 470 (2010).

ThP126

Plasma Oscillations in 2DEG Nanometer Field Effect Transistors for Terahertz Detection

W. Knap[1,2], N.Dyakonova[1], S.Rumyantsev[1,3], M.S. Vitiello[4], D.Coquillat[1], S.Blin[5], F.Teppe[1]

[1]Laboratoire Charles Coulomb Université & TERALAB Montpellier 2 &CNRS (France)

[2]Institue of High Pressure Physics UNIPRESS PAN , 02-845 Warsaw (Poland)

[3]Rensselaer Polytechnic Institute, Troy, New York 12180 USA (USA)

[4]NEST, Istituto Nanoscienze - CNR and Scuola Normale Superiore, 56127 Pisa (Italy)

[5]IES &TERALAB, Universite Montpellier 2 & CNRS, 34950 Montpellier (France)

Two-dimensional electron plasma in nanometre size field effect transistors can oscillate in Terahertz (THz) frequencies, far beyond transistors fundamental cut-of frequencies [1]. We present an overview of some important and recent results concerning the physics of nanometre scale field effect transistors showing that they can be used for the detection of terahertz radiation

The subjects were selected in a way to stress some new aspects/developments rather than purely technological/engineering improvements. The basic physics related problems like temperature dependence of the photoresponse [2], interferences of THz signals leading to helicity sensitive detection are presented [3].

Until now most of works on nanometer FETs detectors were considering only THz imaging applications. We show the progress in overcoming the loading problems and demonstrate first results on the application of nanometre FETs as detectors in wireless communication with signal modulated in GHz range[4]. Finally we present also results from THz detection by grapheme transistors[5]. A possible development of future THz detectors using grapheme structures is also addressed.

References

[1] W. Knap and M. I. Dyakonov, 'Field effect transistors for terahertz applications' in D. Saeedkia, *Handbook of terahertz technology for imaging, sensing and communications*, Cambridge, Woodhead Publishing, 121-155(2013)

[2] Klimenko O A, Knap W, Iniguez B, Coquillat D, Mityagin Y A, Teppe F, Dyakonova N, Videlier H, But D, Lime F, Marczewski J, and Kucharski K *Temperature enhancement of terahertz responsivity of plasma field effect Transistors* J. Appl. Phys. **112**, 014506 (2012)

[3] Drexler C, Dyakonova N, Olbrich P, Karch J, Schafberger M, Karpierz K, Mityagin Yu, Lifshits M B, Teppe F, Klimenko O, Meziani Y M, Knap W and Ganichev S D 2012 Helicity sensitive terahertz radiation detection by field effect transistors *J. Appl. Phys.* **111** 124504 (2012)]

[4] Blin S, Teppe F, Tohme L, Hisatake S, Nouvel P, Coquillat D, Penarier A, Torres J, Knap W, Nagatsuma T *Plasma-Wave Detectors For Terahertz Wireless Communication* IEEE El. Dev. Lett. **33** 1354 (2012)

[5] Vicarelli L, Vitiello M S, Coquillat D, Lombardo A, Ferrari A C, Knap W, Polini M, Pellegrini V and Tredicucci A. Graphene field-effect transistors as room-temperature terahertz detectors, Nature Materials **11** 865(2012)

Electron and hole transport in Ambipolar GaAs devices

A.R. Hamilton [1], J.C.H. Chen [1], Z.K. Keane [1], M.C. Godfrey [1], D.Q. Wang [1], O. Klochan [1], S. Fricke [1], A. M. Burke [1], A.P. Micolich [1], K. Das Gupta [2], 2 F. Sfigakis [2], H. E. Beere [2], D.A. Ritchie [2], D. Reuter [3] and A. D. Wieck [3]

[1] *School of Physics, University of New South Wales, Sydney, NSW 2025, Australia*
[2] *Cavendish Laboratory, University of Cambridge, Cambridge CB3 0HE, United Kingdom*
[3] *Angewandte Festkörperphysik, Ruhr-Universität Bochum, D-44780 Bochum, Germany*

We review recent work on ambipolar undoped GaAs/AlGaAs heterostructure devices, in which the channel can be switched from a high quality 2D electron gas to a 2D hole system simply by changing the top gate bias.

In two-dimensional systems we have performed a direct comparison of the scattering mechanisms of electrons ($\mu_{peak}=4\times10^6$ cm^2/Vs) and holes ($\mu_{peak}=0.8\times10^6$ cm^2/Vs) in the same conduction channel with nominally identical disorder potentials. We find significant discrepancies between electron and hole scattering, with the hole mobility being considerably lower than expected from simple theory [1].

In one-dimensional devices we have studied electron and hole transport in the same quantum point contact. We observe quantized conductance steps, and use source drain biasing to extract the subband spacing for both electrons and holes in the same point contact. [2]

Finally we have used these devices to study the hyperfine coupling of holes with the Ga and As nuclei in the host crystal for the first time [3]. Resistively detected NMR measurements in the quantum Hall regime show that the magnitude of the resistance change and associated NMR peaks in n-type devices is in line with previous measurements, whereas no signal could be detected for p-type devices. This suggests that the hyperfine coupling between holes and nuclei in this type of measurement is much smaller than the electron hyperfine coupling, which could have implications for quantum information processing.

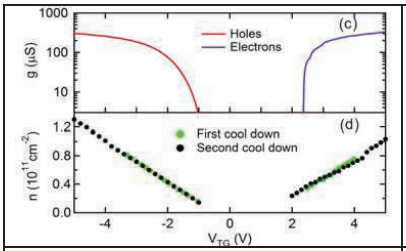

Ambipolar operation of an undoped 2D heterostructure [1].

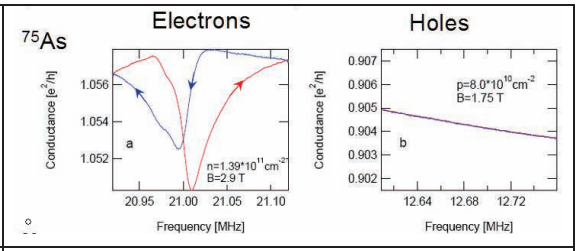

Resistively detected NMR for electrons and holes [3].

[1] J. C. H. Chen *et al*, Appl. Phys. Lett. **100**, 052101 (2012).
[2] J. C. H. Chen *et al*, (unpublished).
[3] Z. K. Keane *et al*, Nano Letters **11**, 3147 (2011).

ThP128

Weak anti-localisation in p-type surface conducting (100) hydrogen-terminated diamond: Proof of a 2DHS

M. T. Edmonds[1], L. H. Willems van Beveren[2], O. Klochan[3], J. Cervenka[2], S. Prawer[2], L. Ley[1,4], A. R. Hamilton[3] and C. I. Pakes[1]

[1] *Department of Physics, La Trobe University, Victoria, Australia*
[2] *School of Physics, The University of Melbourne, Victoria, Australia*
[3] *School of Physics, University of New South Wales, Sydney, New South Wales, Australia*
[4] *Institut für Technische Physik, Universität Erlangen, Erlangen,Germany*

Hydrogen-terminating an insulating diamond and exposing it to air results in electrons being transferred out of the diamond valence band into the adsorbed water layer so that holes accumulate near the diamond surface and give rise to *p*-type surface conductivity. This doping mechanism is known as surface transfer doping and allows doping of diamond without introducing impurities into the diamond lattice [1]. Whether this *p*-type surface conductivity is confined to a two-dimensional hole system (2DHS) has yet to be conclusively proved experimentally, in part because the highest mobility of the holes accumulated at the diamond surface is less than μ~500 $cm^2V^{-1}s^{-1}$.

We have fabricated high quality (100) hydrogen-terminated diamond hall bars, and performed low temperature magneto-transport measurements on the *p*-type surface conducting state. We observe clear weak localization and weak anti-localization effects, which are in excellent agreement with the Hikami-Larkin-Nagaoka model of two-dimensional localization [2]. The extracted phase coherence length obeys a power-law dependence with temperature of $l_\phi \sim T^{-0.45}$ in agreement with the theoretical prediction by Altshuler et al. for 2D systems [3]. This data provides direct evidence for the formation of a two-dimensional hole system at the hydrogen-terminated diamond surface.

The observation of weak anti-localization is a result of the strong spin-orbit interaction present at the diamond surface due to a lack of inversion symmetry that is predicted by DFT calculations. From calculation of the in-plane carrier effective mass the phase and spin coherence times were determined. The presence of spin-orbit interaction at the hydrogen-terminated diamond surface is also discussed, along with the implication for quantum information processors [4] and magnetometers [5] that utilise NV centres located near the hydrogen-terminated diamond surface.

[1] F. Maier, et al., Phys. Rev. Lett. **85**, 3472 (2000).
[2] S. Hikami, et al., Prog. Theor. Phys. **63**, 707 (1980).
[3] B. L. Altshuler, et al., J. Phys. C **15**, 7367 (1982).
[4] J. R. Maze, et al., Nature **455**, 644 (2008).
[5] G. Balasubramanian, et al., Nature **455**, 648 (2008).

Optical properties of ZnO/ZnMgO quantum wells grown by PAMBE

Jacek M. Sajkowski[1], Mieczyslaw A. Pietrzyk[1], Marcin Stachowicz[1], Anna Droba[1], Ewa Przezdziecka[1], Aleksandra Wierzbicka[1], Marcin Syperek[2], Adrian Kozanecki[1]

[1] *Institute of Physics, Polish Academy of Sciences, Al. Lotników 32/46, 02-668, Warsaw, Poland*
[2] *Institute of Physics, Wrocław University of Technology, ul. Wybrzeże Wyspiańskiego 27, 50-370, Wrocław, Poland*

Zinc oxide is considered to be a good candidate for applications in blue and UV optoelectronics due to its properties (3,37 eV direct band gap and high exciton binding energy - 60 meV in bulk ZnO and up to 100 meV in ZnMgO/ZnO/ZnMgO quantum wells). In this work we employ various techniques to investigate optical and structural properties of ZnMgO/ZnO/ZnMgO quantum wells grown by plasma assisted molecular beam epitaxy.

These structures were grown on (0001) sapphire substrates, that were annealed in oxygen prior to the growth. The width of QWs ranged from 2 nm to 9 nm while magnesium content in ZnMgO barrier layers was kept between 10% and 20%. The crystalline quality and surface morphology were investigated both *in situ* (with reflection high energy electron diffraction and *ex situ* (with X-ray diffraction and atomic force microscopy). XRD measurements show good crystalline quality and no phase separation, while RHEED and AFM images confirmed very good flatness of the surface with rms value below 2 nm. Subsequently photoluminescence (PL) and time-resolved photoluminescence (trPL) spectroscopy were used to investigate optical properties of these samples. These measurements allowed us to observe Quantum Confinement Effect in structures with thin QWs (up to 4 nm) and Quantum Confined Stark Effect in thick QWs (above 4 nm). Exemplary results of trPL experiment for structure exhibiting QCSE are shown in figure 1.

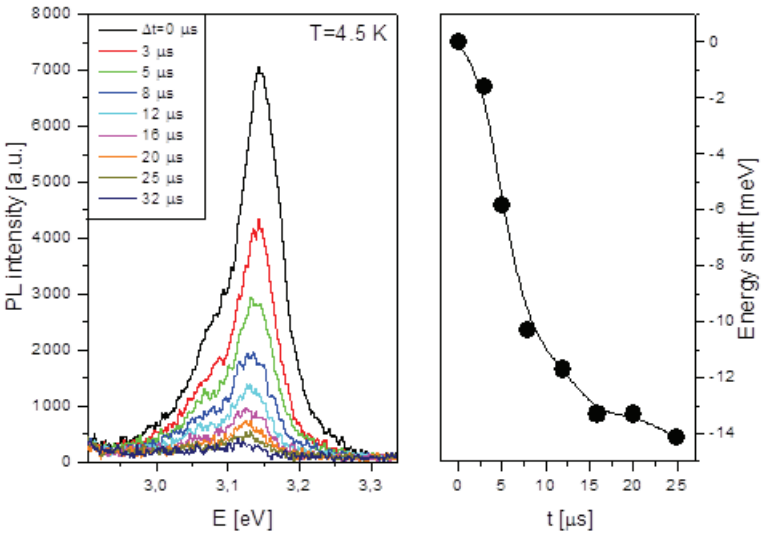

Fig. 1 trPL spectrum and main PL peak energy shift with time for structure with 9 nm QW

ThP130

ab initio Calculations of Optical Absorption in Planar Boron Wheels

Ravindra Shinde[1] and Alok Shukla[1]

[1] *Department of Physics, Indian Institute of Technology Bombay, Mumbai,*

The linear optical absorption spectra of planar boron clusters (B_7 , B_8 and B_9) in wheel shapes are calculated using a systematic all-electron correlated calculation approach. The geometries of these clusters were optimized at the coupled-cluster singles doubles (CCSD) level of theory. With these optimized geometries, excited states were computed using the equation-of-motion coupled cluster singles doubles (EOM-CCSD) approach. This is a popular approach to include the electron correlation in large molecules and clusters at a sophisticated level. Also bench-marking this high-level calculations were done with respect to time-dependent density functional (TDDFT) calculations and configuration interaction singles (CIS) calculations. The nature of optical excitation involved are found to be of collective, plasmonic type, by noticing the contribution of configurations to many body wavefunctions.

Fractionalized Wave Packets from an Artificial Tomonaga-Luttinger Liquid

H. Kamata [1], N. Kumada [2] M. Hashisaka [1], K. Muraki [2], and T. Fujisawa [1]

[1] *Department of Physics, Tokyo Institute of Technology, Meguro, Tokyo, Japan*
[2] *NTT Basic Research Laboratories, NTT Corporation, Atsugi, Kanagawa, Japan*

An elementary charge excitation can appear at a junction of totally different entities, for example an interacting one-dimensional conductor, giving rise to Tomonaga-Luttinger liquid (TLL) behavior, and non-interacting one. An electron with charge, e, injected into the interacting region from the non-interacting one would break up at the junction into the bosonic collective modes of charge density waves with an effective charge, e^*, and the rest charge ($e - e^*$) reflected back to the non-interacting one. Although this process known as charge fractionalization [1] is consistently understood with a momentum-resolved spectroscopy measurement [2], such single elementary excitation process has never been directly observed. Here we employed time-resolved charge detection technique [3] on an artificial spinless TLL formed in two counter-propagating integer quantum Hall edge channels in close proximity to each other. Injection of a charge wave packet to the TLL connected with non-interacting leads causes multiple reflections of the wave packet at the junctions with a significant time interval. The observed wave packets are informative to investigate the correlated charge dynamics in the TLL.

In our sample fabricated from a GaAs/AlGaAs heterostructure, the artificial TLL consists of two counter-propagating edge channels separated by a gate electrode (1 μm in width and 68 μm in length) with a negative gate voltage V_G, allowing no inter-edge tunneling (Fig. 1). A charge injector is located upstream on the right-moving channel while a time-resolved charge detector [3] is located downstream on the left-moving channel. Figure 2 shows observed waveforms for an incident wave packet of charge Q to the TLL region (upper trace) and extracted wave packets of charges $q_\pm$ from the TLL region (lower trace). Injection of charge Q to the left junction generates a fractionalized charge $+rQ$ reflected back in the left-moving lead and an effective charge $(1 - r)Q$ in the TLL, where r is the fractionalization factor. The former is observed as the first packet q_+ while the latter is fractionalized at the right junction to charge $(1 - r^2)Q$ in the right-moving lead and an effective charge $-r(1 - r)Q$ in the TLL. The third fractionalization process arising at the left junction generates charge $-r(1 - r^2)Q$ in the left-moving lead, which is observed as the second packet q_-. The factor r determined by the ratios $q_\pm/Q$ can be quantitatively justified by estimating the interaction parameters with capacitances in realistic quantum Hall devices, and hence, this result indicates that the artificial TLL can be electrostatically controlled.

[1] E. Berg *et al*., Phys. Rev. Lett. **102**, 236402 (2009).
[2] H. Steinberg *et al*., Nature Phys. **4**, 116 (2008).
[3] H. Kamata *et al*., Phys. Rev. B **81**, 085329 (2010).

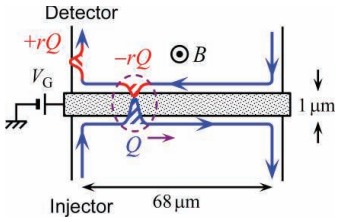

Fig.1: Schematic figure of the artificial TLL and first fractionalization process

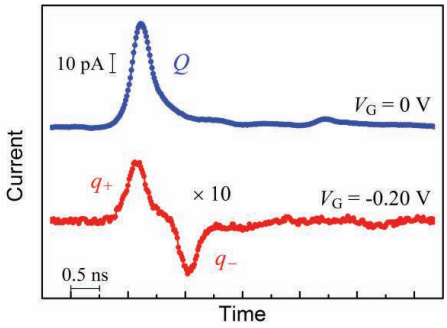

Fig.2: Observed charge waveforms for an incident wave packet Q and extracted wave packets $q_\pm$ from the TLL

ThP132

Spontaneous magnetization of a metal-insulator interface

V.I. Nizhankovskii

International Laboratory of High Magnetic Fields and Low Temperatures, Gajowicka 95, Wroclaw 53-421, Poland

Properties of a metal-insulator interface have essential importance for modern electronics. Some recent results point to an existence of metal-induced states in the energy gap of the insulator predicted in [1]. At an ideal interface these states are extended in the metal and damped in the insulator. Potential disorder results in their localization at the insulator surface and in the appearing of the local magnetic moments [2]. In this way the magnetic flux noise in superconducting quantum interference devices (SQUIDs) was explained [3]. An areal density of the localized electrons required to account for the observed noise magnitude is about $5 \cdot 10^{17}$ m^{-2}.

In the present investigation we directly observed spontaneous magnetization of an eutectic $In_{0.15}Ga_{0.85}$ - sapphire interface.

Excellent wetting of ceramics, glass and other insulators by an eutectic $In_{0.15}Ga_{0.85}$ (melting point 16.5 ^{o}C) is well known. According to [1] high metal-insulator adhesion results from the electron states localized at the insulator surface. As an insulator EPI polished sapphire substrate with orientation $(3\bar{1}3)$, thickness 0.17 mm and area 0.28 cm^2 was used. Small amount ($\sim$ 1 mg) of eutectic was distributed over substrate with a toothpick.

Measurements with a home-built SQUID-magnetometer were done at several temperatures from $T = 4.5$ K up to $T = 309$ K, that is 20 K above the melting point of an eutectic $In_{0.15}Ga_{0.85}$. Magnetic moment of spontaneous magnetization was directed from an insulator to a metal, its density at low temperature corresponds to $1.8 \cdot 10^{18}$ m^{-2} localized spin-1/2 states. Diminishing of the magnetic moment at highest temperature did not exceed 10%.

Influence of a strong magnetic field on the direction of spontaneous magnetization was investigated with a capacitance cantilever (torque magnetometer). These measurements have confirmed the existence of the spontaneous magnetization of a metal-insulator interface, its sign and an order of value. Phase diagram of the spontaneous magnetization on $H - T$ plane spreads above room temperature along the $T-$axis and is restricted to $2 - 2.5$ T along the $H-$axis at $T \leq 100$ K.

Results of these investigations are published in [4, 5].

[1] G. Bordier, C. Noguera, Phys. Rev. B **44**, 6361 (1991).
[2] S. Choi, D. Lee, S. G. Louie, J. Clarke, Phys. Rev. Lett. **103**, 197001 (2009).
[3] S. G. Louie, M. L. Cohen, Phys. Rev. B **13**, 2461 (1976).
[4] V. I. Nizhankovskii, J. Supercond. Nov. Magn. **25**, 447 (2012).
[5] V. I. Nizhankovskii, J. Supercond. Nov. Magn. **26**, 425 (2013).

Photoluminescence at up to 2.2 μm wavelengths from InGaAsBi/AlInAs quantum well

Renata Butkutė, Vaidas Pačebutas, Bronislovas Čechavičius, Ramūnas Nedzinskas, Arūnas Krotkus

[1] *Center for Physical Sciences and Technology, A. Gostauto 11, Vilnius, Lithuania*

III-V semiconducting alloys containing dilute amounts of bismuth have attracted increasing interest due to the large band gap reduction after the introduction of a relatively small content of Bi. It makes bismides promising materials for optoelectronic applications in the near and mid-infrared (MIR) spectral range [1-3]. It is known that the band gap of $GaAs_{1-x}Bi_x$ with $x<0.05$ reduces as fast as ~88 meV/%Bi [4]. Moreover, as the Bi-incorporation affects mainly the valence band, the spin-orbit splitting $\Delta\varepsilon_{SO}$ increases and for $x>0.1$ becomes larger than the energy band gap ε_g suppressing Auger recombination losses as well improving performance characteristics of light emitting bismide-based devices. Photoluminescence (PL) at wavelength of 1.5 μm from $GaAs_{1-x}Bi_x$ layer was already observed [4]. Even longer PL wavelengths (up to 6 μm) can be achieved in lattice-matched with InP substrate quarternary GaInAsBi alloy layers.

In this communication, the first results on GaInAsBi quantum wells will be presented. 5 nm, 10 nm and 20 nm thick $Ga_{0.53}In_{0.47}As_{1-x}Bi_x$ quantum wells were grown on (100) oriented InP:Fe substrates in a SVT-Associates MBE reactor at a temperature of about 240°C. The top and bottom barriers of quantum structures were 50 nm and 100 nm-thick AlInAs lattice-matched with InP. The bismuth content in the wells was nominally 3.7%. Transmission electron microscopy images revealed sharp interfaces between the well and barrier layers and their rather good homogeneity. PL signals with a wavelengths reaching 2.2 μm were observed over the whole temperature range from 4 K to 300K. PL was stronger in thin wells, where relaxation and clustering effects were avoided. For the 5 nm and 10nm thick wells the PL peak energy dependences on the temperature were well described by the Varshni equation with fitting parameters significantly smaller than in other III-V semiconductors. For 20 nm thick well such dependence was "S-shaped" indicating the effects of carrier localization. These results show that bismuth containing compounds could be prospective materials for MIR light sources without antimony.

[1] S. Tixier, M. Adamcyk, T. Tiedje, S. Francoeur, A. Mascarenhas, P. Wei, and F. Schiettekatte, Appl. Phys. Lett. **82**, 2245 (2003).
[2] K. Oe and H. Okamoto, Jpn. J. Appl. Phys., Part 2 **37**, L1283 (1998).
[3] K. Bertulis, A. Krotkus, G. Aleksejenko, V. Pačebutas, R. Adomavičius, G. Molis, and S. Marcinkevičius, Appl. Phys. Lett. **88**, 201112 (2006).
[4] X. Lu, D. A. Beaton, R. B. Lewis, T. Tiedje, and Y. Zhang, Appl. Phys. Lett., 95, 041903 (2009).

ThP134

Structural and magnetic properties of Fe bi-layer on W(110)

I. Zasada and M. Rybicki

Solid State Physics Department, University of Lodz, Poland

The magnetic and structural properties of pseudomorphic iron on tungsten substrate has been studied within the density functional generalized gradient approximation [1]. By studying the spectrum of surface phonons within the direct method, a strong dependence of lattice dynamics on magnetic interaction has been revealed. The ferromagnetic interactions have been found to be crucial element in stabilizing the Fe monolayer on W(110) [1].
In the present work we focus on the crystallographic and magnetic structure of Fe bi-layer on the W(110) surface using LEED technique, DFT and thermodynamic calculations. The structural results of LEED were confirmed by the calculation within the density functional generalized gradient approximation approach implemented in the VASP program. For completeness, we have performed first-principles calculations of the phonon excitation spectrum [2] for the iron bi-layer on the tungsten (110) surface. The stability of the system is analyzed in connection with its magnetic properties. The magnetic moments distribution is than discussed in terms of the thermodynamics of inhomogeneous low-dimensional systems based on a Néel sublattices concept while using a spin 1 Heisenberg Hamiltonian. The model allows us to investigate in a straightforward manner the layer-dependent phenomena. At the end we compare our results with those for Fe monolayer as well as thicker Fe films grown on W(110) surface.

Acknowledgments: This work was supported by Polish government (MNiSW) within the contract No. N N202 259539.

[1] J. Łażewski, P. Piekarz, A. M. Oleś, K. Korecki, and K. Pariński, Phys. Rev. B76, 205427 (2007).
[2] K. Pariński, PHONON software, Cracow, (2007).

Spin–orbit coupling effect on a particle density correlation in a two–dimensional electron gas

M. Kołodziej and G. Harań

Institute of Physics, Politechnika Wrocławska,
ul. Wybrzeże Wyspiańskiego 27, 50-370 Wrocław

Symmetry breaking as an origin of significant physical phenomena, like magnetism or superconductivity, is an important issue in condensed matter physics. Particularly interesting is a presence or a lack of time–reversal and inversion symmetries which determine the symmetry of a superconducting groundstate. Their role has been extensively studied in experiment and theory in non–centrosymmetric superconductors [1]. A unique opportunity to control the time–reversal and inversion symmetry breaking is provided by the spin–orbit coupling interaction in two–dimensional systems where these two symmetries can be lifted by applying external magnetic or electric fields, respectively [2].

The spin–orbit coupling interaction, $\vec{\gamma}(\mathbf{k}) \cdot \hat{\sigma}$, is determined by the scalar product of a gyroscopic vector $\vec{\gamma}(\mathbf{k})$ and the spin operator $\hat{\sigma}$ with $\vec{\gamma}(\mathbf{k}) = \vec{\gamma}(-\mathbf{k})$ representing a time–reversal symmetry breaking and $\vec{\gamma}(\mathbf{k}) = -\vec{\gamma}(-\mathbf{k})$ standing for the inversion symmetry breaking. In both cases the interaction leads to the energy band splitting. We discuss the effect of the above two types of the spin–orbit coupling interaction on a density correlation function in a two–dimensional electron gas and conclude on a possible Cooper pair formation: dominated by the intraband pairing for a broken time–reversal symmetry and with a prevailing interband pairing for a broken inversion symmetry. We also point out that our result can be verified experimentally by the Fourier–transformed scanning tunneling microscopy of a single nonmagnetic impurity in two–dimensional or quasi two–dimensional electron systems [3].

[1] E. Bauer and M. Sigrist, Lecture Notes in Physics **847** (Springer 2011).
[2] M. Sigrist, Lectures on the Physics of Strongly Correlated Systems XIII, ed. A. Avella and F. Mancini (AIP, 2009).
[3] L. Capriotti, D. J. Scalapino, and R. D. Sedgewick, Phys. Rev. B **68**, 014508 (2003).

ThP136

Inelastic light scattering by 2D electronic system with SO coupling in a strong magnetic field

Ritta V. Vitlina [1], Lev I. Magarill [1,2], and Alexander V. Chaplik [1,2]

[1] *Institute of Semiconductor Physics, Siberian Branch, Russian Academy of Sciences, Novosibirsk, 630090 Russia*
[2] *Novosibirsk State University, Novosibirsk, 630090 Russia*

Two-dimensional (2D) system with Bychkov-Rashba type spin-orbit (SO) interaction subjected to a strong perpendicular magnetic field is considered. The magnetic field is supposed to be so high that only zero Landau level is occupied, i.e. $\nu < 2$, where ν is the filling factor. In such a system the intersubband plasmon exists with dispersion law [1]

$$\omega_0(q) = \Delta\sqrt{1+\delta\nu\frac{qa^2}{a_B}\exp(-qa^2/2)},$$

where Δ is the spin sublevel separation, a_B is the Bohr radius, a is the magnetic length, $\delta\nu$ is the filling factor difference of lower and upper spin sublevels.

We consider resonance Raman scattering associated with transitions between spin sublevels. It is shown that the plasmon peak $\omega_0(q)$ in the spectrum of scattered light occurs for arbitrary polarizations of the incident and scattered waves. A specific situation arises if the incident wave is circularly polarized and its wave vector is normal to the structure plane while linearly polarized scattered beam is tilted to the normal. In such a situation the intensity of plasmon peak in scattering cross section contains a term which is sensitive to the sign of the effective Rashba SO constant but is invariant with respect to simultaneous change of the magnetic field direction and incident light chirality. This allows one to experimentally define the sign of the Rashba constant.

[1] R.Z.Vitlina, L.I.Magarill, A.V.Chaplik, JETP, **113**, 282 (2011).

Josephson current suppression due to the spin Hall effect in InAs two-dimensional electron systems

T. Nakamura, Y. Takahashi, Y. Hashimoto, D.H. Yun, S.W. Kim, Y. Iye, and S. Katsumoto

Institute for Solid State Physics, The University of Tokyo 5-1-5 Kashiwanoha, Kashiwa, Chiba 277-8581, Japan

InAs is a narrow gap semiconductor, which provides a low interfacial resistance suitable for the investigation of superconductor/semiconductor junctions [1]. In addition, Rashba type strong spin-orbit coupling (SOC) is expected in two-dimensional electron systems (2DESs) at spatially asymmetric structures of InAs quantum well [2]. Such a strong SOC causes a variety of spin phenomena: spin filtering [3], spin Hall effect [4] etc. SOC does not seem to modify transport property in superconducting junctions so drastically since Cooper pair has no spins and SOC conserves time-reversal symmetry. However, the spin mixing due to SOC changes the superconducting symmetry and furthermore the spin Hall effect induced by currents in the 2DESs affects the characteristics of the superconducting junctions, e.g. Andreev bound states.

In this work, we fabricated Nb/InAs/Nb junctions using InAs modulation doped 2DESs. Figure 1 illustrates a schematic of our junctions. Two Nb electrodes are attached to the 2DES and we can apply a longitudinal current and a transverse current along the Nb/InAs/Nb junction independently and simultaneously. In order to avoid the current leak from Nb electrodes to 2DES electrodes, the Nb-InAs crossing point as kept to the ground level during the measurements by applying positive and negative voltages symmetrically. Figure 2 shows the voltage dependence of the longitudinal conductance with applying several transverse currents. Below 0.3 mV the conductance is enhanced due to the Andreev reflections at the Nb/InAs interfaces and has a peak structure at the zero bias. This sharp zero-bias peak is attributable to Josephson current carried by the Andreev bound states in InAs. With increasing transverse currents, the Andreev reflection keeps the same amplitude, but the zero-bias peak is suppressed, that is, only formation of the Andreev bound states are disturbed by the spin Hall effect.

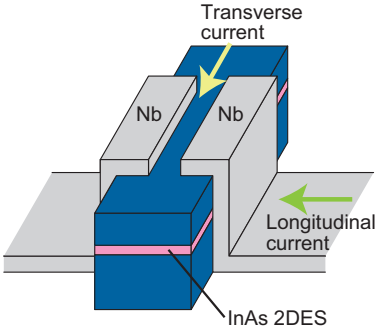

Fig.1. A schematic of Nb/InAs/Nb junctions. The width of the InAs 2DES is 300 nm to 4500 nm.

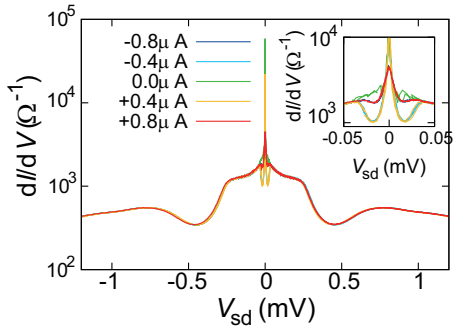

Figure 2. Bias voltage dependence of the differential conductance of a Nb/InAs/Nb junction with a variety of the transverse currents.

[1] T. Schapers, *Superconductor/Semiconductor Junctions* (Springer 2001).
[2] P. Pfeffer and W. Zawadzki, Phys. Rev. B **59**, R5312 (1999).
[3] S.W. Kim, *et al.*, J. Phys. Soc. Jpn. **81**, 054706 (2012).
[4] J. Sinova, *et al.*, Phys. Rev. Lett. **92**, 126603 (2004).

ThP138

The influence of the edge effects on the Hall resistance anomaly

E. M. Kendirlik[1], S. Sirt[1,2], S. B. Kalkan[1] and A. Siddiki[1]

[1] *Department of Physics, Istanbul University, 34134 Istanbul, Turkey*

[2] *Department of Physics, Mimar Sinan Fine Arts University, 34360 Istanbul, Turkey*

At low temperatures and in strong magnetic fields, it is found that the Hall resistance of a two dimensional electron system has plateaus as a function of the number of electrons or magnetic field, and is quantized [1]. However, under these conditions, an unexpected non-monotonic magnetic field B dependence of the Hall resistance at the low-field-end of the quantized plateaus, known as the overshoot effect, remains a puzzle despite both theoretical and experimental efforts. The challenge to utilize the integer quantized Hall effect (IQHE) as a resistance standard would be hindered by such anomalies, especially their physical mechanism is not well understood. This effect had been attributed to the decoupling of the spin-split states within the same Landau level (LL) at odd filling factors by Richter and Wheeler [2] and the scattering between edge states, together with spin-orbit interaction by Komiyama and Nii [3].

In this work,it is reported on systematic experimental findings considering smooth edge defined narrow Hall bars. The overshoot effect observed at the intermediate mobility 2D electron systems are scrutinized and analyzed within the screening theory of the IQHE. We contributed to the understanding of the overshoot effect by performing magneto-transport measurements and investigated the scattering between the edge-edge and edge-bulk evanescent incompressible strips. Unexpectedly, the overshoot effect becomes more pronounced at elevated temperatures, where the Hall bars are defined by shallow chemical etching. In addition, we observe the overshoot effect also at even integer plateaus, which rules out a possible spin dependent explanation, commonly discussed in the literature. All the effect can be elucidated taking into account direct coulomb interaction, namely the screening theory of the IQHE.

[1] K. von Klitzing, G. Dorda and M. Pepper, Phys. Rev. Lett. **45**, 494 (1980).
[2] C. A. Richter and R. G. Wheeler, Surf. Sci. **263**, 270 (1992).
[3] S. Komiyama and H. Nii, Physica B **184**, 7 (1992).

A membrane-based phononic crystal waveguide

D. Hatanaka, I. Mahboob, K. Onomitsu and H. Yamaguchi

NTT Basic Research Laboratories, NTT Corporation, Japan

A phononic crystal is an elastic wave analogue of a photonic crystal. It consists of a periodically-modulated elastic media that results in a bandgap for phonons emerging [1,2]. This can prevent phonons from freely propagating which can enable the development of various phononic crystal devices. However, the phononic crystals reported so far have been passive structures whose elastic properties can only be modulated by changing either the constituent materials or the periodic geometry. In order to realize an active phononic crystal, we fabricated a one dimensional (1D) membrane-based active phononic crystal.

Figure 1 shows an optical microscope image of the 1D phononic crystal and the measurement set-up. It was fabricated by suspending one hundred 30 μm-wide electrically-active membranes ($Al_{0.27}Ga_{0.73}As$ (95 nm)/Si-doped GaAs (100 nm)) [3] by selectively etching the $Al_{0.65}Ga_{0.35}As$ sacrificial layer (3 μm) through 100 equally-spaced holes. This resulted in a 1-mm long waveguide. Application of an alternating voltage to the right-edge membrane induces mechanical oscillations due to the piezoelectric effect. The excited mechanical oscillations can travel in the waveguide and are measured at the left-edge membrane with a He-Ne laser Doppler interferometer. As a preliminary step for the demonstration of its dynamic control, we investigated the frequency response of this 1D phononic crystal in a vector signal analyzer, at room temperature and in a high vacuum when actuated between 0.1-10 MHz as shown in Fig. 2. Both a phononic bandgap (4.5-5.0 MHz) and continuous bands (2.0-4.5 MHz and 5.0-10.0 MHz) are observed. Furthermore, the group velocity of the phonon propagation can be estimated from time domain measurements. These results indicate that this membrane-based 1D phononic crystal can be used as a phononic waveguide which can transfer mechanical energy to any desired direction. The demonstration of a phonon bandgap in a piezoelectric membrane-based phononic waveguide opens up the possibility of on-chip active phononic crystal devices.

[1] R. Martinez-Sala *et al*., Nature **378**, 241 (1995).
[2] Z. Liu *et al*., Science **289**, 1734 (2000).
[3] D. Hatanaka *et al*., Appl. Phys. Lett. **101**, 063102 (2012).

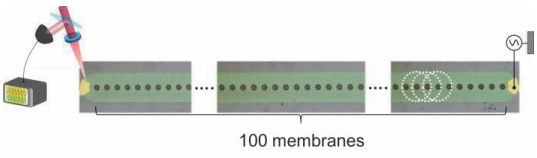

Fig. 1 An optical image of the membrane-based phononic crystal waveguide (green) and the measurement set-up. This waveguide is suspended by removing the sacrificial layer. The dotted circles show a constituent membrane.

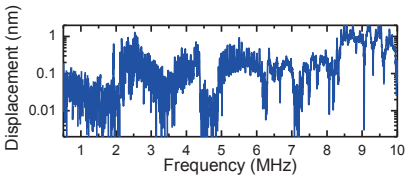

Fig. 2 Frequency response of the membrane-based phononic crystal waveguide when actuating with an amplitude of 0.4 V_{rms}.

Effective g-factors in InAs 2DEGs from THz magneto-photoresponse

M. Pakmehr[1], B. D. McCombe[1], O. Chiatti[2], S. Buchholz[2], S. Fischer[2], C. Heyn[3] and W. Hansen[3]

[1] *Department of Physics, University at Buffalo, The State University of New York*, Amherst, *NY 14260, USA*
[2]*Institut für Physik, Humboldt-Universität, D-12489 Berlin, Germany*
[3]*FG Wachstum, Institut für Angewandte Physik, Universität Hamburg, D-20148 Hamburg, Germany.*

Understanding the effects of spin-orbit interaction in narrow gap semiconductor structures is of interest for both fundamental physics and potential spintronic applications. We have used THz magneto-photoresponse and magnetotransport measurements to probe the high quality 2DEG in a narrow InAs quantum well. Under illumination from several lines of an optically pumped THz laser, the magnetophotoresponse associated with cyclotron resonance (CR) appears in each case as an envelope of the amplitude of the Shubnikov-de Haas oscillations of the 2DEG with a peak near the CR field.[1] We simulated the PR data by a model of resonant carrier heating using the expression for the longitudinal resistivity of a 2DEG and taking the difference between $R_{xx}(B,T)$ in the presence of a resonant temperature profile (laser-on condition), and that with a constant background temperature (laser off) to represent the PR signal. An example of experimental data and a simulation is shown in Fig. 1. In this case there are two magneto- absorption features near CR (inset) – the lower field feature is CR; the origin of the upper feature is not presently understood. The simulations incorporate two lines at the corresponding positions, and both clearly influence the envelope of the oscillations. Clear spin-splitting of the PR oscillations is observed for B > 2.5 T. The SdH oscillations do not show resolved spin-splitting at this carrier density until about 4 T. The photoresponse, a differential temperature electron bolometer effect, generally enhances the visibility of the S-dH oscillations at low fields and the spin–splitting at higher fields. Simulations yield the carrier density, the CR effective mass, scattering times and the g-factor. In the present case for n = 8.84 x 10^{11} cm^{-2}, m* = 0.039 m_e and g = -16, the latter greatly enhanced from the single particle value for this confinement and density, apparently due to many-electron exchange effects. We have also fabricated QPCs in these structures (Fig. 2) using micro-laser photolithography and wet chemical etching, and we will also present PR results for these structures. Work at UB supported by NSF MWN DMR 1008138.

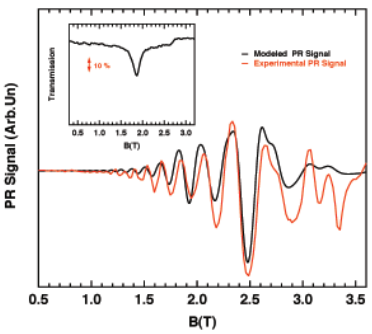

Fig. 1. PR signal at 5.8 meV and 1.8 K vs. B (red) and simulation (black). Inset: magnetotransmission vs. B .

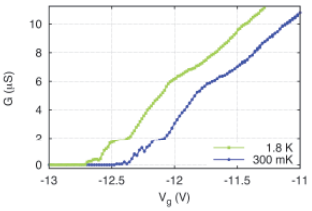

Fig. 2. Conductance vs. in-plane gate voltage showing quantized steps.

[1] M Pakmehr, V. Whiteside, N. Bhandari, et al., Proc. of HMF-20, IOP Journal of Physics:Conference Series, accepted (2012).

Quantum well D^- complexes in a high magnetic field: evidence for their interface nature

V. E. Bisti [1], **A. S. Zhuravlev** [1], **and L. V. Kulik** [1]
[1] *Institute of Solid State Physics RAS, Chernogolovka, Russia*

The spectra of excitations in quasi-two-dimensional systems (high quality GaAs/AlGaAs quantum wells) in a high perpendicular magnetic field are considered experimentally and theoretically. By the method of inelastic light scattering in the spectrum of scattered light two lines were observed. The first line is well-known and is identified as arising due to scattering process involving excitation of spin waves (spin excitons). The second line is new and is identified as resulting from the scattering process with the excitation of $\mathbf{D}^-$ complex. All the excitations studied in this work are spin excitations, and quasi-two-dimensional electrons do not change Landau level. $\mathbf{D}^-$ complex is constructed from two quasi-two-dimensional electrons in the quantum well and positively charged donor impurity. The considered excitation corresponds to the spin-flip of one of the electrons accompanied by a change in the Coulomb interaction. Energies of the singlet and triplet states of the complex in the high-field approximation (all electrons are on the lowest Landau level) are calculated taking into account the interaction energies dependence on the well width. The position of impurity inside the well, outside the well or on the well-barrier interface is considered.

The results demonstrate the switch of the ground state for the barrier $\mathbf{D}^-$ complex from the triplet 1T (higher fields) to the singlet 0S (lower fields) which corresponds to zero energy point in Fig.1. Comparison of the calculations performed for different impurity positions and experimental data leads to a firm conclusion that impurities in such quantum well structures are located at the interface.

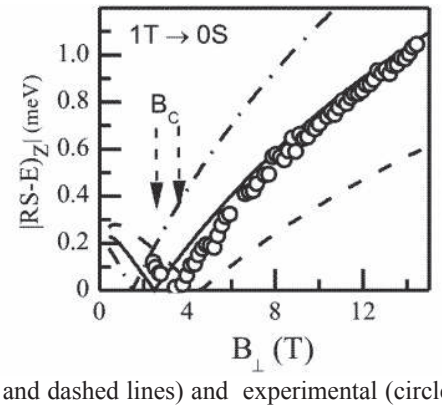

Theoretical (solid and dashed lines) and experimental (circles) correspond to the energies for the excitations between 1T and 0S D- complexes for the well width 20 nm. Solid line represents the calculated data for the barrier D^- complex and coincides with the experimental results. Dashed lines correspond to the calculations with the positive charge located at a distance of 10 nm from both sides of the barrier.

ThP142

Electron-electron interaction correction and magnetoresistance of 2DE system in the parallel field.

A. Yu. Kuntsevich, L. A. Morgun and V.M. Pudalov

P.N. Lebedev Physical Institute RAS, 119991, Leninskiy prosp. 53, Moscow, Russia

Various low density 2D systems demonstrate strong positive magnetoresistance (MR) in the field parallel to the 2D plane [1-3]. This effect is believed to be due to the influence of the Zeeman splitting on electron-electron interactions and is often used to determine the renormalized spin susceptibility [4,5]. The parallel field MR was explained in two different manners, in terms of: (i) diffusive electron-electron interaction correction (EEC) [6,7], and (ii) renormalization of the density of states and single impurity scattering time [8].

Analysis of the resistivity tensor components ρ_{xx} and ρ_{xy} in perpendicular magnetic field was demonstrated earlier [9] to enable extraction of the EEC. Following this ideology, in the present study we use tilting the magnetic field as a powerful tool to distinguish between spin and orbital effects and to explore mechanisms of the parallel field magnetoresistance. We use several Si-MOS disordered 2D electron systems (mobilities μ=1500–5000 cm^2/Vs) with isotropic *g*-factor and thin 2DE layer (<4 nm). EEC is extracted from the simultaneous analysis of both ρ_{xx} and ρ_{xy} components measured in tilted magnetic field up to 15 Tesla, for electron densities (8-30)$\cdot 10^{11}$cm^{-2}, and at temperatures 0.3-30K.

By changing the tilt angle we show that EEC depends on the modulus of magnetic field rather than on its direction, in agreement with theory of the EEC for an isotropic g-factor case. However, the extracted EEC value appears to be an order of magnitude smaller than that required to explain the large MR. This anomalously strong parallel field MR is sharply suppressed by an insignificant, non-quantizing perpendicular field component. The above suppression points to a non-purely Zeeman origin of the parallel field MR.

We also observe a nonlinearity of the Hall resistance (~10%) in low-fields that finds so far no explanation. In total, our findings point at the incompleteness of the existing theory of magnetotransport in interacting and disordered 2D systems: too strong parallel field magnetoresistance, its suppression by perpendicular magnetic field, and the low-field Hall anomaly require an explanation. We believe that these three phenomena are interrelated and originate from a destructive action of the perpendicular field on the localized states coexisting with the 2D electron liquid.

[1] D. Simonian, S.V. Kravchenko, M.P. Sarachik, V.M. Pudalov, Phys. Rev. Lett. **79**, 2304 (1997).
[2] J. Yoon, C. C. Li, D. Shahar, D. C. Tsui, and M. Shayegan, Phys. Rev. Lett. **84**, 4421 (2000).
[3] K.Lai, W. Pan, D.C. Tsui, S.A. Lyon, M. Mühlberger, F. Schäffler, Phys. Rev. B **72**, 081313 (2005).
[4]A.Shashkin, S.V.Kravchenko, V.T. Dolgopolov, T.M.Klapwijk, Phys. Rev. Lett, **87**, 086801 (2001);
[5]S.Vitkalov, K.James, B.Narozhny, M.P.Sarachik, T.M.Klapwijk, Phys. Rev. B **67**, 113310, (2003).
[6] P.A. Lee, T.V. Ramakrishnan, Phys. Rev. B **26** , 4009 (1982).
[7] S. Anissimova, S.V. Kravchenko, A. Punnoose, A.M. Finkel'stein, T.M. Klapwijk, Nature Phys. **3**, 707 (2007).
[8] V. T. Dolgopolov, A. Gold, JETP Letters, **71**,27-30,(2000).
[9] G. M. Minkov, A. V. Germanenko, O. E. Rut, A. A. Sherstobitov, V. A. Larionova, A. K. Bakarov, and B. N. Zvonkov Phys. Rev. B **74**, 045314, (2006).

Coexistence of nearly free and strongly bound trions from magneto-photoluminescence of two-dimensional quantum structures with tunable electron or hole concentration

J. Jadczak [1,3], **L. Bryja** [1], **A. Wójs** [1], **M. Potemski** [2], **P. Plochocka** [3], **F. Liu** [4], **D. R. Yakovlev** [4] **M. Bayer** [4], **D. Reuter** [5], **A. Wieck** [5], **C. A. Nicoll** [6], **I. Farrer** [6] and **D. A. Ritchie** [6]

[1] *Institute of Physics, Wroclaw University of Technology, Wroclaw, Poland*
[2] *Laboratoire National des Champs Magnétiques Intenses, CNRS-UJF-UPS-INSA, Grenoble, France*
[3] *Laboratoire National des Champs Magnétiques Intenses, CNRS, Toulouse, France*
[4] *Experimentelle Physik 2, Technische Universität Dortmund, Dortmund, Germany*
[5] *Lehrstuhl für Angewandte Festkörperphysik, Ruhr-Universität Bochum, Bochum, Germany*
[6] *Cavendish Laboratory, University of Cambridge, Madingley Road, Cambridge, UK*

A dilute two-dimensional (2D) gas of charge carriers in a quantizing perpendicular magnetic field hosts spectacular emergent phenomena exemplified by fractional quantum Hall effect, well-known to depend on both many-body interaction effects and single-particle localization.

We studied coexistence and competition of nearly free and laterally localized radiative excitonic complexes in quantum Hall systems, as revealed in satellite recombination channels activated by their coupling with surrounding nearly free carriers. In contrast to most previous experiments involving 2D electrons we used valence holes whose higher mass appears critical in contrasting the emission signatures from the free and localized charged excitons (trions).

The experiments involve low temperature (T=2–30K), high magnetic field (B=0–23T), polarization resolved (σ^-/σ^+) photoluminescence (PL) on high-quality quantum wells. The key feature was two-beam illumination (photon energies below and above band-gap in the barrier) enabling dynamical tuning of carrier concentration in the acceptor-doped structures – beyond the point of *p*- to *n*-type conversion.

In comparative PL studies of symmetric and asymmetric structures with different widths (w=15–22 nm) and concentrations (tunable, electrons or holes – in the same sample) we were able to identify and understand multiple optical transitions, including nearly free excitons and trions, excitonic complexes bound to charged impurities placed in the well and in the barriers, and their (positive and negative) cyclotron replicas. In particular, we studied the effect of *p*- to *n*-type conversion on those transitions and on the stability of the corresponding complexes.

The most insightful results concern emission from positive trions moving almost freely in the quantum well (X^+) or bound to nearby ionized acceptors in the barrier (AX). We show distinction between X^+ and AX transitions and coexistence of both complexes. As expected, the X^+ shows in the spectra about 1 meV below the exciton X, split into three lines (family of bound states distinguished by spin and angular momentum). The AX is observed far below the X^+, in form of multiple parallel, equidistant, weak lines, corresponding to the acceptors placed on different crystallographic planes in the barrier, characterized by discrete distance from the well. Striking contrast between X^+ and AX lines in their (strong vs nearly absent) dependence of the energy position on the well width. Crucial for the identification of both complexes was also dramatic difference in their binding energy (in contrast to X^- vs DX in previously studied *n*-type wells). Alternative interpretation in terms of AX^- instead of AX will also be discussed.

Samples: GaAs/GaAlAs single quantum wells grown by MBE on (001)-oriented semi-insulating GaAs substrate, Carbon δ-doped in one or both barriers; hole mobility (at T=4.2 K): μ=(1.2-7.4)×10^5 cm^2/Vs; hole concentration (in the dark): p=(1.51–2.4)×10^{11} cm^{-2}.

ThP144

Interference effects on the photoluminescence of AlGaN/GaN quantum wells

M. Ramírez-López [1,2], M. Pérez-Caro[1], Y. L. Casallas-Moreno[1], and M. López-López[1]

[1] *Physics Department, Centro de Investigación y Estudios Avanzados del IPN, Apartado Postal 14-740, México D.F., México 07000*
[2] *Unidad Profesional Interdisciplinaria en Ingeniería y Tecnologías Avanzadas, Av. IPN 2580, Barrio La Laguna Ticomán, Gustavo A. Madero, 07340, México, D.F.*

Group III-nitride semiconductor materials have enabled the design of nanostructures that can operate optically from the infrared to the ultraviolet of the electromagnetic spectrum, which are highly suitable for making electroluminescent devices, sensors and high efficiency solar cells [1].In this work we compared the propierties of AlGaN(50 nm)/GaN(5 nm) quantum wells (QWs) grown on Si(111), with those grown on sapphire substrates by Plasma Assisted Molecular Beam Epitaxy (PAMBE). The nanostructures were characterized structurally by high resolution X-ray diffraction (HRXRD) and scanning electron microscopy (SEM), which show the interfaces of the QWs, and the formation of wurtzite GaN and AlGaN. Optical properties were characterized by photoluminescence (PL), cathodoluminescence (CT) and reflectance (R) spectroscopies. Reflectance spectra show interference oscillations of the different layers, which disappear at the band gap edges of the GaN buffer layer (3.4 eV) and the AlGaN barrier layers (4.4 eV). The PL and CT spectra of the sample grown on sapphire show a strong emission (3 eV), which is consistent with recombination energy determined by self-consistent calculations taking in account a 4 MV/cm built-in electric field and low carrier densities. On the other hand, the sample grown on Si(111) presents a PL spectrum centered at 3 eV, which is modulated by the oscillations that match the reflectance spectrum (Figure 1). In order to understand the modulation of the photoluminescence spectrum, we measured PL and R spectra at different emission angles relative to the normal sample. The modulation peaks have a blue shift (Figure 2) when the angle θ_m at which the spectrum is measured increases because $Cos(\theta_m)$ decrease, and therefore the energy of constructive interference increase according to the interference condition (inset function). From these results we conclude that the photoluminescence modulation is due to the Fabry-Petrot interference of light emitted from the QWs when it is reflected at the GaN/Si(111) and AlGaN/air interfaces, which is not present in the sample grown on sapphire due to its wide band-bap.

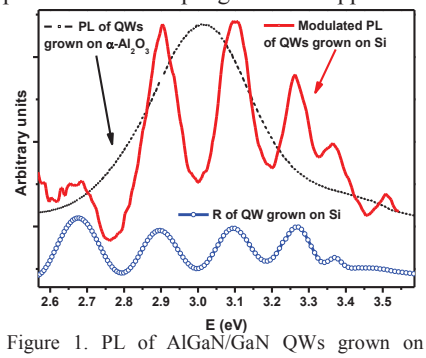

Figure 1. PL of AlGaN/GaN QWs grown on Si (continuous line) and Sapphire (dashed line). Reflectance of QWs grown on Si (open circles).

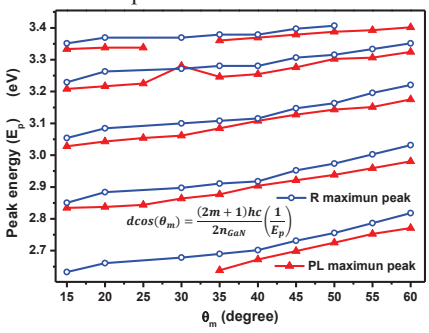

Figure 2. Angle dependence of PL (triangles) and reflectance (open circles) maximum ($\mathbf{E_p}$) for sample grown on Si.

This work was partially suported by CONACYT-SENER project No. 151076 and ICyTDF.

[1] Junqiao Wu, J. Appl. Phys. 106, 01110 (2009)

Orientation efficiency and unavoidable decoherence in optical initialization of hole spins in p-doped quantum wells

Michał Gawełczyk and Paweł Machnikowski

Institute of Physics, Wrocław University of Technology, Wybrzeże Wyspiańskiego 27, 50-370 Wrocław, Poland

Hole spin dynamics in semiconductors is a highly explored field in solid state physics due to its possible applications in rapidly developing field of spintronics. Recently, an optical hole spin initializtion scheme for p-doped quantum well or dot systems via coupling to trion states with sub-picosecond circularly polarized laser pulses was demonstrated [1, 2]. In this theoretical study, we analyze the efficiency of spin initialization and predict the intrinsic spin coherence loss due to the pulse excitation itself as well as the phonon-induced spin dephasing, both taking place on the timescale of the driving laser pulse. Such decay of coherence may be important in future applications but it affects also the results of experiments carried out currently, especially those based on the resonant spin amplification effect [1, 3], where the formation of the observed signal depends essentially on the spin coherence.

Spin states under optical excitation may undergo pure dephasing due to dynamical phonon response to the transient charge evolution [4]. Even if not directly coupled to the reservoir, spin is indirectly dephased through the entangling charge evolution caused by the optical pulse. We show that indeed such a dephasing process is present in the considered system. Morover, we find that the laser pulse itself causes a significant amount of decoherence. Therefeore, some degree of dephasing is unavoidably built into the initialization scheme. Since both the degree of dephasing as well as the orientation efficiency are proportional to the excitation power, it is impossible to reduce the relative loss of coherence by using weak excitation.

Therefore, we focus on the ratio of the degree of dephasing to the achieved orientation effect as a resonable figure of merit and study its dependence on both carrier system and laser pulse parameters. We show that it does not depend on the pulse area but is sensitive to the temperature and detuning. Our results alow us to identify the optimal excitation parameters.

The obtained dependence of the degree of dephasing on detuning is in a qualitative agreement with the recent experimental data [1] for resident hole spins in p-modulation-doped $GaAs/Al_{0.3}Ga_{0.7}As$ single QWs.

[1] M. Kugler, K. Korzekwa, P. Machnikowski, C. Gradl, S. Furthmeier, M. Griesbeck, M. Hirmer, D. Schuh, W. Wegscheider, T. Kuhn, C. Schüller, and T. Korn, Phys. Rev. B **84**, 085327 (2011).
[2] M. Studer, M. Hirmer, D. Schuh, W. Wegscheider, K. Ensslin, and G. Salis, Phys. Rev. B **84**, 085328 (2011).
[3] J. M. Kikkawa and D. D. Awschalom, Phys. Rev. Lett. **80**, 4313 (1998).
[4] A. Grodecka, P. Machnikowski, and J. Förstner, Phys. Rev. A **79**, 042331 (2009).

Andreev reflection in spin-polarized transport through an interacting quantum dot in a hybrid tunneling junction

K. Bocian [1], **W. Rudziński** [1]

[1] *Department of Physics, Adam Mickiewicz University, ul. Umultowska 85, 61-614 Poznań, Poland*

Spin-dependent tunneling through a quantum dot coupled to one ferromagnetic and one superconducting electrodes is studied in the Andreev reflection (AR) regime. Electrical conductance is calculated within the nonequilibrium Green function technique. Effects due to a competition between the Coulomb correlations on the dot, intradot spin-flip processes and Zeeman splitting of the dot discrete level are analyzed in both linear and nonlinear transport regimes. Moreover, the AR phenomenon is studied for different coupling strengths of the dot to the external electrodes and for different magnetizations of the ferromagnetic electrode. It is shown that when a coherent spin rotation is present on the dot, Coulomb interactions may lead to a significant enhancement of the AR tunneling current. A new interference effect due to AR is predicted to appear in the case of a weak intradot repulsion. By contrast, strong Coulomb correlations studied in nonequilibrium situation revealed significant modifications of the AR differential conductance which occurs only in case of spin-polarized transmission. New conditions of the matching of Fermi velocity leading to the perfect AR transmission are formulated in the context of arbitrary Coulomb correlations on the dot. Origin of occurrence of a variety of the multipeak structure of the conductance in equilibrium as well as in nonequilibrium situation is also discussed in detail.

Engineering of type II quantum wells for a broad range of mid infrared emission in interband cascade lasers

K. Ryczko, G. Sęk and J. Misiewicz

Institute of Physics, Wroclaw University of Technology, 50-370 Wroclaw, Poland

Semiconductor lasers emitting in the mid-infrared (MIR) spectral range of 3-8 μm are required for applications in environmental pollution monitoring, medical diagnostics, infrared countermeasures, laser surgery, and gas leakage detection. There exists at least several competing concepts of sources of coherent radiation in MIR including common laser diodes base on type quantum wells (QWs), quantum cascade lasers (QCLs) and interband cascade lasers (ICLs). The main advantage of the latter is combining the potentially possible broad tuning range of the emission, minimized influence of the Auger related carrier losses, and a very low power consumption [1]. However, in order to realize that many parameters of these multilayer structures must be optimized, especially on the side of the active region which is composed of a cascade of type II QWs made of a broken gap materials.

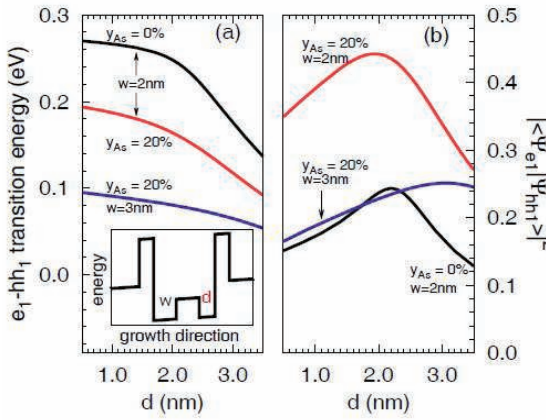

Fig. 1 Effect of type II QW asymmetry (as shown in the inset) and separating barrier composition on the fundamental e1-hh1 transition energy (a), and squared wave function overlap integral.

In this work, we discuss a few possibilities of implementing type-II W-design QW, which allows to preserve the large optical matrix elements in spite of indirect in the real space character of the optical transition. We concentrate on the InAs/GaIn(As)Sb QWs and calculate their fundamental electronic structure properties with respect to the final device performance [2-3]. The calculations are performed within the eight-band k·p theory. We demonstrate the broad range of tunability via the structure parameters modifications, and including the effect of the electric field in order to simulate the operational device conditions. We show that the transition oscillator strength can still be efficiently optimized for wavelengths even beyond 8 μm, if the composition of the separating barrier, which is simultaneously the well for holes, is chosen properly, and for the given range of thickness of InAs layers confining electrons, and the exactly matched structure asymmetry in order to compensate for the effect of the electric field existing in the ICL device. Eventually, detailed prescriptions of the optimized QW designs for certain emission wavelengths are given.

[1] I. Vurgaftman, W. W. Bewley, C. L. Canedy, C. S. Kim, M. Kim, C. D. Merritt, J. Abell, J. R. Lindle, J. R. Meyer, Nature Commun. 2, 585 (2011).

[2] F. Janiak, G. Sęk, M. Motyka, K. Ryczko, J. Misiewicz, A. Bauer, S. Höfling, M. Kamp, A. Forchel, Appl. Phys. Lett. 100, 231908 (2012).

[3] M. Motyka, K. Ryczko, G. Sęk, F. Janiak, J. Misiewicz, A. Bauer, S. Höfling, A. Forchel, Optical Materials 34, 1107 (2012).

Optical properties of type II quantum wells based on GaSb and InAs emitting in a mid infrared range

F. Janiak[1], M. Motyka[2], G. Sęk, K. Ryczko, J. Misiewicz, R. Weih[2], M. Dallner[2]
S. Höfling[2], M. Kamp[2], A. Forchel[2]

[1] *Institute of Physics, Wrocław University of Technology, Wybrzeze Wyspianskiego 27, 50-370 Wrocław, Poland*
[2] *Technische Physik, Physikalisches Institut, Universität Würzburg, Am Hubland, D-97074 Würzburg, Germany*

Mid-infrared semiconductor lasers are continuously increasing their application range during the last years including for instance gas sensing for detection and control of the presence or concentration of harmful gases like CO_2, SOx, NH_3, and many others. The benefits of optical detection methods have been limited mainly by the lack of suitable laser light sources, which have to provide the sensing wavelength in single mode and continuous wave (cw) operation in order to provide the required wavelength and its tunability. Hereby, we present fundamental optical and electronic properties of a type II quantum well system potentially able to cover spectrally the range of 2 to 8 μm, and beyond, and is possible to be integrated in a photonic sensor unit for gas detection.

There will be reviewed the optical properties of investigated type II "W-shaped" structures, deposited on two different substrates – InSb and InAs. It has been investigated structural parameters like as the band offsets importance, and its sensitivity to the layers composition, the active type II transition oscillator strength versus various structure parameters and external factors as temperature or electric field, and the predominating carrier loss mechanisms. For that a combination of several spectroscopic techniques have been used, both emission-like (photoluminescence) and absorption-like (modulated reflectivity spectroscopy) supported by the energy level calculations employing a multiband **kp** model. Eventually, the potential for further material optimization and prospects for the improved device performances will be given.

The work was supported by the EC within Project WideLase No. 318798 of the 7th Framework Program and by the COPERNICUS Award of the Foundation for Polish Science and Deutsche Forschungs Gemeinschaft.

References

[1] F. Janiak et al., Appl. Phys. Lett. **100**, 231908 (2012)

[2] G. Sęk, F. Janiak, Optical Materials **33** 1817 (2011)

[3] M. Motyka, K. Ryczko, G. Sęk, F. Janiak, Optical Materials **34 1107** (2012)

$p \times n$-Type Transverse Thermoelectrics: Driving Perpendicular Heat Flow in Type II Superlattices of InAs/GaSb

M. Grayson [1], Chuanle Zhou [1], S. Birner [2,3,4], Yang Tang [1], and K. Heinselman [1]

[1] *Electrical Engineering and Computer Science, Northwestern University, Evanston, Illinois 60208, USA*
[2] *Walter Schottky Institut, Technische Universität München, 85748 Garching, Germany*
[3] *Institute for Nanoelectronics, Technische Universität München, 80333 Munich, Germany*
[4] *nextnano GmbH, 85586 Poing, Germany*

We introduce a band-engineered transverse thermoelectric with *p*-type Seebeck in one direction and *n*-type orthogonal, resulting in off-diagonal terms that drive heat flow transverse to electrical current [1]. We name such materials $p \times n$ ("p-cross-n") type transverse thermoelectrics. Whereas thermoelectric performance is normally limited by the figure of merit ZT, transverse thermoelectrics can achieve arbitrarily large temperature differences in a single leg Peltier cooler even with inferior *ZT* by being geometrically tapered. Similarly, a single meander line geometry can result in large Seebeck voltage generation, exceeding the optimal performance of a rectangular leg of standard thermoelectric. An intuitive microscopic model is introduced to explain the transverse thermoelectric effect in $p \times n$ materials, which are shown to have advantages for microscale devices and cryogenic temperatures—exactly the regimes where standard longitudinal thermoelectrics fail.

Figure 1 below introduces a microscopic model of a $p \times n$-type semiconductor, with electrons dominating current along the *b*-axis, and holes dominating current along the *a*-axis. The crossed-arrow symbol in the upper right labels the *n* and *p* axes. Transverse thermoelectric behavior is achieved when electrical currents J_x and heat currents Q_y flow at close to 45 degrees relative to the *n*- and *p*- axes, as shown. An expression for the optimal transverse figure of merit $Z_{\perp}T$ and the optimal current/heat flow angle θ is derived.

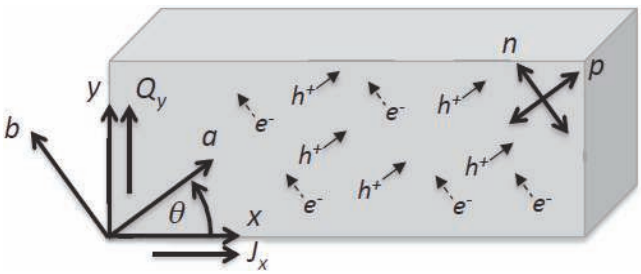

Figure 1. $p \times n$–type transverse thermoelectrics. Materials with *n*-type Seebeck perpendicular to a *p*-type Seebeck (notated with crossed arrows, upper right) can function as transverse thermoelectrics, driving thermoelectric heat flow perpendicular to an applied current.

A band-structure engineering strategy is described, whereby alternating InAs and GaSb layers in a wide-period superlattice can give rise to the desired $p \times n$ Seebeck tensor. A literature survey shows some anisotropic bulk semiconductors also have the necessary $p \times n$–type Seebeck behavior, such as $CsBi_4Te_6$ and $ReSi_{1.75}$.

[1] Chuanle Zhou, S. Birner, Yang Tang, K. Heinselman, and M. Grayson, (accepted to Phys. Rev. Lett. 2013)

Room-temperature TE-polarized intersubband electroluminescence from quantum cascade structures based on InAs/AlInAs quantum dashes

V. Liverini[1], L. Nevou[1], F. Castellano[1,2], A. Bismuto[1], M. Beck[1], F. Gramm[3] and J. Faist[1]

[1] ETH Zürich, Institute for Quantum Electronics, Wolfgang-Pauli-Strasse 16, 8093 Zürich, Switzerland
[1,2]CNR, Istituto Nanoscienze, Piazza dei Cavalieri 12, Pisa, Italy
[3] Electron Microscopy ETH Zurich (EMEZ), ETH Zurich, Wolfgang-Pauli-Strasse 16, 8093 Zürich, Switzerland

The introduction of 3D-confined quantum dots (QDs) or dashes (QDashes) in the active region of Quantum Cascade Lasers (QCLs) would improve their performance by increasing the upper laser state lifetime[1, 2] and allowing for transverse-electric (TE) polarized emission unachievable in quantum-well-based QCLs. Electroluminescence (EL) from QC structures based on InAs/GaAs QDs has already been shown[3, 4], here we demonstrate TE-polarized EL from an in-plane-confined state of InAs/AlInAs QDashes grown in a QC structure based on InAs/AlInAs QDashes[5].

In Fig. 1a, we show the measured TE-polarized intersubband (ISB) absorption from the ground state (|1,1,1>) to the first excited state (|2,1,1>) associated with the lateral confinement due to the width of the dashes (the [110] direction in Fig. 1a insets). The absorption peaked at 89 meV and the extrapolated dipole moment for this transition was 1.7 nm. The QDashes were grown in a QC structure designed to exploit such transition (TEM in the bottom inset of Fig. 1a). The structure was processed as wide ridge lasers and Fig. 1b shows the EL for two devices of the same size but different ridge orientation: one with ridge length along the dash elongation (thick blue line) and the other perpendicular to it (thin blue line). TE-polarized EL was present only for devices processed with ridges parallel to the dash elongation and was centered around 110 meV, in good agreement with the absorption measurements.

The TE EL signal, which was present also at room temperature (inset Fig. 1b), increased with applied bias but no sign of gain could be seen before a negative differential resistance occurred. We will present recent results showing the effect of changes in the active region design.

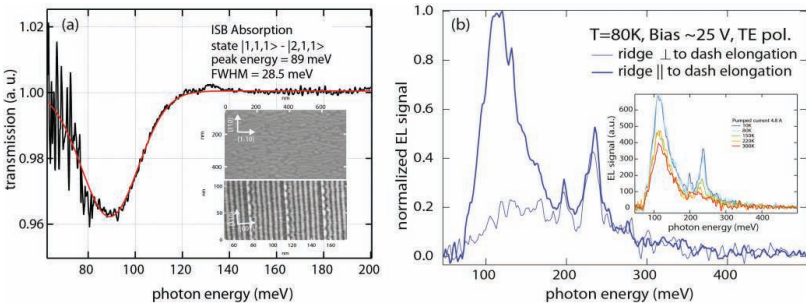

Fig. 1 (a) Black curve, .measured ISB absorption of TE-polarized light by a 50-period stack of InAs/AlInAs QDashes at T=300K. Red curve, Gaussian fit. Inset: (top) SEM of uncapped QDashes, (bottom) TEM image of three periods of the QC structure along the dash width ([110]). (b) 80K TE-polarized EL for the device with ridge length along the dash elongation (thick blue line) and perpendicular to the dash elongation (thin blue line) at a bias of 25 V. Inset: TE-polarized EL measurements up to room temperature for the same current in the device.

[1] R. A. Suris, NATO ASI Ser. E **323** 197 (1996).
[2] C. F. Hsu, J. S. O, P. S. Zory and D. Botez, SPIE: In-Plane Semiconductor Lasers: from Ultraviolet to Midinfrared, **3001** 271 (1997).
[3] S. Anders, L. Rebohle, F. F. Schrey, W. Schrenk, K. Unterrainer and G. Strasser, Appl. Phys. Lett. **82** 3862 (2003).
[4] D. Wasserman, T. Ribaudo, S. A. Lyon, S. K. Lyo and E. A. Shaner, Appl. Phys. Lett. **94** 061101 (2009).
[5] V. Liverini, L. Nevou, F. Castellano, A. Bismuto, M. Beck, F. Gramm and J. Faist, Appl. Phys. Lett. **101** 261113 (2012).

Ambipolar high-mobility transistors in undoped GaAs/AlGaAs quantum wells

A.F. Croxall[1], B. Zheng[1], F. Sfigakis[1], K. Das Gupta[1,2], I. Farrer[1], C.A. Nicoll[1], H.E. Beere[1], and D.A. Ritchie[1]

[1] *Cavendish Laboratory, University of Cambridge, Cambridge CB3 0HE, UK*
[2] *Department of Physics, Indian Institute of Technology Bombay, Mumbai 400076, India*

In an ambipolar device, electrons or holes can be populated on demand in the same conduction channel, with their different properties such as effective mass and spin-orbit coupling. In GaAs/AlGaAs heterostructures, standard modulation doped techniques cannot easily be used as the dopant determines the polarity of the carriers and precludes the formation of the other carrier type. Undoped heterostructures, where the two-dimensional (2D) gas is formed entirely by field effect [1], allow either electrons or holes to populate the channel dependent upon the polarity of the gate voltage, if both n-type and p-type ohmic contacts exist [2]. Unlike in graphene or in carbon nanotubes, there is a 1.5V voltage window between either electron or hole population, (primarily determined by the bandgap of GaAs, 1.52eV).

We have fabricated undoped ambipolar GaAs-based quantum well devices, with different well widths (L=10-25nm) with patterned Ti/Au back and front gates, using a flip-chip process [4, 5]. This method allows a large range of densities to be achieved, *e.g.* from 7×10^{9}cm^{-2} to 5×10^{11}cm^{-2} in a single device with single subband occupation, and without any parallel conduction of any kind. It also enables us to precisely control the wavefunction's position in the quantum well over a wide range, which we characterise by the variable α (Figure 1).

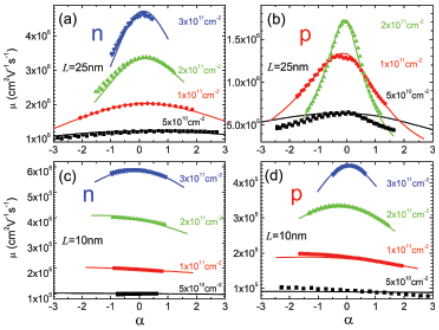

Figure 1: Electron/hole mobilities versus α for L=10nm and 25nm, where $\alpha = (\vec{E}_{front} - \vec{E}_{back})/|(\vec{E}_{front} + \vec{E}_{back})|$.

The change with α of the mobility (points) can be attributed to the relative change of interface roughness scattering from the two interfaces. We have modelled the mobility (solid lines) in the zero temperature limit within the Boltzmann transport formalism [3, 6], with numerically-solved wavefunctions, allowing us to independently characterise the two interfaces. As a growth optimisation tool, the information thus gained on the various scattering mechanisms present will help the development of very high mobility structures.

In conclusion, we have shown an excellent platform for creating high mobility two-dimensional electron (4.7×10^{6}cm^{2}V^{-1}s^{-1} at n=2×10^{11}cm^{-2}) and hole gases (1.8×10^{6} cm^{2}V^{-1}s^{-1} at p=2×10^{11}cm^{-2}), with considerable tunability which may assist the study of fractional quantum Hall states.

[1] B. E. Kane *et al.*, Appl. Phys. Lett. **63**, 2132 (1993).
[2] J. C. H. Chen *et al.*, Appl. Phys. Lett. **100**, 052101 (2012).
[3] A. F. Croxall *et al.*, Appl. Phys. Lett. **102**, 082105 (2013).
[4] K. D. Gupta *et al.*, Semicond. Sci. Technol. **27**, 115006 (2012).
[5] M. V. Weckwerth *et al.*, Superlattices Microstruct. **20**, 561 (1996).
[6] W. Y. Mak *et al.*, Appl. Phys. Lett. **97**, 242107 (2010).

Surface Acoustic Wave-Driven Carrier Dynamics As A Contact-less Probe For Mobilities Of Photogenerated Carriers In Undoped Nanowires

J. B. Kinzel[1], *F. J. R. Schülein*[1], *M. Weiss*[1], *D. Rudolph*[2], *G. Koblmüller*[2], *J. J. Finley*[2], *G. Abstreiter*[2], *A. Wixforth*[1], *H. J. Krenner*[1]

[1] *Lehrstuhl für Experimentalphysik 1, Universität Augsburg, 86150 Augsburg, Germany*
[2] *Walter Schottky Institut, TU München, 85748 Garching, Germany*

We recently applied surface acoustic waves (SAWs) as a fast control mechanism to dynamically modulate the optical emission of single semiconductor nanowires (NWs) at radio frequencies [1]. The underlying processes are strongly dependent on the acoustic amplitude and directly reflect the charge carrier mobilities in the investigated structure. Here we present that our SAW technique provides a contact-less and massively parallel probe for the intrinsic mobilities of electrons and holes in otherwise undoped surface-passivated GaAs/AlGaAs core-shell NWs. To resolve the SAW-driven carrier dynamics, we perform stroboscopic time-correlated single photon counting (s-TCSPC) of the photoluminescence (PL) emission of individual NWs. A typical unperturbed PL transient is plotted in red in Fig. 1(a) showing a mono-exponential decay with a time constant of τ_{PL}= 1.3 ns. When subject to a SAW (f_{SAW} = 194 MHz, P_{SAW} = +5 dBm), we observe a characteristic beating in the PL transient (blue), matching T_{SAW} = 5.1 ns. As expected, this beating shifts in time by $T_{SAW}/2$ as the local acoustic phase is tuned by 180° (green). This observation is a direct fingerprint of the charge carrier dynamics and acoustic charge conveyance within the SAW-induced type-II band edge modulation. As sketched in Fig. 1(b), electrons transfer from the position of the excitation laser (x_0) into the energetically favourable stable points at the minimum of the conduction band. In contrast to electrons, holes remain stationary at the point of photogeneration due to their reduced mobility. $T_{SAW}/2$ later these electrons are conveyed to the position of the holes giving rise to the observed beating. As we further increase the acoustic power, transport of holes sets in. This in turn gives rise to an abrupt and instantaneous quenching of the NW emission. The recorded time transients for different acoustic powers can be reproduced nicely by numerically solving the semi-classical drift and diffusion transport equation for electrons and holes in the SAW-induced potentials. From a direct comparison of the experimental data and the numerical simulation results we determine mobilities of μ_e = 500 cm^2/Vs and μ_h = 50 cm^2/Vs for electrons and holes in the core of the investigated NWs, respectively.

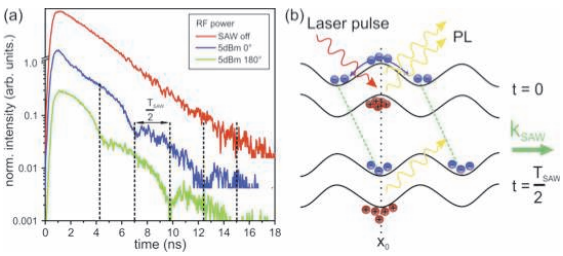

Fig. 1 (a) PL transient of a single GaAs/AlGaAs core-shell NW without SAW (red) and with SAW applied with defined phase shifts (blue, green). (b) Dissociation and acoustic transport of electrons in the SAW-induced type-II bandedge modulation. Spatial overlap of transported electrons and stationary holes gives rise to the observed time-delayed PL emission.

[1] J. B. Kinzel et al., Nano Lett. **11**, 1512-1517 (2011).

Lithographically defined plasmonic bowtie nanoantennas on GaAs and SiO_2 substrates with proximal quantum emitters

K. Schraml [1], G. Bracher [1], M. Spiegl[1], M. Kammerlocher[1], B. Mayer[1], M. Bichler[1], K. Müller[1], M. Kaniber and J.J. Finley[1]

[1] *Walter Schottky Institut, Am Coulombwall 4a, 85748 Garching, Germany*

The local-field enhancements around structured metallic nanoparticles can strongly influence the strength of light-matter interactions over extreme sub-wavelength dimensions. For example, they give rise to strong enhancements of the spontaneous emission yield in hybrid systems that combine metallic nanostructures with proximal emitters and fluorophores [1],[2] and have been predicted to enhance the efficiency of photovoltaic devices [3].

Here, we present the simulation, design and fabrication of gold bowtie nanoantennas on GaAs and SiO_2 using electron beam lithography. We measure the surface plasmon resonance frequency (λ_{SPR}), characterize the impact of geometrical parameters and test the influence of the antenna on the radiative properties of proximal quantum emitters. Two different samples were fabricated with plasmonic nanostructures; (i) on SiO_2 decorated with implanted CdSe nanocrystals and (ii) on GaAs with near surface self-assembled InGaAs quantum dots. As shown in fig 1 (inset), high quality nanostructures with feed-gaps and tip radii as small as $d = 10$ nm (see fig 1) were realized, with simulated field enhancement factors of 10^3-$10^4\times$. White light reflectivity was used to determine λ_{SPR} and demonstrate that it can be continuously tuned in the range $1\mu m \geq \lambda_{SPR} \geq 700\,nm$ by reducing the nano-triangle size from $s = 200$ nm to 100 nm. This directly shifts λ_{SPR} into the range of optical activity of colloidal CdSe nanocrystals (~640 nm). For nano-antennas on GaAs, the much higher refractive index of the substrate ($n_{GaAs} = 3.5$ c.f. $n_{SiO_2} = 1.5$) shifts λ_{SPR} by ~300 nm to longer wavelength for similar structure sizes. On GaAs substrates, λ_{SPR} could be tuned into the emission range of InGaAs quantum dots (900 nm to 950 nm) opening the way to probe coupling phenomena. First investigations of the influence of such plasmonic bowtie antennas on the linear and non-linear optical properties of CdSe and InGaAs proximal quantum emitters will be presented and characterized as a function of the feed-gap size and the surface plasmon resonance wavelength.

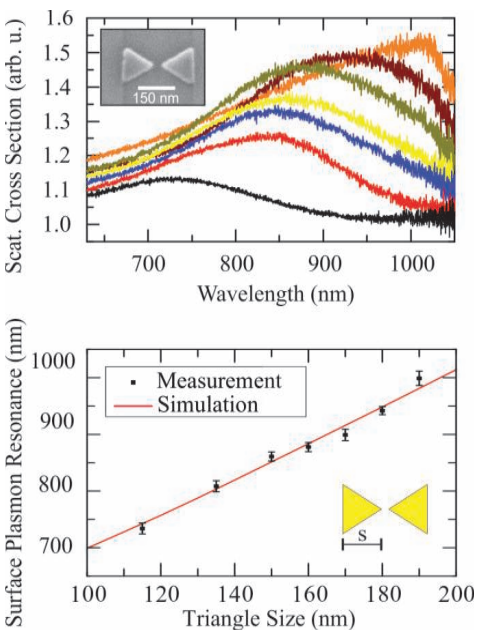

Fig. 1: Typical measurements and FDTD simulation of surface plasmon resonances for a 35nm thick gold bowtie nanoantennas on glass as a function of triangle size. The inset shows a SEM picture of a typical structure investigated.

[1] A. Kinkhabwala et al., Nature Photonics 3, 654-657 (2009)
[2] P.P. Pompa et al., Nature Nanotechnology 1, 126-130 (2006)
[3] H. A. Atwater & A. Polman, Nature Materials 9, 205-213 (2010)

Two-photon lasing in the dispersive regime of cavity QED

C. Sanchez-Munoz[1], E. del Valle[1], A. Gonzalez-Tudela[1], S. Lichtmannecker[2], K. Mueller[2], A. Buse[2], C. Tejedor[1], J.J. Finley[2] and F.P. Laussy[2]

[1] *Departamento de Física Teórica de la Materia Condensada, Facultad de Ciencias, Universidad Autónoma de Madrid, E-28049 Madrid, Spain*
[2] *Walter Schottky Institut, Technische Universitt Mnchen, Am Coulombwall 3, D-85748, Garching, Germany*

Semiconductor nanostructures are the main candidates for being sources of special photon states. In this contribution, we consider the dispersive regime of a coherently excited quantum dot embedded in a microcavity. At certain resonant frequencies of the coherent excitation, quantum superpositions of the ground state and n-photon Fock states inside the cavity are obtained, observed as peaks in the cavity populations and the correlation functions.

We focus on the case of possible lasing emission of photon pairs by using a joint master equation description and Monte Carlo simulations. We show that the system can be brought to emit light in a regime in which the dominant emission corresponds to two correlated, successive photons (within a coherence time provided by the cavity decay rate). Such emission dominates over all other types of emission, in particular, that of single uncorrelated photons.

An analysis of the various regimes of operation around this two-photon resonance is carried out to discuss the adequacy of the standard correlation functions (such as $g^{(2)}(\tau)$) to describe the light actually emitted by the system; in particular, we show that extremely large values of bunching are not a guarantee of a useful two-photon emission.

Prospects of higher n-photon laser devices and figures of merits for technological applications, such as quantum lithography, are discussed.

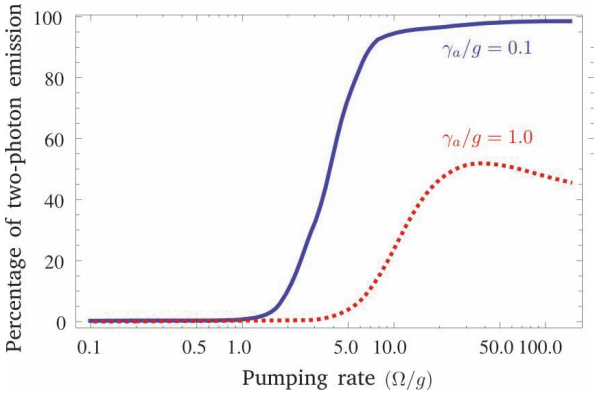

Figure 1: Fraction of two-photon emission over all other types of emission as a function of pumping in a cavity QED system with a low (dotted red) and high (solid blue) Q factor of the cavity. In a good enough system, all the light is emitted as two-photons, thereby realizing a pure two-photon laser.

Capillary driven strain-free synthesis of epitaxial PbTe/CdTe quantum dots for min-infrared devices

G. Springholz, I. Daruka, H. Groiss, F. Schäffler, A. Hochreiner, A.Khiar, M.Eibelhuber

Institut for Semiconductor Physics, Johannes Kepler University, A-4040 Linz, Austria

Self-assembled semiconductor quantum dots are commonly produced by strain-driven Stranski-Krastanow growth of strained-layer heteroepitaxy. The resulting quantum dots have been widely employed for visible and near-infrared photonics but efficient mid-infrared emission has been difficult to achieve due strain-induced type II band alignments. As a solution, we have invented a strain-free synthesis method that is based on capillary driven phase separation and nano-precipitation rather than on epitaxial strain [1]. This method has been applied to the PbTe/CdTe model system, which is a combination of a narrow gap IV-VI semiconductor with a wide gap II-VI semiconductor, featuring identical lattice constants but different crystal structures. As shown by Fig. 1, due to phase separation, 2D PbTe/CdTe epilayers grown by molecular beam epitaxy onto GaAs (001) transform into isolated quantum dots during post annealing. The resulting QDs show highly symmetric shapes and their size is well controlled. This leads to an exceedingly wide tunability of emission over the whole 1.5 to 4 µm wavelength region [1], well suited for optoelectronic device applications.

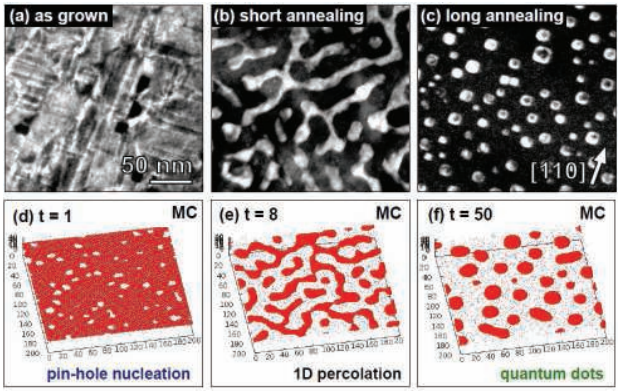

Figure 1: Formation of PbTe/CdTe nanocrystals by capillary driven nanoprecipitation from intially 2D epitaxial PbTe layers embedded in CdTe.
Top: Pan-view TEM images for (a-c) as grown, short and long annealed sample.
Bottom: Coarse grain Monte Carlo simulation of the topological transition, revealing the three characteristic transformation stages.

To unravel the mechanism involved in this synthesis method, in the present work we have developed a Monte Carlo model that accounts for thermodynamics by appropriate choice of the nearest and next-nearest neighboring bond energies. As demonstrated by Fig. 1, this model captures all essential features observed by *in situ* TEM annealing experiments, namely, the initial nucleation of interpenetrating pin-holes in the 2D epilayers that rapidly grow in size to form a one-dimensional percolation network, which then subsequently split up further into isolated QDs (*cf.* lower part of Fig. 1). Further annealing leads to coarsening by Ostwald ripening. As demonstrated by our calculation, this *topological transition* is driven by interface-energy minimization of the two phase system and the key kinetic parameters of this process are identified. Quantitative comparison of the size distribution, density and shapes shows excellent agreement between calculations and experimental data, including also the results from optical measurements. Based on the energetics, we propose a generic analytic model that predicts the size of the quantum dots as a function of the initial structure parameters that can be applied to arbitrary material systems.

[1] H. Groiss *et al*., APL **91** 222106(2007). A. Hochreiner *et al*., APL **98** 021106(2011); APL **100**, 113112 (2012).
[2] H. Groiss, I. Daruka *et al*., submitted.

In-situ electron-beam lithography of deterministic nanophotonic structures using low temperature cathodoluminescence spectroscopy

M. Gschrey, F. Gericke, R. Schmidt, A. Schüssler, J.-H. Schulze, T. Heindel, S. Rodt, A. Strittmatter, and S. Reitzenstein

Institut für Festkörperphysik, Technische Universität Berlin, Hardenbergstraße 36, D-10623 Berlin, Germany

Single semiconductor quantum dots (QDs) integrated within microcavity structures are a promising tool for the development of non-classical light sources for optical quantum technology. For maximum performance of such quantum devices, the coupling between a target QD and the optical mode of the microcavity needs to be precisely controlled, both spatially *and* spectrally. To achieve spatial alignment, the growth of site-controlled QDs has received great attention. However, these QDs still suffer from a reduced optical quality if compared to standard self-organized QDs. Moreover, for a fully deterministic device it will be vital to ensure spectral alignment which can be achieved by in-situ lithography techniques.

In this work, we report on a novel, fully-deterministic nanophotonic device technology using high-resolution electron-beam in-situ lithography. Our approach combines low-temperature cathodo-luminescence (CL) spectroscopy with high-resolution electron-beam writing of nanostructures and is demonstrated by patterning single-QD mesa structures.

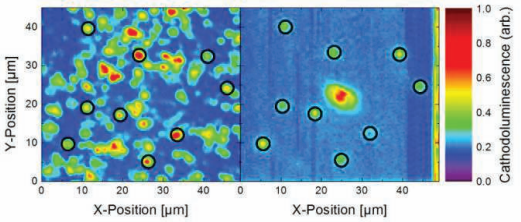

Fig. 1: CL-intensity maps before (a) and after (b) fabrication of single-QD mesa structures. Black circles in (a) mark the selected QDs that are integrated into the sub-µm mesa structures.

The in-situ lithography process starts by spin-coating a planar GaAs sample containing InGaAs QDs in the active layer with the standard electron beam resist PMMA. Subsequently, the sample is mapped by CL to select target QDs and to determine precisely their position and their emission wavelength. A respective CL intensity map is depicted in Fig. 1a). It shows CL emission from a number of QDs, nine of which are selected (indicated by black circles) for in-situ lithography. The CL-selection step is performed at low electron-beam dose to avoid an over-exposure of the resist. Next, we define sub-µm sized mesa structures on the resist which are precisely aligned to the selected QDs. The structures are written at a higher electron dose to locally invert the resist. In this configuration the exposed resist acts as an etch mask which allows us to realize sub-µm photonic structures with nm-accuracy.

To verify the positioning process of deterministically patterned single-QD mesas, another CL-mapping was performed. The associated CL intensity-map is shown in Fig. 1b) and nicely demonstrates that all mesa-structures are at the pre-selected positions, and that 90% of them are optically active. The optical properties are studied in more detail via micro-photoluminescence measurements at low temperature. We observe resolution-limited single-QD emission linewidths of 17 µeV, verifying the high optical quality of our nanophotonic structures. Single-photon emission is verified by second-order correlation measurements on single emission lines, resulting in $g^{(2)}(0) = 0.02$.

Author Index

G

L